SEAFLOWER BIOSPHERE RESERVE: NEW FINDINGS AND TRENDS IN THE LARGEST CARIBBEAN MARINE PROTECTED AREA

EDITED BY: Juan Armando Sanchez, Sonia Bejarano and Santiago Herrera
PUBLISHED IN: Frontiers in Marine Science

frontiers Research Topics

frontiers

ISSN 1664-8714
ISBN 978-2-88971-836-8
DOI 10.3389/978-2-88971-836-8

About Frontiers

Frontiers is more than just an open-access publisher of scholarly articles: it is a pioneering approach to the world of academia, radically improving the way scholarly research is managed. The grand vision of Frontiers is a world where all people have an equal opportunity to seek, share and generate knowledge. Frontiers provides immediate and permanent online open access to all its publications, but this alone is not enough to realize our grand goals.

Frontiers Journal Series

The Frontiers Journal Series is a multi-tier and interdisciplinary set of open-access, online journals, promising a paradigm shift from the current review, selection and dissemination processes in academic publishing. All Frontiers journals are driven by researchers for researchers; therefore, they constitute a service to the scholarly community. At the same time, the Frontiers Journal Series operates on a revolutionary invention, the tiered publishing system, initially addressing specific communities of scholars, and gradually climbing up to broader public understanding, thus serving the interests of the lay society, too.

Dedication to Quality

Each Frontiers article is a landmark of the highest quality, thanks to genuinely collaborative interactions between authors and review editors, who include some of the world's best academicians. Research must be certified by peers before entering a stream of knowledge that may eventually reach the public - and shape society; therefore, Frontiers only applies the most rigorous and unbiased reviews.
Frontiers revolutionizes research publishing by freely delivering the most outstanding research, evaluated with no bias from both the academic and social point of view. By applying the most advanced information technologies, Frontiers is catapulting scholarly publishing into a new generation.

What are Frontiers Research Topics?

Frontiers Research Topics are very popular trademarks of the Frontiers Journals Series: they are collections of at least ten articles, all centered on a particular subject. With their unique mix of varied contributions from Original Research to Review Articles, Frontiers Research Topics unify the most influential researchers, the latest key findings and historical advances in a hot research area! Find out more on how to host your own Frontiers Research Topic or contribute to one as an author by contacting the Frontiers Editorial Office: frontiersin.org/about/contact

SEAFLOWER BIOSPHERE RESERVE: NEW FINDINGS AND TRENDS IN THE LARGEST CARIBBEAN MARINE PROTECTED AREA

Topic Editors:
Juan Armando Sanchez, University of Los Andes, Colombia
Sonia Bejarano, Leibniz Centre for Tropical Marine Research (ZMT), Germany
Santiago Herrera, Lehigh University, United States

Citation: Sanchez, J. A., Bejarano, S., Herrera, S., eds. (2021). SeaFlower Biosphere Reserve: New Findings and Trends in the Largest Caribbean Marine Protected Area. Lausanne: Frontiers Media SA. doi: 10.3389/978-2-88971-836-8

Table of Contents

frontiers in Marine Science

EDITORIAL
published: 15 October 2021
doi: 10.3389/fmars.2021.772150

Editorial: SeaFlower Biosphere Reserve: New Findings and Trends in the Largest Caribbean Marine Protected Area

Juan Armando Sánchez[1]*, *Sonia Bejarano*[2] and *Santiago Herrera*[3]

[1] Biological Sciences, University of Los Andes, Bogotá, Colombia, [2] Leibniz Centre for Tropical Marine Research (LG), Bremen, Germany, [3] Department of Biological Sciences, Lehigh University, Bethlehem, PA, United States

Keywords: coral reefs and islands, Caribbean, SeaFlower biosphere reserve, San Andrés, Providencia and Santa Catalina Islands, Colombia

Editorial on the Research Topic

SeaFlower Biosphere Reserve: New Findings and Trends in the Largest Caribbean Marine Protected Area

OPEN ACCESS

Edited and reviewed by:
Laura Airoldi,
University of Padova Chioggia Hydrobiological Station, Italy

***Correspondence:**
Juan Armando Sánchez
juansanc@uniandes.edu.co

Specialty section:
This article was submitted to Marine Conservation and Sustainability, a section of the journal Frontiers in Marine Science

Received: *07 September 2021*
Accepted: *20 September 2021*
Published: *15 October 2021*

Citation:
Sánchez JA, Bejarano S and Herrera S (2021) Editorial: SeaFlower Biosphere Reserve: New Findings and Trends in the Largest Caribbean Marine Protected Area. Front. Mar. Sci. 8:772150. doi: 10.3389/fmars.2021.772150

The SeaFlower Biosphere Reserve-SFBR is home to the most developed coral reefs in the Caribbean Sea and some of the few atolls and barrier reefs in the Atlantic Ocean (Geister, 1992). In what was perhaps the first scientific study in this area, John Milliman highlighted the prolific development of coral reefs in Albuquerque, Courtown (Bolivar), Serrana, and Quitasueño, the four atolls that surround the islands of San Andrés, Providencia, and Santa Catalina (Milliman, 1969). The archipelago's reefs likely remained in good condition over the following two decades, whether these were relatively remote or close to inhabited islands. The first expeditions led by INVEMAR in the mid-90's revealed both the enormous coral-dominated areas of these structurally complex reefs and their evident deterioration in coral health with the presence of diseases and partially dead corals (Diaz et al., 1996; Zea et al., 1998). People's awareness of these changes and threats was a motivation to establish a reserve. The Raizal community–descending from European, African, and indigenous people that kept their language and culture–together with the local environmental authority (CORALINA), and in collaboration with international scientific institutions, promoted the establishment of the SeaFlower Biosphere Reserve in the year 2000. The Reserve is considered an exemplary case of participatory mapping and zonation worldwide (Friedlander et al., 2003). Today, the SeaFlower Biosphere Reserve management plan remains the roadmap for sustainable development in the archipelago.

This special topic compiles 13 scientific studies conducted by 72 authors, 55 of whom are Colombians. This is a remarkable effort given the remoteness and financial challenges associated with conducting research in the Global South. Collectively, these studies considered biodiversity levels and ecosystem functioning in the Reserve, emphasizing detecting accelerated environmental changes in recent years. Several tropical storms recently impacted the study area, including Iota (2020), a category five hurricane from which its inhabitants are still recovering. Understanding environmental change and strengthening social-ecological resilience are essential objectives for this region to prosper sustainably.

New biodiversity assessments presented in this topic found 263 previously unreported species. The biodiversity knowledge of the SFBR is increasing in numbers, proving to be an important setting for invertebrates and marine fish that requires further exploration. Of the 138 echinoderms found in the Reserve so far, 10 species were new records (Borrero-Pérez et al.). Similarly, Acero et al. reported 220 species of fish for the first time in the Reserve. These add up to 411 species, approximately a quarter of the total species found in the greater Caribbean when added to previous records. In mesophotic coral ecosystems, between 40 and 115 m deep, Sánchez, González-Zapata et al. found a complete replacement of the community of corals, octocorals, and black corals, totaling 33 species, all new records for the area, and in the case of *Stylaster duchassaingi* is the southernmost record of the species. In contrast, some octocorals may be new to science. Alvarez-Yela et al. also contributed with an original aspect of the Reserve's biodiversity, the microbiomes of some corals, sponges, and sediments; a starting point for the study of microbial diversity in the remote Serrana atoll. These contributions identified new knowledge gaps, including the structure, biodiversity, and functioning of deeper reef environments and coral-associated microbiota.

Other contributions focused on ecosystem functioning and large-scale oceanographic processes. Idárraga-García and León found that in a single atoll (Roncador), there are geomorphological features such as canyons that point at previously unknown flows of matter and energy between shallow and deep ecosystems, as well as large landslides. The SeaFlower Biosphere Reserve occupies a prominent area within the Caribbean basin that is characterized by its heterogeneity in connectivity patterns. Lopera et al. demonstrate that some areas within the SFBR act as larval sinks (e.g., Serranilla, Providencia, Quitasueño, and Serrana), whereas the primary larval sources are found in the northern region of the Reserve (e.g., Serranilla, Alicia, and Nuevo). Populations of queen conch at Serrana bank, as presented by Ardila et al., are as numerous as the most preserved areas in the Caribbean (e.g., Bahamas) and sustain a well-managed artisanal fishery. Ramirez-Gallego and Barrientos-Muñoz found that Serrana and Serranilla comprise hope areas for the endangered populations of loggerhead and hawksbill turtles, where they regularly nest. In addition, Barragán-Barrera et al. found that although studies on dolphins of the genus *Stenella* suggest they prefer coastal waters, observations around the Reserve suggest that for *S. attenuata* and *S. longirostris* these remote and oceanic environments are equally important for their populations. These results constitute new knowledge for the management of the Reserve and its marine resources.

In line with global trends, the SFBR changes have accelerated in the last three decades, resulting in severe coral reef degradation. According to Sánchez, Gómez-Corrales et al. the percent cover of reef-building corals and coralline algae in Serrana and Roncador has decreased abruptly while the cover of leafy algae has increased significantly since 1995. In both areas, these changes have been accompanied by an increase in octocoral densities. According to Bernal-Sotelo et al., key species of reef-building corals, such as the pillar coral *Dendrogyra cylindrus* in Providencia, have declined in percent cover and abundance since the beginning of the century, practically in the absence of recruitment. Further, Lizcano-Sandoval et al. recorded reduced skeletal densities in *Orbicella faveolata* over the last decades. A combination of global and local factors may be working in synergy to explain the decline of reef-building corals in the SFBR. Against this concerning backdrop, Guerra-Vargas et al. find that seagrasses in San Andrés hold enormous potential for removing atmospheric carbon dioxide and sustain higher ecosystem service levels when they occur next to coral reefs. There are many reasons to act decisively to halt the sources of coral reef decline in SFBR. The need to mitigate local stressors and continue advocating for reductions in greenhouse gas emissions globally is clear. The SFBR, however, needs further studies addressing social-ecological issues to understand resilience patterns, including timely assessments of coral reef fisheries.

The SFBR is a natural laboratory for the study and conservation of coral and island ecosystems. International scientific support is urgently needed to explore its deep-sea environments, which are practically unknown. This special topic constitutes a milestone in open marine science within a marine protected area in a country with little tradition of sharing raw data. Collectively, it was a great effort for the authors, the FMR team, and the dedication of the reviewers that allowed us not only to maintain scientific rigor but also to improve the quality of the manuscripts.

AUTHOR CONTRIBUTIONS

JS wrote the editorial with inputs from SB and SH. All authors read and approved the manuscript.

FUNDING

This Research Topic was encouraged and partially supported by the ColombiaBIO-Colciencias (Convenio 341-2016, Universidad de los Andes-Comisión Colombiana del Océano-CCO) and Corporación para el Desarrollo Sostenible del Departamento Archipiélago de *San Andrés* Providencia y Santa Catalina, CORALINA-Universidad de los Andes (Convenios No. 13, 2014 and No. 21, 2015). Many contributions were part of the SeaFlower Expeditions (2015–2016) organized and sponsored by Comisión Colombiana del Océano-CCO/Dimar (J. M. Soltau, J. Sintura, A. Chadid, R. Carranza, and their team), Colombian Navy (ARC Providencia and crew, Serrana Expedition), Coralina (N. Bolaños, E. Castro, and their team), Secretaría de Pesca y Agricultura (Gobernación del Departamento de San Andrés, Providencia y Santa Catalina), ColombiaBIO-MinCiencias (F. García, L. Ayala, and team).

REFERENCES

Diaz, J. M., Diaz, G., Garzon-Ferreira, J., Geister, J., Sánchez, J. A., and Zea S. (1996). *Atlas de los Arrecifes Coralinos del Caribe Colombiano. I. Archipiélago de San Andrés y Providencia*. Santa Marta: Invemar.

Friedlander, A., Sladek-Nowlis, J., Sánchez, J. A., Appeldoorn, R., Usseglio, P., Mccormick, C., et al. (2003). Designing effective marine protected areas in old providence and Santa Catalina Islands, San Andrés Archipelago, Colombia, using biological and sociological information. *Conserv. Biol.* 17, 1769–1784. doi: 10.1111/j.1523-1739.2003.00338.x

Geister, J. (1992). Modern reef development and Cenozoic evolution of an oceanic island/reef complex: Isla de Providencia (Western Caribbean Sea, Colombia). *Facies* 27, 1–69.

Milliman, J. D. (1969). Four Southwestern Caribbean Atolls: Courtown Cays, Albuquerque Cays, Roncador Bank and Serrana Bank. *Atoll Res. Bull.* 129, 1–26. doi: 10.5479/si.00775630.129.1

Zea, S., Geister, J., Garzón-Ferreira, J., and Díaz, J. (1998). *Biotic Changes in the Reef Complex of San Andrés Island (Southeastern Caribbean Sea, Columbia) Occuring Over Nearly Three Decades*. Washington, DC: Smithsonian Inst.

Conflict of Interest: The authors declare that the research was conducted in the absence of any commercial or financial relationships that could be construed as a potential conflict of interest.

frontiers in Marine Science

ORIGINAL RESEARCH
published: 17 January 2019
doi: 10.3389/fmars.2018.00513

Decadal Change in the Population of *Dendrogyra cylindrus* (Scleractinia: Meandrinidae) in Old Providence and St. Catalina Islands, Colombian Caribbean

Katherine Bernal-Sotelo[1], Alberto Acosta[2] and Jorge Cortés[3,4]*

[1] Posgrado en Biología, Universidad de Costa Rica, San José, Costa Rica, [2] UNESIS, Departamento de Biología, Pontificia Universidad Javeriana, Bogotá, Colombia, [3] Centro de Investigación en Ciencias del Mar y Limnología (CIMAR), Universidad de Costa Rica, San José, Costa Rica, [4] Escuela de Biología, Universidad de Costa Rica, San José, Costa Rica

OPEN ACCESS

Edited by:
Sonia Bejarano, Leibniz Centre for Tropical Marine Research (LG), Germany

Reviewed by:
Jose M. Fariñas-Franco, National University of Ireland Galway, Ireland
Bernhard Riegl, Nova Southeastern University, United States

***Correspondence:**
Katherine Bernal-Sotelo
jkatherinebs@gmail.com

Specialty section:
This article was submitted to Marine Conservation and Sustainability, a section of the journal Frontiers in Marine Science

Received: *11 July 2018*
Accepted: *21 December 2018*
Published: *17 January 2019*

Citation:
Bernal-Sotelo K, Acosta A and Cortés J (2019) Decadal Change in the Population of Dendrogyra cylindrus (Scleractinia: Meandrinidae) in Old Providence and St. Catalina Islands, Colombian Caribbean. Front. Mar. Sci. 5:513. doi: 10.3389/fmars.2018.00513

The IUCN considers the stony coral *Dendrogyra cylindrus* as vulnerable. However, there is insufficient information on its population structure and dynamics, conservation status, or extinction risk and population decreases have been inferred from observations of habitat degradation. In 2002 and 2012, surveys using manta tows, circular plots and satellite images were performed in Old Providence and Santa Catalina Islands (Seaflower Biosphere Reserve) to determine changes in the condition and structure of a local population of *D. cylindrus* and its habitat. Size-frequency histograms were asymmetric and leptokurtic, showing positive distribution induced by colony fragmentation, which is indicative of reef degradation. Signs of degradation were more evident in 2012, when partial mortality of living tissue in the parent colony yielded 96.6% of the asexually produced fragments. Most of the fragments were from larger colonies (≥115 cm), which exhibited the highest partial and total mortality (>50%). Three of the four benthic habitats used by the species in 2002 were seen in 2012, but with reduced areas. The results suggest that the reduction of living tissue, the dominance of colonies produced asexually, and reduced size of fragments limit population growth and species viability in an unfavorable and changing habitat within this marine protected area (MPA) of the southwestern Caribbean. In the west of the reef complex of Old Providence, a synergy of multiple stressors could cause the habitat degradation and the fragmentation of colonies, limiting the potential recovery of the species and therefore the ability to create a healthy, genetically diverse and resilient population. Thus, these stressors must be minimized to prevent local extinction. Monitoring the population trends and recording sexual recruitment continues to be vital to understand the larvae's habitat selection and determine whether these habitats are suitable for the survival of coral recruits. Other stressors to be monitored include anchor damage, diseases and bleaching. We recommend the MPA management program to include specific plans of conservation, recovery and restoration for coral reef builders species like *D. cylindrus*.

Keywords: *Dendrogyra cylindrus*, population size distribution, habitat, partial mortality, fragmentation

INTRODUCTION

Dendrogyra cylindrus Ehrenberg, 1834 is a stony coral with a restricted distribution in the Caribbean. Despite its low abundance in its habitat, this species' construction of vertical cylindrical columns makes it conspicuous in reefs (INVEMAR, 2010), covering significant horizontal and vertical extensions, and reaching heights of two to three meters (Almy and Carrion, 1963; Prahl and Erhardt, 1985). This species' characteristic vertical growth increases the habitat's three-dimensionality (Acosta and Acevedo, 2006), fostering local biodiversity and making it an excellent reef builder. *D. cylindrus* reproduces both asexually and sexually, releasing sperm and incubating fecundated eggs (Szmant, 1986; Richmond and Hunter, 1990; Marhaver et al., 2015). This coral is slow growing, 0.8–2 cm/year (Hughes, 1987; Hudson and Goodwin, 1997), long-lived, and can compete for space due to its asexual reproduction strategy (Hughes and Tanner, 2000; Darling et al., 2012). *D. cylindrus* is usually found at depths between 5 and 12 m, as part of fringing reefs along the sheltered shores of Caribbean islands, where the substrate is mainly sand and consolidated dead coral colonized by octocorals, mixed coral, and sponges (Prahl and Erhardt, 1985; Geister and Díaz, 1997; Díaz et al., 2000; Acosta and Acevedo, 2006). In Colombia, the habitat of *D. cylindrus* has been reported exclusively in the Seaflower Biosphere Reserve which is a marine protected area (MPA). Within this MPA, the reef complex of Old Providence Island hosts more than 90% of the total Colombian *D. cylindrus* population.

The Seaflower Biosphere Reserve was declared as an MPA in 2005 and covers all the Archipelago of San Andres and it includes the islands and cays of Providence, San Andrés, Bolivar, Alburquerque, Quitasueño, Serrana and Roncador. The reserve has created specific areas where particular activities are allowed or prohibited to safeguard the marine ecosystems. Although there are no coral management and conservation plans, there is a reef monitoring program, but it does not include a detailed monitoring of *D. cylindrus* population structure. In Old Providence Island, the only protected area is the McBean Lagoon National Natural Park in the northeast, where very few colonies of *D. cylindrus* remain.

The species' limited sexual reproduction (Acosta and Acevedo, 2006; Brainard et al., 2011), asynchronous spawning (Marhaver et al., 2015) and propensity to fragmentation, bleaching and diseases contribute to its vulnerability. White plague is a highly virulent disease that affects this species and destroys tissue; type I destroys 3.1 mm day^{-1} and type II destroys 3.3 mm day^{-1} (Richardson et al., 1998; Weil, 2004). Its low reproductive output limits population connectivity and recovery within the metapopulation (Rockwood, 2006). These factors, combined with low juvenile survival rates, low observed recruitment, and, possibly, low frequency of reproductive colonies, have the potential to decrease population growth (Aronson et al., 2008).

According to Acosta and Acevedo (2006), the population could be maintained via asexual reproduction by fragmentation using two mechanisms. First, columns of the colony break off and fall and in some cases the ramet fixes to the substrate creating columns by positive phototropism, which allows it to grow vertically and horizontally. Alternatively, the living tissue on the columns dies by natural causes, leaving patches of live tissue on the skeleton, and creating physically isolated fragments (Meesters et al., 1997; Hughes and Tanner, 2000). Excess fragmentation, however, results in constant loss of parent colony live tissue (Lirman, 2000; Cooper et al., 2009), which is expensive to regenerate, high fragment mortality (Hughes and Jackson, 1980; Chadwick-Furman et al., 2000), reduction of average colony size (e.g., *Orbicella annularis* Pante et al., 2008; Alvarado-Chacón and Acosta, 2009b), and an imbalance in the relative proportion of size classes, resulting in lower population growth (Vandermeer and Goldberg, 2003).

The 2017 IUCN Red List of Threatened Species (Aronson et al., 2008) and NOAA (2014) list *D. cylindrus* as a vulnerable species because of its declining populations caused by the degradation and destruction of reef habitats (Wilkinson, 2008). The IUCN recommends research on population abundance and trends, ecology and habitat status, threats and resilience, restoration and management of new protected areas. Despite the IUCN's suggestion, population structure analyses are still scarce for most stony corals, and *D. cylindrus* is no exception. Besides, it is unknown how disturbances in the last decade have altered the structure and colonization habitat of *D. cylindrus* on Caribbean coral reefs (Aronson et al., 2008).

Given that the changes in the abundance and distribution over time can be an indication of the health of populations of *D. cylindrus,* as well as their sustainability in the ecosystem, in this study we evaluate the changes in its population structure and habitat over a decade in the reefs of Old Providence and St. Catalina Islands, which are part of the Seaflower Biosphere Reserve MPA.

MATERIALS AND METHODS

Study Site

Surveys were conducted in the Old Providence and St. Catalina Islands reef complex in the Archipelago of San Andrés, Colombian Caribbean (**Figure 1**). This archipelago is part of the Seaflower MPA, which was recognized by UNESCO as a Biosphere Reserve. The islands have a shallow marine platform with a 285.2 km^2 reef complex (Díaz et al., 2000). The study area covered the shallow reef complex (1–15 m depth) that surrounds the islands.

The data obtained by Acosta and Acevedo (2006) in 2002 was used as a baseline to evaluate the change in population structure for *D. cylindrus* in 2012. The manta tow technique, which consist of towing a diver with a small boat to produce a general description of large areas of the reef (Rogers et al., 1994), was used to locate and create a spatial distribution map, using zigzag band transects and covering 1.6 km^2. In places where more than four colonies were observed, 60 m-diameter circular plots were set *in situ* to measure the size and condition of colonies and fragments (**Figure 1**). A total of 20 plots were assessed. The center point of each plot was georeferenced. The 2002 study determined that the habitat and areas with the highest population density were to the west of the islands. This information was used to

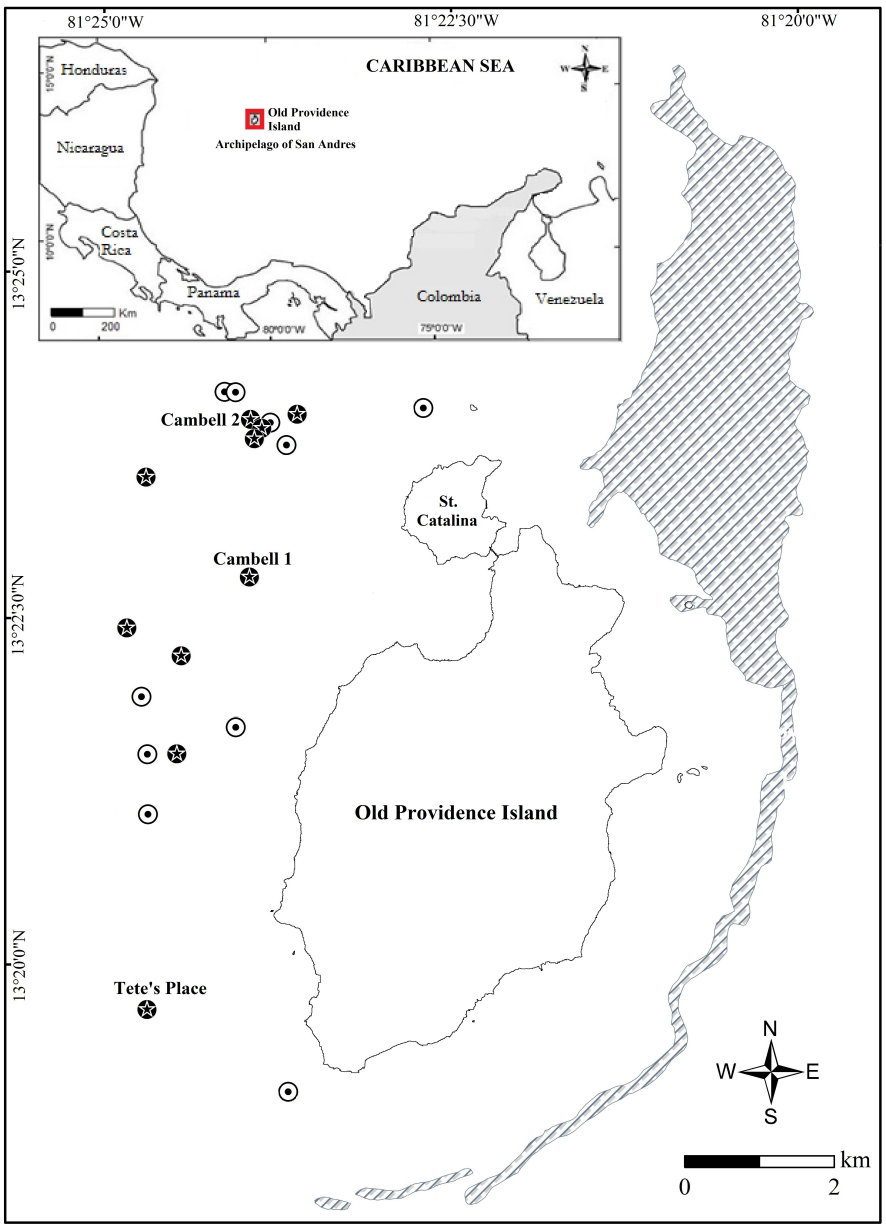

FIGURE 1 | Study area in Old Providence and St. Catalina Islands. Black circles with stars: plots where colonies were found in 2002 and 2012. White circles with dots: plots where colonies were found in 2002, but not in 2012. Barrier reef: striped area east of the islands. Cambell 1, Cambell 2, and Tete's Place are popular dive sites.

plan the 2012 sampling. The same 20 plots surveyed in 2002 were resampled, all west of the islands where some of the best-known dive sites are located (**Figure 1**). No live colonies of *D. cylindrus* were found in ten of the 2012 plots; only skeletal remains existed, despite extending the diameter of the plots to 70 m to confirm the absence of live colonies (**Figure 1**).

Population Structure Analysis

The population structure for *D. cylindrus* was determined by measuring the size of the individuals (colonies and fragments) and constructing size-frequency histograms. The maximum height (cm) of each colony and the maximum length (cm) of each fragment were measured and then classified into size classes. The fragments could have two origins, as explained above: (a) physical detachment from the parent colony, where fragments were lying horizontally on the substrate around the colony, or (b) partial mortality of the parent colony, where remaining live tissue generated clones (fragments) on the standing colony. The colonies and fragments were grouped into ten categories according to their size following the Sturges Rule (Llinás and Rojas, 2006). Size-class distribution diagrams were created for the entire population, as well as for colonies and fragments separately

to verify their respective contribution to the distribution based on the absolute frequency of individuals in each size class.

Population structure changes between 2002 and 2012 were assessed by comparing the size-class distribution diagrams, calculating their asymmetry (α3) and kurtosis (α4), which were used as base parameters to evaluate the bias of the two curves (skewness and peakedness relative to a normal distribution). We also compared the absolute frequencies of the colonies and fragments by size class, as well as the total average size of the colonies and fragments (height and length, respectively) by applying non-parametric Mann–Whitney *U* and *Z* tests and the Kolmogorov–Smirnov tests for two samples. Additionally, we calculated descriptive statistics [mode, geometric mean, and coefficient of variation (CV)] to analyze size variability, in this case, colony height and fragment length.

Colony Condition

To determine the condition of the colonies and determine how the condition changed over time, we measured the partial mortality of each colony by identifying the lesions that physically separated part of the live tissue from the rest. We also measured the frequency of colonies with signs of white syndromes (i.e., bleaching and white diseases), as well as erosion at the base of the colony, manifested by a thinning of the colony base that can lead to a toppling. After using these three variables (i.e., average partial mortality by colony, absolute frequency of colonies with white syndromes, and absolute frequency of colonies with erosion at the base) to determine the condition of colonies, we compared the results between 2002 and 2012 using the Mann–Whitney *U* test. Non-parametric tests were employed because the Kolmogorov–Smirnov test with the Lilliefors correction and Levene test showed non-normality and non-homogeneity of variances of the five dependent variables both untransformed, and after being transformed by square root, log, natural log and Box-Cox.

Habitat Change

We identified the habitats used by *D. cylindrus* in the shallow reef complex (<15 m depth) using the landscape units previously produced by Bernal-Sotelo (2015) for 2000 and 2012, as well as the georeferenced points of the circular plots. This identification was carried out by placing the georeferenced points on each of the maps to visualize the distribution areas of *D. cylindrus*. Using ArcGIS 10.0 and the shapefile maps of Bernal-Sotelo (2015), we assessed the relationship between the potential area of use of each habitat (i.e., the total area of each habitat where the species is present and which corresponds to the area that could potentially be colonized by *D. cylindrus*) and the active use observed in each habitat (i.e., the absolute frequency of colonies and fragments present in each plot and habitat). Similarly, we counted the number of times that *D. cylindrus* populations and their habitat changed within 10 years, and calculated the percentages of change in both cases. We then quantified the relationship between the rate of change of *D. cylindrus* populations and the rate of habitat change. Using the HaviStat 1.0 program (Montenegro and Acosta, 2008), we estimated Bailey's confidence intervals for each year to evaluate whether the species used any of the habitats, and analyzed the changes in use by creating graphs of potential area and frequency of observed use.

RESULTS

Population Structure Analysis

In 2002, 283 individuals of *D. cylindrus* were quantified (20 plots, 0.06 km^2), of which 213 were colonies and 70 were fragments (Acosta and Acevedo, 2006). In contrast, in 2012, 846 individuals were recorded, of which 261 were colonies and 585 were fragments (present in only ten plots, 0.03 km^2). In 2012, the number of fragments increased by 515 in comparison to 2002 (an increase of 313%) which explains the relative increase in population after ten years. There were significant differences in the size of the total population (colonies and fragments) between 2002 and 2012 (*U* and Z_{K-S}: $p < 0.05$, $n = 1129$). In both years, the size-frequency histograms were skewed to the right, showing a leptokurtic distribution (>3: 2002 = 3.7 and 2012 = 8.9), and had positive asymmetry (>0: 2002 = 1 and 2012 = 2.2). This trend was emphasized in 2012 (**Figure 2**). In 2002, ∼65% of the colonies and fragments were in the first four size classes (<15.1–75 cm), while in 2012, ∼60% of the total the population were in these classes (**Figure 2**). The average size of the colonies and fragments in 2012 was smaller than in 2002, but had a higher coefficient of variation compared to 2002 (**Table 1**).

Colony frequency and height in all size classes were similar in 2002 and 2012 (*U* and Z_{K-S}: $p > 0.05$, $n = 474$), showing a leptokurtic distribution (α_4: 2002 = 3.5, 2012 = 4.3) and positive asymmetry (α_3: 2002 = 0.9, 2012 = 1.3). In both years, most of the colonies (2002 = 67.6%, 2012 = 70.5%) were in the first five size classes (**Figure 2**). The colonies in 2012 were 4.7 cm higher (on average) than those in 2002 (**Table 1**). The frequency and length in all size classes of fragments changed significantly between 2002 and 2012 (*U* and Z_{K-S}: $p < 0.05$, $n = 655$). The distribution of fragment sizes was also leptokurtic (>3) and had positive asymmetry (>0); this trend was heightened in 2012 (α_4: 2002 = 4.6, 2012 = 6.0; α_3: 2002 = 1.2, 2012 = 1.6). In 2002, ∼70% of the fragments were in the first four size classes, while in 2012, ∼78% were in the first two categories (**Figure 2**). The fragments in 2002 were, on average, larger than those in 2012 by 22.7 cm, a decrease of 47.3% (**Table 1**). This size reduction occurred because 96.6% of the fragments in 2012 were clones (living tissue surrounded by the skeleton), while in 2002 this type of fragmentation only represented 30% of the total. The fragments on the columns were smaller than the fragments lying on the substrate near the colony.

Colony Condition

The number of colonies affected by some level of partial mortality in 2012 (61.3%) was significantly greater (*U*: $p = 0.03$, $n = 474$) than in 2002 (56.8%; **Figure 3**). In addition, partial colony mortality was higher in 2012 (25% ± 32.8%) than in 2002 (15.3% ± 21.9%). However, in both years, partial mortality had higher average values in the larger size categories (**Figure 3**). Partial mortality was significantly higher in 2012 than in 2002 in the largest size classes: 135.1–155 cm (*U*: $p = 0.001$, $n = 23$),

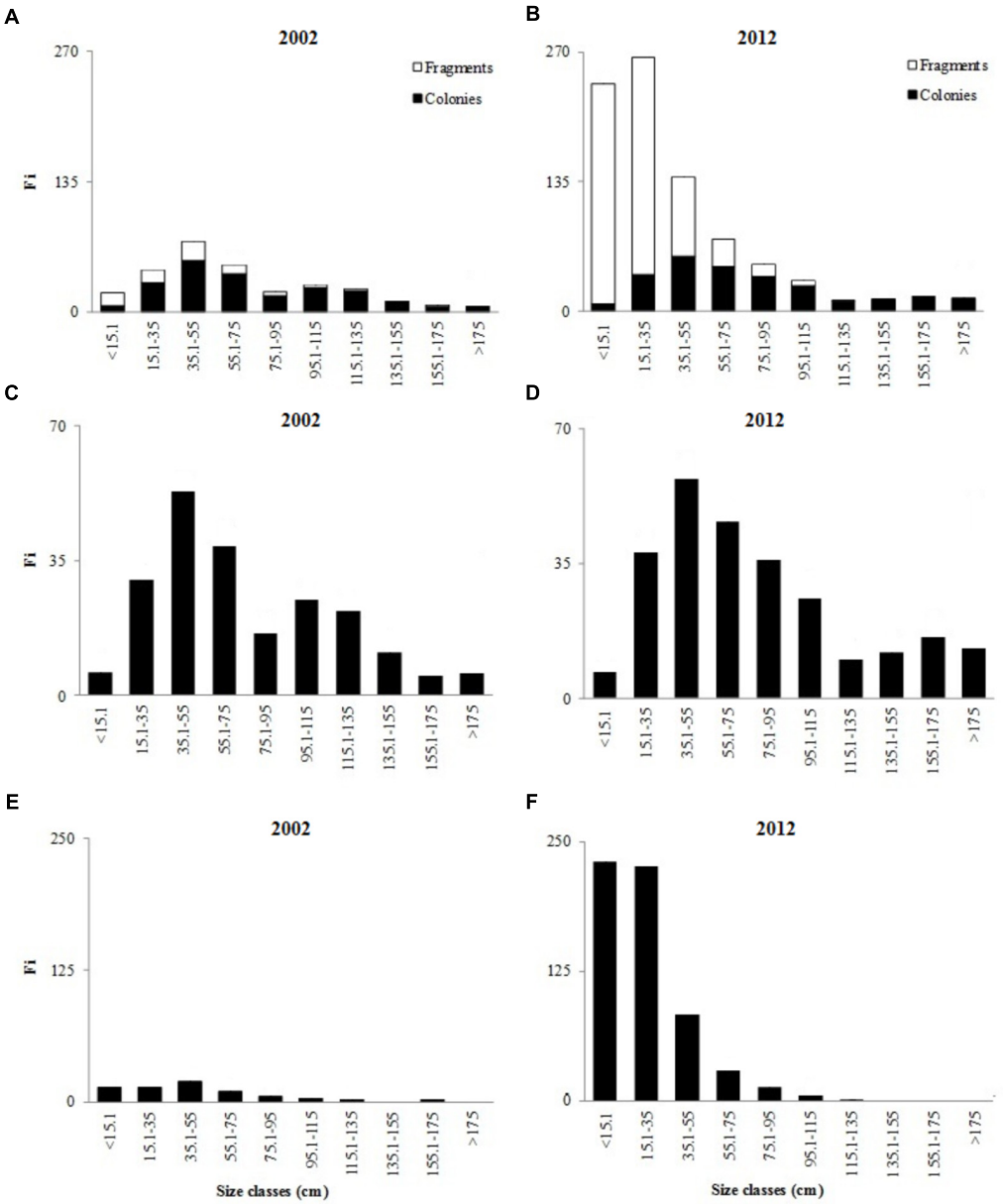

FIGURE 2 | *Dendrogyra cylindrus* population structure in terms of the frequency of colonies and/or fragments per size class. Total population (including colonies and fragments) in 2002 and 2012 **(A,B)**. Colony contribution per size class in 2002 and 2012 **(C,D)**. Relative contribution of fragments to the size classes in 2002 and 2012 **(E,F)**. Fi: absolute frequency.

155.1–175 cm (U: $p = 0.02$, $n = 21$), and >175 cm (U: $p = 0.02$, $n = 19$). In 2012, the colonies in these three classes had an average of 50–80% dead tissue, while in 2002 the percent of dead tissue did not exceed 27% (**Figure 3**).

The frequency of white syndromes in 2012 was lower compared to 2002, but the difference was not statistically significant (U: $p = 0.1$, $n = 474$). However, the number of colonies with erosion at the base was significantly different (U: $p = 0$, $n = 474$); more than 50% of colonies in 2002 were eroded, while in 2012, the percentage of colonies with eroded bases did not exceed 25% (**Table 2**). The most significant differences in frequency of erosion were found in three size classes: 75.1–95 cm (U: $p = 0.01$, $n = 52$), 115.1–135 cm (U: $p = 0.03$, $n = 32$), and 135.1–155 cm (U: $p = 0.04$, $n = 23$) (**Table 2**). The most notable change was observed in the 115.1–135 cm class, which went from 17 colonies with erosion in 2002 to only three colonies in 2012.

Habitat Change

In 2002, *D. cylindrus* was present in four habitats of the reef complex, defined by the association of *D. cylindrus* with other dominant benthic species and substrate types (**Figure 4**, *sensu* Bernal-Sotelo, 2015). These habitats are represented

TABLE 1 | Temporal comparison of the average size of colonies and fragments comprising the population of *Dendrogyra cylindrus*, measured as height of colonies and length of fragments in 2002 and 2012.

Year	Population	n	Mean	Geometric mean (cm)	Mode (cm)	CV
2002	Colonies + Fragments	283	68.5 ± 44.6	53.5	40	0.65
	Colonies	213	75.2 ± 45.0	62	40	0.59
	Fragments	70	48.0 ± 36.5	34.2	40	0.76
2012	Colonies + Fragments	846	42.1 ± 41.8	27.3	8	0.99
	Colonies	261	79.9 ± 51.7	64.9	80	0.64
	Fragments	585	25.3 ± 20.3	18.5	8	0.8

n: frequency; CV: coefficient of variation.

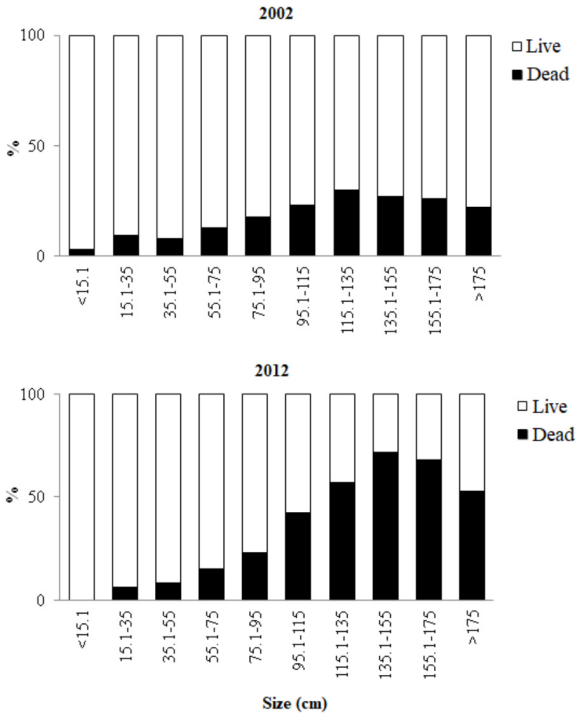

FIGURE 3 | Mean proportion of live and dead tissue among colonies within each size class in 2002 (*n* = 213) and 2012 (*n* = 261).

TABLE 2 | Absolute frequency of colonies of *D. cylindrus* with white syndromes or erosion at the base in 2002 and 2012.

Size classes (cm)	White syndromes		Erosion at base	
	2002	2012	2002	2012
<15.1	0	0	1	0
15.1–35	1	1	11	5
35.1–55	5	0	19	11
55.1–75	1	2	16	12
75.1–95	2	0	12	7
95.1–115	3	0	17	10
115.1–135	3	0	17	3
135.1–155	2	1	9	4
155.1–175	1	0	4	6
>175	2	0	3	6
Σ	20	4	109	64
%	9.4	1.5	51.2	24.5

Σ*: sum; %: proportion to total colonies; n 2002 = 213; n 2012 = 261.*

in **Figure 4** with the following numbers: 4 (IB: *Acropora palmata-Pseudodiploria strigosa*, *Millepora* spp.-dead coral, sand and octocorals-macroalgae), 10 (FR: *Agaricia* spp.-mixed corals, sponges-macroalgae and octocorals-antipatharia), 13 (FRp-Lp: Macroalgae, sand, octocorals and dead coral), and 26 (FR-BR-L: Sand and macroalgae). In 2002, 46.2% of sampling plots were in habitat 13, and 38.5%, were in habitat 10. In 2012, *D. cylindrus* was found in three habitats, two of them new (transformed from the original benthic composition): 11 (FR: Cyanobacteria, macroalgae-dead coral and mixed corals-octocorals-sand) and 12 (FRp: Dead coral, *Orbicella* spp.-mixed coral, macroalgae, sand and octocorals); and the species remained in habitat 13. Both habitat 11 and habitat 13 each had 42.9% of the sampling plots. In 2012, only dead colonies and eroded skeletons of *D. cylindrus* were found in habitats 4, 10, and 26 (**Figure 4**). The deterioration of habitat 4 was reflected in the loss of >70% of calcifying organisms (stony corals and hydrocorals), especially, *A. palmata,* as well as by the increase of more than 95% of dead coral coverage. Habitat 10 in 2002 was transformed into habitat 11 in 2012, because of the dominance of cyanobacteria, a new benthic component, which in habitat 11 covered 31.9%.

According to Bailey's confidence intervals, the population of *D. cylindrus* on the island primarily used habitat 13 because, in both years, it was the habitat with the highest potential area (2002 = 5.7 km^2, 2012 = 4.4 km^2) and the habitat with the highest observed use (2002 = 132 individuals, 2012 = 411 individuals), which means that the species used the most available habitat (**Figure 5**). Habitat 13, where most of the population of *D. cylindrus* was concentrated, was characterized by the dominance of components such as macroalgae, sand, octocorals, and dead coral, mainly on the leeward fore-reef terrace. Mixed sponges and octocorals (habitat 10) were also found to a lesser extent in 2002.

The unfavorable change in habitat was also reflected in the change of population's size class structure (**Table 3**). Habitat 13 lost 23% of its area for *D. cylindrus*. This generated a population change 11 times greater than in 2002, largely because fragmentation followed partial mortality, whereas habitat 10 lost a relatively smaller area (8.4%) and had a relatively lower

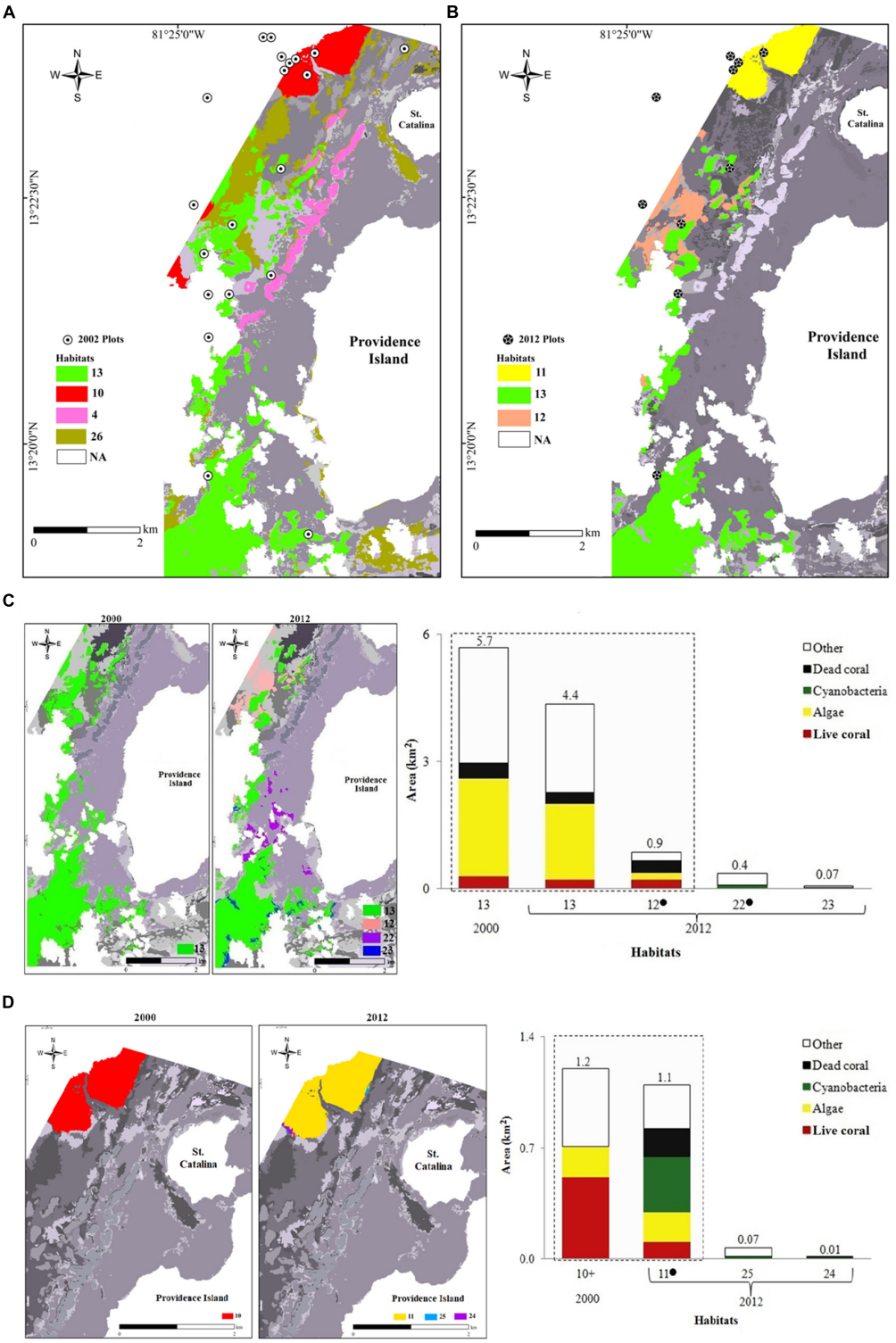

FIGURE 4 | Habitats where *D. cylindrus* was present in the Old Providence reef complex and their changes over time: **(A)** 2002 and **(B)** 2012. Detailed changes in habitat 13 **(C)** and habitat 10 **(D)**. Map legends are organized from habitats where *D. cylindrus* had the highest frequency (habitats 11 and 13) to habitats where *D. cylindrus* had the lowest frequency (habitats 12 and 26). In c and d, the 2000 and 2012 maps show changes in habitat distribution. Cumulative bar plots on the right show the changes in the total area and the area covered by the main components of each habitat. "•" indicate habitat exclusive of 2012, whereas habitats without symbols were present in both years. The bars within dotted boxes represent the habitats corresponding to coral communities. The area (km^2) of each habitat is presented on each bar. Other components: octocorals, rubble and sand. 4 = IB: *A. palmata-P. strigosa*, *Millepora* spp.-dead coral, sand and

(Continued)

FIGURE 4 | Continued
octocorals-macroalgae. 10 = FR: *Agaricia* spp.-mixed corals, sponges-macroalgae and octocorals-antipatharia. 11 = FR: Cyanobacteria, macroalgae-dead coral and mixed corals-octocorals-sand. 12 = FRp: Dead coral, *Orbicella* spp.-mixed corals, macroalgae, sand and octocorals. 13 = FRp-Lp: Macroalgae, sand, octocorals and dead coral. 22 = L: Sand, cyanobacteria and octocorals. 23 = FR-BR-L: Sand, macroalgae, rubble and octocorals, 24 FR-BR-L: Cyanobacteria and sand. 24 = FR-BR-L: Cyanobacteria and sand. 25 FR-BR-L: Sand and cyanobacteria. 26 = FR-BR-L: Sand and macroalgae. The first letters of each habitat refer to the geomorphological zone and the type of reef (when it is a coral formation). IB = Internal reef barrier. BR = Backreef terrace. FR = Forereef terrace. FRp = Patch reef on the forereef terrace. L = Lagoon. Lp = Reef in patch (or strip) of the lagoon. In grayscale are the areas where *D. cylindrus* was not observed. "+" indicate habiat exclusive of 2002.

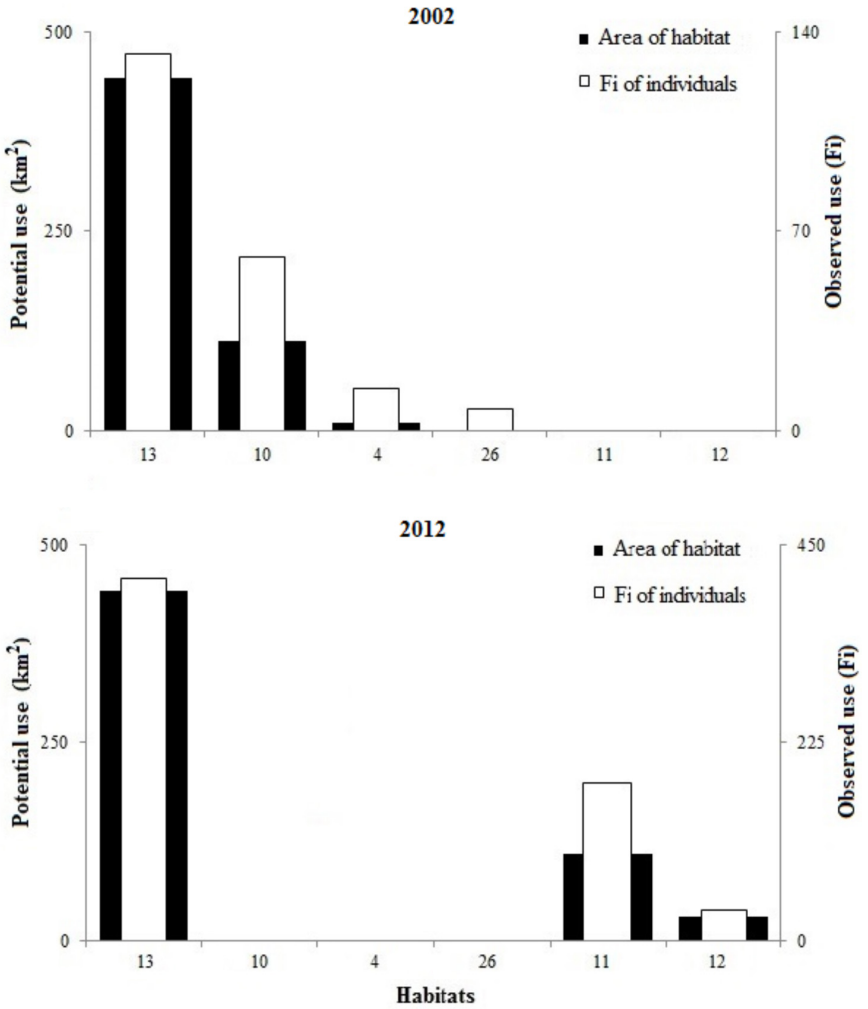

FIGURE 5 | Habitat used by individual *D. cylindrus* (including colonies and fragments), in terms of absolute frequency (Fi, white) and area of the six potential habitats (black), in 2002 and 2012.

population growth (6.1 times). Habitats 4 and 26 were not analyzed because of the low number of colonies and fragments present in the two samples (n was not representative for a change analysis).

DISCUSSION

The right-skewed size distribution reported for most coral populations is usually considered an indicator of stable to moderately deteriorated environments (Bak and Meesters, 1998; Meesters et al., 2001; Smith et al., 2005), where the populations are recovering as a result of successful sexual recruitment (Bak and Meesters, 1999; Cooper et al., 2009; Rodríguez-Martínez et al., 2010). However, the increase in positive skew over time for *D. cylindrus* in Old Providence indicates the opposite; a response to a modified environment created an increase in the frequency of smaller sizes produced by fragmentation or fission, resulting from partial mortality with fragments remaining fixed to a parental colony that is slowly dying while standing (**Figure 6**).

TABLE 3 | Relationship between *D. cylindrus* population and habitat change (bold).

Habitat		2002	2012	Change in terms of		Area of greatest change
				Number of times	%	
13	Colonies (Fi)	104	188	1.8		
	Fragments (Fi)	28	257	9.2		
	Total	132	445	**11**		
	Area (km^2)	5.7	4.4		**–23.4**	
	Composition		Dead coral			Northwest
			Cyanobacteria			Southwest
	Habitat fragmentation		3			
10	Colonies	38	38	0		
	Fragments	23	141	6.1		
	Total	61	179	**6.1**		
	Area (km^2)	1.3	1.1		**–8.4**	
	Composition		Cyanobacteria and Dead coral			Northwest
	Habitat fragmentation		3			

Because the colonies and fragments occupy the same space, although the original habitat changes, the number of colonies and fragments present on each habitat in 2012 were calculated as follows: for colonies = 180 colonies of habitat 13 + 8 colonies of habitat 12, and 38 colonies of habitat 10 + 0 colonies of habitat 11; for fragments = 231 fragments of habitat 13 + 26 fragments of habitat 12, and 0 fragments of habitat 10 + 141 fragments of habitat 11.

In 2012, 96.6% of the total fragments quantified were the result of partial colony mortality. This value surpasses reports of fragmentation for branching species like *A. palmata* that presented 40% of colonies fragmented after storms (Lirman, 2000) or for massive species such as *O. annularis*, which, in the Virgin Islands had 9% of colonies undergoing fission by partial mortality (Edmunds and Elahi, 2007). The increase in the average partial mortality per colony of *D. cylindrus* (2002 = 15.3% and 2012 = 25.0%) indicates that the Old Providence reefs are no longer in good condition; mortality even exceeds the expected values for highly degraded areas (Fong and Glynn, 2001; Bauman et al., 2013).

Larger colonies of *D. cylindrus* (>115.1 cm) were the most affected by partial and total mortality, contributing to the majority of fragments. The direct relationship between colony size and partial mortality has also been reported for other species from the Pacific and Caribbean (Babcock, 1991; Pante et al., 2008; Bauman et al., 2013). Partial mortality could be a strategy to maximize the area:volume ratio in a colony facing adverse environmental conditions, as less energy is required to sustain a smaller area of living tissue (Hughes and Tanner, 2000; Alvarado-Chacón and Acosta, 2009b). However, a smaller area of living tissue in *D. cylindrus* (–9.7% in 2012) may result in a reduction of sexual reproduction (van Woesik and Jordán-Garza, 2011). This situation is further exacerbated in the smaller fragments of *D. cylindrus*, which must invest the energy that was destined for reproduction to repair damaged tissue and compete against invaders.

The absence of sexual recruits could be explained by the lower coverage of *D. cylindrus* living tissue, which limits the reproductive output of the species (Marhaver et al., 2015). The absence of recruits affects the recovery by self-seeding, as observed by Hughes and Tanner (2000) and Alvarado-Chacón and Acosta (2009a) for other corals. Lack of recruitment could also be attributed to the reproductive biology of this species, which involves asynchronous spawning and rapid embryonic development (Marhaver et al., 2015), possibly preventing dispersal and crossbreeding between populations. Thus, the probability of recovery of this declining population in Old Providence by importing larvae from other populations is unlikely. Besides, the closest *D. cylindrus* population is 70 km away in Quitasueño Bank (Díaz et al., 2000). Therefore, the viability of the species on the island is dependent on the self-recruitment of large reproductive colonies, which are precisely the ones being lost.

Coral population skewness caused by asexual reproduction have been associated with factors such as temperature (Bauman et al., 2013), diseases (Edmunds and Elahi, 2007), overgrowth of macroalgae and cyanobacteria (Hughes and Tanner, 2000; Edmunds and Elahi, 2007), bioerosion (Fong and Glynn, 1998; McClanahan et al., 2008), eutrophication (Lewis, 1997), hurricanes (Bythell et al., 1993; Taylor et al., 2007), and sedimentation (Pante et al., 2008). All of these stressors have been observed in Old Providence in the last decades and affect the various size classes differently. The cumulative effect of these multiple stressors may explain the demise of *D. cylindrus* colonies present in the ten sampling plots with only skeletal remains of this species.

The prevalence and severity of coral diseases in the Caribbean have been intensified by factors such as eutrophication, sewage inputs and water temperature (Santavy et al., 2001; Weil, 2004; Cooper et al., 2009). This was not observed in the Old Providence reefs, where the incidence of white syndromes in *D. cylindrus* decreased from 9.4% in 2002 to 1.5% in 2012. Possible explanations for this result include a more intense impact of bleaching (in 2005 and 2010) and white diseases in the past. *D. cylindrus* is considered to have medium resistance to white plague and bleaching

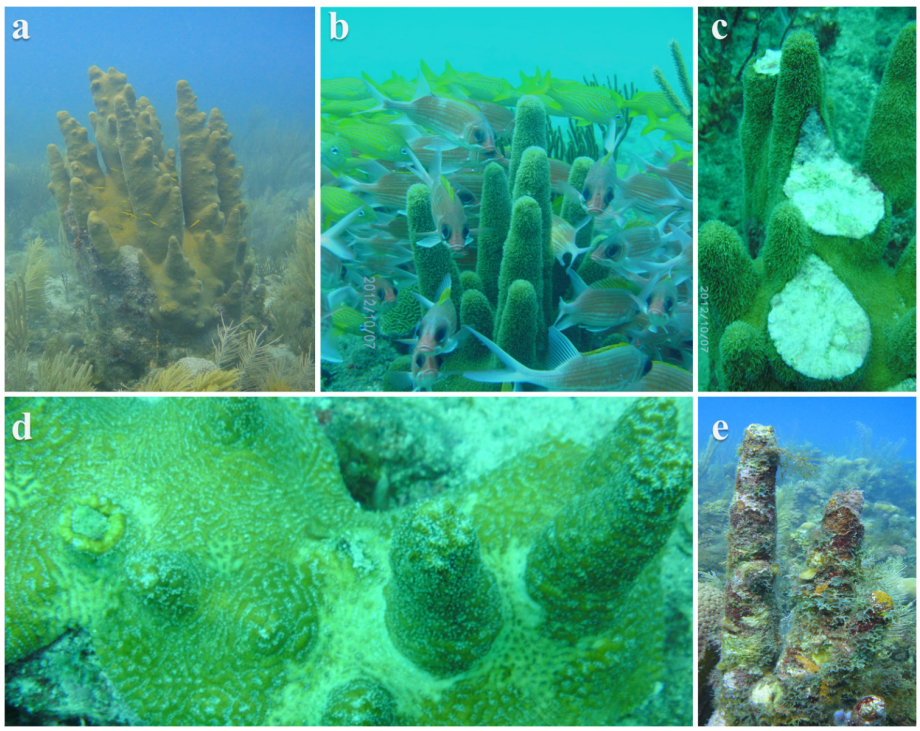

FIGURE 6 | Colonies of *D. cylindrus* in different condition including: **(a)** healthy, **(b)** healthy with associated fauna, **(c)** fragmented due to anchors breakage, **(d)** with tissue mortality at the base likely to lead to fragmentation, and **(e)** dead and colonized by macroalgae and sponges.

(Ward et al., 2006; Quinn and Kojis, 2008; Bruckner and Hill, 2009). For example, in Florida (Jaap, 1985), Honduras (Riegl et al., 2009), Jamaica (Quinn and Kojis, 2008) and Puerto Rico (Bruckner and Hill, 2009) from 1983 to 2008, 0–8% of *D. cylindrus* colonies experienced bleaching, whereas >40% of *Acropora* spp., *Agaricia* spp., *Helioseris cucullata*, *O. annularis*, *Porites* spp. and *Siderastrea siderea* colonies experienced bleaching.

The highest frequency of colonies with erosion at the base in 2002 (51.2% vs. 24.5% in 2012) may be explained by the presence of bioeroders such as *Diadema antillarum* (Acosta and Acevedo, 2006). In 2002, this urchin was found in the proximity of 13.8% of the colonies with signs of erosion, while in 2012, the urchins were only present in 3.8% of colonies. Also, in 2012, there was less associated fauna with the colonies, an indicator of deterioration of the system and reduced habitat quality. Echinoids of the genus *Diadema* and *Echinometra* can exert an adverse effect on *Pocillopora* spp., *Porites* spp. and also on massive corals through the mechanical abrasion caused by their spines and because they feed on living tissue and calcium carbonate, weakening the bases of the colonies (Glynn, 1988; Guzmán, 1988; Bak, 1994).

The cumulative effect of multiple stressors is the key factor affecting coral survival around the world (McClanahan et al., 2008). This was observed in this study at Old Providence where habitats 10 and 13 are located (habitats most used by *D. cylindrus*). Human population density is highest on the west coast of Old Providence (>1000 people/km^2). This area contains 95% of dive sites, as well as high tourist use, and the Santa Isabel pier (Vides and Sierra-Correa, 2003; Vivas-Aguas et al., 2012). This implies a higher risk of contamination and physical damage (e.g., anchoring) to colonies. The west coast of Old Providence is also the area with the majority of permanent and occasional freshwater streams and where the sanitary landfill that discharges leachate to the sea is located. Furthermore, in Old Providence wastewater is discharged directly into the sea or disposed of in septic tanks that leak liquid waste into the sea (Vivas-Aguas et al., 2012). These stressors contribute to nutrient enrichment and decrease water quality. The average concentration of dissolved inorganic nitrogen and phosphorus (DIN and DIP) in Old Providence (Vivas-Aguas et al., 2012) indeed exceeded the corals' limit of physiological stress (DIN = 14 μg l^{-1}, DIP = 62 μg l^{-1}; Fabricius, 2005).

The excess of nutrient loading has caused cyanobacteria and macroalgae to proliferate in Old Providence (Puyana et al., 2015). The habitat considered typical for *D. cylindrus* has changed because of the growth and dominance of cyanobacteria in habitat 10, which led to its transformation after ten years into habitat 11, where 31.9% of coverage was benthic cyanobacteria. This finding agrees with Ford et al. (2018) who found that mats of cyanobacteria have become prevalent on different reefs of the world, playing an important role in the ecosystem degradation. During blooms, planktonic cyanobacteria also affect the living tissue of *D. cylindrus* (Puyana et al., 2015). Benthic cyanobacteria colonize skeletal areas exposed between coral fragments, competing for space with

living tissue (Ritson-Williams et al., 2005; Kuffner et al., 2006). Competition decreases the individual growth rate of remaining tissue and colonies by up to 30% in places with low water quality (Vermeij and Bak, 2002; Edmunds, 2007). *D. cylindrus* colonies at Old Providence were 4.7 cm higher in 2002 than in 2012, so colonies around the island may grow 0.47 mm per year (assuming a constant growth rate), which is lower than 0.8–2 cm/year (Hughes, 1987; Hudson and Goodwin, 1997).

Surviving colonies and fragments of *D. cylindrus* are enduring suboptimal conditions when we compare their current habitat quality with previous decades (Prahl and Erhardt, 1985; Geister and Díaz, 1997). Biogenetic simplification of the habitat or dominance of some unwanted components was the primary driver of the decrease in abundance and density of the associated fauna, as well as the loss of functional and taxonomic diversity (Bustamante et al., 2017). We argue this is the case in Old Providence, with a higher fragmentation of colonies in locations with a higher loss of usable habitat area used by *D. cylindrus*. For example, habitat 13 lost 23.4% of its suitable area in 10 years and had the number of colonies and fragments increase by 11 times in 2012 than in 2002.

Our results suggest that *D. cylindrus* populations in Colombia are under high extinction risk, and should be considered as extremely vulnerable. The fragmentation of colonies and habitat transformation is a consequence of the synergy of multiple stressors that can limit the potential recovery of the species in changing habitats. These stressors must be minimized to prevent the species' local extinction, especially in the west of Old Providence. Therefore, to reduce the local stressors and help improve the resilience of local *D. cylindrus* populations to climate change, we suggest the following mediation efforts: (a) the improvement of water quality; (b) the evaluation of management strategies effectiveness of the Seaflower MPA and the regulation of land- and water-based activities; (c) the monitoring of population tendencies and recording of sexual recruitment to understand the larvae's habitat selection and whether these habitats are suitable for recruit survival; (d) the monitoring of natural (e.g., hurricanes, temperature change) and anthropic stressors (e.g., anchors, diving, eutrophication), that can affect the species to collect evidence of the cause-effect relationships and for evidence-based decision making; and (e) the formulation of conservation, recovery and restoration plans that are specific for coral reef builders species like *D. cylindrus* and can be included in the MPA program. The Seaflower MPA currently has a no-take management zone (García et al., 2005), but diving and tourism activities have not been limited, which implies a risk to coral due to anchoring (**Figure 6**). The results of these mediation efforts should benefit not only *D. cylindrus*, but other species and habitats within the MPA, and will contribute to a greater understanding of larval habitat selection and recruitment habitat potential that will enhance the future *D. cylindrus* populations in Colombia.

AUTHOR CONTRIBUTIONS

KB-S, AA, and JC conceptualized the study and wrote the final manuscript. KB-S and AA did the field work. KB-S analyzed the data, performed the geographical component and structured the document with the supervision of AA and JC. AA made a complementary analysis of the species habitat use.

FUNDING

This work was supported by the University of Costa Rica (FR-082), Javeriana University (004318), and CONARE-CeNAT (Costa Rica) student grant.

ACKNOWLEDGMENTS

The work was done with the permits of CORALINA (001-2012) and PNN McBean Lagoon (001-2013). We are grateful to CIMAR (Universidad de Costa Rica), INVEMAR, CORALINA, Catalina Benavides, Ana Fonseca, Trigal Velásquez, Julián González, members of PRIAS-CeNAT and Sirius dive shop. We thank to Lillian R. McCormick for the English review and to the reviewers who helped us to improve the quality of the manuscript.

REFERENCES

Acosta, A., and Acevedo, A. (2006). "Population structure and colony condition of *Dendrogyra cylindrus* (Anthozoa: Scleractinia) in Providencia Island, Colombia Caribbean," in *Proceedings Of the 10th International Coral Reef Symposium*, Okinawa, 1605–1610.

Almy, C., and Carrion, T. (1963). Shallow-water stony corals of Puerto Rico. *Carib. J. Sci.* 3, 133–162

Alvarado-Chacón, E. M., and Acosta, A. (2009a). Fertilidad y fecundidad de *Montastraea annularis* en un arrecife degradado. *Bol. Invest. Mar. Cost.* 38, 91–108.

Alvarado-Chacón, E. M., and Acosta, A. (2009b). Population size-structure of the reef-coral *Montastraea annularis* in two contrasting reefs of a marine protected area in the southern Caribbean Sea. *Bull. Mar. Sci.* 85, 61–76.

Aronson, R., Bruckner, A., Moore, J., Precht, B., and Weil, E. (2008). *Acropora palmata, Dendrogyra cylindrus, Montastraea annularis, Montastraea faveolata, Montastraea franksi. The IUCN Red List of Threatened Species Version 2014.3*

Babcock, R. C. (1991). Comparative demography of three species of *Scleractinian* corals using age- and size-dependent classifications. *Ecol. Monogr.* 61, 225–244. doi: 10.2307/2937107

Bak, R. P. M. (1994). Sea urchin bioerosion on coral reefs: place in the carbonate budget and relevant variables. *Coral Reefs* 13, 99–103. doi: 10.1007/BF00300768

Bak, R. P. M., and Meesters, E. H. (1998). Coral population structure: the hidden information of colony size-frequency distributions. *Mar. Ecol. Prog. Ser.* 162, 301–306. doi: 10.3354/meps162301

Bak, R. P. M., and Meesters, E. H. (1999). Population structure as a response of coral communities to global change. *Am. Zool.* 39, 56–65. doi: 10.1093/icb/39.1.56

Bauman, A. G., Pratchett, M. S., Baird, A. H., Riegl, B., Heron, S. F., and Feary, D. A. (2013). Variation in the size structure of corals is related to environmental extremes in the Persian Gulf. *Mar. Environ. Res.* 84, 43–50. doi: 10.1016/j.marenvres.2012.11.007

Bernal-Sotelo, J. K. (2015). *Cambio Espacio-Temporal (2000-2012) del Complejo Arrecifal de las Islas de Providencia y Santa Catalina, Caribe colombiano*. M.Sc. thesis, Universidad de Costa Rica, San Pedro.

Brainard, R. E., Birkeland, C., Eakin, C. M., McElhany, P., Miller, M. W., Patterson, M., et al. (2011). *Status Review Report of 82 Candidate Coral Species Petitioned Under the U.S. Endangered Species Act. Tech. Memo.* NOAA-TM-NMFS-PIFSC-27. Honolulu, HI: NOAA.

Bruckner, A. W., and Hill, R. L. (2009). Ten years of change to coral communities off Mona and Desecheo Islands, Puerto Rico, from disease and bleaching. *Dis. Aquat. Organ.* 87, 19–31. doi: 10.3354/dao02120

Bustamante, M., Tajadura, J., Díez, I., and Saiz-Salinas, J. I. (2017). The potential role of habitat-forming seaweeds in modeling benthic ecosystem properties. *J. Sea Res.* 130, 123–133. doi: 10.1016/j.seares.2017.02.004

Bythell, J. C., Gladfelter, E. H., and Bythell, M. (1993). Chronic and catastrophic natural mortality of three common Caribbean reef corals. *Coral Reefs* 12, 143–152. doi: 10.1007/BF00334474

Chadwick-Furman, N. E., Goffredo, S., and Loya, Y. (2000). Growth and population dynamic model of the reef coral *Fungia granulosa* Klunzinger, 1879 at Eilat, northern Red Sea. *J. Exp. Mar. Biol. Ecol.* 249, 199–218. doi: 10.1016/S0022-0981(00)00204-5

Cooper, T. F., Gilmour, J. P., and Fabricius, K. E. (2009). Bioindicators of changes in water quality on coral reefs: review and recommendations for monitoring programs. *Coral Reefs* 28, 589–606. doi: 10.1007/s00338-009-0512-x

Darling, E. S., Alvarez-Filip, L., Oliver, T. A., McClanahan, T. R., and Côté, I. M. (2012). Evaluating life-history strategies of reef corals from species traits. *Ecol. Lett.* 15, 1378–1386. doi: 10.1111/j.1461-0248.2012.01861.x

Díaz, J. M., Barrios, L. M., Cendales, M. H., Garzón-Ferreira, J., Geister, J., López-Victoria, M., et al. (2000). *Áreas Coralinas de Colombia*. Santa Marta: INVEMAR.

Edmunds, P. J. (2007). Evidence for a decadal-scale decline in the growth rates of juvenile scleractinian corals. *Mar. Ecol. Prog. Ser.* 341, 1–13. doi: 10.3354/meps341001

Edmunds, P. J., and Elahi, R. (2007). The demographics of a 15-year decline in cover of the Caribbean reef coral *Montastraea annularis*. *Ecol. Monogr.* 77, 3–18. doi: 10.1890/05-1081

Ehrenberg, C. G. (1834). *Beiträge zur physiologischen Kenntniss der Corallenthiere im Allgemeinen, und Besonders des Rothen Meeres, nebst einem Versuche zur Physiologischen Systematik Derselben*, Vol. 1. Berlin: Abhandlungen der Königlichen Akademie der Wissenschaften, 225–380. Available at: http://bibliothek.bbaw.de/bibliothek-digital/digitalequellen/schriften/anzeige?band=07-abh/1832-1&seite:int=00000243

Fabricius, K. E. (2005). Effects of terrestrial runoff on the ecology of corals and coral reefs: review and synthesis. *Mar. Pollut. Bull.* 50, 125–146. doi: 10.1016/j.marpolbul.2004.11.028

Fong, P., and Glynn, P. W. (1998). A dynamic size-structured population model: does disturbance control size structure of a population of the massive coral *Gardineroseris planulata* in the Eastern Pacific? *Mar. Biol.* 130, 663–674. doi: 10.1007/s002270050288

Fong, P., and Glynn, P. W. (2001). Population abundance and size-structure of an Eastern Tropical Pacific reef coral after the 1997-98 ENSO: a simulation model predicts field measures. *Bull. Mar. Sci.* 69, 187–202.

Ford, A. K., Bejarano, S., Nugues, M. M., Visser, P. M., Albert, S., and Ferse, S. C. A. (2018). Reefs under siege-the rise, putative drivers, and consequences of benthic cyanobacterial mats. *Front. Mar. Sci.* 5, 1–15. doi: 10.3389/fmars.2018.00018

García, M. I., Howard, M., Charris, S., Hawkins, E., Taylor, M., Prada, M. C., et al. (2005). *Plan de Manejo del ÁREA Marina Protegida Seaflower, Parte II. (Informe del proyecto Caribbean Archipelago - Biosphere Reserve: Regional Marine Protected Area System CO-GM-P066646)*. San Andrés: GEF-TOC-CORALINA.

Geister, J., and Díaz, J. M. (1997). "A field guide to oceanic barrier and atolls of the southwestern Caribbean (San Andrés y Providencia)," in *Proceedings of the 8th International. Coral Reef Symposium*, Panama.

Glynn, P. W. (1988). El Niño warming, coral mortality and reef framework destruction by echinoid bioerosion in the eastern Pacific. *Galaxea* 7, 129–160.

Guzmán, H. M. (1988). Distribución y abundancia de organismos coralívoros en los arrecifes coralinos de la Isla del Caño, Costa Rica. *Rev. Biol. Trop.* 36, 191–207.

Hudson, J. H., and Goodwin, W. B. (1997). "Restoration and growth rate of hurricane damaged pillar coral (*Dendrogyra cylindrus*) in the Key Largo National Sanctuary, Florida,". in *Proceedings of the 8th International. Coral Reef Symposium, Smithsonian Tropical Research Institute*, Panama, 567–570.

Hughes, T. P. (1987). Skeletal density and growth form of corals. *Mar. Ecol. Prog. Ser.* 35, 259–266. doi: 10.3354/meps035259

Hughes, T. P., and Jackson, J. B. C. (1980). Do corals lie about their age? some demographic consequences of partial mortality, fission and fusion. *Science* 209, 713–715. doi: 10.1126/science.209.4457.713

Hughes, T. P., and Tanner, J. E. (2000). Recruitment failure life histories, and long-term decline of Caribbean corals. *Ecology* 81, 2250–2263. doi: 10.1890/0012-9658(2000)081[2250:RFLHAL]2.0.CO;2

INVEMAR (eds) (2010). *Corales Escleractíneos de Colombia*. Santa Marta: Instituto de Investigaciones Marinas y Costeras José Benito Vives de Adréis.

Jaap, W. C. (1985). "An epidemic zooxanthellae expulsion during 1983 in the lower Florida Keys coral reefs: hyperthermic etiology," in *Proceedings of the. 5th International. Coral Reef Symposium*, Tahiti, 143–148.

Kuffner, I., Walters, L., Becerro, M., Paul, V., Ritson-Williams, R., and Beach, K. (2006). Inhibition of coral recruitment by macroalgae and cyanobacteria. *Mar. Ecol. Prog. Ser.* 323, 107–117. doi: 10.3354/meps323107

Lewis, J. B. (1997). Abundance, distribution and partial mortality of the massive coral *Siderastrea siderea* on degrading coral reefs at Barbados, West Indies. *Mar. Pollut. Bull.* 34, 622–627. doi: 10.1016/S0025-326X(96)00184-1

Lirman, D. (2000). Fragmentation in the branching coral *Acropora palmata* (Lamarck): growth, survivorship, and reproduction of colonies and fragments. *J. Exp. Mar. Biol. Ecol.* 251, 41–57. doi: 10.1016/S0022-0981(00)00205-7

Llinás, H., and Rojas, C. (2006). *Estadística Descriptiva y Distribuciones de Probabilidad*. Barranquilla: Ediciones Uninorte.

Marhaver, K. L., Vermeij, M. J. A., and Medina, M. M. (2015). Reproductive natural history and successful juvenile propagation of the threatened Caribbean Pillar Coral *Dendrogyra cylindrus*. *BMC Ecol.* 15, 1–11. doi: 10.1186/s12898-015-0039-7

McClanahan, T. R., Ateweberhan, M., and Omukoto, J. (2008). Long-term changes in coral colony size distributions on Kenyan reefs under different management regimes and across the 1998 bleaching event. *Mar. Biol.* 153, 755–768. doi: 10.1007/s00227-007-0844-4

Meesters, E. H., Hilterman, M., Kardinaal, E., Keetman, M., de Vries, M., and Bak, R. P. M. (2001). Colony size-frequency distributions of scleractinian coral populations: spatial and interspecific variation. *Mar. Ecol. Prog. Ser.* 209, 43–54. doi: 10.3354/meps209043

Meesters, E. H., Wesseling, I., and Bak, R. P. M. (1997). Coral colony tissue damage in six species of reef-building corals: partial mortality in relation with depth and surface area. *J. Sea. Res.* 37, 131–144. doi: 10.1016/S1385-1101(96)00004-4

Montenegro, J. A., and Acosta, A. (2008). HaviStat© v1.0: aplicación para evaluar uso y preferencia de hábitat. *PANAMJAS* 3, 2–4.

NOAA (2014). *Endangered and Threatened Wildlife and Plants: Final Listing Determinations on Proposal to List 66 Reef-Building Coral Species and to Reclassify Elkhorn and Staghorn Corals. Final rule*. Miami, FL: National Oceanic and Atmospheric Administration.

Pante, E., King, A., and Dustan, P. (2008). Short-term decline of a Bahamian patch reef coral community: rainbow gardens reef 1991-2004. *Hydrobiologia* 596, 121–132. doi: 10.1007/s10750-007-9062-9

Prahl, H., and Erhardt, H. (1985). *Colombia: Corales y Arrecifes Coralinos*. Bogotá: Fondo FEN.

Puyana, M., Acosta, A., Bernal-Sotelo, K., Velásquez-Rodríguez, T., and Ramos, F. (2015). Spatial scale of cyanobacterial blooms in old providence island, colombian caribbean. *Univ. Sci.* 20, 83–105. doi: 10.11144/Javeriana.SC20-1.sscb

Quinn, N., and Kojis, B. (2008). The recent collapse of a rapid phase-shift reversal on a Jamaican north coast coral reef after the 2005 bleaching event. *Rev. Biol. Trop.* 56 (Suppl. 1), 149–159.

Richardson, L. L., Goldberg, W. M., Carlton, R. G., and Halas, J. C. (1998). Coral disease outbreak in the Florida Keys: Plague type II. *Rev. Biol. Trop.* 46, 187–198.

Richmond, R. D., and Hunter, C. L. (1990). Reproduction and recruitment of corals: comparison among the Caribbean, the Tropical Pacific and the Red Sea. *Mar. Ecol. Prog. Ser.* 60, 185–203. doi: 10.3354/meps060185

Riegl, B., Purkis, S. J., Keck, J., and Rowlands, G. P. (2009). Monitored and modeled coral population dynamics and the refuge concept. *Mar. Pollut. Bull.* 58, 24–38. doi: 10.1016/j.marpolbul.2008.10.019

Ritson-Williams, R., Paul, V., and Bonito, V. (2005). Marine benthic cyanobacteria overgrow coral reef organisms. *Coral Reefs* 24:629. doi: 10.1007/s00338-005-0059-4

Rockwood, L. L. (2006). *Introduction to Population Ecology*. Oxford: Blackwell Publ.

Rodríguez-Martínez, R. E., Ruíz-Renteria, F., van Tussenbroek, B., Barba-Santos, G., Escalante-Mancera, E., Jordán-Garza, G., et al. (2010). Environmental state and tendencies of the puerto morelos Caricomp site, Mexico. *Rev. Biol. Trop.* 58 (Suppl. 3), 23–43.

Rogers, C. S., Garrison, G., Grober, R., Hillis, Z. M., and Franke, M. A. (1994). *Coral reef monitoring manual for the Caribbean and Western Atlantic*. St. John: National Park Service.

Santavy, D. L., Mueller, E., Peters, E. C., MacLaughlin, L., Porter, J. W., Patterson, K. L., et al. (2001). Quantitative assessment of coral diseases in the Florida keys: strategy and methodology. *Hydrobiologia* 460, 39–52. doi: 10.1023/A:1013194422440

Smith, L. D., Devlin, M., Haynes, D., and Gilmour, J. P. (2005). A demographic approach to monitoring the health of coral reefs. *Mar. Pollut. Bull.* 51, 399–407. doi: 10.1016/j.marpolbul.2004.11.021

Szmant, A. M. (1986). Reproductive ecology of Caribbean reef corals. *Coral Reefs* 5, 43–54. doi: 10.1007/BF00302170

Taylor, E., Hernández, D., Howard, F., Peñaloza, G., Posada, S., Howard, N., et al. (2007). Impacto en los arrecifes de coral ocasionados por el huracán Beta en la plataforma insular de Old Providencie y Santa Catalina. *Bol. Cient. CIOH* 25, 71–77. doi: 10.26640/01200542.25.71_77

van Woesik, R., and Jordán-Garza, A. G. (2011). Coral populations in a rapidly changing environment. *J. Exp. Mar. Biol. Ecol.* 408, 11–20. doi: 10.1016/j.jembe.2011.07.022

Vandermeer, J. H., and Goldberg, D. E. (2003). *Population Ecology First Principles*. Princeton, NJ: Princeton University Press.

Vermeij, M. J. A., and Bak, R. P. M. (2002). "Inferring demographic processes from population size structure in corals," in *Proceedings of the 9th International Coral Reef Symposium,* Bali, 589–593.

Vides, M., and Sierra-Correa, P. (2003). *Atlas de Paisajes Costeros de Colombia*. Santa Marta: INVEMAR.

Vivas-Aguas, L. J., Garay, J. A., Espinosa, L., Abdulazis, P., Bent, O., Osorio, L., et al. (2012). "Calidad ambiental en las islas de San Andrés, Providencia y Santa Catalina", in *Atlas de la Reserva de Biósfera Seaflower Archipiélago de San Andrés, Providencia y Santa Catalina*, eds D. I. Gómez-López, C. Segura-Quintero, P. C. Sierra-Correa, and J. Garay-Tinoco (Santa Marta: INVEMAR), 60–85.

Ward, J., Rypien, K., Bruno, J., Harvell, C., Jordán-Dahlgren, E., Mullen, K., et al. (2006). Coral diversity and disease in Mexico. *Dis. Aquat. Organ.* 69, 23–31. doi: 10.3354/dao069023

Weil, E. (2004). "Coral reef diseases in the Wider Caribbean" in *Coral Health and Disease*, eds E. Rosenberg, and Y. Loya (New York, NY: Springer), 35–68. doi: 10.1007/978-3-662-06414-6_2

Wilkinson, C. (2008). *Status of Coral Reefs of the World*. Townsville, TSV: Global Coral Reef Monitoring Network and Rainforest Research Centre.

Conflict of Interest Statement: The authors declare that the research was conducted in the absence of any commercial or financial relationships that could be construed as a potential conflict of interest.

frontiers in Marine Science

ORIGINAL RESEARCH
published: 08 February 2019
doi: 10.3389/fmars.2019.00038

Climate Change and Atlantic Multidecadal Oscillation as Drivers of Recent Declines in Coral Growth Rates in the Southwestern Caribbean

Luis D. Lizcano-Sandoval[1,2†], Ángela Marulanda-Gómez[2†], Mateo López-Victoria[2] and Alberto Rodriguez-Ramirez[3†]*

[1] Posgrado de Ciencias del Mar y Limnología, Universidad Nacional Autónoma de México, Puerto Morelos, Mexico, [2] Department of Natural Sciences and Mathematics, Pontificia Universidad Javeriana Cali, Cali, Colombia, [3] Global Change Institute, The University of Queensland, St. Lucia, QLD, Australia

Historical records of growth rates of the key Caribbean reef framework-building coral *Orbicella faveolata* can be fundamental not only to understand how these organisms respond to environmental changes but also to infer future responses of reef ecosystems in a changing world. While coral growth rates have been widely documented throughout the Caribbean, the drivers of coral growth variability remain poorly understood. Here, we provide a record spanning 53 years (1963–2015) of the coral growth parameters for five *O. faveolata* core samples collected at Serrana Atoll, inside the Seaflower Biosphere Reserve, Colombian Caribbean. Coral cores were extracted from reefs isolated from direct anthropogenic impacts, and growth estimations (skeletal density, linear extension, and calcification rates) were derived using computerized tomography. Master records of coral growth parameters were evaluated to identify long-term trends and to relate growth responses with sea surface temperature (SST), the Atlantic Multi-decadal Oscillation (AMO), North Atlantic Oscillation (NAO) and Southern Oscillation indexes, aragonite saturation state (Ω_{arag}), and degree heating months (DHM). We found significant negative relationships between density and mean SST, maximum SST, AMO, and DHM. Moreover, density showed significant positive correlations with NAO and Ω_{arag}. Extension rate did not show significant correlations with any environmental variable. However, there were significant negative correlations between calcification and maximum SST, AMO, and DHM. Trends of coral growth indicated a significant reduction in density and calcification over time, which were best explained by changes in Ω_{arag}. Inter-annual declines in calcification and density up to 25% (relative to historical mean) were associated to the impacts of previously recorded mass bleaching events (1998, 2005, and 2010). Our study provides further evidence that AMO and Ω_{arag} are important drivers affecting coral growth rates in the Southwestern Caribbean. Therefore, we suggest upcoming variations of AMO and future trajectories of Ω_{arag} in the Anthropocene could have a substantial influence on future disturbances, ecological process and responses of the Caribbean reefs.

Keywords: coral growth parameters, Atlantic Multi-decadal Oscillation, ocean acidification, coral reefs, *Orbicella faveolata*, Serrana Atoll

OPEN ACCESS

Edited by:
Sonia Bejarano, Leibniz Centre for Tropical Marine Research (LG), Germany

Reviewed by:
Chiara Lombardi, Italian National Agency for New Technologies, Energy and Sustainable Economic Development (ENEA), Italy
Henrique Cabral, Irstea Centre de Bordeaux, France

****Correspondence:***
Mateo López-Victoria
malov@javerianacali.edu.co; malov@puj.edu.co

†Present address:
Luis D. Lizcano-Sandoval, College of Marine Science, University of South Florida, St. Petersburg, FL, United States
Ángela Marulanda-Gómez Department of Freshwater and Marine Ecology, Institute of Biodiversity and Ecosystem Dynamics (IBED), The University of Amsterdam, Amsterdam, Netherlands
Alberto Rodriguez-Ramirez, Marine Palaeoecology Lab, School of Biological Sciences, The University of Queensland, St. Lucia, QLD, Australia

Specialty section:
This article was submitted to Marine Ecosystem Ecology, a section of the journal Frontiers in Marine Science

Received: *19 September 2018*
Accepted: *23 January 2019*
Published: *08 February 2019*

Citation:
Lizcano-Sandoval LD, Marulanda-Gómez Á, López-Victoria M and Rodriguez-Ramirez A (2019) Climate Change and Atlantic Multidecadal Oscillation as Drivers of Recent Declines in Coral Growth Rates in the Southwestern Caribbean. Front. Mar. Sci. 6:38. doi: 10.3389/fmars.2019.00038

INTRODUCTION

Interpreting coral growth records is critical to identifying responses of coral reefs to environmental conditions over time and to predict future trajectories of these ecosystems (Pandolfi, 2011). For instance, the annual density banding of massive coral skeletons allows retrospective analysis of different coral growth parameters such as skeletal density, linear extension and calcification rates (Lough and Barnes, 1992). Because coral growth responses are determined by changes in environmental conditions (Lough and Cooper, 2011), it is possible to associate the variability in annual growth with previously known environmental and climatic conditions and disturbances (Bessat and Buigues, 2001; Lough, 2008; Carilli et al., 2010). While coral growth is controlled by several environmental factors such as seawater temperature, light, carbonate saturation state, wave energy and turbidity (Lough and Barnes, 2000; Cruz-Piñón et al., 2003; Fabricius, 2005; Marubini et al., 2008; Tanzil et al., 2009; Yan et al., 2011), drivers of recent observed declines in coral growth parameters require further investigation (Lough and Cantin, 2014). Reductions in coral growth rates of massive corals have been linked to bleaching events (Carilli et al., 2009a,b), SST increase (Cantin et al., 2010; Tanzil et al., 2013), attributed to ocean acidification (Crook et al., 2013; D'Olivo et al., 2013), and to the combination of warming and ocean acidification (Cooper et al., 2008; De'ath et al., 2009). Results are, however, inconsistent across broad spatial scales.

Several studies in the Caribbean have documented a wide variability among species and reef habitats in the response of coral growth rates to environmental conditions, thus complicating accurate region-wide predictions of future climatic impacts on coral reefs. Guzman et al. (2008) linked declines in growth rates of the coral *Siderastrea siderea* to runoff and sedimentation derived from the construction of the Panama Canal. Reefs subject to chronic anthropogenic stressors in the Mesoamerican Reef (MR) displayed suppressed growth rates of massive *Orbicella faveolata* for several years after the 1998 mass bleaching event (Carilli et al., 2009a). In contrast, for inshore *O. faveolata* colonies from the Florida Keys, growth rates recovered quickly (∼within 1 year) after thermal stress (Manzello et al., 2015). Also MR coral reefs experiencing thermal variability appear to enhance the tolerance of corals to thermal stress, as skeletal rates of *Siderastrea siderea* were not affected in back reef and nearshore colonies compared to colonies within more thermally stable fore reef environments, in which a significant decline in skeletal extension was found (Castillo et al., 2011, 2012). Evaluating calcification rates and SST trends from MR, Carricart-Ganivet et al. (2012) found *Porites astreoides* to be more sensitive to increasing temperature than *O. faveolata* and *O. franksi*. Furthermore, Crook et al. (2013) documented a significant decrease in calcification rates of *P. astreoides* concomitant with a natural gradient in pH and aragonite saturation (Ω_{arag}) on the MR. Considering that declines in coral growth parameters seem to be primarily temperature-related rather than attributable to ocean acidification (Lough and Cantin, 2014), negative impacts on coral growth rates are excepted under future ocean warming. Yet, responses of growth parameters under the combined effects of ocean warming and acidification are not well understood for the Caribbean.

The modulating effect of climatic cycles such as the Atlantic Multi-decadal Oscillation (AMO) on coral records has also been identified as an important driver of coral growth rates in the Caribbean (Hetzinger et al., 2008). However, the identification of primary drivers of coral growth that are modulated by decadal climate variability requires more attention (Lough and Cantin, 2014). Evidence of multidecadal variability in annual coral growth rates has been documented for *S. siderea* in Belize and the Bahamas (Saenger et al., 2009), and Mexico (Vásquez-Bedoya et al., 2012); and for *O. faveolata* in Florida (Helmle et al., 2011). Furthermore, reanalyzing previously published coral growth records from Belize (*O. faveolata*) and Panama (*S. siderea*), Kwiatkowski et al. (2013) found that variations in growth rates between 1880 and 2000 displayed a decadal variability which was linked to regional climatic drivers (i.e., volcanic and anthropogenic aerosol emissions) rather than global drivers (i.e., climate change or ocean acidification). Thus, coral records from remote reefs, isolated from direct anthropogenic influence (e.g., coastal development and contamination, eutrophication, particulate organic matter, tourism) can be useful to clarify sources of decadal climate variability and support understanding of past and future climatic impacts on the Caribbean coral reefs.

Here, we provide the first decadal-scale record (1963–2015) of coral growth parameters from *O. faveolata* colonies that grew on patch reefs isolated from direct anthropogenic impacts at Serrana Atoll, Southwestern Caribbean. Growth parameters such as skeletal density, linear extension and calcification rates were evaluated to identify long-term trends and to relate growth responses with SST, AMO, The North Atlantic Oscillation (NAO) and Southern Oscillation (SOI) indexes, aragonite saturation states (Ω_{arag}), and degree heating months (DHM). This analysis provides insight into how corals from an isolated Caribbean reef responded to environmental and climatic conditions over the last 50 years, and how they are likely to respond to a changing ocean.

MATERIALS AND METHODS

Coral Collection

Five cores from the massive coral *Orbicella faveolata* were collected on SCUBA at 4–9 m depth in lagoonal patch reefs of Serrana Atoll, inside the Seaflower Biosphere Reserve, Colombian Caribbean (**Figure 1**), during August 2016. Each coral core was extracted using an underwater pneumatic hand drill supplied with compressed air. Coral colonies were drilled along the maximum vertical growth axis (Helmle and Dodge, 2011). Cores were 6 cm in diameter and 0.6–0.9 m long (**Table 1**). A polystyrene ball was inserted and fixed with epoxy resin into the core hole to avoid colonization by boring organisms, diseases on exposed surfaces and promote coral tissue recovery.

Growth Rates

The cores were rinsed with freshwater and then oven dried for 24 h at 50–60°C. A GE LightSpeed VCT 64 (General Electric Company) computerized tomography (CT) scanner was

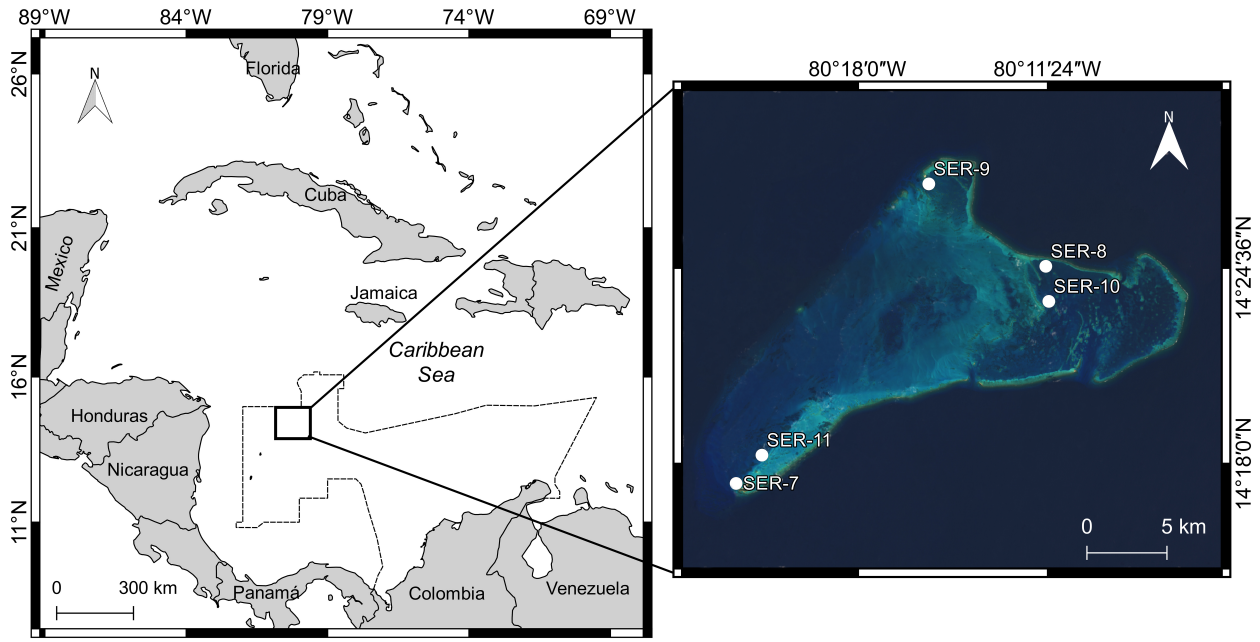

FIGURE 1 | Location of the Serrana Atoll in the Colombian Caribbean (dashed line). Sampling sites are indicated by white dots with the corresponding core code shown. Satellite image obtained and edited from the Landsat 8 OLI/TIRS C1 L-1 dataset (https://earthexplorer.usgs.gov/), taken on March 4, 2018.

TABLE 1 | Location and details of *O. faveolata* colonies used in this study.

Core ID	Latitude	Longitude	Depth (m)	Timespan	Density (g cm^{-3})	Extension (cm year^{-1})	Calcification (g cm^{-2} year^{-1})
SER-7	14°17′20.2″N	80°22′14.0″W	6	1974–2015	1.12 ± 0.13	0.87 ± 0.19	0.97 ± 0.22
SER-8	14°24′39.1″N	80°11′28.4″W	9	1969–2015	1.01 ± 0.18	1.03 ± 0.19	1.02 ± 0.23
SER-9	14°27′25.6″N	80°15′32.3″W	4	1963–2015	1.35 ± 0.21	1.00 ± 0.21	1.33 ± 0.27
SER-10	14°23′28.3″N	80°11′22.1″W	5	1971–2015	0.93 ± 0.16	1.12 ± 0.28	1.04 ± 0.33
SER-11	14°18′17.3″N	80°21′20.2″W	6	1963–2015	0.93 ± 0.09	0.79 ± 0.16	0.72 ± 0.13

Growth parameters are means ± SD of the respective timespans.

used to image the coral cores along with an aragonite step-wedge standard obtained from the shell of the giant clam *Tridacna maxima* (see **Supplementary Information**). The solid aragonite standard with known density was used to estimate coral density. The software RadiAnt DICOM Viewer 4.0 was used to view the DICOM files obtained from the CT scan and generate multi-planar reconstructions of all coral cores. Coronal and sagittal planes were examined to choose one image for each core, respectively. By using this method, the alternate pattern of horizontal density bands (high and low density) in the coral skeleton were visualized from different angles and slices. A density banding pattern is important to follow the vertical growth of massive corals and construct the coral chronology (see **Supplementary Information**). Skeletal density was calculated following the method by Carricart-Ganivet and Barnes (2007) for X-ray images, adapted to CT scan images (see **Supplementary Information**). Linear extension was measured between contiguous years or high-to-high density bands. Each coral year is formed by a pair of bands, corresponding to high and low density bands. Calcification rates were estimated as the product of skeletal density and linear extension rate. These three growth characteristics are sensitive to environmental changes and their variations are recorded in the coral skeleton (Barnes and Lough, 1996).

Annual growth values (i.e., density, extension and calcification) of each coral core were derived from the averaged measurements made in one transect, of both the coronal and sagittal planes, along the vertical growth axis of the coral colony. Master chronologies of skeletal density, linear extension and calcification were constructed averaging the annual values of the five cores, therefore the number of cores contributing to a specific year varied through the maser chronology (**Table 1**). To detect trends in growth parameters over time, linear regressions were applied to the master chronologies. Coefficients of variation (CV) were calculated for each growth parameter to demonstrate the inter-annual variability irrespective of differences in the means (Helmle et al., 2011). Annual density, extension and calcification rates were correlated to examine the relationship between coral growth parameters. Significance level for correlations was $\alpha = 0.05$. In addition, master chronologies of the standardized

anomalies (STDA) were obtained for each growth parameter. STDA consisted of the annual values minus the mean (over the period 1963–2015), divided by the standard deviation (Helmle et al., 2011). The five standardized chronologies were then averaged to create a single standardized record. As a result, the inherent variability of each core was accounted for, and a regional signal was detected (Jones et al., 2009; Grove et al., 2013).

Drivers of Growth Variability and Environmental Records

To explore potential drivers of growth variability, annual means, minimum, and maximum of sea surface temperature (SST), DHM, Ω_{arag}, AMO, Southern Oscillation Index (SOI) and NAO, were correlated with annual values of skeletal density, linear extension and calcification rates (Pearson's correlations). Additionally, growth responses to thermal stress were assessed by plotting growth master chronologies and annual changes of growth parameters against DHM. Annual changes in growth parameters were calculated as the percentage of change relative to the 1963–2015 mean values. Finally, master chronologies of STDA were plotted against SST and AMO to comparatively evaluate long-term trends. A 13-year smoothing was applied to STDA and SST data to reduce inter-annual variability and facilitate the comparison of both time series.

SST was obtained from the 1° × 1° gridded HadISST1 dataset (Rayner et al., 2003) centered on 13.5°–14.5°N and 79.5°–80.5°W. The AMO was calculated from the Kaplan SST dataset (Enfield et al., 2001), which is an index of North Atlantic temperatures. The NAO and SOI indexes were constructed from normalized sea level pressure differences between the Azores–Iceland (Jones et al., 1997) and Darwin–Tahiti (Ropelewski and Jones, 1987), respectively. These indices are typically associated with climatic changes at large scales both in the Pacific and Atlantic oceans (i.e., ENSO events).

Aragonite saturation state (Ω_{arag}) data were extracted from the NOAA Coral Reef Watch (CRW) Experimental Ocean Acidification Product Suite (OAPS) for the period 1988–2011 centered on 15°–16°N and 79°–81°W (Gledhill et al., 2008). The Ω_{arag} data used here was 1°N adjacent to the area where Serrana Atoll is located.

DHM were calculated using the SST monthly data from HadISST on the same grid, in a similar manner to the degree heating weeks (DHW) used by NOAA Coral Reef Watch to predict coral bleaching. Thermal stress is considered to occur when temperatures surpass the bleaching threshold, which is established as 1°C above the mean of the climatological month with the highest temperature (Liu et al., 2006). However, for the HadISST dataset DHM were calculated as the annual sum of the difference between average monthly SSTs that exceeded the long-term maximum monthly mean (Carilli et al., 2010).

To further explore potential drivers of growth variability, a distance-based linear model (DISTLM) using a resemblance matrix of master chronologies values of density, calcification and extension (based on Euclidean distance), and forward selection, was adopted (Legendre and Anderson, 1999; Anderson et al., 2008). Forward selection adds one variable at a time to the model, selecting the variable that produces the greatest improvement in the value of adjusted r^2 at each step. We used adjusted r^2 as the selection criterion instead of r^2 as we aimed to include only variables that significantly explained variation in the model. This method was applied to the time period 1988–2011, including as explanatory variables DHM, AMO, Ω_{arag}, and NAO (data sets available for this period). DISTLM results provide a marginal test, fitting each variable individually (ignoring all other variables), and a sequential test, fitting each variable one at a time, restricted to the variables that were already included in the model (Anderson, 2003; Anderson et al., 2008). In addition, for the period 1963–2015, we applied the DISTML only to evaluate the individual contribution of each variable (marginal test) as our set of explanatory variables for this period were temperature-based (redundant variables). DISTLM analysis were performed in PERMANOVA+ package for PRIMER v6.

RESULTS

Coral Growth

Over the period 1963–2015, the coral *Orbicella faveolata* of Serrana Atoll presented an overall mean ± SD skeletal density of 1.08 ± 0.08 g cm^{-3}, linear extension rate of 0.96 ± 0.11 cm $year^{-1}$ and calcification rate of 1.02 ± 0.12 g cm^{-2} $year^{-1}$. Mean values for individual cores are shown in **Table 1**. The CV was 7% for density, 12% for extension rate and 12% for calcification rate. Extension rate was positively related to calcification rate ($r = 0.82$, $p < 0.001$, $n = 53$), calcification rate was positively related to density rate ($r = 0.29$, $p = 0.04$, $n = 53$) and density rate was negatively related to extension rate ($r = -0.28$, $p = 0.04$, $n = 53$). Skeletal density and calcification rate increased significantly over time (**Figure 2A**, $r^2 = 0.16$, $p = 0.004$, $n = 53$; $r^2 = 0.10$, $p = 0.021$, $n = 53$, respectively), whereas no significant change was observed in linear extension rate ($r^2 = 0.003$, $p = 0.698$, $n = 53$).

Drivers of Growth Variability

Mean ± SD of environmental conditions in Serrana Atoll were SST of 28.04 ± 0.31°C for the period 1963–2015, and Ω_{arag} of 4.06 ± 0.09 for the period 1988–2011.

Skeletal density was negatively related to the mean SST, maximum SST, AMO, and DHM, based on coral growth master chronologies and environmental records (**Table 2**). In contrast, density was positively related to the NAO and Ω_{arag}. Extension rate was not related to any of the environmental variables. However, there were significant negative correlations between calcification and maximum SST, AMO, and DHM. The 13-year smoothed anomalies of coral growth master chronologies tended to show opposite variation patterns to SST and AMO (**Figure 3**).

Thermal stress in recent decades has been recurrent and intense (**Figure 2B**). Peaks of DHM in 1998, 2005, 2010 and 2015, coincident with El Niño events, had a negative effect on coral growth parameters. Reductions up to 25% (2005), 13% (2010), and 15% (2005) in calcification, extension and density, respectively, were detected (**Figure 4**). However, high DHM values observed before 1997, as in 1969, showed no negative effects on coral growth. During the period 1963–1997, thermal

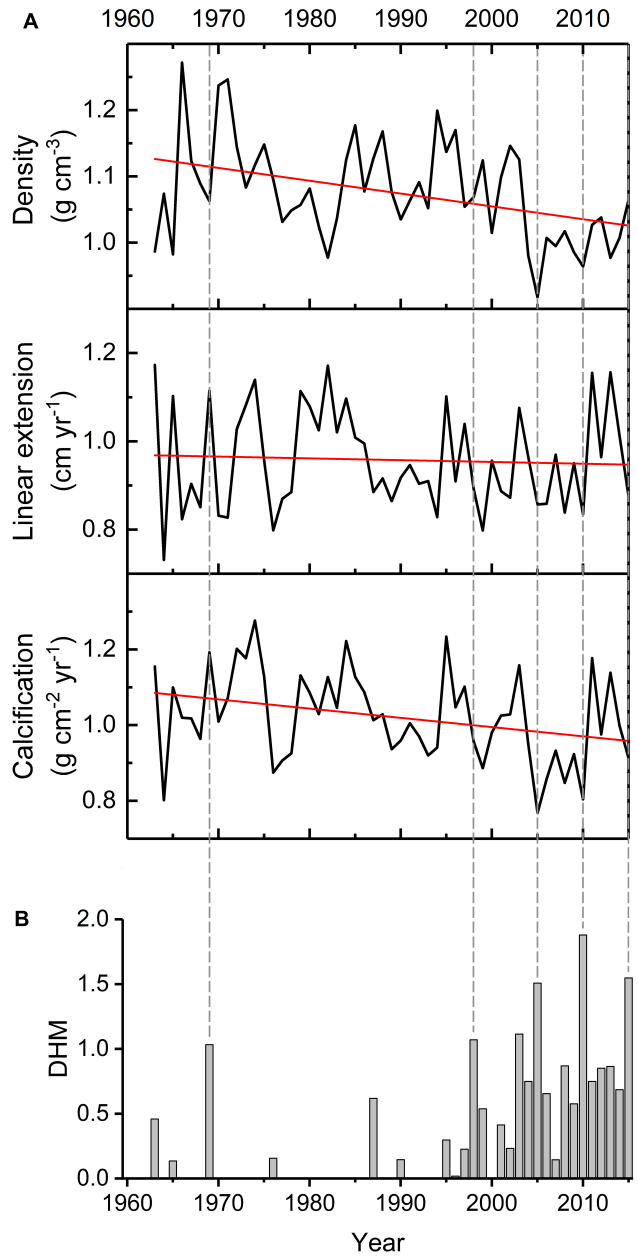

FIGURE 2 | Coral growth master chronologies during 1963–2015 for Serrana Atoll (black solid lines) **(A)**. Trends (red solid lines) are significant for density (r^2 = 0.16, p = 0.004, n = 53) and calcification (r^2 = 0.10, p = 0.021, n = 53), but not for extension (r^2 < 0.00, p = 0.698, n = 53). The thermal stress index given by degree heating months (DHM) are represented by gray bars **(B)**. Dashed lines indicate the years (1969, 1998, 2005, 2010, and 2015) with the highest DHM values.

stress events were sporadic, and did not explained important reductions in growth parameters (e.g., 1964, 1976 and 1977).

DISTLM analysis for the period 1963–2015 did not identify a predominant predictor explaining most of the variation in the master chronologies (see marginal test, **Table 3**). For the period 1988–2011, the variation in coral density was mainly explain

TABLE 2 | Pearson correlations of coral growth parameters with environmental variables during 1963–2015 (n = 53), and 1988–2011 for Ω_{arag} (n = 24).

	Density	Extension	Calcification
SST mean	***r* = −0.43, *p* = 0.001**	r = 0.07, p = 0.599	r = −0.21, p = 0.125
SST max	***r* = −0.37, *p* = 0.007**	r = −0.03, p = 0.843	***r* = −0.27, *p* = 0.050**
SST min	r = −0.23, p = 0.097	r = 0.07, p = 0.607	r = −0.11, p = 0.415
AMO	***r* = −0.41, *p* = 0.003**	r = −0.09, p = 0.514	***r* = −0.36, *p* = 0.009**
DHM	***r* = −0.44, *p* = 0.001**	r = −0.05, p = 0.728	***r* = −0.30, *p* = 0.029**
NAO	***r* = 0.28, *p* = 0.045**	r = 0.09, p = 0.541	r = 0.22, p = 0.116
SOI	r = 0.13, p = 0.341	r = −0.08, p = 0.556	r = 0.04, p = 0.795
Ω_{arag}	***r* = 0.61, *p* = 0.002**	r = −0.11, p = 0.621	r = 0.24, p = 0.265

Bold values are significant at p < 0.05.

by Ω_{arag}, which accounted for 37% of the total variation (see marginal and sequential tests, **Tables 4**, **5**).

DISCUSSION

Located far away from direct anthropogenic disturbances, corals from Serrana Atoll allow a clear identification of environmental and climatic signatures on growth rates. Here we present a 53-year record of coral growth parameters for *O. faveolata* for remote Southwestern Caribbean reefs. To the best of our knowledge, this is the first record of its kind for this region of the Caribbean, complementing the geographic coverage of previous studies and providing new insights into the understanding of coral growth responses in a period characterized by human-induced environmental and climatic changes (1963–2015).

Overall, coral growth records from Serrana Atoll indicate that calcification processes for *O. faveolata* have suffered disparate changes over the last 50 years, mainly associated to thermal stress, and occurring more frequently during recent decades. While the values of growth parameters of *O. faveolata* are within the ranges found for other Caribbean reefs (Dodge and Brass, 1984; van Veghel and Bosscher, 1995; Gischler and Oschmann, 2005; Helmle et al., 2011; Manzello et al., 2015), the CVs (7–12%) observed suggest important inter-annual variations in growth responses to environmental conditions. Indeed, between 1963 and 1990 growth parameters were characterized by positive anomalies. However, in the last 20 years negative anomalies have dominated the variability of growth parameters (**Figure 3**). Although values of CV were low in comparison to those reported by Helmle et al. (2011) for *O. faveolata* in Florida, probably reflecting latitudinal differences as well as lesser variability in environmental conditions in Serrana Atoll during the last decades, it is highly likely that thermal stress caused significant inter-annual variations over the studied period.

Degree heating months showed a negative effect on calcification rates during 1998, 2005 and 2010, coinciding with severe coral bleaching events in the region (Hughes et al., 2017). Signatures of bleaching on coral growth parameters include an increase in skeletal density and a marked reduction in extension and calcification rates (Carilli et al., 2009a). Corals growing in clear and oligotrophic waters are highly vulnerable to changes in temperature and thermal stress, which can result

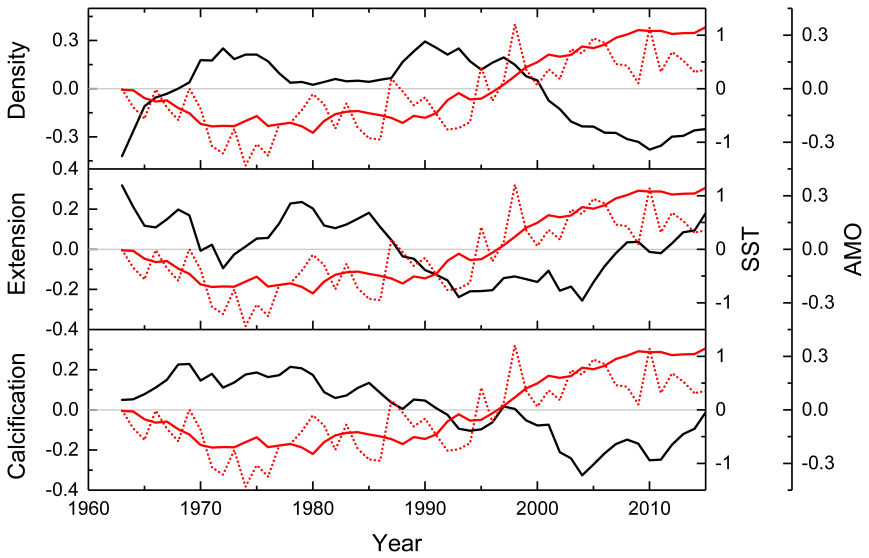

FIGURE 3 | Coral growth, SST and AMO correlations. Values of coral growth parameters (black solid lines) and SST (red solid lines) are presented as 13-year smoothed standardized anomalies (STDA). AMO is represented by red dotted lines. Density and calcification are negatively correlated with cyclical temperature trends.

in mass coral bleaching (Hughes et al., 2017), and significant decreases in their growth parameters (Carilli et al., 2009a,b). Whilst we cannot relate every single decline in growth parameters to thermal stress, we highlight that bleaching-induced impacts on growth parameters were unprecedented before 1997, and more frequent in recent years, corresponding with bleaching events linked to global warming (Hughes et al., 2018). Nevertheless, the magnitude of declines in Serrana Atoll were relatively small when compared to those in Belize during the 1998 bleaching, where *O. faveolata* corals showed pronounced decreases in extension and calcification rates (over four standard deviations outside the mean more chronology) and even interruption of growth (Carilli et al., 2009a). This outcome suggests that *O. faveolata* corals at Serrana Atoll, isolated from direct chronic human impacts (e.g., pollution, costal development, tourism), seem to have responded better to recent bleaching events than Belizean counterparts. This observation supports the hypothesis that corals with higher local anthropogenic stressors present reduced coral resistance to bleaching or thermal tolerance (Carilli et al., 2009a, 2010).

The significant relationships between growth parameters provide insights into historical growth strategies of *O. faveolata* at Serrana Atoll. We found a strong positive relationship between extension and calcification, and weaker relationships between extension and density (negative), and density and calcification (positive). These correlations are usually used to infer how corals invest increased availability of resources for calcification in extension or density (Carricart-Ganivet, 2007). While previous studies report that skeletal density tends to be the primary driver of variations in calcification for *O. faveolata* (Carricart-Ganivet, 2004), here extension was the key driver. This indicates that the growth strategy of the corals is favoring extension rather than the skeletal density at Serrana Atoll, as the extension did not showed a declining trend, but instead was strong related with the skeletal calcification rate. We argue that corals at Serrana Atoll are investing their calcification resources into maintaining extension as a response to a reduction of Ω_{arag}, attributed to ocean acidification in recent years (see below for details), and long-term increases in SST. This growth response seems to correspond to the "stretching" modulation phenomenon (in a temporal context) postulated by Carricart-Ganivet and Merino (2001), in which corals respond to environmental stress by extending their skeletons and maintaining calcification. This was clearly observed during the last decade (**Figure 3**), where despite the decline in density, both extension and calcification did not decline and remained relatively unchanged.

The most significant responses detected in growth parameters were the long-term decreases in skeletal density and calcification rates, and the absence of a temporal trend in extension rates. The downward trend in density was mainly linked to a decline in Ω_{arag} (**Table 2** and **Figure 5**) and, to a lesser extent, to warmer conditions in recent decades, which in turn could affect calcification responses. For the studied period (1963–2015) moderate to weak relationships were observed between density and the environmental variables considered (mainly SST related). The DISTML analysis indicated that temperature-based explanatory variables explained a modest part of the observed variability in density (<19%), suggesting that there are additional factors implicated in the declining trend. For the period 1998–2011, the DISTLM analysis identified that Ω_{arag} explained most of the variability observed in density. Thus, it is reasonable to suppose that long-term declining trends in density and calcification were modulated by a decrease in Ω_{arag}, the latter attributed to ocean acidification (Gledhill et al., 2008). Other studies have found that ocean acidification has a direct effect on skeletal density but not on linear extension rates (Tambutté et al., 2015; Mollica et al., 2018) as observed in our coral cores. Similarly to Kleypas (1999) and Helmle et al. (2011), we argue that Ω_{arag} has not yet reached a critical threshold needed to negatively

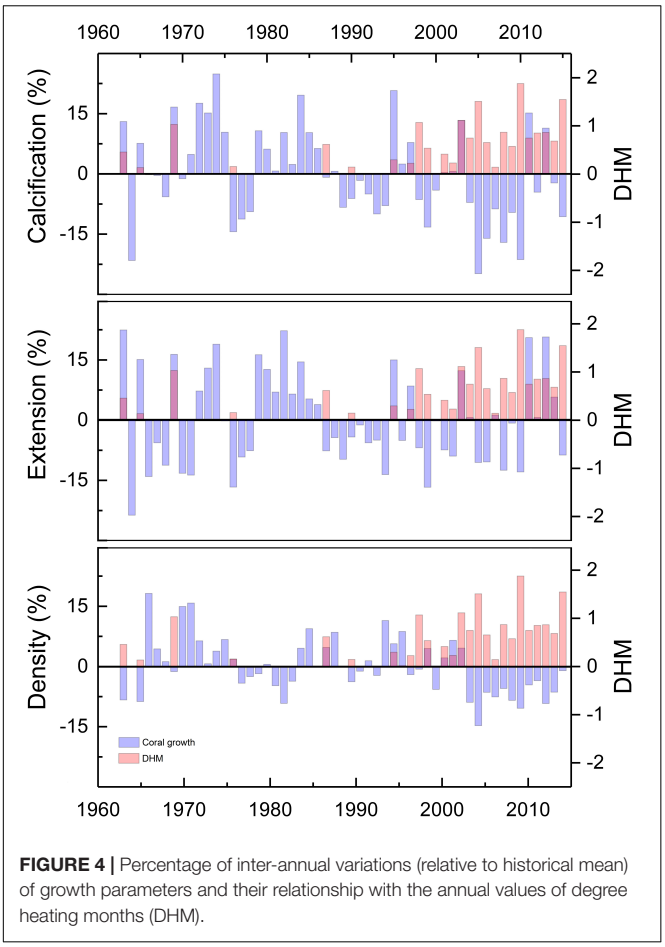

FIGURE 4 | Percentage of inter-annual variations (relative to historical mean) of growth parameters and their relationship with the annual values of degree heating months (DHM).

TABLE 3 | DISTLM marginal test for the period 1963–2015.

Variable	SS (trace)	Pseudo-F	*p*-value	Proportion
		Density		
DHM	0.06	12.31	0.002	**0.19**
SST (°C)	0.05	11.35	0.003	**0.18**
AMO	0.05	10.01	0.003	**0.16**
NAO	0.02	4.21	0.045	**0.08**
SOI	0.01	0.92	0.356	0.02
		Extension		
DHM	0.00	0.10	0.734	0.00
SST (°C)	0.00	0.28	0.561	0.01
AMO	0.01	0.43	0.494	0.01
NAO	0.01	0.38	0.527	0.01
SOI	0.00	0.35	0.574	0.01
		Calcification		
DHM	0.07	5.00	0.027	0.09
SST (°C)	0.03	2.43	0.129	0.05
AMO	0.09	7.45	0.013	**0.13**
NAO	0.04	2.56	0.118	0.05
SOI	0.00	0.07	0.798	0.00

Significant proportions of explained variation ($p < 0.05$) are given in bold.

TABLE 4 | Results of the marginal test for the period 1988–2011 performed by DISTLM forward analysis.

Variable	SS (trace)	Pseudo-F	*p*-values	Proportion
		Density		
DHM	0.03	8.74	0.009	**0.28**
Ω_{arag}	0.04	12.69	0.003	**0.37**
AMO	0.02	5.51	0.030	**0.20**
NAO	0.04	9.59	0.007	**0.30**
		Extension		
DHM	0.00	0.11	0.748	0.01
Ω_{arag}	0.00	0.25	0.623	0.01
AMO	0.00	0.03	0.861	0.00
NAO	0.00	0.00	0.974	0.00
		Calcification		
DHM	0.03	2.98	0.100	0.12
Ω_{arag}	0.02	1.30	0.268	0.06
AMO	0.01	0.67	0.409	0.03
NAO	0.03	2.22	0.185	0.09

Significant proportions of explained variation ($p < 0.05$) are given in bold.

impact linear extension. Nevertheless, ocean acidification is an increasing threat for corals as ongoing reduction in carbonate ion concentration will lead to less dense and more fragile coral skeletons (Fantazzini et al., 2015; Tambutté et al., 2015; Mollica et al., 2018), compromising reef ecosystem function within decades (Kleypas and Yates, 2009; Albright et al., 2018). Some models predict an average 12.4% decline in skeletal density for *Porites* corals globally by the end of the century due to ocean acidification (Mollica et al., 2018). In light of the decreasing trends documented here and global predictions of decreasing coral density, we speculate that ocean acidification will play a major role in coral calcification at Serrana Atoll (and elsewhere within the coralline complexes from the Seaflower Reserve) in the near future.

Our study provides further evidence concerning the multi-decadal variability in coral growth rates in the Caribbean (Hetzinger et al., 2008; Helmle et al., 2011). Particularly we found a significant negative correlation of the skeletal density and calcification with AMO, and no relationship between extension and AMO. The majority of studies only report the relationship between AMO and extension, identifying a positive correlation for locations such as Belize and Panama (Kwiatkowski et al., 2013), and negative correlations in Mexico (Vásquez-Bedoya et al., 2012), Bahamas and Belize (Saenger et al., 2009), and Florida (Helmle et al., 2011). In Florida, Helmle et al. (2011) found a positive relationship between density and AMO, and no relationship with calcification, contrary to our finding. These varying outcomes do not diminish the importance of multi-decadal variability in coral growth rates in the Caribbean but underline the need to improve our understanding of the significant role of the AMO in influencing coral growth rates in the region. As previous AMO analyses were based on coral records up to only 2000 (Helmle et al., 2011; Kwiatkowski et al., 2013), just after the AMO shifted from a cold to a warm phase (Zhang and Delworth, 2006), our master chronologies add crucial data to infer coral growth responses in such warm AMO phases.

TABLE 5 | Results of sequential test for the period 1988–2011 performed by DISTLM forward analysis.

Variable	Adjusted r^2	SS (trace)	Pseudo-F	*p*-Value	Proportion	Cumul.
			Density			
Ω_{arag}	0.336880	4.45E-02	12.685	0.001	**0.37**	0.37
			Extension			
Ω_{arag}	−0.033651	2.10E-03	0.25123	0.616	0.01	0.01
			Calcification			
DHM	0.079387	3.50E-02	2.9834	0.106	0.12	0.12
AMO	0.084099	1.30E-02	1.1132	0.339	0.04	0.16
NAO	0.106950	1.75E-02	1.5372	0.226	0.06	0.22
Ω_{arag}	0.185130	3.03E-02	2.919	0.111	0.10	0.33

Significant proportions of explained variation ($p < 0.05$) are given in bold. Cumul, cumulative proportion of explained variation.

In our study area, long-term trends of skeletal density and calcification varied inversely to AMO, with positive anomalies during the cold phase of the AMO (1965–1995), and negative anomalies during the last warm phase after 1995 (Zhang and Delworth, 2006).

The master chronologies analyzed provide key details regarding the latest trends of coral growth parameters that can support predictions of future trajectories of coral growth and calcification processes for the Southwestern Caribbean. Since 2010, calcification and extension rates have shown baseline averages, but density values remain below the long-term average (negative anomalies). We attribute this to ocean acidification given that Ω_{arag} apparently contributed to the declining trend observed for density. Thus, although long-term calcification processes at Serrana Atoll have been modulated by SST oscillations at decadal scales (AMO), it appears that in the most recent phase of the AMO decreasing Ω_{arag} dominated the effect of SST. The ocean acidification and temperature oscillations controlled by AMO are therefore important to understand how coral growth parameters may respond to those oscillations in the coming decades. Climatic predictions indicate the oceans will continue to acidify, negatively affecting coral reefs by reducing carbonate ion concentrations which result in corals with more fragile skeletons and more susceptible to bioerosion (Kleypas, 1999; van Woesik et al., 2013; Mollica et al., 2018). Temperature is another key variable that is expected to continue increasing and threatening corals (Meissner et al., 2012). However, temperature stress on Caribbean reefs might be less in coming decades than in recent years (1990–2015). According to historical ocean temperature oscillations it has been suggested that in the following decades these oscillations will shift from a warm phase (the present) to a cold phase (Klöwer et al., 2014; McCarthy et al., 2015; Frajka-Williams et al., 2017; Page, 2017). In spite of this, models indicate that most coral reefs will suffer marked deterioration over the next few decades, even reducing global warming to 2°C and under the optimistic assumption of corals undergoing thermal adaptation (Frieler et al., 2012). Calcification might be oscillating in response to the AMO, however, the decline in Ω_{arag} will be critical for coral growth. Consequently, the prediction of future responses of Caribbean reefs has to consider the combined role of warming, AMO variability and ocean acidification on coral growth and calcification processes.

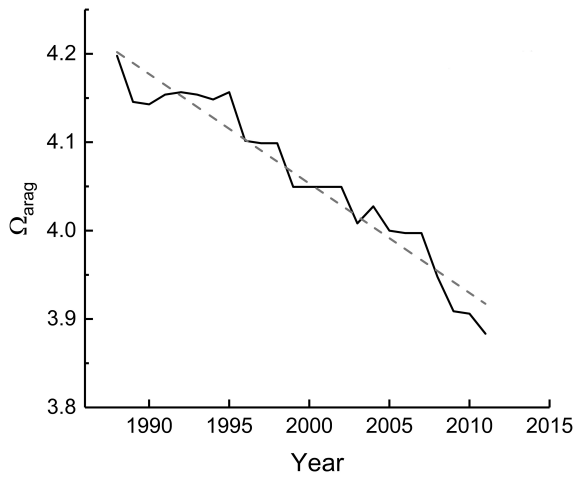

FIGURE 5 | Aragonite saturation state (Ω_{arag}) in the vicinity of Serrana Atoll, during 1988–2011 (solid line). The dashed line indicates a significant tendency ($r^2 = 0.94$, $p < 0.001$) described by the equation $y = 28.815 - 0.012x$.

AUTHOR CONTRIBUTIONS

LL-S processed and analyzed the cores, performed statistical analyses, and contributed to manuscript writing. ÁM-G contributed to core processing and analysis. ML-V collected the samples, processed and analyzed the cores, and contributed to manuscript writing. AR-R analyzed the cores, performed statistical analyses, contributed to manuscript writing, and directed the work. All authors participated in study conception and design.

FUNDING

This work was funded by the Pontificia Universidad Javeriana Cali. The field trip was conducted during the Seaflower Scientific Expedition-Serrana 2016, supported by the Colombian Government, under the leadership of the Colombian Oceans' Commission (CCO), and with logistic support from the

Colombian Navy. Additional funding was provided by the Administrative Department of Science, Technology and Innovation (Colciencias), under the Colombia-BIO program (Agreement 341–2016, between Universidad de los Andes and Comisión Colombiana del Océano).

ACKNOWLEDGMENTS

We thank the Colombian authorities leading the Scientific Expeditions to the Seaflower Biosphere Marine Reserve, in particular the Colombian Oceans' Commission (CCO), the Colombian Navy, and the Corporation for the Sustainable Development of the Archipelago of San Andrés, Providencia and Santa Catalina (Coralina). Of great importance was the logistic support during the field trip provided by the crew members from Coralina, and by Juliana Sintura. The Hospital Universitario del Valle (HUV) and its personnel kindly helped us with CT-scan images acquisition. We thank Adam Suchley for his comments on a previous version of this manuscript. This research was performed under the framework of a collaborative research between the Global Change Institute, the University of Queensland, and the Department of Natural Sciences and Mathematics, from the Pontificia Universidad Javeriana Cali.

SUPPLEMENTARY MATERIAL

The Supplementary Material for this article can be found online at: https://www.frontiersin.org/articles/10.3389/fmars.2019.00038/full#supplementary-material

REFERENCES

Albright, R., Takeshita, Y., Koweek, D. A., Ninokawa, A., Wolfe, K., Rivlin, T., et al. (2018). Carbon dioxide addition to coral reef waters suppresses net community calcification. *Nature* 555, 516–519. doi: 10.1038/nature25968

Anderson, M., Gorley, R. N., and Clarke, K. (2008). *PERMANOVA+ for Primer: Guide to Software and Statistical Methods*. Plymouth: PRIMER-E Ltd.

Anderson, M. J. (2003). *Distlm Forward: A Fortran Computer Program to Calculate a Distance-Based Multivariate Analysis for a Linear Model using Forward Selection*. Auckland: Department of Statistics, University of Auckland.

Barnes, D. J., and Lough, J. M. (1996). Coral skeletons: storage and recovery of environmental information. *Glob. Chang. Biol.* 2, 569–582. doi: 10.1111/j.1365-2486.1996.tb00068.x

Bessat, F., and Buigues, D. (2001). Two centuries of variation in coral growth in a massive *Porites* colony from moorea (French Polynesia): a response of ocean-atmosphere variability from south central Pacific. *Palaeogeogr. Palaeoclimatol. Palaeoecol.* 175, 381–392. doi: 10.1016/S0031-0182(01)00381-9

Cantin, N. E., Cohen, A. L., Karnauskas, K. B., Tarrant, A. M., and McCorkle, D. C. (2010). Ocean warming slows coral growth in the central red sea. *Science* 329, 322–325. doi: 10.5061/dryad.9g182

Carilli, J. E., Norris, R. D., Black, B., Walsh, S. M., and Mcfield, M. (2010). Century-scale records of coral growth rates indicate that local stressors reduce coral thermal tolerance threshold. *Glob. Chang. Biol.* 16, 1247–1257. doi: 10.1111/j.1365-2486.2009.02043.x

Carilli, J. E., Norris, R. D., Black, B. A., Walsh, S. M., and McField, M. (2009a). Local stressors reduce coral resilience to bleaching. *PLoS One* 4:e6324. doi: 10.1371/journal.pone.0006324

Carilli, J. E., Prouty, N. G., Hughen, K. A., and Norris, R. D. (2009b). Century-scale records of land-based activities recorded in mesoamerican coral cores. *Mar. Pollut. Bull.* 58, 1835–1842. doi: 10.1016/j.marpolbul.2009.07.024

Carricart-Ganivet, J. P. (2004). Sea surface temperature and the growth of the west atlantic reef-building coral *Montastraea annularis*. *J. Exp. Mar. Bio. Ecol.* 302, 249–260. doi: 10.1016/j.jembe.2003.10.015

Carricart-Ganivet, J. P. (2007). Annual density banding in massive coral skeletons: result of growth strategies to inhabit reefs with high microborers' activity? *Mar. Biol.* 153, 1–5. doi: 10.1007/s00227-007-0780-3

Carricart-Ganivet, J. P., and Barnes, D. J. (2007). Densitometry from digitized images of X-radiographs: methodology for measurement of coral skeletal density. *J. Exp. Mar. Bio. Ecol.* 344, 67–72. doi: 10.1016/j.jembe.2006.12.018

Carricart-Ganivet, J. P., Cabanillas-Terán, N., Cruz-Ortega, I., and Blanchon, P. (2012). Sensitivity of calcification to thermal stress varies among genera of massive reef-building corals. *PLoS One* 7:e32859. doi: 10.1371/journal.pone.0032859

Carricart-Ganivet, J. P., and Merino, M. (2001). Growth responses of the reef-building coral *Montastraea annularis* along a gradient of continental influence in the southern gulf of Mexico. *Bull. Mar. Sci.* 68, 133–146.

Castillo, K. D., Ries, J. B., and Weiss, J. M. (2011). Declining coral skeletal extension for forereef colonies of *Siderastrea siderea* on the mesoamerican barrier reef system, southern belize. *PLoS One* 6:e14615. doi: 10.1371/journal.pone.0014615

Castillo, K. D., Ries, J. B., Weiss, J. M., and Lima, F. P. (2012). Decline of forereef corals in response to recent warming linked to history of thermal exposure. *Nat. Clim. Chang.* 2, 756–760. doi: 10.1038/nclimate1577

Cooper, T. F., De'ath, G., Fabricius, K. E., and Lough, J. M. (2008). Declining coral calcification in massive *Porites* in two nearshore regions of the northern great barrier reef. *Glob. Chang. Biol.* 14, 529–538. doi: 10.1111/j.1365-2486.2007.01520.x

Crook, E. D., Cohen, A. L., Rebolledo-Vieyra, M., Hernandez, L., and Paytan, A. (2013). Reduced calcification and lack of acclimatization by coral colonies growing in areas of persistent natural acidification. *Proc. Natl. Acad. Sci. U.S.A.* 110, 11044–11049. doi: 10.1073/pnas.1301589110

Cruz-Piñón, G., Carricart-Ganivet, J. P., and Espinoza-Avalos, J. (2003). Monthly skeletal extension rates of the hermatypic corals *Montastraea annularis* and *Montastraea faveolata*: biological and environmental controls. *Mar. Biol.* 143, 491–500. doi: 10.1007/s00227-003-1127-3

De'ath, G., Lough, J. M., and Fabricius, K. E. (2009). Declining coral calcification on the great barrier reef. *Science* 323, 116–119. doi: 10.1126/science.1165283

Dodge, R. E., and Brass, G. W. (1984). Skeletal extension, density and calcification of the reef coral, *Montastrea annularis*: St. Croix, U.S. Virgin Islands. *Bull. Mar. Sci.* 34, 288–307.

D'Olivo, J. P., McCulloch, M. T., and Judd, K. (2013). Long-term records of coral calcification across the central great barrier reef: assessing the impacts of river runoff and climate change. *Coral Reefs* 32, 999–1012. doi: 10.1007/s00338-013-1071-8

Enfield, D. B., Mestas-NuÑez, A. M., and Trimble, P. J. (2001). The Atlantic multidecadal oscillation and its relationship to rainfall and river flows in the continental U.S.A. *Geophys. Res. Lett.* 28, 2077–2080. doi: 10.1029/2000GL012745

Fabricius, K. E. (2005). Effects of terrestrial runoff on the ecology of corals and coral reefs: review and synthesis. *Mar. Pollut. Bull.* 50, 125–146. doi: 10.1016/j.marpolbul.2004.11.028

Fantazzini, P., Mengoli, S., Pasquini, L., Bortolotti, V., Brizi, L., Mariani, M., et al. (2015). Gains and losses of coral skeletal porosity changes with ocean acidification acclimation. *Nat. Commun.* 6:7785. doi: 10.1038/ncomms8785

Frajka-Williams, E., Beaulieu, C., and Duchez, A. (2017). Emerging negative atlantic multidecadal oscillation index in spite of warm subtropics. *Sci. Rep.* 7:11224. doi: 10.1038/s41598-017-11046-x

Frieler, K., Meinshausen, M., Golly, A., Mengel, M., Lebek, K., Donner, S. D., et al. (2012). Limiting global warming to 2°C is unlikely to save most coral reefs. *Nat. Clim. Chang.* 3, 165–170. doi: 10.1038/nclimate1674

Gischler, E., and Oschmann, W. (2005). Historical climate variation in Belize (Central America) as recorded in scleractinian coral skeletons. *Palaios* 20, 159–174. doi: 10.2210/palo.2004.p04-09

Gledhill, D. K., Wanninkhof, R., Millero, F. K., and Eakin, M. (2008). Ocean acidification of the greater caribbean region 1996-2006. *J. Geophys. Res.* 113, C10031. doi: 10.1029/2007JC004629

Grove, C. A., Zinke, J., Peeters, F., Park, W., Scheufen, T., Kasper, S., et al. (2013). Madagascar corals reveal a multidecadal signature of rainfall and river runoff since 1708. *Clim. Past* 9, 641–656. doi: 10.5194/cp-9-641-2013

Guzman, H. M., Cipriani, R., and Jackson, J. B. C. (2008). Historical decline in coral reef growth after the panama canal. *Ambio* 37, 342–346. doi: 10.1579/07-A-372.1

Helmle, K. P., and Dodge, R. E. (2011). "Sclerochronology," in *Encyclopedia of Modern Coral Reefs*, ed. D. Hopley (Berlin: Springer), 958–966. doi: 10.1007/978-90-481-2639-2_22

Helmle, K. P., Dodge, R. E., Swart, P. K., Gledhill, D. K., and Eakin, C. M. (2011). Growth rates of florida corals from 1937 to 1996 and their response to climate change. *Nat. Commun.* 2:215. doi: 10.1038/ncomms1222

Hetzinger, S., Pfeiffer, M., Dullo, W. C., Keenlyside, N., Latif, M., and Zinke, J. (2008). Caribbean coral tracks atlantic multidecadal oscillation and past hurricane activity. *Geology* 36, 11–14. doi: 10.1130/G24321a.1

Hughes, T. P., Anderson, K. D., Connolly, S. R., Heron, S. F., Kerry, J. T., Lough, J. M., et al. (2018). Spatial and temporal patterns of mass bleaching of corals in the Anthropocene. *Science* 359, 80–83. doi: 10.1126/science.aan8048

Hughes, T. P., Kerry, J. T., Álvarez-Noriega, M., Álvarez-Romero, J. G., Anderson, K. D., Baird, A. H., et al. (2017). Global warming and recurrent mass bleaching of corals. *Nature* 543, 373–377. doi: 10.1038/nature21707

Jones, P. D., Briffa, K. R., Osborn, T. J., Lough, J. M., van Ommen, T. D., Vinther, B. M., et al. (2009). High-resolution palaeoclimatology of the last millennium: a review of current status and future prospects. *Holocene* 19, 3–49. doi: 10.1177/0959683608098952

Jones, P. D., Jonsson, T., and Wheeler, D. (1997). Extension to the north atlantic oscillation using early instrumental pressure observations from gibraltar and south-west Iceland. *Int. J. Climatol.* 17, 1433–1450. doi: 10.1002/(SICI)1097-0088(19971115)17:13<1433::AID-JOC203>3.0.CO;2-P

Kleypas, J. A. (1999). Geochemical consequences of increased atmospheric carbon dioxide on coral reefs. *Science* 284, 118–120. doi: 10.1126/science.284.5411.118

Kleypas, J. A., and Yates, K. K. (2009). Coral reefs and ocean acidification. *Oceanography* 22, 108–117. doi: 10.5670/oceanog.2009.101

Klöwer, M., Latif, M., Ding, H., Greatbatch, R. J., and Park, W. (2014). Atlantic meridional overturning circulation and the prediction of north atlantic sea surface temperature. *Earth Planet. Sci. Lett.* 406, 1–6. doi: 10.1016/j.epsl.2014.09.001

Kwiatkowski, L., Cox, P. M., Economou, T., Halloran, P. R., Mumby, P. J., Booth, B. B. B., et al. (2013). Caribbean coral growth influenced by anthropogenic aerosol emissions. *Nat. Geosci.* 6, 362–366. doi: 10.1038/ngeo1780

Legendre, P., and Anderson, M. J. (1999). Distance-based redundancy analysis: testing multispecies responses in multifactorial ecological experiments. *Ecol. Monogr.* 69, 1–24. doi: 10.1890/0012-9615(1999)069[0001:DBRATM]2.0.CO;2

Liu, G., Strong, A. E., Skirving, W. J., and Arzayus, L. F. (2006). "Overview of NOAA coral reef watch program's near-real-time satellite global coral bleaching monitoring activities," in *Proceedings of the 10th International Coral Reef Symposium*, (Okinawa), 1783–1793.

Lough, J. M. (2008). Coral calcification from skeletal records revisited. *Mar. Ecol. Prog. Ser.* 373, 257–264. doi: 10.3354/meps07398

Lough, J. M., and Barnes, D. J. (1992). Comparisons of skeletal density variations in *Porites* from the central great barrier reef. *J. Exp. Mar. Bio. Ecol.* 155, 1–25. doi: 10.1016/0022-0981(92)90024-5

Lough, J. M., and Barnes, D. J. (2000). Environmental controls on growth of the massive coral *Porites*. *J. Exp. Mar. Bio. Ecol.* 245, 225–243. doi: 10.1016/S0022-0981(99)00168-9

Lough, J. M., and Cantin, N. E. (2014). Perspectives on massive coral growth rates in a changing ocean. *Biol. Bull.* 226, 187–202. doi: 10.1086/BBLv226n3p187

Lough, J. M., and Cooper, T. F. (2011). New insights from coral growth band studies in an era of rapid environmental change. *Earth Sci. Rev.* 108, 170–184. doi: 10.1016/j.earscirev.2011.07.001

Manzello, D. P., Enochs, I. C., Kolodziej, G., and Carlton, R. (2015). Recent decade of growth and calcification of *Orbicella faveolata* in the florida keys: an inshore-offshore comparison. *Mar. Ecol. Prog. Ser.* 521, 81–89. doi: 10.3354/meps11085

Marubini, F., Ferrier-Pages, C., Furla, P., and Allemand, D. (2008). Coral calcification responds to seawater acidification: a working hypothesis towards a physiological mechanism. *Coral Reefs* 27, 491–499. doi: 10.1007/s00338-008-0375-6

McCarthy, G. D., Haigh, I. D., Hirschi, J., Grist, J. P., and Smeed, D. A. (2015). Ocean impact on decadal atlantic climate variability revealed by sea-level observations. *Nature* 521, 508–512. doi: 10.1038/nature14491

Meissner, K. J., Lippmann, T., and Sen Gupta, A. (2012). Large-scale stress factors affecting coral reefs: open ocean sea surface temperature and surface seawater aragonite saturation over the next 400 years. *Coral Reefs* 31, 309–319. doi: 10.1007/s00338-011-0866-8

Mollica, N. R., Guo, W., Cohen, A. L., Huang, K.-F., Foster, G. L., Donald, H. K., et al. (2018). Ocean acidification affects coral growth by reducing skeletal density. *Proc. Natl. Acad. Sci. U.S.A.* 115, 1754–1759. doi: 10.1073/pnas.1712806115

Page, N. J. (2017). The coming cooling: usefully accurate climate forecasting for policy makers. *Energy Environ.* 28, 330–347. doi: 10.1177/0958305X16686488

Pandolfi, J. M. (2011). "The Paleoecology of Coral Reefs," in *Coral Reefs: An Ecosystem in Transition*, eds Z. Dubinsky and N. Stambler (Berlin: Springer), 13–24. doi: 10.1007/978-94-007-0114-4_2

Rayner, N. A., Parker, D. E., Horton, E. B., Folland, C. K., Alexander, L. V., and Rowell, D. P. (2003). Global analyses of sea surface temperature, sea ice, and night marine air temperature since the late nineteenth century. *J. Geophys. Res.* 108:4407. doi: 10.1029/2002JD002670

Ropelewski, C. F., and Jones, P. D. (1987). An extension of the tahiti–darwin southern oscillation index. *Mon. Weather Rev.* 115, 2161–2165. doi: 10.1175/1520-0493(1987)115<2161:AEOTTS>2.0.CO;2

Saenger, C., Cohen, A. L., Oppo, D. W., Halley, R. B., and Carilli, J. E. (2009). Surface-temperature trends and variability in the low-latitude north atlantic since 1552. *Nat. Geosci.* 2, 492–495. doi: 10.1038/ngeo552

Tambutté, E., Venn, A. A., Holcomb, M., Segonds, N., Techer, N., Zoccola, D., et al. (2015). Morphological plasticity of the coral skeleton under CO2-driven seawater acidification. *Nat. Commun.* 6:7368. doi: 10.1038/ncomms8368

Tanzil, J., Brown, B., Tudhope, A., and Dunne, R. (2009). Decline in skeletal growth of the coral *Porites lutea* from the andaman sea, south thailand between 1984 and 2005. *Coral Reefs* 28, 519–528. doi: 10.1007/s00338-008-0457-5

Tanzil, J. T., Brown, B. E., Dunne, R. P., Lee, J. N., Kaandorp, J. A., and Todd, P. A. (2013). Regional decline in growth rates of massive *Porites* corals in Southeast Asia. *Glob. Chang. Biol.* 19, 3011–3023. doi: 10.1111/gcb.12279

van Veghel, M. L., and Bosscher, H. (1995). Variation in linear growth and skeletal density within the polymorphic reef building coral *Montastraea annularis*. *Bull. Mar. Sci.* 56, 902–908.

van Woesik, R., van Woesik, K., and van Woesik, L. (2013). Effects of ocean acidification on the dissolution rates of reef-coral skeletons. *PeerJ* 1, e208. doi: 10.7717/peerj.208

Vásquez-Bedoya, L. F., Cohen, A. L., Oppo, D. W., and Blanchon, P. (2012). Corals record persistent multidecadal SST variability in the Atlantic Warm Pool since 1775 AD. *Paleoceanography* 27, A3231. doi: 10.1029/2012PA002313

Yan, H., Sun, L., Wang, Y., Huang, W., Qiu, S., and Yang, C. (2011). A record of the southern oscillation index for the past 2,000 years from precipitation proxies. *Nat. Geosci.* 4, 611–614. doi: 10.1038/ngeo1231

Zhang, R., and Delworth, T. L. (2006). Impact of atlantic multidecadal oscillations on India/Sahel rainfall and Atlantic hurricanes. *Geophys. Res. Lett.* 33:L17712. doi: 10.1029/2006GL026267

Conflict of Interest Statement: The authors declare that the research was conducted in the absence of any commercial or financial relationships that could be construed as a potential conflict of interest.

frontiers in Marine Science

ORIGINAL RESEARCH
published: 12 February 2019
doi: 10.3389/fmars.2019.00010

Ecological Niche Modeling of Three Species of *Stenella* Dolphins in the Caribbean Basin, With Application to the Seaflower Biosphere Reserve

Dalia C. Barragán-Barrera[1,2], Karina Bohrer do Amaral[3]*, Paula Alejandra Chávez-Carreño[4], Nohelia Farías-Curtidor[1], Rocío Lancheros-Neva[1,5], Natalia Botero-Acosta[1], Paula Bueno[6], Ignacio Benites Moreno[3,7], Jaime Bolaños-Jiménez[8,9], Laurent Bouveret[10], Delma Nataly Castelblanco-Martínez[11,12], Jolanda A. Luksenburg[13,14], Julie Mellinger[10], Roosevelt Mesa-Gutiérrez[15], Benjamin de Montgolfier[16], Eric A. Ramos[12,17], Vincent Ridoux[18] and Daniel M. Palacios[19]**

[1] Fundación Macuáticos Colombia, Medellín, Colombia, [2] Laboratorio de Ecología Molecular de Vertebrados Acuáticos, Department of Biological Sciences, Universidad de los Andes, Bogotá, Colombia, [3] Laboratório de Sistemática e Ecologia de Aves e Mamíferos Marinhos, Instituto de Biociências, Universidade Federal do Rio Grande do Sul, Porto Alegre, Brazil, [4] Independent Researcher, La Paz, Mexico, [5] Parques Nacionales Naturales de Colombia, Bogotá, Colombia, [6] WWF Colombia, Bogotá, Colombia, [7] Centro de Estudos Costeiros, Limnológicos e Marinhos, Universidade Federal do Rio Grande do Sul, Imbé, Brazil, [8] Asociación Civil Sea Vida, Aragua, Venezuela, [9] Instituto de Ciencias Marinas y Pesquerías, Universidad Veracruzana, Veracruz, Mexico, [10] Observatoire des Mammifères Marins de l'Archipel Guadeloupéen, Archipelago's Guadeloupe, France, [11] Consejo Nacional de Ciencia y Tecnología, University of Quintana Roo, Chetumal, Mexico, [12] Fundación Internacional para la Naturaleza y la Sostenibilidad, Chetumal, Mexico, [13] Institute of Environmental Sciences, Leiden University, Leiden, Netherlands, [14] Department of Environmental Science and Policy, George Mason University, Fairfax, VA, United States, [15] Duke Marine Laboratory, Nicholas School of the Environment, Duke University, Durham, NC, United States, [16] Aquasearch, Sainte-Luce, France, [17] The Graduate Center, City University of New York, New York, NY, United States, [18] Observatoire PELAGIS, Université de La Rochelle, La Rochelle, France, [19] Marine Mammal Institute and Department of Fisheries and Wildlife, Oregon State University, Newport, OR, United States

OPEN ACCESS

Edited by:
Santiago Herrera,
Lehigh University, United States

Reviewed by:
Lindsay Porter,
University of St Andrews, United Kingdom
Samuel Georgian,
Marine Conservation Institute, United States

***Correspondence:**
Dalia C. Barragán-Barrera
daliac.barraganbarrera@gmail.com
Karina Bohrer do Amaral
karinabohrerdoamaral@gmail.com
Daniel M. Palacios
daniel.palacios@oregonstate.edu

Specialty section:
This article was submitted to Marine Conservation and Sustainability, a section of the journal Frontiers in Marine Science

Received: 31 July 2018
Accepted: 11 January 2019
Published: 12 February 2019

Citation:
Barragán-Barrera DC, do Amaral KB, Chávez-Carreño PA, Farías-Curtidor N, Lancheros-Neva R, Botero-Acosta N, Bueno P, Moreno IB, Bolaños-Jiménez J, Bouveret L, Castelblanco-Martínez DN, Luksenburg JA, Mellinger J, Mesa-Gutiérrez R, de Montgolfier B, Ramos EA, Ridoux V and Palacios DM (2019) Ecological Niche Modeling of Three Species of Stenella Dolphins in the Caribbean Basin, With Application to the Seaflower Biosphere Reserve. Front. Mar. Sci. 6:10. doi: 10.3389/fmars.2019.00010

Dolphins of the genus *Stenella* occur in pelagic waters of both tropical and warm-temperate oceans. Three species, the Atlantic spotted dolphin (*Stenella frontalis*), the pantropical spotted dolphin (*S. attenuata*), and the spinner dolphin (*S. longirostris*) are abundant worldwide, but in the Caribbean Basin they have been poorly studied and information on their distribution patterns is scarce. Specifically, in Colombia's remote Seaflower Biosphere Reserve (SFBR) *S. attenuata* has been reported occasionally, but *S. frontalis* and *S. longirostris* have never been recorded before. To address this information gap, an ecological niche modeling approach was used to determine the potential distribution patterns of these three dolphin species in the region. Records of these species for the Caribbean Basin were compiled, including both published and unpublished data. Environmental information, including bathymetry, bathymetric slope, distance to shore, sea surface temperature, sea surface salinity, and chlorophyll-*a* concentration was gathered from public databases (MARSPEC and Bio-ORACLE) in raster format. The maximum entropy algorithm (Maxent) for modeling species' geographic distributions with presence-only data was used. After filtering the data, 210 records of *S. attenuata*, 204 of *S. frontalis*, and 80 of *S. longirostris* were used to run models. The best configuration for each model was chosen based on the $\Delta AICc$ criterion. For all three species, the final ecological niche models returned *AUC*

test values higher than 0.8, indicating satisfactory model performance. The resulting potential distribution maps suggested that areas closest to continental shorelines of the Caribbean Basin and surrounding islands had the highest environmental suitability for all species (>70%). All models reported high environmental suitability for *S. attenuata* and *S. longirostris* in the SFBR, mainly in the southernmost part surrounding San Andrés and Providence Archipelago. Assessment of niche overlap from the predictions of species distributions using the similarity statistic and pairwise map overlap indicated that *S. frontalis* and *S. longirostris* had niches slightly more similar in comparison to *S. attenuata*. As this was a first effort to fill a gap in our understanding of the distribution of species in the genus *Stenella* in the Caribbean Basin, further studies are necessary using both niche modeling and biological/ecological approaches.

Keywords: *Stenella*, potential distribution area, Caribbean Basin, Seaflower Biosphere Reserve, Maxent, ecological niche modeling, niche overlap

INTRODUCTION

The ocean comprises 70% of the planet and offers a wide range of habitats to marine life (e.g., Spalding et al., 2012; Kelley et al., 2016). These different habitats are characterized by gradients in sea surface temperature (SST), sea surface salinity (SSS), productivity, and topography at both broad and local scales (Redfern et al., 2006), playing an important role to explain distribution patterns of marine top predators such as cetaceans (e.g., Baumgartner et al., 2001; Palacios et al., 2013b). Dolphins of the genus *Stenella* (Gray, 1866) are common in tropical, subtropical, and temperate waters worldwide. Because of such wide distribution patterns, they are often considered "umbrella species," since any conservation efforts made on their behalf benefit many other species within their habitat (Jefferson et al., 2008).

Although the taxonomy of *Stenella* remained unclear until the 1980s, the five species that make up the genus are now well characterized. The genus is considered a non-monophyletic assemblage (see Perrin et al., 2013), with some species being more related to *Tursiops* (Leduc et al., 1999). While the *Stenella* species have great dispersal capacity, they exhibit significant distribution changes in response to seasonal variation in oceanographic conditions (Reilly, 1990; Moreno et al., 2005). Additionally, some species within the genus are considered sympatric throughout their distribution, although at an individual level they appear to have distinct environmental requirements at regional scales (e.g., Baumgartner et al., 2001; Davis et al., 2002; do Amaral et al., 2015).

The Atlantic spotted dolphin (*S. frontalis*), endemic to the Atlantic Ocean, is distributed mainly in areas closer to continental shelves and surrounding islands (Perrin et al., 1987; Davis et al., 1998; do Amaral et al., 2015). The pantropical spotted dolphin (*S. attenuata*) and the spinner dolphin (*S. longirostris*) are more widely distributed in the Atlantic, Indian, and Pacific Oceans (Jefferson et al., 2008), and appear to have similar patterns of habitat use that favor their presence over deeper waters (Davis et al., 1998, 2002; Baumgartner et al., 2001; do Amaral et al., 2015). Although these three species have been previously reported in the Caribbean Basin (e.g., Caldwell et al., 1971; Mignucci-Giannoni, 1998; Pardo et al., 2009; Palacios et al., 2013b; Niño-Torres et al., 2015; Ramos et al., 2016), little is known about their habitat preferences and spatial distribution in coastal or oceanic areas. Hence, it is important to identify areas where these species are likely to be found in order to direct research and improve management measures.

Particularly in Colombia's Caribbean Sea, cetacean research has been limited, with most studies focusing on specific coastal mainland locations, including Santa Marta (Pardo and Palacios, 2006; Fraija et al., 2009; Pardo et al., 2009), Bay of Cispatá (García and Trujillo, 2004), Gulf of Morrosquillo (Palacios et al., 2013b), and La Guajira (Combatt and González, 2007; Palacios et al., 2012; Farías-Curtidor et al., 2017). To date, almost no research effort has been conducted in the remote oceanic region surrounding the Archipelago of San Andrés, Providencia and Santa Catalina (Pardo et al., 2009; Palacios et al., 2013b). Located in this region, the Seaflower Biosphere Reserve (SFBR) is one of the largest marine reserves in the western hemisphere, containing the most extensive open-ocean coral reefs in the Caribbean Sea (Mow et al., 2007; Coralina-Invemar, 2012). This unique marine ecosystem is highly biodiverse (Taylor et al., 2013) and may be of importance for cetaceans. However, given the remoteness of the region and the prevalence of windy conditions, the development of systematic visual surveys necessary to assess cetacean abundance and distribution has been logistically and financially challenging.

To date, at least 22 species of marine mammals have been confirmed to occur in the Colombian Caribbean, including 18 odontocetes (Palacios et al., 2013b). Within the SFBR, pantropical spotted dolphins, bottlenose dolphins (*Tursiops truncatus*), false killer whales (*Pseudorca crassidens*), and sperm whales (*Physeter macrocephalus*) are all confirmed species (Pardo et al., 2009; Barragán-Barrera et al., 2017). Stranding reports in the San Andrés Archipelago also indicate the presence of pygmy or dwarf sperm whales (*Kogia* sp.) (Palacios et al., 2013b) and Cuvier's beaked whales (*Ziphius cavirostris*) (Prieto-Rodríguez, 1988; Vidal, 1990). However, the area can potentially host several other species, including Atlantic spotted dolphins, spinner dolphins, striped dolphins (*S. coeruleoalba*), short-finned pilot whales

(*Globicephala macrorhynchus*), killer whales (*Orcinus orca*), and even humpback whales (*Megaptera novaeangliae*) (Pardo et al., 2009; Palacios et al., 2013b; Bolaños-Jiménez et al., 2014).

Ecological niche modeling is a widely used tool to predict cetaceans' distribution and understand the ecological precursors (Redfern et al., 2006; Gregr et al., 2013; Palacios et al., 2013a). These models can also be implemented to assess areas of high conservation priority and identify key areas for research on interactions between humans and wildlife (Bailey and Thompson, 2009). For the Caribbean Basin, the use of advanced geospatial analysis tools has the potential to improve the current comprehension of cetacean distribution patterns and the environmental factors influencing them. However, these analyses have never been conducted in the region, despite some studies being developed in the adjacent Gulf of Mexico (e.g., Davis et al., 1998, 2002; Baumgartner et al., 2001) and the Western South Atlantic Ocean (e.g., do Amaral et al., 2015). Since 2014, Colombia has been carrying out scientific cruises in the SFBR to assess the local biodiversity of the islands (Murillo, 2014). Despite cetaceans having been taken into account in these efforts, in practice the Colombian Program of Marine Fauna Observers has been the main source of this type of information in recent times (Palacios et al., 2013b). Research efforts could be optimized if uncertainty regarding cetacean occurrence and distribution in the Reserve is overcome.

With the aim of determining the potential distributions of spotted and spinner dolphins throughout the Caribbean Basin, and more specifically within the SFBR, we adopted an ecological niche modeling approach. Because absence data are generally not available for oceanic dolphins and the offshore limits of their distributions are unknown, we used a presence-only method to predict the potential distribution of these species (Robinson et al., 2017). The chosen method was maximum entropy (Phillips et al., 2006), which has been applied successfully on species with limited data (Wisz et al., 2008; Elith et al., 2011). Furthermore, this method has been successfully used with cetaceans (Derville et al., 2018), and has already been used to predict the potential distribution of *Stenella* species in the Western South Atlantic (do Amaral et al., 2015). We hypothesized that these species have different distribution patterns as a consequence of distinct environmental requirements, as has been found in adjacent regions such as the Gulf of Mexico and the Western South Atlantic. In addition to overcoming the prevailing information gaps, our results could contribute to the understanding of the effectiveness of the SFBR in protecting top predators such as dolphins, and to identify other areas that deserve protection throughout the Caribbean Basin.

MATERIALS AND METHODS

Study Area

The geographical extent of the models and the background sampling was restricted to the Caribbean Basin (59°24′W–89°21′W and 7°42′N–22°41′N). The Caribbean is a semi-enclosed tropical sea adjacent to the Atlantic Ocean (Müller-Karger et al., 1989; Aguirre, 2014). Although the area is influenced by the discharge of the Amazon and Orinoco rivers, it is generally considered oligotrophic and homogeneous despite seasonal upwelling events (Müller-Karger et al., 1989; Criales-Hernández et al., 2006; Arévalo-Martínez and Franco-Herrera, 2008; Chollett et al., 2012; Rueda-Roa and Muller-Karger, 2013), and the influence of the warm Caribbean Current (Aguirre, 2014).

Within the Caribbean Basin, the SFBR is located in oceanic waters of the Colombian Exclusive Economic Zone (80°39′W–82°17′W and 11°56′N–13°55′N) (Coralina-Invemar, 2012) (**Figure 1**). The Reserve was created as the first Colombian Marine Protected Area and was declared as a UNESCO Biosphere Reserve in November 2000 (Taylor et al., 2013). It has an area of around 65,000 km^2 and encompasses the San Andrés, Providencia and Santa Catalina Archipelago (**Supplementary Figure S1**) (Taylor et al., 2013). The SFBR is a highly biodiverse region, containing more than 77% of the shallow coral reefs of Colombia, as well as other coastal/marine ecosystems such as atolls, beaches, sandy bottoms, mangroves, and seagrass beds (Coralina-Invemar, 2012; Taylor et al., 2013).

Environmental Data

Environmental layers used in the modeling were selected after reviewing previous cetacean niche modeling studies (e.g., Baumgartner et al., 2001; Cañadas et al., 2002; Davis et al., 2002; do Amaral et al., 2015; Tobeña et al., 2016; Gomez et al., 2017). The selected layers included both static and dynamic variables for all three species (**Table 1**). Dynamic variables used in this study included SST, chlorophyll-*a* concentration (Chl-a), diffuse attenuation (Da), and SSS. Static layers included bathymetry, slope and distance to shore (**Table 1**). Environmental layers representing SST, SSS and Chl-a were included as two different metrics: the annual mean and the annual range (the differences between annual maximum and minimum). For Da, only the annual mean was included because annual range was not available.

Raster layers of dynamic and static information data were gathered from the public database Bio-Oracle (Oceans Rasters for Analysis of Climate and Environment) (Tyberghein et al., 2012) and MARSPEC (Ocean Climate Layers from Marine Spatial Ecology) (Sbrocco and Barber, 2013). While the Bio-Oracle public database carried raster layers of Chl-a and Da at the 9.2 km resolution, the remaining layers were available in the MARSPEC public database at 1 km resolution. All layers were cropped to encompass the study area and adjusted to a common resolution of 9.2 km per grid cell using the raster package (Hijmans, 2017) in R 3.4.2 (R Core Team, 2018). The correlation among layers was investigated using the function pairs in the raster package. Only layers with correlation coefficient below 0.7 were included in the ecological niche models (Dormann et al., 2013) (**Supplementary Figure S2**). A principal component analysis (PCA) was performed to visualize the environmental heterogeneity across the study area using the rasterPCA function from Rstoolbox package (Leutner and Horning, 2016) (**Supplementary Figure S3**).

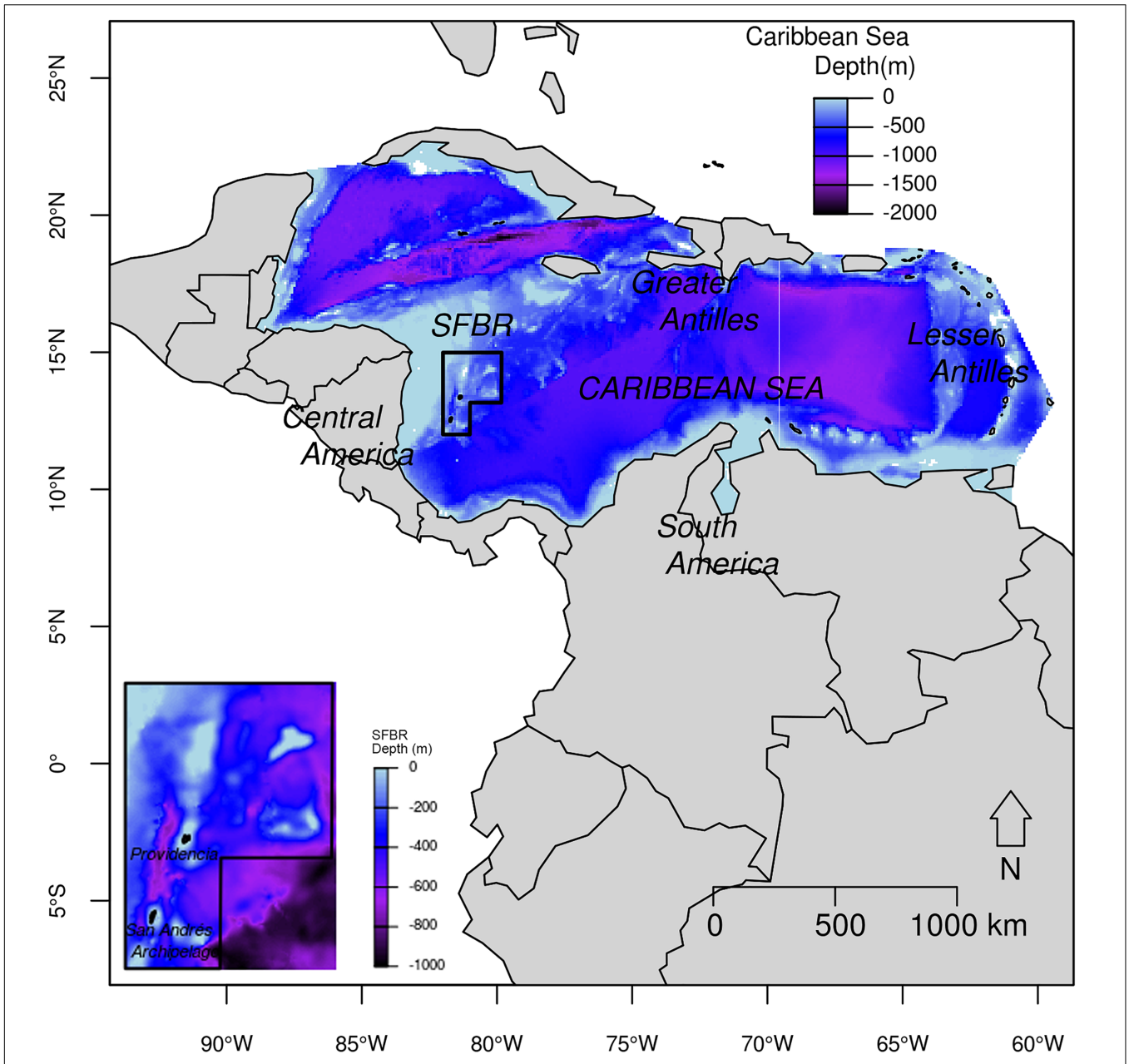

FIGURE 1 | Study area with the location of Seaflower Biosphere Reserve (polygon in bold black line). Inset provides a zoom in the Seaflower Biosphere Reserve and indicates the main islands.

Occurrence Data

Georeferenced sighting data for Atlantic spotted dolphins, pantropical spotted dolphins, and spinner dolphins occurring between 1981 and 2016 in the Caribbean Basin, were compiled from several sources: published records, unpublished data, and the Sistema de Información Ambiental Marina (SIAM[1]) operated by the Instituto de Investigaciones Marinas y Costeras (INVEMAR, Colombia's Marine and Coastal Research Institute). These occurrence data were collected through different seasons and years, during both systematic and opportunistic marine wildlife observations. Only confirmed sightings correctly identified at the species level as *Stenella* were included.

After scrutinizing, filtering, cleaning duplicate records and removing some of the bias by subsampling records (see Hijmans and Elith, 2017), a total of 494 records were included: 210 sightings of pantropical spotted dolphins, 204 Atlantic spotted dolphins, and 80 spinner dolphins (**Table 2** and **Figure 2**). The dataset used for this study is presence-only, meaning that absences (such as survey track lines) were not considered (Franklin, 2009). A subset of records (20%) was used as testing

[1]http://siam.invemar.org.co

TABLE 1 | List of environmental variables used in this study and their respective source, original grid resolution, and unit of measurement.

Environmental variables	Source	Unit	Original resolution
Bathymetry (depth of the seafloor)	MARSPEC	m	1 km
Distance to shore	MARSPEC	km	1 km
Bathymetric slope	MARSPEC	degrees	1 km
Mean annual chlorophyll-*a* concentration	Bio-Oracle	mg/m^3	9 km
Annual range in chlorophyll-*a* concentration	Bio-Oracle	mg/m^3	9 km
Mean annual diffuse attenuation	Bio-Oracle	m^{-1}	9 km
Mean annual sea surface salinity	MARSPEC	psu	1 km
Annual range in sea surface salinity	MARSPEC	psu	1 km
Mean annual sea surface temperature	MARSPEC	°C	1 km
Annual range in sea surface temperature	MARSPEC	°C	1 km

data as explained below, and the remaining was used as training data.

Ecological Niche Modeling

We used a presence-only approach to model the distribution of *Stenella* species in the Caribbean Basin. Specifically, we used the maximum entropy (Maxent) algorithm (Phillips et al., 2017) to model the potential distribution of the three species. Maxent estimates the geographic range of a species by finding the distribution that has the maximum entropy constrained by the environmental conditions at recorded occurrence locations (Phillips et al., 2017). Maxent predicts environmental suitability, with better conditions represented by higher values (Phillips et al., 2006). This method tends to predict the largest possible suitable area consistent with the data (Merow et al., 2013). While careful consideration of the limitations and biases in the data must be taken, Maxent performs well when compared to presence-absence models (Derville et al., 2018).

In order to build the Maxent species distribution models, we used the Maxent function available within the dismo version 1.1-4 package in R (Hijmans et al., 2017). Maxent model settings were defined through the ENMevaluate function of the ENMeval package (Muscarella et al., 2014), which provided species-specific settings to generate models, such as feature classes and standardized multiplier values. The model with the lowest value of the Akaike's Information Criterion corrected for small samples sizes (*AICc*) reflects both model's goodness-of-fit and complexity (Muscarella et al., 2014). We used the block as data partitioning method, which splits the data into four bins based on lines of latitude and longitude to divide occurrence localities as equally as possible (Muscarella et al., 2014). For model validation, we adopted the values of the area under the receiver-operator (ROC) curve (*AUC*) as indicators of the predictive skill of the model (Phillips et al., 2006), where *AUC* closest to a value of 1 would be a perfect model and *AUC* = 0.5 would indicate that the model performed no better than random.

Twenty percent of the sightings for each species were randomly selected as test data sets to evaluate the fit of the model and its predictive power through the evaluate function in the dismo package. Maps were exported in raster format with continuous values and were interpreted from a percentage of environmental suitability ranging from unsuitable (0%) to highly suitable (100%). For visualization purposes of the potential distributions of these three species across the study area in a binary map of presence/absence, these were built based on the threshold of equal test sensitivity and specificity.

Statistical Comparisons of Distribution Patterns

We tested the null hypothesis that each species had similar distributions of the environmental variables using the non-parametric Kruskal–Wallis test followed by the Dunn test available in the dunn package (Dinno, 2017). The range and distributional properties of the environmental layers where species were recorded were represented as boxplots.

Comparative similarity measures among *Stenella* species and the niche identity test implemented in the dismo package were computed. Specifically, we estimated the "*D*" and "*I*" similarity statistics of Warren et al. (2008) using the functions niche overlap from predictions of species' distributions, where the resulting values ranges from 0 (no overlap) to 1 (the distributions are identical). We tested the null hypothesis that the ecological niche models of each species pair were identical using the function nicheEquivalency based on 499 randomizations. To visualize the degree of spatial overlap between the *Stenella* species distributions, we overlapped binary maps for the three pairwise combinations of species using the crop function in the raster package.

TABLE 2 | The ecological niche models with the best configuration for each species, the number of training and testing data, the *AUC* testing values and the relative contributions of the major environmental variables to the Maxent models with dynamic and static variables.

Species	Feature classes and regularization multipliers values	Training data	Testing data	*AUC* testing	Variable contribution (%)
Atlantic spotted dolphin	LQHP RM 3.5	163	41	0.852	Distance (30.49%) Mean Chl-a (22.88%) Bathymetry (22.68%)
Pantropical spotted dolphin	LQH RM 2.5	168	42	0.856	Distance (29.63%) Mean Chl-a (19.66%) Range SST (16.27%)
Spinner dolphin	H RM 2.5	64	16	0.854	Distance (57.94%) Mean Chl-a (26.84%) Slope (10.63%)

L, linear; Q, quadratic; H, hinge; P, product; RM, regularization multiplier.

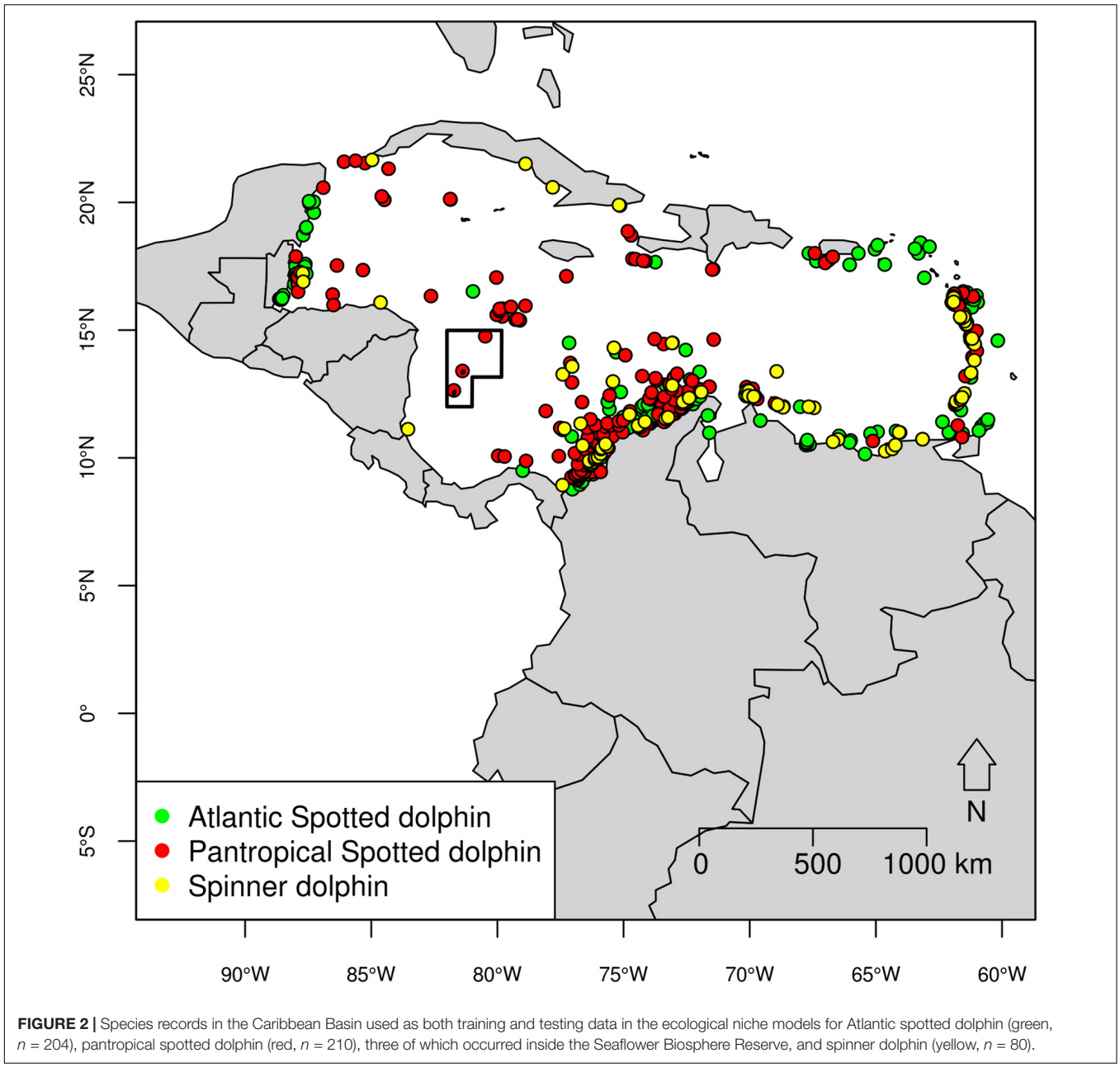

FIGURE 2 | Species records in the Caribbean Basin used as both training and testing data in the ecological niche models for Atlantic spotted dolphin (green, $n = 204$), pantropical spotted dolphin (red, $n = 210$), three of which occurred inside the Seaflower Biosphere Reserve, and spinner dolphin (yellow, $n = 80$).

RESULTS

Ecological Niche Modeling

Ecological niche models were built based on seven uncorrelated environmental layers: bathymetry, distance to shore, slope, Mean SSS, Mean SST and Mean Chl-a, as well as Range SST. In total, 887 records of *Stenella* species were compiled (**Supplementary Table S1**), and after data cleaning 494 were kept (**Table 2** and **Figure 2**).

The model with the best configuration for each species is presented in **Table 2**. Ecological niche models incorporating dynamic and static variables returned *AUC* test values higher than 0.85 for all three species, indicating that these models had a good performance. In general, distance to shore and Mean Chl-a were the environmental variables that contributed the most within all models (**Table 2**). The potential geographic range of distribution for each species, as predicted by the best models, is shown in **Figures 3–5**.

Atlantic Spotted Dolphin Ecological Niche Model

The predicted potential distribution map for the Atlantic spotted dolphin indicated that the areas closest to continental shorelines had the highest environmental suitability (>70%). Specifically a high suitability area was found mainly in the coastal region off mainland Colombia and more broadly, along the southeastern Caribbean, with oceanic areas and

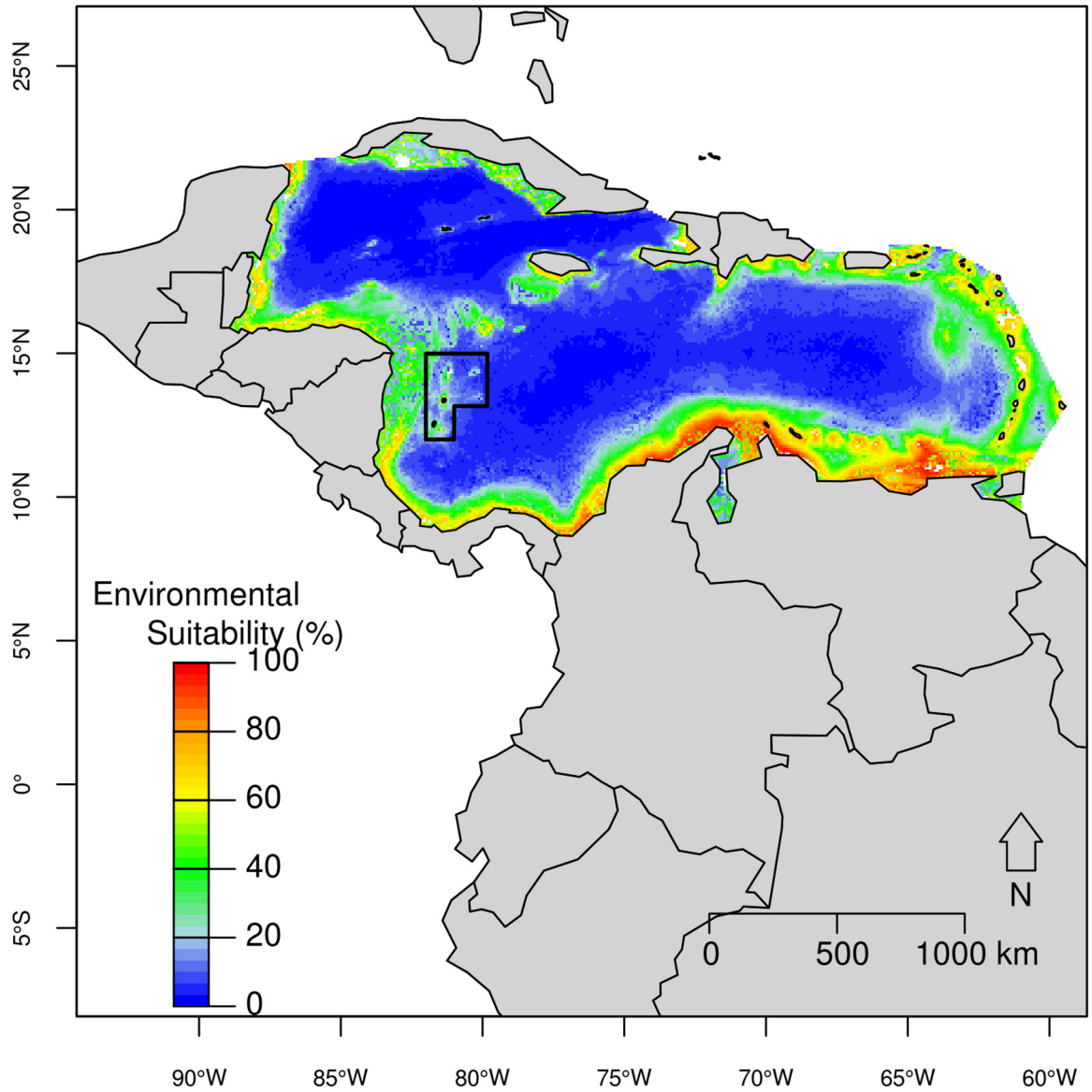

FIGURE 3 | Predicted potential distribution for the Atlantic spotted dolphin in the Caribbean Basin from the best ecological niche model. Red colors indicate highest habitat suitability and blue lowest suitability.

particularly the SFBR presenting a low environmental suitability (**Figure 3**). High environmental suitability (higher than 80%) was observed in areas with bathymetry ranging from 9 m to 1,067 m (median = 77 m); distance to shore between 1 km and 12 km (median = 4 km); slope ranging from 1° to 113° (median = 24°); Mean SST between 25 and 27°C (median = 26.9°C); Range SST between 1.89 and 3.34°C (median = 2.55°C); Mean SSS ranging from 34.3 to 36.1 psu (median = 34.7 psu); and Mean Chl-a between 0.12 and 1.68 mg/m^3 (median = 0.64 mg/m^3).

Pantropical Spotted Dolphin Ecological Niche Model

An environmental suitability higher than 60% was predicted for the pantropical spotted dolphin across most of the Caribbean Basin, but mainly closer to the continent and nearby islands, including the SFBR (**Figure 4**). Records with suitability higher than 80% ranged in depth from 58 m to 2,215 m (median = 813 m); distance to shore between 3 km and 72 km (median = 42 km); slope ranging from 2° to 120° (median = 26°); Mean SST between 25.6 and 28.3°C; Range SST was between 1.1 and 4.1°C (median = 1.3°C); Mean SSS around 35 psu; and Mean Chl-a ranging from 0.12 to 1.12 mg/m^3 (median = 0.21). In the SFBR, environmental suitability around 60% was detected within the southern portion of the Reserve.

Spinner Dolphin Ecological Niche Model

The highest suitability (>70%) for spinner dolphins was predicted in waters surrounding islands or seamounts, and with

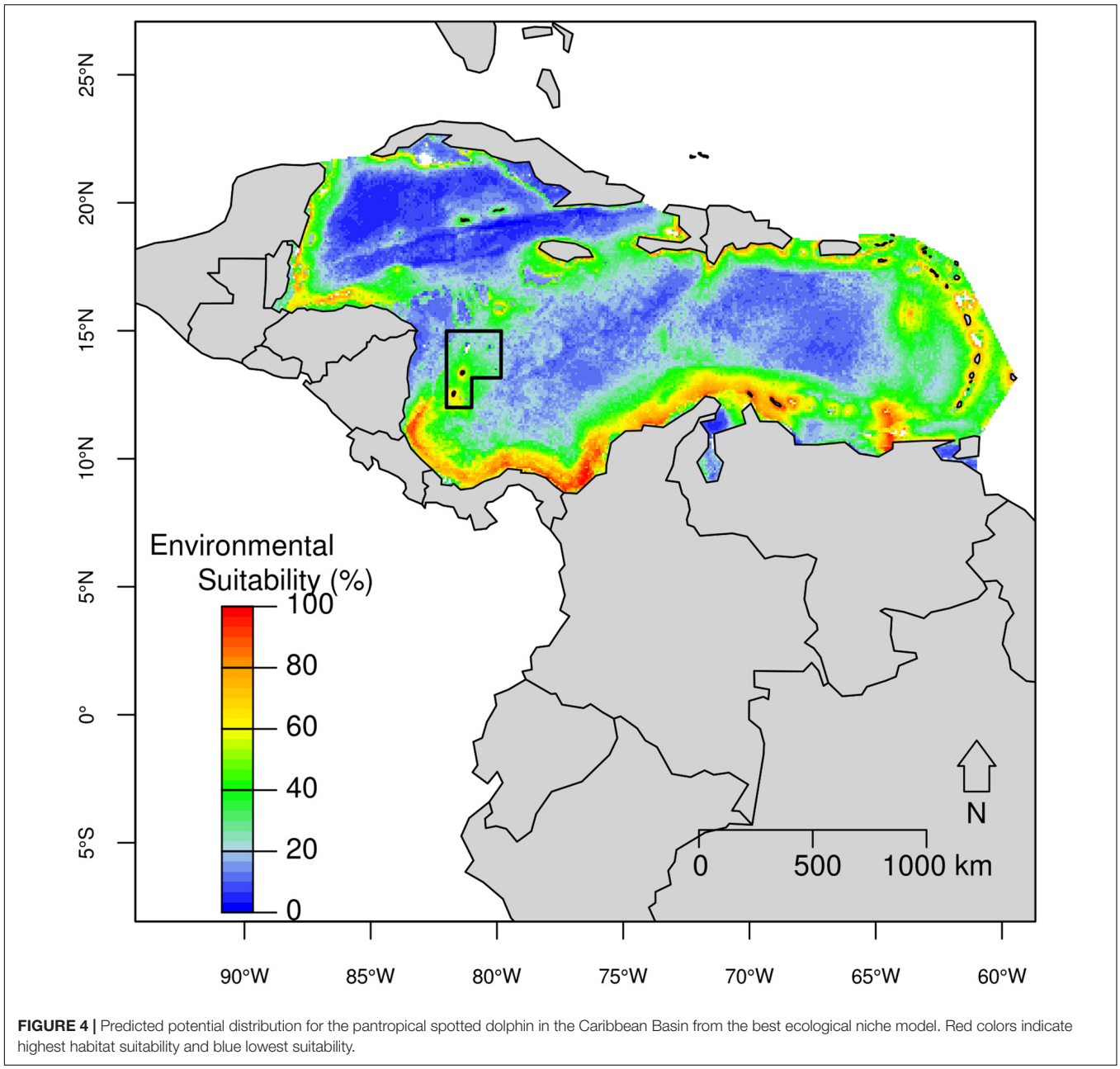

FIGURE 4 | Predicted potential distribution for the pantropical spotted dolphin in the Caribbean Basin from the best ecological niche model. Red colors indicate highest habitat suitability and blue lowest suitability.

a steeper slope (**Figure 5**), in almost all coastal areas in the Caribbean including surrounding islands. High environmental suitability (over 80%) corresponded to areas with bathymetry ranging from 30 m to 1,599 m (median = 620 m); distance to shore between 1 km and 9 km (median = 5 km); slope ranging from 1° to 165° (median = 106.5°); Mean SST between 25.4 and 27.7°C (median = 27.2°C); Range SST between 2.14 to 4°C (median = 2.5°C); Mean SSS ranging from 34.6 to 35.9 psu (median = 35.1 psu); and Mean Chl-a between 0.11 and 1.7 mg/m^3 (median = 0.38 mg/m^3). The SFBR exhibited a high habitat suitability for spinner dolphins, primarily around the insular region, where environmental suitability reached 72% (e.g., around San Andrés Island).

Niche Overlap and Identity Test

Pairwise overlap for the three *Stenella* species is presented in **Table 3**. We found high "*I*" and "*D*" similarity statistic scores for all pairwise comparisons, indicating that ecological niches were broadly similar among Atlantic spotted dolphins, pantropical spotted dolphins, and spinner dolphins in the Caribbean Basin. Niche identity tests did not reject the null hypotheses that assumed the niches were identical between pairwise *Stenella* species comparisons (**Table 3**).

However, our results indicated that while the distribution of Atlantic spotted dolphins and spinner dolphins showed the highest statistical similarity, Atlantic and pantropical spotted dolphins shared the lowest similarity values. In general, all three

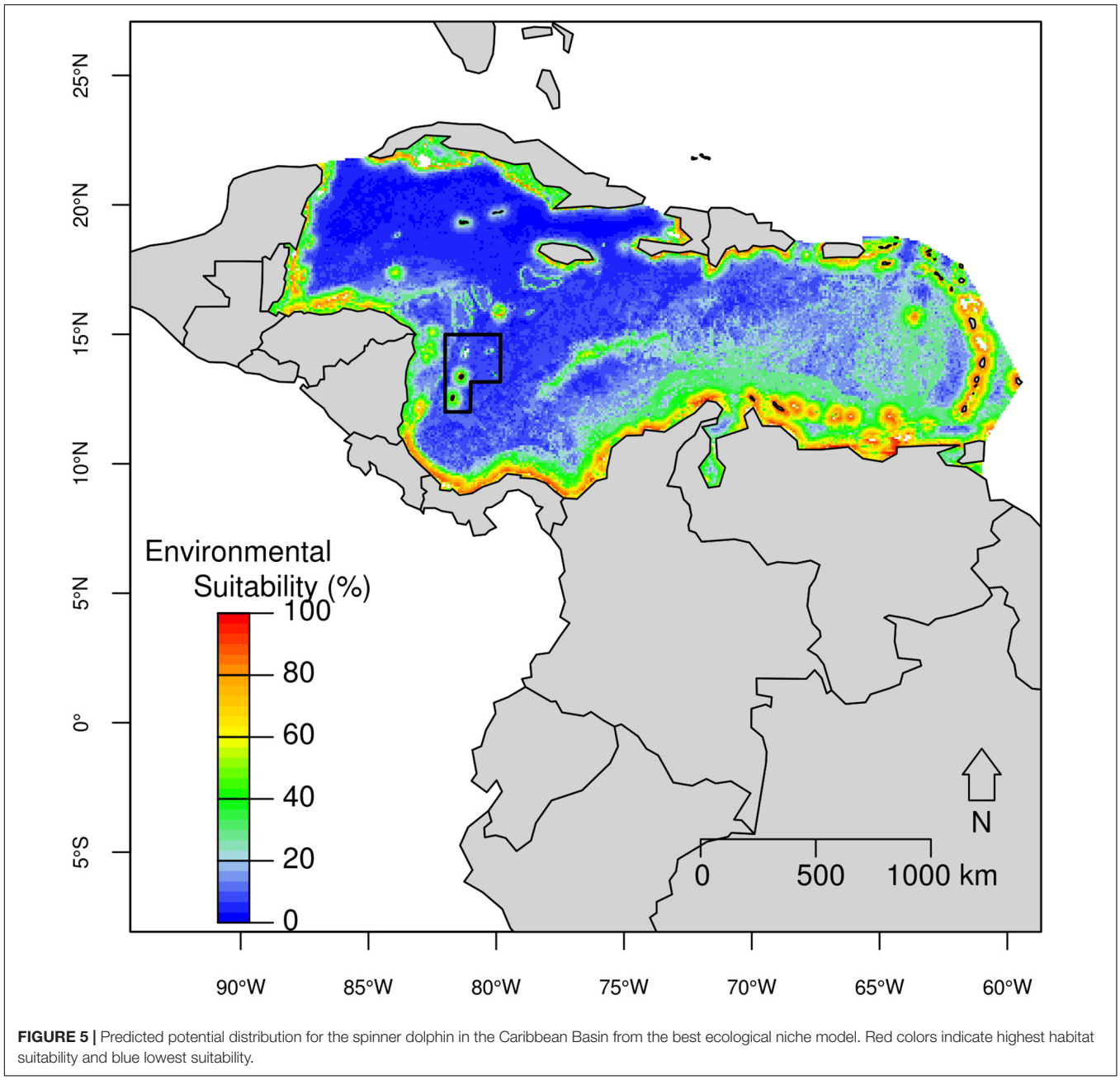

FIGURE 5 | Predicted potential distribution for the spinner dolphin in the Caribbean Basin from the best ecological niche model. Red colors indicate highest habitat suitability and blue lowest suitability.

TABLE 3 | Metrics obtained in niche overlap comparison and niche identity tests conducted pairwise between *Stenella* species.

	Niche overlap		Niche identity	
Pairwise combinations	***D* similarity statistics**	***I* similarity statistics**	***D* similarity statistics**	***I* similarity statistics**
Atlantic spotted dolphin *versus* pantropical spotted dolphin	0.73	0.94	0.71 (*p*-value = 1)	0.92 (*p*-value = 1)
Atlantic spotted dolphin *versus* spinner dolphin	0.80	0.96	0.76 (*p*-value = 0.99)	0.95 (*p*-value = 0.98)
Pantropical spotted dolphin *versus* spinner dolphin	0.78	0.96	0.67 (*p*-value = 0.99)	0.90 (*p*-value = 1)

species coincided in some areas, according to the overlap map based on the threshold of equal test sensitivity and specificity (**Table 4** and **Figures 6–8**). All species overlapped in their distributions in coastal areas of the southern and southeastern Caribbean off Colombia, Venezuela, and surrounding areas in the Antilles, as well as in the SFBR. Nonetheless, while

TABLE 4 | Threshold of equal test sensitivity and specificity obtained for each model generated among three *Stenella* species in the Caribbean Basin.

Species	Threshold of equal test sensitivity and specificity
Atlantic spotted dolphin	0.432
Pantropical spotted dolphin	0.516
Spinner dolphin	0.365

the distribution of pantropical spotted dolphins included more oceanic waters around 1,000 m deep, spinner dolphins appeared to occupy areas closer to island chains, and Atlantic spotted dolphins appeared to be more restricted to coastal/neritic waters.

Statistical Comparisons of Environmental Variables

The median values of the environmental variables for each species indicated significant interspecific differences (**Table 5** and **Figure 9**). The null hypothesis of equal medians for bathymetry, distance to shore, slope, Mean Chl-a, Mean SST and Range SST was rejected (Kruskal–Wallis test, $p < 0.05$).

Pantropical spotted dolphins had the highest median bathymetry, distance to shore, Mean SST, and the lowest median Mean Chl-a. In other words, pantropical spotted dolphins occupied areas of low phytoplankton biomass, and deeper (up to about 1,000 m) and warmer waters. Atlantic spotted dolphins and pantropical spotted dolphins differed in relation to bathymetry,

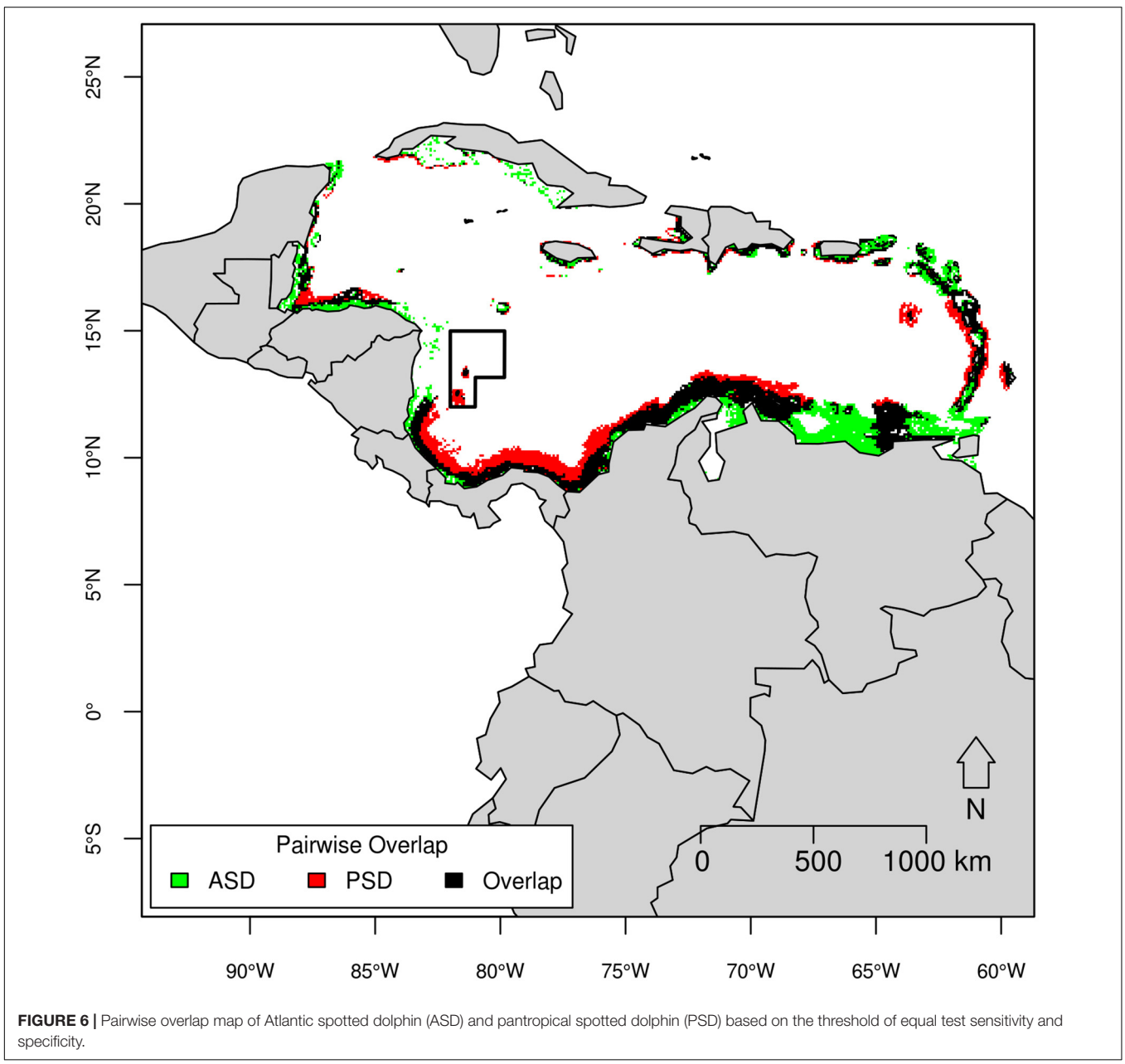

FIGURE 6 | Pairwise overlap map of Atlantic spotted dolphin (ASD) and pantropical spotted dolphin (PSD) based on the threshold of equal test sensitivity and specificity.

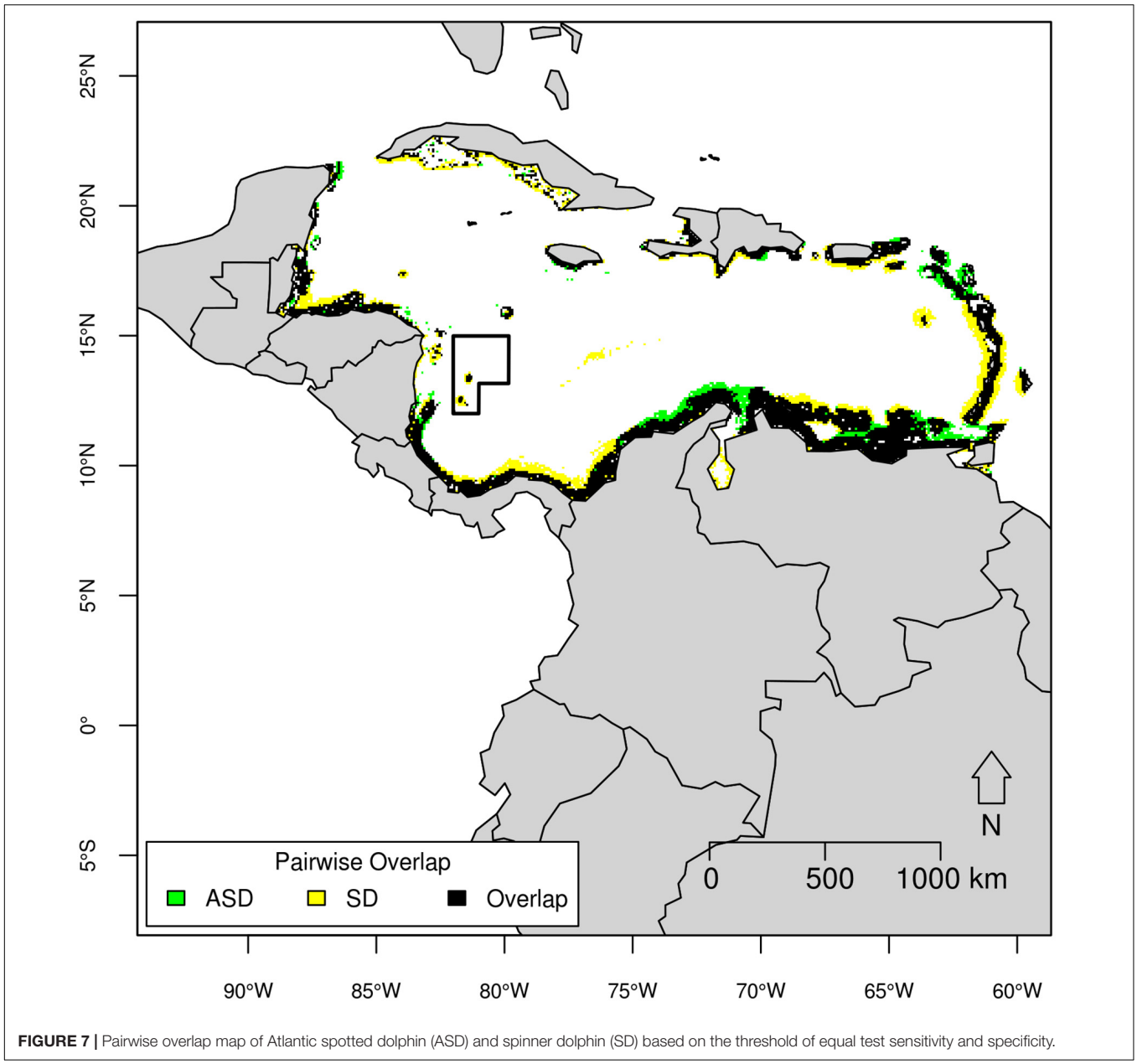

FIGURE 7 | Pairwise overlap map of Atlantic spotted dolphin (ASD) and spinner dolphin (SD) based on the threshold of equal test sensitivity and specificity.

slope, distance to shore, Range SST and Mean Chl-a, with the former occurring in shallow waters closer to the shore, with lower slope values and Mean SST but higher productivity. Likewise, spinner dolphins occurred in areas surrounding the coast, with more phytoplankton biomass, and in shallower waters, although in regions characterized by a steeper slope.

DISCUSSION

This study established a series of potential "baseline" ecological niche models for Atlantic spotted dolphins, pantropical spotted dolphins and spinner dolphins. These models were used for assessing their distribution patterns in the Caribbean Basin, particularly in the SFBR. In this study, we provide the first characterization of the environmental niches of three *Stenella* species and their potential distributional patterns in the Caribbean Basin. Our findings show that distance to coastline and Mean Chl-a play an important role that influences the potential distribution of these three species in the region.

Species of *Stenella* are widely distributed in the Caribbean Basin, yet their patterns have been poorly studied. Small delphinids of the genus *Stenella* carry out long-range movements of up to 2,500 km (Reilly, 1990), presumably associated with prey availability dynamics (Davis et al., 2002). In fact, ecological niches for dolphins appear to be defined by variables that affect distribution and abundance of resources they rely upon (Baumgartner et al., 2001; MacLeod et al., 2008).

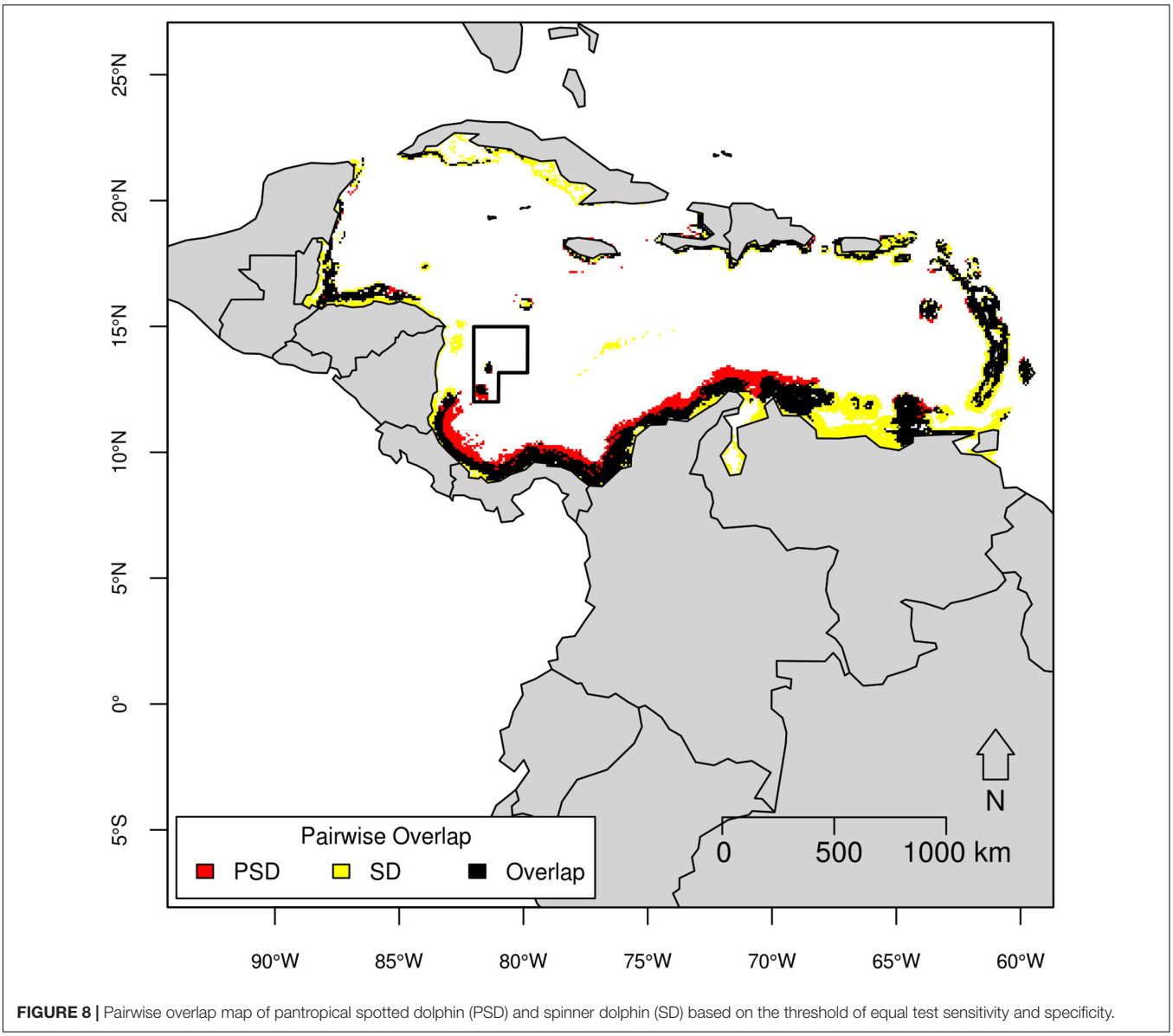

FIGURE 8 | Pairwise overlap map of pantropical spotted dolphin (PSD) and spinner dolphin (SD) based on the threshold of equal test sensitivity and specificity.

The availability of dolphin prey depends mainly on primary productivity, which is highly variable in the oligotrophic waters of the Caribbean Basin (Corredor, 1979; Müller-Karger and Aparicio, 1994; Aguirre, 2014). In the first part of the year, primary productivity concentrates along the continental coasts of Colombia and Venezuela, while shifting to Caribbean islands such as Puerto Rico, the Virgin Islands and the Antilles in the second part (Müller-Karger et al., 1989; Müller-Karger and Aparicio, 1994). This variability enables *Stenella* species, such as pantropical spotted dolphins and spinner dolphins, to exploit oceanic and deeper-water environments given their long-distance movement capabilities.

TABLE 5 | Results of the Kruskal–Wallis test for comparing environmental variables between Atlantic spotted dolphins, pantropical spotted dolphins and spinner dolphins.

Environmental variable	Kruskal–Wallis (X^2)	*p*-value
Bathymetry	40.567	1.552e-09
Distance to shore	18.999	7.487e-05
Bathymetric slope	8.1875	0.01668
Mean annual sea surface temperature	17.65	0.000147
Annual range in sea surface temperature	14.7705	0.0006203
Mean annual sea surface salinity	4.84	0.08892
Mean annual chlorophyll-a concentration	35.297	2.165e-08

Coastal-marine ecosystems such as coral reefs and seagrass beds host a high biodiversity and productivity that provide food resources for local and oceanic biological communities. The SFBR appears to be an important area for dolphins in the Caribbean Basin not only because it contains the largest open-ocean coral reefs in the Caribbean, but because it also holds extensive and healthy seagrass beds (Taylor et al., 2013). Consequently, the overlap in the ecological niche of pantropical spotted dolphins

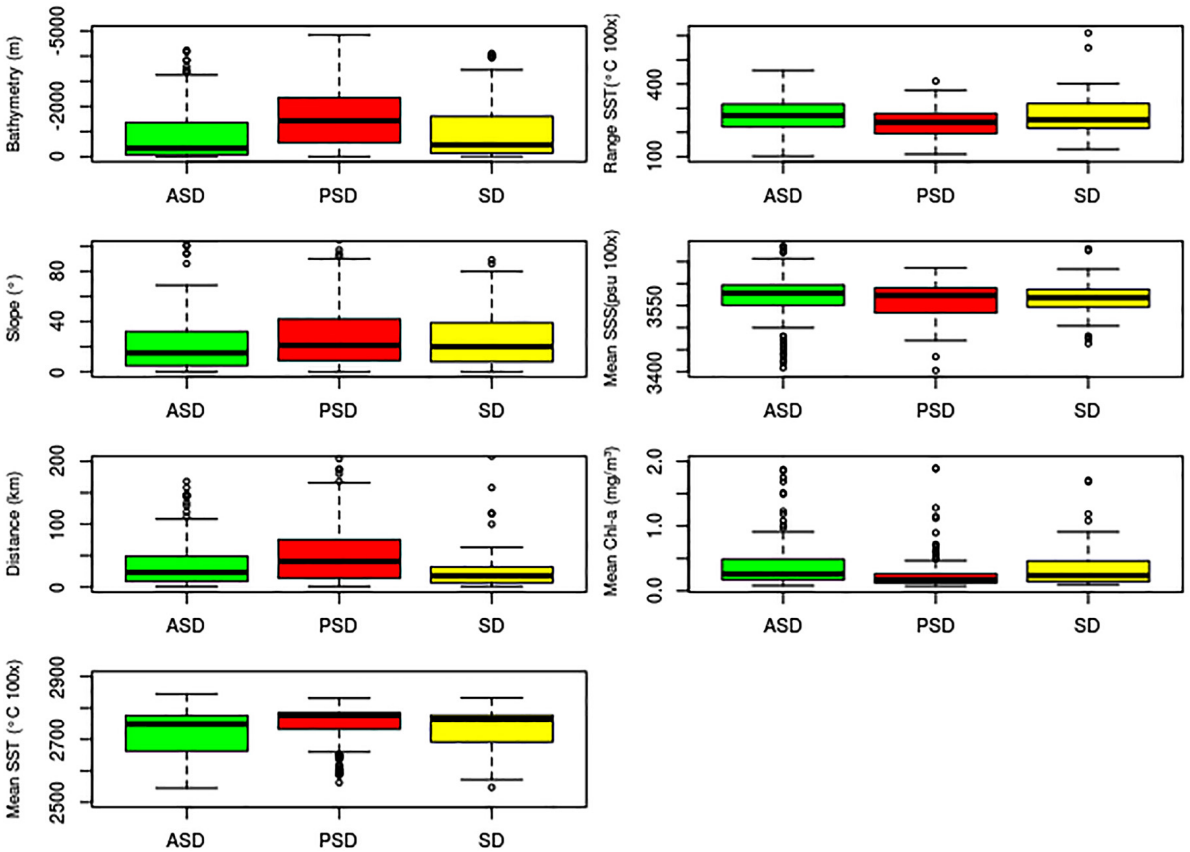

FIGURE 9 | Box plots of values extracted from environmental layers for Atlantic spotted dolphins (ASD), pantropical spotted dolphins (PSD) and spinner dolphins (SD) in the Caribbean Basin. The thick horizontal line inside each box represents the median; the upper and lower borders of the box are the 25th and 75th percentiles; the 5th and 95th percentiles are represented by the error bars; small circles are outliers.

and spinner dolphins in the area is not surprising. In contrast, Atlantic spotted dolphins primarily inhabit coastal environments throughout most of their range, a distribution pattern similar to the one previously described in the Western South Atlantic Ocean by do Amaral et al. (2015). Productive coral reefs and seagrass beds are also found along the Colombian mainland coast, notably in Morrosquillo Gulf, the Rosario and San Bernardo Archipelago, Santa Marta, and the Tayrona region (Garzón-Ferreira et al., 2001).

Water temperature has been shown to be an important attribute of cetaceans' ecological niches (MacLeod, 2009). In the Caribbean Basin, the southern region along the coast of Colombia and Venezuela exhibits low SST associated with coastal upwelling, mainly off La Guajira region (Colombia) in the central Caribbean and around Margarita Island (Venezuela) in the eastern Caribbean (Gordon, 1967; Müller-Karger et al., 1989; Andrade et al., 2003; Andrade and Barton, 2005; Lonin et al., 2010; Paramo et al., 2011). This upwelling generates a high primary productivity (Corredor, 1979; Andrade et al., 2003; Andrade and Barton, 2005; Criales-Hernández et al., 2006; Arévalo-Martínez and Franco-Herrera, 2008; Lonin et al., 2010) that has been related to the occurrence of other dolphin species in the area (Farías-Curtidor et al., 2017). Considering that low SST was an important descriptor of habitat suitability for Atlantic spotted dolphins, it is not surprising that they were preferentially found in Caribbean environments defined by shallow waters with lower temperatures and elevated primary productivity.

Bathymetry is another important predictor of Atlantic spotted dolphin habitats in the Caribbean Basin. Similar to what has been reported for the Gulf of México and the Western South Atlantic Ocean, this species showed a preference for shallower waters along the Colombian Caribbean (Davis et al., 1998; do Amaral et al., 2015). Atlantic spotted dolphins feed preferentially on coastal prey (Perrin et al., 1994), so their presence in shallow waters is frequent (Davis et al., 1998, 2002). These coastal habits could suggest that this species is not very cosmopolitan in the Atlantic Ocean, showing restricted movements across northern and southern portions of this ocean. Genetic studies have shown that individuals from the Colombian Caribbean are closely related to those population units from locations as far as west and east north Atlantic (Mesa-Gutiérrez et al., 2015); while populations from Azores and Madeira, which show high connectivity between them (Quérouil et al., 2010), resulted closely related to those from the Western North Atlantic and Brazil (Caballero et al., 2013; Mesa-Gutiérrez et al., 2015). Additionally, Atlantic spotted dolphins along the Brazilian coast

also show genetic (Caballero et al., 2013) and morphological divergence (Moreno et al., 2005) associated with differences in environmental conditions between southern and northern Brazilian populations (do Amaral et al., 2015). Furthermore, Atlantic spotted dolphin populations along the east coast of the United States and Gulf of Mexico show significant population structure due mainly to an extensive continental shelf that promotes differential habitat structuring and hence, the aggregation of resources in specific zones to be exploited (Adams and Rosel, 2006). All these evidences suggest that environmental conditions associated with coastal habitats could drive differentiation between Atlantic spotted dolphins across the Atlantic Ocean although more studies are needed to support this assumption.

Similar to Atlantic spotted dolphins, spinner dolphins occur in productive regions surrounding coastlines but with steeper slopes, mainly near islands (**Figure 7**). Indeed, the niche for these two species overlapped in much of coastal areas around the Caribbean Basin, except in waters surrounding islands such as in the SFBR, which is characterized by a pronounced slope (mean = 4.5°). The slope had a considerable contribution for the spinner dolphin model, preferred by this species due to the vertical and horizontal migration of mesopelagic fish considered an important part of their diet (Benoit-Bird and Au, 2003; Thorne et al., 2012).

Pantropical spotted dolphins also appeared to prefer waters around islands, but are present in deeper waters, as reported in the Gulf of Mexico (Davis et al., 1998) and in the Western South Atlantic (do Amaral et al., 2015). SST had a considerable contribution to the species' model, indicating that offshore pantropical spotted dolphins are usually found in warm tropical waters, as reported previously in the Western South Atlantic (do Amaral et al., 2015).

Although the *Stenella* species analyzed here showed differences in their environmental requirements in the Caribbean Basin, in general both spotted and spinner dolphins occupied similar habitats in the region. It has been suggested that Atlantic spotted dolphins and pantropical spotted dolphins are sympatric in the Atlantic Ocean (Perrin and Hohn, 1994). Likewise, associations between pantropical spotted dolphins and spinner dolphins have been documented in the Atlantic (Silva et al., 2005). However, do Amaral et al. (2015) suggested that *Stenella* dolphins, particularly the three species considered for the current study, could exhibit niche partitioning and spatial segregation in the Western South Atlantic. Davis et al. (1998) also reported differences in distribution of these three *Stenella* species along the Gulf of Mexico. These differences have been related not only to oceanographic conditions (do Amaral et al., 2015), but also to prey distribution and feeding preferences among *Stenella* species (Davis et al., 2002). However, in areas where nutrients are scarce, feeding preferences facilitate that small cetaceans share their habitat (Davis et al., 2002). In the Caribbean Basin, Atlantic spotted, pantropical and spinner dolphins seem to overlap much more in their distributions, particularly in high-productivity areas.

These findings generate special concern regarding climate change due to the effects on marine and coastal productive ecosystems such as coral reefs. Particularly, these ecosystems have been heavily affected in the Caribbean Basin (Connell, 1997; Pandolfi et al., 2003), allowing the increase in macroalgae coverage (Mumby et al., 2007) and the consequent decreases in local biodiversity. Similarly, prey distribution could be affected due to increases in water temperature (Learmonth et al., 2006; MacLeod, 2009). These shifts in prey availability can affect distributional patterns on dolphins in the Caribbean Basin (Learmonth et al., 2006; MacLeod, 2009; Ramos et al., 2016), which could force them to spend more time traveling in oceanic waters looking for resources.

While oceanic areas in the Caribbean Basin appear to be potentially important for *Stenella* dolphins, most studies have taken place in coastal waters. Therefore, the distribution patterns suggested in this study, based only on sightings, do not predict suitable habitat beyond the known records of *Stenella* in the Caribbean Basin. Although efforts have increased in the region to advance marine mammal research, there is still a large knowledge gap to improve the management of such species. Areas of very low coverage (like the center of Western Caribbean where no research has been done) could contribute to the habitat close to shore and of specific depths being deemed highly suitable. This is the case for the SFBR, which is an oceanic area poorly studied with regarding marine mammals. This Reserve holds high local biodiversity related to coastal marine ecosystems that are potentially important for dolphins' distribution as foraging hotspots. The SFBR appears to be more suitable in its southern portion for pantropical and spinner dolphins, mainly around the islands, but their ecological and oceanographic conditions could allow the occurrence of other small cetacean species. Future research should focus on this protected area, to assess if it should be considered as a priority area for cetacean species in the Caribbean Basin.

AUTHOR CONTRIBUTIONS

DB-B, PC-C, NF-C, RL-N, PB, JB-J, LB, DC-M, JL, JM, RM-G, BdM, ER, VR, and DP contributed to the acquisition of field data. DB-B, KBA, and NF-C organized the data and compiled the literature. DB-B and KBA conceived and designed the experiments, analyzed the data, and wrote the manuscript. KBA performed the experiments. DB-B, KBA, PC-C, NB-A, IM, JB-J, DC-M, JL, RM-G, BdM, ER, and DP contributed to the manuscript writing. All authors have approved the final version of the manuscript.

ACKNOWLEDGMENTS

We thank the Colombian Program of Marine Fauna Observers, and acknowledge the collaboration of all the observers, captains, and crew members of seismic vessels. Special thanks to Comisión Colombiana del Océano, Armada Nacional de Colombia, ARC Providencia crew, and Universidad de los Andes for their

logistic support during the Scientific Seaflower Expedition Cayo Serrana Island 2016. DB-B received a small grant provided by Cetacean Society International to participate in this expedition (2015). Fieldwork in Colombia was also supported by the Society for Marine Mammalogy (DB-B, 2014), the "Proyecto Semilla – 2013-2 Call for Funding of Research Category: Master and Doctoral students, project 'Genetic structure and diversity of bottlenose dolphins *Tursiops truncatus* (Montagu, 1821) (Cetacea: Delphinidae) in La Guajira, Colombian Caribbean"' from Universidad de los Andes (DB-B, 2014), the "Proyecto Semilla – 2015-1 Call for Funding of Research Category: Master and Doctoral students, project 'Occurrence, distribution and preliminary genetic status of delphinids in La Guajira, Colombian Caribbean"' from Universidad de los Andes (DB-B, 2015), and the Rufford Small Grant Foundation (NF-C, 2016). KBA received a Ph.D. degree scholarships from Coordenação de Aperfeiçoamento de Pessoal de Nível Superior (CAPES) (process 1395438). Finally, we really appreciate the comments that reviewers have provided to the manuscript, which have been valuable and useful to improve the final version.

SUPPLEMENTARY MATERIAL

The Supplementary Material for this article can be found online at: https://www.frontiersin.org/articles/10.3389/fmars.2019.00010/full#supplementary-material

REFERENCES

Adams, L. D., and Rosel, P. E. (2006). Population differentiation of the Atlantic spotted dolphin (*Stenella frontalis*) in the western North Atlantic, including the Gulf of Mexico. *Mar. Biol.* 148, 671–681. doi: 10.1007/s00227-005-0094-2

Aguirre, R. (2014). Spectral reflectance analysis of the caribbean sea. *Geofís. Int.* 53, 385–398.

Andrade, C., and Barton, D. (2005). The guajira upwelling system. *Cont. Shelf Res.* 25, 1003–1022. doi: 10.1016/j.csr.2004.12.012

Andrade, C. A., Barton, E. D., and Mooers, C. N. K. (2003). Evidence for an Eastward Flow along the Central and South American Caribbean Coast. *J. Geophys. Res.* 108, C6–C3185. doi: 10.1029/2002JC001549

Arévalo-Martínez, D. L., and Franco-Herrera, A. (2008). Características oceanográficas de la surgencia frente a la Ensenada de Gaira, Departamento de Magdalena, época seca menor de 2006. *Bol. Invest. Mar. Cost.* 37, 131–162.

Bailey, H., and Thompson, P. M. (2009). Using marine mammal habitat modelling to identify priority conservation zones within a marine protected area. *Mar. Ecol. Prog. Ser.* 378, 279–287. doi: 10.3354/meps07887

Barragán-Barrera, D. C., Farías-Curtidor, N., Do Amaral, K., Lancheros-Neva, R., Botero-Acosta, N., and Bueno, P. (2017). "Registro del delfín manchado pantropical (*Stenella attenuata*) en la Isla Cayo Serrana y su distribución potencial en el Caribe," in *Oral presentation from the Coloquio de Resultados Expedición Científica Seaflower* 2016, (Isla Cayo Serrana).

Baumgartner, M. F., Mullin, K. D., May, L. N., and Leming, T. D. (2001). Cetacean habitats in the northern Gulf of Mexico. *Fish. Bull.* 99, 219–239.

Benoit-Bird, K. J., and Au, W. W. L. (2003). Prey dynamics affect foraging by a pelagic predator (*Stenella longirostris*) over a range of spatial and temporal scales. *Behav. Ecol. Sociobiol.* 53, 364–373.

Bolaños-Jiménez, J., Mignucci-Giannoni, A., Blumenthal, J., Bogomolni, A., Casas, J. J., Henríquez, A., et al. (2014). Distribution, feeding habits and morphology of killer whales *Orcinus orca* in the Caribbean Sea. *Mammal Rev.* 44, 177–189. doi: 10.1111/mam.12021

Caballero, S., Santos, M. C. O., Sanches, A., and Mignucci-Giannoni, A. A. (2013). Initial description of the phylogeography, population structure and genetic diversity of Atlantic spotted dolphins from Brazil and the Caribbean, inferred from analyses of mitochondrial and nuclear DNA. *Biochem. Syst. Ecol.* 48, 263–270. doi: 10.1016/j.bse.2012.12.016

Caldwell, D. K., Caldwell, M. C., Rathjen, W. F., and Sullivan, J. R. (1971). Cetaceans from the Lesser Antillean island of St. *Vincent. Fish. Bull.* 69, 303–312.

Cañadas, A., Sagarminaga, R., and García-Tiscar, S. (2002). Cetacean distribution related with depth and slope in the Mediterranean waters off southern Spain. *Deep Sea Res. Part I Oceanogr. Res. Pap.* 49, 2053–2073. doi: 10.1016/S0967-0637(02)00123-1

Chollett, I., Müller-Karger, F. E., Heron, S. F., Skirving, W., and Mumby, P. J. (2012). Seasonal and spatial heterogeneity of recent sea surface temperature trends in the Caribbean Sea and southeast Gulf of Mexico. *Mar. Pollut. Bull.* 64, 956–965. doi: 10.1016/j.marpolbul.2012.02.016

Combatt, J. A., and González, E. (2007). *Ocurrencia y distribución del delfín nariz de botella Tursiops truncatus (Montagu, 1821) en las costas de Dibulla, Baja Guajira, durante el período de agosto a diciembre de 2005*. dissertation/bachelor's thesis, Universidad de Bogotá Jorge Tadeo Lozano, Santa Marta.

Connell, J. H. (1997). Disturbance and recovery of coral assemblages. *Coral Reefs.* 16, S101–S113. doi: 10.1007/s003380050246

Coralina-Invemar (2012). "Atlas de la Reserva de Biósfera Seaflower," in *Archipiélago de San Andrés, Providencia y Santa Catalina. Santa Marta: Instituto de Investigaciones Marinas y Costeras "José Benito Vives De Andréis" -INVEMAR- y Corporación para el Desarrollo Sostenible del Archipiélago de San Andrés*, eds D. Gómez-López I, C. Segura-Quintero, P. C. Sierra-Correa, and J. Garay-Tinoco (Coralina: Providencia y Santa Catalina -CORALINA).

Corredor, J. E. (1979). Phytoplankton response to low level nutrient enrichment through upwelling in the Colombian Caribbean Basin. *Deep Sea Res. Part A Oceanogr. Res. Pap.* 26, 731–741. doi: 10.1016/0198-0149(79)90010-4

Criales-Hernández, M. C., García, C. B., and Wolff, M. (2006). Flujos de biomasa y estructura de un ecosistema de surgencia tropical en La Guajira, Caribe colombiano. *Rev. Biol. Trop.* 54, 1257–1282. doi: 10.15517/rbt.v54i4.14399

Davis, R. W., Fargion, G. S., May, N., Lemig, T. D., Baumgartner, M., Evans, W. E., et al. (1998). Physical habitat of the cetaceans along the continental slope in the north central and western Gulf of Mexico. *Mar. Mamm. Sci.* 14, 490–507. doi: 10.1111/j.1748-7692.1998.tb00738.x

Davis, R. W., Ortega-Ortiz, J. G., Ribic, C. A., Evans, W. E., Biggs, D. C., Ressler, P. H., et al. (2002). Cetacean habitat in the northern oceanic Gulf of Mexico. *Deep Sea Res. Part I Oceanogr. Res. Pap.* 49, 121–142. doi: 10.1016/S0967-0637(01)00035-8

Derville, S., Torres, L., Iovan, C., and Garrigue, C. (2018). Finding the right fit: comparative cetacean distribution models using multiple data sources and statistical approaches. *Divers. Distrib.* 24, 1657–1673. doi: 10.1111/ddi.12782

Dinno, A. (2017). *Dunn.test: Dunn's Test of Multiple Comparisons Using Rank Sums. R package version 1.3.5*. Available at: https://CRAN.R-project.org/package=dunn.test

do Amaral, K. B., Alvares, D. J., Heinzelmann, L., Borges-Martins, M., Siciliano, S., and Moreno, I. B. (2015). Ecological niche modeling of *Stenella* dolphins (Cetartiodactyla: delphinidae) in the southwestern Atlantic Ocean. *J. Exp. Mar. Bio. Ecol.* 472, 166–179. doi: 10.1016/j.jembe.2015.07.013

Dormann, C. F., Elith, J., Bacher, S., Buchmann, C., Carl, G., Carré, G., et al. (2013). Collinearity: a review of methods to deal with it and a simulation study evaluating their performance. *Ecography* 36, 27–46. doi: 10.1111/j.1600-0587.2012.07348.x

Elith, J., Phillips, S. J., Hastie, T., Dudík, M., Chee, Y. E., and Yates, C. J. (2011). A statistical explanation of MaxEnt for ecologists. *Divers. Distrib.* 17, 43–57. doi: 10.1111/j.1472-4642.2010.00725.x

Farías-Curtidor, N., Barragán-Barrera, D. C., Chávez-Carreño, P. A., Jiménez-Pinedo, C., Palacios, D., Caicedo, D., et al. (2017). Range extension for the common dolphin (*Delphinus* sp.) to the Colombian Caribbean, with taxonomic implications from genetic barcoding analysis. *PLoS One* 12:e0171000. doi: 10.1371/journal.pone.0171000

Fraija, N., Flórez-González, L., and Jáuregui, A. (2009). Cetacean occurrence in the Santa Marta region, Colombian Caribbean. *Lat. Am. J. Aquat. Mamm.* 7, 69–73.

Franklin, J. (2009). *Mapping Species Distributions: Spatial Inference and Prediction*. Cambridge: Cambridge University Press.

García, C., and Trujillo, F. (2004). Preliminary observations on habitat use patterns of the Marine Tucuxi, *Sotalia fluviatilis*, in Cispatá Bay, Colombian Caribbean Coast. *Lat. Am. J. Aquat. Mamm.* 3, 53–59. doi: 10.5597/lajam00048

Garzón-Ferreira, J., Rodríguez-Ramírez, A., Bejarano-Chavarro, S., Navas-Camacho y, R., and Reyes-Nivia, C. (2001). "Estado de los arrecifes coralinos en Colombia," in *INVEMAR Informe del Estado de los Ambientes Marinos y Costeros en Colombia*, eds G. H. Ospina-Salazar and A. Acero (Santa Marta: Serie de publicaciones periódicas INVEMAR), 29–40.

Gomez, C., Lawson, J., Kouwenberg, A.-L., Moors-Murphy, H., Buren, A., Fuentes-Yaco, C., et al. (2017). Predicted distribution of whales at risk: identifying priority areas to enhance cetacean monitoring in the Northwest Atlantic Ocean. *Endang. Species Res.* 32, 437–458. doi: 10.3354/esr00823

Gordon, A. L. (1967). Circulation of the Caribbean Sea. *J. Geophys. Res.* 72, 6207–6223. doi: 10.1029/JZ072i024p06207

Gregr, E. J., Baumgartner, M. F., Laidre, K. L., and Palacios, D. M. (2013). Marine mammal habitat models come of age: the emergence of ecological and management relevance. *Endanger. Species Res.* 22, 205–212. doi: 10.3354/esr00476

Hijmans, R. (2017). *raster: Geographic Data Analysis and Modeling. R package version 2.6-7*. Available at: https://CRAN.R-project.org/package=raster

Hijmans, R., and Elith, J. (2017). *Species Distribution Modeling With R*. Available at: https://cran.r-project.org/web/packages/dismo/vignettes/sdm.pdf

Hijmans, R. J., Phillips, S., Leathwick, J. R., and Elith, J. (2017). *dismo: Species Distribution Modeling. R package version 1.1-4*. Available at: https://CRAN.R-project.org/package=dismo

Jefferson, T. A., Webber, M. A., and Pitman, R. L. (2008). *Marine Mammals of the World: A Comprehensive Guide to Their Identification*. Oxford: Elsevier, Academic Press.

Kelley, J., Brown, A., Therkildsen, N., and Foote, A. (2016). The life aquatic: advances in marine vertebrate genomics. *Nat. Rev. Genet.* 17, 523–534. doi: 10.1038/nrg.2016.66

Learmonth, J. A., MacLeod, C. D., Santos, M. B., Pierce, G. J., Crick, H. Q. P., and Robinson, R. A. (2006). Potential effects of climate change on marine mammals. *Oceanogr. Mar. Biol.* 44, 431–464. doi: 10.1201/9781420006391.ch8

Leduc, R. G., Perrin, W. F., and Dizon, A. E. (1999). Phylogenetic relationships among the delphinid cetaceans based on full cytochrome b sequences. *Mar. Mamm. Sci.* 15, 619–648. doi: 10.1111/j.1748-7692.1999.tb00833.x

Leutner, B., and Horning, N. (2016). *Tools for Remote Sensing Data Analysis. The Comprehensive R Archive Network*. Available at: https://cran.r-project.org/web/packages/RStoolbox/RStoolbox.pdf

Lonin, S. A., Hernández, J. L., and Palacios, D. M. (2010). Atmospheric events disrupting coastal upwelling in the southwestern Caribbean. *J. Geophys. Res.* 115:C06030. doi: 10.1029/2008JC005100

MacLeod, C. D. (2009). Global climate change, range changes and potential implications for the conservation of marine cetaceans: a review and synthesis. *Endanger. Species Res.* 7, 125–136. doi: 10.3354/esr00197

MacLeod, C. D., Mandleberg, L., Schweder, C., Bannon, S. M., and Pierce, G. J. (2008). A comparison of approaches for modelling the occurrence of marine animals. *Hydrobiologia* 612, 21–32. doi: 10.1016/j.prevetmed.2012.11.005

Merow, C., Smith, M. J., and Silander, J. A. Jr. (2013). A practical guide to MaxEnt for modeling species' distributions: what it does, and why inputs and settings mater. *Ecography* 36, 1058–1069. doi: 10.1111/j.1600-0587.2013.07872.x

Mesa-Gutiérrez, R., Barragán-Barrera, D. C., Chávez-Carreño, P., Farías-Curtidor, N., and Caballero, S. (2015). "Population structure of the Atlantic spotted dolphin (*Stenella frontalis*) in La Guajira, Colombian Caribbean," in *Abstract retrieved from the 21st Biennial Conference on The Biology of Marine Mammals*, (San Francisco, CA).

Mignucci-Giannoni, A. A. (1998). Zoogeography of cetaceans off Puerto Rico and the Virgin Islands. *Caribb. J. Sci.* 34, 173–190.

Moreno, B. I, Zerbini, A. N., Danilewicz, D., Santos, M. C. O., Simões-Lopes, P. C., Laílson-Brito, J. Jr., et al. (2005). Distribution and habitat characteristics of dolphins of the genus *Stenella* (Cetacea: delphinidae) in the southwest Atlantic Ocean. *Mar. Ecol. Prog. Ser.* 300, 229–240. doi: 10.3354/meps300229

Mow, J. M., Taylor, E., Howard, M., Bained, M., Connolly, E., and Chiquillo, M. (2007). Collaborative planning and management of the San Andres Archipelago's coastal and marine resources: a short communication on the evolution of the Seaflower marine protected area. *Ocean Coast. Manage.* 50, 209–222. doi: 10.1016/j.ocecoaman.2006.09.001

Müller-Karger, F. E., and Aparicio, R. (1994). Mesoscale processes affecting phytoplankton abundance in the southern Caribbean Sea. *Cont. Shelf Res.* 14, 199–221. doi: 10.1016/0278-4343(94)90013-2

Müller-Karger, F. E., McClain, C. R., Fisher, T. R., Esaias, W. E., and Varela, R. (1989). Pigment distribution in the Caribbean Sea: observations from space. *Prog. Oceanogr.* 23, 23–64. doi: 10.1016/0079-6611(89)90024-4

Mumby, P. J., Hastings, A., and Edwards, H. J. (2007). Thresholds and the resilience of Caribbean coral reefs. *Nature* 450, 98–101. doi: 10.1038/nature06252

Murillo, C. I. (2014). "Reserva de Biósfera Seaflower," in *Construyendo País Marítimo*, eds C. G. Linares, N. J. Machuca and S. H. Reyes (Bogotá, CO: Comisión Colombiana del Océano), 138–145.

Muscarella, R., Galante, P. J., Soley-Guardia, M., Boria, R. A., Kass, J. M., Uriarte, M., et al. (2014). ENMeval: an R package for conducting spatially independent evaluations and estimating optimal model complexity for Maxent ecological niche models. *Methods Ecol. Evol.* 5, 1198–1205. doi: 10.1111/2041-210X.12261

Niño-Torres, C. A., García-Rivas, M., del, C., CastelblancoMartínez, D. N., Padilla-Saldiar, J. A., Blanco-Parra, M., et al. (2015). Aquatic mammals from the Mexican Caribbean: a review. *Hidrobiologica* 25, 143–154. doi: 10.1007/978-1-4614-6898-1_3

Palacios, D. M., Farías-Curtidor, N., Jiménez-Pinedo, C., Castellanos, L., Gärtner, A., Gómez-Salazar, C., et al. (2012). "Range extension for the long-beaked common dolphin (*Delphinus capensis*) to the Colombian Caribbean," in *Paper SC/64/SM20 Presented to the IWC Scientific Committee Annual Meeting*, (Panama), 6.

Palacios, D. M., Baumgartner, M. F., Laidre, K. L., and Gregr, E. J. (2013a). Beyond correlation: integrating environmentally and behaviourally mediated processes in models of marine mammal distributions. *Endanger. Species Res.* 22, 191–203. doi: 10.3354/esr00558

Palacios, D. M., Gärtner, A., Caicedo, D., Farías, N., Jiménez-Pinedo, C., Curcio-Valencia, J., et al. (2013b). "Mamíferos acuáticos de la región Caribe colombiana," in *Diagnóstico del Estado de conocimiento y conservación de los mamíferos acuáticos en Colombia*, eds F. Trujillo, A. Gärtner, D. Caicedo, and M. C. Diazgranados (Bogotá, CO: Ministerio de Ambiente y Desarrollo Sostenible, Fundación Omacha, Conservación Internacional, and WWF), 94–127.

Pandolfi, J. M., Bradbury, R. H., Sala, E., Hughes, T. P., Bjorndal, K. A., Cooke, R. G., et al. (2003). Global trajectories of the long-term decline of coral reef ecosystems. *Science* 301, 955–958. doi: 10.1126/science.1085706

Paramo, J., Correa, M., and Núñez, S. (2011). Evidencias de desacople físico-biológico en el sistema de surgencia en La Guajira, Caribe colombiano. *Rev. Biol. Mar. Oceanogr.* 46, 421–430. doi: 10.4067/S0718-19572011000300011

Pardo, M., and Palacios, D. (2006). Cetacean occurrence in the Santa Marta Region, Colombian Caribbean, 2004-2005. *Lat. Am. J. Aquat. Mamm.* 5, 129–134. doi: 10.5597/lajam00105

Pardo, M. A., Mejía-Fajardo, A., Beltrán-Pedreros, S., Trujillo, F., Kerr, I., and Palacios, D. M. (2009). Odontocete sightings collected during offshore cruises in the western and Southwestern Caribbean Sea. *Lat. Am. J. Aquat. Mamm.* 7, 57–62. doi: 10.5597/lajam00135

Perrin, W. F., Caldwell, D. K., and Caldwell, M. C. (1994). "Atlantic spotted dolphin *Stenella frontalis* (G. Cuvier, 1829)," in *Handbook of Marine Mammals*, eds S. H. Ridgway and R. Harrison (San Diego, CA: Academic Press), 173–190.

Perrin, W. F., and Hohn, A. A. (1994). "Pantropical spotted dolphin *Stenella attenuata*," in *The First Book of Dolphins*, eds S. H. Ridgway and R. Harrison (San Diego, CA: Academic Press), 71–98.

Perrin, W. F., Mitchell, E. D., Mead, J. G., Caldwell, D. K., Caldwell, M. C., Bree, P. J., et al. (1987). Revision of the spotted dolphins, *Stenella* spp. *Mar. Mamm. Sci.* 3, 99–170. doi: 10.1111/j.1748-7692.1987.tb00158.x

Perrin, W. F., Rosel, P. E., and Cipriano, F. (2013). How to contend with paraphyly in the taxonomy of the delphinine cetaceans? *Mar. Mamm. Sci.* 29, 567–588. doi: 10.1111/mms.12051

Phillips, S. J., Anderson, R. P., Dudík, M., Schapire, R. E., and Blair, M. E. (2017). Opening the black box: an open-source release of Maxent. *Ecography* 40, 887–893. doi: 10.1111/ecog.03049

Phillips, S. J., Anderson, R. P., and Schapire, R. E. (2006). Maximum entropy modeling of species geographic distributions. *Ecol. Model.* 190, 231–259. doi: 10.1016/j.ecolmodel.2005.03.026

Prieto-Rodríguez, M. (1988). Reporte de algunos cetáceos del Caribe Colombiano. *Bol. Fac. Biol. Mar. UJTL* 8, 30–40.

Quérouil, S., Freitas, L., Cascão, I., Alves, F., Dinis, A., Almeida, J. R., et al. (2010). Molecular insight into the population structure of common and spotted dolphins inhabiting the pelagic waters of the Northeast Atlantic. *Mar. Biol.* 157, 2567–2580. doi: 10.1007/s00227-010-1519-0

Ramos, E. A., Castelblanco-Martínez, D. N., Niño-Torres, C. A., Jenko, K., and Gomez, N. A. (2016). A review of the aquatic mammals of Belize. *Aquat. Mamm.* 42, 476–493. doi: 10.1578/AM.42.4.2016.476

R Core Team (2018). *R: A Language and Environment for Statistical Computing*. Vienna: R Foundation for Statistical Computing. Available at: https://www.R-project.org/

Redfern, J., Ferguson, M., Becker, E., Hyrenbach, K., Good, C. P., Barlow, J., et al. (2006). Techniques for cetacean–habitat modeling. *Mar. Ecol. Prog. Ser.* 310, 271–295. doi: 10.3354/meps310271

Reilly, S. B. (1990). Seasonal changes in distribution and habitat differences among dolphins in the eastern tropical Pacific. *Mar. Ecol. Prog. Ser.* 66, 1–11. doi: 10.3354/meps066001

Robinson, N. M., Nelson, W. A., Costello, M. J., Sutherland, J. E., and Lundquist, C. J. (2017). A systematic review of marine-based Species Distribution Models (SDMs) with recommendations for best practice. *Front. Mar. Sci.* 4:421. doi: 10.3389/fmars.2017.00421

Rueda-Roa, D. T., and Muller-Karger, F. E. (2013). The southern Caribbean upwelling system: sea surface temperature, wind forcing and chlorophyll concentration patterns. *Deep Sea Res. Part I Oceanogr. Res. Pap.* 78, 102–114. doi: 10.1016/j.dsr.2013.04.008

Sbrocco, E., and Barber, P. H. (2013). MARSPEC: ocean climate layers for marine spatial ecology. *Ecology* 94, 979–979. doi: 10.1890/12-1358.1

Silva, J. M. Jr., Silva, F. J. L., and Sazima, I. (2005). Rest, nurture, sex, release, and play: diurnal underwater behaviour of the spinner dolphin at Fernando de Noronha Archipelago,SW Atlantic. *J. Ichthyol. Aquat. Biol.* 9, 161–176.

Spalding, M., Agostini, V., Rice, J., and Grant, S. (2012). Pelagic provinces of the world: a biogeographic classification of the world's surface pelagic waters. *Ocean Coast. Manage.* 60, 19–30. doi: 10.1016/j.ocecoaman.2011.12.016

Taylor, E., Baine, M., Killmer, A., and Howard, M. (2013). Seaflower marine protected area: governance for sustainable development. *Mar. Policy* 41, 57–64. doi: 10.1016/j.marpol.2012.12.023

Thorne, L. H., Johnston, D. W., Urban, D. L., Tyne, J., Bejder, L., Baird, R. W., et al. (2012). Predictive modeling of spinner dolphin *Stenella longirostris* resting habitat in the Main Hawaiian Islands. *PLoS One* 7:e43167. doi: 10.1371/journal.pone.0043167

Tobeña, M., Prieto, R., Machete, M., and Silva, M. A. (2016). Modeling the potential distribution and richness of cetaceans in the Azores from Fisheries Observer Program data. *Front. Mar. Sci.* 3:202. doi: 10.3389/fmars.2016.00202

Tyberghein, L., Verbruggen, H., Pauly, K., Troupin, C., Mineur, F., and De Clerck, O. (2012). Bio-ORACLE: a global environmental dataset for marine species distribution modelling. *Glob. Ecol. Biogeogr.* 21, 272–281. doi: 10.1111/j.1466-8238.2011.00656.x

Vidal, O. (1990). Lista de los mamíferos acuáticos de Colombia. *Inf. Mus. Mar. UJTL* 37, 1–18.

Warren, D. L., Glor, R. E., Turelli, M., and Funk, D. (2008). Environmental niche equivalency versus conservatism: quantitative approaches to niche evolution. *Evolution* 62, 2868–2883. doi: 10.1111/j.1558-5646.2008.00482.x

Wisz, M. S., Hijmans, R. J., Li, J., Peterson, A. T., Graham, C. H., and Guisan, A. (2008). Effects of sample size on the performance of species distribution models. *Divers. Distrib.* 14, 763–773. doi: 10.1111/j.1472-4642.2008.00482.x

Conflict of Interest Statement: The authors declare that the research was conducted in the absence of any commercial or financial relationships that could be construed as a potential conflict of interest.

frontiers in Marine Science

ORIGINAL RESEARCH
published: 25 February 2019
doi: 10.3389/fmars.2019.00077

Unraveling the Underwater Morphological Features of Roncador Bank, Archipelago of San Andres, Providencia and Santa Catalina (Colombian Caribbean)

Javier Idárraga-García and Hermann León*

Oceanographic and Hydrographic Research Center of Colombia, Cartagena, Colombia

In this study, we present the first detailed description of the morphology of the Roncador Bank deep underwater environments, located in the central sector of the SeaFlower Biosphere Reserve (Archipelago of San Andres, Providencia and Santa Catalina-ASAPSC, Republic of Colombia). The analysis was carried out from multibeam bathymetric information recently acquired by the Oceanographic and Hydrographic Research Center of Colombia (CIOH), and the subsequent creation of a 35 m-resolution digital terrain model, which was the main input for the geomorphological mapping. The results allowed to determine that Roncador Bank corresponds to a seamount of highly irregular contour, reaching a height up to 2,350 m with respect to the surrounding seafloor. The volcanic edifice that makes up the seamount is bounded to the south and east by two escarpments, which are tectonically related with the Southern Roncador and Eastern Roncador faults, respectively. We were able to determine that these faults are currently active and that recently have generated earthquakes of magnitudes up to 6.0, which has important implications for the estimated seismic risk in the ASAPSC. This situation allowed to infer that the volcanic processes that formed the Roncador volcano were controlled by the presence of major faults on the seabed. The steep slope gradients (up to 40°) of the escarpments effectively concentrate erosive processes, leading to the development of a dense gully network and extensive slope deposits in the hillsides. Also, we identified debris-avalanche deposits indicating the occurrence of partial collapses of Roncador, which shows that gravity-driven mass transport processes have played an important role in the edifice shaping. These large-scale underwater landslide events may have the capacity to generate tsunamis, so it is necessary to carry out specific studies to analyze their tsunamigenic potential. Finally, the mapping and detailed description of Roncador seamount morphological features, such as pinnacles, escarpments, hummocky terrains, ridges, gullies and canyons, reported in this study are key to advance in the basic knowledge on the geology and geomorphology of the ASAPSC, and have direct implications for future specific research on the characterization of deep ecosystems, geohazards, natural resources, and territory planning.

Keywords: submarine geomorphology, SeaFlower Biosphere Reserve, western Caribbean, Roncador Bank, multibeam bathymetry

OPEN ACCESS

Edited by:
Santiago Herrera,
Lehigh University, United States

Reviewed by:
Federico Di Traglia,
Università degli Studi di Firenze, Italy
Aggeliki Georgiopoulou,
University College Dublin, Ireland
Jon J. Major,
United States Geological Survey, United States

****Correspondence:***
Javier Idárraga-García
jidarragag@unal.edu.co

Specialty section:
This article was submitted to Marine Conservation and Sustainability, a section of the journal Frontiers in Marine Science

Received: *29 August 2018*
Accepted: *11 February 2019*
Published: *25 February 2019*

Citation:
Idárraga-García J and León H (2019) Unraveling the Underwater Morphological Features of Roncador Bank, Archipelago of San Andres, Providencia and Santa Catalina (Colombian Caribbean). Front. Mar. Sci. 6:77. doi: 10.3389/fmars.2019.00077

INTRODUCTION

The investigation of the seabed geomorphology, i.e., the forms, processes and evolution of submarine landscapes, has become a powerful tool to characterize the renewable and non-renewable marine resources, such as marine ecosystems, fisheries, hydrocarbons, deep sea minerals, among others. Also, knowing the submarine morphology is key to the assessment of geohazards, and to the marine and coastal spatial planning, including the operation of offshore infrastructure, the appointment of protected areas, and the implementation of environmental programs.

The Archipelago of San Andres, Providencia and Santa Catalina (ASAPSC) is located in the western sector of the Caribbean Sea and belongs to the Republic of Colombia (**Figure 1**). This archipelago has an area of 180,000 km^2 approximately (Coralina-Invemar, 2012), and includes the SeaFlower Biosphere Reserve (SBR), one of the most important protected marine areas in the western hemisphere. The ASAPSC comprises two oceanic islands (San Andres and Providencia-Santa Catalina) and a group of atolls and coral banks (Albuquerque, Este-Sureste, Roncador, Quitasueño, Serrana, Serranilla, and Bajo Nuevo, among others), most of which emerge permanently as cays, which support the highest density of corals in the Caribbean Sea. In spite of the well-known importance of the SBR from the biological, ecological and productive point of view, very little is known about its physical aspects, especially on the geological structure and the geomorphological features of the islands and banks in their deep submarine environments.

In this paper, we took advantage of recently acquired multibeam bathymetric information to illuminate and describe, for the very first time, the submarine geomorphology of Roncador Bank, located in the central sector of the ASAPSC. The results presented here are not only important for improving the basic knowledge of the geological and geomorphological origin and evolution of the ASAPSC, but also constitute the basis for carrying out studies of geohazards, mineral resources, and marine ecosystems, and for establishing policies for their exploitation, protection and conservation.

GEOLOGIC AND OCEANOGRAPHIC CONTEXT OF THE ASAPSC AND RONCADOR BANK

Roncador Bank is located in the ASAPSC, in the northwestern sector of the Colombian Caribbean, approximately 140 km to the east of Providencia Island and 205 km to the northeast of San Andres Island (**Figure 1**). Geologically, the ASAPSC is part of the province known as Lower Nicaraguan Rise (LNR) (Holcombe et al., 1990), which is considered as a crustal block limited by the Pedro Escarpment to the northwest and the Hess Escarpment to the southeast (Holcombe et al., 1990; Mauffret and Leroy, 1997). Case et al. (1990), based on the analysis of multichannel seismic data concluded that the LNR is composed of oceanic crust. Alternatively, Mauffret and Leroy (1997) found that this province is underlain by an oceanic plateau. Milliman and Supko (1968) superimposed geomagnetic data over the bathymetry in the area of the San Andres Island and found a direct relationship, which is especially pronounced at Este-Sureste atoll. According to these authors, this suggests the presence of deep-seated volcanic cones under the limestone caps of the atolls and of the San Andres Island. The volcanic origin of these formations is further supported by a basaltic pebble that was dredged from a depth of approximately 700 m in the area of the Albuquerque Bank, and by the presence of a prominent platform recognized throughout the area, which can represent the remnants of wave-cut volcanoes, later covered by a thick sediment cover (Milliman and Supko, 1968).

From the few geological studies carried out in the ASAPSC area, it has been concluded that the atolls, islands and coral banks may have originated by volcanic activity during Early Cenozoic times (Geister and Díaz, 2007). In this scenario, subsidence and simultaneous capping of these volcanoes by shallow-water carbonate layers from Cenozoic through Quaternary gave rise to the formation of the shallow banks and atolls of the archipelago (Geister and Díaz, 2007). Most of the banks, atolls and islands of the ASAPSC exhibit a NNE-SSW orientation, suggesting a possible NNE-trending submarine fault zone, which controlled the location of volcanic material on the seafloor. Additionally, the presence of some atolls and elongated islands with a NW-SE trend also suggests the existence of fault zones oriented to the NW underlying these structures.

On the other hand, the geological knowledge of Roncador Bank is quite limited, and what little information is available is restricted to its shallowest part. Roncador is an elongated atoll with an overall NW-SE trend, reaching a maximum amplitude of about 6 km and a length of approximately 13 km (Geister and Díaz, 2007). This bank forms the base of Roncador Cay, a vegetated islet located in the northern sector, formed by the accumulation of coarse coral debris (Geister and Díaz, 2007); its dimensions are 482 m in length and 290 in width (Tabares et al., 2009). The geomorphology of Roncador reef complex has been well characterized by Milliman (1969), and Geister and Díaz (2007). These authors stated that Roncador has a windward fore-reef terrace that is somewhat narrower and deepens more rapidly than that of any of the other ASAPSC atolls. The peripheral reef is continuous only on the windward side (Geister and Díaz, 2007). The lagoon terrace is considerably shallower than that of the other atolls in the area; the depths within the lagoon basin reach approximately 18 m, with an average of 10–12 m (Milliman, 1969; Geister and Díaz, 2007). According to Milliman (1969), the lagoon basin is completely open to the west, with the exception of the southernmost sector, where a few elongated, shallow patch reefs form a discontinuous peripheral reef to the southwest.

The prevailing surface current in the Caribbean Sea, known as the Caribbean Current, is a high-speed flow (>25 cm/s) from E to W, and forms a large counterclockwise eddy in the southwestern sector of the Caribbean (Geister and Díaz, 2007) (**Figure 1**). According to Hallock et al. (1988), the persistent northward flow of this current through large gaps and narrow open seaways of the Nicaraguan Rise is a key oceanographic and environmental factor that controls the sedimentary processes on the western platforms of the rise. The Caribbean Current is

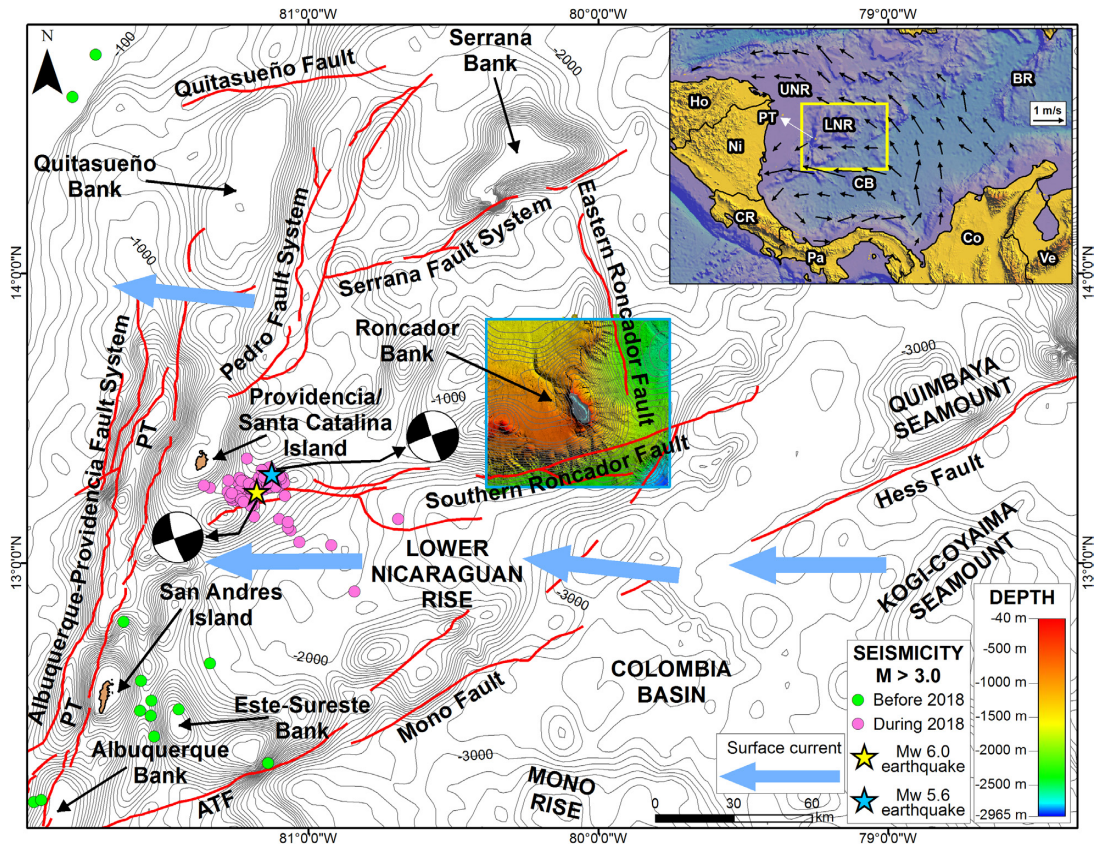

FIGURE 1 | Location of Roncador Bank in the Archipelago of San Andres, Providencia and Santa Catalina (ASAPSC) as indicated by the DTM in the blue box. The regional fault systems are shown as red lines and the instrumental seismicity (M > 3) is indicated by green and pink circles. The blue and yellow starts correspond to the Mw 5.6 and Mw 6.0 earthquakes occurred in 2018 with their focal mechanisms as reported by the Colombia National Seismological Network. The flow of surface currents (Caribbean current) around Roncador is represented by the thick blue arrows (Coralina-Invemar, 2012). The isobaths spacing is 100 m. The inset in the upper right corner shows the location of the ASAPSC area in western Caribbean, where the directions of the Caribbean surface current are indicated by the thin black arrows (Coralina-Invemar, 2012). PT, Providencia Trough; ATF, Albuquerque-Turmeque Fault; LNR, Lower Nicaraguan Rise; UNR, Upper Nicaraguan Rise; BR, Beata Ridge; CB, Colombia Basin; Ho, Honduras; Ni, Nicaragua; CR, Costa Rica; Pa, Panama; Co, Colombia; Ve, Venezuela.

divided just between the islands and cays in such a way that a part (∼60%) continues its journey toward the Cayman Sea and the rest recirculates toward the southwestern Caribbean, forming the Colombia-Panama Gyre, whose waters flow to the south of the ASAPSC (Coralina-Invemar, 2012). The surface currents in the ASAPSC are distorted by the continuous arrival of eddies that rotate in both directions and travel with the Caribbean Current. These eddies are deformed between the walls and escarpments of the archipelago seamounts (Coralina-Invemar, 2012). According to Coralina-Invemar (2012), in the archipelago, the Caribbean Surface Water (CSW) reaches a depth between 50 and 75 m and is characterized by its low salinity. A second water mass, the Subtropical Subsurface Water (SSW), with a maximum salinity, is located between 150 and 200 m, followed by a water body known as Subantarctic Intermediate Water (SIW) that has the minimum salinity between 600 and 900 m. Finally, the North Atlantic Deep Water (NADW) is located in the deepest parts of the area. Unfortunately, the behavior of these deep currents (flow directions and velocities) in the ASAPSC area is currently unknown.

DATA AND METHODS

The acquisition of multibeam bathymetric data in the Roncador area was carried out in 2017 on board the research vessel ARC Malpelo, which is operated by the Center for Oceanographic and Hydrographic Research of Colombia (CIOH), using a Kongsberg EM 302 system with a frequency of 30 kHz. This expedition was part of a huge initiative, led by the General Maritime Directorate of Colombia (DIMAR), to map the entire seabed of the ASAPSC, with the purpose of advancing knowledge of the geology and geomorphology of the Colombian Caribbean underwater environments.

After applying some corrections to the raw depth soundings, a digital terrain model (DTM) was generated with a spatial resolution of 35 m. In order to support our morphological observations and interpretations, we carried out some standard morphometric calculations. These DEM-derived products were obtain using the software ArcGIS 10.3.1, and include the hillshade, slope, aspect, and profile and plan curvature models.

Hillshade is a raster generated from elevation data that provides a shaded surface depending on the angle and azimuth of a hypothetical illumination source, and is typically displayed underneath the transparent bathymetry to enhance visualization of elevation data. The terrain slope is defined as the maximum rate of change in a cell value (elevation) relative to the neighboring cells, and its resulting raster shows the steepest gradient in degrees ranging between 0° (horizontal) and 90° (vertical) (Jenness, 2013). The aspect map shows the azimuth direction at which the maximum slope is achieved (Favalli and Fornaciai, 2017). Since the aspect represents the azimuthal direction of the gravity force component tangential to the surface, generally it is accepted that aspect indicates the flow line direction (Olaya, 2009). The profile curvature is defined as the rate of change of slope measured in a vertical plane oriented along the gradient line (e.g., Olaya, 2009). A negative value indicates convex slopes, while a positive value indicates concave surfaces. Consequently, a value close or equal to zero indicates flat or uniform surfaces. The profile curvature runs parallel to the terrain maximum slope and affects the acceleration or deceleration of flow down the slope (e.g., Wood, 1996; Olaya, 2009; Di Traglia et al., 2014). The planform curvature (commonly called plan curvature) is perpendicular to the direction of the maximum slope. Here, a positive value indicates that the surface is sidewardly convex, and a negative value indicates that the surface is sidewardly concave. A value close or equal to zero indicates flat or uniform surfaces. The plan curvature runs perpendicular to the terrain maximum slope and affects the convergence and divergence of flow down the slope (e.g., Olaya, 2009; Favalli and Fornaciai, 2017).

We also used seafloor backscatter information, which were acquired concurrently with the bathymetry. Our analysis was only qualitative with the aim of evaluating the nature of the substrate, mainly in terms of lithology, roughness and heterogeneities, and to differentiate depositional and erosional areas.

GENERAL PHYSIOGRAPHY OF RONCADOR BANK

The area covered by the bathymetric survey around Roncador Bank extends between latitudes 13.2° and 13.8°, and longitudes −79.7° and −80.4°, covering about 4,800 km^2. The information allowed us to determine that the depths in the zone vary between −40 and −2,965 m (**Figure 2**). The shallowest values (<−2,000 m) are observed in the central and northwestern sectors, whereas deeper values (>−2,000 m) are found to the south and east of the study area (**Figure 2**). It is also clear that the deep and shallow sectors are separated by a zone of closely spaced isobaths with a general tendency W–E observed at 13.3°N, which exhibits an abrupt direction shift at −80°W to continue with a general tendency N–S (**Figure 2**). In **Figure 3A**, this zone shows the steepest slope angles (between 25° and 40°).

The aspect (or slope direction) map allowed us to differentiate four sectors with contrasting characteristics (**Figure 3B**): the southern sector where slopes oriented within the SE and SW quadrants (azimuth between 90° and 270°) are predominant; the northeast sector which exhibits slopes oriented mainly to the east, with minor variations to the ENE and ESE; the north-central and southeastern sectors where slopes are oriented preferentially to the NW (average azimuth of 315°); and a northwestern sector which exhibits slopes oriented north and northwest.

GEOMORPHOLOGY OF RONCADOR BANK

Morphologically, Roncador corresponds to an irregular-shaped seamount which reaches a maximum height of about 2,350 m with respect to the adjacent relatively flat seafloor. There are several distinct morphologic elements that characterize Roncador Seamount (**Figure 4**): escarpments; slope deposits; archipelagic apron; pinnacles (volcanic remnants); hummocky terrains; terrain with small-scale scarps and ridges; major ridges; and canyons.

Escarpments

One of the most prominent geoforms identified in the study area corresponds to a zone of major escarpments, occurring in the southern sector with a general tendency W–E, which suddenly shifts their trend to continue with an S–N direction (**Figures 2**, **3A–D**, **4**, **6B,D**, **8A,C**). These escarpments show steep slopes, with angles varying between 18° and 25°, but locally reaching values of 40°, and oriented toward the SE, SW, ENE, and ESE (**Figures 3A,B**). One of the most important features of these escarpments is the presence of very complex longitudinal and transverse profiles, as a result of the occurrence of numerous small, narrow and deeply incised gullies (**Figures 4**, **5A–C**, **6B–D**, **8A,C**, **9A–D**). This situation is evident in the profile and plan curvature maps shown in **Figures 3C,D**, where concave and convex forms are repetitive along the escarpment hillsides. In particular, the profile curvature map of the southern escarpment (**Figure 5B**) differentiates very well its upper limit, where it is bounded by a relatively regular, gentle sloping surface that extends to the north. The crest of the escarpment is very irregular in plan view; it is evident by an abrupt slope break (**Figure 5B**) and occurs at depths ranging from −790 to −600 m. In contrast, the lower limit of the escarpment is not so evident in the profile curvature map (**Figure 5B**). This is due to the fact that the escarpment foothill is partially covered by slope deposits, and therefore the slope change is not as strong as in the escarpment's upper part. On the other hand, the plan curvature map (**Figure 5C**) clearly delineates the dense gully network present in the southern escarpment. From this map it is evident that the gullies are arranged in a dendritic pattern, and that most of them originate at the slope break that forms the escarpment crest (**Figure 5C**). Only two gullies have heads extending beyond the upper part of the escarpment, incising the relatively flat surface located to the north (**Figures 5A,C**). The gullies reach depths up to 300 m beneath the escarpment seafloor. From the backscatter data, shown in **Figures 7B–D**, it is observed that, in general, the upper part of the escarpments exhibit high reflectivity, being higher in the eastern escarpment,

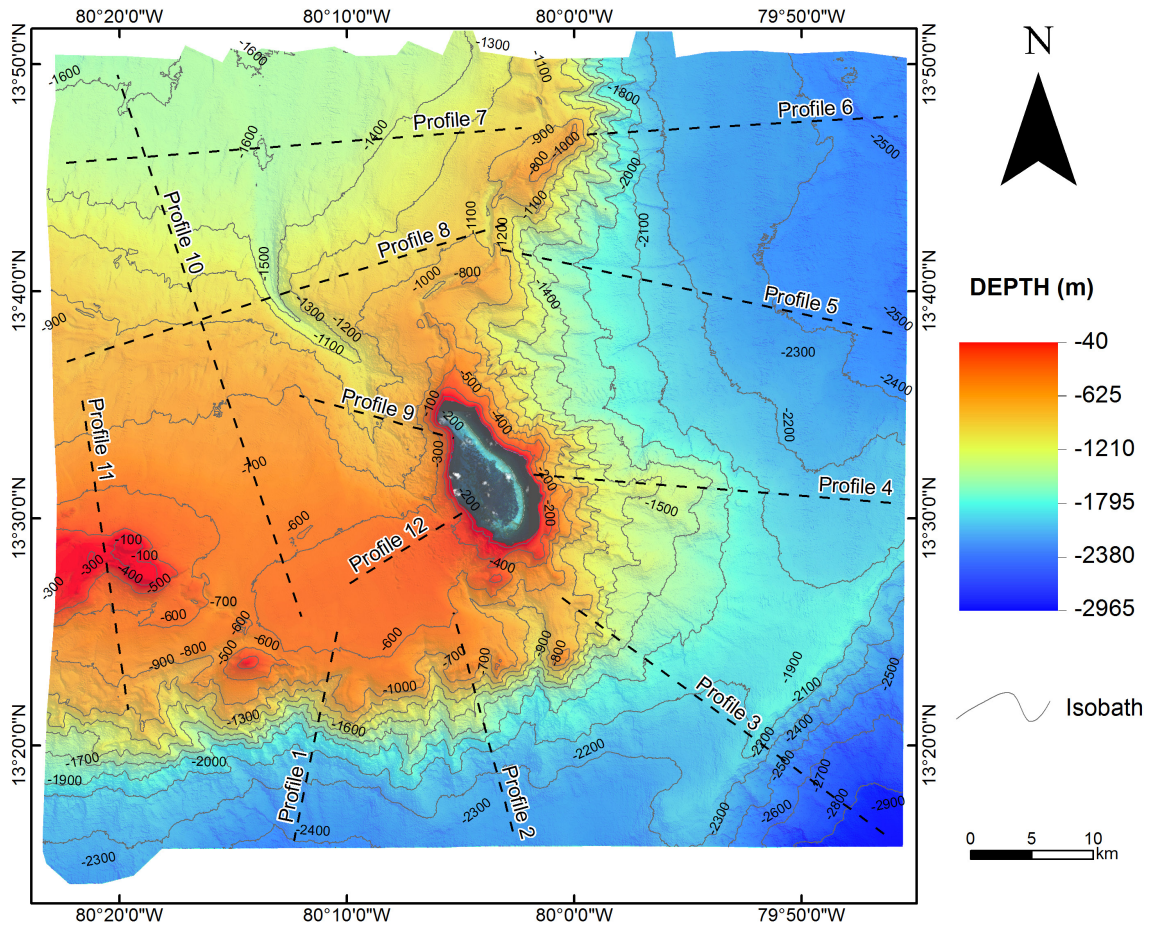

FIGURE 2 | Bathymetric model, with gray scale hillshade behind, of Roncador Bank and adjacent areas. The sector exhibiting the greater depths (> −2,000 m) is observed to the south and east of the study area, whereas the shallower depths (< −2,000 m) predominate in the central and northwestern sectors. The black dashed lines indicate the profiles shown in **Figure 9**. The isobaths spacing is 100 m. The satellite image covers the reef constructions shallower than –40 m and the permanently emerged areas (cays).

which implies that volcanic rock and/or limestone crop out there. On the other hand, the middle and lower parts of the escarpments exhibit medium to low reflectivity, implying the presence of softer sea bottom, which is consistent with the occurrence of slope deposits (**Figures 7B–D**).

As is observed in the slope and profile curvatures maps (**Figures 3A,C**), at the top of the eastern escarpment, there is a depression-like feature, slightly sinuous, trending SW–NE. This depression is very narrow (maximum width of 1,000 m), deepens to 200 m below the surrounding seafloor, and reaches a length of about 18 km (**Figures 6A,D**). The backscatter signal of this feature is characterized by high values, indicating a highly reflective seafloor (**Figures 7A,D**). This acoustic response indicates that erosive processes predominate, exposing a hard substrate (volcanic rock and/or limestone), and that sediment cover is scarce or absent.

We also infer that Roncador southern and eastern escarpments are tectonically controlled by the activity of two regional faults, named Southern Roncador Fault and Eastern Roncador Fault, respectively. These faults are recognized on the seafloor as very strong lineaments (**Figures 4**, **6B–D**). The Southern Roncador Fault comprises two traces that are oblique to the general direction of the escarpment, and exhibit a strike ranging between N72°E and N80°E; the Eastern Roncador Fault strikes between N5°W and N20°W (**Figures 4**, **6B–D**).

Slope Deposits

A belt of landforms with low gradients (less than 8°), and geometries of cones and lobes of different sizes and shapes is observed at the foot of the escarpments described above (**Figures 4**, **6B–D**, **8A,C**). From their morphology, and the fact that they occur at the escarpments foothills, they are interpreted as slope deposits.

Based on the bathymetry data, we were able to differentiate up to 21 individual depositional bodies, which in most cases seem to be bounded by gullies and channels. The individual areas of these deposits vary between 9 and 138 km^2, and their surfaces are commonly irregular due to the presence of minor scarps and ridges (**Figures 4**, **6B–D**, **9A–E,K**). Such textures may have originated as a result of compressional deformation and/or

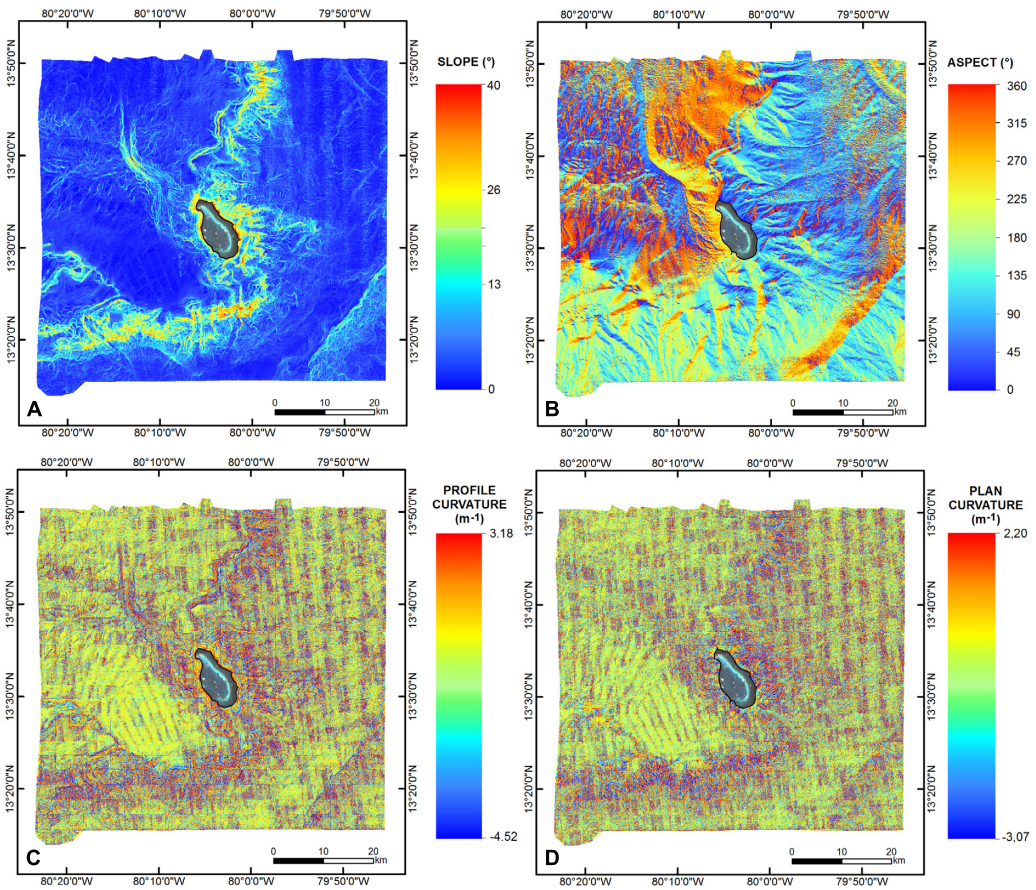

FIGURE 3 | (A) Terrain slope model, where a zone exhibiting the steepest slope angles bounds Roncador seamount to the south and east. **(B)** Aspect (or slope direction) model. **(C)** Profile curvature model. **(D)** Plan curvature model. The satellite image covers the reef constructions shallower than –40 m and the permanently emerged areas (cays).

collapse of the material during the deposition. The backscatter signal shows that the slope deposits have intermediate to low reflectivity, implying that they are mostly composed mostly of fine-grained sediment, with minor quantities of coarser sediment mainly located at their proximal sectors (**Figures 7B–D**).

Archipelagic Apron

This geoform is characterized by a very smooth relief, which deepens with a maximum slope of 5°. It is observed in the southeastern and eastern sectors as a relatively flat surface that bounds the slope deposits in deeper areas. Also, it extends from the top of the escarpments to the northwest of the study zone with a gentle slope of about 3° (**Figures 4**, **6B–D**, **8A–D**, **9B,D,F,G,J,L**). The acoustic reflectivity of the apron surface (**Figures 7C,D**) is very low, which suggests that this sedimentary body is likely the product of fine-grained, hemipelagic sedimentation, although some bottom current-driven sedimentation should not be discarded.

Canyon

In the central part of the zone, there is bathymetric expression of a canyon of significant dimensions. This conduit, known as Roncador Canyon, originates on the western side of the bank, and extends for about 35 km toward the northwest, where it flows into a small fan at a depth of −1,580 m approximately (**Figures 4**, **6A**, **8B,D**, **9H,I**). The proximal part of this canyon is partially covered by deposits having a hummocky structure (**Figures 4**, **6A**, **8B,D**, **9I**), inferred to be debris-flow deposits. Roncador Canyon is up to 430 m deep with respect to the adjacent submarine relief, and exhibits a marked V cross section that varies between symmetrical and strongly asymmetric, with canyon walls reaching maximum slope values between 20° and 35° (**Figures 3A**, **9H,I**). The profile curvature map, shown in **Figure 3C**, delineates very well the canyon margins, and shows that the middle and distal reaches have constant widths, varying between 2.5 and 3 km. By contrast, the proximal reach of the canyon exhibits the largest width, with values between 7.5 and 8.7 km. The thalweg of the Roncador canyon is characterized by a high backscatter signal (**Figure 7A**), which is evidence that the bottom of the canyon is devoid of sediment. Also, the proximal reach exhibits intermediate values in the seafloor reflectivity (**Figure 7A**) due to the presence of extensive debris flow deposits, mainly on the eastern hillside.

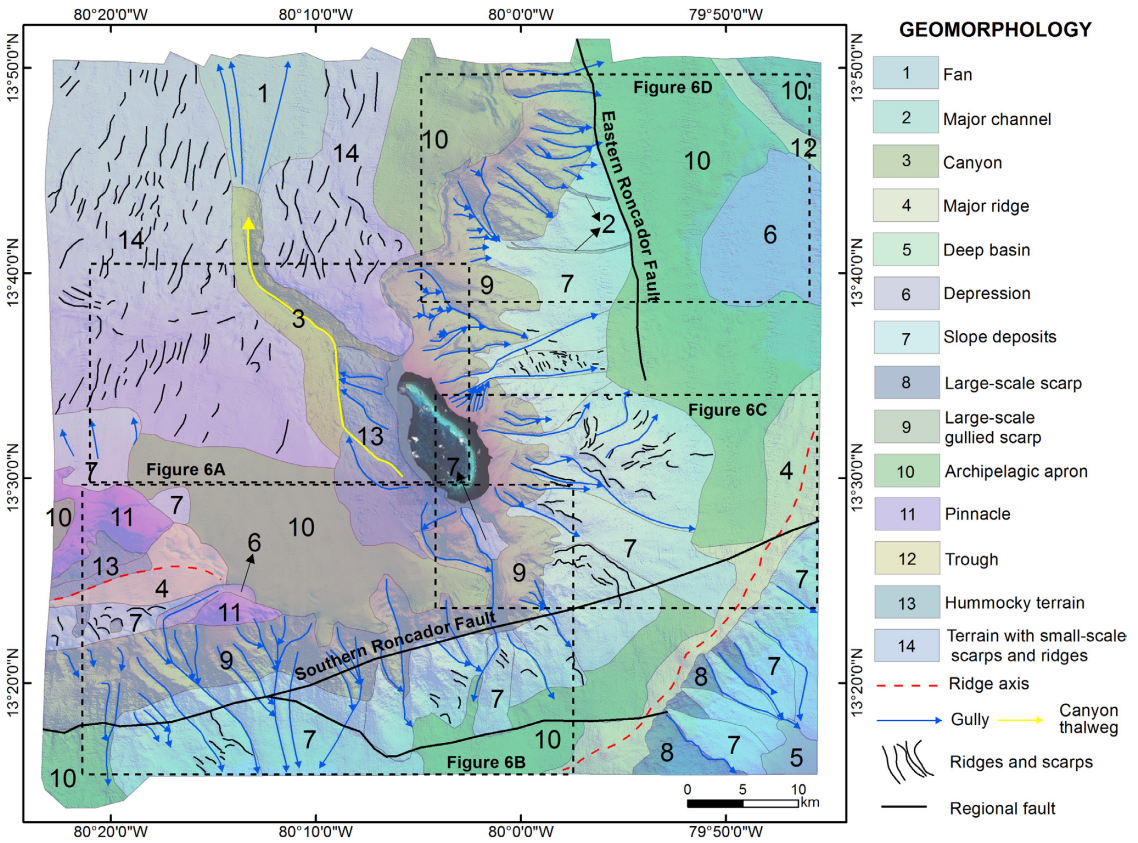

FIGURE 4 | Submarine geomorphological map of Roncador Bank and adjacent areas, where the main geomorphic features are shown. The satellite image covers the reef constructions shallower than –40 m and the permanently emerged areas (cays). The boxes indicate the location of **Figure 6**. See text for detailed description.

Pinnacles

Here, we refer to pinnacles as geoforms associated with cone-shaped elevations mounted on the top of a major submarine feature. We were able to identify two pinnacles in the southwestern sector of the study zone, which are interpreted as remnants of volcanic edifices (**Figures 4**, **6B**, **8A,B,D**, **9K**). This is supported by the backscatter image shown in **Figure 7B**, which provides evidence of a high reflective seafloor associated with these two pinnacles. The pinnacle located to the south rises over the top of the Roncador southern escarpment, reaching a height of 450 m above the surrounding seafloor; its base has a length of about 18.8 km, and its slopes exhibit a complex shape, with both concave and convex profiles. The second pinnacle is located to the northwest of the first pinnacle, and it raises over the archipelagic apron reaching a height of approximately 550 m (**Figures 4**, **6B**); its base has a length of about 44 km, and also exhibits an asymmetrical profile, with both concave and convex slopes (**Figure 9K**). Its slopes have an average angle of 15°, but locally can reach up to 25°.

Hummocky Terrain

This terrain is characterized by a very irregular and rough texture, due to the presence of numerous blocks (or rock fragments) of various sizes deposited on the slopes of major geoforms by mass wasting processes (**Figures 4**, **6A**, **8B,D**, **9I**). The blocks can reach several tens of meters of height and exhibit very irregular shapes. The most prominent hummocky terrain of the study area is located on the western flank of Roncador seamount, extending to a maximum depth of about −1,100 m, where it appears to be partially filling the proximal reach of the Roncador Canyon eastern wall (**Figures 4**, **6A**, **8B,D**, **9I**). The backscatter signal shows a mixture of intermediate and high reflectivity values (**Figure 7A**). The higher values indicate the blocks or rock fragments, and the intermediate values represent the finer sediment of the deposit. This terrain is interpreted as debris flow deposits produced by a partial collapse of the western margin of Roncador volcanic edifice, and reaches an area of 93.8 km^2. Furthermore, a smaller hummocky terrain is observed in the southern part of the northernmost volcanic pinnacle, with an area of approximately 24 km^2 (**Figures 4**, **6B**, **7B**).

Terrain With Small-Scale Ridges and Scarps

In the northwesternmost sector of the study area there is a surface with a general smooth (<5°), northward-oriented slope, which exhibits a distinctive irregular relief due to the presence of a series of minor scarps and ridges (**Figures 4**, **6A**, **8B,D**, **9H,J**). These features exhibit a preferential N-NNE strike, although locally

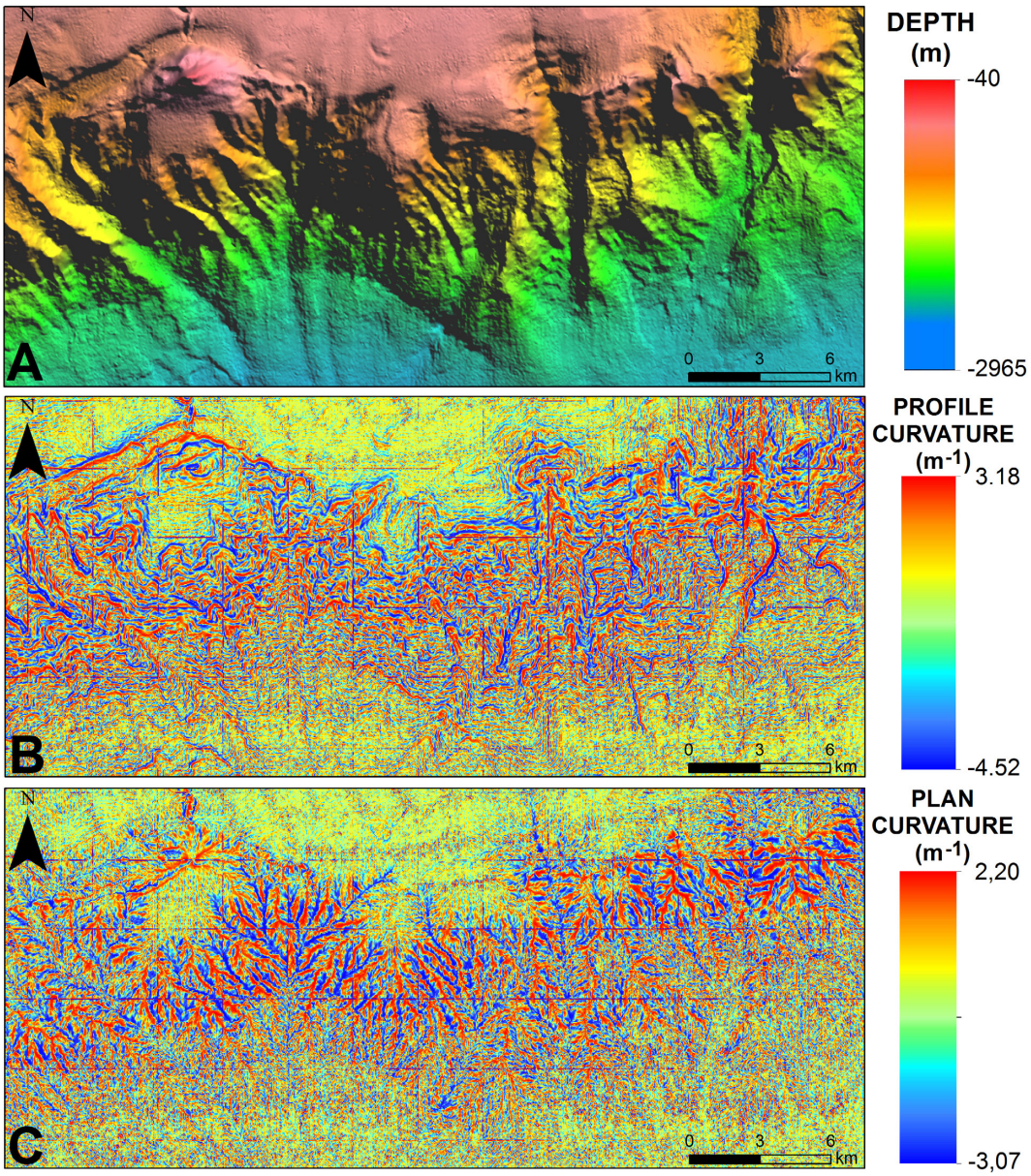

FIGURE 5 | Detail of Roncador southern escarpment. **(A)** Bathymetric model. **(B)** Profile curvature model. **(C)** Plan curvature model. See text for detailed description.

some are arranged with a general direction E–W (**Figure 3B**). These irregularities can reach maximum heights of several tens of meters above the surrounding seafloor. This terrain occupies about 812 km^2, but it is important to clarify that this geoform extends to the north, outside the area covered by this study.

Major Ridges

In the southeastern sector of the study area, a SW–NE-elongated positive relief is observed, which does not exceed 150 m in height above the surrounding seafloor (**Figures 4**, **6C**, **8A,C**, **9C**). This ridge is bounded to the southeast by an escarpment that extends toward greater depths outside the study area, and that is partially covered by slope deposits. The ridge presents a strongly asymmetrical cross section with steeper slopes toward the southeast (inclination between 10° and 20°) and smoother slopes to the northwest (inclination < 5°) (**Figures 3A,B**).

DISCUSSION

According to the few geological and geomorphological studies conducted, it has been proposed that the LNR, the geological province where the ASAPSC is located, is composed of oceanic-type crust, with the peculiarity that it has been affected by intense

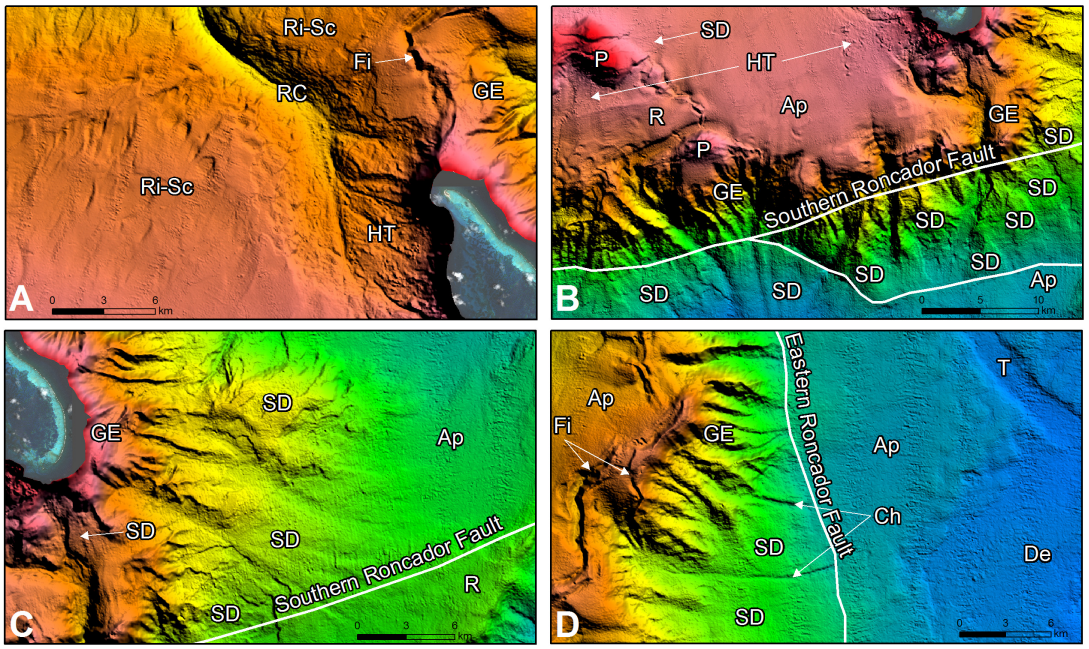

FIGURE 6 | Detail of some of the most important geoforms associated with Roncador Bank. **(A)** Northwestern sector of Roncador where a hummocky terrain (HT) is identified in the proximal reach of the Roncador Canyon (RC). **(B)** Southern escarpment of Roncador where a series of gullies and slope deposits (SD) are present. This escarpment is controlled by the Southern Roncador Fault. At the top of the escarpment, there are two pinnacles (P). **(C)** Gullied escarpment (GE) in the southeastern sector of Roncador, and extensive slope deposits (SD) at the foothills. **(D)** Eastern escarpment of Roncador which is controlled by the Eastern Roncador Fault. At the top of the escarpment, a fissure (Fi) is identified. The satellite image covers the reef constructions shallower than –40 m and the permanently emerged areas (cays). Ri-SC, terrain with minor ridges and scarps corresponding to large-scale landslides deposits; R, ridge; Ap, archipelagic apron; De, depression; T, trough; Ch, channel. See **Figure 4** for location.

volcanism since Cenozoic times. In this sense, Geister (1992) and Geister and Díaz (2007) reported the common presence of geological features such as seamounts and volcanoes with a preferential NE–SW orientation. Additionally, on Providencia Island, volcanic rocks crop out, including basalts and trachytes (Mitchell, 1955; Wadge and Wooden, 1982; Geister, 1992). Although from the middle of the last century it has been known that the islands, atolls and banks that make up the ASAPSC lie on a basement of volcanic origin, very little is known about the geomorphological features that these formations exhibit in the deep environments, beyond the outer limit of shallower reef constructions. In this work, we contribute to the advance of the geological knowledge of the ASAPSC, by means of the detailed geomorphological description of Roncador Bank from newly acquired multibeam bathymetric data.

Our analysis allowed us to identify and map a series of geomorphological features in the Roncador Bank area, which are the product of volcanic, erosive and depositional processes that have interacted during the geological history of the bank. Roncador corresponds to a seamount, which is one of the several volcanic edifices that make up the ASAPSC. This seamount is limited to the south and east by two escarpments, with general directions E–W and N–S, respectively, which are controlled tectonically by two regional faults: Southern Roncador Fault and Eastern Roncador Fault. Two facts lead us to affirm that these two faults are probably active. The first is that both structures are recognized in the bathymetry as strong lineaments, even when they go through the slope deposits and sedimentary apron. Thus, the faults seem not to be buried by the most recent sedimentation. However, as an alternative, this situation could be the consequence of a very low sedimentation rate in the area, i.e., there is not enough sediment to bury the faults since their last activity, or perhaps bottom currents remove any sediment that is being deposited. The second fact is that although in the Roncador area itself there is no recorded seismicity, the Southern Roncador Fault to the west of the analyzed zone does have earthquake activity (**Figure 1**). During October and November 2018, a seismic swarm of more than 400 earthquakes occurred, the largest at magnitude 6.0, as reported by the Colombia National Seismological Network (CNSN). The focal mechanisms obtained by the CNSN for the Mw 6.0 earthquake and a Mw 5.6 aftershock indicate left-lateral faulting, which is consistent with the Caribbean intraplate strike-slip tectonics previously reported by several authors (Burke et al., 1984; Mann and Burke, 1984; Carvajal-Arenas and Mann, 2018). Such activity not only proves the active character of the Southern Roncador Fault but recognizes its seismogenic potential, and therefore the implication for the seismic risk in the ASAPSC.

The presence of currently active faults supports the hypothesis previously raised by some authors (e.g., Geister, 1992; Geister and Díaz, 2007) that the construction of the ASAPSC volcanic edifices was strongly controlled by regional tectonic structures. In

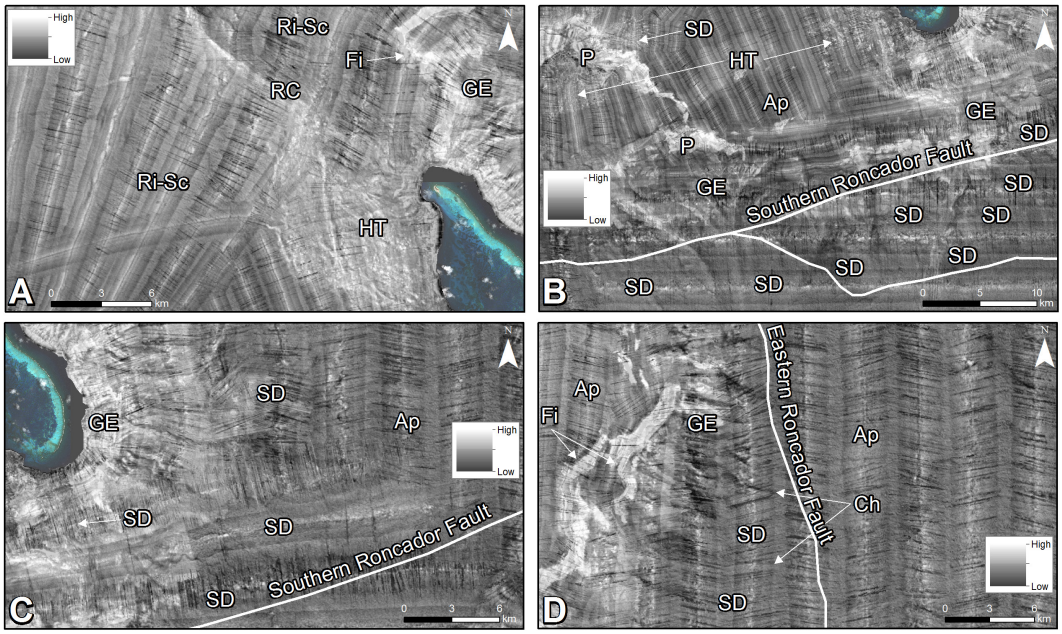

FIGURE 7 | Backscatter signal of the seafloor in the same sector shown in **Figure 6**. **(A)** In the northwestern sector of Roncador, the hummocky terrain (HT) is characterized by a mixture of intermediate and high values of seafloor reflectivity. The thalweg of Roncador Canyon (RC), the gullied escarpment (GE) and the fissure (Fi) exhibit high backscatter values. **(B)** Southern escarpment of Roncador where the slope deposits (SD) show low backscatter signal, demonstrating their depositional character. The two pinnacles (P) at the top of the escarpment exhibit high values of reflectivity. **(C)** Gullied escarpment (GE) in the southeastern sector of Roncador characterized by very high backscatter, and extensive slope deposits (SD) at the foothills exhibiting intermediate to low acoustic reflectivity. **(D)** A fissure (Fi) at the top of the eastern escarpment of Roncador is evident by very high backscatter values. The satellite image covers the reef constructions shallower than –40 m and the permanently emerged areas (cays). Ri-SC, terrain with minor ridges and scarps corresponding to large-scale landslides deposits; Ap, archipelagic apron; Ch, channel. See **Figure 4** for location.

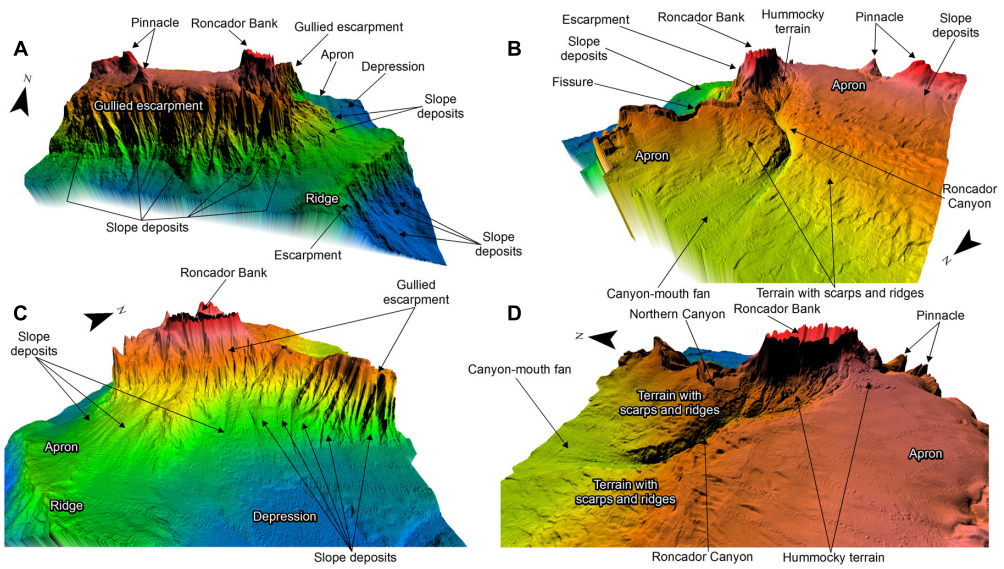

FIGURE 8 | General 3D views of Roncador Bank and adjacent areas where the main identified geoforms are highlighted. **(A)** View from the south. **(B)** View from the northwest. **(C)** View from the east. **(D)** View from the west. Vertical exaggeration is by 8. See text for detailed description.

this sense, the Roncador seamount was built by the accumulation of volcanic material on the seabed, which took advantage of the presence of large fractures (Southern and Eastern Faults) to penetrate the oceanic crust and extrude to the surface. The narrow and deep depression identified in the northern sector of Roncador, along the top of the eastern escarpment, probably

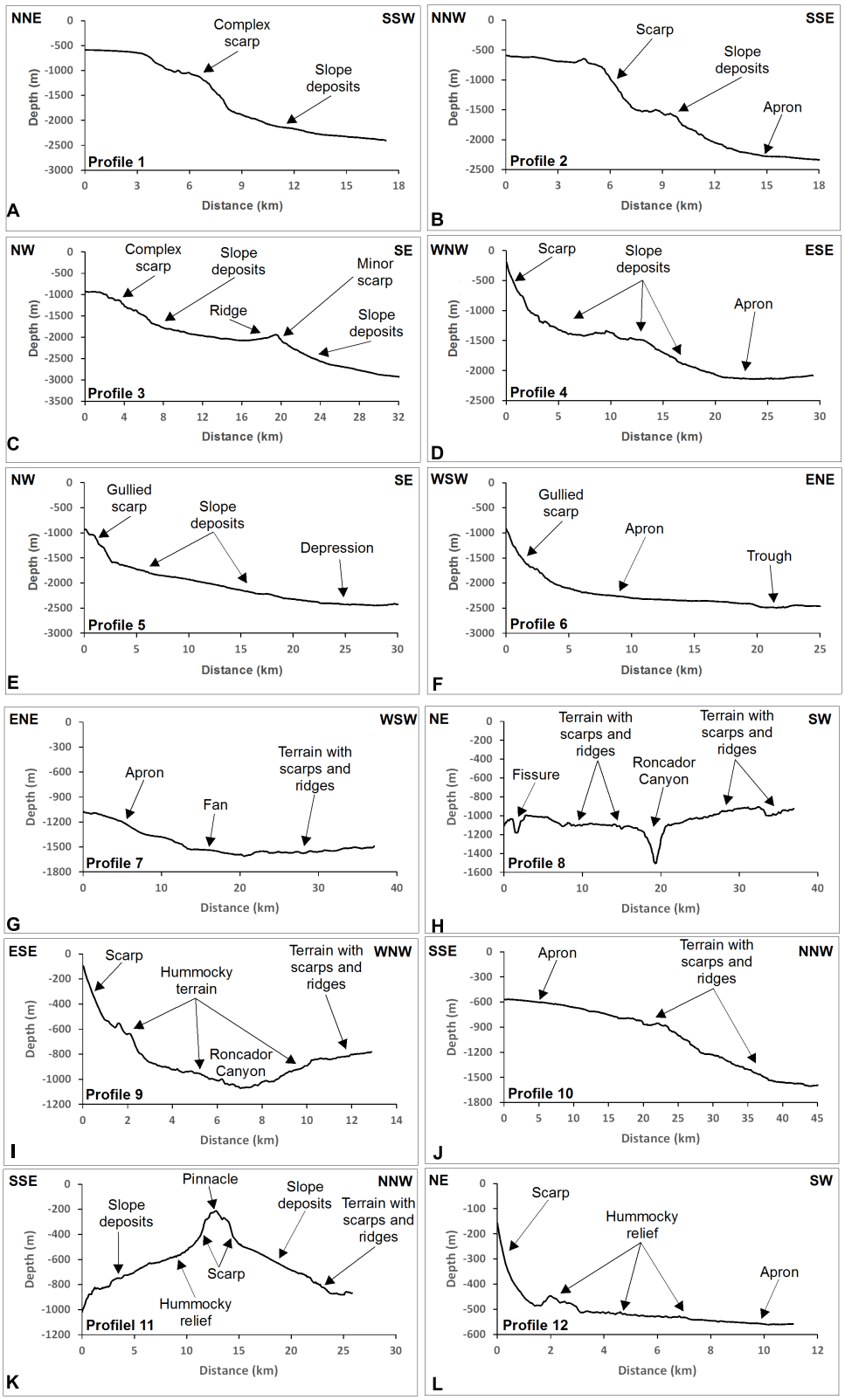

FIGURE 9 | Bathymetric profiles showing the main geomorphological features of Roncador Bank and adjacent areas. **(A–C)** Southern escarpment. **(D–F)** Eastern escarpment. **(G–I)** Northwestern sector. **(J–L)** Western sector. See **Figure 2** for the profiles location.

corresponds to a volcanic fissure, that is, a fracture filled by volcanic material.

On the other hand, the presence of a series of embayments along the upper flanks and a belt of slope deposits along the lower parts of the escarpments provide evidence that erosion and sedimentation processes have been important in the evolution of the Roncador volcanic edifice. In fact, erosive processes seem to prevail over the upper and middle parts of the Roncador escarpments, which in consequence results in active supplying of sediments downslope. Some authors have suggested that the overall slope geometry relates to the underlying lithology and to the prevailing sediment transport mechanisms (e.g., Adams et al., 1998; Adams and Schlager, 2000). For example, Adams and Kenter (2014) established that concave slope profiles are common in carbonate settings, as this type of lithology tends to build steeper slopes than their siliciclastic counterparts. The observation of some concave profiles in both southern and eastern escarpments of Roncador (**Figures 9B,D,F,I,L**), in association with the presence of steep slopes and high to intermediate backscatter intensities, indicates that the upper flanks are predominantly made of hard substrate, limestone and/or volcanic rock. Also, some bathymetric profiles clearly show the change from a zone exhibiting concave, steep slopes to a zone showing convex, gentler slopes or, in some cases, alternating concave-convex slopes (**Figures 9B,D,L**). This marks the transition from an erosive regime in the upper part of the escarpments to a depositional regime toward the seamount base. The steep slopes of the escarpments (up to 40°) favors the concentration of mass wasting processes, which is evident by the occurrence of a dense network of gullies parallel to the slope. These gullies serve as conduits for the sedimentary material that moves from the shallower parts to the foot of the seamount, where it is deposited forming sediment bodies in the form of lobes and cones.

Development and survival of submarine canyons rely on the availability of a proximal source of sediment, and appropriate sediment transport mechanisms, such as ocean currents and mass wasting (Normandeau et al., 2014; Puig et al., 2014). We have determined that the Roncador Canyon originates on the northwestern flank of Roncador edifice and runs to the northwest for approximately 35 km. Therefore, the proximal and direct sediment source for the canyon is the western slope of the seamount and atoll rim, which implies that downslope erosive flows have played a role in the canyon evolution. The canyon upper reach is covered by an extensive debris-avalanche deposit, recognized by its typical hummocky morphology. This deposit is incised by a series of gullies which flow into the Roncador Canyon. From our analysis, we were able to infer that Roncador western flank have been, and likely are actively providing sediments downslope to Roncador Canyon, by means of the gullies, which act as channels funneling sediment from the upper parts of the atoll toward the canyon. Two facts further support this hypothesis. First, the high backscatter intensities observed along the gullies and the canyon thalweg (**Figure 7A**), implying that these conduits are sediment starved. Second, the presence of a fan in the canyon mouth (**Figures 8B,D**), produced by depositation of the sediment transported through the gullies and canyon. Roncador Canyon and its feeder gullies, as well as the gully networks present in the southern and eastern escarpments of Roncador edifice originated from gravity flows whose source could be mass wasting processes and/or cascading, dense-water flows. The first is supported by the common observation of slide scars in the heads of gullies and canyons. The presence of several water masses in the Roncador area, the CSW up to 50–75 m depth and the SSW between 150 and 200 m (Coralina-Invemar, 2012), accounts for the possibility of dense-water flows. The depth range of the transition between these two water masses is very similar to the depth of the atoll outer rim where the shelf-break is located. Several works have reported the strong influence of dense water cascades-triggered gravity flows in the formation and evolution of gullies and canyons (e.g., Canals et al., 2006; Micallef and Mountjoy, 2011).

It is widely established from numerous studies (e.g., Rebesco et al., 2014; Ercilla et al., 2016) that bottom currents strongly shape the seafloor through erosion, transport and deposition. In the ASAPSC area, Coralina-Invemar (2012) has reported the existence of at least four water masses: CSW, SSW, SIW, and NADW. Although the depth ranges to which these water bodies extend are relatively well constrained, their present-day circulation patterns (directions and velocities) have not yet been measured, particularly the deeper flows, such as SIW and NADW. Thus, it is necessary to undertake physical oceanography studies to characterize the dynamic behavior of deep water flows in order to establish the significance of bottom current processes in shaping the ASAPSC deep-sea morphology. Having in mind that water masses that circulate in modern oceans and seas are able to transport sediment over long distances, and their bottom component can re-suspend and advect eroded seafloor (Ercilla et al., 2016), the link between the ASAPSC deep currents and some morphological features described in Roncador area (such as escarpments, sedimentary aprons, canyons and gullies, among others) should be addressed.

It is well known that seamounts or volcanic islands are highly susceptible to partial collapses of their edifices, mainly due to the high slope gradients, intense fracturing, chemical weathering associated with volcanic processes, earthquake activity, among other causes (Fairbridge, 1950; Ui, 1983; Siebert, 1984). Commonly, this type of collapse produces debris avalanches, whose deposits typically exhibit hummocky morphology (e.g., Moore et al., 1989; Le Friant et al., 2009). In this study, we identified a terrain with hummocky structure located in the western sector of Roncador, evidence of a partial collapse of that sector of the seamount. Geister and Díaz (2007) reported that the Roncador western platform margin is formed by an almost continuous vertical to overhanging cliff plunging from an 18 m deep shelf-edge into the ocean, which appears to have formed by break-off of the outer shelf margins. Here, the atoll rim is characterized by a major arcuate bight-like geometry, widely recognized as the morphological expression of large submarine failures (Fairbridge, 1950; Terry and Goff, 2013).

In contrast to the Roncador southern and eastern flanks, which are limited by large escarpments, toward the northwestern sector the seamount extends through a relatively gentle surface with irregular relief due to the presence of multiple minor

scarps and ridges. This terrain could correspond to an extensive sedimentary deposit product of the collapse of the Roncador northwestern flank, where the scarps and ridges may represent deformational structures generated at the moment of the material deposition. Detailed studies are necessary to confirm or refute this hypothesis.

Regarding potential geohazards, the recognition of a partial collapse event of the Roncador volcanic edifice implies the possible occurrence of landslide-triggered tsunamis in the geological past. This hypothesis is further supported by the presence of very large limestone boulders on the Roncador western outer reef flat, which must have been deposited by extremely high-energy events, such as tsunamis, although storm surges should not be discarded. Other platform margin failures, evidenced by a series of steep escarpments, have been identified in the southeastern sector of San Andres Island, the northwestern sector of Providencia Island, and the western flank of Serrana bank (Geister and Díaz, 2007). For all these previous cases, Idárraga-García et al. (under review) identified the corresponding landslide deposits in the deeper marine areas. The occurrence of a tsunami event today could have an important impact on the neighboring and densely populated islands of San Andres, Providencia and Santa Catalina, so it is very important to promote detailed analysis of the tsunamigenic potential in the area, related mainly to underwater landslide events.

According to Rogers (1994), seamounts have been thought to play an important role in patterns of marine biogeography, support high biodiversity and host unique biological communities. Differences in seamount seabed morphology influence hydrodynamic flow patterns and therefore the deposition of sediment and organic matter (Clark et al., 2010). In Roncador, we have determined that the seamount is limited to the south and east by two escarpments, which exhibit steep slopes (between 18° and 25°, locally reaching 40°) that are mostly bare rock. The same characteristics are shared by the two volcanic pinnacles located to the southwest of the study zone. There is growing evidence that submarine features exhibiting abrupt slope angles host a variety of species assemblages as well as high abundances of certain species of cold-water corals (Huvenne et al., 2011; Robert et al., 2015, 2017). This situation has an effect in the distribution and abundance of benthic and sessile fauna in Roncador, and it is an issue that must be studied in detail, since at present there is no research that addresses the close relationship between geomorphology and the biological communities in the SeaFlower zone, at least in its deep environments.

Also, in this work we reported and described in detail some other morphologic features which have important implications on future biodiversity and ecosystem research in the archipelago. For example, the Roncador Canyon, which runs for approximately 35 km and exhibits maximum widths of 8.7 km and depths of 430 m beneath the surrounding seafloor. It is well known that unusual physical oceanographic conditions inside submarine canyons increase suspended particulate matter concentrations and transport of organic matter from coastal zones to the deep ocean (Bosley et al., 2004; Genin, 2004; Canals et al., 2006). These processes are responsible for enhancing both pelagic and benthic productivity inside canyon habitats as well as biodiversity of many benthic faunal groups (Rowe et al., 1982; Vetter et al., 2010). Also, there is increasing evidence of how canyons benefit and support fisheries (Yoklavich et al., 2000), enhance carbon sequestration and storage (Epping et al., 2002; Canals et al., 2006; Masson et al., 2010), provide nursery and refuge sites for other marine life, including vulnerable ecosystems and essential fish-habitats such as cold-water corals and sponge fields (De Leo et al., 2010; Fernandez-Arcaya et al., 2013; Davies et al., 2014). Therefore, the Roncador Canyon should be considered as a geomorphological feature of primary interest to establish its influence on the circulation patterns of deep sea currents, and consequently its relationship with the presence of certain types of ecosystems.

CONCLUSION

The analysis of high-resolution bathymetric information acquired recently in the SBR (Archipelago of San Andres, Providencia and Santa Catalina) allowed us to describe in detail the underwater morphology of Roncador Bank and adjacent areas. The results obtained in this study support the volcanic origin of the Roncador seamount and the influence of faults (e.g., Roncador Southern Fault and Roncador Eastern Fault) on the ocean floor that acted as zones of weakness that allowed the volcanic material to penetrate the oceanic crust and reach the surface. We suggest that these faults are probably active and therefore seismogenic potential that must be analyzed in order to better assess the seismic risk for the ASAPSC. Also, we were able to determine that erosion and sedimentation processes have played an important role in the evolution of Roncador area. Debris-avalanche deposits were identified as a result of partial collapses of the volcanic edifice. Such mass-wasting has not only acted as shaping agents for the seamount morphology, but also as potential generators of tsunamis in the geological past. Due to this, detailed studies must be carried out to advance the knowledge of geohazards due to landslide-related tsunamis.

Finally, the results presented here contribute significantly to the basic knowledge of the geology and geomorphology of Roncador and adjacent areas, with direct applications in ecosystem characterization, geohazards assessment, and territory management.

AUTHOR CONTRIBUTIONS

HL carried out the pre-processing of the raw multibeam data and prepared the DTMs. He also contributed to the preparation of the manuscript. JI-G carried out the geological interpretation of the bathymetric data and prepared the figures and the manuscript.

FUNDING

This study was funded by the Administrative Department of Science, Technology and Innovation of Colombia (COLCIENCIAS) by means of the National Program for Financing Science, Technology and Innovation "Francisco

José de Caldas" and "Colombia BIO" project. JI-G thanks COLCIENCIAS for funding his postdoctoral position at the Oceanographic and Hydrographic Research Center of Colombia (CIOH).

ACKNOWLEDGMENTS

This research was developed within the framework of the National Plan for Scientific Expeditions "SeaFlower." We are very grateful with DIMAR-CIOH for the permission to use the multibeam bathymetric dataset. We deeply thank the scientific crew onboard the vessel ARC Malpelo for the acquisition and preprocessing of the bathymetry data. Also, many thanks to the Editors of the special topic "SeaFlower Biosphere Reserve: New Findings and Trends in the Largest Caribbean Marine Protected Area" for giving us the opportunity to publish our work, and to the reviewers for the suggestions made to improve the manuscript.

REFERENCES

Adams, E. W., and Kenter, J. A. (2014). So different, yet so similar: comparing and contrasting siliciclastic and carbonate slopes. Deposits, architecture and controls of carbonate margin, slope and basinal settings. *SEPM Spec. Publ.* 105, 14–25.

Adams, E. W., and Schlager, W. (2000). Basic types of submarine slope curvature. *J. Sediment. Res.* 70, 814–828. doi: 10.1306/2DC4093A-0E47-11D7-8643000102C1865D

Adams, E. W., Schlager, W., and Wattel, E. (1998). Submarine slopes with an exponential curvature. *Sediment. Geol.* 117, 135–141. doi: 10.1016/S0037-0738(98)00044-X

Bosley, K. L., Lavelle, J. W., Brodeur, R. D., Wakefield, W. W., Emmett, R. L., Baker, E. T., et al. (2004). Biological and physical processes in and around Astoria Submarine Canyon, Oregon, USA. *J. Mar. Syst.* 50, 21–37. doi: 10.1016/j.jmarsys.2003.06.006

Burke, K., Cooper, C., Dewey, J. F., Mann, P., and Pindell, J. L. (1984). Caribbean tectonics and relative plate motions. *Geol. Soc. Am. Bull.* 162, 31–63. doi: 10.1130/MEM162-p31

Canals, M., Puig, P., Durrieu de Madron, X., Heussner, S., Palanques, A., and Fabres, J. (2006). Flushing submarine canyons. *Nature* 444, 354–357. doi: 10.1038/nature05271

Carvajal-Arenas, L. C., and Mann, P. (2018). Western Caribbean intraplate deformation: defining a continuous and active microplate boundary along the San Andres rift and Hess Escarpment fault zone, Colombian Caribbean Sea. *AAPG Bull.* 102, 1523–1563. doi: 10.1306/12081717221

Case, J. E., MacDonald, W. D., and Fox, P. J. (1990). "Caribbean crustal provinces: seismic and gravity evidence," in *The Geology of North America*, Vol. H, eds G. Dengo and J. E. Case (Boulder, CO: The Geological Society of America), 15–36.

Clark, M. R., Rowden, A. A., Schlacher, T., Williams, A., Consalvey, M., Stocks, K. I., et al. (2010). The ecology of seamounts: structure, function, and human impacts. *Ann. Rev. Mar. Sci.* 2, 253–278. doi: 10.1146/annurev-marine-120308-081109

Coralina-Invemar (2012). *Atlas De La Reserva De Biósfera SeaFlower. Archipiélago De San Andrés, Providencia Y Santa Catalina. Instituto De Investigaciones Marinas Y Costeras "José Benito Vives De Andréis" INVEMAR- Y Corporación para el Desarrollo Sostenible Del Archipiélago De San Andrés, Providencia Y Santa Catalina -CORALINA-. Serie De Publicaciones Especiales De INVEMAR # 28.* Colombia: Santa Marta, 180.

Davies, J. S., Howell, K. L., Stewart, H. A., Guinan, J., and Golding, N. (2014). Defining biological assemblages (biotopes) of conservation interest in the submarine canyons of the south west approaches (offshore United Kingdom) for use in marine habitat mapping. *Deep Sea Res. II Top. Stud. Oceanogr.* 104, 208–229. doi: 10.1016/j.dsr2.2014.02.001

De Leo, F. C., Smith, C. R., Rowden, A. A., Bowden, D. A., and Clark, M. R. (2010). Submarine canyons: hotspots of benthic biomass and productivity in the deep sea. *Proc. R. Soc. Lond. B Biol. Sci.* 277, 2783–2792. doi: 10.1098/rspb.2010.0462

Di Traglia, F., Morelli, S., Casagli, N., and Garduño Monroy, V. H. (2014). Semi-automatic delimitation of volcanic edifice boundaries: validation and application to the cinder cones of the Tancitaro-Nueva Italia region (Michoacán-Guanajuato Volcanic Field, Mexico). *Geomorphology* 219, 152–160. doi: 10.1016/j.geomorph.2014.05.002

Epping, E., van der Zee, C., Soetaert, K., and Helder, W. (2002). On the oxidation and burial of organic carbon in sediments of the Iberian margin and Nazaré Canyon (NE Atlantic). *Prog. Oceanogr.* 52, 399–431. doi: 10.1016/S0079-6611(02)00017-4

Ercilla, G., Juan, C., Hernández-Molina, F. J., Bruno, M., Estrada, F., Alonso, B., et al. (2016). Significance of bottom currents in deep-sea morphodynamics: an example from the Alboran Sea. *Mar. Geol.* 378, 157–170. doi: 10.1016/j.margeo.2015.09.007

Fairbridge, R. W. (1950). Landslide patterns on oceanic volcanoes and atolls. *Geog. J.* 45, 84–88. doi: 10.2307/1789022

Favalli, M., and Fornaciai, A. (2017). Visualization and comparison of DEM-derived parameters. application to volcanic areas. *Geomorphology* 290, 69–84. doi10.1016/j.geomorph.2017.02.029

Fernandez-Arcaya, U., Rotllant, G., Ramirez-Llodra, E., Recasens, L., Aguzzi, J., and Flexas, M. D. M. (2013). Reproductive biology and recruitment of the deep-sea fish community from the NW Mediterranean continental margin. *Prog. Oceanogr.* 118, 222–234. doi: 10.1016/j.pocean.2013.07.019

Geister, J. (1992). Modern reef development and Cenozoic evolution of an oceanic island/reef complex: isla de Providencia (western Caribbean Sea, Colombia). *Facies* 27, 1–69. doi: 10.1007/BF02536804

Geister, J., and Díaz, J. M. (2007). *Reef Environments and Geology of an Oceanic Archipelago: San Andres, Old Providence and Sta. Catalina (Caribbean Sea, Colombia)*. Colombia: Boletín Geológico Instituto Nacional de Investigaciones Geológico Mineras de, 142.

Genin, A. (2004). Bio-physical coupling in the formation of zooplankton and fish aggregations over abrupt topographies. *J. Mar. Syst.* 50, 3–20. doi: 10.1016/j.jmarsys.2003.10.008

Hallock, P., Hine, A. C., Vargo, G. A., Elrod, J. A., and Jaap, W. C. (1988). Platforms of the nicaraguan rise: examples of the sensitivity of carbonate sedimentation to excess trophic resources. *Geology* 16, 1104–1107. doi: 10.1130/0091-7613(1988)016<1104:POTNRE>2.3.CO;2

Holcombe, T. L., Ladd, J. W., Westbrook, G., Edgar, N. T., and Bowland, C. L. (1990). "Caribbean marine geology: ridges and basins of the plate interior," in *The Geology of North America*, Vol. H, eds G. Dengo and J. E. Case (Boulder, CO: The Geological Society of America:), 231–306.

Huvenne, V. A. I., Tyler, P. A., Masson, D. G., Fisher, E. H., Hauton, C., Hühnerbach, V., et al. (2011). A picture on the wall: innovative mapping reveals cold-water coral refuge in submarine canyon. *PLoS One* 6:e28755. doi: 10.1371/journal.pone.0028755

Jenness, J. (2013). *DEM Surface Tools for ArcGIS (Version 2.1.399)*. Available at: http://www.jennessent.com/arcgis/surface_area.htm

Le Friant, A., Boudon, G., Arnulf, A., and Robertson, R. E. A. (2009). Debris avalanche deposits offshore St. Vincent (West Indies): impact of flank-collapse events on the morphological evolution of the island. *J. Volcanol. Geotherm. Res.* 179, 1–10. doi: 10.1016/j.jvolgeores.2008.09.022

Mann, P., and Burke, K. (1984). Neotectonics of the Caribbean. *Rev. Geophys. Space Phys.* 22, 309–362. doi: 10.1029/RG022i004p00309

Masson, D. G., Huvenne, V. A. I., de Stigter, H. C., Wolff, G. A., Kiriakoulakis, K., and Arzola, R. G. (2010). Efficient burial of carbon in a submarine canyon. *Geology* 38, 831–834. doi: 10.1130/G30895.1

Mauffret, A., and Leroy, S. M. (1997). Seismic stratigraphy and structure of the Caribbean igneous province. *Tectonophysics* 283, 61–104. doi: 10.1016/S0040-1951(97)00103-0

Micallef, A., and Mountjoy, J. J. (2011). A topographic signature of a hydrodynamic origin for submarine gullies. *Geology* 39, 115–118. doi: 10.1130/G31475.1

Milliman, J. D. (1969). Four southwestern caribbean atolls: courtown cays, albuquerque cays, roncador bank and serrana bank. *Atoll Res. Bull.* 129, 1–26. doi: 10.5479/si.00775630.129.1

Milliman, J. D., and Supko, P. R. (1968). On the geology of san andres island, western caribbean. *Geol. En Mijnbouw* 47, 102–105.

Mitchell, R. C. (1955). Geologic and petrographic notes on the colombian islands of la providencia and san andres, west indies. *Geol. En Mijnbouw* 17, 76–83.

Moore, J. G., Clague, D. A., Holcomb, R. T., Lipman, P. W., Normark, W. R., and Torresan, M. E. (1989). Prodigious submarine landslides on the hawaiian ridge. *J. Geophys. Res.* 94, 17465–17484. doi: 10.1029/JB094iB12p17465

Normandeau, A., Lajeunesse, P., St-Onge, G., Bourgault, D., Drouin, S. S.-O., Senneville, S., et al. (2014). Morphodynamics in sediment-starved inner-shelf submarine canyons (Lower St. Lawrence Estuary, Eastern Canada). *Mar. Geol.* 357, 243–255. doi: 10.1016/j.margeo.2014.08.012

Olaya, V. (2009). "Basic land-surface parameters," in *Geomorphometry: Concepts, Software, Applications, Developments in Soil Science*, eds T. Hengl and H. I. Reuter (Amsterdam: Elsevier), 141–169.

Puig, P., Palanques, A., and Martín, J. (2014). Contemporary sediment-transport processes in submarine canyons. *Annu. Rev. Mar. Sci.* 6, 53–77. doi: 10.1146/annurev-marine-010213-135037

Rebesco, M., Hernández-Molina, J., van Rooij, D., and Wåhlin, A. (2014). Contourites and associated sediments controlled by deep-water circulation processes: state-of-the-art and future considerations. *Mar. Geol.* 352, 111–154. doi: 10.1016/j.margeo.2014.03.011

Robert, K., Huvenne, V. A. I., Georgiopoulou, A., Jones, D. O. B., Marsh, L., Carter, G. D. O., et al. (2017). New approaches to high-resolution mapping of marine vertical structures. *Sci. Rep.* 7:9005. doi: 10.1038/s41598-017-09382-z

Robert, K., Jones, D. O. B., Tyler, P. A., Van Rooij, D., and Huvenne, V. A. I. (2015). Finding the hotspots within a biodiversity hotspot: finescale biological predictions within a submarine canyon using high-resolution acoustic mapping techniques. *Mar. Ecol.* 36, 1256–1276. doi: 10.1111/maec.12228

Rogers, A. D. (1994). The biology of seamounts. *Adv. Mar. Biol.* 30, 305–351. doi: 10.1016/S0065-2881(08)60065-6

Rowe, G. T., Polloni, P. T., and Haedrich, R. L. (1982). The deep-sea macrobenthos on the continental margin of the Northwest Atlantic Ocean. *Deep Sea Res. A* 29, 257–278. doi: 10.1016/0198-0149(82)90113-3

Siebert, L. (1984). Large volcanic debris avalanches: characteristics of source areas, deposits, and associated eruptions. *J. Volcanol. Geotherm. Res.* 22, 163–197. doi: 10.1016/0377-0273(84)90002-7

Tabares, N., Soltau, J., Díaz, J., David, D., and Landazábal, E. (2009). *Características Geomorfológicas Del Relieve Submarino En El Caribe Colombiano. En: Dimar-CIOH (Eds). Geografía Submarina Del Caribe Colombiano. Serie de Publicaciones Especiales*, Vol. 4. Colombia: CIOH, 150.

Terry, J. P., and Goff, J. (2013). One hundred and thirty years since darwin: 'Reshaping' the theory of atoll formation. *Holocene* 23, 615–619. doi: 10.1177/0959683612463101

Ui, T. (1983). Volcanic dry avalanche deposits—identification and comparison with nonvolcanic debris stream deposits. *J. Volcanol. Geotherm. Res.* 18, 135–150. doi: 10.1016/0377-0273(83)90006-9

Vetter, E. W., Smith, C. R., and De Leo, F. C. (2010). Hawaiian hotspots: enhanced megafaunal abundance and diversity in submarine canyons on the oceanic islands of Hawaii. *Mar. Ecol.* 31, 183–199. doi: 10.1111/j.1439-0485.2009.00351.x

Wadge, G., and Wooden, J. (1982). Late Cenozoic alkaline volcanism in the northwestern caribbean: tectonic setting and Sr isotopic characteristics: earth and planet. *Sci. Lett.* 57, 35–46. doi: 10.1016/0012-821X(82)90171-6

Wood, J. (1996). *The Geomorphological Characterization of Digital Elevation Models*. Ph.D. thesis, University of Leicester, UK, 185.

Yoklavich, M. M., Greene, H. G., Cailliet, G. M., Sullivan, D. E., Lea, R. N., and Love, M. S. (2000). Habitat associations of deep-water rock fishes in a submarine canyon: an example of a natural refuge. *Fish. Bull. Natl. Ocean. Atmosphere. Adm.* 98, 625–641.

Conflict of Interest Statement: The authors declare that the research was conducted in the absence of any commercial or financial relationships that could be construed as a potential conflict of interest.

frontiers in Marine Science

ORIGINAL RESEARCH
published: 26 February 2019
doi: 10.3389/fmars.2019.00073

Steady Decline of Corals and Other Benthic Organisms in the SeaFlower Biosphere Reserve (Southwestern Caribbean)

Juan Armando Sánchez†, Matías Gómez-Corrales†, Lina Gutierrez-Cala, Diana Carolina Vergara, Paula Roa, Fanny L. González-Zapata, Mariana Gnecco, Nicole Puerto, Lorena Neira and Adriana Sarmiento*

Laboratorio de Biología Molecular Marina (BIOMMAR), Departamento de Ciencias Biológicas, Facultad de Ciencias, Universidad de los Andes, Bogotá, Colombia

OPEN ACCESS

Edited by:
Rochelle Diane Seitz, College of William & Mary, United States

Reviewed by:
Carlos Jimenez, Enalia Physis Environmental Research Centre (ENALIA), Cyprus
Nikolaos V. Schizas, University of Puerto Rico at Mayagüez, Puerto Rico

***Correspondence:**
Juan Armando Sánchez
juansanc@uniandes.edu.co

† These authors have contributed equally to this work

Specialty section:
This article was submitted to Marine Conservation and Sustainability, a section of the journal Frontiers in Marine Science

Received: *31 July 2018*
Accepted: *08 February 2019*
Published: *26 February 2019*

Citation:
Sánchez JA, Gómez-Corrales M, Gutierrez-Cala L, Vergara DC, Roa P, González-Zapata FL, Gnecco M, Puerto N, Neira L and Sarmiento A (2019) Steady Decline of Corals and Other Benthic Organisms in the SeaFlower Biosphere Reserve (Southwestern Caribbean). Front. Mar. Sci. 6:73. doi: 10.3389/fmars.2019.00073

Coral reef decline persists as a global issue with ties to climate change and human footprint. The SeaFlower Biosphere reserve includes some of the most isolated oceanic coral reefs in the Southwestern Caribbean, which provide natural experiments to test global and/or basin-wide factors affecting coral reefs. In this study, we compared coral and other substrate cover (algae, cyanobacteria, and octocorals), along population densities of keystone urchin species from two atolls (Serrana and Roncador Banks), during 1995, 2003, and 2015/2016. We also surveyed benthic foraminifera as a water quality proxy for coral growth in the last period. A steady reduction in coral cover was clearly observed at Roncador's lagoon, but not at Serrana's reefs, with significant differences between 1995 and 2015/2016. Percent cover of fleshy algae decreased significantly also at Roncador between 1995 and 2003 but did not change notably from 1995 to 2016 at Serrana. However, both Banks exhibited a loss in crustose coralline algae from 2003 to 2015/2016. Likewise, a reduction in bottom complexity, measured as bottom rugosity, was evident between 1995 and 2003. Roncador Bank had unprecedented high octocoral densities, which increased almost threefold from 2003 to 2015. In contrast, urchin densities were low in Roncador; only *Diadema antillarum* increased from 2003 to 2016 in Serrana Bank. The Foraminifera in Reef Assessment and Monitoring (FORAM) Index (FI) in the two Banks was below the range expected for healthy coral reefs. Although both Banks follow a reduction in CCA and CA cover, Roncador Bank also faces an alarming decline in coral cover, urchins and bottom complexity (rugosity) in contrast to increases in octocoral densities and potential loss of resilience and eutrophication suggested by the FI index. These unexpected findings led us to consider and discuss potential outcomes, where these reefs deteriorate (i.e., erode and drown) providing ideal conditions for octocoral growth. Hence, it is of utmost urgency to start monitoring reef budgets, octocorals and nutrient sources.

Keywords: coral reefs, coral decline, Caribbean, algae cover, FORAM index, octocoral community, atoll, SeaFlower

INTRODUCTION

Marine biodiversity reaches its highest complexity in coral reefs. These formidable tropical ecosystems account for at least 30% of marine biodiversity at an extent of less than 1% of the planet's surface (Roberts et al., 2002). In addition to offering a seascape of indescribable beauty, they provide significant economic benefits to countries where they are found (Costanza et al., 1997), as well as providing coastal protection from storms (i.e., hurricanes) and waves (i.e., tsunamis) (Foster et al., 2013). Direct and indirect economic profit from tourism provided the exploitation of coral reef ecosystems around the world surpass 36 billion dollars a year (Spalding et al., 2017). Yet, coral reefs face unprecedented environmental challenges (Camp et al., 2018). Thermal anomalies in the oceans lead to coral bleaching and mortality (Hughes et al., 2003; Eakin et al., 2010). Of greatest concern, the increase of atmospheric carbon dioxide (CO_2) concentration alters seawater chemistry leading to ocean acidification, which includes adverse effects on the calcification rates of marine organisms including corals (Orr et al., 2005; Hoegh-Guldberg et al., 2007). These processes act in synergy with the human footprint, particularly increasing sewage and overexploitation, which reduces the resilience of marine ecosystems like coral reefs (Mumby, 2009; Graham et al., 2013; Wiedenmann et al., 2013). Failure to protect coral reefs will affect millions of livelihoods worldwide and provoke unparalleled rapid biodiversity losses in the years to come.

Biodiversity loss encompasses all marine coastal organisms (Hooper et al., 2012), in which coral reefs have become an emblematic instance of this global trend of ecosystem degradation. Recent trends, altering the composition of species assemblages at coastal marine environments (Dornelas et al., 2014), have raised new concerns about marine conservation because the emerging species turnover corresponds to less favorable ecosystem states in terms of productivity and services for humans (Pandolfi and Lovelock, 2014). Not understanding how marine communities react to many agents of deterioration and stress, climate change and human footprint, for example, prevents us from stopping degradation, managing and restoring vulnerable ecosystems like coral reefs (López-Angarita et al., 2014). In corals reefs, resilience and trophic functions appear greatly compromised (Jackson et al., 2001; Hughes et al., 2010). The worse-case scenario, in declining coral reefs, predicts high erosion and rising sea-levels leading to drowned reef structures with a few calcareous corals surviving and the hard bottom cover dominated by fleshy algae (Hughes et al., 2003; Hoegh-Guldberg et al., 2007, 2017; Perry et al., 2018). Are Caribbean coral reefs reaching this state?

The key players in coral reefs are set between top-down, grazing, and bottom-up, nutrient input controls (Littler et al., 2006). This relative dominance model allows an ideal coral-dominated shallow reef, including crustose coralline algae, under high grazing and low nutrient input (Littler and Littler, 2007). The worst case-scenario, under high nutrient input and low grazing, predicts a macroalgae dominated reef (Ledlie et al., 2007; Slattery and Lesser, 2014) or a sponge-dominated state, where dissolved organic matter is processed fueling higher trophic levels (De Goeij et al., 2013; McMurray et al., 2018). Reef decline in the Caribbean can be traced back to the time of Columbus, where reduction of herbivores like green turtles started, and more recently with the extinction of the monk seal and the mass mortalities of the black sea urchins and corals (Lessios et al., 1984; Hughes, 1994; Jackson, 1997). Basin-wide, Caribbean coral cover shrunk to 10% in less than three decades (Gardner et al., 2003). A combination of thermal anomalies, leading to coral bleaching and mortality (Eakin et al., 2010), overfishing of larger herbivores like parrotfishes (Paddack et al., 2009; Mumby et al., 2012; Loh et al., 2015), human footprint (Appeldoorn et al., 2016), including coastal pollution and eutrophication (Mora, 2008), and more recent invasive species (Lesser and Slattery, 2011; Albins and Hixon, 2013), reduced the resilience of coral reefs in the Caribbean like no other region in the world (Jackson et al., 2014).

Increased nutrient and sediment load in coastal areas are recognized as major drivers of coral reef deterioration worldwide (Fabricius, 2011; Sherman et al., 2016). In addition, coastal pollution can lead to disturbances in the coral microbiome and disease-related mortality (Klaus et al., 2007; Montilla et al., 2016). Traditional methods to evaluate reef condition do not effectively reflect the current water quality in terms of nutrients, due to a delayed response by the long-lived coral community and the associated costs of long-term monitoring (Cooper et al., 2009). Recently, the benthic foraminiferal assemblage has emerged as an economic and reliable alternative to assess water quality to support growth of symbiotic and calcifying organisms on coral reefs (Hallock et al., 2003). The "Foraminifera in Reef Assessment and Monitoring (FORAM) Index" (FI), is an efficient and cost-effective measure of water and sediment quality based on the assemblage of foraminiferal shells (Hallock, 2012). On oligotrophic and clear waters with abundance of hypercalcifying mixotrophs, such as hard corals, the shells of larger (symbiont-bearing) foraminifera account for a high proportion of sediment composition (Hallock, 1999). When nutrients increase the shells of smaller heterotrophic species dominate the assemblage, if conditions lead to accumulation of organic matter, stress-tolerant or opportunistic taxa can abound (Cockey et al., 1996).

Roncador and Serrana (locally known as "Islas Cayo," hereafter referred as Banks) comprise two of the few true Darwinian atolls in the Caribbean (**Figure 1**). Surrounded by depths of over two thousand meters, these atolls enclose shallow lagoons (5–15 m), where most of the coral growth stands (Milliman, 1969; Diaz et al., 1996b). An atoll is the climax of an oceanic coral reef complex developing on an extinct volcano (Darwin, 1842). The network-like distribution of patch reefs in these lagoons respond to their positioning with respect to the lagoonal terrace, a sand Bank off the back reef, and the water motion exposure (Geister and Díaz, 1996). These Banks have the same fractal patterning formed by corals at Indo-Pacific atolls' lagoons (Blakeway and Hamblin, 2015), which remarks the singularity of this type of reef formation in Caribbean reefs. This rare coral patch formation composed mostly of *Orbicella* (instead of *Acropora* in the Indo-Pacific) species (*O. annularis*, *O. faveolata* and *O. franksi*) with some colonies attaining large sizes (Diaz et al., 1996a; Sánchez et al., 2005; Foster et al., 2013). This habitat includes a different community of benthic

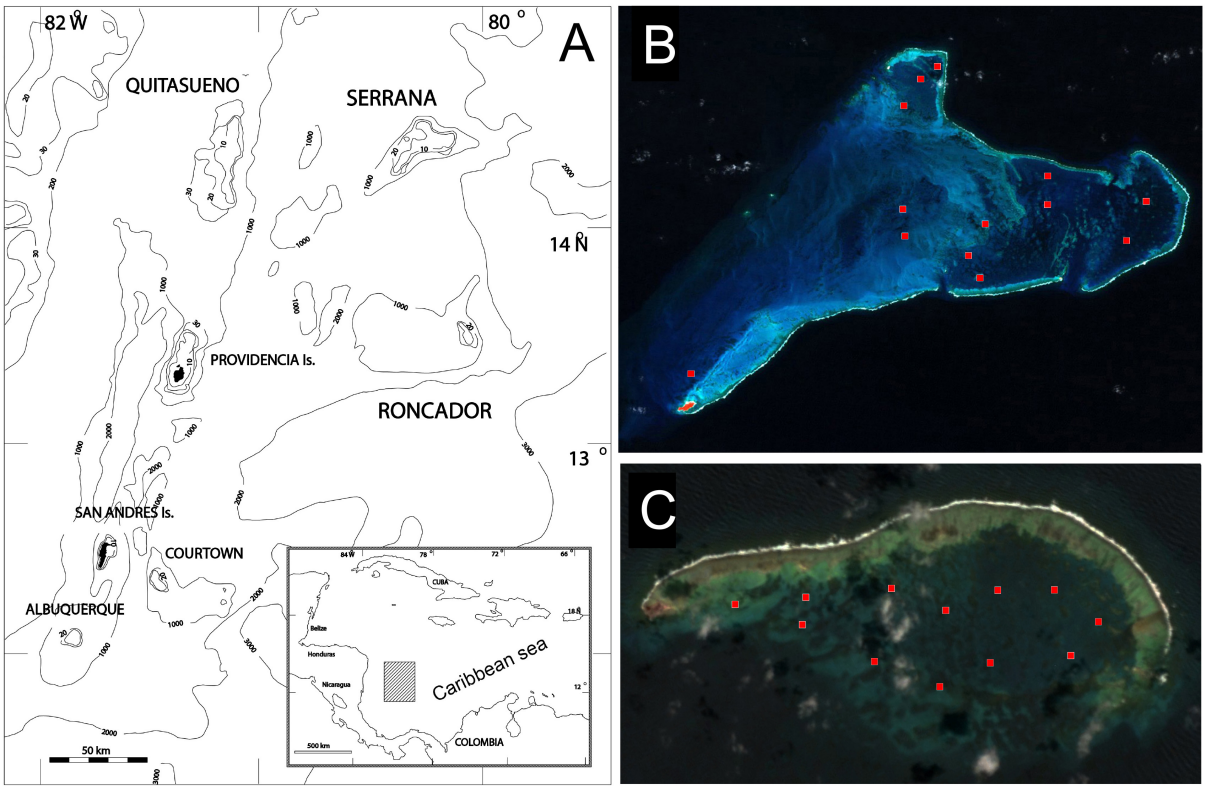

FIGURE 1 | Study area. **(A)** Partial map of the Southwestern Caribbean showing the geographical location of the studied Banks in the San Andrés, Providencia and Santa Catalina Archipelago (Colombia) and details of the study sites: **(B)** Serrana (2016) and **(C)** Roncador Banks (2015) (red squares, exact positions in the **Supplementary Table 1**) (Images from NASA).

organisms and fish compared to the deepest, most exposed external environments of the atolls and barrier reefs of the area (Sánchez et al., 1997a; Díaz-Pulido et al., 2004; Velásquez and Sánchez, 2015; Sánchez, 2016; Gonzalez-Zapata et al., 2018).

The SeaFlower Biosphere Reserve is the largest Marine Protected Area (MPA) in the Caribbean and the second in Latin-America (Guarderas et al., 2008). These include islands and cays, two barrier-reef systems and seven atolls similar to Roncador and Serrana (Diaz et al., 1996a; Sánchez et al., 2005). The geographic zoning of the MPA was the result of an exemplary collaboration between scientists, politicians, and community involvement since 1999 to 2005 (Friedlander et al., 2003; Sánchez et al., 2005; Schrope, 2008; Taylor et al., 2013; Ramirez, 2016). Due to the extension of the MPA, however, the area is rarely explored beyond the larger Islands, San Andrés, Providencia and Santa Catalina (Taylor et al., 2013). Quantitative surveys of corals and other benthic organisms began with scientific expeditions led by the research groups of Invemar funded by Colciencias in 1994–1995 (Diaz et al., 1996b; Sánchez et al., 1997a, 1998; Díaz-Pulido et al., 2004), following by planning of the MPA (Coralina- Gobernación del Archipiélago de San Andrés, Providencia y Santa Catalina-The Ocean Conservancy) between 2000 and 2003 (Friedlander et al., 2003; Sánchez et al., 2005) and recently thanks to a nation-wide interest (SeaFlower Expeditions: Comisión Colombiana del Océano-CCO/Dimar, Coralina, Gobernación del Archipiélago de San Andrés, Providencia y Santa Catalina [Secretaria de Pesca y Agricultura], ColombiaBIO-Colciencias and diverse Colombian universities and ONGs). This research aimed to study trends in coral and other substrate cover between similar sites in the lagoons within Serrana and Roncador Banks, using previously available data from 1995 to 2003 and combining it with data taken during the years 2015 and 2016. In addition, we estimated the FI to assess the effect of nutrient concentration on Serrana (2016) and Roncador (2015) Banks to support recruitment and proliferation of calcifying, photosynthesizing holobionts. These surveys spanned 20 years of change in Caribbean reefs, which provide an unprecedented long-term account of ecosystem trends in some of the most isolated reefs in the region.

MATERIALS AND METHODS

Study Area

Roncador Bank is an elongated atoll of about 13 km in length (NW-SW) and 6.5 km wide. The peripheral windward reef extends without interruption along its entire length (∼11 km), with considerable stretches of its crest emerging at low tides (**Figures 1A,B**). Serrana Bank is an extended Bank of triangular shape, originated from an annular atoll, which was partially dissected to leeward by subsidence of the sea floor. This

Bank measures 15.5 km in the SW-NE direction and 33.4 km in the W-N direction, where a well-developed, 50 km long, peripheral reef encloses a large lagoon basin by the N, E, and S, that connects by the W to the open sea (**Figure 1B**) (Milliman, 1969; Diaz et al., 1996a; Geister and Díaz, 1996; Díaz et al., 2000; Sánchez et al., 2005; Taylor et al., 2013). We revisited the area during September 2015 (Roncador, 12 sites: **Figure 1A**) and August 2016 (Serrana, 13 sites: **Figure 1B**). Details of sampling sites during May 1995 (Díaz-Pulido et al., 2004), April–May 2003 (Sánchez et al., 2005) and 2015/2016 (this study) are included in the **Supplementary Table 1**. The surveyed sites during 2015/2016 were positioned as close as possible to the previous expeditions using GPS coordinates (see **Supplementary Table 1**). The sheltered environments in these atolls include the highest relief environments in the lagoon and leeward terrace, with the largest coral cover and colony sizes (e.g., **Figure 2**).

Algae and Coral Cover

Algal and coral (scleractinian) percentage cover, as well as reef rugosity values were included from two previous studies taken in 1995 and 2003 (Díaz-Pulido et al., 2004; Sánchez et al., 2005). We measured reef rugosity as an environmental variable indicator of wave-motion energy and the chronic disturbance effect of waves (Aronson and Precht, 1995). Rugosity, a measurement of bottom topography also known as simple surface roughness index, which acts as a proxy of reef degradation (Bozec et al., 2015), was estimated from the ratio of linear length of a chain that was laid out in a straight line along the bottom following all the vertical relief to its length when stretched out 10 m (Sánchez et al., 1997b). We used a modified band transect technique (Dodge et al., 1982; Etnoyer et al., 2010) to estimate algae and coral cover during 2015 at Roncador and 2016 at Serrana. Equivalent methods for cover estimation were used in 1995 and 2003 surveys (Díaz-Pulido et al., 2004; Sánchez et al., 2005). At each site (See **Figures 1A,B** and **Supplementary Table 1** for details) a 25 m × 1 m band was surveyed using a 50 × 50 cm photoquadrat, which facilitated the quantification of the benthic components. Following the 2003 survey (Sánchez et al., 2005), the 50 × 50 cm quadrat was positioned four times in a square fashion to complete a 1 × 1 m quadrat, that was surveyed at 10 random points, to complete a total of 10 m^2 per band. For each site, algal and coral cover were estimated manually by digitizing the areas from the photo quadrats using ImageJ (Schneider et al., 2012; López-Angarita et al., 2014). Benthic cover was categorized as follows, hard coral (HC), crustose coralline algae (CCA), calcareous algae (CA), fleshy algae (FA), cyanobacteria (CB), other invertebrates, sponges, octocorals, rock, rubble and sand (see **Supplementary Table 1**). Hard corals included scleractinian and other hard corals such as *Millepora* spp. and *Stylaster roseus*. Algae genera for CA included *Amphiroa*, *Halimeda*, *Galaxaura* and *Penicillus*. Algae belonging to genera *Turbinaria*, *Caulerpa*, *Dyctiota*, *Lobophora*, *Mycrodictium* and *Sargassum* composed the FA category. We evaluated cover percentage differences in HC, CCA, CA, FA, CB and rugosity index (RI) per site at a mid-water reefs at Roncador (12–23 m) and shallow reefs at Serrana (2–13 m) across the 3 years of sampling, by obtaining bootstrapped (n = 1000 with replacement) confidence intervals (95% CI) for each mean (see **Supplementary Table 3**), to smooth confounding effects due to differences in sampling unbalanced sample sizes, repeated measures and seasonal variability. Data for cover percentage comparisons at Roncador mid-water reefs came from 8 stations (12–22 m) in 1995, 14 stations (12–23 m) in 2003 and 13 stations (8–18 m) in 2015. Likewise, data for the above comparisons at Serrana shallow reefs came from 12 stations (3–13 m) in 1995, 36 stations (2–13 m) in 2003 and 13 stations (2–11 m) in 2016.

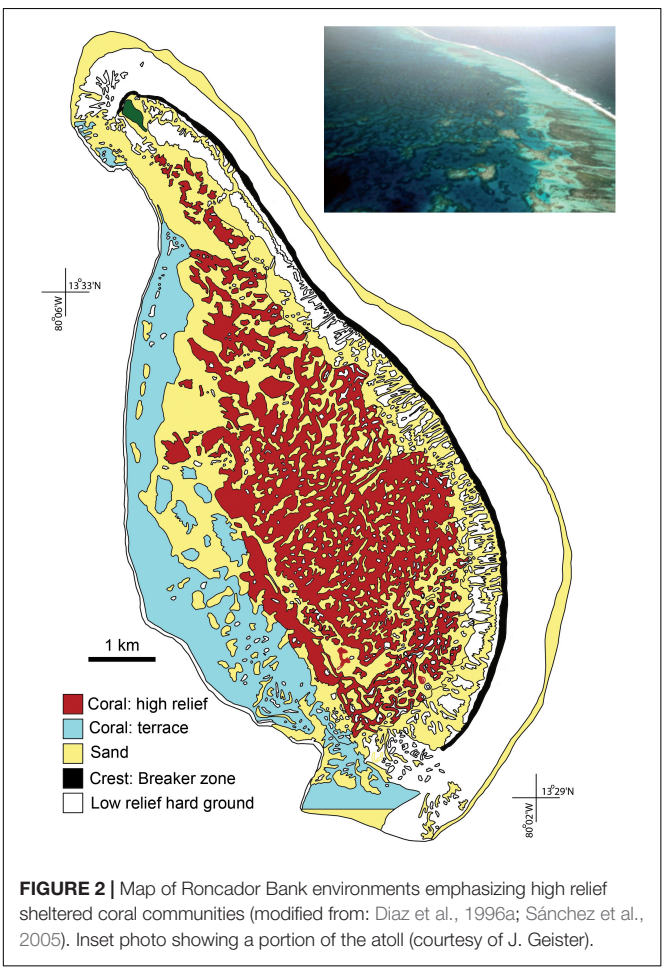

FIGURE 2 | Map of Roncador Bank environments emphasizing high relief sheltered coral communities (modified from: Diaz et al., 1996a; Sánchez et al., 2005). Inset photo showing a portion of the atoll (courtesy of J. Geister).

Octocoral Densities

In situ estimates of octocoral density in the quadrats were made by counting the individual erect colonies within each quadrat and then averaging the density values of the 10 random points for each surveyed station following the same methods as in 2003 (Sánchez and Wirshing, 2005; Sánchez et al., 2005; Etnoyer et al., 2010) (see **Supplementary Table 4**). Octocoral density changes were assessed by obtaining bootstrapped (n = 1000 with replacement) confidence intervals (95% CI) for each mean value (see **Supplementary Table 3**) at Roncador between 2003 and 2015, and Serrana between 2003 and 2016.

FORAM Index (FI)

During the expeditions to Roncador (2015) and Serrana (2016) Banks, samples of superficial sandy sediment were collected at four different sites in each Bank (6–12 m). The samples were stored in plastic containers (20 ml), fixed with absolute ethanol, subsequently dried (>24 h, 60°C) and thoroughly mixed. From each sample, we took a 0.1 g subsample, placed it in a 90 mm-diameter petri dish and examined it using a Leica EZ4 stereoscope. We removed and counted all foraminifera until a minimum of 150 individuals were found in all the samples combined for each station, excluding heavily worn and reworked specimens. The tests were placed onto cardboard micropaleontological faunal slides, counted, identified by genus and sorted into three functional groups: symbiont-bearing, opportunistic and other small heterotrophic taxa; the proportions of each functional groups were then used to calculate the average FI (Hallock et al., 2003). The FI ranges from 1 to 10, where FI < 2 indicates unfavorable conditions for coral growth, 2 < FI < 4 represents the limit for coral growth and unsuitable for recovery and FI > 4 permits coral growth and recovery.

Sea Urchin Densities

Sea urchin densities, namely of *Diadema antillarum* and *Echinometra viridis*, were estimated by counting the number of urchins within each quadrat along the transect, then averaging the density values for each surveyed station following the same methods as in 2003 (Coyer et al., 1993; Sánchez and Wirshing, 2005; Sánchez et al., 2005) (see **Supplementary Table 6**). We compared Sea urchin density by obtaining bootstrapped (n = 1000 with replacement) confidence intervals (95% CI) for each mean (see **Supplementary Table 3**) at Roncador between 2003 and 2015, and Serrana between 2003 and 2016.

RESULTS

Algae and Coral Cover

Roncador Bank mid-water reefs experienced a mean decline in CCA (10.13%) and FA (53.41%), but not HC (22.58%), from 1995 to 2015 (CCA: 2.15%, FA: 28.88%, HC: 9.85%). Mean CB increased significantly from 1995 (1.73%) to 2003 (13.20%) but decreased in 2015 (3.99%) close to its 1995 value. Mean CA did not change significantly over the three periods surveyed (6.51, 7.89, and 3.99%) at this Bank. Meanwhile, mean CCA in Serrana Bank shallow reefs from 1995 (5.05%) lowered significantly to 0.25% in 2016. During 2003 mean FA (48.53%) and HC (35.73%) reduced significantly as compared to 2003 period (FA: 25.83%, HC: 19.24%) in this Bank, but not when compared to 2016 (FA: 43.24%, HC: 20.88%). Mean CB significantly raised from 1995 (0.58%) to 2003 (9.15%) but fell back to 1.97% in 2016. (**Figure 3**, see **Supplementary Tables 1–3** for complete data sets). Cover by CA fell down from 6.5% in 1995 to 3.9% in 2015 at Roncador mid-water reefs, and from 7.3 to 3.2% at Serrana shallow reefs for the 1995–2016 period. CB reached its highest cover during 2003 at both Banks, 13.2% at Roncador and 9.2% at Serrana, while remaining below 5% at Roncador in 1995/2015 and 2% at Serrana in 1995/2016. CCA diminished from 10.1% in 1995 to 2.2% in 2015 at Roncador, and from 5.1 to 0.3% at Serrana from 1995 to 2016. FA was the highest at Roncador during 1995 with 53.4% but diminished by 24.5% in 2015, with a slight decline of 2.8% from 2003 to 2015. Similarly, HC cover at this Bank decrease from 22.6% in 1995 to 14.9% in 2003, and to 9.9% during 2016; a continuous reduction in HC cover of 12.7% over 20 years. FA at Serrana fluctuated from 48.5% in 1995 down to 25.8% in 2003 and then up to 43.2% in 2016. However, despite a 21.5% HC mean reduction at Serrana shallow reefs from 1995 to 2003, its HC cover did not differ significantly between 1995 and 2016, when reached a mean of 20.9%.

Based on the surveys performed in 1995 at Roncador Bank mid-water reefs (Díaz-Pulido et al., 2004), a total of 20.0% HC cover was attributed to *Orbicella franksi*, *Agaricia agaricites, O. annularis, Pseudodiploria strigosa, Colphophyllia natans, Siderastrea siderea, Montastraea cavernosa, Millepora alcicornis* and *Porites porites*. Comparing the datasets from the 2003 surveys taken at Roncador Bank, all previously reported species were present and dominant at mid-water reefs, with the exception of *P. astreoides* and *M. cavernosa*, but all species with an overall lower coral cover (15.5%). During 2015, the main coral species were *O. annularis, O. faveolata, A. agaricites*, *P. astreoides* and *O. franksi*. These species remained as the most abundant species despite an apparent decline of HC cover (12.7%) when compared to the 1995 dataset from Roncador Bank. On the other hand, Serrana Bank showed an apparent trend of loss and posterior recovery of HC cover. In 1995 this Bank's 32% of HC cover was represented by *Orbicella* spp., *A. agaricites, S. siderea*, *C. natans, Diploria labyrinthiformis* and *P. strigosa*. In 2003, *Orbicella* spp., *A. agaricites, S. siderea* along *P. astreoides* and *P. porites*, composed 15.5% of HC cover at this Bank. Lastly, in 2016 *O. annularis*, *O. faveolata*, *S. siderea*, *P. astreoides* and *Agaricia* spp. colonies composed over 17.0% of HC cover at Serrana shallow reefs, where *O. annularis* was the main responsible for the increase in mean HC cover, along the appearance of *Agaricia* spp. colonies in the quadrats.

There was an apparent decrease in rugosity at both Banks when comparing data sets between 1995 and 2003. However, there was not an apparent change in rugosity when comparing the datasets between 2003 and those taken in 2015/2016. (**Figure 4**). A 52 and 55% reduction of rugosity occurred at Roncador mid-water and Serrana shallow reefs from 1995 to 2015 and 2016, respectively.

Octocoral Densities

The density in Roncador ranged between 3.5 and 15.1 ind m^{-2} in 2003 and 11.3–68.5 ind m^{-2} in 2015, the highest value for Serrana only reached 13.9 ind m^{-2} in a survey during 2003 (see **Suplemmentary Table 4**). Although the octocoral densities between Roncador and Serrana showed strong spatial variation, their temporal patterns within surveyed sites are more complex. The highest value for octocoral density reported for 2003 was 15.1 ind m^{-2}, while in 2015 was 68.5 ind m^{-2}, almost 5 times the highest value in 2003. At Roncador Bank, octocoral density increased from 11.2 ind m^{-2} during 2003 to 36.4 ind m^{-2} in 2015, a 225% increment. Contrarily, Serrana Bank did not change its octocoral density over a 11-year span, with 1.9 ind m^{-2} in

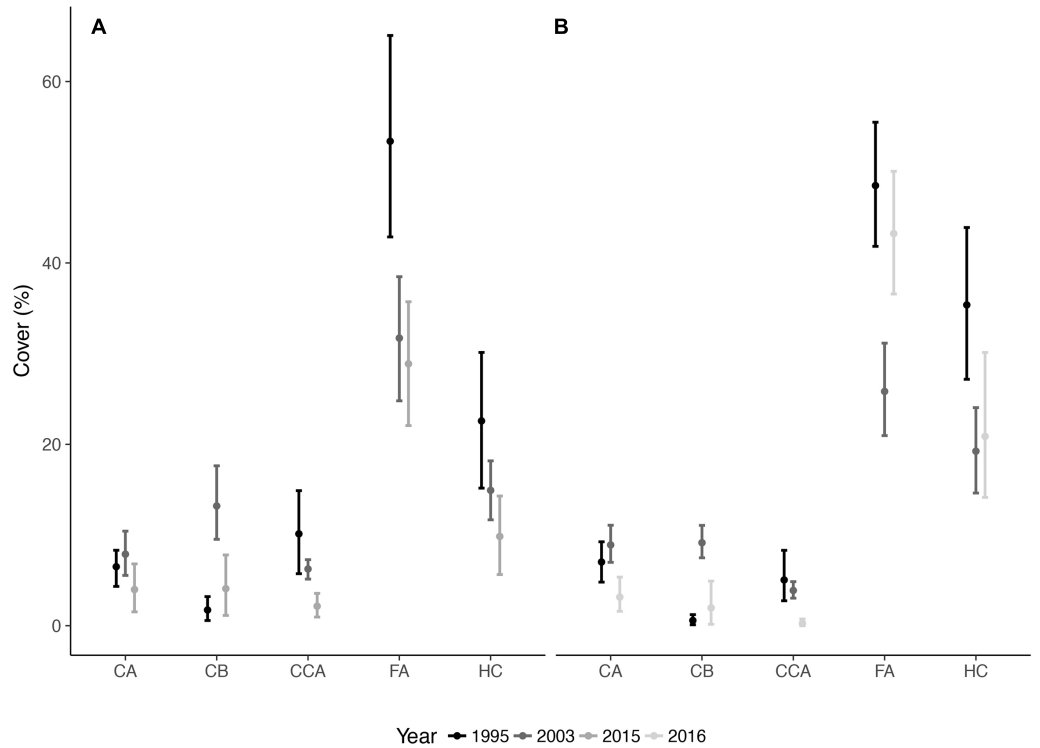

FIGURE 3 | Calcareous algae (CA), cyanobacteria (CB), crustose coralline algae (CCA), fleshy algae (FA) and hard coral (HC) cover (%) means with 95% CI for the data collected for three periods at **(A)** Roncador (1995–2003–2015) and **(B)** Serrana (1995–2003–2016) Banks.

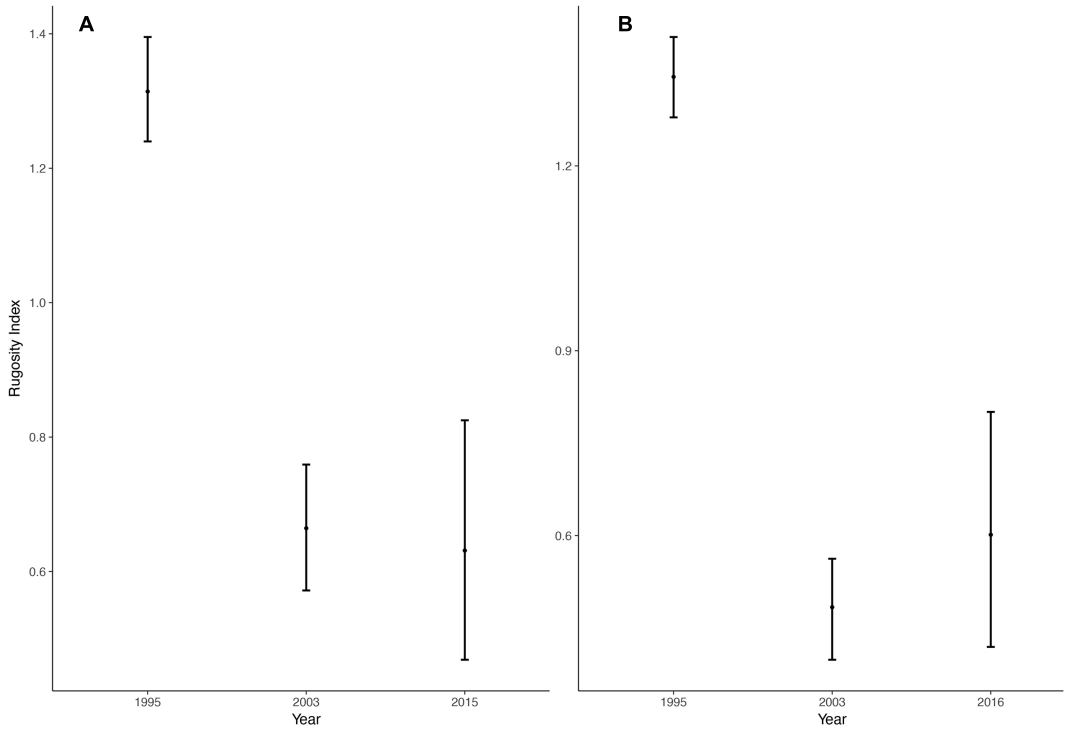

FIGURE 4 | Bottom complexity. Rugosity index means with 95% CI for three periods at **(A)** Roncador and **(B)** Serrana Banks.

2003 to 1.5 ind m^{-2} in 2016 (**Figure 5A**). In general, density values for Serrana were lower than Roncador, which included a peak value reaching 13.9 ind m^{-2} in 2003 and 6.5 ind m^{-2} in 2016. The sites where octocoral densities increased were located inside the reef lagoon. Serrana had the lowest values with low variation among sites (**Figure 5A**). Although, we did not survey densities per species, at both Banks *Antillogorgia bipinnata* was overall the most abundant gorgonian coral followed by the soft coral *Briareum asbestinum* and plexaurid gorgonians belonging to the genera *Plexaura, Pseudoplexaura* and *Eunicea*.

FORAM Index (FI)

We examined a total of 8 sediment samples, counted 1363 foraminifera tests and identified 34 genera at both Banks: 7 symbiont-bearing, 3 opportunistic and 24 other small heterotrophic. The most abundant genera for each functional

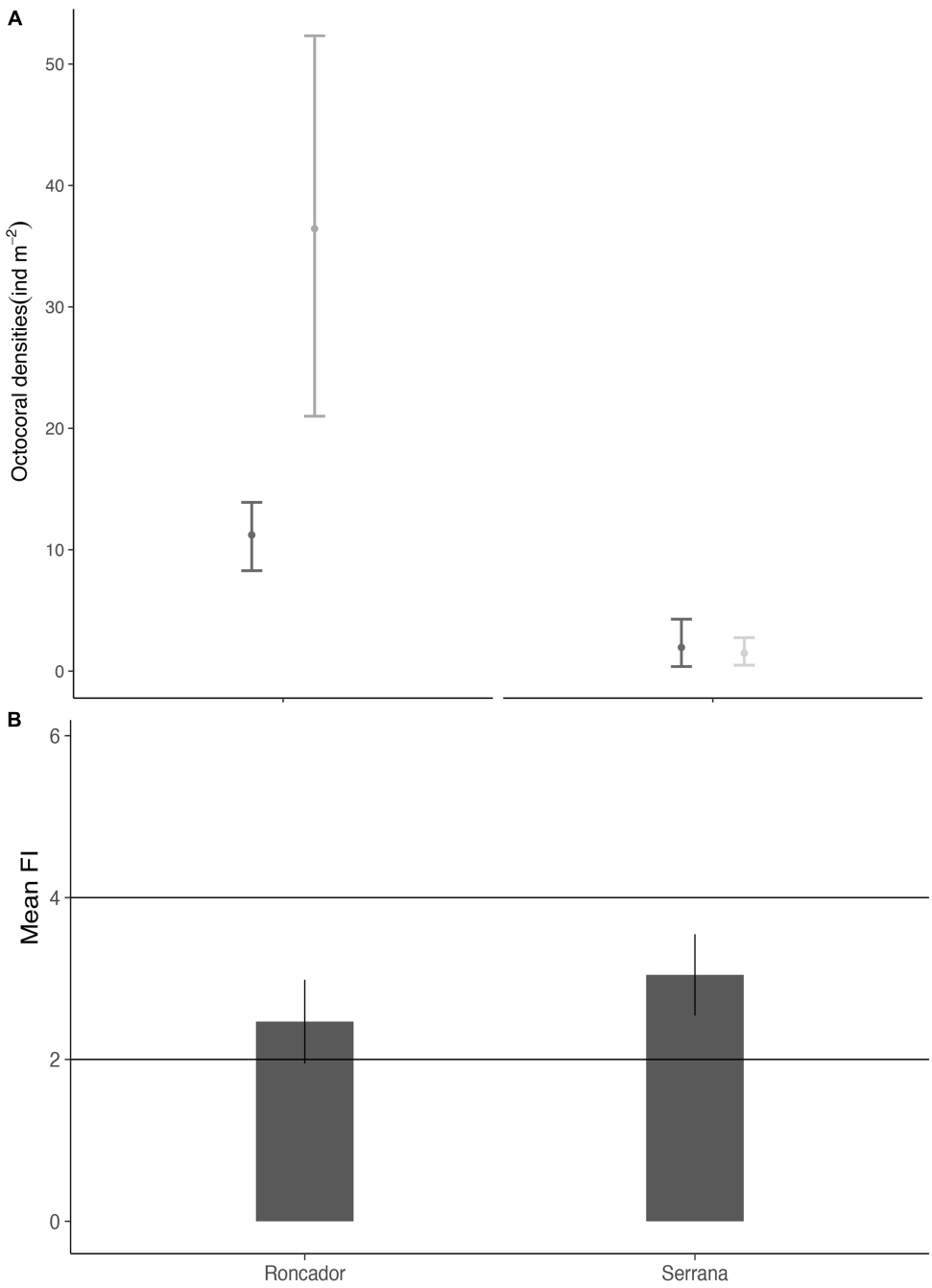

FIGURE 5 | Octocoral and Benthic foraminifera abundance. **(A)** Octocoral densities (ind m^{-2}) means with 95% CI in Roncador and Serrana during 2003 and 2015/2016. **(B)** The average FI ± SD for Roncador 2015 and Serrana 2016. Horizontal lines represent critical point for analysis (Hallock et al., 2003)].

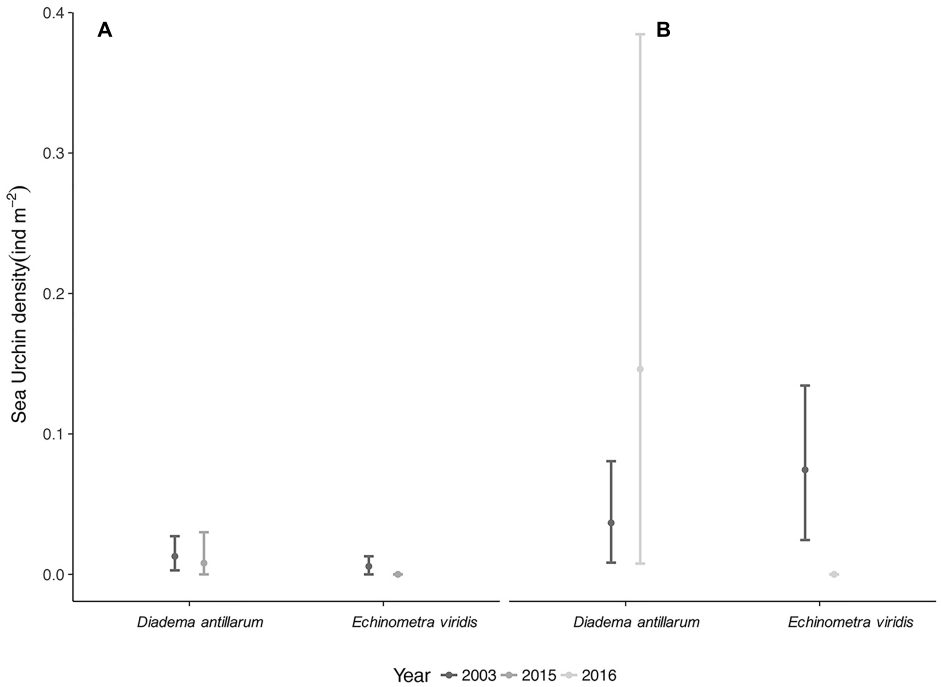

FIGURE 6 | Sea Urchin abundance. Species mean density (ind m^{-2}) with 95% CI for two periods at **(A)** Roncador 2003/2005 and **(B)** Serrana Banks 2003/2016.

group were *Laevipeneroplis*, *Bolivina* and *Triloculina*, respectively (See **Supplementary Table 5**). The small heterotrophic taxa dominated the foraminifera community with 86% of all individuals, followed by 10% of symbiont-bearing and 4% of opportunistic. The average FI found for Roncador was 2.5 and 3 for Serrana (**Figure 5B**).

Sea Urchin Densities

Urchins were seldom found at both Serrana and Roncador Banks, sometimes absent in many sites during 2015 and 2016 surveys. Similar densities of the sea urchin *D. antillarum* were found at Roncador during 2003 (0.01 ind m^{-2}) with respect to 2015 (0.01 ind m^{-2}), while its density was higher in Serrana 2016 (0.15 ind m^{-2}) than in 2003 (0.04 ind m^{-2}). Despite these trends, sea urchin density did not change significantly over those periods (**Figures 6A,B**). On the contrary, no individual of *E. viridis* was recorded in Roncador 2015 and Serrana 2016, showing a reduction in its density when compared to 2003 (see **Supplementary Table 6**).

DISCUSSION

Our results demonstrate a significant reduction in CCA and HC percent cover, which included massive (*Orbicella* spp.) and encrusting/smaller (*Agaricia* spp., *P. astreoides*) reef building species, particularly at Roncador Bank mid water-reefs. Likewise, a reduction in benthic complexity (rugosity), was evident between 1995 and 2003 at both Roncador and Serrana atolls. The Banks were different in terms of gorgonian densities, whit a nearly one order of magnitude higher in Roncador and a trend to increase. Sea urchin densities were overall low at both Banks. The FI at both Banks, a proxy of water quality and reef resilience, was below the range expected for coral reefs, which are apparently isolated from human waste water and/or sources of eutrophication (FI $>$ 4). FI values found, between 2 and 4, corresponded to reefs with water conditions from marginal to unsuitable for recovery of coral communities after disturbance (Hallock et al., 2003). This means nutrient availability does not favor the recruitment and growth of mixotrophic and calcifying organisms like hard corals (Hallock, 2012), compromising reef health in the long term. Those values are common at fringing reefs along the continental coast of Colombia affected by constant runoff and nutrient input from pollution (Velásquez et al., 2011; López-Angarita et al., 2014). Although both Banks show a decrease in CA and CCA, Roncador Bank mid-water reefs additionally face an alarming decline in overall coral cover. The correspondence of declining CCA, FA and general coral cover, water quality and bottom complexity (rugosity) with increases in octocoral is even more alarming in an already declining reef system.

Although remote reefs represent an exemplary case to assess reef health, due to its isolation from direct human disturbances, our results evidenced a clear decline in CCA an overall HC cover from 1995 to 2015 at Roncador mid-water reefs. During the year 2003, a mass mortality of hard corals was also observed in the lagoon of Serrana Bank (Sánchez et al., 2010), whereas coral in Roncador appeared healthier that year (Sánchez et al., 2005). Rugosity for both Roncador and Serrana Banks decreased dramatically between 1995 and 2003. The 1997–1998

El Niño Southern Oscillation led to mass coral bleaching and subsequently coral mortalities as well as the appearance of numerous diseases affecting corals (Weil, 2004), which most likely also impacted the two Banks. In terms of direct external effects, these reefs face the Caribbean current, NW direction, and at least part of the year receive diluted waters influenced by fresh-water runoff from the continental coast (Beier et al., 2017). Coastal waters coming from the Colombian coast are increasingly polluted with nutrients coming from rivers, which promotes coral degradation and harmful algae blooms (Restrepo et al., 2006; Coronado-Franco et al., 2018). Moreover, direct impacts from continental eutrophic waters on these Banks are likely. Complex seasonal water circulation around the archipelago (Garay et al., 1987) can also transport nutrients from the nearby island of San Andrés, where overpopulation and eutrophication is on the rise (Gavio et al., 2010; Mancera-Pineda et al., 2014). In addition, regional currents may be introducing alien objects or drifters, which can contribute as a source or external organic and inorganic material into San Andres (Mancera-Pineda et al., 2014), The case in point of drifters demonstrates that external threats can have detrimental impacts to isolated reef sites such as Serrana and Roncador.

The models of coral degradation usually consider a shift from coral to algae dominance in degrading coral reefs (Mumby, 2009; Graham et al., 2013; Slattery and Lesser, 2014), a signal not clearly evidenced in our study area. It is important to mention that detailed observations on Serrana and Roncador reefs, made over 50 years ago (1966), describe these reef communities as both coral and CCA-dominated, which included abundant stands of species today endangered like *Acropora cervicornis* and *A. palmata*, and only mentioning a reduction on fish abundances in comparison to observation from 1945 (Milliman, 1969). Coral and CCA percent cover decreased at Roncador mid-water reefs whereas only CCA decreased at Serrana shallow reefs which kept CCA, FA and HC close to their values in 1995. A pattern unexpected in an area devoid of direct human influence, which follow the world-wide decline of marine wilderness (Jones et al., 2018) and coral reef degradation (Bruno and Valdivia, 2016). The rise of slimy cyanobacterial mats, as those observed in these Caribbean reefs, comprise another phase shift related to increases in both eutrophication and water temperature during the last 40 years (De Bakker et al., 2017). In addition, large predator fishes, such as groupers, have been depleted by unsustainable fisheries throughout the entire SeaFlower reserve (Prada et al., 2007), with Roncador bank exhibiting the lowest abundance values in the archipelago (Hooker et al., 2011). Overall, corals reefs are experimenting a more complex degradation scenario than previously thought, where even far-flung reefs seem to be unable to cope with large-scale stressor such as global warming/sea level rise and ocean acidification (Perry et al., 2013, 2018). This situation could be acting in synergy with the tectonic activity leading to subsidence in the Caribbean (Khan et al., 2017), which could be different between Serrana and Rocandor Banks. In fact, Roncador Bank has been predicted to be more vulnerable to sea-level rise impacts than Serrana (Andrade et al., 2011). In addition, the small size of Roncador Bank, together with strong water motion, coral degradation and eutrophication, makes it prone to erosion and sediment loss, which suggest a similar reef demise as the case of Serranilla Bank (Triffleman et al., 1992). An interpretation of coral reefs declining, in both coral and algae whereas octocorals thrive, needs a more complex scenario with multiple stressors, where ocean acidification, sea-level and reef erosion should be taken into account (Pendleton et al., 2016).

A strong differentiation between octocoral densities from Roncador and Serrana Banks, on a spatial and temporal scale, was clearly found. Overall, density values in Roncador mid-water reefs were almost five times higher than those in Serrana shallow reefs, reaching up to 68.5 ind m^{-2} whereas the highest in the later was 13.9 ind m^{-2} (see **Supplementary Table 3**). These values are consistent with previous studies reporting similar ranges (2.95–20.6 ind m^{-2}) for octocoral densities recently estimated in the Caribbean (Privitera-Johnson et al., 2015), except for station 17 in Roncador that showed unusually higher density than those previously reported (68.5 ind m^{-2}). Interestingly, Roncador mid-water reefs showed higher mean octocoral densities (see **Supplementary Table 4**) than those reported in many Caribbean regions (Etnoyer et al., 2010; Sánchez, 2016) and those (9 ind m^{-2}) reported for SE Sulawesi assemblages (Rowley, 2018). It is widely known that habitat complexity significantly affects the assembly of benthic communities (Sánchez et al., 1997a) and in this study we see a dramatic decrease in habitat complexity through the measured rugosity index. Since these indexes reflect the growth dynamics of hard corals and reef erosion (Bozec et al., 2015), we can conclude that the percent cover of scleractinian community has been receding in the last years, whereas changes in octocoral densities tend to increase. This is a striking pattern because if hard coral cover continues to decrease and octocorals increase, or at least remain constant; it means that their relative abundance in the community increases as well, and such trend could dominate the community in a hypothetical phase shift scenario altering the functional and trophic structure of the reef community (Norström et al., 2009; Lenz et al., 2015). These growing gorgonian assemblages can also change in composition due to the relative abundance of associate predators (e.g., *Cyphoma*) or species susceptibility to diseases (Sánchez, 2016).

In the last two decades Caribbean reefs have experienced thermal anomalies of up to 16 weeks as during 2005 and 2010, including coral bleaching throughout the province and scleractinian coral mortality, coinciding with the record of hurricanes, with four category 5 hurricanes, including Katrina (Wilkinson and Souter, 2008; Eakin et al., 2010). However, gorgonian corals (Octocorallia), one of the features of the Caribbean reef province, exhibited negligible mortality and high resilience after bleaching (Lasker and Sánchez, 2002; Lasker, 2003; Prada et al., 2010). Octocorals have also shown to be very resistant to ocean acidification in experimental settings (Enochs et al., 2016), even below saturation of $\Omega_{calcite}$ (Gómez et al., 2015). Other octocorals, such as the soft coral species of the Red Sea, have also shown resistance to high pCO_2 values due to the protective properties of their tissues (Gabay et al., 2013, 2014). In short, octocorals, due to their resistance to bleaching and acidification, together with a heterothrophic feeding strategy in most Caribbean species (Baker et al., 2015; Sánchez et al., 2019),

should be included in the list of climate change/human footprint survivors. Yet, these organisms have been rarely considered as reef-building corals, although a large colony can contribute as much calcium carbonate, at its holdfast, as a small scleractinian coral species (Kocurko, 1987). Octocoral-dominated reefs already exists at naturally acidified waters (Inoue et al., 2013). Should we consider an octocoral-algae phase shift in Caribbean reefs?

CONCLUSION

Although both Banks followed a loss in coral cover, topographic complexity (rugosity) and resilience (FI index), Roncador Bank mid-water reefs face a steady decline. These unexpected findings led us to consider the scenario of some of these reefs starting to lose complexity, whereas providing ideal conditions for octocoral recruitment, settlement, successful establishment and subsequent growth. Other SeaFlower reef complexes, like San Andrés Island, have already shown the effects of coastal erosion and eutrophication (Gavio et al., 2010). Situations predicted to increase with the human footprint and under a climate change scenario (Schönberg et al., 2017), hence bioerosion and reef budgets are rarely considered in monitoring programs (Perry et al., 2013). Serrana Bank shallow reefs, a larger reef-complex with signs of HC recovery, provides some hope in terms of its withstanding HC cover, yet a more detailed monitoring is needed.

Another concern is the apparent eutrophication of the Banks as seen in the coral/algae abundances and FORAM index. Due to lack of information, foreign sources of nutrients should not be ignored and deserve further study. Yet, a more likely scenario could be related with the cycle of dissolved organic carbon (DOC), fleshy algae and the microbial community (Pawlik et al., 2016), which maintains the algal competitive abundance and promotes coral degradation (Haas et al., 2016). Coral diseases are prevalent in the two Banks and mass mortalities have been observed in Serrana Bank (Sánchez et al., 2005, 2010). Monitoring the sources of nutrients in these Banks, along with the other components of reef resilience (i.e., herbivorous fish), can bring important information for, urgently needed, adaptive management in these deteriorating coral reefs.

The implications of high octocoral densities in Roncador are of the utmost importance for understanding the future of Caribbean reefs. First it is important to note that Roncador mid-water reefs, and even Serrana shallow reefs, show significantly lower densities of sponges as compared to continental reefs (Zea, 2001), where increased suspended particles promote sponge abundance and dominance (Valderrama and Zea, 2003; Loh et al., 2015). Novel community assemblages may include new trophic and habitat provisioning opportunities (Lugo et al., 2000) and could even transform the storm resistance regimes (Lenz et al., 2015). To fully understand the nature of octocoral densities, as well as how environmental conditions change by high octocoral abundances, it is paramount to set a baseline of recruitment survivorship and dynamics in future monitoring programs. Specifically, future studies in the area should address the hypothesis of the stock-recruitment within the octocoral canopy (Privitera-Johnson et al., 2015), which suggests that once larvae leave the parental colonies, they will get caught up beneath the canopy of the octocoral community promoting settlement and eventually densities of adult colonies.

Caribbean atolls, such as Roncador and Serrana Banks, developed remarkable areas of high relief coral communities in their lagoons and terraces (e.g., **Figure 2**), but today live coral cover averages less than 10% at Roncador mid-water reefs, when in 1995 was 22.6%, and less than 21% at Serrana shallow reefs, when in 1995 was 35.4%. These Banks, isolated from human populations and rivers, comprised the climax of thousands of years of a reef-building process, which is disappearing in the last few decades in the absence of a clear causal explanation. The fate of these and many coral reefs in the Caribbean are beyond alarming. The need of more sophisticated means of reef monitoring, including reef budgets and nutrients (i.e., carbon sources), is urgently needed toward adaptive management of Caribbean MPAs.

AUTHOR CONTRIBUTIONS

JS conceived the study. FG-Z, LG-C, and MGn collected the samples. FG-Z, LG-C, NP, PR, LN, MGn, DV, and AS processed the imagery. MG-C analyzed the samples. MG-C, PR, LG-C, and DV performed the data analyses. JS and MG-C wrote the manuscript with contributions from LG-C and DV. All authors edited the manuscript before submission.

FUNDING

This work was supported by the ColombiaBIO-Colciencias (Convenio 341-2016, Universidad de los Andes- Comisión Colombiana del Océano-CCO) and Corporación para el Desarrollo Sostenible del Departamento Archipiélago de *San Andrés* Providencia y Santa Catalina, CORALINA-Universidad de los Andes (Convenios No. 13, 2014 and No. 21, 2015). Additional Funding sources included COLCIENCIAS (Grant No. 120465944147) and Vicerrectoría de Investigaciones, Programas de Investigación (*Completando la teoría del origen de las especies de Darwin: especiación ecológica en octocorales, desde niños a doctores*) (UniAndes).

ACKNOWLEDGMENTS

We greatly acknowledge the SeaFlower Expeditions (2015–2016) organizers and sponsors: Comisión Colombiana del Océano-CCO/Dimar (J. Soltau, J. Sintura, A. Chadid, R. Carranza and their team), Colombian Navy (ARC Providencia and crew, Serrana Expedition), Coralina (N. Bolaños, Erik Castro and their team), Secretaria de Pesca y Agricultura (Gobernación del departamento de San Andrés, Providencia y Santa Catalina), ColombiaBIO-Colciencias (F. García, L. Ayala and team). Centro de Servicios Compartidos, Universidad de los Andes, efficiently managed resources for the Serrana expedition. We

express great appreciation to T. González and A. Iñiguez for contributing in the field and/or processing digital imagery and estimating coral cover. Members of BIOMMAR, and O. Ruíz and J. Andrade who helped with logistics. Comments and criticism from three reviewers greatly improved the corrected manuscript.

SUPPLEMENTARY MATERIAL

The Supplementary Material for this article can be found online at: https://www.frontiersin.org/articles/10.3389/fmars.2019.00073/full#supplementary-material

REFERENCES

Albins, M. A., and Hixon, M. A. (2013). Worst case scenario: potential long-term effects of invasive predatory lionfish (*Pterois volitans*) on atlantic and caribbean coral-reef communities. *Environ. Biol. Fishes* 96, 1151–1157. doi: 10.1007/s10641-011-9795-1

Andrade, C. A., Pinzón, V. M., and Manzanillo, I. (2011). Effects of sea-level rise due to climatic changes on the beaches of the Cays of the San Andres Archipelago. *Sci. Bull.* 29, 62–74.

Appeldoorn, R., Ballantine, D., Bejarano, I., Carlo, M., Nemeth, M., Otero, E., et al. (2016). Mesophotic coral ecosystems under anthropogenic stress: a case study at Ponce, Puerto Rico. *Coral Reefs* 35, 63–75. doi: 10.1007/s00338-015-1360-5

Aronson, R. B., and Precht, W. F. (1995). Landscape patterns of reef coral diversity: a test of the intermediate disturbance hypothesis. *J. Exp. Mar. Biol. Ecol.* 192, 1–14. doi: 10.1016/0022-0981(95)00052-S

Baker, D. M., Freeman, C. J., Knowlton, N., Thacker, R. W., Kim, K., and Fogel, M. L. (2015). Productivity links morphology, symbiont specificity and bleaching in the evolution of Caribbean octocoral symbioses. *ISME J.* 9, 2620–2629. doi: 10.1038/ismej.2015.71

Beier, E., Bernal, G., Ruiz-Ochoa, M., and Barton, E. D. (2017). Freshwater exchanges and surface salinity in the Colombian basin, Caribbean Sea. *PLoS One* 12:e0182116. doi: 10.1371/journal.pone.0182116

Blakeway, D., and Hamblin, M. G. (2015). Self-generated morphology in lagoon reefs. *PeerJ* 3:e935. doi: 10.7717/peerj.935

Bozec, Y.-M., Alvarez-Filip, L., and Mumby, P. J. (2015). The dynamics of architectural complexity on coral reefs under climate change. *Glob. Change Biol.* 21, 223–235. doi: 10.1111/gcb.12698

Bruno, J. F., and Valdivia, A. (2016). Coral reef degradation is not correlated with local human population density. *Sci. Rep.* 6:29778. doi: 10.1038/srep29778

Camp, E. F., Schoepf, V., Mumby, P. J., Hardtke, L. A., Rodolfo-Metalpa, R., Smith, D. J., et al. (2018). The future of coral reefs subject to rapid climate change: lessons from natural extreme environments. *Front. Mar. Sci.* 5:4. doi: 10.3389/fmars.2018.00433

Cockey, E., Hallock, P., and Lidz, B. H. (1996). Decadal-scale changes in benthic foraminiferal assemblages off Key Largo, Florida. *Coral Reefs* 15, 237–248. doi: 10.1007/BF01787458

Cooper, T. F., Gilmour, J. P., and Fabricius, K. E. (2009). Bioindicators of changes in water quality on coral reefs: review and recommendations for monitoring programmes. *Coral Reefs* 28, 589–606. doi: 10.1007/s00338-009-0512-x

Coronado-Franco, K. V., Selvaraj, J. J., and Mancera Pineda, J. E. (2018). Algal blooms detection in Colombian Caribbean Sea using MODIS imagery. *Mar. Pollut. Bull.* 133, 791–798. doi: 10.1016/j.marpolbul.2018.06.021

Costanza, R., d'Arge, R., de Groot, R., Farber, S., Grasso, M., Hannon, B., et al. (1997). The value of the world's ecosystem services and natural capital. *Nature* 387, 253–260. doi: 10.1038/387253a0

Coyer, J. A., Ambrose, R. F., Engle, J. M., and Carroll, J. C. (1993). Interactions between corals and algae on a temperate zone rocky reef: mediation by sea urchins. *J. Exp. Mar. Biol. Ecol.* 167, 21–37. doi: 10.1016/0022-0981(93)90181-M

Darwin, C. (1842). *The Structure and Distribution of Coral Reefs*. Berkeley, CA: University of California Press, 214.

De Bakker, D. M., Van Duyl, F. C., Bak, R. P., Nugues, M. M., Nieuwland, G., and Meesters, E. H. (2017). 40 Years of benthic community change on the Caribbean reefs of Curaçao and Bonaire: the rise of slimy cyanobacterial mats. *Coral Reefs* 36, 355–367. doi: 10.1007/s00338-016-1534-9

De Goeij, J. M., Van Oevelen, D., Vermeij, M. J., Osinga, R., Middelburg, J. J., de Goeij, A. F., et al. (2013). Surviving in a marine desert: the sponge loop retains resources within coral reefs. *Science* 342, 108–110. doi: 10.1126/science.1241981

Díaz, J. M., Barrios, L. M., Cendales, M. H., Garzón-Ferreira, J., Geister, J., Parra-Velandia, F., et al. (2000). Áreas coralinas de Colombia. Invemar.

Diaz, J. M., Diaz, G., Garzon-Ferreira, J., Geister, J., Sánchez, J. A., and Zea, S. (1996a). *Atlas de los Arrecifes Coralinos del Caribe colombiano. I. Archipiélago de San Andrés y Providencia*. Santa Mart: INVEMAR.

Diaz, J. M., Sánchez, J. A., Garzon-Ferreira, J., and Zea, S. (1996b). Morphology and marine habitats from two southwestern Caribbean atolls: albuquerque and Courtown. *Atoll Res. Bull.* 435, 1–33.

Díaz-Pulido, G., Sánchez, J. A., Zea, S., Díaz, J. M., et al. (2004). Esquemas de distribución espacial en la comunidad bentónica de arrecifes coralinos continentales y oceánicos del Caribe colombiano. *Rev. Acad. Colomb. Cienc. Exactas* 108, 337–347.

Dodge, R. E., Logan, A., and Antonius, A. (1982). Quantitative reef assessment studies in Bermuda: a comparison of methods and preliminary results. *Bull. Mar. Sci.* 32, 745–760.

Dornelas, M., Gotelli, N. J., McGill, B., Shimadzu, H., Moyes, F., Sievers, C., et al. (2014). Assemblage time series reveal biodiversity change but not systematic loss. *Science* 344, 296–299. doi: 10.1126/science.1248484

Eakin, C. M., Morgan, J. A., Heron, S. F., Smith, T. B., Liu, G., Alvarez-Filip, L., et al. (2010). Caribbean corals in crisis: record thermal stress, bleaching, and mortality in 2005. *PLoS One* 5:e13969. doi: 10.1371/journal.pone.0013969

Enochs, I. C., Manzello, D. P., Wirshing, H. H., Carlton, R., and Serafy, J. (2016). Micro-CT analysis of the Caribbean octocoral *Eunicea flexuosa* subjected to elevated p CO 2. *ICES J. Mar. Sci. J. Cons.* 73, 910–919. doi: 10.1093/icesjms/fsv159

Etnoyer, P., Wirshing, H., and Sánchez, J. A. (2010). Rapid assessment of octocoral diversity and habitat on Saba Bank, Netherlands antilles. *PLoS One* 5:e10668. doi: 10.1371/journal.pone.0010668

Fabricius, K. E. (2011). "Factors determining the resilience of coral reefs to eutrophication: a review and conceptual model," in *Coral Reefs: An Ecosystem in Transition*, eds Z. Dubinsky and N. Stambler (Berlin: Springer), 493–505.

Foster, N. L., Baums, I. B., Sánchez, J. A., Paris, C. B., Chollett, I., Agudelo, C. L., et al. (2013). Hurricane-driven patterns of clonality in an ecosystem engineer: the Caribbean coral *Montastraea annularis*. *PLoS One* 8:e53283. doi: 10.1371/journal.pone.0053283

Friedlander, A., Sladek-Nowlis, J., Sánchez, J. A., Appeldoorn, R., Usseglio, P., Mccormick, C., et al. (2003). Designing effective marine protected areas in old providence and santa catalina islands, san andrés archipelago, colombia, using biological and sociological information. *Conserv. Biol.* 17, 1769–1784. doi: 10.1111/j.1523-1739.2003.00338.x

Gabay, Y., Benayahu, Y., and Fine, M. (2013). Does elevated p CO_2 affect reef octocorals? *Ecol. Evol.* 3, 465–473. doi: 10.1002/ece3.351

Gabay, Y., Fine, M., Barkay, Z., and Benayahu, Y. (2014). Octocoral tissue provides protection from declining oceanic pH. *PLoS One* 9:e91553. doi: 10.1371/journal.pone.0091553

Garay, J., Francisco, C., Carlos, A., and Jairo, A. (1987). Estudio oceanográfico del área insular y oceánica del Caribe colombiano de San Andrés y Providencia y cayos vecinos. *CIOH Sci. Bull.* 9:33.

Gardner, T. A., Cote, I. M., Gill, J. A., Grant, A., and Watkinson, A. R. (2003). Long-term region-wide declines in Caribbean corals. *Science* 301, 958–961. doi: 10.1126/science.1086050

Gavio, B., Palmer-Cantillo, S., and Mancera, J. E. (2010). Historical analysis (2000–2005) of the coastal water quality in San Andrés Island, sea flower biosphere reserve, Caribbean Colombia. *Mar. Pollut. Bull.* 60, 1018–1030. doi: 10.1016/j.marpolbul.2010.01.025

Geister, J., and Díaz, J. M. (1996). "A field guide to the atolls and reefs of San Andres and Providencia (Colombia)," in *Proceedings of the 8th International Coral Reef Symposium*, Panama City, 235–236.

Gómez, C. E., Paul, V. J., Ritson-Williams, R., Muehllehner, N., Langdon, C., and Sánchez, J. A. (2015). Responses of the tropical gorgonian coral *Eunicea fusca* to ocean acidification conditions. *Coral Reefs* 34, 451–460. doi: 10.1007/s00338-014-1241-3

Gonzalez-Zapata, F. L., Bongaerts, P., Ramírez-Portilla, C., Adu-Oppong, B., Walljasper, G., Reyes, A., et al. (2018). Holobiont diversity in a reef-building coral over its entire depth range in the mesophotic zone. *Front. Mar. Sci.* 5:29. doi: 10.3389/fmars.2018.00029

Graham, N. A., Bellwood, D. R., Cinner, J. E., Hughes, T. P., Norström, A. V., and Nyström, M. (2013). Managing resilience to reverse phase shifts in coral reefs. *Front. Ecol. Environ.* 11, 541–548. doi: 10.1890/120305

Guarderas, A. P., Hacker, S. D., and Lubchenco, J. (2008). Current status of marine protected areas in latin america and the caribbean. *Conserv. Biol.* 22, 1630–1640. doi: 10.1111/j.1523-1739.2008.01023.x

Haas, A. F., Fairoz, M. F. M., Kelly, L. W., Nelson, C. E., Dinsdale, E. A., Edwards, R. A., et al. (2016). Global microbialization of coral reefs. *Nat. Microbiol.* 1:16042. doi: 10.1038/nmicrobiol.2016.42

Hallock, P. (1999). "Symbiont-bearing Foraminifera," in *Modern Foraminifera*, ed. B. K. S. Gupta (Dordrecht: Springer), 123–139.

Hallock, P. (2012). "The FoRAM index revisited: uses, challenges, and limitations," in *Proceedings of the 12th International Coral Reef Symposium*, Cairns.

Hallock, P., Lidz, B. H., Cockey-Burkhard, E. M., and Donnelly, K. B. (2003). "Foraminifera as bioindicators in coral reef assessment and monitoring: the FORAM index," in *Coastal Monitoring through Partnerships*, eds B. D. Melzian, V. Engle, M. McAlister, and S. S. Sandhu (Berlin: Springer), 221–238.

Hoegh-Guldberg, O., Mumby, P. J., Hooten, A. J., Steneck, R. S., Greenfield, P., Gomez, E., et al. (2007). Coral reefs under rapid climate change and ocean acidification. *Science* 318, 1737–1742. doi: 10.1126/science.1152509

Hoegh-Guldberg, O., Poloczanska, E. S., Skirving, W., and Dove, S. (2017). Coral reef ecosystems under climate change and ocean acidification. *Front. Mar. Sci.* 4:158. doi: 10.3389/fmars.2017.00158

Hooker, H., Santos-Martinez, A., and Taylor, E. (2011). "Abundancias de grandes serranidos en la reserva de biosfera seaflower," in *Proceedings of the 64th Gulf and Caribbean Fisheries Institute*, Puerto Morelos, 237–240.

Hooper, D. U., Adair, E. C., Cardinale, B. J., Byrnes, J. E., Hungate, B. A., Matulich, K. L., et al. (2012). A global synthesis reveals biodiversity loss as a major driver of ecosystem change. *Nature* 486, 105–108. doi: 10.1038/nature11118

Hughes, T. P. (1994). Catastrophes, phase shifts, and large-scale degradation of a caribbean coral reef. *Science* 265, 1547–1551. doi: 10.1126/science.265.5178.1547

Hughes, T. P., Baird, A. H., Bellwood, D. R., Card, M., Connolly, S. R., Folke, C., et al. (2003). Climate change, human impacts, and the resilience of coral reefs. *Science* 301, 929–933. doi: 10.1126/science.1085046

Hughes, T. P., Graham, N. A. J., Jackson, J. B. C., Mumby, P. J., and Steneck, R. S. (2010). Rising to the challenge of sustaining coral reef resilience. *Trends Ecol. Evol.* 25, 633–642. doi: 10.1016/j.tree.2010.07.011

Inoue, S., Kayanne, H., Yamamoto, S., and Kurihara, H. (2013). Spatial community shift from hard to soft corals in acidified water. *Nat. Clim. Change* 3, 683–687. doi: 10.1038/nclimate1855

Jackson, J. B. C. (1997). Reefs since Columbus. *Coral Reefs* 16, S23–S32. doi: 10.1007/s003380050238

Jackson, J. B. C., Donovan, M. K., Cramer, K. L., and Lam, V. V. (2014). *Status and Trends of Caribbean Coral Reefs*. Washington, D.C: Global Coral Reef Monitoring Network.

Jackson, J. B. C., Kirby, M. X., Berger, W. H., Bjorndal, K. A., Botsford, L. W., Bourque, B. J., et al. (2001). Historical overfishing and the recent collapse of coastal ecosystems. *Science* 293, 629–638. doi: 10.1126/science.1059199

Jones, K. R., Klein, C. J., Halpern, B. S., Venter, O., Grantham, H., Kuempel, C. D., et al. (2018). The location and protection status of earth's diminishing marine wilderness. *Curr. Biol.* 28, 2506.e3–2512.e3. doi: 10.1016/j.cub.2018.06.010

Khan, N. S., Ashe, E., Horton, B. P., Dutton, A., Kopp, R. E., Brocard, G., et al. (2017). Drivers of holocene sea-level change in the caribbean. *Quat. Sci. Rev.* 155, 13–36. doi: 10.1016/j.quascirev.2016.08.032

Klaus, J. S., Janse, I., Heikoop, J. M., Sanford, R. A., and Fouke, B. W. (2007). Coral microbial communities, zooxanthellae and mucus along gradients of seawater depth and coastal pollution. *Environ. Microbiol.* 9, 1291–1305. doi: 10.1111/j.1462-2920.2007.01249.x

Kocurko, M. J. (1987). Shalow-water octocorallia and related submarine lithification, San Andres island, Colombia, *Tex. J. Sci.* 39, 349–365.

Lasker, H. R. (2003). Zooxanthella densities within a Caribbean octocoral during bleaching and non-bleaching years. *Coral Reefs* 22, 23–26.

Lasker, H. R., and Sánchez, J. A. (2002). "Allometry and astogeny of modular organisms," in *Reproductive Biology of Invertebrates Progress in Asexual Reproduction*, ed. R. N. Hughes (New York, NY: John Wiley), 207–253.

Ledlie, M. H., Graham, N. A. J., Bythell, J. C., Wilson, S. K., Jennings, S., Polunin, N. V. C., et al. (2007). Phase shifts and the role of herbivory in the resilience of coral reefs. *Coral Reefs* 26, 641–653. doi: 10.1007/s00338-007-0230-1

Lenz, E. A., Bramanti, L., Lasker, H. R., and Edmunds, P. J. (2015). Long-term variation of octocoral populations in St. John, US Virgin Islands. *Coral Reefs* 34, 1099–1109. doi: 10.1007/s00338-015-1315-x

Lesser, M. P., and Slattery, M. (2011). Phase shift to algal dominated communities at mesophotic depths associated with lionfish (*Pterois volitans*) invasion on a Bahamian coral reef. *Biol. Invasions* 13, 1855–1868. doi: 10.1007/s10530-011-0005-z

Lessios, H. A., Robertson, D. R., and Cubit, J. D. (1984). Spread of diadema mass mortality through the caribbean. *Science* 226, 335–337. doi: 10.1126/science.226.4672.335

Littler, M. M., and Littler, D. S. (2007). Assessment of coral reefs using herbivory/nutrient assays and indicator groups of benthic primary producers: a critical synthesis, proposed protocols, and critique of management strategies. *Aquat. Conserv. Mar. Freshw. Ecosyst.* 17, 195–215. doi: 10.1002/aqc.790

Littler, M. M., Littler, D. S., and Brooks, B. L. (2006). Harmful algae on tropical coral reefs: bottom-up eutrophication and top-down herbivory. *Harmful Algae* 5, 565–585. doi: 10.1016/j.hal.2005.11.003

Loh, T.-L., McMurray, S. E., Henkel, T. P., Vicente, J., and Pawlik, J. R. (2015). Indirect effects of overfishing on Caribbean reefs: sponges overgrow reef-building corals. *PeerJ* 3:e901. doi: 10.7717/peerj.901

López-Angarita, J., Moreno-Sánchez, R., Maldonado, J. H., and Sánchez, J. A. (2014). Evaluating linked social-ecological systems in marine protected areas. *Conserv. Lett.* 7, 241–252. doi: 10.1111/conl.12063

Lugo, A. E., Rogers, C. S., and Nixon, S. W. (2000). Hurricanes, coral reefs and rainforests: resistance, ruin and recovery in the Caribbean. *Ambio* 29, 106–115. doi: 10.1579/0044-7447-29.2.106

Mancera-Pineda, J. E., Montalvo-Talaigua, M., and Gavio, B. (2014). Potentially toxic dinoflagellates associated to drift in san andres Island, international biosphere reservation – Seaflower. *Caldasia* 36, 139–156. doi: 10.15446/caldasia.v36n1.43896

McMurray, S. E., Stubler, A. D., Erwin, P. M., Finelli, C. M., and Pawlik, J. R. (2018). A test of the sponge-loop hypothesis for emergent Caribbean reef sponges. *Mar. Ecol. Prog. Ser.* 588, 1–14. doi: 10.3354/meps12466

Milliman, J. D. (1969). Four southwerstern caribbean atolls: courtown cays, alburquerque cays, Roncador Bank and Serrana Bank. *Atoll Res. Bull.* 129, 1–41. doi: 10.5479/si.00775630.129.1

Montilla, L. M., Ramos, R., García, E., and Cróquer, A. (2016). Caribbean yellow band disease compromises the activity of catalase and glutathione S-transferase in the reef-building coral *Orbicella faveolata* exposed to anthracene. *Dis. Aquat. Organ.* 119, 153–161. doi: 10.3354/dao02980

Mora, C. (2008). A clear human footprint in the coral reefs of the Caribbean. *Proc. R. Soc. Lond. B Biol. Sci.* 275, 767–773. doi: 10.1098/rspb.2007.1472

Mumby, P. J. (2009). Phase shifts and the stability of macroalgal communities on Caribbean coral reefs. *Coral Reefs* 28, 761–773. doi: 10.1007/s00338-009-0506-8

Mumby, P. J., Steneck, R. S., Edwards, A. J., Ferrari, R., Coleman, R., Harborne, A. R., et al. (2012). Fishing down a Caribbean food web relaxes trophic cascades. *Mar. Ecol. Prog. Ser.* 445, 13–24. doi: 10.3354/meps09450

Norström, A., Nyström, M., Lokrantz, J., and Folke, C. (2009). Alternative states on coral reefs: beyond coral-macroalgal phase shifts. *Mar. Ecol. Prog. Ser.* 376, 295–306. doi: 10.3354/meps07815

Orr, J. C., Fabry, V. J., Aumont, O., Bopp, L., Doney, S. C., Feely, R. A., et al. (2005). Anthropogenic ocean acidification over the twenty-first century and its impact on calcifying organisms. *Nature* 437, 681–686. doi: 10.1038/nature04095

Paddack, M. J., Reynolds, J. D., Aguilar, C., Appeldoorn, R. S., Beets, J., Burkett, E. W., et al. (2009). Recent region-wide declines in Caribbean reef fish abundance. *Curr. Biol.* 19, 590–595. doi: 10.1016/j.cub.2009.02.041

Pandolfi, J. M., and Lovelock, C. E. (2014). Novelty trumps loss in global biodiversity. *Science* 344, 266–267. doi: 10.1126/science.1252963

Pawlik, J. R., Burkepile, D. E., and Thurber, R. V. (2016). A vicious circle? Altered carbon and nutrient cycling may explain the low resilience of caribbean coral reefs. *BioScience* 66, 470–476. doi: 10.1093/biosci/biw047

Pendleton, L. H., Hoegh-Guldberg, O., Langdon, C., and Comte, A. (2016). Multiple stressors and ecological complexity require a new approach to coral reef research. *Front. Mar. Sci.* 3:36. doi: 10.3389/fmars.2016.00036

Perry, C. T., Alvarez-Filip, L., Graham, N. A. J., Mumby, P. J., Wilson, S. K., Kench, P. S., et al. (2018). Loss of coral reef growth capacity to track future increases in sea level. *Nature* 558, 396–400. doi: 10.1038/s41586-018-0194-z

Perry, C. T., Murphy, G. N., Kench, P. S., Smithers, S. G., Edinger, E. N., Steneck, R. S., et al. (2013). Caribbean-wide decline in carbonate production threatens coral reef growth. *Nat. Commun.* 4:1402. doi: 10.1038/ncomms2409

Prada, C., Weil, E., and Yoshioka, P. M. (2010). Octocoral bleaching during unusual thermal stress. *Coral Reefs* 29, 41–45. doi: 10.1007/s00338-009-0547-z

Prada, M., Castro, E., Puello, E., Pomare, M., Penaloza, G., James, L., et al. (2007). Threats to the grouper population due to fishing during reproductive seasons in the san andres and providencia archipelago, Colombia. *Proc. Gulf Caribbean Fish. Inst*. 58, 270–275.

Privitera-Johnson, K., Lenz, E. A., and Edmunds, P. J. (2015). Density-associated recruitment in octocoral communities in St. John, US Virgin Islands. *J. Exp. Mar. Biol. Ecol.* 473, 103–109. doi: 10.1016/j.jembe.2015.08.006

Ramirez, L. F. (2016). Marine protected areas in Colombia: advances in conservation and barriers for effective governance. *Ocean Coast. Manage.* 125, 49–62. doi: 10.1016/j.ocecoaman.2016.03.005

Restrepo, J. D., Zapata, P., Díaz, J. M., Garzón-Ferreira, J., and García, C. B. (2006). Fluvial fluxes into the Caribbean Sea and their impact on coastal ecosystems: the magdalena river, Colombia. *Glob. Planet. Change* 50, 33–49. doi: 10.1016/j.gloplacha.2005.09.002

Roberts, C. M., McClean, C. J., Veron, J. E., Hawkins, J. P., Allen, G. R., McAllister, D. E., et al. (2002). Marine biodiversity hotspots and conservation priorities for tropical reefs. *Science* 295, 1280–1284. doi: 10.1126/science.1067728

Rowley, S. J. (2018). Environmental gradients structure gorgonian assemblages on coral reefs in SE Sulawesi, Indonesia. *Coral Reefs* 37, 609–630. doi: 10.1007/s00338-018-1685-y

Sánchez, J. A. (2016). "Diversity and evolution of octocoral animal forests at both sides of tropical america," in *Marine Animal Forests*, eds S. Rossi, L. Bramanti, A. Gori, and C. Orejas Saco del Valle (Cham: Springer International Publishing), 1–33.

Sánchez, J. A., Díaz, J. M., and Zea, S. (1997a). Gorgonian communities in two contrasting environments on oceanic atolls of the southwestern Caribbean. *Bull. Mar. Sci.* 61, 453–465.

Sánchez, J. A., Zea, S., and Diaz, J. M. (1997b). Gorgonian communities of two contrasting environments from oceanic Caribbean atolls. *Bull. Mar. Sci.* 61, 61–72.

Sánchez, J. A., Dueñas, L. F., Rowley, S. J., González, F. L., Vergara, D. C., Montaño-Salazar, S. M., et al. (2019). "Gorgonian corals (39)," in *Mesophotic Coral Ecosystems Coral Reefs of the World,* eds Y. Loya et al. (Basel:Springer Nature), 727–745. doi: 10.1007/978-3-319-92735-0_39

Sánchez, J. A., Herrera, S., Navas-Camacho, R., Rodríguez-Ramírez, A., Herron, P., Pizarro, V., et al. (2010). White plague-like coral disease in remote reefs of the Western Caribbean. *Rev. Biol. Trop.* 58, 145–154. doi: 10.15517/rbt.v58i1.20031

Sánchez, J. A., Pizarro, V., Acosta-De-Sanchez, A. R., Castillo, P. A., Herron, P., Martinez, J. C., et al. (2005). Evaluating coral reef benthic communities in remote atolls (quitasueno, serrana, and roncador banks) to recommend marine-protected areas for the seaflower biosphere reserve. *Atoll Res. Bull.* 531, 1–66. doi: 10.5479/si.00775630.531.1

Sánchez, J. A., and Wirshing, H. H. (2005). A field key to the identification of tropical western Atlantic zooxanthellate octocorals (Octocorallia?: Cnidaria). *Caribb. J. Sci.* 41, 508–522.

Sánchez, J. A., Zea, S., and Díaz, J. M. (1998). Patterns of octocoral and black coral distribution in the oceanic barrier reef-complex of providencia Island, Southwestern Caribbean. *Caribb. J. Sci.* 34, 250–264.

Schneider, C. A., Rasband, W. S., and Eliceiri, K. W. (2012). NIH Image to ImageJ: 25 years of image analysis. *Nat. Methods* 9:671. doi: 10.1038/nmeth.2089

Schönberg, C. H. L., Fang, J. K. H., Carreiro-Silva, M., Tribollet, A., and Wisshak, M. (2017). Bioerosion: the other ocean acidification problem. *ICES J. Mar. Sci.* 74, 895–925. doi: 10.1093/icesjms/fsw254

Schrope, M. (2008). Conservation: providential outcome. *Nat. News* 451, 122–123. doi: 10.1038/451122a

Sherman, C., Schmidt, W., Appeldoorn, R., Hutchinson, Y., Ruiz, H., Nemeth, M., et al. (2016). Sediment dynamics and their potential influence on insular-slope mesophotic coral ecosystems. *Cont. Shelf Res.* 129, 1–9. doi: 10.1016/j.csr.2016.09.012

Slattery, M., and Lesser, M. P. (2014). Allelopathy in the tropical alga *Lobophora variegata* (Phaeophyceae): mechanistic basis for a phase shift on mesophotic coral reefs? *J. Phycol.* 50, 493–505. doi: 10.1111/jpy.12160

Spalding, M., Burke, L., Wood, S. A., Ashpole, J., Hutchison, J., and zu Ermgassen, P. (2017). Mapping the global value and distribution of coral reef tourism. *Mar. Policy* 82, 104–113. doi: 10.1016/j.marpol.2017.05.014

Taylor, E., Baine, M., Killmer, A., and Howard, M. (2013). Seaflower marine protected area: governance for sustainable development. *Mar. Policy* 41, 57–64. doi: 10.1016/j.marpol.2012.12.023

Triffleman, N. J., Hallock, P., and Hine, A. C. (1992). Morphology, sediments, and depositional environments of a small carbonate platform; Serranilla Bank, Nicaraguan Rise, Southwest Caribbean Sea. *J. Sediment Res.* 62, 591–606. doi: 10.1306/D426796A-2B26-11D7-8648000102C1865D

Valderrama, D., and Zea, S. (2003). Esquemas de distribución de esponjas arrecifales (Porifera) del noroccidente del golfo de Urabá, Caribe sur, Colombia. *Bol. Investig. Mar. Costeras* 32, 37–56.

Velásquez, J., López-Angarita, J., and Sánchez, J. A. (2011). Evaluation of the FORAM index in a case of conservation. *Biodivers. Conserv.* 20, 3591–3603. doi: 10.1007/s10531-011-0152-7

Velásquez, J., and Sánchez, J. A. (2015). Octocoral species assembly and coexistence in Caribbean coral reefs. *PLoS One* 10:e0129609. doi: 10.1371/journal.pone.0129609

Weil, E. (2004). "Coral reef diseases in the wider Caribbean," in *Coral Health and Disease*, eds E. Rosenberg and Y. Loya (Berlin: Springer), 35–68. doi: 10.1007/978-3-662-06414-6_2

Wiedenmann, J., D'Angelo, C., Smith, E. G., Hunt, A. N., Legiret, F.-E., Postle, A. D., et al. (2013). Nutrient enrichment can increase the susceptibility of reef corals to bleaching. *Nat. Clim. Change* 3, 160–164. doi: 10.1038/nclimate1661

Wilkinson, C., and Souter, D. (2008). *Status of Caribbean Coral Reefs after Bleaching and Hurricanes in 2005*. Townsville: Global Coral Reef Monitoring Network, and Reef and Rainforest Research Center.

Zea, S. (2001). Patterns of sponge (Porifera, Demospongiae) distribution in remote, ocenic reef complexes of the southwestern Caribbean. *Rev. Acad. Colomb. Cienc. Exactas Físicas Nat.* 25, 579–592.

Conflict of Interest Statement: The authors declare that the research was conducted in the absence of any commercial or financial relationships that could be construed as a potential conflict of interest.

frontiers in Marine Science

DATA REPORT
published: 02 April 2019
doi: 10.3389/fmars.2019.00113

Fish Biodiversity in Three Northern Islands of the Seaflower Biosphere Reserve (Colombian Caribbean)

Arturo Acero P.[1]*, *Jose Julian Tavera*[2], *Andrea Polanco F.*[3] and *Nacor Bolaños-Cubillos*[4]

[1] Instituto de Estudios en Ciencias del Mar, CECIMAR, Universidad Nacional de Colombia, Santa Marta, Colombia, [2] Grupo de Investigación SEyBA, Laboratorio de Ictiología, Departamento de Biología, Universidad del Valle, Cali, Colombia, [3] Museo de Historia Natural marina de Colombia, Programa de Biodiversidad, Instituto de Investigaciones Marinas y Costeras Invemar, Santa Marta, Colombia, [4] Corporación para el Desarrollo Sostenible del Archipiélago de San Andrés, San Andrés, Colombia

Keywords: inventory, new records, fish species, Actinopterygii, Chondrichthyes, Roncador, Serrana, Serranilla

OPEN ACCESS

Edited by:
Sonia Bejarano,
Leibniz Centre for Tropical Marine Research (LG), Germany

Reviewed by:
Badi Raymundo Samaniego, University of the Philippines Los Baños, Philippines
Andres López-Perez, Universidad Autónoma Metropolitana, Mexico
Hudson Tercio Pinheiro, California Academy of Sciences, United States

***Correspondence:**
Arturo Acero P.
aacerop@unal.edu.co

Specialty section:
This article was submitted to Marine Evolutionary Biology, Biogeography and Species Diversity, a section of the journal Frontiers in Marine Science

Received: *21 September 2018*
Accepted: *25 February 2019*
Published: *02 April 2019*

Citation:
Acero P A, Tavera JJ, Polanco F A and Bolaños-Cubillos N (2019) Fish Biodiversity in Three Northern Islands of the Seaflower Biosphere Reserve (Colombian Caribbean). Front. Mar. Sci. 6:113. doi: 10.3389/fmars.2019.00113

BACKGROUND

The archipelago of San Andres, Providence and Santa Catalina was declared by the United Nations Educational, Scientific and Cultural Organization (UNESCO) as the Seaflower Biosphere Reserve in the year 2000. With 180,000 km^2, the archipelago boasts a variety of ecosystems and relatively high levels of biodiversity within the region. In light of the urgent need to appraise the value of marine biodiversity within the reserve and understand its role in contributing to food security for the resident human population, the Colombian government has organized three annual expeditions to three different northern islands. The dataset presented here summarizes the information on fish biodiversity collected in three of the reserve's northern islands, namely Roncador, Serrana, and Serranilla during 2015–2017. In order to include all the information about the Colombian northern islands of the archipelago, data from Quitasueño were also added despite is has not been visited yet by this series of annual expeditions.

DATA DESCRIPTION

Study Area

The archipelago of San Andres, Old Providence and Santa Catalina (Colombia) occupies a relatively small, yet important portion of the central western Caribbean Sea between 82 and 86°W meridians and 12 and 16°N parallels. The three main islands are populated by "raizales" (i.e., an Afrocolombian ethnic group mainly dedicated to fishing and trade among the islands of the reserve), mainland Colombians, and foreigners. According to the national laws, fishing is only allowed for raizales, yet enforcement is weak and illegal fishing by fleets from Jamaica, Nicaragua, Honduras, and others, is common. Enforcement is particularly challenging on the smallest islands of the reserve, as these are patrolled by an often small number of officials and vessels of the Colombian naval force. The archipelago encompasses about three fourths of the more than one hundred Colombian coralline formations. Since 2014 the Colombian government through the Comisión Colombiana del Océano (CCO) has carried out three annual scientific expeditions to the reserve visiting one island at a time. To date, three northern islands have been intensively surveyed, namely Roncador in 2015 (13.533333 N, −80.05 W), Serrana in 2016 (14.383333 N, −80.2 W), and Serranilla in 2017 (15.833333 N, −79.833333 W).

Methods

Here we compile a fish biodiversity dataset for Roncador, Serrana, and Serranilla from various sources. The first one is a published checklist of species ($n = 653$) distributed in 121 families constructed based on 28 papers (peer-reviewed and non-peer-reviewed) published since 1944, as well as on unpublished data gathered by the authors over the past two decades (Bolaños-Cubillos et al., 2015). The second source corresponds to a series of unpublished biological records which are partially available at the Biodiversity Information System of Colombia (SIB Colombia) and were collected during the 2015, 2016, and 2017 Seaflower Expeditions (Acero, 2018; Acero et al., 2018; Polanco, 2018). The third and last source comprised a list of species found on the deep shelves and upper slopes of the islands of the reserve (Polanco, 2015; Robertson and Van Tassell, 2015). For the sake of completeness, all information available from Quitasueño (the only northern island of this archipelago not visited yet by these series of expeditions), usually from Robertson and Van Tassell (2015) or from unpublished short visits by Colombian scientist, is included.

During the expeditions organized by the CCO data were collected by scuba diving as well as snorkeling over a total of 250 man-hours of underwater observation, using the 30-min timed free swim method in depths ranging between 0 and 35 m. As our main objective was to focus on species richness, six ecological units (INVEMAR-ANH, 2012) were surveyed, namely Octocoral-Sponges, Macroalgae-Octocoral-Sponge Meadows, Bioturbated Sediment—Calcareous Algae, Leafy Algae over Rubble, *Acropora palmata*-Octocorals, Seagrass Meadow and Encrusting Algae-Encrusting Sponge-Octocoral, and Coral Mixture. Specimens collected or photographed by several expedition members were also identified and included. In the case of Serranilla, seven species were recorded by video cameras during the project "Elasmobranch diversity and abundance estimates using baited remote underwater video stations" developed by Colombia Azul Foundation, Universidad de los Andes, and Florida International University. Scientific names of species follow the Catalog of Fishes (Eschmeyer et al., 2018) and the classification follows Eschmeyer et al. (2018) for cartilaginous fishes and Betancur-R et al. (2017) for bony fishes.

Description of the Dataset

The dataset presented here comprises a depurated inventory of the fish species reported from Roncador, Serrana, and Serranilla (the three of them already visited by the recent CCO expeditions), as well as from Quitasueño, the largest and westernmost island, which has not been yet visited by the CCO expeditions. The dataset includes all the fish species observed during the expeditions carried out between 2015 and 2017 (**Table 1**) plus the reports previously published in Bolaños-Cubillos et al. (2015), Polanco (2015), and Robertson and Van Tassell (2015). The six fields included per species within this dataset are listed and described in detail below.

Taxon ID and Scientific Name ID: This field includes a unique and stable-through-time alphanumeric identifier (taxonomic identifier) provided by Life Science Identifier (LSID), recovered from World Register of Marine Species (WoRMS) (AphiaID).

Basis of record: As the data set includes records based on human observations, machine observations (Baited Remote Underwater Video Stations - BRUVs) or preserved specimens this field contains this specific information for each species.

Bibliographic Citation: This field includes the reference that explicitly reports the species on the northern islands of the Seaflower Biosphere Reserve.

Reference: URLs associated to georeferenced occurrences of the species found in the dataset.

Locality: Specific localities where the species have been recorded in the northern islands are presented in this field. Four localities were defined considering the islands Quitasueño, Roncador, Serrana, Serranilla, and a locality named North for species found on the northern area among the banks.

Locality ID: The Marine Regions Geographic Identifier (MRGID) provided by mariregions.org for each island and the MRGID for the Seaflower Marine Protected Area for the locality named "North."

Outcomes and Discussion

A total of 411 species are recorded here for our study area, that is the northern islands of the reserve (i.e., Roncador, Serrana, and Serranilla) and the westernmost island Quitasueño. Considering that a total of 1,694 fish species (including shelf and slope fishes) are reported for the Greater Caribbean region (Robertson and Van Tassell, 2015), our study area harbors 24% (i.e., close to one fourth) of the region's fish species richness. Fifty four percent of the species reported here (i.e., 220) were inventoried by the authors (**Table 1**) during expeditions to Roncador in 2015 ($n = 140$), Serrana in 2016 ($n = 155$), and Serranilla in 2017 ($n = 166$). With 1,577 fish species reportedly native to and resident in the shallow waters (<100 m) of the Greater Caribbean (Robertson and Van Tassell, 2015), our findings demonstrated that just three of the smallest islands of the reserve encompass a remarkable proportion (i.e., 14%) of Greater Caribbean marine fish species richness. This high diversity is concentrated in an area less than 5% of Greater Caribbean extension. Interestingly, only 42% species ($n = 92$) were common to the three islands. When clustering sites based on fish community structure using the Jaccard index of similarity, relatively low values are observed between pairs of islands indicating that each island harbors relatively distinct fish communities. The fish faunas of Roncador and Serrana, for instance, are 62% similar, and those of Roncador and Serranilla are alike only by 52%. This result emphasizes the urgent need to protect the valuable and unique fish assemblages of these and other small islands and banks comprising the archipelago.

Another point worth remarking is the consistent absence (or at least rarity) of several large-bodied, commercially valuable species throughout the reserve threatened by overfishing (Chasqui et al., 2017). Most striking is the absence of the Nassau grouper, *Epinephelus striatus*, one of the most typical large epinephelines of Caribbean coral reefs (Bent-Hooker, 2012).

TABLE 1 | Inventory of the species observed in three of the northern islands of the Reserve Roncador, Serrana and Serranilla with some additional records from Quitasueño and the northern water territories.

Family and species	Location	References
CHIMAERIDAE		
Chimaera cubana	North	Bolaños-Cubillos et al., 2015
GINGLYMOSTOMATIDAE		
Ginglymostoma cirratum	Roncador, Serrana, Serranilla	Bolaños-Cubillos et al., 2015; Acero, 2018; Acero et al., 2018
LAMNIDAE		
Isurus oxyrinchus	North	Bolaños-Cubillos et al., 2015
SCYLIORHINIDAE		
Scyliorhinus retifer	Quitasueño	Robertson et al., 2015
TRIAKIDAE		
Mustelus canis insularis	North	Bolaños-Cubillos et al., 2015
CARCHARHINIDAE		
Carcharhinus acronotus	Serranilla	Bolaños-Cubillos et al., 2015; Acero et al., 2018
Carcharhinus altimus	North	Bolaños-Cubillos et al., 2015
Carcharhinus falciformis	North	Bolaños-Cubillos et al., 2015
Carcharhinus leucas	North	Bolaños-Cubillos et al., 2015
Carcharhinus limbatus	North	Bolaños-Cubillos et al., 2015
Carcharhinus obscurus	North	Bolaños-Cubillos et al., 2015
Carcharhinus perezii	Roncador, Serrana, Serranilla	Bolaños-Cubillos et al., 2015; Fundación Colombia Azul et al., 2017
Carcharhinus plumbeus	North	Bolaños-Cubillos et al., 2015
Galeocerdo cuvier	Serranilla	Bolaños-Cubillos et al., 2015; Fundación Colombia Azul et al., 2017
Negaprion brevirostris	Serranilla	Bolaños-Cubillos et al., 2015; Acero et al., 2018
Prionace glauca	North	Bolaños-Cubillos et al., 2015
Rhizoprionodon porosus	North	Bolaños-Cubillos et al., 2015
Rhizoprionodon terraenovae *D	Serranilla	Fundación Colombia Azul et al., 2017
SPHYRNIDAE		
Sphyrna lewini	Serrana	Bolaños-Cubillos et al., 2015
Sphyrna mokarran	Serranilla	Bolaños-Cubillos et al., 2015; Fundación Colombia Azul et al., 2017
HEXANCHIDAE		
Heptranchias perlo	North	Bolaños-Cubillos et al., 2015
Hexanchus nakamurai	North	Bolaños-Cubillos et al., 2015
SQUALIDAE		
Squalus cubensis	North	Bolaños-Cubillos et al., 2015
NARCINIDAE		
Narcine bancroftii	North	Bolaños-Cubillos et al., 2015
RHINOBATIDAE		
Pseudobatos percellens	Serrana, Serranilla	Bolaños-Cubillos et al., 2015; Acero et al., 2018
RAJIDAE		
Fenestraja sinusmexicanus	Quitasueño	Polanco, 2015
Leucoraja garmani	Quitasueño	Polanco, 2015
UROTRYGONIDAE		
Urobatis jamaicensis	Serrana	Bolaños-Cubillos et al., 2015
DASYATIDAE		
Hypanus americanus	Roncador, Serrana, Serranilla	Bolaños-Cubillos et al., 2015; Acero et al., 2018
Hypanus sabinus *D	Serranilla	Acero et al., 2018
MYLIOBATIDAE		
Aetobatus narinari	Serrana	Bolaños-Cubillos et al., 2015
MEGALOPIDAE		
Megalops atlanticus	North	Bolaños-Cubillos et al., 2015
ALBULIDAE		
Albula vulpes	Serrana, Serranilla	Bolaños-Cubillos et al., 2015; Acero et al., 2018
CONGRIDAE		
Conger esculentus	North	Bolaños-Cubillos et al., 2015
Heteroconger longissimus	Roncador, Serrana	Bolaños-Cubillos et al., 2015
Pseudophichthys splendens	Quitasueño	Polanco, 2015
Rhynchoconger gracilior	Quitasueño	Polanco, 2015
MURAENIDAE		
Anarchias similis	Quitasueño	Robertson et al., 2015
Echidna catenata	Roncador, Serranilla	Bolaños-Cubillos et al., 2015; Acero et al., 2018
Enchelycore nigricans	North	Bolaños-Cubillos et al., 2015
Gymnothorax conspersus	North	Bolaños-Cubillos et al., 2015
Gymnothorax funebris	Roncador, Serranilla	Bolaños-Cubillos et al., 2015; Acero et al., 2018
Gymnothorax maderensis	North	Bolaños-Cubillos et al., 2015
Gymnothorax miliaris	Roncador, Serrana, Serranilla	Bolaños-Cubillos et al., 2015; Acero et al., 2018
Gymnothorax moringa	Roncador, Serrana, Serranilla	Bolaños-Cubillos et al., 2015; Acero et al., 2018
Gymnothorax vicinus	Roncador, Serranilla	Bolaños-Cubillos et al., 2015; Acero et al., 2018
Uropterygius macularius	North	Bolaños-Cubillos et al., 2015
NETTASTOMATIDAE		
Hoplunnis macrura	Quitasueño	Robertson et al., 2015
Hoplunnis tenuis	Quitasueño	Polanco, 2015
OPHICHTHIDAE		
Ahlia egmontis	Serranilla	Bolaños-Cubillos et al., 2015; Acero et al., 2018
Callechelys bilinearis	North	Bolaños-Cubillos et al., 2015
Myrichthys breviceps	Serranilla	Bolaños-Cubillos et al., 2015; Acero et al., 2018
Myrichthys ocellatus	North	Bolaños-Cubillos et al., 2015
Myrophis platyrhynchus	Quitasueño	Robertson et al., 2015
Ophichthus ophis	Serranilla	Acero et al., 2018
Ophichthus spinicauda	North	Bolaños-Cubillos et al., 2015

(Continued)

TABLE 1 | Continued

Family and species	Location	References
CHLOPSIDAE		
Kaupichthys hyoproroides	North	Bolaños-Cubillos et al., 2015
MORINGUIDAE		
Moringua edwardsi	North	Bolaños-Cubillos et al., 2015
CLUPEIDAE		
Harengula humeralis	North	Bolaños-Cubillos et al., 2015
Jenkinsia lamprotaenia	North	Bolaños-Cubillos et al., 2015
Jenkinsia majua	North	Bolaños-Cubillos et al., 2015
ENGRAULIDAE		
Anchoa lamprotaenia	North	Bolaños-Cubillos et al., 2015
ARGENTINIDAE		
Glossanodon pygmaeus	Quitasueño	Robertson et al., 2015
SYNODONTIDAE		
Saurida brasiliensis	Quitasueño	Robertson et al., 2015
Saurida caribbaea	Quitasueño	Polanco, 2015
Saurida normani	North	Bolaños-Cubillos et al., 2015
Synodus intermedius	Roncador, Serrana	Bolaños-Cubillos et al., 2015
Synodus synodus	Serranilla	Bolaños-Cubillos et al., 2015; Acero et al., 2018
CHLOROPHTHALMIDAE		
Chlorophthalmus agassizi	Quitasueño	Polanco, 2015
PARAZENIDAE		
Cyttopsis rosea	Quitasueño	Polanco, 2015
Parazen pacificus	Quitasueño	Polanco, 2015
ZENIONTIDAE		
Zenion hololepis	Quitasueño	Polanco, 2015
GRAMMICOLEPIDIDAE		
Xenolepidichthys dalgleishi	Quitasueño	Polanco, 2015
MERLUCCIIDAE		
Steindachneria argentea	Quitasueño	Polanco, 2015
Merluccius albidus	Quitasueño	Polanco, 2015
POLYMIXIIDAE		
Polymixia lowei	North	Bolaños-Cubillos et al., 2015
BERYCIDAE		
Beryx splendens	Quitasueño	Polanco, 2015
TRACHICHTHYIDAE		
Hoplostethus occidentalis	Quitasueño	Polanco, 2015
HOLOCENTRIDAE		
Holocentrus adscensionis	Roncador, Serrana, Serranilla	Bolaños-Cubillos et al., 2015; Acero, 2018; Acero et al., 2018
Holocentrus rufus	Roncador, Serrana, Serranilla	Bolaños-Cubillos et al., 2015; Acero, 2018; Acero et al., 2018
Myripristis jacobus	Roncador, Serrana, Serranilla	Bolaños-Cubillos et al., 2015; Acero, 2018; Acero et al., 2018
Ostichthys trachypoma	North	Bolaños-Cubillos et al., 2015
Neoniphon marianus	Roncador, Serrana, Serranilla	Bolaños-Cubillos et al., 2015; Acero, 2018; Acero et al., 2018

(Continued)

TABLE 1 | Continued

Family and species	Location	References
Sargocentron coruscum	North	Bolaños-Cubillos et al., 2015
Sargocentron vexillarium	Roncador, Serrana, Serranilla	Bolaños-Cubillos et al., 2015; Acero et al., 2018
OPHIDIIDAE		
Lepophidium entomelan	North	Bolaños-Cubillos et al., 2015
Lepophidium kallion	North	Polanco, 2015
Lepophidium marmoratum	North	Bolaños-Cubillos et al., 2015
Lepophidium staurophor	North	Bolaños-Cubillos et al., 2015
Neobythites marginatus	Quitasueño	Polanco, 2015
Neobythites multiocellatus	Quitasueño	Robertson et al., 2015
APOGONIDAE		
Apogon binotatus	North	Bolaños-Cubillos et al., 2015
Apogon lachneri	Serrana	Bolaños-Cubillos et al., 2015
Apogon maculatus	Roncador, Serrana, Serranilla	Bolaños-Cubillos et al., 2015; Acero et al., 2018
Apogon pseudomaculatus	North	Bolaños-Cubillos et al., 2015
Apogon quadrisquamatus	Serranilla	Bolaños-Cubillos et al., 2015; Acero et al., 2018
Apogon townsendi	Serrana, Serranilla	Bolaños-Cubillos et al., 2015; Acero et al., 2018
Astrapogon puncticulatus	North	Bolaños-Cubillos et al., 2015
Astrapogon stellatus	North	Bolaños-Cubillos et al., 2015
Phaeoptyx conklini	North	Bolaños-Cubillos et al., 2015
Paroncheilus affinis	Quitasueño	Robertson et al., 2015
GOBIIDAE		
Bathygobius soporator	North	Bolaños-Cubillos et al., 2015
Coryphopterus dicrus	Roncador	Bolaños-Cubillos et al., 2015
Coryphopterus eidolon	Roncador	Bolaños-Cubillos et al., 2015
Coryphopterus lipernes	North	Bolaños-Cubillos et al., 2015
Coryphopterus personatus	Roncador, Serrana, Serranilla	Bolaños-Cubillos et al., 2015; Acero et al., 2018
Coryphopterus tortugae	Roncador, Serrana, Serranilla	Bolaños-Cubillos et al., 2015; Acero et al., 2018
Cryptopsilotris batrachodes *MP	Serranilla	Acero et al., 2018
Elacatinus evelynae	Roncador, Serrana	Bolaños-Cubillos et al., 2015
Elacatinus horsti	Roncador, Serrana	Bolaños-Cubillos et al., 2015
Elacatinus illecebrosus	Roncador	
Elacatinus lori	North	Bolaños-Cubillos et al., 2015
Elacatinus louisae	Roncador, Serranilla	Bolaños-Cubillos et al., 2015; Acero et al., 2018
Elacatinus prochilos	Serrana, Serranilla	Bolaños-Cubillos et al., 2015; Acero et al., 2018
Elacatinus serranilla	Serranilla	Robertson et al., 2015
Gnatholepis thompsoni	Serranilla	Bolaños-Cubillos et al., 2015; Acero et al., 2018
Nes longus	North	Bolaños-Cubillos et al., 2015

(Continued)

TABLE 1 | Continued

Family and species	Location	References
Risor ruber	North	Bolaños-Cubillos et al., 2015
Tigrigobius dilepis	Roncador	Bolaños-Cubillos et al., 2015
Varicus bucca	Serrana	Robertson et al., 2015
AULOSTOMIDAE		
Aulostomus maculatus	Roncador, Serrana, Serranilla	Bolaños-Cubillos et al., 2015; Acero, 2018; Acero et al., 2018
FISTULARIIDAE		
Fistularia tabacaria *	Serranilla	Acero et al., 2018
SYNGNATHIDAE		
Bryx dunckeri	North	Bolaños-Cubillos et al., 2015
Microphis lineatus	North	Bolaños-Cubillos et al., 2015
Syngnathus pelagicus	Roncador	
DACTYLOPTERIDAE		
Dactylopterus volitans	Serranilla	Bolaños-Cubillos et al., 2015; Acero et al., 2018
CALLIONYMIDAE		
Callionymus bairdi	North	Bolaños-Cubillos et al., 2015
Foetorepus agassizi	Quitasueño	Polanco, 2015
MULLIDAE		
Mulloidichthys martinicus	Roncador, Serrana, Serranilla	Bolaños-Cubillos et al., 2015; Acero, 2018; Acero et al., 2018
Pseudupeneus maculatus	Roncador, Serrana, Serranilla	Bolaños-Cubillos et al., 2015; Acero, 2018; Acero et al., 2018
GEMPYLIDAE		
Gempylus serpens	North	Bolaños-Cubillos et al., 2015
Nealotus tripes	North	Bolaños-Cubillos et al., 2015
Promethichthys prometheus	Quitasueño	Polanco, 2015
NOMEIDAE		
Nomeus gronovii	North	Bolaños-Cubillos et al., 2015
SCOMBRIDAE		
Acanthocybium solandri	Serrana	Bolaños-Cubillos et al., 2015
Euthynnus alletteratus	North	Bolaños-Cubillos et al., 2015
Katsuwonus pelamis	North	Bolaños-Cubillos et al., 2015
Scomberomorus cavalla	North	Bolaños-Cubillos et al., 2015
Scomberomorus regalis	North	Bolaños-Cubillos et al., 2015
Thunnus atlanticus	North	Bolaños-Cubillos et al., 2015
Thunnus obesus	North	Bolaños-Cubillos et al., 2015
POLYNEMIDAE		
Polydactylus virginicus	North	Bolaños-Cubillos et al., 2015
SPHYRAENIDAE		
Sphyraena barracuda	Roncador, Serrana, Serranilla	Bolaños-Cubillos et al., 2015; Acero, 2018; Acero et al., 2018
Sphyraena picudilla	Roncador, Serrana	
CARANGIDAE		
Alectis ciliaris	North	Bolaños-Cubillos et al., 2015
Caranx bartholomaei	Roncador, Serrana, Serranilla	Bolaños-Cubillos et al., 2015; Acero et al., 2018
Caranx crysos	Roncador, Serrana, Serranilla	Bolaños-Cubillos et al., 2015; Acero, 2018; Acero et al., 2018
Caranx hippos	Serranilla	Bolaños-Cubillos et al., 2015; Acero et al., 2018
Caranx latus	Roncador, Serrana, Serranilla	Bolaños-Cubillos et al., 2015; Acero et al., 2018
Caranx lugubris	Roncador, Serrana	Bolaños-Cubillos et al., 2015
Caranx ruber	Roncador, Serrana, Serranilla	Bolaños-Cubillos et al., 2015; Acero, 2018; Acero et al., 2018
Decapterus macarellus	Serrana, Serranilla	Bolaños-Cubillos et al., 2015; Acero et al., 2018
Decapterus punctatus	Serranilla	Bolaños-Cubillos et al., 2015; Acero et al., 2018
Elagatis bipinnulata	Roncador, Serrana, Serranilla	Bolaños-Cubillos et al., 2015; Acero et al., 2018
Seriola dumerili	North	Bolaños-Cubillos et al., 2015
Seriola fasciata	Serranilla	Bolaños-Cubillos et al., 2015; Acero et al., 2018
Seriola rivoliana	Roncador, Serranilla	Bolaños-Cubillos et al., 2015; Acero et al., 2018
Trachinotus falcatus	North	Bolaños-Cubillos et al., 2015
Trachinotus goodei	Roncador, Serrana	Bolaños-Cubillos et al., 2015
CORYPHAENIDAE		
Coryphaena hippurus	Roncador, Serrana	Bolaños-Cubillos et al., 2015
ECHENEIDAE		
Echeneis naucrates	Serranilla	Bolaños-Cubillos et al., 2015; Acero et al., 2018
Echeneis neucratoides	North	Bolaños-Cubillos et al., 2015
Phtheirichthys lineatus	North	Bolaños-Cubillos et al., 2015
Remora brachyptera	Serrana	Robertson et al., 2015
RACHYCENTRIDAE		
Rachycentron canadum	North	Bolaños-Cubillos et al., 2015
BOTHIDAE		
Bothus lunatus	Roncador, Serranilla	Bolaños-Cubillos et al., 2015; Acero et al., 2018
PARALICHTHYIDAE		
Ancylopsetta microctenus	Quitasueño	Polanco, 2015
Citharichthys dinoceros	Quitasueño	Polanco, 2015
GRAMMATIDAE		
Gramma loreto	Roncador, Serrana, Serranilla	Bolaños-Cubillos et al., 2015; Acero, 2018; Acero et al., 2018
Gramma melacara	Roncador, Serrana	Bolaños-Cubillos et al., 2015
OPISTOGNATHIDAE		
Opistognathus aurifrons	Roncador, Serrana, Serranilla	Bolaños-Cubillos et al., 2015; Acero et al., 2018
Opistognathus maxillosus	North	Bolaños-Cubillos et al., 2015
Opistognathus whitehursti	North	Bolaños-Cubillos et al., 2015
POMACENTRIDAE		
Abudefduf saxatilis	Roncador, Serrana, Serranilla	Bolaños-Cubillos et al., 2015; Acero, 2018; Acero et al., 2018
Abudefduf taurus	Roncador	Bolaños-Cubillos et al., 2015
Chromis cyanea	Roncador, Serrana, Serranilla	Bolaños-Cubillos et al., 2015; Acero, 2018; Acero et al., 2018

(Continued)

TABLE 1 | Continued

Family and species	Location	References
Chromis insolata	Roncador	Bolaños-Cubillos et al., 2015
Chromis multilineata	Roncador, Serrana, Serranilla	Bolaños-Cubillos et al., 2015; Acero et al., 2018
Microspathodon chrysurus	Roncador, Serrana, Serranilla	Bolaños-Cubillos et al., 2015; Acero et al., 2018
Stegastes adustus	Roncador, Serranilla	Bolaños-Cubillos et al., 2015; Acero et al., 2018
Stegastes diencaeus	Roncador, Serrana, Serranilla	Bolaños-Cubillos et al., 2015; Acero, 2018; Acero et al., 2018
Stegastes leucostictus	Roncador, Serrana, Serranilla	Bolaños-Cubillos et al., 2015; Acero, 2018; Acero et al., 2018
Stegastes partitus	Roncador, Serrana, Serranilla	Bolaños-Cubillos et al., 2015; Acero, 2018; Acero et al., 2018
Stegastes planifrons	Roncador, Serrana, Serranilla	Bolaños-Cubillos et al., 2015; Acero et al., 2018
Stegastes xanthurus	Roncador, Serrana	Bolaños-Cubillos et al., 2015; Acero, 2018
ATHERINIDAE		
Atherina harringtonensis	Serranilla	Bolaños-Cubillos et al., 2015; Acero et al., 2018
Atherinomorus stipes	North	Bolaños-Cubillos et al., 2015
BELONIDAE		
Ablennes hians	North	Bolaños-Cubillos et al., 2015
Platybelone argalus argalus	North	Bolaños-Cubillos et al., 2015
Strongylura notata	North	Bolaños-Cubillos et al., 2015
Tylosurus acus acus	North	Bolaños-Cubillos et al., 2015
Tylosurus crocodilus crocodilus	North	Bolaños-Cubillos et al., 2015
EXOCOETIDAE		
Cheilopogon cyanopterus	Quitasueño	Robertson et al., 2015
Cheilopogon exsiliens	North	Bolaños-Cubillos et al., 2015
Cheilopogon melanurus	North	Bolaños-Cubillos et al., 2015
Cypselurus comatus	North	Robertson et al., 2015
Exocoetus obtusirostris	Quitasueño	Robertson et al., 2015
Exocoetus volitans	Quitasueño	Robertson et al., 2015
Hirundichthys affinis	North	Bolaños-Cubillos et al., 2015
Parexocoetus hillianus	North	Bolaños-Cubillos et al., 2015
Prognichthys occidentalis	North	Bolaños-Cubillos et al., 2015
HEMIRAMPHIDAE		
Hemiramphus balao	North	Robertson et al., 2015
Hemiramphus brasiliensis	Serranilla	Bolaños-Cubillos et al., 2015; Acero et al., 2018
MUGILIDAE		
Mugil curema	North	Bolaños-Cubillos et al., 2015
Mugil trichodon	North	Bolaños-Cubillos et al., 2015
GOBIESOCIDAE		
Gobiesox punctulatus	Serranilla	Bolaños-Cubillos et al., 2015
BLENNIIDAE		
Entomacrodus nigricans	North	Bolaños-Cubillos et al., 2015
Ophioblennius macclurei	Roncador, Serrana, Serranilla	Bolaños-Cubillos et al., 2015; Acero et al., 2018
CHAENOPSIDAE		
Acanthemblemaria aspera *	Serrana	
Acanthemblemaria maria *	Serranilla	Acero et al., 2018
Acanthemblemaria spinosa *	Serrana	
Emblemaria caycedoi	North	Bolaños-Cubillos et al., 2015
Emblemariopsis sp. *	Serrana	
Lucayablennius zingaro	Roncador, Serrana	Bolaños-Cubillos et al., 2015
LABRISOMIDAE		
Brockius albigenys	North	Bolaños-Cubillos et al., 2015
Gobioclinus bucciferus	North	Bolaños-Cubillos et al., 2015
Gobioclinus gobio	North	Bolaños-Cubillos et al., 2015
Gobioclinus guppyi	North	Bolaños-Cubillos et al., 2015
Brockius nigricinctus	Serranilla	Bolaños-Cubillos et al., 2015; Acero et al., 2018
Labrisomus nuchipinnis	Serranilla	Bolaños-Cubillos et al., 2015; Acero et al., 2018
Malacoctenus aurolineatus	Roncador, Serrana	Bolaños-Cubillos et al., 2015
Malacoctenus boehlkei	Roncador, Serrana	Bolaños-Cubillos et al., 2015
Malacoctenus erdmani	Serrana	
Malacoctenus gilli	Serranilla	Bolaños-Cubillos et al., 2015; Acero et al., 2018
Malacoctenus macropus	Roncador, Serranilla	Bolaños-Cubillos et al., 2015; Acero et al., 2018
Malacoctenus triangulatus	Roncador, Serrana, Serranilla	Bolaños-Cubillos et al., 2015; Acero et al., 2018
CHAENOPSIDAE		
Stathmonotus gymnodermis *MP	Serranilla	Acero et al., 2018
TRIPTERYGIIDAE		
Enneanectes pectoralis	North	Bolaños-Cubillos et al., 2015
CAPROIDAE		
Antigonia capros	North	Bolaños-Cubillos et al., 2015
Antigonia combatia	Quitasueño	Polanco, 2015
GERREIDAE		
Eucinostomus argenteus	North	Bolaños-Cubillos et al., 2015
Eucinostomus lefroyi *	Serranilla	Acero et al., 2018
Gerres cinereus	North	Bolaños-Cubillos et al., 2015
HAEMULIDAE		
Anisotremus surinamensis	Serranilla	Bolaños-Cubillos et al., 2015; Acero et al., 2018
Anisotremus virginicus	North	Bolaños-Cubillos et al., 2015
Brachygenys chrysargyreus	Roncador, Serrana, Serranilla	Bolaños-Cubillos et al., 2015; Acero et al., 2018
Haemulon album	Roncador, Serrana, Serranilla	Bolaños-Cubillos et al., 2015; Acero, 2018; Acero et al., 2018

(Continued)

TABLE 1 | Continued

Family and species	Location	References
Haemulon aurolineatum	Serrana, Serranilla	Bolaños-Cubillos et al., 2015; Acero et al., 2018
Haemulon carbonarium	Roncador, Serrana, Serranilla	Bolaños-Cubillos et al., 2015; Acero et al., 2018
Haemulon flavolineatum	Roncador, Serrana, Serranilla	Bolaños-Cubillos et al., 2015; Acero, 2018; Acero et al., 2018
Haemulon macrostomum	Serrana	Bolaños-Cubillos et al., 2015
Haemulon melanurum	Serrana, Serranilla	Bolaños-Cubillos et al., 2015; Acero, 2018; Acero et al., 2018
Haemulon parra	Serrana, Serranilla	Bolaños-Cubillos et al., 2015; Acero et al., 2018
Haemulon plumierii	Roncador, Serrana, Serranilla	Bolaños-Cubillos et al., 2015; Acero, 2018; Acero et al., 2018
Haemulon sciurus	Serrana	Bolaños-Cubillos et al., 2015
Haemulon striatum	North	Bolaños-Cubillos et al., 2015
Haemulon vittatum	Serrana	Bolaños-Cubillos et al., 2015
LUTJANIDAE		
Apsilus dentatus	North	Bolaños-Cubillos et al., 2015
Etelis oculatus	North	Bolaños-Cubillos et al., 2015
Lutjanus analis	Serrana, Serranilla	Bolaños-Cubillos et al., 2015; Acero et al., 2018
Lutjanus apodus	Roncador, Serrana, Serranilla	Bolaños-Cubillos et al., 2015; Acero, 2018; Acero et al., 2018
Lutjanus buccanella	North	Bolaños-Cubillos et al., 2015
Lutjanus cyanopterus	North	Bolaños-Cubillos et al., 2015
Lutjanus griseus	Serrana	Bolaños-Cubillos et al., 2015
Lutjanus jocu	Roncador, Serrana	Bolaños-Cubillos et al., 2015
Lutjanus mahogoni	Roncador, Serrana, Serranilla	Bolaños-Cubillos et al., 2015; Acero, 2018; Acero et al., 2018
Lutjanus purpureus	North	Bolaños-Cubillos et al., 2015
Lutjanus synagris	Serrana, Serranilla	Bolaños-Cubillos et al., 2015; Acero et al., 2018
Lutjanus vivanus	North	Bolaños-Cubillos et al., 2015
Ocyurus chrysurus	Roncador, Serrana, Serranilla	Bolaños-Cubillos et al., 2015; Acero et al., 2018
Pristipomoides macrophthalmus	North	Bolaños-Cubillos et al., 2015
Rhomboplites aurorubens	North	Bolaños-Cubillos et al., 2015
MALACANTHIDAE		
Caulolatilus cyanops	North	Bolaños-Cubillos et al., 2015
Malacanthus plumieri	Roncador, Serrana, Serranilla	Acero, 2018; Acero et al., 2018
POMACANTHIDAE		
Centropyge argi	Serranilla	Bolaños-Cubillos et al., 2015; Acero et al., 2018
Holacanthus ciliaris	Roncador, Serrana, Serranilla	Bolaños-Cubillos et al., 2015; Acero, 2018; Acero et al., 2018
Holacanthus tricolor	Roncador, Serrana, Serranilla	Bolaños-Cubillos et al., 2015; Acero, 2018; Acero et al., 2018
Pomacanthus arcuatus	Roncador, Serrana, Serranilla	Bolaños-Cubillos et al., 2015; Acero, 2018; Acero et al., 2018
Pomacanthus paru	Roncador, Serrana, Serranilla	Bolaños-Cubillos et al., 2015; Acero et al., 2018

(Continued)

TABLE 1 | Continued

Family and species	Location	References
PRIACANTHIDAE		
Cookeolus japonicus	North	Bolaños-Cubillos et al., 2015
Heteropriacanthus cruentatus	Roncador, Serrana, Serranilla	Bolaños-Cubillos et al., 2015; Acero et al., 2018
Priacanthus arenatus *	Serranilla	Acero et al., 2018
SCIAENIDAE		
Equetus lanceolatus	Roncador, Serranilla	Bolaños-Cubillos et al., 2015; Acero et al., 2018
Equetus punctatus	Serrana, Serranilla	Bolaños-Cubillos et al., 2015; Acero, 2018; Acero et al., 2018
Pareques acuminatus	Serrana, Serranilla	Bolaños-Cubillos et al., 2015; Acero, 2018; Acero et al., 2018
URANOSCOPIDAE		
Kathetostoma cubana	North	Polanco, 2015
LABRIDAE		
Bodianus rufus	Roncador, Serrana, Serranilla	Bolaños-Cubillos et al., 2015; Acero et al., 2018
Clepticus parrae	Roncador, Serrana, Serranilla	Bolaños-Cubillos et al., 2015; Acero, 2018; Acero et al., 2018
Doratonotus megalepis *	Serranilla	Acero et al., 2018
Halichoeres bivittatus	Roncador, Serrana, Serranilla	Bolaños-Cubillos et al., 2015; Acero et al., 2018
Halichoeres cyanocephalus	Serranilla	Bolaños-Cubillos et al., 2015; Acero et al., 2018
Halichoeres garnoti	Roncador, Serrana, Serranilla	Bolaños-Cubillos et al., 2015; Acero, 2018; Acero et al., 2018
Halichoeres maculipinna	Roncador, Serrana, Serranilla	Bolaños-Cubillos et al., 2015; Acero et al., 2018
Halichoeres pictus	Serranilla	Bolaños-Cubillos et al., 2015; Acero et al., 2018
Halichoeres poeyi	Serrana, Serranilla	Bolaños-Cubillos et al., 2015; Acero et al., 2018
Halichoeres radiatus	Roncador, Serrana, Serranilla	Bolaños-Cubillos et al., 2015; Acero et al., 2018
Lachnolaimus maximus	Roncador, Serrana	Bolaños-Cubillos et al., 2015
Thalassoma bifasciatum	Roncador, Serrana, Serranilla	Bolaños-Cubillos et al., 2015; Acero, 2018; Acero et al., 2018
Xyrichthys martinicensis	Roncador	Bolaños-Cubillos et al., 2015
Xyrichthys novacula	North	Bolaños-Cubillos et al., 2015
Xyrichthys splendens	Roncador, Serrana, Serranilla	Bolaños-Cubillos et al., 2015; Acero et al., 2018
SCARIDAE		
Cryptotomus roseus	North	Bolaños-Cubillos et al., 2015
Nicholsina usta	Serranilla	Bolaños-Cubillos et al., 2015; Acero et al., 2018
Scarus coelestinus	Roncador, Serrana, Serranilla	Bolaños-Cubillos et al., 2015; Acero et al., 2018
Scarus coeruleus	North	Bolaños-Cubillos et al., 2015
Scarus guacamaia	North	Bolaños-Cubillos et al., 2015
Scarus iseri	Roncador, Serrana, Serranilla	Bolaños-Cubillos et al., 2015; Acero, 2018; Acero et al., 2018
Scarus taeniopterus	Roncador, Serrana, Serranilla	Bolaños-Cubillos et al., 2015; Acero, 2018; Acero et al., 2018

(Continued)

TABLE 1 | Continued

Family and species	Location	References
Scarus vetula	Roncador, Serrana, Serranilla	Bolaños-Cubillos et al., 2015; Acero, 2018; Acero et al., 2018
Sparisoma atomarium	Roncador, Serrana, Serranilla	Bolaños-Cubillos et al., 2015; Acero, 2018; Acero et al., 2018
Sparisoma aurofrenatum	Roncador, Serrana, Serranilla	Bolaños-Cubillos et al., 2015; Acero, 2018; Acero et al., 2018
Sparisoma chrysopterum	Roncador, Serrana, Serranilla	Bolaños-Cubillos et al., 2015; Acero, 2018; Acero et al., 2018
Sparisoma radians	Serranilla	Bolaños-Cubillos et al., 2015; Acero et al., 2018
Sparisoma rubripinne	Roncador, Serrana, Serranilla	Bolaños-Cubillos et al., 2015; Acero et al., 2018
Sparisoma viride	Roncador, Serrana, Serranilla	Bolaños-Cubillos et al., 2015; Acero, 2018; Acero et al., 2018
LOBOTIDAE		
Lobotes surinamensis	North	Bolaños-Cubillos et al., 2015
EPHIPPIDAE		
Chaetodipterus faber	North	Bolaños-Cubillos et al., 2015
SPARIDAE		
Calamus bajonado	North	Bolaños-Cubillos et al., 2015
Calamus calamus	Roncador, Serrana, Serranilla	Bolaños-Cubillos et al., 2015; Acero, 2018; Acero et al., 2018
CHAETODONTIDAE		
Chaetodon capistratus	Roncador, Serrana, Serranilla	Bolaños-Cubillos et al., 2015; Acero, 2018; Acero et al., 2018
Chaetodon ocellatus	Roncador, Serrana, Serranilla	Bolaños-Cubillos et al., 2015; Acero, 2018; Acero et al., 2018
Chaetodon sedentarius	Serranilla	Bolaños-Cubillos et al., 2015; Acero et al., 2018
Chaetodon striatus	Roncador, Serrana, Serranilla	Bolaños-Cubillos et al., 2015; Acero, 2018; Acero et al., 2018
Prognathodes aculeatus	Roncador, Serrana	Bolaños-Cubillos et al., 2015
ANTENNARIIDAE		
Antennarius pauciradiatus *	Roncador	
*Histrio histrio**	Roncador	Bolaños-Cubillos et al., 2015
OGCOCEPHALIDAE		
Dibranchus atlanticus	Quitasueño	Polanco, 2015
Malthopsis gnoma	Quitasueño	Polanco, 2015
Ogcocephalus pumilus	Quitasueño	Robertson et al., 2015
Zalieutes mcgintyi	Quitasueño	Polanco, 2015
TRIACANTHODIDAE		
Hollardia hollardi	Quitasueño	Polanco, 2015
Parahollardia schmidti	Quitasueño	Polanco, 2015
DIODONTIDAE		
Chilomycterus antillarum *	Serrana	Acero, 2018
Diodon holocanthus	Serrana, Serranilla	Bolaños-Cubillos et al., 2015; Acero et al., 2018
Diodon hystrix	Roncador, Serrana, Serranilla	Bolaños-Cubillos et al., 2015; Acero et al., 2018
TETRAODONTIDAE		
Canthigaster rostrata	Roncador, Serrana, Serranilla	Bolaños-Cubillos et al., 2015; Acero, 2018; Acero et al., 2018
Sphoeroides dorsalis	Quitasueño	Robertson et al., 2015
Sphoeroides spengleri	Serrana, Serranilla	Bolaños-Cubillos et al., 2015; Polanco, 2018
BALISTIDAE		
Balistes capriscus	Roncador	
Balistes vetula	Roncador, Serrana, Serranilla	Bolaños-Cubillos et al., 2015; Acero, 2018; Acero et al., 2018
Canthidermis maculata	North	Bolaños-Cubillos et al., 2015
Canthidermis sufflamen	Serrana, Serranilla	Bolaños-Cubillos et al., 2015; Acero, 2018; Acero et al., 2018
Melichthys niger	Serrana, Serranilla	Bolaños-Cubillos et al., 2015; Acero et al., 2018
Xanthichthys ringens	North	Bolaños-Cubillos et al., 2015
MONACANTHIDAE		
Aluterus scriptus	Serrana, Serranilla	Bolaños-Cubillos et al., 2015; Acero et al., 2018
Cantherines macrocerus	Roncador, Serrana, Serranilla	Bolaños-Cubillos et al., 2015; Acero, 2018; Acero et al., 2018
Cantherines pullus	Roncador, Serrana, Serranilla	Bolaños-Cubillos et al., 2015; Acero et al., 2018
Monacanthus ciliatus *	Serranilla	Acero et al., 2018
Monacanthus tuckeri	North	Bolaños-Cubillos et al., 2015
Stephanolepis setifer *	Roncador	
OSTRACIIDAE		
Acanthostracion polygonius	Roncador, Serrana, Serranilla	Bolaños-Cubillos et al., 2015; Acero et al., 2018
Acanthostracion quadricornis	Serrana, Serranilla	Bolaños-Cubillos et al., 2015; Acero et al., 2018
Lactophrys bicaudalis	Roncador, Serrana, Serranilla	Bolaños-Cubillos et al., 2015; Acero et al., 2018
Lactophrys trigonus	Roncador	Bolaños-Cubillos et al., 2015
Lactophrys triqueter	Roncador, Serrana, Serranilla	Bolaños-Cubillos et al., 2015; Acero, 2018; Acero et al., 2018
ACANTHURIDAE		
Acanthurus chirurgus	Roncador, Serrana, Serranilla	Bolaños-Cubillos et al., 2015; Acero, 2018; Acero et al., 2018
Acanthurus coeruleus	Roncador, Serrana, Serranilla	Bolaños-Cubillos et al., 2015; Acero, 2018; Acero et al., 2018
Acanthurus tractus	Roncador, Serrana, Serranilla	Bolaños-Cubillos et al., 2015; Acero, 2018; Acero et al., 2018
ACROPOMATIDAE		
Synagrops bellus	Quitasueño	Polanco, 2015
Synagrops spinosus	Quitasueño	Polanco, 2015
Synagrops trispinosus	Quitasueño	Polanco, 2015
PEMPHERIDAE		
Pempheris schomburgkii	Serrana, Serranilla	Bolaños-Cubillos et al., 2015; Acero et al., 2018
CIRRHITIDAE		
Amblycirrhitus pinos	Roncador, Serrana, Serranilla	Bolaños-Cubillos et al., 2015; Acero et al., 2018
KYPHOSIDAE		
Kyphosus cinerascens *	Serrana, Serranilla	Acero et al., 2018
Kyphosus sectatrix	Roncador, Serrana, Serranilla	Acero et al., 2018

(Continued)

TABLE 1 | Continued

Family and species	Location	References
Kyphosus vaigiensis	Serrana, Serranilla	Bolaños-Cubillos et al., 2015; Acero et al., 2018
PERCOPHIDAE		
Bembrops anatirostris	Quitasueño	Polanco, 2015
Bembrops macromma	Quitasueño	Polanco, 2015
Bembrops magnisquamis	Quitasueño	Polanco, 2015
Bembrops ocellatus	Quitasueño	Polanco, 2015
Bembrops quadrisella	Quitasueño	Polanco, 2015
SERRANIDAE		
Alphestes afer	North	Bolaños-Cubillos et al., 2015
Bullisichthys caribbaeus	Quitasueño	Polanco, 2015
Cephalopholis cruentata	Roncador, Serrana, Serranilla	Bolaños-Cubillos et al., 2015; Acero, 2018; Acero et al., 2018
Cephalopholis fulva	Roncador, Serrana, Serranilla	Bolaños-Cubillos et al., 2015; Acero, 2018; Acero et al., 2018
Epinephelus adscensionis	North	Bolaños-Cubillos et al., 2015
Epinephelus guttatus	Roncador, Serrana	Bolaños-Cubillos et al., 2015
Epinephelus itajara	Roncador	Bolaños-Cubillos et al., 2015
Epinephelus morio	North	Bolaños-Cubillos et al., 2015
Epinephelus striatus	North	Bolaños-Cubillos et al., 2015
Hypoplectrus aberrans	Roncador, Serrana, Serranilla	Bolaños-Cubillos et al., 2015; Acero et al., 2018
Hypoplectrus indigo	Roncador, Serranilla	Bolaños-Cubillos et al., 2015; Acero et al., 2018
Hypoplectrus maculiferus	Serrana	
Hypoplectrus chlorurus	Serrana	Bolaños-Cubillos et al., 2015
Hypoplectrus gummigutta	North	Bolaños-Cubillos et al., 2015
Hypoplectrus guttavarius	Serrana	Bolaños-Cubillos et al., 2015
Hypoplectrus nigricans	Roncador, Serrana, Serranilla	Bolaños-Cubillos et al., 2015; Acero, 2018; Acero et al., 2018
Hypoplectrus providencianus	Roncador, Serrana, Serranilla	Bolaños-Cubillos et al., 2015; Acero et al., 2018
Hypoplectrus puella	Roncador, Serrana, Serranilla	Bolaños-Cubillos et al., 2015; Acero et al., 2018
Hypoplectrus randallorum	North	Bolaños-Cubillos et al., 2015
Hypoplectrus unicolor	Roncador, Serrana, Serranilla	Bolaños-Cubillos et al., 2015; Acero et al., 2018
Hyporthodus flavolimbatus	North	Bolaños-Cubillos et al., 2015
Hyporthodus mystacinus	North	Bolaños-Cubillos et al., 2015
Hyporthodus niveatus	North	Bolaños-Cubillos et al., 2015
Liopropoma rubre	Serrana	Bolaños-Cubillos et al., 2015
Mycteroperca bonaci	Serrana	Bolaños-Cubillos et al., 2015
Mycteroperca interstitialis	Roncador, Serrana	Bolaños-Cubillos et al., 2015
Mycteroperca phenax	Roncador	
Mycteroperca tigris	Roncador, Serrana	Bolaños-Cubillos et al., 2015
Mycteroperca venenosa	Roncador, Serrana	Bolaños-Cubillos et al., 2015; Acero, 2018
Paranthias furcifer	North	Bolaños-Cubillos et al., 2015
Plectranthias garrupellus	Serrana	Robertson et al., 2015
Pronotogrammus martinicensis	Serrana	Polanco, 2015
Pseudogramma gregoryi	North	Bolaños-Cubillos et al., 2015
Rypticus saponaceus	Roncador, Serranilla	Bolaños-Cubillos et al., 2015; Acero et al., 2018
Serranus baldwini	Serrana, Serranilla	Bolaños-Cubillos et al., 2015; Acero et al., 2018
Serranus flaviventris	Quitasueño	Robertson et al., 2015
Serranus tabacarius	Roncador, Serrana, Serranilla	Bolaños-Cubillos et al., 2015; Acero et al., 2018
Serranus tigrinus	Roncador, Serrana, Serranilla	Bolaños-Cubillos et al., 2015; Acero, 2018; Acero et al., 2018
Serranus tortugarum *	Serranilla	Polanco, 2018
SCORPAENIDAE		
Pontinus castor	North	Robertson et al., 2015
Pterois volitans	Roncador, Serrana, Serranilla	Bolaños-Cubillos et al., 2015; Acero, 2018; Acero et al., 2018
Scorpaena plumieri	Roncador, Serrana	
SETARCHIDAE		
Ectreposebastes imus	Quitasueño	Polanco, 2015
Setarches guentheri	Quitasueño	Polanco, 2015
PERISTEDIIDAE		
Peristedion brevirostre	North	Robertson et al., 2015
Peristedion greyae	Quitasueño	Polanco, 2015
Peristedion longispatha	Quitasueño	Polanco, 2015
Peristedion truncatum	Quitasueño	Polanco, 2015
TRIGLIDAE		
Bellator brachychir	Quitasueño	Polanco, 2015
Bellator militaris	Quitasueño	Robertson et al., 2015

*Species with asterisk (*) correspond to new reports for the area. Species with asterisk (*D) or (*MP) corresponds to contributions of Diego Cardeñosa, PhD candidate Stony Brook University and Professors Paula Quiceno y Mario Londoño, Universidad de Antioquia, respectively. Species observed during the Seaflower Expedition (2015–2017) field work including in the reference (Fundación Colombia Azul et al., 2017; Acero, 2018; Acero et al., 2018; Polanco, 2018).*

High levels of overfishing are also apparent for large-bodied parrotfishes. The rarity of the blue parrotfish *Scarus coeruleus*, and the absence of the rainbow parrotfish *S. guacamaia*, suggest that these have been likely extirpated from the islands for several decades (Acero and Polanco, 2017). Serranilla has particularly depleted grouper populations. The yellowmouth grouper *Mycteroperca interstitialis*, the tiger grouper *M. tigris*, and the yellowfin grouper *M. venenosa*, for instance, have never been observed by any contemporary researcher in that island. Other relatively valuable fishes such as the greater amberjack *Seriola dumerili*, the permit *Trachinotus falcatus*, and the jolthead

porgy *Calamus bajonado* are also commercially extinct or very close to extinct throughout the reserve.

The reserve is, however, a natural laboratory where several actively speciating groups show high species richness. About two thirds of the 18 recognized species of *Hypoplectrus*, a genus of small hermaphroditic serranids endemic to the Greater Caribbean, occur in the reserve with at least nine of them on the northern islands. *Elacatinus*, a genus of cleaning and sponge dwelling gobies also endemic to the western tropical Atlantic, includes 35% of its 20 recognized species on the reserve reefs, five of them in them occurring on the northern islands. Those genera, as well as several others, must be studied in detail to help understand Caribbean connectivity patterns and develop suitable management strategies.

Lastly, 9% ($n = 19$) of the species detected during the CCO Colombian expeditions are new reports for the reserve or at least to its northern part. These species are distributed in 15 families, namely Carcharhinidae (*Rhizoprionodon terraenovae*), Dasyatidae (*Hypanus sabinus*), Gobiidae (*Cryptopsilotris batrachodes*), Fistulariidae (*Fistularia tabacaria*), Chaenopsidae (*Acanthemblemaria aspera*, *A. maria*, *A. spinosa*, *Emblemariopsis* sp.), Labrisomidae (*Stathmonotus gymnodermis*), Gerreidae (*Eucinostomus lefroyi*), Priacanthidae (*Priacanthus arenatus*), Labridae (*Doratonotus megalepis*), Antennariidae (*Antennarius pauciradiatus*, *Histrio histrio*), Diodontidae (*Chilomycterus antillarum*), Monacanthidae (*Monacanthus ciliatus*, *Stephanolepis setifer*), Kyphosidae (*Kyphosus cinerascens*), and Serranidae (*Serranus tortugarum*). Obtaining such high percentage of new reports through a relatively limited sampling effort indicates that if scientific fish ichthyocides were used the biodiversity of this unique Caribbean region will be more thoroughly evaluated and perhaps currently reported levels would most likely increase.

DATA AVAILABILITY

The dataset "Fish biodiversity in three northern islands of the Seaflower Biosphere Reserve (Colombian Caribbean)," which includes the most recently updated list of species in the northern area of the reserve, was assembled using the Darwin Core standard (DwC) and is available through the Integrated Publishing Tool of the Ocean Biogeographic Imation System (OBIS) and the Global Biodiversity Information Facility (GBIF) Colombian nodes (SIBM-SIB Colombia) (IPT link: https://ipt.biodiversidad.co/sibm/resource?r=fish_biodiversity_northern_islands_seaflower_biosphere_reserve_colombian_caribbean; GBIF Portal: http://www.gbif.org/dataset/d8e8b1bf-0b56-4cc0-bf75-c9283fad4aa2; DOI: http://doi.org/10.15472/ygq6i9, http://doi.org/10.15472/7rocx4). Future updates of this list will be published in the latter repository. Changes incorporated to each new version of the list will be summarized in the respective metadata section of the electronic resource.

AUTHOR CONTRIBUTIONS

AA, JT, AP, and NB-C built the database. AA, AP, and JT contributed to the writing and correction of the manuscript. AP and AA devised the data set. All the four authors reviewed the final version of the manuscript and contributed to the discussion.

FUNDING

This research was supported by Universidad Nacional de Colombia, Universidad del Valle, INVEMAR, Coralina, and CCO through Colombia BIO–Colciencias project, agreement No. 341 of 2017 with the aim of joining efforts to characterize the biodiversity in areas of scientific interest with poor biological information in order to strengthen the scientific collections and the generation of genetic information of Colombian biodiversity. Projects involved: Biodiversidad íctica de la Isla Cayo Serrana durante la Expedición Seaflower 2016–Seaflower Expedition 2016, Universidad Nacional de Colombia, Universidad dela Valle, Coralina; Biodiversidad íctica de la Isla Cayo Serranilla durante la Expedición Seaflower 2017–Seaflower Expedition 2017, Universidad Nacional de Colombia, Universidad dela Vallle, INVEMAR, Coralina; Evaluación física y biológica de las unidades ecológicas someras en la isla Cayo Serranilla de la Reserva de Biósfera–Seaflower–Seaflower Expedition 2017, INVEMAR, Coralina.

ACKNOWLEDGMENTS

Authors thanks the CCO which organized the expeditions. Diego Cardeñosa, Sabrina Monsalve, Camila Cáceres, Mario Londoño and Paula Quiceno whom contributed with new reports. Valeria Pizarro, J. D. González, and J. Prato contributed with photographic records. Alfredo Abril, A. Pérez, N. Howard Archibold contributed with information in the field. Erika Montoya who help us with the data managment. Contribution No.467, Inst. de Estudios en Ciencias del Mar (Cecimar); Invemar Contrib. No. 1215.

REFERENCES

Acero, P. A. (2018). *Biodiversidad íctica de la Isla Cayo Serrana durante la Expedición Seaflower 2016 - Proyecto Colombia BIO*. Version 2.4. Universidad Nacional de Colombia. Occurrence dataset. doi: 10.15472/awzfyz

Acero, P. A., and Polanco, F. A. (2017). Biodiversidad íctica de los mares colombianos: riqueza amenazada. *Rev. Acad. Colomb. Cienc. Ex. Fis. Nat*. 41, 200–212. doi: 10.18257/raccefyn.480

Acero, P. A., Polanco, F. A., Tavera, J. J., and Bola-os-Cubillos, N. (2018). *Universidad Nacional de Colombia*. Available online at: https://ipt.biodiversidad.co/sibm/resource?r=fish_biodiversity_northern_islands_seaflower_biosphere_reserve_colombian_caribbean

Bent-Hooker, H. (2012). *Los grandes serránidos de la Reserva de Biosfera Seaflower, Caribe insular colombiano: evaluación de la pesca y de las agregaciones reproductivas*. Master thesis, Universidad Nacional de Colombia, Sede Caribe, San Andrés Isla.

Betancur-R, R., Wiley, E. O., Arratia, G., Acero, P. A., Bailly, N., Miya, M., et al. (2017). Phylogenetic classification of bony fishes. *BMC Evol. Biol*. 17:162. doi: 10.1186/s12862-017-0958-3

Bolaños-Cubillos, N., Abril, A., Bent Hooker, H., Caldas, J. P., and Acero, P. A. (2015). Lista de peces conocidos del archipiélago de San Andrés, Providencia

y Santa Catalina, Reserva de Biosfera Seaflower, Caribe occidental colombiano. *Bol. Invest. Mar. Cost.* 44, 127–162. doi: 10.25268/bimc.invemar.2015.44.1.24

Chasqui, V. L., Polanco, F. A., Acero, P. A., Mejía-Falla, P. A., Navia, A. F., Zapata, L. A., et al. (eds.). (2017). Libro rojo de peces marinos de Colombia. Serie Publicaciones Generales Invemar 93. (Santa Marta: Instituto de Investigaciones marinas y Costeras INVEMAR, Ministerio de Ambiente y Desarrollo Sostenible), 552 p.

Eschmeyer, W. N., Fricke, R., and van der Laan, R. (eds.). (2018). *Catalog of Fishes: Genera, Species, References*. Available online at: http://researcharchive.calacademy.org/research/ichthyology/catalog/fishcatmain.asp (Accessed September 21, 2018).

Fundación Colombia Azul, Universidad de los Andes, and Florida International University (2017). *Elasmobranquios de la Isla Cayo Serranilla durante la Expedición Seaflower 2017 - Proyecto Colombia BIO*. Versión 1.0. 95 registros, aportados por: Cardeósa C, Monsalve S y Cáceres C. Conjunto de datos/Registros biológicos. Available online at: http://ipt.biodiversidad.co/sibm/resource?r=fca_elasmo_seaflower_2017

INVEMAR-ANH (2012). *Línea Base Ambiental en el Área de Régimen Común Jamaica - Colombia Como Aporte al Aprovechamiento Sostenible de los Recursos Marinos Compartidos*. Convenio 016-2010 ANH-Invemar. (Santa Marta), 774 p. Available online at: http://anh.invemar.org.co/cotros-productos

Polanco, F. A. (2015). *Dynamics of the Continental Slope Demersal Fish Community in the Colombian Caribbean*. Dissertation/Doctoral thesis, Universidad Nacional de Colombia and Justus Liebig University, Giessen, 189 p.

Polanco, F. A. (2018). Instituto de Investigaciones Marinas y Costeras - INVEMAR. Available online at: https://ipt.biodiversidad.co/sibm/resource?r=peces_unidades_ecologicas_someras_serranilla2017-proyecto_colombia_bio&amp https://ipt.biodiversidad.co/sibm/resource?r=peces_unidades_ecologicas_someras_serranilla2017-proyecto_colombia_bio&amp

Robertson D. R., Peña E. A., Posada J. M., Claro R. (2015) *Peces Costeros del Gran Caribe: sistema de Información en línea. Version 1.0 Instituto Smithsonian de Investigaciones Tropicales*. Balboa: República de Panamá

Robertson, D. R., and Van Tassell, J. (2015). *Shorefishes of the Greater Caribbean: Online Information System*. Version 1.0 Smithsonian Tropical Research Institute, Balboa.

Conflict of Interest Statement: The authors declare that the research was conducted in the absence of any commercial or financial relationships that could be construed as a potential conflict of interest.

frontiers in Marine Science

DATA REPORT
published: 17 April 2019
doi: 10.3389/fmars.2019.00188

Echinoderms of the Seaflower Biosphere Reserve: State of Knowledge and New Findings

Giomar H. Borrero-Pérez[1], Milena Benavides-Serrato[2], Néstor H. Campos[2], Elizabeth Galeano-Galeano[3], Brigitte Gavio[3,4], Jairo Medina[3] and Alfredo Abril-Howard[3]*

[1] Programa de Biodiversidad, Museo de Historia Natural Marina de Colombia, Instituto de Investigaciones Marinas y Costeras Invemar, Santa Marta, Colombia, [2] CECIMAR, Universidad Nacional de Colombia, Sede Caribe, Santa Marta, Colombia, [3] Universidad Nacional de Colombia, Sede Caribe, San Andrés, Colombia, [4] Universidad Nacional de Colombia, Sede Bogotá, Bogotá, Colombia

Keywords: taxonomic inventory, new records, distribution patterns, Crinoidea, Asteroidea, Ophiuroidea, Echinoidea, Holothuroidea

OPEN ACCESS

Edited by:
Sonia Bejarano, Leibniz Centre for Tropical Marine Research (LG), Germany

Reviewed by:
Renata Alitto, Campinas State University, Brazil
Carolina Bastidas, Massachusetts Institute of Technology, United States

****Correspondence:***
Giomar H. Borrero-Pérez
giomar.borrero@invemar.org.co; giomarborrero@gmail.com

Specialty section:
This article was submitted to Marine Evolutionary Biology, Biogeography and Species Diversity, a section of the journal Frontiers in Marine Science

Received: *21 September 2018*
Accepted: *26 March 2019*
Published: *17 April 2019*

Citation:
Borrero-Pérez GH, Benavides-Serrato M, Campos NH, Galeano-Galeano E, Gavio B, Medina J and Abril-Howard A (2019) Echinoderms of the Seaflower Biosphere Reserve: State of Knowledge and New Findings. Front. Mar. Sci. 6:188. doi: 10.3389/fmars.2019.00188

BACKGROUND

Echinoderms are a charismatic marine invertebrate group that stand out for their beauty and color, but also for several attributes. Their morphological and biological characteristics represent innovations and particularities in animal evolution. Several species have proven to be key in the functioning of ecosystems and therefore in their conservation. Besides, some sea cucumbers and sea urchins are used for human consumption, being currently highly commercially important. In this paper we summarize the list of echinoderms in the SeaFlower Biosphere Reserve (SFBR) and their distribution patterns, including shallow and deep species. The SFBR was declared in November 2000 by UNESCO, and covers the extension of the department of Colombia "Archipiélago de San Andrés, Providencia y Santa Catalina," which has an approximate area of 180,000 km^2 of which <1% is emerged (CORALINA-INVEMAR, 2012). Within the SFBR is the Marine Protected Area Seaflower with 65,018 km^2, declared in 2005 and divided in three sections: a northern section (37,522 km^2) that includes Quitasueño, Serrana and Roncador as well as multiple deep submerged banks; a central section (12,716 km^2) that includes Providencia and Santa Catalina; and a southern section (14,780 km^2) encompassing San Andrés, Bolívar and Albuquerque among other banks (**Figure 1**). Although the sections share similar environments dominated by corals, transparent waters and oceanic features, each one has particular dynamics of fishing exploitation, which make them to require specific management actions (CORALINA-INVEMAR, 2012). To compile the data presented in this study we reviewed literature, specimen's records from museums, open access databases, and the species collected during recent samplings made in 2011 by Universidad Nacional de Colombia-Sede Caribe and the Seaflower Expeditions 2016 and 2017. This dataset provides a baseline for echinoderm species composition and geographic distribution, thus expanding the knowledge on biodiversity within the SFBR as part of the current SeaFlower Expeditions. It is essential to continue efforts to access these remote areas at SFBR, implement the use of new tools to evaluate their biodiversity (such as DNA barcoding) and define priority research topics for the conservation of marine biodiversity in this strategically located reserve.

DATA DESCRIPTION

Data Collection

We report here the dataset entitled "Echinoderms from the SeaFlower Biosphere Reserve" which updates the checklist presented by Borrero-Pérez et al. (2016) including new records from unpublished results of samplings conducted in 2011 by Universidad Nacional de Colombia-Sede Caribe, the Seaflower Expeditions 2016 and 2017, and open-access databases.

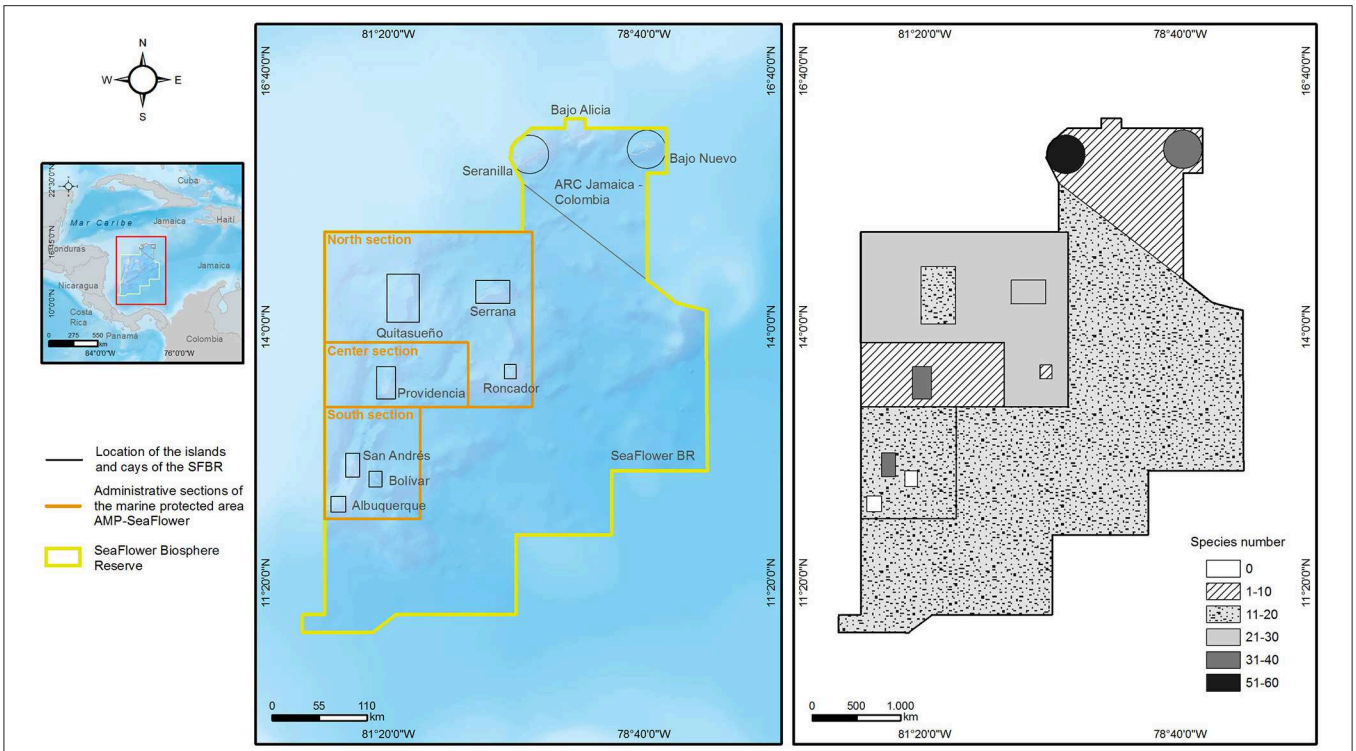

FIGURE 1 | Location of the SeaFlower Biosphere Reserve (SFBR), indicating the locations considered in the Checklist (left) and comparing the number of species registered in each one (right).

A descriptive analysis of species richness and spatial distribution patterns was made and some outcomes are presented.

This dataset compiles the lists of echinoderm species recorded within the SFBR and derived from: (i) Peer reviewed papers or published reports of several investigations, most of them supported by voucher specimens deposited at Museo de Historia Natural Marina de Colombia (MHNMC-INVEMAR), available through the Sistema de Información sobre Biodiversidad Marina (SIBM), and at the National Museum of Natural History (NMNH) (Clark, 1939; Quiñones, 1981; Clark and Downey, 1992; CORALINA, 2001; Diaz et al., 2003; García et al., 2003; Vélez, 2003; García-Hanse and Álvarez-León, 2007; Lasso, 2007a,b; Mejía-Ladino et al., 2008; Benavides-Serrato et al., 2011, 2013; Abril-Howard et al., 2012; Borrero-Pérez et al., 2012; INVEMAR-ANH, 2012; Vega-Sequeda et al., 2015; INVEMAR-SIBM a[1], b[2], c[3]; NMNH[4]); (ii) The Ocean Biogeographic Information System (OBIS) data base; (iii) The Global Biodiversity of Information Facility (GBIF) data base; (iv) Biological records available at SIB Colombia reporting the unpublished results of samplings made in 2011 and the results of several projects developed during the Seaflower Expeditions 2016 and 2017 (UNAL (Universidad Nacional de Colombia), 2016; Benavides-Serrato et al., 2018a,b; Borrero-Pérez, 2018). The search at GBIF database was conducted using two polygons including the SFBR: Polygon 1 (−80 W 11.8 N,−78 W 11.8 N, −78 W 16.2 N, −80 W 16.2 N, −80 W 11.8 N), Polygon 2 (−82 W 11 N, −80 W 11 N, −80 W 15 N, −82 W 15 N, −82 W 11 N). Using this search criteria we recovered new information formerly recorded as present in Nicaragua. The following nine fields are presented per species in this dataset:

taxonID and scientificNameID: These fields include a unique and stable-through-time alphanumeric identifier (taxonomic identifier) AphiaID provided by World Register of Marine Species (WoRMS).

locality: Specific localities were the species have been recorded in the SFBR are presented in this field. Fourteen localities were defined (**Figure 1**) considering the largest islands San Andrés (1), and Providencia and Santa Catalina (2); the Cay Islands Serranilla (3), Bajo Nuevo (4), Quitasueño (5), Serrana (6), Roncador (7), Albuquerque (8) and Bolivar (9); the Joint Regime Area Jamaica-Colombia (ARC Jamaica-Colombia, in Spanish) (10); the administrative sections of the SeaFlower marine protected area: North section (11), Central section (12) and South section (13) (CORALINA-INVEMAR, 2012), that were used to locate

[1]INVEMAR -SIBM a. *Acceso en línea en*. Available online at: http://siam.invemar.org.co/sibm-busqueda-avanzada. Ecorregión SAN. Consultado en: 29-06-2015

[2]INVEMAR-SIBM b. *Acceso en línea en*. Available online at: http://siam.invemar.org.co/sibm-busqueda-avanzada. Proyecto Expedición Providencia I. Consultado en: 19-09-2018.

[3]INVEMAR-SIBM c. *Acceso en línea en*. Available online at: http://siam.invemar.org.co/sibm-busqueda-avanzada. Proyecto ANH ARC Jamaica. Consultado en: 17-07-2018

[4]NMNH. *National Museum of Natural History. Acceso en línea en*. Available online at: http://collections.nmnh.si.edu/search/iz/. Consultado en: 23-06-2015

the species not recorded in the area near the islands or cays; and finally, the locality Seaflower BR (14), where all the recorded species outside of the previously mentioned localities and sections were located.

locationID and coordinates: Fields based on the Marine regions Gazetteer (http://www.marineregions.org/gazetteer.php).

catalogNumber and collectionCode: These fields list cataloged lots available for each species, indicating the museums were they are deposited.

basisOfRecord: This field indicates PreservedSpecimens and HumanObservations, which includes records from literature.

bibliographicCitation: This field includes the reference that explicitly mentions the species in the RBSF, usually with voucher specimens.

References: This field includes references that have compiled echinoderm species records in the SFBR or in the Colombian Caribbean Sea.

institutionCode: This field includes the name (or acronym) in use by the institution having custody of the object(s) or information referred to in the record.

eventDate: This field includes the date of collection of the specimens recorded. Wherever the exact collection date is unknown, a comment appears in the field **eventRemarks**.

Echinoderms Species and Distribution Patterns

A total of 148 echinoderm species were found within the SFBR. Ophiuroidea was the most species-rich class (44 species), followed by Asteroidea (38), Echinoidea (31), Holothuroidea (26) and finally Crinoidea (9). Considering the revision by Borrero-Pérez et al. (2016) as a baseline, there are 23 new records for the SFBR; eight of them are shallow water species based on unpublished results of samplings made in 2011 by UNAL and SeaFlower Expeditions 2016, 2017 at Quitasueño, Roncador, Serrana and Serranilla (Benavides-Serrato et al., 2018a,b; Borrero-Pérez, 2018); and 15 are deep water species located mostly in SeaFlower BR (13 species) and in the North section (2) localities, recorded from GBIF data base. As these deep species were assigned to Nicaragua, they were not considered in previous publications. The majority of these deep water specimens were collected by research vessels Alaminos and Gyre during the 1960's and 1970's (Prestridge, 2016). On a smaller scale, the importance of the expeditions carried out recently is reflected, considering that the increase in the number of species for Quitasueño and Serrana was 80%, Serranilla 25%, and Roncador was 100% (**Table 1**).

The echinoderms recorded for the first time in the SFBR are the shallow water species: *Astropecten duplicatus*, ***Copidaster lymani***, *Ophioderma cinerea*, *Ophiolepis impressa*, *Ophiolepis paucispina*, *Arbacia punctulata*, *Mellita quinquiesperforata*, *Brissus unicolor*; and the deep water species: *Plinthaster dentatus, Zoroaster fulgens,* ***Hymenaster modestus, Litonotaster intermedius, Dytaster insignis, Benthopecten simplex, Calyptraster personatus, Ophiothrix pallida, Deima validum validum, Mesothuria verrilli, Mesothuria maroccana,*** *Molpadia cubana,* ***Psychropotes depressa, Benthodytes typica,*** and ***Benthodytes lingua*** (**Table 1**). Ten of these species (in bold), are also first records for the Colombian Caribbean Sea.

The highest number of species were recorded in shallow waters near San Andrés (36 species), and Providencia and Santa Catalina islands (37), which is expected given their accessibility and the greatest sampling effort in those islands. However, Serranilla which is the farthest locality from Colombian continent cost, is currently the richest with 54 species. This locality has been sampled several times and this number of species includes shallow and deep environments. Some of the Serranilla records came from research cruises previous to 1970's; from expeditions carried out by INVEMAR in 2011 to characterize shallow and deep ecosystems (INVEMAR-ANH, 2012; Vega-Sequeda et al., 2015); and from the recent Seaflower Expedition in 2017 (Benavides-Serrato et al., 2018b; Borrero-Pérez, 2018). Albuquerque and Bolivar, located nearest to San Andres, showed no echinoderm records (**Figure 1**; **Table 1**).

Although deep environments have been relatively less studied in the SFBR, except by the research project focused on ARC Jamaica-Colombia (INVEMAR-ANH, 2012), 48% of the species currently recorded in the SFBR are distributed only or mainly below 200 m in depth. These species records are the result of some sampling stations of research cruises like the R/V Albatross (1884), Presidential Cruise (1938), R/V Oregon (1957, 1964), R/V Pillsbury (1971), R/V Alaminos, and R/V Gyre during the 1960's and 1970's. The samples of these cruises are deposited mostly in the Smithsonian NMNH and most of them were included in the catalogs of the echinoderms of Colombia and other publications (Clark, 1939; Clark and Downey, 1992; Benavides-Serrato et al., 2011; Borrero-Pérez et al., 2012; Prestridge, 2016). Given that samples from R/V Gyre during the 1960's and 1970's were assigned to Nicaragua they had not been considered in previous publications (Orrell and Hollowell, 2018).

Most of the deep water species (75%) have a single record in the reserve, which is expected considering that samplings at deep water are restricted to some of the deep banks in the SFBR, such as those sampled around Serranilla and Bajo Nuevo by INVEMAR-ANH (2012); or restricted to some stations during the research cruises previously mentioned. In the case of shallow water species, 42% (32 species) have a single record (one locality), 42% (32 species) 2 to 4, and 16% (13 species) 5 to 10 records. Among them only 17 species (22%) are distributed throughout the reserve, recorded in several localities or at least in Serranilla and/or Bajo Nuevo (the northernmost localities) and in one locality of the South section. These species are the sea star *Oreaster reticulatus* (reported in 4 localities), the brittle stars *Ophiocoma echinata* (7), *Ophiothrix oerstedii* (6), *Ophioderma appressa* (6) and *O. rubicunda* (4); the sea urchins *Diadema antillarum* (8), *Eucidaris tribuloides* (7), *Echinometra lucunter lucunter* (7), *E. viridis* (6), *Tripneustes*

TABLE 1 | Species of echinoderms of the SeaFlower Biosphere Reserve.

Species	South section	San Andrés	Bolivar	Albuquerque	Central section	Providencia and Santa Catalina	North section	Quitasueño	Serrana	Roncador	Bajo Nuevo	Serranilla	ARC Jamaica-Colombia	SeaFlower Biosphere Reserve
Caryometra atlantidis											X			
Trichometra cubensis							X				X			
Davidaster discoideus		X												
Davidaster rubiginosus		X				X								
Crinometra brevipinna											X			
Stylometra spinifera											X			
Endoxocrinus (Endoxocrinus) parrae parrae											X			
Democrinus conifer							X							
Democrinus rawsonii							X							
Luidia alternata alternata												X		
Luidia barbadensis							X							
Luidia clathrata												X		
Luidia senegalensis												X		
Astropecten americanus							X							
Astropecten antillensis												X		
Astropecten articulatus												X		
Astropecten cingulatus							X							
*Astropecten duplicatus**								**R**						
Astropecten nitidus							X							
Dytaster insignis*														**R**
Persephonaster echinulatus					X									
Pseudarchaster gracilis gracilis					X									
Benthopecten simplex*														**R**
Cheiraster (Barbadosaster) echinulatus							X							
Cheiraster (Christopheraster) mirabilis					X									
Asterinides folium	X													

(Continued)

TABLE 1 | Continued

Species	South section	San Andrés	Bolivar	Albuquerque	Central section	Providencia and Santa Catalina	North section	Quitasueño	Serrana	Roncador	Bajo Nuevo	Serranilla	ARC Jamaica-Colombia	SeaFlower Biosphere Reserve
Stegnaster wesseli	X													
Marginaster pectinatus											X			
Anthenoides peircei							X				X			
Apollonaster yucatanensis														X
Circeaster americanus					X		X							
Nymphaster arenatus					X		X							
Rosaster alexandri							X							
Linckia bouvieri									X					
Linckia guildingi						X						**R**		
Ophidiaster guildingi						X			**R**					
Tamaria halperni								X	X			X		
Oreaster reticulatus		X				X			**R**			X		
Copidaster lymani *												**R**		
*Plinthaster dentatus**							**R**							
*Litonotaster intermedius**														**R**
*Calyptraster personatus**														**R**
Hymenaster modestus*														**R**
Pteraster militaroides militaroides					X									
Echinaster (Othilia) brasiliensis									X					
Henricia antillarum							X						X	
*Zoroaster fulgens**														**R**
Astrophyton muricatum						X						X		
Ophiomyxa flaccida						X								
Ophiacantha bidentata											X		X	
Ophiocamax hystrix											X			
Ophiomitra valida											X		X	
Ophiopristis hirsuta											X	X	X	
Ophiotreta cf. sertata											X		X	
Ophiocoma echinata	X	X				X		**R**	**R**	**R**		**R**		
Ophiocoma pumila								**R**	**R**			X		
Ophiocoma wendtii						X		**R**	**R**			**R**		

(Continued)

TABLE 1 | Continued

Species	South section	San Andrés	Bolivar	Albuquerque	Central section	Providencia and Santa Catalina	North section	Quitasueño	Serrana	Roncador	Bajo Nuevo	Serranilla	ARC Jamaica-Colombia	SeaFlower Biosphere Reserve
Bathypectinura heros											X			
Ophioderma appressa	X	X				X		**R**	**R**			**R**		
Ophioderma brevicauda		X												
Ophioderma brevispina												X		
*Ophioderma cinerea**									**R**			**R**		
Ophioderma rubicunda		X						**R**	**R**			**R**		
Ophiopaepale goesiana											X			
Ophiomyces frutectosus											X			
Amphiodia pulchella		X				X								
Amphiodia trychna		X												
Amphipholis gracillima		X												
Amphipholis januarii		X				X								
Amphipholis squamata		X				X								
Amphiura stimpsonii		X												
Microphiopholis atra												X		
Ophionephthys limicola		X												
Ophiophragmus pulcher		X				X								
Ophiostigma isocanthum		X				X								
Ophiostigma siva		X				X								
Ophiothrix (Ophiothrix) angulata		X				X								
Ophiothrix lineata												X		
Ophiothrix (Ophiothrix) oerstedii	X	X				X			**R**		X	X		
Ophiothrix pallida*							**R**							
Ophiothrix (Acanthophiothrix) suensoni						X				**R**	X	X		
Ophiactis savignyi		X												
Ophionereis reticulata						X			**R**		X	**R**		
Ophiolepis elegans		X												
*Ophiolepis impressa **								**R**	**R**	**R**		**R**		
*Ophiolepis paucispina**												**R**		

(Continued)

TABLE 1 | Continued

Species	South section	San Andrés	Bolivar	Albuquerque	Central section	Providencia and Santa Catalina	North section	Quitasueño	Serrana	Roncador	Bajo Nuevo	Serranilla	ARC Jamaica-Colombia	SeaFlower Biosphere Reserve
Ophiothyreus goesi								X						
Ophiomusium acuferum											X		X	
Ophiomusium eburneum											X			
Ophiomusium testudo											X	X		
Ophiomusium validum											X			
Eucidaris tribuloides		X				X		X	**R**		X	X	X	
Stylocidaris affinis							X							
Stylocidaris lineata											X	X		
Araeosoma belli							X							
Aspidodiadema jacobyi							X							
Diadema antillarum	X	X				X		**R**	**R**		X	X	X	
Bathysalenia goesiana											X	X		
*Arbacia punctulata**								**R**						
Coelopleurus floridanus									X					
Trigonocidaris albida											X		X	
Lytechinus variegatus variegatus		X				X						X		
Lytechinus williamsi		X												
Tripneustes ventricosus	X	X				X		**R**	**R**			X		
Echinometra lucunter lucunter	X	X				X		**R**	**R**		X	X		
Echinometra viridis		X				X		**R**	**R**		X	X		
Echinoneus cyclostomus		X												
Clypeaster lamprus							X	X						
Clypeaster rosaceus		X				X						X		
Clypeaster subdepressus		X												
Echinocyamus grandiporus						X					X	X		
Encope emarginata												X		
Leodia sexiesperforata	X					X						**R**		
*Mellita quinquiesperforata**									**R**					
Conolampas sigsbei							X				X			

(Continued)

TABLE 1 | Continued

Species	South section	San Andrés	Bolivar	Albuquerque	Central section	Providencia and Santa Catalina	North section	Quitasueño	Serrana	Roncador	Bajo Nuevo	Serranilla	ARC Jamaica-Colombia	SeaFlower Biosphere Reserve
*Brissus unicolor**												**R**		
Meoma ventricosa ventricosa						X			**R**			X		
Plagiobrissus grandis		X												
Palaeobrissus hilgardi											X	X		
Linopneustes longispinus							X							
Agassizia excentrica											X			
Heterobrissus hystrix							X							
Ocnus suspectus												X		
Thyonella sabanillaensis												X		
Pentamera pulcherrima												X		
Lissothuria braziliensis												X		
Astichopus multifidus									**R**			X		
Isostichopus badionotus		X				X		**R**	**R**			X	X	
Deima validum validum*														**R**
Actinopyga agassizii						X						**R**		
Holothuria (Cystipus) cubana						X								
Holothuria (Halodeima) floridana		X				X								
Holothuria (Halodeima) grisea												X		
Holothuria (Halodeima) mexicana		X				X		**R**	**R**	**R**	X	X		
Holothuria (Platyperona) parvula	X											**R**		
Holothuria (Selenkothuria) glaberrima	X											X		
Holothuria (Thymiosycia) arenicola												X		
Holothuria (Thymiosycia) impatiens						X								

(Continued)

TABLE 1 | Continued

Species	South section	San Andrés	Bolivar	Albuquerque	Central section	Providencia and Santa Catalina	North section	Quitasueño	Serrana	Roncador	Bajo Nuevo	Serranilla	ARC Jamaica-Colombia	SeaFlower Biosphere Reserve
Holothuria (Thymiosycia) thomasi						X			**R**					
Holothuria (Vaneyothuria) lentiginosa									X					
*Mesothuria verrilli**														**R**
Mesothuria maroccana*														**R**
Euapta lappa												X		
Synaptula hydriformis		X				X								
*Molpadia cubana**														**R**
Psychropotes depressa*														**R**
Benthodytes typica*														**R**
Benthodytes lingua*														**R**
Total species by Borrero-Pérez et al. (2016)	11	36	0	0	6	37	20	4	5	0	34	40	10	0
Total first records per locality							2	14	22	4		14		13
Total	11	36	0	0	6	37	22	18	27	4	34	54	10	13

X indicates presence of the species accounted by Borrero-Pérez et al. (2016); R indicates first records for a locality; asterisk (*) in the species column indicates new records for SeaFlower Biosphere Reserve; and bold letter denote new records for Colombian Caribbean Sea.

ventricosus (6), *Clypeaster rosaceus* (3), *Leodia sexiesperforata* (3) and *Lytechinus variegatus variegatus* (3); and the sea cucumbers *Holothuria mexicana* (7), *Isostichopus badionotus* (6), *H. parvula* (2), and *H. glaberrima* (2). Most of these species are also the most frequent, being recorded in more than 4 localities, and some of them occur in large densities. However, little is known about the local population densities and distribution of some species (e.g., *Diadema antillarum*) that have proven to be key in the functioning of reef ecosystems (Lessios, 2016) and *I. badionotus* and *H. mexicana* currently considered the most commercially important sea cucumbers in the Caribbean Sea (Guzman and Guevara, 2002; Toral-Granda, 2008). The high percentage of species records only in one locality likely are related with sampling effort. For example the widely-distributed and common family Amphiuridae is almost restricted to San Andres and Providencia and Santa Catalina Islands localities. Most amphiurids live buried in soft bottoms or hidden in different structures, extending their arms toward the surface to feed (Hendler et al., 1995). The records of this family in the SFBR come from a single study focused on this group using a specific sampling technique. More samplings are needed to complete the inventory and to better understand the spatial pattern of echinoderm diversity, including localities where the species composition is practically unknown, such as Albuquerque and Bolivar cays, and focusing on different habitats.

Knowledge on the geographic distribution of Echinoderm species throughout the SFBR is a prerequisite to understand the spatial patterns of larval connectivity and the role of SFBR in the Caribbean-wide Echinoderm population dynamics. Based on this knowledge it will be possible to define priority research topics for the conservation of marine biodiversity in this strategically located reserve for the Caribbean Sea. Currently, only the 53% of the species previously registered in the Colombian Caribbean (Benavides-Serrato et al., 2013), and 27% of the species from the Caribbean Sea and the Gulf of Mexico (Alvarado-Barrientos and Solís-Marín, 2013) are recorded in the SFBR.

Finally, most of the species (88%) included in this study have vouchers deposited in several biological collections, mostly in the Museo de Historia Natural Marina de Colombia (MHNMC-INVEMAR), the National Museum of Natural History-Smithsonian (NMNH-Smithsonian), and others, making a more reliable inventory. Physical evidence of each species is fundamental in taxonomy because it allows to unify criteria for the identification, especially of species or groups with variable characteristics, and dubious identifications.

Re-Use Potential

The checklist presented here provides an updated inventory of echinoderm species from the SFBR including published and unpublished records obtained through a comprehensive literature, museum collections, open-access databases records and recent samplings in the reserve. Future taxonomic and biogeographic studies will greatly benefit from this baseline of echinoderms species of these remote areas, which despite their strategic location have generally been included in inventories of countries or larger regions. The dataset presents the catalog numbers of the voucher for each species, facilitating any taxonomic revision that could be needed.

DATA AVAILABILITY

The dataset "Echinoderms from the SeaFlower Biosphere Reserve" that includes the complete list of species was assembled using the Darwin Core standard (DwC) and is available through the Integrated Publishing Tool of the OBIS and GBIF Colombian nodes (SIBM–SIB Colombia) (IPT SIBM OBIS Colombia link: https://ipt.biodiversidad.co/sibm/resource?r=echinoderms_from_the_seaflower_biosphere_reserve; DOI: https://doi.org/10.15472/iipeom; GBIF: https://www.gbif.org/dataset/5a39c87c-9d97-4282-b3a9-e2c292b4729d). Future updates of the list will be published in the latter repository. Changes incorporated to each new version of the list will be summarized in the respective metadata section of the electronic resource.

AUTHOR CONTRIBUTIONS

GHB-P, MB-S, NC, EG-G, BG, JM, and AA-H collected and identified echinoderm samples during the last expeditions to Quitasueño, Roncador, Serrana and Serranilla (2011, 2016 and 2017). GHB-P and MB-S collected and processed the information for the biological records and the checklist dataset. GHB-P compile the complete checklist dataset, performed the descriptive analyses and wrote the manuscript. GHB-P, MB-S, NC, EG-G, BG, JM, and AA-H reviewed and approved the manuscript.

FUNDING

This work was supported by INVEMAR, Universidad Nacional de Colombia (UNAL), Comisión Colombiana del Océano, through Colombia BIO-Colciencias project, agreement No. 341 of 2017; and UNAL-Sede Caribe, Gobernación Departamental de San Andrés, Providencia y Santa Catalina and Corporación Autónoma Regional-CORALINA, agreement No. 021 of 2011. Projects involved: Aproximación a la diversidad de equinodermos en los cayos del norte, Reserva de Biosfera Seaflower—Universidad Nacional 2011; Estado del conocimiento de equinodermos en isla Cayo Serrana: biodiversidad y conectividad en el mar Caribe—Expedición Seaflower, 2016, Universidad Nacional de Colombia, INVEMAR; Caracterización de la epifauna y macrobentos (0–800 m) de Isla Cayo Serranilla y áreas aledañas–Expedición Seaflower 2017, Universidad Nacional de Colombia, INVEMAR; Evaluación física y biológica de las unidades ecológicas someras en la Isla Cayo Serranilla de la Reserva de Biósfera Seaflower–Expedicion SeaFlower, 2017, INVEMAR, Coralina.

ACKNOWLEDGMENTS

We thank the people who organized and participated in SeaFlower Expeditions that helped enrich the inventories. T. Forbes, J. D. González, and V. Pizarro contributed with some photographic records. A. Polanco and A. Merchán helped during field trips and projects development. E. Montoya assisted the datasets elaboration (SIBM) and S. Millán, LABSIS-INVEMAR, helped with the map. Two reviewers for their suggestions to improve the manuscript. Contribution No. INVEMAR: 1215; and CECIMAR: 486.

REFERENCES

Abril-Howard, A., Bolaños, N., Machacón, I., Lasso, J., Gómez, D. I., and Ward, V. (2012). Actualización del conocimiento de los ecosistemas marinos en la Reserva de Biósfera Seaflower, con énfasis en las islas de San Andrés y Providencia," in *Atlas de la Reserva de Biósfera Seaflower. Archipiélago de San Andrés, Providencia y Santa Catalina*, eds D. I. Gómez-López, C. Segura-Quintero, P. C. Sierra-Correa, and J. Garay-Tinoco (CORALINA-INVEMAR, 2012. Instituto de Investigaciones Marinas y Costeras "José Benito Vives De Andréis" -INVEMAR- y Corporación para el Desarrollo Sostenible del Archipiélago de San Andrés, Providencia y Santa Catalina–CORALINA, Serie de Publicaciones Especiales de INVEMAR 28), 129–157.

Alvarado-Barrientos, J. J., and Solís-Marín, F. A. (eds) (2013). *Echinoderm Research and Diversity in Latin America*. Berlin; Heidelberg: Springer-Verlag.

Benavides-Serrato , M., Borrero-Pérez, G. H., Merchán-Cepeda, A., and Campos, N. H. (2018b). *Caracterización de la Epifauna y Macrobentos (0-800 m) de Isla Cayo Serranilla y Áreas aledañas: Equinodermos Primera Fase 2017. v1. Dataset/Occurrence.* Universidad Nacional de Colombia. Available online at: https://ipt.biodiversidad.co/sibm/resource?r=serranilla2017&v$=$1.0. doi: 10.15472/lbjyx0

Benavides-Serrato, M., Borrero-Pérez, G. H., Cantera, J. R., Cohen-Rengifo, M., and Neira, R. (2013). "Echinoderms of Colombia," in *Echinoderm Research and Diversity in Latin America*, eds J. J. Alvarado-Barrientos, and F. A. Solís-Marín (Berlin; Heidelberg: Springer-Verlag), 145–182.

Benavides-Serrato, M., Borrero-Pérez, G. H., and Díaz-Sánchez, C. M. (2011). *Equinodermos del Caribe Colombiano I: Crinoidea, Asteroidea y Ophiuoridea. Serie de Publicaciones Especiales de Invemar* 22. Santa Marta.

Benavides-Serrato, M., Gavio, B., Galeano, E., Medina, J., and Abril-Horward, A. (2018a). *Diversidad de Equinodermos en los Cayos del Norte, Reserva de Biósfera SeaFlower, 2011. v1. Dataset/Occurrence.* Universidad Nacional de Colombia. Available online at: https://ipt.biodiversidad.co/sibm/resource?r=cayosnorte2011&v$=$1.0. doi: 10.15472/ygq6i9

Borrero-Pérez, G. H. (2018). *Equinodermos_unidades_ecologicas_someras_Serranilla2017-Seflower-Proyecto_Colombia_BIO. v1. Dataset/Occurrence.* Instituto de Investigaciones Marinas y Costeras – INVEMAR. Available online at: https://ipt.biodiversidad.co/sibm/resource?r=equinodermos_unidades_ecologicas_someras_serranilla2017-seaflower-proyecto_colombia_bio. doi: 10.15472/kfevgp

Borrero-Pérez, G. H., Benavides-Serrato, M., and Díaz-Sánchez, C. M. (2012). *Equinodermos del Caribe Colombiano II: Echinoidea y Holothuroidea. Serie de Publicaciones Especiales de Invemar No. 30*. Santa Marta. Available online at: http://www.invemar.org.co/redcostera1/invemar/docs/10454EQII__web.pdf

Borrero-Pérez, G. H., Díaz-Sánchez, C. M., and Benavides-Serrato, M. (2016). "Equinodermos. Invertebrados innovadores," in *Biodiversidad del mar de Los Siete Colores*, *Serie de Publicaciones Generales del INVEMAR No. 84, Santa Marta – Colombia),* eds M. D. Vides, E. C. Alonso, and N. Bolaños (Instituto de Investigaciones Marinas y Costeras–INVEMAR y Corporación para el Desarrollo Sostenible del Archipiélago de San Andrés, Providencia y Santa Catalina-CORALINA), 156–177. Available online at http://cinto.invemar.org.co/sai/app/pdf/biodiversidad-del-mar-de-los-siete-colores-web.pdf

Clark, A. M., and Downey, M. E. (1992). *Starfishes of the Atlantic. Natural History Museum Publications*. London: Chapman and Hall.

Clark, H. (1939). Echinoderms (other than holothurians) collected on the Presidential cruise of 1938. *Smithsonian Miscellaneous Collections*, 98, 1–18.

CORALINA (2001). *Plan de Manejo Ambiental Old Point Regional Mangrove Park 2001-2011. Documento Discusión*. San Andrés: CORALINA.

CORALINA-INVEMAR (2012). "Atlas de la reserva de Biósfera Seaflower. Archipiélago de San Andrés, providencia y Santa Catalina," in *Serie de Publicaciones Especiales de INVEMAR* No. 28, eds D. I. Gómez-López, C. Segura-Quintero, P. C. Sierra-Correa, and J. Garay-Tinoco (Santa Marta: Instituto de Investigaciones Marinas y Costeras "José Benito Vives De Andréis"-INVEMAR y Corporación para el Desarrollo Sostenible del Archipiélago de San Andrés, Providencia y Santa Catalina-CORALINA) Available online at http://www.invemar.org.co/redcostera1/invemar/docs/10447AtlasSAISeaflower.pdf

Diaz, J. M., Barrios, L. M., and Gomez, D. I. (eds). (2003). *Las Praderas de Pastos Marinos de Colombia: Estructura y Distribución de un Ecosistema Estratégico*. Serie *Publicaciones Especiales No. 10.* Santa Marta: INVEMAR.

García, M. I., McCormick, C., Chow, R., Peñaloza, G., Connolly, E., Mitchell, A., et al. (2003). *Plan de Manejo del Área Marina Protegida Seaflower - Parte I. Proyecto Caribbean Archipelago Biosphere Reserve: Regional Marine Protected Area System CO-GM-P*066646. San Andrés Isla San Andrés Isla: GEF–TOC–CORALINA.

García-Hanse, I., and Álvarez-León, R. (2007). Macroflora y macrofauna asociadas al cordón arrecifal de Little Reef (Isla de San Andrés, Colombia). *Revista Luna Azul* 25, 61–77. doi: 10.17151/luaz.2007.25.5

Guzman, H. M., and Guevara, C. (2002). Population structure, distribution and abundance of three commercial species of sea cucumber (Echinodermata) in Panama. *Caribbean J. Sci.* 38, 230–238.

Hendler, G., Miller, J., Pawson, D., and Porter, M. (1995). *Echinoderms of Florida and the Caribbean Sea Stars, Sea Urchins and Allies*. Washington, DC: Smithsonian Institution Press.

INVEMAR-ANH (2012). *Línea Base Ambiental en el Área de Régimen Común Jamaica-Colombia Como Aporte al Aprovechamiento Sostenible de los Recursos Marinos Compartidos, Informe Técnico Final*. Santa Marta: INVEMAR-ANH.

Lasso, Z. J. (2007a). *Informe de gestión y acciones del Old Point Regional Mangrove Park. Proyecto "Protección y Conservación de Los Recursos de la Biodiversidad y de los Ecosistemas Estratégicos en la Reserva de la Biosfera Seaflower." Documento de Discusión.* CORALINA.

Lasso, Z. J. (2007b). *Las Acciones Desarrolladas por la Corporación Para Lograr la Recuperación, Conservación, Protección y uso Sostenible de los Recursos Naturales Presentes en los Manglares del Parque Regional Old Point, Incluyendo Evaluación Técnica y Participativa de la Implementación del Parque Regional. Proyecto Protección y Conservación de los recursos de la biodiversidad y de los ecosistemas estratégicos dentro de la Reserva de Biosfera Seaflower. Informe Técnico*. CORALINA.

Lessios, H. A. (2016). The great *Diadema antillarum* die-off: 30 years later. *Annu. Rev. Mar. Sci.* 8, 1.1–1.17. doi: 10.1146/annurev-marine-122414-033857

Mejía-Ladino, L. M., Gómez, D. I., Montoya-Cadavid, E., and Navas-Camacho, R. (2008). *Actualización de la Línea Base de Flora y Fauna Marina y Costera del Parque Regional Old Point. Informe Técnico Final.* Santa Marta.

Orrell, T., and Hollowell, T. (2018). *NMNH Extant Specimen Records. Version* 1.19. *Occurrence dataset*. National Museum of Natural History, Smithsonian Institution. Available online at: https://doi.org/10.15468/hnhrg3 accessed via GBIF.org on 2018-07-23.

Prestridge, H. (2016). *Biodiversity Research and Teaching Collections - TCWC Marine Invertebrates. Version 5.1. Occurrence Dataset*. Texas A&M University Biodiversity Research and Teaching Collections. Available online at https://doi.org/10.15468/dfrwoh accessed via GBIF.org on 2018-07-23.

Quiñones, R. (1981). "Lista preliminar de los equinodermos," in *Informe Sobre los Resultados de la Expedición a las Islas de Providencia y Santa Catalina*, ed B. Werding, J. Garzón, and S. Zea (Santa Marta: Invemar), 35–45.

Toral-Granda, V. (2008). "Population status, fisheries and trade of sea cucumbers in Latin America and the Caribbean," in *A Global Review of Fisheries and Trade Sea Cucumbers*, eds V. Toral-Granda, A. Lovatelli, and M. Vasconcellos (Rome: AO Fisheries and Aquaculture Technical Paper. No. 516), 211–229.

UNAL (Universidad Nacional de Colombia), Instituto de Investigaciones Marinas y Costeras "José Benito Vives de Andreis", Universidad del Magdalena, Universidad Jorge Tadeo Lozano, Pontifica Universidad Javeriana, Fundación Malpelo y Otros Ecosistemas Marinos, et al. (2016). *Caracterización de equinodermos de Serrana durante la Expedición Seaflower 2016. Versión 1.1. 39 registros, aportados por: Benavides M, Campos N, Bustos D, Perez D, Howard A, Pizarro D, Forbes, T, González JD. Conjunto de datos/Registros biológicos*. Available online at: https://ipt.biodiversidad.co/sib/resource?r=unal_equinodermos_seaflower_2016. doi: 10.15472/3fz5b3

Vega-Sequeda, J., Díaz-Sánchez, C. M., Gómez-Campo, K., López-Londoño, T., Díaz-Ruiz, M., and Gómez-López, D. I. (2015). Biodiversidad marina en Bajo Nuevo, Bajo Alicia y Banco Serranilla, Reserva de Biosfera Seaflower. *Boletín Investigaciones Marinas Costeras* 44, 199–224. Available online at: http://cinto.invemar.org.co/ojs/index.php/boletin/article/view/27/26. doi: 10.25268/bimc.invemar.2015.44.1.27

Vélez, C. (2003). *Estrellas Quebradizas Infaunales (Echinodermata: Ophiuroidea) Asociadas a Fondos Blandos Someros de las Islas de San Andrés y Providencia*. Bogotá: Tesis Biólogo Marino, Universidad de Bogotá Jorge Tadeo Lozano.

Conflict of Interest Statement: The authors declare that the research was conducted in the absence of any commercial or financial relationships that could be construed as a potential conflict of interest.

frontiers in Marine Science

ORIGINAL RESEARCH
published: 26 June 2019
doi: 10.3389/fmars.2019.00338

Microbial Diversity Exploration of Marine Hosts at Serrana Bank, a Coral Atoll of the Seaflower Biosphere Reserve

Astrid Catalina Alvarez-Yela[1], Jeanneth Mosquera-Rendón[1], Alejandra Noreña-P[1], Marco Cristancho[2] and Diana López-Alvarez[1]*†*

[1] Centro de Bioinformática y Biología Computacional BIOS, Manizales, Colombia, [2] Vicerrectoría de Investigación, Universidad de los Andes, Bogotá, Colombia

OPEN ACCESS

Edited by:
Santiago Herrera,
Lehigh University, United States

Reviewed by:
Rika Anderson,
Carleton College, United States
James Davis Reimer,
University of the Ryukyus, Japan

***Correspondence:**
Astrid Catalina Alvarez-Yela
catalina.alvarez@bios.co;
catalinaalvarezy@gmail.com
Diana López-Alvarez
dianalopez430@gmail.com

†Present address:
Diana López-Alvarez,
Facultad de Ciencias Agropecuarias,
Universidad Nacional de Colombia,
Palmira, Colombia

Specialty section:
This article was submitted to Marine Conservation and Sustainability, a section of the journal Frontiers in Marine Science

Received: 31 July 2018
Accepted: 03 June 2019
Published: 26 June 2019

Citation:
Alvarez-Yela AC, Mosquera-Rendón J, Noreña-P A, Cristancho M and López-Alvarez D (2019) Microbial Diversity Exploration of Marine Hosts at Serrana Bank, a Coral Atoll of the Seaflower Biosphere Reserve. Front. Mar. Sci. 6:338. doi: 10.3389/fmars.2019.00338

Microorganisms represent nearly 90% of ocean biomass and are fundamental for the functioning and health of marine ecosystems due to their integral contribution to biogeochemical cycles and biological processes. In marine environments, microorganisms exist as microbial communities in the water column, benthonic substrates, and macroorganisms, where they establish symbiotic interactions and fulfill their ecological roles. Such interactions can have a harmful or beneficial impact on the hosts depending on the emergent properties of the communities, their taxonomic structure, and functionality. To evaluate these features, culture independent approaches like metabarcoding have been developed and have hugely contributed to the characterization of marine microbial diversity. The present study was aimed to explore the structure and metabolic functionality of microbial communities associated to marine hosts at the Serrana Bank, a coral atoll part of the Seaflower Biosphere Reserve (Archipelago of San Andrés, Old Providence and Saint Catalina, Colombia). We found a highly diverse microbial assemblage associated with the corals *Siderastrea siderea*, *Colpophyllia natans*, and *Orbicella annularis*, the sponge *Haliclona* sp. and sediment from Isla de los Pájaros lagoon. However, the coral *Porites astreoides* had significantly lower bacterial diversity and a different community composition. Proteobacteria was the most abundant phylum within bacterial communities in the evaluated hosts, except in *P. astreoides*, where Cyanobacteria was the predominant group. Firmicutes, Actinobacteria, Bacteroidetes, Acidobacteria, Chloroflexi, and Gemmatimonadetes were also identified within all microbiomes, but their dominance varied between hosts. Additionally, the most abundant group among the fungi communities associated with *O. annularis*, *S. siderea*, and *C. natans* was Ascomycota, but significant differences between clasess and order were observed among hosts. Finally, functional profiles revealed that the principal microbial functions were focused on membrane transport, carbohydrates, amino acids and energy metabolism, replication, and translation processes. A significant higher metabolic functionality was found in the sponge microbiome in comparison to the coral microbial communities.

Keywords: seaflower, microbial diversity, marine hosts, amplicons, symbiotic interactions

INTRODUCTION

In marine environments, microorganisms represent nearly 90% of the biomass, are responsible for up to 98% of primary marine productivity, and are key players in mass and energy fluxes through biogeochemical processes (carbon, nitrogen, sulfur cycling, etc.) (Caron, 2005; Sogin et al., 2006). It is estimated that up to 3.5×10^{30} microorganisms live on the oceanic subsurface establishing complex communities. They can be found in the water column as plankton, in benthonic substrates, and adhered to macroorganisms (Glöckner et al., 2012; Grossart et al., 2013).

Among the macroorganisms that inhabit marine ecosystems, corals and sponges are a major component and they have existed for millions of years as structural and functional pieces. Coral reefs have an immense biodiversity, which can be compared to that of the tropical rain forest and contributes largely to the primary productivity in marine environments (Cárdenas et al., 2012). Sponges play a functional role in coral reefs in several ways: they enhance coral survival by binding corals to the reef frame, mediate regeneration of physical impacts on reefs by temporary stabilization of carbonate rubble, and take part in nutrient cycling through microbial symbionts (Bell, 2008). These organisms not only contribute to the global ocean productivity but also provide nutrients and shelter for other organisms (Wulff, 2006; Coker et al., 2014). Corals, sponges, and other marine organisms have been exposed to both natural and anthropogenic threats: in Colombia, 60% of coral reefs are at risk, 20% may disappear in the next decade, 19% have been destroyed, and 15% are in a critical conservation status (Galeano et al., 2016). These threats have led to a decline of their populations and changes in the associated microbiota living in their surface (Riegl et al., 2009).

The microbiome has an impact on its host, which could be harmful or beneficial depending on its microbial structure and functionality (Konopka, 2009; Kellogg et al., 2014). Microbial communities interact and establish symbiotic associations at the surface of macroorganisms. When there are shifts in the composition of these communities, hosts have several impacts including changes in the intake of nutrients, absorption of light (biofilm formation), and interaction with potential pathogens (Webster et al., 2008; Wahl et al., 2012; Zhang et al., 2015).

One of the major limitations to study structure and functionality of marine microbial communities has been the inability to cultivate around 99% of the microorganisms (Delmont et al., 2011). Advances in molecular biology and sequencing technologies have led to the development of new approaches including metabarcoding and metagenomics to overcome this limitation (Streit and Schmitz, 2004; Pavan-Kumar et al., 2015). These approaches have contributed to the knowledge that microbes represent a pivotal role on earth in terms of phylogenetic and functional diversity (Debnath et al., 2007; Dionisi et al., 2012; Glöckner et al., 2012). Metabarcoding studies on marine hosts like macro-algae, corals, and sponges have shown that microbial communities are not distributed randomly; their prevalence depends on a species-specific structure (Lachnit et al., 2011; Morrow et al., 2012) which can change in response to environmental factors or host features such as age, diseases, and physiological state (Lachnit et al., 2011; Lawler et al., 2016).

The Seaflower Biosphere Reserve, located in the Colombian Caribbean sea, covers an extension of 65.018 km^2 of a marine protected area (MPA) created to preserve the biodiversity of the Archipelago of San Andrés, Old Providence, and Saint Catalina (Comisión Colombiana del Oceáno, 2015). The reserve encompasses three inhabited islands and several cays, banks, and atolls. One of these banks is Serrana Bank (14°23′00″ N, 80°16′00″ W), a reef complex located 150 km northwest of Old Providence Island (**Figure 1**). It has seven cays of which only the southwest cay "Serrana" (500 m × 200 m) has established vegetation (Díaz et al., 1996); another cay "Isla de los Pájaros" has a small extension, but it is an important station for hundreds of migrating birds species.

The reserve is a place largely unexplored within the third largest barrier reef of the world (Comisión Colombiana del Oceáno, 2015). Its great biodiversity includes more than 407 fish species, 48 hard corals, 54 soft corals, and 130 sponges. Starting in 2014, scientific explorations to generate knowledge about this diverse ecosystem have been launched. To date these explorations have contributed to the characterization of its flora and fauna, and the evaluation of the oceanographic and meteorological aspects of the reserve (Howard, 2006).

To our knowledge, no studies have been undertaken to characterize marine microbial diversity, or to evaluate microbiomes associated with specific macroorganisms on any ecosystem of the Seaflower Biosphere Reserve. The aim of this study was to assess the diversity, taxonomic structure, and potential metabolic functionality of microbial communities (bacteria and fungi) associated with two marine hosts by 16S rRNA and ITS gene metabarcoding on the Serrana Bank, one of the unexplored areas of the reserve.

METHODOLOGY AND TOOLS

Experimental Design and Sampling

Serrana is an extensive reef complex, with a 37 km × 30 km dimension, including the insular platform. There is a lagoon with numerous seaweed patches and sea grass beds, which are highly productive. There is a secondary barrier, long and narrow, with the coral *Acropora palmata* as the dominant species, creating a quiet environment with reef patches (*Montastraea*) covering 60% of the deep bottom. Other coral species including *Agaricia agaricites*, *Porites* spp., *Mycetophyllia ferox*, *Diploria* spp., and *Siderastrea siderea* are also frequent in this coral reef habitat (Howard et al., 2004).

Our aim was to identify and analyze microbiomes associated with corals, algae, and sponges inhabiting the reserve. In addition, we collected a sample from sediment from a cay lagoon to compare its microbial composition and diversity with that of the macroorganisms sampled. All samples were collected by triplicate.

Eight microbial samples associated to corals were collected by scuba diving, at depths ranging from 7 to 12 m (**Supplementary Table S1**). Mucus on the surface of corals was collected using sterile syringes (10 ml). The mucus was gently

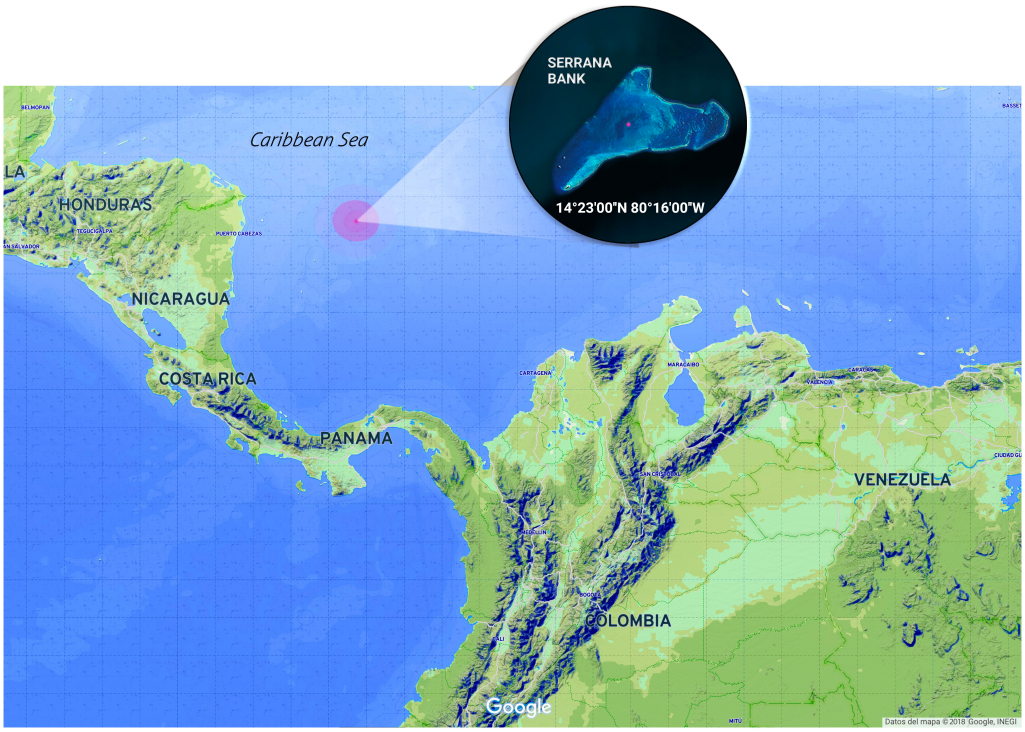

FIGURE 1 | Serrana Bank location at the Seaflower Biosphere Reserve (Colombia). Samples collection area (red dot). Image edited from Google.

shaken using the plastic tip of syringes to get rid of the viscous material and reduce pumping of seawater. Nitrile gloves were worn during collection to reduce human bacterial contamination and syringes were capped after collection to prevent further seawater contamination. The collected mucus was transferred to 2 ml tubes within the next hour and preserved in 70% alcohol. Samples were stored at 4°C for further analyses.

Six microbial samples associated to algae and one associated to sponges were collected by snorkeling and scuba diving, at depths ranging from 3 to 12 m (**Supplementary Table S1**). These specimens were collected by hand and stored in sterile plastic bags for 3 h. At the beach, samples were preserved in 70% alcohol and kept at 4°C for further analyses.

A sediment sample from the "Isla de los Pájaros" cay lagoon was collected during the expedition. This sample was collected at 0.5 m depth by hand, wearing nitrile gloves, stored immediately in 2 ml tubes with 70% alcohol, and cooled down for further analyses. The complete metadata associated with collected samples is described in **Supplementary Table S1**.

DNA Extraction and Sequencing

Total community DNA was extracted using the GeneJET Genomic DNA Purification Kit, GeneJET Plant Genomic DNA Purification Kit, and DNeasy Plant Mini Kit, according to manufacturer's instructions with some required modifications (pressure changes, mechanical fragmentation, and cell lysis). DNA quality was evaluated by electrophoresis in agarose gels and spectrophotometry.

Amplicon library preparation and sequencing were performed by Novogene[1], Chula Vista, CA, United States. The V4 hypervariable region of the 16S rRNA gene was amplified with the primers 515F/806R (5′-GTGCCAGCMGCCGCGGTAA-3′/5′-GGACTACHVGGGTWTCTAAT-3′), and for some samples, the ITS2 region was also amplified using the primers ITS3/ITS4 (5′-GCATCGATGAAGAACGCAGC-3′/5′-TCCTCCGCTTATTGATATGC-3′). All PCR reactions were carried out in 30 μl total volume with 15 μl of Phusion® High-Fidelity PCR Master Mix (New England Biolabs), 0.2 μM of forward and reverse primers, and 10 ng template DNA. Thermal cycling consisted of initial denaturation at 98°C for 1 min, followed by 30 cycles of denaturation at 98°C for 10 s, annealing at 50°C for 30 s, elongation at 72°C for 30 s, and a final cycle at 72°C for 5 min. Libraries were sequenced using the Illumina HiSeq platform (Q30 > 80%) to obtain 250 bp paired reads (**Table 1**).

Amplicon Analyses

Taxonomic analyses were performed using QIIME 2 release 2017.9[2]. The raw sequences quality control was ran with DEMUX plugin and reads were trimmed to a length of 250 bp using the DADA2 plugin. Filtered sequences were aligned and clustered into operational taxonomic units (OTUs) and assigned to clusters using a QIIME feature, which uses a Naive Bayes classifier to

[1]https://en.novogene.com/
[2]https://qiime2.org/

TABLE 1 | Metadata associated to the samples collected and sequenced at the Seaflower Biosphere Reserve.

Species	Depth (m)	Coordinates		Collection date	Dataset code	Amplicon analysis
Orbicella annularis	11	14°23′51.8″ N	80°08′10.1″ W	24 August 2016	CO1	ITS
Siderastrea siderea	9	14°27′40.6″ N	80°00′26.3″ W	25 August 2016	CO2	16S and ITS
Porites astreoides	12	14°23′07.3″ N	80°07′51.0″ W	24 August 2016	CO3	16S
Colpophyllia natans	10	14°27′23.4″ N	80°14′09.5″ W	24 August 2016	CO4	ITS
Haliclona sp.	7	14°17′18.4″ N	80°11′53.9″ W	25 August 2016	ES1	16S
Isla de los Pájaros sediment	0.5	14°27′40.6″ N	80°15′40.7″ W	23 August 2016	SE1	16S

map each sequence to taxonomy. The classifier was trained on a qiime-compatible Silva database (release 119), Greengenes (Greengenes v13_5), and UNITES reference databases with 97% similarity. Statistical analyses were computed in R using the qiime2R v.0.99.1[3], and phyloseq (McMurdie and Holmes, 2013), a common tool for ecological analyses of microbiome data in R/Bioconductor; abundance plots were computed with ggplot2 (Wickham, 2016), retrieving the 20 most abundant classification groups (phylum, class, order, and family). Diversity indexes (Observed Shannon, Simpson) and rarefaction curves were calculated and constructed and, beta-diversity estimates were calculated within QIIME using Bray–Curtis distance between samples. Principal coordinate analyses (PCoA) and non-metric multidimensional scaling (NMDS) were computed from the resulting distance matrices to compress dimensionality into two-dimensions, enabling visualization of sample relationships.

Additionally, Phylogenetic Investigation of Communities by Reconstruction of Unobserved States (PICRUSt) was used to predict the functional profiles of microbial communities associated to hosts (Langille et al., 2013). Because PICRUSt uses "closed-reference" OTU for prediction, the filter_otus_from_otu_table.py script was used to get an output compatible with the OTUs table generated with QIIME 2. Function profiles were created based on the KEGG functional annotations and the output table was collapsed at KO level 2 to identify pathways significantly different among samples. One-way ANOVA with 999 permutations ($P < (0.05)$, and pairwise Tukey's tests were estimated. Relative abundances of KEGG level 2 gene ontologies were plotted in R using ggplot2.

RESULTS

Sixteen samples were collected as part of the Seaflower Scientific Expedition 2016 (**Supplementary Table S1**), 8 from corals, 6 from algae, 1 from sponge, and 1 from the lagoon sediment. DNA extraction was unsuccessful for 10 of these samples; hence, the final 16S analysis was limited to four samples, and the ITS tests were restricted to three samples (**Table 1**). The sequenced microbiomes are in association with:

Orbicella annularis (CO1): *O. annularis* is a coral belonging to the family Merulinidae found between 1.5 and 82 m depth, and it is generally the most abundant coral up to 10 m of depth in semi-protected coral reefs, lagoons, and in the upper part of reef pendants (Reed, 1985). *O. annularis* colonies are massive, columnar, or flat; corallites can be flush with the surface or they can be conic. Its septa are uniformly arranged, alternating large and short septa, and its columellas are small and compact, and its color varies between brown and yellow (Ellis and Solander, 1786). This coral is considered an endangered species, its populations have decreased over 50% in the last 30 years through diseases and bleaching effects, and other factors of anthropogenic origin (Edmunds, 2015).

Siderastrea siderea (CO2): *S. siderea*, also known as the massive starlet coral, belongs to the family Siderastreidae found generally in depths between 0.5 and 2 m, forming reef patches toward the inner side of the reef. Its colonies are hemispheric or encrusting, some with >2 m in diameter, with more than 48 radial elements directed in a 45° pendant toward the columella. Its septa are highly compact shaping a soft surface; calices measure from 4 to 5 mm in diameter. It has a brown color with reddish tones (Ellis and Solander, 1786).

Porites astreoides (CO3): *P. astreoides* is a very common coral belonging to the family Poritidae that can be found in almost every reef environment, ranging from shallow to deep zones. This coral can be massive, laminar, or subnodular, covered by little protuberances or smooth; its colonies are hemispheric, flattened, or encrusting, generally not >60 cm in diameter; its calices measure from 1.25 to 1.5 mm in diameter, its 12 radial elements are porous, and its columella is also porous and very small with rough denticles in the septa. *P. astreoides* has a light green to yellowish brown color, and it adapts to different growth patterns; it is generally small but it can also cover extensions that reach several meters (Green et al., 2008).

Colpophyllia natans (CO4): *C. natans* belongs to the family Mussidae, it lives in large colonies which can measure >1 m in diameter. The largest colonies commonly have a regular hemispheric shape, while smaller colonies have a plane disc shape. In some cases, valleys of the coral extend completely across the colony or can be sub-divided into smaller series; valleys and walls are large measuring up to 2 cm width, walls usually present grooves along the cups, and there is a clear limit between the wall and the valley. Its septa have identical thickness and they have less than 12 septa per centimeter. The columella is discontinuous and thin, less than a quarter of the valleys thickness. This coral inhabits the upper part of reefs and slopes up to 50 m depth; ridges are generally brown and valleys are green, brown, or whitish (De-Kluijver et al., 2016).

Haliclona sp. (ES1): The genus *Haliclona* groups the encrusting-type sponges belonging to the family Chalinidae,

[3]https://github.com/jbisanz/qiime2R

which is normally found anchored to rocks and branches of coral reefs. Sponges have been widely studied and recognized as the largest sources of marine bioactive secondary metabolites, which represent up to 40% of all known natural marine products (Lee et al., 2001). Many of these metabolites have been linked with a microbial origin (Haygood et al., 1999; Lozada and Dionisi, 2015). In the case of *Haliclona* spp., at least 190 secondary metabolites have been identified exhibiting biological activities like antibiotic, antifungal, antimicrobial, antimalarial, cytotoxic activities, among others (Yu et al., 2006; Hoppers et al., 2015). Several of these compounds are produced by their associated microbiota, which make microbiomes the key players in the functional capabilities of sponges (Kennedy et al., 2009; Khan et al., 2011, 2014).

"Isla de los Pájaros" Sediment (SE1): Cayo Pájaro is a small island located at the Serrana reef complex and it is recognized as a stopover for thousands of migrating birds. It has a little lagoon with a rocky bottom, which is used as a hydration source for inhabitant birds of Serrana Bank and other Seaflower Reserve cays.

After sequencing, a total of 639,010 reads were obtained from the samples sequenced by 16S and 190,008 passed quality filters. Likewise, 517.769 reads were generated from the ITS sequencing of which 254,224 were quality accepted. These reads were used to perform the metabarcoding analysis.

Bacterial Profiling of Marine Hosts at Seaflower

The 16S reads were assigned to 35 different bacterial phyla, 95 classes, 134 orders, 196 families, and 282 genera (**Supplementary Table S1**). Proteobacteria was the most abundant phylum in *S. siderea* (39.35%), *Haliclona* sp. (38.88%), and the sediment microbiomes (65.43%), in contrast to *P. astreoides*, where bacteria from the phylum Cyanobacteria were predominant (32.17%). Firmicutes, Actinobacteria, Bacteroidetes, Acidobacteria, Chloroflexi, and Gemmatimonadetes were also identified, but they showed different dominance between hosts (**Figure 2A**). In addition, among the archaeal groups, three different phyla, five classes, seven orders, four families, and four genera were found. Crenarchaeota (0.16–1.21%) and Euryarchaeota (<1%) were identified as the predominant archaeal phyla.

The taxonomic assignments, class and order, showed that dominant groups were very different between hosts (**Figures 2B,C**). The two more abundant classes within the Proteobacteria group were Gamma and Alphaproteobacteria. Bacilli and Clostridia were predominant within the Firmicutes group and Chloroplast was the most dominant class of the Cyanobacteria group. Actinobacteria and Acidimicrobiia were the predominant classes within Actinobacteria. The dominant class from Bacteroidetes was Bacteroidia, and Gemm-2 was identified as the most common class from the Gemmatimonadetes group. Additionally, the most represented classes within the Acidobacteria group were Sva0725 and Solibacteres, and Anaerolineae and SAR202 the most abundant classes within the Chloroflexi group.

Taxonomic assignments showed that the most predominant orders among the microbiomes associated to marine hosts were Streptophyta, Rhodobacterales, Unclassified Gemm-2, Sphingomonadales, Actinomycetales, Bacillales, HTCC2188, Acidimicrobiales, Pseudomonadales, and Lactobacillales. Rhodospirillales, Sva0725, Clostridiales, Rhizobiales, Caldilineales, Thiohalorhabdales, Marinicellales, and Oceanospirillales were also abundant among hosts. Family classification related to these groups is shown in **Figure 2D**.

Bacterial Community Composition Associated With *Siderastrea siderea* (CO2)

A total of 19 bacterial orders, 125 genera, and 34 species were identified to be specific for *S. siderea* (**Supplementary Figure S1**). Among the archaeal orders, *vadinCA11* and *Methanobrevibacter* were associated to these groups. The metabarcoding analysis showed that Proteobacteria (39.35%), Firmicutes (21.13%), and Actinobacteria (20.18%) were the predominant phyla associated with this coral. A smaller proportion of Bacteroidetes (7.61) Chloroflexi (2.84%), Cyanobacteria (2.53%), Acidobacteria (1.71%), Gemmatimonadetes (1.01%), PAUC34f (0.95%), Planctomycetes (0.53%), Verrucomicrobia (0.48%), Nitrospirae (0.38%), and Spirochaetes (0.34%) were found within the microbiome. Gammaproteobacteria (21.58%), Bacilli (17.56%), Actinobacteria (16.66%), and Alphaproteobacteria (14.23%) were the dominant bacterial classes in association with this coral species, while Actinomycetales (19.86%) and Bacillales (14.08%) were the predominant orders in this host. Bacterial species included *Shewanella algae*, *Janthinobacterium lividum*, *Candidatus Portiera*, *Acinetobacter johnsonii*, *Pseudomonas viridiflava*, *Bacteroides barnesiae*, *Pseudomonas fragi*, *Lactococcus garvieae*, and *Acinetobacter guillouiae*.

Bacterial Community Composition Associated With *Porites astreoides* (CO3)

A total of 4 orders, 29 genera, and 6 species were found to be specific for *P. porites* (**Supplementary Figure S1**). Cyanobacteria (32.17%) and Firmicutes (21.99%) were the predominant phyla within the microbiome associated to this coral species, followed by Proteobacteria (21.24%) and Bacteroidetes (16.35%). Chloroplast (34.27%), Gammaproteobacteria (14.49%), Bacteroidia (12.65%), Bacilli (12.21%), and Clostridia (11.21%) were found as the main classes on this coral host. Streptophyta (41.96%), Bacteroidales (15.49%), Clostridiales (13.68%), and Lactobacillales (10.48%) were identified as the dominant orders. For this coral it was possible to identify 78 genera including, Streptophyta-related genera, *Thermomonas*, *Flavisolibacter*, *Acinetobacter*, *Ramlibacter*, *Lactobacillus*, and *Vibrio* and the species *A. guillouiae*, *C. Portiera*, *Prevotella melaninogenica*, *Corynebacterium variabile*, and *Vibrio* sp.

Bacterial Community Composition Associated With *Haliclona* sp. (ES1)

A total of two orders, four genera, and four species were found to be specific for *Haliclona* sp. (**Supplementary Figure S1**). For this group of sponges, Proteobacteria (38.88%) was the most abundant associated phylum, followed by Chloroflexi

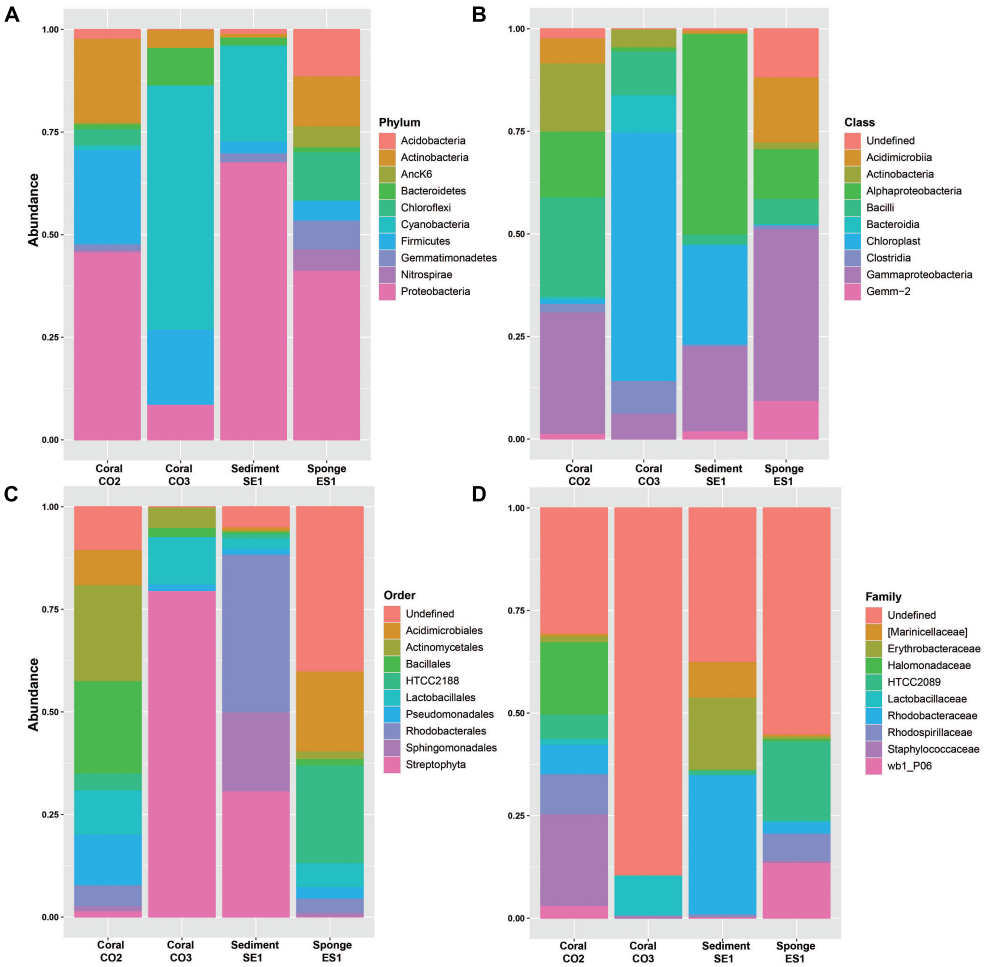

FIGURE 2 | Relative abundances of bacterial microorganisms in marine hosts at the Seaflower Biosphere Reserve. **(A)** Phylum. **(B)** Class. **(C)** Order. **(D)** Family.

(12.36%), Actinobacteria (11.28%), Acidobacteria (10.33%), and Gemmatimonadetes (6.24%). A significant number of Nitrospirae (4.66%), Firmicutes (4.55%), and AncK6 (4.48%) was also identified. Gammaproteobacteria (28.54%), Acidimicrobia (10.72%), and Alphaproteobacteria (8.45%) were the dominant classes.

HTCC2188 (15.92%), Acidimicrobiales (13.09%), Sva0725 (6.45%), Caldilineales (6.44%%), Thiohalorhabdales (6.03%), Rhodospirillales (5.48%), and Chromatiales (4.98%) were identified as the predominant orders associated to this sponge species, HTCC2089 (14.14%), wb1_P06 (9.97%), Rhodospirillaceae (4.94%), and Rhodobacteraceae (1.99%) as the most abundant families, and *A. johnsonii*, *S. algae*, *Sphingomonas yabuuchiae*, *Acinetobacter lwoffii*, *P. fragi*, *Bacteroides plebeius*, *P. viridiflava*, and *Prevotella copri* as some of the species identified.

Bacterial Community Composition Associated With "Isla de los Pájaros" Sediment (SE1)

A total of 21 orders, 27 genera, and 2 species were found to be specific for the sediment (**Supplementary Figure S1**). Proteobacteria (65.43%) was the most abundant microbial group in association with the sediment, while less frequently Cyanobacteria (17.13%), Planctomyces (3.66%), Bacteroidetes (2.96%), Firmicutes (2.28%), and Gemmatimonadetes (1.91%) were found. Alphaproteobacteria (48.42%), Gammaproteobacteria (20.33%), and Chloroplast (18.19%) were identified as the predominant classes within the microbiome. Rhodobacterales (33.62%), Streptophyta (21.56%), Sphingomonadales (16.21%), Marinicellales (6.92%), Alteromonadales (4.13%), Rhizobiales (2.92%), and Thiotrichales (2.03%) were the predominant orders and *Rhodopirellula baltica*, *Octadecabacte antarcticus*, *Tunicatimonas pelagia*, *A. johnsonii*, *Anaerospora hongkongensis*, *S. yabuuchiae*, *Brevibacterium aureum*, and *Rubidimonas crustatorum* were some of the identified species.

Eukaryotic Profiling of Marine Hosts at Seaflower

ITS reads were assigned to 2 fungi phyla, 11 different classes, 28 orders, 46 families, 56 genera, and 42 species

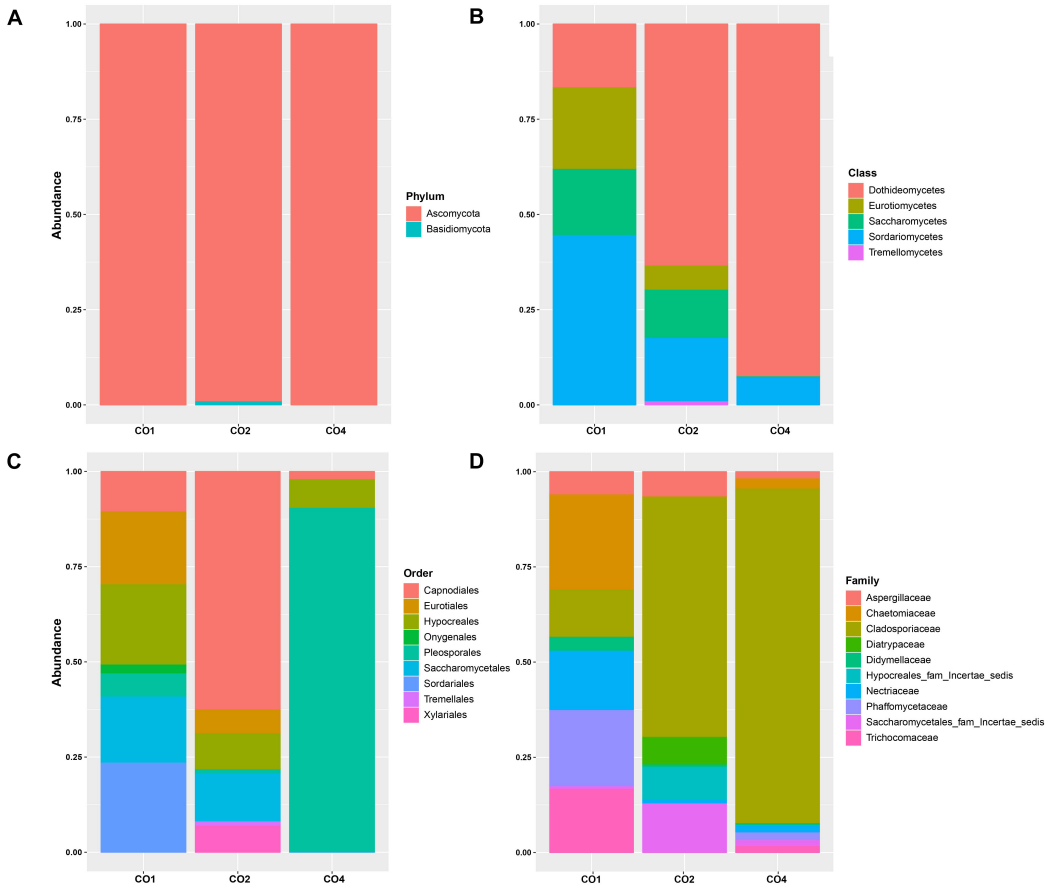

FIGURE 3 | Relative abundances of eukaryotic microorganisms in marine hosts at the Seaflower Biosphere Reserve. **(A)** Phylum. **(B)** Class. **(C)** Order. **(D)** Family.

(**Supplementary Table S3**). The most abundant phylum among the microbial communities associated to *O. annularis*, *S. siderea*, and *C. natans* was Ascomycota (83.85%, 97.41%, and 99.40%, respectively) and Basidiomycota (3.64%, 2.26%, and 0.02%, respectively) had a very low representation among microbiomes (**Figure 3A**). Dothideomycetes, Sordariomycetes, Eurotiomycetes, Saccharomycetes, and Tremellomycetes were the predominant classes within the identified phyla (**Figure 3B**).

The most frequent orders were different among hosts, with Pleosporales, Capnodiales, Sordariales, Hypocreales, Eurotiales, Saccharomycetales, Onygenales, Xylariales, and Tremellames as the predominant orders within microbiomes (**Figure 3C**). Family classification related to these groups is shown in **Figure 3D**.

Eukaryotic Community Composition Associated With *Orbicella annularis* (CO1)

A total of two orders, seven genera, and four species were found to be specific for *O. annularis* (**Supplementary Figure S2**). Ascomycota (83.85%) was the predominant group within the microbiome of *O. annularis*. Sordariomycetes (42.35%), Saccharomycetes (15.32%) and Eurotiomycetes (12.73%) were identified as the dominant fungi classes, while Dothideomycetes (9.14%) was also identified as abundant. Among the orders Sordariales (28.41%), Hypocreales (21.06%), and Saccharomycetales (18.63%) were the dominant groups, and *Cyberlindnera rhodanensis*, *Mycothermus thermophilus*, *Purpureocillium lilacinum*, *Trichoderma virens*, and *Fusarium solani* were identified as common fungal species.

Eukaryotic Community Composition Associated With *Siderastrea siderea* (CO2)

A total of 10 fungi orders, 25 genera, and 23 species were found to be specific for *S. siderea* (**Supplementary Figure S2**). The eukaryotic communities identified in this study were limited to Ascomycota (97.41%) and Basidiomycota (2.26%) groups, in contrast to previous studies in which Microsporidia, Chytridiomycota, and Entomophthoromycota were detected as the most abundant phyla within the coral microbiome (Wang et al., 2018). Among the observed classes, Dothideomycetes (55.44%) and Sordariomycetes (18.13%) were the predominant classes but unlike other samples, Orbiliomycetes (0.47%) and Lecanoromycetes (0.08%) were also identified in association with this host. The more abundant eukaryotic orders were Capnodiales (49.90%), Saccharomycetales (12.29%), Hypocreales (9.36%), and Pleosporales (8.94%), with presence of the

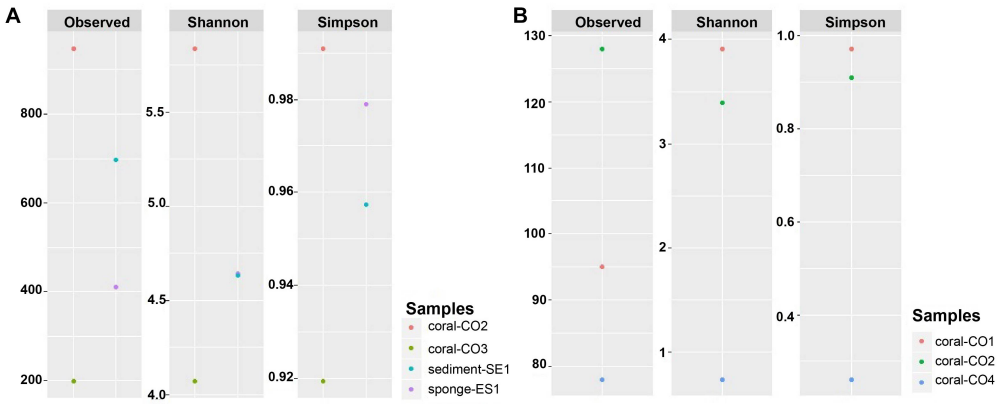

FIGURE 4 | Alpha diversity indexes of microbial communities in marine hosts at the Seaflower Biosphere Reserve. **(A)** Bacterial and archaeal communities. **(B)** Eukaryotic communities.

species like *Acremonium alternatum*, *Leptographium bistatum*, *Cladosporium sphaerospermum*, *Sarocladium glaucum*, and *Meyerozyma guilliermondii*.

Eukaryotic Community Composition Associated With *Colpophyllia natans* (CO4)

A total of one order, three genera, and two species were found to be specific for *C. natans* (**Supplementary Figure S2**). The analysis of the eukaryotic communities associated with this species revealed that Ascomycota was the most abundant phylum (99.40%), and Basidiomycota had a low representation within the microbiome (0.02%). Dothideomycetes was the dominant class with more that 90% of the microbial assignations. Pleosporales (89.82%) was the main order, and a minor representation of Hypocreales (7.23%) and Capnodiales (1.89%) was observed. ITS profiling revealed the presence of the species *Cyberlindner rhodanensis*, *F. solani*, *Candida sake*, *Thermomyces lanuginosus*, and *Strelitziana eucalypti* in this host.

Diversity of Microbial Communities at the Seaflower Biosphere Reserve

The observed OTUS and Simpson's diversity index results showed a higher bacterial taxonomic diversity within the microbiome associated with *S. siderea* (0.99), followed by the sponge (0.98) and the sediment samples (0.96). *P. astreoides* showed microbial communities with lower diversity (0.92) (**Figure 4A**). Regarding eukaryotic characterization, *O. annularis* showed high diversity (0.97) while *C. natans* showed a very low diversity in comparison to the other coral species (0.26) (**Figure 4B**).

Using Shannon's index, higher evenness was observed in the microbiota associated with *S. siderea* (>5.83). *P. astreoides* showed the lowest evenness within its microbial diversity (4.07). *Haliclona* sp. and the sediment revealed a similar evenness associated to their taxonomic composition (4.64) (**Figure 4A**). Higher evenness of the eukaryotic communities was found in *O. annularis* (3.90), and *C. natans* showed the lowest evenness within its microbiome (0.74) (**Figure 4B**).

Alpha diversity rarefaction plots indicated that the abundance of bacterial or eukaryotic taxa associated to marine hosts has been widely surveyed at the maximum number of sequences read, except for *P. astreoides*, which did not reach an asymptote shape (**Supplementary Figure S3**). The diversity found in this coral was likely to be highly under-represented due to the low number of reads. Rarefaction plots also proved that the most diverse microbiota was associated with *S. siderea*.

The NMDS diagram showed that communities from Coral-CO3 were separated from the others, by the *x*-axis. However, the *y*-axis did not show a clear separation of the samples Coral-CO2 and Sponge-ES1. On the other hand, the PCoA showed a separation between four microbial community's samples. The first axis divides the samples Coral-CO2 and Sponge-ES1 from other samples, containing 53.9% of the total variation, and the second axis explains the 26.4% of the variation, clustering the coral samples (**Figure 5A**). The PCoA and NMDS analyses for the fungi microbiomes showed a separation between three microbial community's samples. For NMDS plot, communities from CO2 and CO4 were clearly separated from CO1, by the *x*-axis, on PCoA, the first axis divides the sample CO4 from CO2 and CO1 containing 56.5% of the total variation, while the second axis explains the 43.5% of the variation (**Figure 5B**). Because of the low number of samples that were compared, we consider that these analyses are not conclusive, but they do contribute to a possible understanding of the complexities of trophic interactions.

Preliminary Metabolic Profiling of Microbial Communities Associated With Marine Hosts at Seaflower

Functional community profiles were obtained for metagenomes associated with *S. siderea*, *P. astreoides*, *Haliclona* sp., and the sediment. Predicted functional groups showed that there was not a significant change on metabolic functionality assignments between hosts except for amino acid ($F = 2071$, $p < 0.05$), and carbohydrate metabolism ($F = 408$, $p < 0.05$). For amino

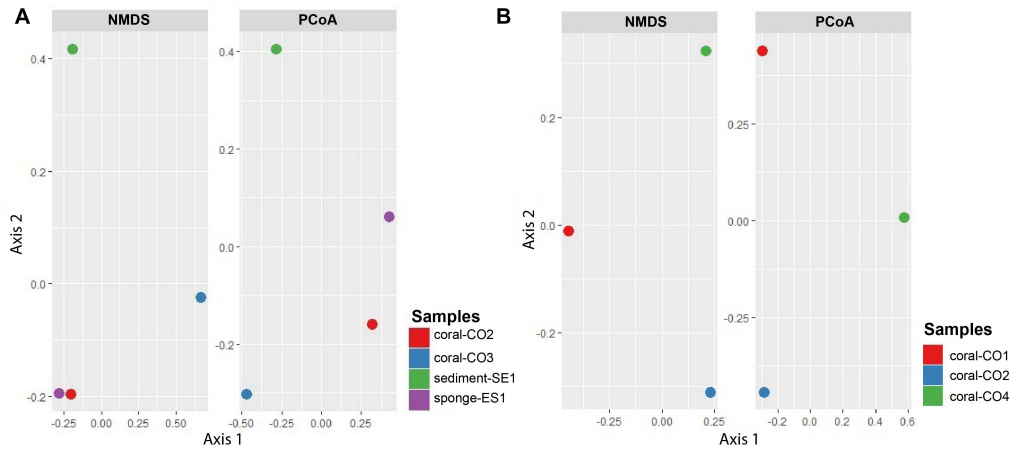

FIGURE 5 | NMDS and principal coordinates analysis (PCoA) of metagenomes associated with hosts at the Seaflower Biosphere Reserve. **(A)** Bacterial and archaeal communities. **(B)** Eukaryotic communities.

acid metabolism, the sponge had a larger number of metabolic processes, in comparison with the sediment and the corals. Among the carbohydrate metabolism, more pathways were assigned to the sponge and the sediment, while the corals had a lower assignment of pathways. Metabolic profiling revealed that the principal microbial functions are focused on membrane transport, carbohydrates, amino acids, and energy metabolism, as well as replication and translation processes (**Figure 6**).

DISCUSSION

Metabarcoding using next-generation sequencing has been used for large-scale biodiversity analyses (Pavan-Kumar et al., 2015) and can be useful for biodiversity monitoring in environments that are undergoing rapid climate-related changes, such as ocean warming and eutrophication of coastal environments. We reported the first taxonomic survey of microbial communities associated to corals, a marine sponge, and sediment at Serrana Bank, an atoll of the Seaflower Biosphere Reserve. This survey provides an opportunity to investigate local patterns of diversity of sessile taxa. Although we collected 16 samples, it was unfortunate that just a small number produced DNA of high quality for sequencing. Ten samples did not fulfill DNA quality controls due to contamination with proteins (260/280 < 2), which can be a result of cross contamination with the host tissue residues. However, we decided to go ahead with the sequencing given that this was the first set of available samples with information on the microbiome composition of marine hosts at this reserve. We are certain that the study of the microbiomes associated to macroorganisms in Serrana Bank is an important complement to the collected information on the flora and the fauna that populates this ecosystem. We identified 1.776 OTUs assigned to bacteria and 227 OTUs assigned to fungi. Although this amount is not as big as in other studies performed in coral reefs (Rohwer et al., 2002; Hernandez-Agreda et al., 2017), it helped to gain insights about the microbial diversity associated to some marine hosts at the Serrana Bank.

We discovered differences in the presence/absence of microbial communities associated to corals, the sponge, and the sediment, with unique OTUS associated to every host (**Supplementary Figures S1**, **S2**). Most of the OTUs identified are common coral and sponge holobionts, for instance, alpha and gamma proteobacteria usually dominate the bacterial communities in corals, as well as Firmicutes, Bacteroidetes, Actinobacteria, and Acidobacteria. However, the species vary according to the host, age, health status, and the surrounding micro-environment (Hernandez-Agreda et al., 2017). Among the eukaryotic groups found within the microbiomes, Ascomycota was the major representative. This phyla is considered as an obligate fungi in corals (Raghukumar and Ravindran, 2012). Studies of fungi as marine symbionts have mainly focused in their role as pathogenic agents. However, they can also contribute to skeletal biomineralization, net bioerosion reduction, resistance to environmental stress, UV damage protection, among others (Ainsworth et al., 2017). The classes Dothideomycetes, Sordariomycetes, Eurotiomycetes, Saccharomycetes, and Tremellomycetes found in this study are commonly reported in marine environments (Xu et al., 2014). Important differences were identified in the microbiota of *P. astreoides*, where Cyanobacteria was the most abundant group. These groups have been reported in marine ecosystems fulfilling ecological roles, like nutrient cycling between macroorganisms and the water column (Dinsdale et al., 2008; Glöckner et al., 2012). Relative abundances of species within taxonomic phyla, classes, and orders differed among all samples.

The archaeal groups identified in the surveyed hosts included extremophile species (hyperthermophiles, mesophilic, psychrophilic, halophilic, methanogenic, etc.), acknowledged as the most abundant archaea in marine environments (Madigan and Martinko, 2005). Species of *Candidatus*, *Nitrososphaera*, and *Nitrosopumilus*, associated to the hosts, are widespread ammonia-oxidizing archaea (AOA), and key players in

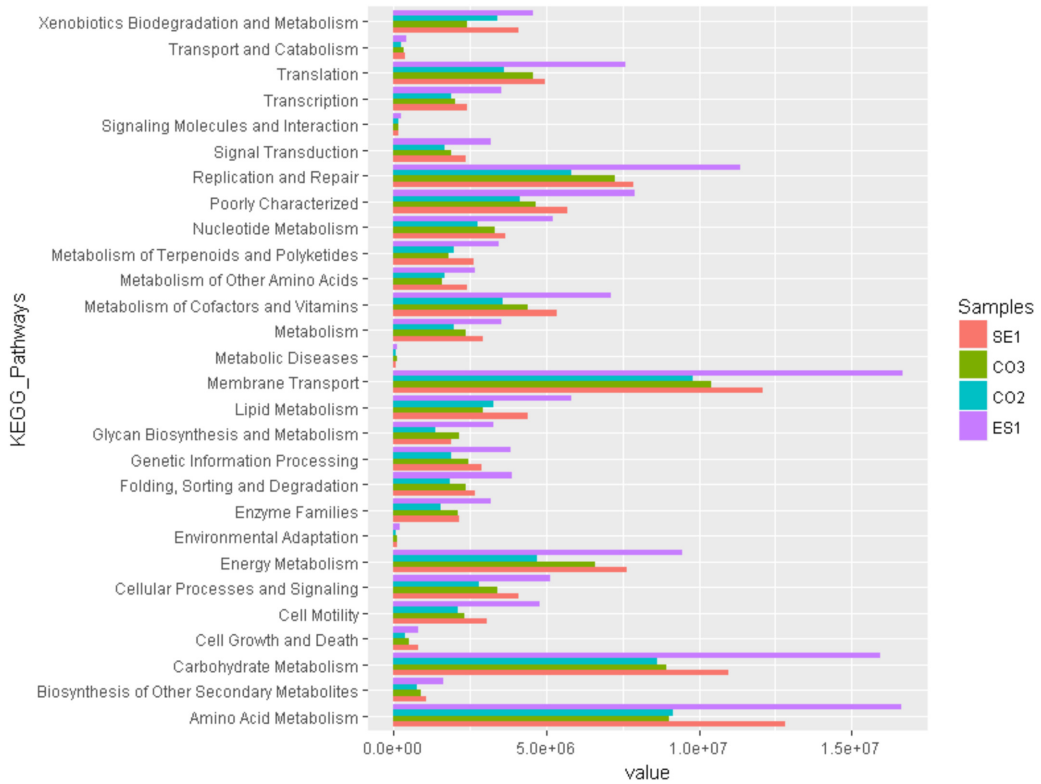

FIGURE 6 | Predictive functional profiling of microbial communities associated with *S. siderea*, *P. astreoides*, *Haliclona* sp., and Isla de los Pájaros sediment at the Seaflower Biosphere Reserve.

nitrification processes due to their metabolic versatility and adaptability (Spang et al., 2012).

Bacterial Community Composition Associated With *Siderastrea siderea* (CO2)

Our results match and complement the findings of previous diversity studies reported for *S. siderea*, where identical microbial phyla and classes were identified (Cárdenas et al., 2012; Kellogg et al., 2014). Within these groups, important bacterial species were found playing a common role in reducing nitrate to nitrite, degrading aromatic compounds, and oxidizing sulfur, ammonia, and carbon, among others (Dinsdale et al., 2008; Sun et al., 2016).

It has been reported that in diseased *S. siderea*, there is an increase in Alphaproteobacteria and decrease in Gammaproteobacteria (Cárdenas et al., 2012). Furthermore, *Corynebacterium* and *Acinetobacter* are known as potential pathogens in corals due to their association with the dark spot syndrome in these organisms (Sweet et al., 2013). We found a high number of both groups of bacteria, as well as the presence of *Corynebacterium* and *Acinetobacter*, so at this point, it is not possible to make assumptions about the health of the coral, but it is likely that the coral could be in an early disease state. The number of bacteria genera identified in this study was lower than previously reported for this host (600 vs. 222) (Kellogg et al., 2014). However, this might be a consequence of the limitations of the software and databases used to do the taxonomic assignments.

Bacterial Community Composition Associated With *Porites astreoides* (CO3)

Our findings differ from some studies previously reported, in which Proteobacteria, Bacteroidetes, and Acidobacteria were the dominant phyla, while Oceanospirillales was the most abundant order (Wegley et al., 2007; Morrow et al., 2012). Our findings show in contrast that Cyanobacteria represented more than 30% of the microbial communities associated to *P. astreoides*. Cyanobacteria are oxy-photosynthetic bacteria that have dominated marine environments and play an essential role in modern coral reef ecosystems by forming a major component of epiphytic, epilithic, and endolithic communities, as well as of microbial mats. Theses bacteria also provide nitrogen to the coral reef ecosystems through nitrogen fixation. On the other hand, Cyanobacteria have been found forming pathogenic microbial consortia in association with other microbes on living coral tissues, causing coral tissue lysis and death, which have contributed to considerable declines in coral reefs (Charpy et al., 2010). It has been observed that a great abundance of Cyanobacteria, Bacteroidetes, Firmicutes, and Actinobacteria is related with black band disease (Barneah et al., 2007) and dark

spot syndrome in corals (Sweet et al., 2013). However, when we searched for genera and species that have been associated specifically to dark spot syndrome (Oscillatoria) (Sweet et al., 2013) and black band disease (*Cyanobacterium*, *Oscillatoria*, *Phormidium*, and *Pseudoscillatoria*) (Frias-Lopez et al., 2003), none of these specific taxa were identified. It should be noted that a large number of OTUs do not present identification up to genus (**Supplementary Tables S2**, **S3**), so we need to be careful in the interpretation of the sequence comparison results, until the databases are better populated.

Among the identified genera, the usually dominant genus *Endozoicomonas* was not found in our study. Although there is not a clear consistency between community shifts in microbiomes associated with healthy and diseased corals (Kellogg et al., 2014), it has been suggested that *Endozoicomonas* is an obligate member of a healthy microbiome of *P. astreoides* and its loss and reduction has been observed in some specimens, along with a decrease in Oceanospirillales (Mouchka et al., 2010; Morrow et al., 2012; Meyer et al., 2014). This could suggest that this coral was in a diseased state. In addition, *Vibrio* was only found in *P. astreoides*, and not the other hosts. *Acinetobacter* and *Vibrio* have been commonly associated with marine organisms, and have also been recognized as pathogens in invertebrates and corals (Ben-Haim et al., 2003; Kellogg et al., 2014; Wang et al., 2015). A similar result was found in corals with unusual lesions, where a negative correlation was found between *Endozoicomonas* and members of the Vibrionaceae family which have been recognized as opportunistic pathogens (Meyer et al., 2014).

Overall, results revealed differences between the microbiome compositions previously described for *P. astroides* (Rodriguez-Lanetty et al., 2013). These differences are characterized by the higher abundance of Cyanobacteria within the microbial community, the lower representation of Oceanospirillales, the absence of *Endozoicomonas*, and the identification of *Acinetobacter* and *Vibrio* as possible opportunistic species in association with the coral. Our results could reflect the current health status of this marine host in Serrana bank, but also could be a consequence of the low number of reads that were obtained for this coral. Additional samples should be sequenced to fully characterize this microbiome and generate more accurate conclusions about their association with the coral host.

Bacterial Community Composition Associated With *Haliclona* sp. (ES1)

The bacterial phyla identified in this host have been previously found in association with different marine sponges and with *Haliclona* sp. (Khan et al., 2014; Jasmin et al., 2015) although their abundance is slightly different. These microorganisms are important because they fulfill critical ecological roles regarding nutrient acquisition, processing of metabolic waste, host defense, secondary metabolites production, and stabilization of the sponge skeleton (Hentschel, 2003). Interestingly, representatives of Acidobacteria, Chloroflexi, and Gemmatimonadetes are indicative of high microbial-abundant (HMA) sponges (Jiang et al., 2007; Khan et al., 2011), which suggest that the assessed sponge had a significant microbial abundance, where most of the identified taxa are related with healthy organisms. Also, marine Actinomycetes have been commonly associated to *Haliclona* species, where they represent an important microbial diversity, and an extensive metabolic potential for obtaining novel compounds such as polyketides (Jiang et al., 2007; Khan et al., 2011).

Because most of the taxonomic assignments for this host were not completed to the family level (database restrictions), it was difficult to complete assignations to specific genera and species. This limited our search for microorganisms that have been described as potential source of bioactive secondary metabolites (*Streptomyces*, *Haliea*, *Nocardiopsis*, *Micromonospor*, *Cytophaga*, *Pseudoalteromonas*, *Verrucosispora*, *Pseudovibrio*, and *Bacillus*) (Jiang et al., 2007; Kennedy et al., 2009).

Bacterial Community Composition Associated With "Isla de los Pájaros" Sediment (SE1)

The prevalence of Proteobacteria classes has been previously described on superficial lakes and marine sediment microbiomes as main drivers of biogeochemical cycling of carbon, nitrogen, and sulfur, and as the source of variations in nutrient content of water (Hongxiang et al., 2008; Franco et al., 2017). Cyanobacteria are found in lagoons and soft muddy floors forming associations with photosynthetic bacteria, sulfur bacteria, and other microorganisms. Biological N_2 fixation has been described as one of the most important contribution of Cyanobacteria, where they also represent an organic source for planktonic and benthic heterotrophic organisms (Charpy et al., 2010).

Taxa identified in this sample show that the lagoon's water contains microorganisms that are contributing to nutrient content and cycling in water, being a significant source of hydration for birds that use this place as a stopover in their migration. Nevertheless, the microbiome associated with the sediment sample showed the lowest bacterial taxonomic diversity. This was an unusual finding, since sediments of different origin seem to have a large microbial diversity in comparison with host-associated communities (Thompson et al., 2017). In this case, the high temperatures that are reached in the lake ($>20°C$), due to its shallowness, could expain this decreased richness (Milici et al., 2016). Since no general relationship between temperature and richness has been established (Hendershot et al., 2017), we would need to analyze additional samples to confirm this result and the factors that influence this lower microbial diversity on the sediment of this lagoon.

Eukaryotic Community Composition Associated With *Orbicella annularis* (CO1)

Several genera found in this study contain species described as saprophytes in corals including *Aspergillus sydowii* and *C. sphaerospermum* that have been reported in this species (Kendrick et al., 1982) but were not identified in this study. Additionally, the species *F. solani* has been reported as an

important pathogen in marine organisms (Raghukumar and Ravindran, 2012) and it was found in this coral host. It would be premature to make inferences about the health status of this host, but it is important to highlight that some of the identified taxa have been associated to diseased organisms.

Eukaryotic Community Composition Associated With *Colpophyllia natans* (CO4)

Fungal biomass constituted up to 0.05% of the weight of the corals and are apparently an important component of this group of organisms (Raghukumar and Ravindran, 2012). Previous microscopic studies have shown that endolithic–Ascomycetes-like fungi are ubiquitously found across several genera of healthy corals. In contrast, other fungi such as *Aspergillus* spp. are known as coral pathogens (Kim et al., 2000, 2006; Alker et al., 2001). Fungi in coral holobionts are involved in carbon and nitrogen metabolism by conversion of nitrate and nitrite to ammonia, which enable nitrogen cycling within the host (Wegley et al., 2007). Coral-associated microbes have been involved in biogeochemical cycling, particularly nitrogen, sulfur, and phosphorus cycles, and they have been positively associated with coral health and the resilience of coral reef ecosystems (Sun et al., 2016). These features make fungi key players within the coral microbiomes and their functionality.

Diversity Analyses of Microbial Communities Associated With Marine Hosts

Results from observed OTUs and Simpson diversity indexes showed that the microbiota associated to the marine hosts is highly diverse, and it has a considerable species richness. The most diverse bacterial communities were found associated with *S. siderea*, and the least diverse were in association with *P. porites*. The most diverse eukaryotic community was found associated with *S. siderea* and the least diverse was in association with *C. natans*.

The Shannon index showed that bacterial communities associated with *S. siderea* had a random distribution in terms of species evenness. In contrast, communities associated with *P. astreoides* were dominated by a few abundant species, of Cyanobacteria. *O. annularis* and *S. siderea* microbiomes harbor eukaryotic communities with an even taxa representation. For the microbiome associated with *C. natans*, just a few eukaryotic groups were highly represented while others were underrepresented.

Rarefaction analysis was appropriate for the characterization of microbial diversity in the studied hosts. It would be convenient to identify rare species interacting in a smaller proportion with these macroorganisms (Gotelli and Colwell, 2001). For *P. astreoides*, additional sequencing efforts are required to fully characterize its microbiome.

Principal component analysis suggested that the composition of microbial communities was different between hosts but given the low sample number it is necessary to confirm this with a study that includes a larger number of specimens and replicates. This supports the idea that there are some species-specific relationships, as it has been suggested for some sponges and corals (Taylor et al., 2007; Morrow et al., 2012).

Potential Metabolic Functionality of Microbial Communities

Most functional subsystems were represented in all samples. The metabolic pathways identified within the marine microbiomes included membrane transport; transformation of carbon, nitrogen, phosphorus, and sulfur macromolecules (carbohydrate metabolism, amino acid metabolism, energy metabolism); and cell division processes (replication and repair, translation). Membrane transport systems are needed for the uptake of substrates that are present in the environment and can be used by microorganisms and marine hosts. Carbohydrate, amino acid, energy metabolism, replication, and translation processes are coupled because macromolecules are broken to produce energy and basic compounds for the synthesis of new essential biological structures (Karlsson, 2012). These processes also guarantee the correct mass fluxes through the biogeochemical cycles within the marine ecosystem (Caron, 2005; Glöckner et al., 2012). Functions of surveyed microbial communities in this study are involved in cofactors and vitamin metabolism, and in xenobiotics biodegradation. In vitamin metabolism, the production of porphyrin, chlorophyll, pantothenate, and CoA is fundamental for cellular development. Xenobiotic biodegradation includes the degradation of recalcitrant pools of organic matter such as benzoates, caprolactam, and polycyclic hydrocarbons, which are known to be toxic substances in different ecosystems (Dinsdale et al., 2008).

The described functional profiles can be related to the potential that has been attributed to marine microbes, in providing nutritional by-products, proteins, essential vitamins, and nitrogenous compounds to hosts (Xu and Gordon, 2003; Lesser, 2004; Croft et al., 2005), as well as their ability to transform polluting substances in association with macroorganisms (Wahl et al., 2012; Grossart et al., 2013).

Potential activities related to amino acid and carbohydrate metabolism were more abundant in sponges than in corals. This could be a consequence of the high potential of sponges to produce bioactive compounds, and to harbor a larger arsenal of microbial metabolic pathways. The range of compounds that can be isolated from *Haliclona* sp. and its microbiome includes steroids, terpenoids, polyacetylenes, alkaloids, cyclic peptides, unsaturated fatty acids, and polyketides (Yu et al., 2006). Previous studies had suggested that coral-associated microbes have a lower functional diversity because they rarely include processes associated with secondary metabolism, virulence pathways, cell signaling, and membrane transport pathways. These pathways did not show a significant difference in corals microbial communities identified in our study.

CONCLUSION

We report the first taxonomic survey of microbial communities associated with corals, a marine sponge, and sediment at Serrana

Bank, an atoll of the Seaflower Biosphere Reserve. Although total OTUs assignment was lower compared to other studies performed in coral reefs, our results provide insights about the microbial diversity associated with several marine hosts at the Serrana Bank. We found that the bacterial and eukaryotic community structures are different between hosts. Despite the fact that the same phyla are dominant (Proteobacteria, Firmicutes, Actinobacteria, Bacteroidetes, and Acidobacteria from bacteria; Ascomycota for Eukarya), the relative abundances of each group vary among corals, the sponge, and the sediment. This is recurrent at all taxonomic levels (class, order, family).

Our results showed that *S. siderea* harbors a higher bacterial diversity (richness and evenness) than the sponge and sediment. This finding was unsual, because host-associated communities have been found to be less diverse than sediments. Hence, additional analyses are necessary in order to confirm this result and the driving factors for this shift.

Additionally, important differences were identified in the microbiota of *P. astreoides,* where Cyanobacteria was the predominant phylum, and opportunistic species (*Vibrio* and *Acinetobacter*) were identified. These species could indicate a disease status for the coral, but concise conclusions cannot be drawn at this point. It is yet to be proved if human intervention, climate change, or other factors might be playing a role in the decline of this coral in the reserve. Since the diversity found in this coral was likely to be under-represented, due to the low number of reads, additional samples should be sequenced to fully characterize this microbiome and generate more accurate conclusions about their association with the coral host.

Regarding eukaryotic characterization, *O. annularis* showed a higher diversity than *S. siderea* and *C. natans*. Overall, the fungi found in association with each host are an important component of their holobionts, because they influence the health status, carbon and nitrogen cycling, and resilience of coral reef ecosystems.

Finally, potential metabolic functionality was evaluated for some hosts. Our results revealed that the sponge microbiome had a significantly higher number of metabolic activities (amino acid and carbohydrate metabolism) in comparison to corals. This result could be associated with the HMA found in the sponge. In general, we found functional evidence of energy production, cell reproduction, and nutrient cycling within the marine ecosystem.

The implementation of continuous monitoring of the wellbeing of this Caribbean ecosystem is crucial and it must include the study of microbial communities associated with its macroorganisms. In our study, metabarcoding data from these microbial communities generated a set of OTUs that could be potentially used for effective biodiversity monitoring through time. Extended surveys of biodiversity changes in the Seaflower Biosphere reserve will be a critical action for the application of proper management practices.

AUTHOR CONTRIBUTIONS

MC and AA-Y participated in the conception and design of the study. AA-Y collected the data. AA-Y, JM-R, AN-P, and DL-A performed the analyses and interpretation of the results. AA-Y, AN-P, DL-A, and MC wrote the manuscript. All authors read, commented, and approved the manuscript.

FUNDING

This work was co-funded by the Department of Science, Technology, and Innovation (COLCIENCIAS) through the program Colombia BIO, the Comisión Colombiana del Oceáno under the program "Seaflower Scientific Expedition" and by the Centro de Bioinformática y Biología Computacional BIOS.

ACKNOWLEDGMENTS

The authors extend their appreciation to Valeria Pizarro from the Fundación Malpelo; Lizette Quan and Paula Quinceno from the Universidad de Antioquia; and to Juliana Sintura from the Comisión Colombiana del Océano for their collaboration during the species identification and sampling activities of this research.

SUPPLEMENTARY MATERIAL

The Supplementary Material for this article can be found online at: https://www.frontiersin.org/articles/10.3389/fmars.2019.00338/full#supplementary-material

REFERENCES

Ainsworth, T. D., Fordyce, A. J., and Camp, E. F. (2017). The other microeukaryotes of the coral reef microbiome. *Trends Microbiol.* 25, 980–991. doi: 10.1016/j.tim.2017.06.007

Alker, A. P., Smith, G. W., and Kim, K. (2001). Characterization of *Aspergillus sydowii* (Thom et Church), a fungal pathogen of Caribbean sea fan corals. *Hydrobiologia* 460, 105–111. doi: 10.1023/A:1013145524136

Barneah, O., Ben-Dov, E., Kramarsky-Winter, E., and Kushmaro, A. (2007). Characterization of black band disease in Red Sea stony corals. *Environ. Microbiol.* 9, 1995–2006. doi: 10.1111/j.1462-2920.2007.01315.x

Bell, J. J. (2008). The functional roles of marine sponges. *Estuar. Coast. Shelf Sci.* 79, 341–353. doi: 10.1016/j.ecss.2008.05.002

Ben-Haim, Y., Thompson, F. L., Thompson, C. C., Cnockaert, M. C., Hoste, B., Swings, J., et al. (2003). Vibrio coralliilyticus sp. nov., a temperature-dependent pathogen of the coral *Pocillopora damicornis*. *Int. J. Syst. Evol. Microbiol.* 53, 309–315. doi: 10.1099/ijs.0.02402-2400

Cárdenas, A., Rodriguez-R, L. M., Pizarro, V., Cadavid, L. F., and Arévalo-Ferro, C. (2012). Shifts in bacterial communities of two caribbean reef-building coral species affected by white plague disease. *ISME J.* 6, 502–512. doi: 10.1038/ismej.2011.123

Caron, D. A. (2005). Marine microbial ecology in a molecular world?: what does the future hold? *Scentia Mar.* 69 (Suppl) 97–110. doi: 10.3989/scimar.2005.69s197

Charpy, L., Palinska, K. A., Casareto, B., Langlade, M. J., Suzuki, Y., Abed, R. M. M., et al. (2010). Dinitrogen-fixing cyanobacteria in microbial mats of two shallow coral reef ecosystems. *Microb. Ecol.* 59, 174–186. doi: 10.1007/s00248-009-9576-y

Coker, D. J., Wilson, S. K., and Pratchett, M. S. (2014). Importance of live coral habitat for reef fishes. *Rev. Fish Biol. Fish*. 24, 89–126. doi: 10.1007/s11160-013-9319-9315

Comisión Colombiana del Oceáno (2015). *Aportes al conocimiento de la Reserva de Biósfera Seaflower*. Bogota: Comisión Colombiana del Oceáno.

Croft, M. T., Lawrence, A. D., Raux-Deery, E., Warren, M. J., and Smith, A. G. (2005). Algae acquire vitamin B12 through a symbiotic relationship with bacteria. *Nature* 438, 90–93. doi: 10.1038/nature04056

Debnath, M., Paul, A K., and Bisen, P. S. (2007). Natural bioactive compounds and biotechnological potential of marine bacteria. *Curr. Pharm. Biotechnol*. 8, 253–260. doi: 10.2174/138920107782109976

De-Kluijver, M., Gijswijt, G., De-Leon, R., and Da-Cunda, I. (2016). *Marine Species Identification Portal. Boulder Brain Coral (Colpophyllia natans)*. Available at: http://species-identification.org/species.php?species_group=caribbean_diving_guide&id=305 (accessed June 20, 2018).

Delmont, T. O., Robe, P., Clark, I., Simonet, P., and Vogel, T. M. (2011). Metagenomic comparison of direct and indirect soil DNA extraction approaches. *J. Microbiol. Methods* 86, 397–400. doi: 10.1016/j.mimet.2011.06.013

Díaz, J. M., Díaz-Pulido, G., Garzón-Ferreira, J., Geister, J., Sánchez M J. A., and Zea, S. (1996). *Atlas de los Arrecifes Coralinos del Caribe Colombiano. I. Complejos Arrecifales oceánicos*. Santa Marta: Serie Publicaciones Especiales Invemar.

Dinsdale, E. A., Edwards, R. A., Hall, D., Angly, F., Breitbart, M., Brulc, J. M., et al. (2008). Functional metagenomic profiling of nine biomes. *Nature* 452, 629–632. doi: 10.1038/nature06810

Dionisi, H., Lozada, M., and Oliviera, N. L. (2012). Bioprospection of marine microorganisms: biotechnological applications and methods. *Rev. Argent Microbiol*. 44, 49–60. doi: 10.1590/S0325-75412012000100010

Edmunds, P. J. (2015). A quarter-century demographic analysis of the Caribbean coral, *Orbicella annularis*, and projections of population size over the next century. *Limnol. Oceanogr.* 60, 840–855. doi: 10.1002/lno.10075

Ellis, J., and Solander, D. C. (1786). *The Natural History of Many Curious and Uncommon Zoophytes?: Collected from Various Parts of the Globe*. London?: Printed for Benjamin White and Son... and Peter Elmsly.

Franco, D. C., Signori, C. N., Duarte, R. T. D., Nakayama, C. R., Campos, L. S., and Pellizari, V. H. (2017). High prevalence of gammaproteobacteria in the sediments of admiralty bay and north bransfield basin, Northwestern Antarctic Peninsula. *Front. Microbiol.* 8:153. doi: 10.3389/fmicb.2017.00153

Frias-Lopez, J., Bonheyo, G. T., Jin, Q., and Fouke, B. W. (2003). Cyanobacteria associated with coral black band disease in caribbean and indo-pacific reefs. *Appl. Environ. Microbiol.* 69, 2409–2413. doi: 10.1128/AEM.69.4.2409-2413.2003

Galeano, E., Gomez, D. I., Navas, R., Alonso, D., Zarza-González, E., Cano-Correa, M., et al. (2016). *Reporte del Estado de los Arrecifes Coralinos y Pastos Marinos en Colombia (2014-2015) Proyecto COL75241, PIMS # 3997, Diseño e implementación de un Subsistema Nacional de Áreas Marinas Protegidas (SAMP) en Colombia*. Santa Marta: Serie de publicaciones Generales del Invemar.

Glöckner, F. O., Stal, L., Sandaa, R. A., Gasol, J. M., O'Gara, F., Hernandez, F., et al. (2012). "Marine Microbial Diversity and its role in Ecosystem Functioning and Environmental Change. Marine Board Position Paper 17" in *Marine Board Position Paper 17*., eds N. McDonough and J.-B. Calewaert (Belgium: European Scientific Foundation), 84. doi: 10.13140/RG.2.1.5138.6400

Gotelli, N. J., and Colwell, R. K. (2001). Quantifying biodiversity: procedures and pitfalls in the measurement and comparison of species richness. *Ecol. Lett*. 4, 379–391. doi: 10.1046/j.1461-0248.2001.00230.x

Green, D. H., Edmunds, P. J., and Carpenter, R. C. (2008). Increasing relative abundance of *Porites astreoides* on Caribbean reefs mediated by an overall decline in coral cover. *Mar. Ecol. Prog. Ser.* 359, 1–10. doi: 10.3354/meps07454

Grossart, H. P., Riemann, L., and Tang, K. W. (2013). Molecular and functional ecology of aquatic microbial symbionts. *Front. Microbiol.* 4:59 doi: 10.3389/fmicb.2013.00059

Haygood, M. G., Schmidt, E. W., Davidson, S. K., and Faulkner, D. J. (1999). Microbial symbionts of marine invertebrates: opportunities for microbial biotechnology. *J. Mol. Microbiol. Biotechnol.* 1, 33–43.

Hendershot, J. N., Read, Q. D., Henning, J. A., Sanders, N. J., and Classen, A. T. (2017). Consistently inconsistent drivers of microbial diversity and abundance at macroecological scales. *Ecology* 98, 1757–1763. doi: 10.1002/ecy.1829

Hentschel, U. (2003). Microbial diversity of marine sponges. *Prog. Mol. Subcell Biol.* 68, 365–372. doi: 10.1007/978-3-642-55519-0_3

Hernandez-Agreda, A., Gates, R. D., and Ainsworth, T. D. (2017). Defining the core microbiome in Corals' microbial soup. *Trends Microbiol.* 25, 125–140. doi: 10.1016/j.tim.2016.11.003

Hongxiang, X., Min, W., Xiaogu, W., Junyi, Y., and Chunsheng, W. (2008). Bacterial diversity in deep-sea sediment from northeastern Pacific Ocean. *Acta Ecol. Sin.* 28, 479–485. doi: 10.1016/S1872-2032(08)60026-60028

Hoppers, A., Stoudenmire, J., Wu, S., and Lopanik, N. B. (2015). Antibiotic activity and microbial community of the temperate sponge, Haliclona sp. *J. Appl. Microbiol.* 118, 419–430. doi: 10.1111/jam.12709

Howard, M. (2006). *Evaluation Report Seaflower Biosphere Reserve Implementation: The First Five Years 2000–2005*. Waltham, MA: Brandeis University.

Howard, M., Valeria, P., and Mow, J. M. (2004). Ethnic and biological diversity within the seaflower biosphere reserve. *Int. J. Isl. Aff.* 13, 109–114.

Jasmin, C., Anas, A., and Nair, S. (2015). Bacterial diversity associated with cinachyra cavernosa and haliclona pigmentifera, cohabiting sponges in the coral reef ecosystem of gulf of mannar, Southeast Coast of India. *PLoS One* 10:e0123222. doi: 10.1371/journal.pone.0123222

Jiang, S., Sun, W., Chen, M., Dai, S., Zhang, L., Liu, Y., et al. (2007). Diversity of culturable actinobacteria isolated from marine sponge Haliclona sp. *Antonie van Leeuwenhoek* 92, 405–416. doi: 10.1007/s10482-007-9169-z

Karlsson, T. (2012). *Carbon and Nitrogen Dynamics in Agricultural Soils Model Applications at Different Scales in Time and Space*. Uppsala: Acta Universitatis agriculturae Sueciae.

Kellogg, C. A., Piceno, Y. M., Tom, L. M., DeSantis, T. Z., Gray, M. A., and Andersen, G. L. (2014). Comparing bacterial community composition of healthy and dark spot-affected *Siderastrea sidereain* Florida and the Caribbean. *PLoS One* 9:e108767. doi: 10.1371/journal.pone.0108767

Kendrick, B., Risk, M. J., Michaelides, J., and Bergman, K. (1982). Amphibious microborers: bioeroding fungi isolated from corals. *Bull. Mar. Sci.* 32, 862–867.

Kennedy, J., Baker, P., Piper, C., Cotter, P. D., Walsh, M., Mooij, M. J., et al. (2009). Isolation and analysis of bacteria with antimicrobial activities from the marine sponge haliclona simulans collected from irish waters. *Mar. Biotechnol.* 11, 384–396. doi: 10.1007/s10126-008-9154-9151

Khan, S. T., Komaki, H., Motohashi, K., Kozone, I., Mukai, A., Takagi, M., et al. (2011). Streptomyces associated with a marine sponge Haliclona sp.; biosynthetic genes for secondary metabolites and products. *Environ. Microbiol.* 13, 391–403. doi: 10.1111/j.1462-2920.2010.02337.x

Khan, S. T., Musarrat, J., Alkhedhairy, A. A., and Kazuo, S. (2014). Diversity of bacteria and polyketide synthase associated with marine sponge Haliclona sp. *Ann. Microbiol.* 64, 199–207. doi: 10.1007/s13213-013-0652-7

Kim, K., Alker, A. P., Shuster, K., Quirolo, C., and Harvell, C. D. (2006). Longitudinal study of aspergillosis in sea fan corals. *Dis. Aquat. Organ.* 69, 95–99. doi: 10.3354/dao069095

Kim, K., Harvell, C. D., Kim, P. D., Smith, G. W., and Merkel, S. M. (2000). Fungal disease resistance of Caribbean sea fan corals (*Gorgonia* spp.). *Mar. Biol.* 136, 259–267. doi: 10.1007/s002270050684

Konopka, A. (2009). What is microbial community ecology? *ISME J.* 3, 1223–1230. doi: 10.1038/ismej.2009.88

Lachnit, T., Meske, D., Wahl, M., Harder, T., and Schmitz, R. (2011). Epibacterial community patterns on marine macroalgae are host-specific but temporally variable. *Environ. Microbiol.* 13, 655–665. doi: 10.1111/j.1462-2920.2010.02371.x

Langille, M. G. I., Zaneveld, J., Caporaso, J. G., McDonald, D., Knights, D., Reyes, J. A., et al. (2013). Predictive functional profiling of microbial communities using 16S rRNA marker gene sequences. *Nat. Biotech.* 31, 814–821. doi: 10.1038/nbt.2676

Lawler, S. N., Kellogg, C. A., France, S. C., Clostio, R. W., Brooke, D., and Ross, S. W. (2016). Coral-associated bacterial diversity is conserved across two deep-sea anthothela species. *Front. Microbiol.* 7:458. doi: 10.3389/fmicb.2016.00458

Lee, Y., Lee, J., and Lee, H. (2001). Microbial symbiosis in marine sponges. *J. Microbiol.* 39, 254–264

Lesser, M. P. (2004). Discovery of symbiotic nitrogen-fixing cyanobacteria in corals. *Science* 305, 997–1000. doi: 10.1126/science.1099128

Lozada, M., and Dionisi, H. M. (2015). "Microbial bioprospecting in marine environments," in *Springer Handbook of Marine Biotechnology. Springer Handbooks*. ed. S. K Kim (Springer: Heidelberg).

Madigan, M. T., and Martinko, J. M. (2005). *Brock Biology of Microorganisms*. 11 ed. Upper Saddle River, NJ: Prentice Hall.

McMurdie, P. J., and Holmes, S. (2013). phyloseq: an R package for reproducible interactive analysis and graphics of microbiome census data. *PLoS One* 8:e61217. doi: 10.1371/journal.pone.0061217

Meyer, J. L., Paul, V. J., and Teplitski, M. (2014). Community shifts in the surface microbiomes of the coral porites astreoides with unusual lesions. *PLoS One* 9:e100316. doi: 10.1371/journal.pone.0100316

Milici, M., Tomasch, J., Wos-Oxley, M. L., Wang, H., Jáuregui, R., Camarinha-Silva, A., et al. (2016). Low diversity of planktonic bacteria in the tropical ocean. *Sci. Rep.* 6:19054. doi: 10.1038/srep19054

Morrow, K. M., Moss, A. G., Chadwick, N. E., and Liles, M. R. (2012). Bacterial associates of two caribbean coral species reveal species-specific distribution and geographic variability. *Appl. Environ. Microbiol.* 78, 6438–6449. doi: 10.1128/AEM.01162-1112

Mouchka, M. E., Hewson, I., and Harvell, C. D. (2010). Coral-associated bacterial assemblages: current knowledge and the potential for climate-driven impacts. *Integr. Comp. Biol.* 50, 662–674. doi: 10.1093/icb/icq061

Pavan-Kumar, A., Gireesh-Babu, P., and Lakra, W. S. (2015). DNA metabarcoding: a new approach for rapid biodiversity assessment. *J. Cell Sci. Mol. Biol.* 2:111

Raghukumar, C., and Ravindran, J. (2012). Fungi and their role in corals and coral reef ecosystems. *Biol. Mar. Fungi* 53 89–113. doi: 10.1007/978-3-642-23342-5_5

Reed, J. K. (1985). "Deepest distribution of Atlantic hermatypic corals discovered in the Bahamas," in *Proceedings of the Fifth International Coral Reef Congress*, Tahiti.

Riegl, B., Bruckner, A., Coles, S. L., Renaud, P., and Dodge, R. E. (2009). Coral reefs. *Ann. N. Y. Acad. Sci.* 1162, 136–186. doi: 10.1111/j.1749-6632.2009.04493.x.

Rodriguez-Lanetty, M., Granados-Cifuentes, C., Barberan, A., Bellantuono, A. J., and Bastidas, C. (2013). Ecological inferences from a deep screening of the complex bacterial consortia associated with the coral, *Porites astreoides*. *Mol. Ecol.* 22, 4349–4362. doi: 10.1111/mec.12392

Rohwer, F., Seguritan, V., Azam, F., and Knowlton, N. (2002). Diversity and distribution of coral-associated bacteria. *Mar. Ecol. Prog. Ser.* 243, 1–10. doi: 10.3354/meps243001

Sogin, M. L., Morrison, H. G., Huber, J. A., Welch, D. M., Huse, S. M., Neal, P. R., et al. (2006). Microbial diversity in the deep sea and the underexplored "rare biosphere." *Proc. Natl. Acad. Sci. U.S.A.* 103, 12115–12120. doi: 10.1073/pnas.0605127103

Spang, A., Poehlein, A., Offre, P., Zumbrägel, S., Haider, S., Rychlik, N., et al. (2012). The genome of the ammonia-oxidizing candidatus nitrososphaera gargensis: insights into metabolic versatility and environmental adaptations. *Environ. Microbiol.* 14, 3122–3145. doi: 10.1111/j.1462-2920.2012.02893.x

Streit, W. R., and Schmitz, R. A. (2004). Metagenomics - the key to the uncultured microbes. *Curr. Opin. Microbiol.* 7, 492–498. doi: 10.1016/j.mib.2004.08.002

Sun, W., Anbuchezhian, R., and Li, Z. (2016). "Association of Coral-Microbes, and the Ecological Roles of Microbial Symbionts in Corals," in *The Cnidaria, Past, Present and Future*.eds S. Goffredo and Z Dubinsky (Switzerland: Springer International Publishing)

Sweet, M., Burn, D., Croquer, A., and Leary, P. (2013). Characterisation of the bacterial and fungal communities associated with different lesion sizes of dark spot syndrome occurring in the coral stephanocoenia intersepta. *PLoS One* 8:e62580. doi: 10.1371/journal.pone.0062580

Taylor, M. W., Radax, R., Steger, D., and Wagner, M. (2007). Sponge-associated microorganisms: evolution, ecology, and biotechnological potential. *Microbiol. Mol. Biol. Rev.* 71, 295–347. doi: 10.1128/MMBR.00040-06

Thompson, L. R., Sanders, J. G., McDonald, D., Amir, A., Ladau, J., Locey, K. J., et al. (2017). A communal catalogue reveals Earth's multiscale microbial diversity. *Nature* 551, 457–463. doi: 10.1038/nature24621

Wahl, M., Goecke, F., Labes, A., Dobretsov, S., and Weinberger, F. (2012). The second skin: ecological role of epibiotic biofilms on marine organisms. *Front. Microbiol.* 3:292. doi: 10.3389/fmicb.2012.00292

Wang, L., Chen, Y., Huang, H., Huang, Z., Chen, H., and Shao, Z. (2015). Isolation and identification of *Vibrio campbellii* as a bacterial pathogen for luminous vibriosis of *Litopenaeus vannamei*. *Aquac. Res.* 46, 395–404. doi: 10.1111/are.12191

Wang, L., Shantz, A. A., Payet, J. P., Sharpton, T. J., Foster, A., Burkepile, D. E., et al. (2018). Corals and their microbiomes are differentially affected by exposure to elevated nutrients and a natural thermal anomaly. *Front. Mar. Sci.* 5:101. doi: 10.3389/fmars.2018.00101

Webster, N. S., Xavier, J. R., Freckelton, M., Motti, C. A., and Cobb, R. (2008). Shifts in microbial and chemical patterns within the marine sponge Aplysina aerophoba during a disease outbreak. *Environ. Microbiol.* 10, 3366–3376. doi: 10.1111/j.1462-2920.2008.01734.x

Wegley, L., Edwards, R., Rodriguez-Brito, B., Liu, H., and Rohwer, F. (2007). Metagenomic analysis of the microbial community associated with the coral Porites astreoides. *Environ. Microbiol.* 9, 2707–2719. doi: 10.1111/j.1462-2920.2007.01383.x.

Wickham, H. (2016). *ggplot2: Elegant Graphics for Data Analysis*. New York, NY: Springer-Verlag.

Wulff, J. L. (2006). Ecological interactions of marine sponges. *Can. J. Zool.* 84, 146–166. doi: 10.1139/z06-019

Xu, J., and Gordon, J. I. (2003). Honor thy symbionts. *Proc. Natl. Acad. Sci. U.S.A.* 100, 10452–10459. doi: 10.1073/pnas.1734063100

Xu, W., Pang, K. L., and Luo, Z. H. (2014). High fungal diversity and abundance recovered in the deep-sea sediments of the pacific ocean. *Microb. Ecol.* 68, 688–698. doi: 10.1007/s00248-014-0448-448

Yu, S., Deng, Z., Proksch, P., and Lin, W. (2006). Oculatol, oculatolide, and A-nor sterols from the sponge haliclona oculat a. *J. Nat. Prod.* 69, 1330–1334. doi: 10.1021/np0600494

Zhang, Y. Y., Ling, J., Yang, Q. S., Wang, Y. S., Sun, C. C., Sun, H. Y., et al. (2015). The diversity of coral associated bacteria and the environmental factors affect their community variation. *Ecotoxicology* 24, 1467–1477. doi: 10.1007/s10646-015-1454-1454

Conflict of Interest Statement: The authors declare that the research was conducted in the absence of any commercial or financial relationships that could be construed as a potential conflict of interest.

frontiers in Marine Science

DATA REPORT
published: 06 September 2019
doi: 10.3389/fmars.2019.00536

Corals in the Mesophotic Zone (40–115 m) at the Barrier Reef Complex From San Andrés Island (Southwestern Caribbean)

Juan Armando Sánchez[1], Fanny L. González-Zapata[1], Luisa F. Dueñas[2], Julio Andrade[1], Ana Lucía Pico-Vargas[1], Diana Carolina Vergara[1], Adriana Sarmiento[1] and Nacor Bolaños[3]*

[1] Departamento de Ciencias Biológicas, Facultad de Ciencias, Laboratorio de Biología Molecular Marina-BIOMMAR, Universidad de los Andes, Bogotá, Colombia, [2] Departamento de Biología, Facultad de Ciencias, Universidad Nacional de Colombia, Sede Bogotá, Bogotá, Colombia, [3] Corporación para el Desarrollo Sostenible del Archipiélago De San Andrés, Providencia y Santa Catalina (CORALINA), San Andrés, Colombia

Keywords: Mesophotic Coral Ecosystem (MCE), coral, octocoral, black coral, stylaster, scleractinia, San Andrés Island, Caribbean

OPEN ACCESS

Edited by:
Zhijun Dong,
Yantai Institute of Coastal Zone Research (CAS), China

Reviewed by:
Xiubao Li,
Hainan University, China
Carolina Bastidas,
Massachusetts Institute of Technology, United States

****Correspondence:***
Juan Armando Sánchez
juansanc@uniandes.edu.co

Specialty section:
This article was submitted to Marine Evolutionary Biology, Biogeography and Species Diversity, a section of the journal Frontiers in Marine Science

Received: *05 June 2019*
Accepted: *15 August 2019*
Published: *06 September 2019*

Citation:
Sánchez JA, González-Zapata FL, Dueñas LF, Andrade J, Pico-Vargas AL, Vergara DC, Sarmiento A and Bolaños N (2019) Corals in the Mesophotic Zone (40–115 m) at the Barrier Reef Complex From San Andrés Island (Southwestern Caribbean). Front. Mar. Sci. 6:536. doi: 10.3389/fmars.2019.00536

BACKGROUND

Shallow reefs in the SeaFlower Biosphere Reserve, even at the remotest bank atolls, are showing a steady decline in coral cover overall health condition during the last 20 years (Sánchez et al., 2019b). Mesophotic Coral Ecosystems (MCEs), located between 30 and >150 m of water depth, may act as a refuge of coral populations due to favorable conditions in this less altered environment (Bongaerts et al., 2010). Particularly, in our study area, San Andres Island, populations of corals reaching the lower (>60 m) mesophotic zone, 40–90 m, such as *Agaricia undata* exhibit genetic connectivity throughout its depth range (Gonzalez-Zapata et al., 2018a), supporting this zone as a major reef-building coral refuge. It has been suggested that depending on the type of endosymbiont, corals can acclimatize to deeper depths (Ziegler et al., 2015), which was in fact observed in the bacterial population from *A. undata* in San Andrés Island (Gonzalez-Zapata et al., 2018a). In addition, many species of fish, corals, and other invertebrates from shallow reefs are also found in mesophotic reefs and it is proposed that these populations could contribute to the recovery of affected populations in shallower areas following a disturbance (Kramer et al., 2019).

There are potential new species of corals and associated species, including common shallow-water fauna, in mesophotic reefs (Luck et al., 2013; Petrescu et al., 2014), which urges studies surveying coral diversity at these depths. However, these reefs have been rarely explored below 60 m in water depth. The dataset presented in this study, provide the first exploration of the mesophotic zone (40–120 m deep) in an oceanic barrier reef complex (SeaFlower Biosphere Reserve), San Andrés Island, Southwestern Caribbean. The dataset presented here includes the collection information, and community composition of corals *sensu lato* (stony corals, hydrocorals, black corals, and octocorals). The ultimate goal was to contribute to the understanding of sensible and vulnerable environments, in the SeaFlower Biosphere reserve, in which San Andrés Island is immersed.

DATA COLLECTION

We concentrated the study in the fore-reef slope of San Andrés Island barrier reef complex near the location called "Trampa de Tortugas" or "Trampa Tortuga," which offered a number of logistic advantages. The site bears a shelter to anchor the supporting boat despite its location on the

TABLE 1 | Specimens comprising the mesophotic coral dataset (Cnidaria: Anthozoa and Hydrozoa).

IN-ANDES	Code	Species	Depth (m)	Site	Sdate
		Black corals (Anthipatharia)			
4128	SAI206	*Antipathes atlantica* (Gray, 1857) (C)	40	Trampa deTortugas	11/04/15
4205	SAI128	*Antipathes furcata* (Gray, 1857) (A)	70	Trampa deTortugas	11/04/15
4466	SAI153	*Antipathes* sp. (Pallas, 1976) (C)	85	Trampa deTortugas	11/04/15
4467	SAI184	*Antipathes* sp. (Pallas, 1976)	40	Trampa deTortugas	11/04/15
4468	SAI185	*Antipathes* sp. (Pallas, 1976)	40	Trampa deTortugas	11/04/15
4469	SAI186	*Antipathes* sp. (Pallas, 1976)	40	Trampa deTortugas	11/04/15
4470	SAI187	*Antipathes* sp. (Pallas, 1976)	40	Trampa deTortugas	11/04/15
4164	SAI205	*Rhipidipathes colombiana* (Opresko and Sánchez, 1997) (R)	40	Trampa deTortugas	11/04/15
4324	SAI131	*Stichopathes lutkeni* (Brook, 1889) (A)	70	Trampa deTortugas	11/04/15
4325	SAI142	*Stichopathes lutkeni* (Brook, 1889)	85	Trampa deTortugas	11/04/15
4327	SAI150	*Stichopathes lutkeni* (Brook, 1889)	85	Trampa deTortugas	11/04/15
4328	SAI151	*Stichopathes lutkeni* (Brook, 1889)	85	Trampa deTortugas	11/04/15
4339	SAI171	*Stichopathes lutkeni* (Brook, 1889)	40	Trampa deTortugas	11/04/15
4340	SAI172	*Stichopathes lutkeni* (Brook, 1889)	40	Trampa deTortugas	11/04/15
4330	SAI174	*Stichopathes lutkeni* (Brook, 1889)	40	Trampa deTortugas	11/04/15
4341	SAI180	*Stichopathes lutkeni* (Brook, 1889)	40	Trampa deTortugas	11/04/15
4334	SAI190	*Stichopathes lutkeni* (Brook, 1889)	40	Trampa deTortugas	11/04/15
4335	SAI196	*Stichopathes lutkeni* (Brook, 1889)	40	Trampa deTortugas	11/04/15
4323	SAI104	*Stichopathes lutkeni* (Brook, 1889)	70	Trampa deTortugas	10/04/15
4394	SAI095	*Stichopathes occidentalis* (Gray, 1860) (A)	70	Trampa deTortugas	10/04/15
4395	SAI103	*Stichopathes occidentalis* (Gray, 1860)	70	Trampa deTortugas	10/04/15
4337	SAI120	*Stichopathes occidentalis* (Gray, 1860)	100	Trampa deTortugas	10/04/15
4396	SAI130	*Stichopathes occidentalis* (Gray, 1860)	70	Trampa deTortugas	11/04/15
4397	SAI132	*Stichopathes occidentalis* (Gray, 1860)	70	Trampa deTortugas	11/04/15
4374	SAI140	*Stichopathes occidentalis* (Gray, 1860)	85	Trampa deTortugas	11/04/15
4376	SAI144	*Stichopathes occidentalis* (Gray, 1860)	85	Trampa deTortugas	11/04/15
4379	SAI149	*Stichopathes occidentalis* (Gray, 1860)	85	Trampa deTortugas	11/04/15
4381	SAI156	*Stichopathes occidentalis* (Gray, 1860)	85	Trampa deTortugas	11/04/15
4382	SAI157	*Stichopathes occidentalis* (Gray, 1860)	85	Trampa deTortugas	11/04/15
4383	SAI168	*Stichopathes occidentalis* (Gray, 1860)	85	Trampa deTortugas	11/04/15
4385	SAI189	*Stichopathes occidentalis* (Gray, 1860)	40	Trampa deTortugas	11/04/15
4386	SAI191	*Stichopathes occidentalis* (Gray, 1860)	40	Trampa deTortugas	11/04/15
4388	SAI193	*Stichopathes occidentalis* (Gray, 1860)	40	Trampa deTortugas	11/04/15
4389	SAI194	*Stichopathes occidentalis* (Gray, 1860)	40	Trampa deTortugas	11/04/15
4391	SAI200	*Stichopathes occidentalis* (Gray, 1860)	40	Trampa deTortugas	11/04/15
4812	SAI081	*Stichophates* sp. (C)*	115	Trampa deTortugas	10/04/15
4579	SAI083	*Stichophates* sp.	115	Trampa deTortugas	10/04/15
4580	SAI094	*Stichophates* sp.	70	Trampa deTortugas	10/04/15
4581	SAI108	*Stichophates* sp.	90	Trampa deTortugas	10/04/15
4582	SAI111	*Stichophates* sp.	90	Trampa deTortugas	10/04/15
4585	SAI141	*Stichophates* sp.	85	Trampa deTortugas	11/04/15
4586	SAI148	*Stichophates* sp.	85	Trampa deTortugas	11/04/15
4587	SAI158	*Stichophates* sp.	85	Trampa deTortugas	11/04/15
4588	SAI166	*Stichophates* sp.	85	Trampa deTortugas	11/04/15
4589	SAI167	*Stichophates* sp.	85	Trampa deTortugas	11/04/15
4590	SAI195	*Stichophates* sp.	40	Trampa deTortugas	11/04/15
4592	SAI207	*Stichophates* sp.	40	Trampa deTortugas	11/04/15
4249	SAI010	*Tanacetipathes hirta* (Gray, 1857) (C)	67	Blue Wall	14/01/15

(Continued)

TABLE 1 | Continued

IN-ANDES	Code	Species	Depth (m)	Site	Sdate
4253	SAI159	*Tanacetipathes hirta* (Gray, 1857)	85	Trampa deTortugas	11/04/15
		Reef building corals (Scleractinia)			
4302	SAI098	*Agaricia fragilis* (Dana, 1848) (C)	70	Trampa deTortugas	10/04/15
4303	SAI119	*Agaricia fragilis* (Dana, 1848)	80	Trampa deTortugas	10/04/15
4305	SAI188	*Agaricia fragilis* (Dana, 1848)	40	Trampa deTortugas	11/04/15
4741	SAI178	*Agaricia* sp. (R)	40	Trampa deTortugas	11/04/15
4739	SAI116	*Agaricia* sp.	80	Trampa deTortugas	10/04/15
4300	SAI033	*Agaricia undata* (Ellis and Solander, 1786) (A)	80	Trampa deTortugas	15/01/15
4738	SAI101	*Agaricia undata* (Ellis and Solander, 1786)	70	Trampa deTortugas	10/04/15
4199	SAI118	*Agaricia undata* (Ellis and Solander, 1786)	80	Trampa deTortugas	10/04/15
4740	SAI134	*Agaricia undata* (Ellis and Solander, 1786)	45	Trampa deTortugas	11/04/15
4301	SAI034	*Agaricia undata* (Ellis and Solander, 1786)	80	Trampa deTortugas	15/01/15
7244	SAI603	*Balanophyllia cyathoides* (Pourtalès, 1871) (A)	70	Trampa deTortugas	10/04/15
4479	SAI127	*Javania cailleti* (Duchassaing and Michelotti, 1864) (R)	110	Trampa deTortugas	10/04/15
4426	SAI117	*Mycetophyllia reesi* (Wells, 1973) (R)	80	Trampa deTortugas	10/04/15
4427	SAI121	*Mycetophyllia reesi* (Wells, 1973)	100	Trampa deTortugas	10/04/15
4428	SAI125	*Mycetophyllia reesi* (Wells, 1973)	110	Trampa deTortugas	10/04/15
4477	SAI071	*Phacelocyathus flos* (Pourtalès, 1878) (R)	70	Trampa deTortugas	16/01/15
4430	SAI096	*Thalamophyllia riisei* (Duchassaing and Michelotti, 1864) (A)	70	Trampa deTortugas	10/04/15
4431	SAI100	*Thalamophyllia riisei* (Duchassaing and Michelotti, 1864)	70	Trampa deTortugas	10/04/15
7242	SAI601	*Thalamophyllia riisei* (Duchassaing and Michelotti, 1864)	70	Trampa deTortugas	10/04/15
7243	SAI602	*Thalamophyllia riisei* (Duchassaing and Michelotti, 1864)	70	Trampa deTortugas	10/04/15
		Lace corals (Hydrozoa: Stylasteridae)			
4187	SAI064	*Stylaster duchassaingi* (Pourtalès, 1867) (C)	95	Trampa deTortugas	16/01/15
4188	SAI107	*Stylaster duchassaingi* (Pourtalès, 1867) (C)	90	Trampa deTortugas	10/04/15
		Gorgonian corals (Octocorallia)			
4262	SAI039	*Antillogorgia hystrix* (Bayer, 1961) (C)	60	Trampa deTortugas	15/01/15
4642	SAI032	*Caliacis nutans* (Duchassaing and Michelotti, 1864) (C)	80	Trampa deTortugas	15/01/15
4139	SAI105	*Ellisella barbadensis* (Duchassaing and Michelotti, 1864) (A)	90	Trampa deTortugas	10/04/15
4143	SAI162	*Ellisella barbadensis* (Duchassaing and Michelotti, 1864)	85	Trampa deTortugas	11/04/15
4137	SAI025	*Ellisella barbadensis* (Duchassaing and Michelotti, 1864)	80	Trampa deTortugas	15/01/15
4140	SAI106	*Ellisella barbadensis* (Duchassaing and Michelotti, 1864)	90	Trampa deTortugas	10/04/15
4141	SAI109	*Ellisella barbadensis* (Duchassaing and Michelotti, 1864)	90	Trampa deTortugas	10/04/15
4142	SAI160	*Ellisella barbadensis* (Duchassaing and Michelotti, 1864)	85	Trampa deTortugas	11/04/15
4190	SAI001	*Ellisella elongata* (Pallas, 1766) (R)	67	Blue Wall	14/01/15
4440	SAI110	*Ellisella schmitti* (Bayer, 1961) (A)	90	Trampa deTortugas	10/04/15
4498	SAI090	*Ellisella* sp. (R)*	115	Trampa deTortugas	10/04/15
4499	SAI092	*Ellisella* sp.	115	Trampa deTortugas	10/04/15
4409	SAI027	*Eunicea pinta* (Bayer and Deichmann, 1958) (C)	80	Trampa deTortugas	15/01/15
4410	SAI036	*Eunicea pinta* (Bayer and Deichmann, 1958)	60	Trampa deTortugas	15/01/15
4411	SAI176	*Eunicea* sp. (C)*	40	Trampa deTortugas	11/04/15
4412	SAI177	*Eunicea* sp.	40	Trampa deTortugas	11/04/15
4369	SAI022	*Hypnogorgia pendula* (Duchassaing and Michelotti, 1864) (C)	80	Trampa deTortugas	15/01/15
4639	SAI023	*Hypnogorgia pendula* (Duchassaing and Michelotti, 1864)	80	Trampa deTortugas	15/01/15
4640	SAI024	*Hypnogorgia pendula* (Duchassaing and Michelotti, 1864)	80	Trampa deTortugas	15/01/15
4641	SAI028	*Hypnogorgia pendula* (Duchassaing and Michelotti, 1864)	80	Trampa deTortugas	15/01/15
4646	SAI137	*Hypnogorgia* sp. (C)*	85	Trampa deTortugas	11/04/15
4208	SAI009	*Nicella goreaui* (Bayer, 1973) (C)	67	Blue Wall	14/01/15
4219	SAI087	*Nicella goreaui* (Bayer, 1973)	115	Trampa deTortugas	10/04/15
4220	SAI155	*Nicella goreaui* (Bayer, 1973)	85	Trampa deTortugas	11/04/15

(Continued)

TABLE 1 | Continued

IN-ANDES	Code	Species	Depth (m)	Site	Sdate
4221	SAI164	*Nicella goreaui* (Bayer, 1973)	85	Trampa deTortugas	11/04/15
4680	SAI112	*Nicella toeplitzae* (Viada and Cairns, 2007) (R)	80	Trampa deTortugas	10/04/15
4194	SAI089	*Swiftia exserta* (Ellis and Solander, 1786) (C)	115	Trampa deTortugas	10/04/15
4665	SAI050	*Thelogorgia studeri* (Bayer, 1991) (C)	95	Trampa deTortugas	16/01/15
4666	SAI052	*Thelogorgia studeri* (Bayer, 1991)	95	Trampa deTortugas	16/01/15
4667	SAI057	*Thelogorgia studeri* (Bayer, 1991)	95	Trampa deTortugas	16/01/15
4668	SAI058	*Thelogorgia studeri* (Bayer, 1991)	95	Trampa deTortugas	16/01/15
4669	SAI136	*Thelogorgia studeri* (Bayer, 1991)	85	Trampa deTortugas	11/04/15
4643	SAI056	*Thesea sp.* (Duchassaing and Michelotti, 1860) (C)	95	Trampa deTortugas	16/01/15
4647	SAI161	*Thesea* sp. (Duchassaing and Michelotti, 1860)	85	Trampa deTortugas	11/04/15
4648	SAI163	*Thesea* sp. (Duchassaing and Michelotti, 1860)	85	Trampa deTortugas	11/04/15
4349	SAI008	*Villogorgia nigrescens* (Duchassaing and Michelotti, 1860) (A)	67	Blue Wall	14/01/15
4350	SAI030	*Villogorgia nigrescens* (Duchassaing and Michelotti, 1860)	80	Trampa deTortugas	15/01/15
4351	SAI031	*Villogorgia nigrescens* (Duchassaing and Michelotti, 1860)	80	Trampa deTortugas	15/01/15
4352	SAI035	*Villogorgia nigrescens* (Duchassaing and Michelotti, 1860)	80	Trampa deTortugas	15/01/15
4353	SAI053	*Villogorgia nigrescens* (Duchassaing and Michelotti, 1860)	95	Trampa deTortugas	16/01/15
4660	SAI055	*Villogorgia nigrescens* (Duchassaing and Michelotti, 1860)	95	Trampa deTortugas	16/01/15
4354	SAI135	*Villogorgia nigrescens* (Duchassaing and Michelotti, 1860)	85	Trampa deTortugas	11/04/15

*IN-ANDES: museum catalog number. Code, collector number. Species, Depth (meter), Site at San Andrés Island (SeaFlower Biosphere Reserve) and Date collected (day/month/year). Information per species: (A) Abundant, (C) Common, and (R) rare. *Potentially new species.*

fore-reef terrace. In addition, this site provides the only accessible glimpse of the oldest slope of the barrier-reef complex of San Andrés (Geister, 1975; Díaz et al., 1995; Diaz et al., 1996). We explored the reef using Close-Circuit Rebreather (CCR) (Megalodon, Inner Space Systems) and hypoxic trimix techniques (e.g., 11% Oxygen and 60% Helium) with complete bail-out support for each diver. At the site, we installed a mooring block at 24 m as a gas station that had high oxygen bail-outs (O_2 96%) and from where we tied a 200 m long reel down to a depth of 114 m. The reel was used to safely explore down the site and to have an easy return to shallower waters. Seven dives were planned with a maximum of 20–30 min of bottom time and the longest dives spanned 133–328 min including decompression stops. The sampling included digital imagery (Nikon^{TM} D7000, Nikkor micro 60 mm lens, Sea & Sea^{TM} YS-D1 strobe, and Aquatica^{TM} AD7000 housing) and 113 voucher specimens (dry and ethanol 96%), which were deposited at Museo de Historia ANDES (Bogotá, Colombia) (**Table 1**).

Coral Identifications

All specimens were examined under the optical and/or compound microscope for morphological identification and contrasted against species keys (if available) and/or taxonomic descriptions. For scleractinian corals we used Cairns, 2000; for Stylasteridae Cairns et al., 1986; for black corals Opresko and Sánchez, 2005; for octocorals Bayer, 1961; Bayer and Grasshoff, 1994, 1995; Sánchez and Wirshing, 2005; Sánchez, 2009. In addition, several species accounts for Colombia were also useful in species identification (Flórez et al., 2010; Chacón-Gómez et al., 2012; Santodomingo et al., 2013). When needed, Scanning Electron Microscopy (SEM) images were obtained at the microscopy laboratory in the Universidad de los Andes to increase the certainty of identifications.

DATASET OUTCOMES AND DISCUSSION

The dataset included 113 specimens from 33 species collected below 40 m (8 black corals, 1 lace coral, 8 scleractinian corals, and 16 gorgonian corals: **Table 1**). Exploring "Trampa de Tortugas," we noticed the disappearance of most reef-building corals and zooxanthellate octocorals at different depths. Some reef-building corals, notably *Mycethophyllia reesi*, *Agaricia undata, A. fragilis,* and *Madracis* sp., distributed well into the lower mesophotic zone (∼90 m) and are characterized by an increase in the presence of the euendolithic algae *Ostreobium*, which is clearly observable at the colony surface (Gonzalez-Zapata et al., 2018b). These colonial corals are replaced below 80 m by azooxanthellate cup corals, including *Javania cailleti, Phacelocyathus flos, Balanophyllia cyathoides,* and *Thalamophyllia riisei* forma *solida* (**Figure 1**). A noteworthy observation was the presence of *Ostreobium* at the basal portion of *T. riisei* cup-corals.

The lower mesophotic reef is also the habitat of many unique black corals (e.g., *Rhipidipathes colombiana* and *Tanacetipathes hirta*) and hydrocorals (*Stylaster duchassaingi*) but the most abundant group are azoxanthellate octocorals mostly from the Plexauridae family (Sánchez, 2017; Sánchez et al., 2019a). The species replacement is enhanced by short terraces intertwined with abrupt steps at every 10 m starting at 60, 90, 100, and 115 m, at "Trampa Tortuga" reef in San Andrés Island. On the

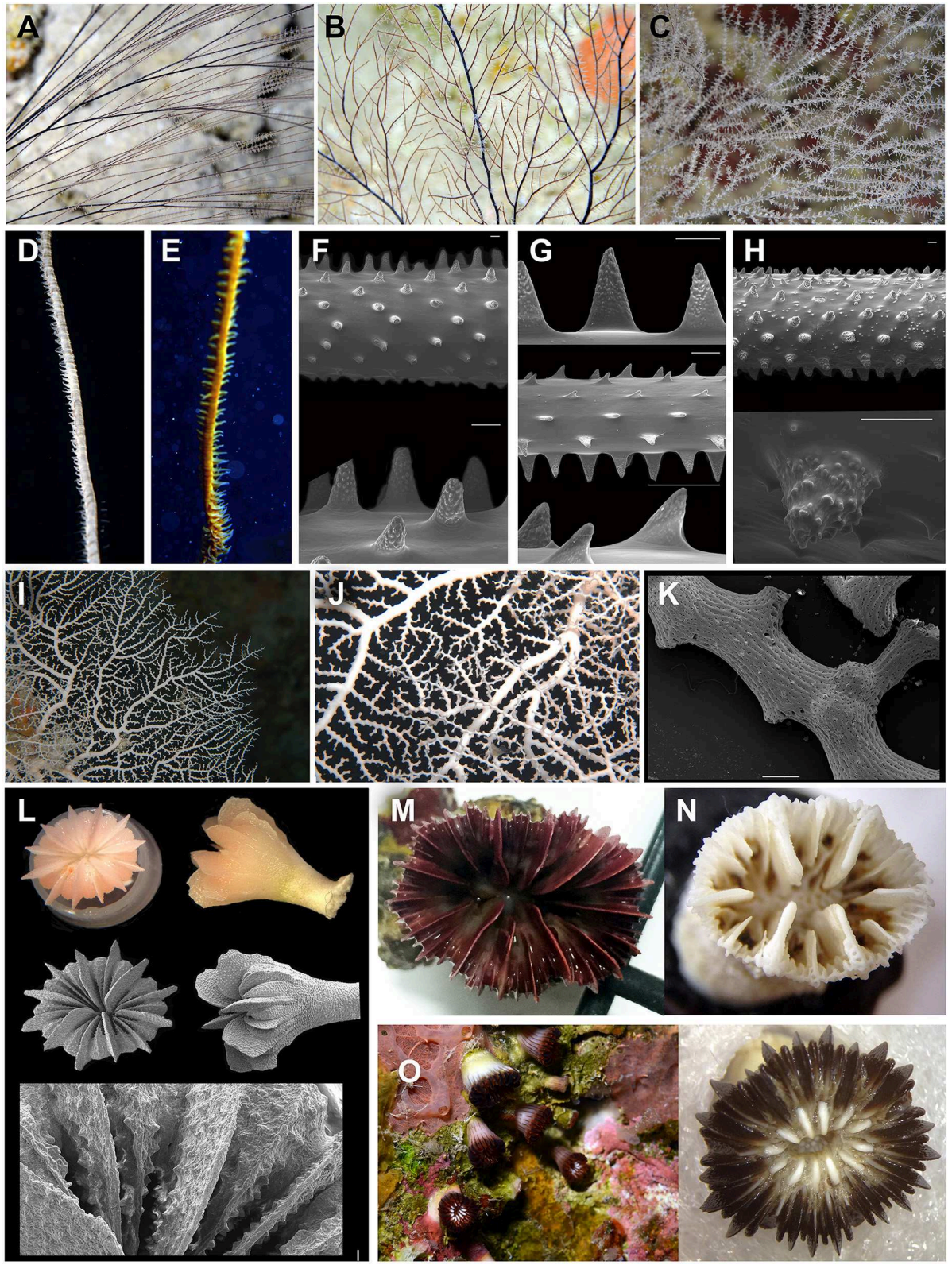

FIGURE 1 | Selected corals in the lower mesophotic zone (45–70 m) at San Andrés Island (SeaFlower Biosphere reserve). **(A–H)** Black corals. **(A)** *Antipathes furcata*, **(B,C)** *Antipathes atlantica*, **(D,E)** *Stichopathes* spp. **(F)** *Stichopathes lutkeni*; **(G)** *S. occidentalis*; **(H)** *Stichopathes* sp. (probably undescribed species or not reported

(Continued)

FIGURE 1 | yet for the Caribbean) (scales **F–H** scale 200 and 50 μm for details). **(I–K)** *Stylaster duchassaingi* Pourtalès, 1867 **(I,J)**. Colonies at Trampa Tortuga, 90 m. **(K)** Scanning Electron Microscopy (SEM) images detail of terminal branches (scale 500 μm). **(L)** Cup coral *Thalamophyllia riisei* forma *solida,* voucher samples from Trampa Tortuga, San Andrés, optical, and SEM, including a costae detail. **(M)** Cup corals *Javania cailleti* (left) **(N)** *Balanophyllia cyathoides* (right), voucher specimen from Trampa Tortuga, San Andrés. **(O)** Cup coral *Phacelocyathus flos*, voucher from Trampa Tortuga, San Andrés. Corals at 55 m and voucher specimen.

leeward side of the Island, there is parallel slope sand corridor (mostly from *Halimeda copiosa* flocks) following the reef slope, which end at about 60–80, where the reef growth continues. The deepest zooxanthellate gorgonian coral was *Antillogorgia hystrix* (65 m), followed by *Eunicea pinta* (55 m). Occasionally, *Muricea laxa*, *A. bipinnata,* and *A. americana* were seen at depths of about 40 m. These zooxanthellate octocorals share habitat with some azooxanthellate octocorals such as *Iciligorgia schrammi* and diverse ellisellids (Sánchez et al., 2019a).

Black corals (Antipatharia) are also common from 30 m down to the lower mesophotic area (Bo et al., 2019). The most abundant black corals are *Antipathes furcata* (**Figure 1A**)*, A. caribbeana, A. atlantica* (**Figure 1B**)*, Plumapathes pennacea, Stichopathes lutkeni,* and *S. occidentalis*. Wire corals, *Stichopathes* spp., with colonies reaching more than 2 m long were seen in high densities of to have more than 10 colonies per square meter (**Figures 1C,D**). Below 70 m, the aforementioned black corals are less seen and other species emerge such as *Rhipidipathes colombiana*, first seen off the Colombian coast (Opresko and Sánchez, 2005), and *Tanacetipathes hirta*. There is also a great amount of wire corals from species we could not identify and probably comprise new undescribed species. Despite the clear characters of *S. lutkeni* and *S. occidentalis* under the electron microscope, there were specimens, *Stichopathes* sp., with conspicuously smaller spines not found in any other species described for this region (**Figure 1H**).

The most unexpected finding comprised a number of new records for several deep-sea corals, which have been usually found on deeper waters. *Stylaster duchassaingi* Pourtalès, 1867, a hydrocoral (Stylasteridae) was observed from 80 to 115 m forming seafan colonies up to 40 cm in height (**Figures 1I–K**). This is the southernmost record of the species and one of the shallower observations in its range. *Stylaster roseus* is commonly observed in the same reef but above 40 m (JAS, personal observation). San Andrés Island is the only coral reef complex so far in the Caribbean with two documented species of *Stylaster*.

As expected, the exploration of the lower mesophotic zone uncovered a great amount of new species records and potential discoveries (e.g., *Stichopathes* sp.). In addition, this is the first time that many of the species have been ever seen and photographed in their natural environment (Sánchez et al., 2019a). Continuing research in this environment will enrich the ecology, systematics, and conservation of understudied corals such as cup corals. For instance, the *Thallamophyllia riisei* cup coral found in San Andrés is extremely different to the reported *T. riisei* from the Colombian coast (Flórez et al., 2010), which is colonial with great differences in morphological traits. It is worth mention that this is the product of only seven dives (and <140 min of total bottom time) for San Andres Island.

REUSE POTENTIAL

The specimens collected and properly curated (deposited and INANDES in Bogota, Colombia) comprise a valuable resource for further systematic studies in several groups of corals, which could comprise new species. In addition, it is important to mention that the specimens in this data report have not been monitored in the past, giving the logistic constraints of deep-sea diving. As the interest in MCEs increases biodiversity data becomes crucial for comparisons.

DATA AVAILABILITY

The datasets for this study can be found at https://ipt.biodiversidad.co/cr-sib/resource.do?r=0359_mesofoticos_20190729, titled "Biodiversidad y Conectividad de los arrecifes mesofóticos (30–120 m) de la costa Caribe colombiana". The data presented here corresponds to coral specimens (Cnidaria: Anthozoa andHydrozoa) collected between 40 and 115 m in the mesophotic corals ecosystems from San Andrés Island (SeaFlower Biosphere Reserve).

AUTHOR CONTRIBUTIONS

JS, LD, JA, and NB conceived the study. JS, JA, and NB collected the data. FG-Z, AS, DV, AP-V, and JS identified and processed the material. JS wrote the report with the help of LD, FG-Z, and NB. All authors read and accepted the manuscript.

FUNDING

This work was supported by an agreement between Corporación para el Desarrollo Sostenible del Departamento Archipiélago de *San Andrés* Providencia y Santa Catalina, CORALINA-Universidad de los Andes (Convenios No. 13, 2014 and No. 21, 2015: *Protección y conservación de los recursos de la biodiversidad y de los ecosistemas estratégicos dentro de la Reserva de Biosfera Seaflower* Fondo de Compensación Ambiental FCA del Ministerio de Ambiente y Desarrollo Sostenible). Additional funding was possible thanks to the University of Los Andes (Vicerrectoría de Investigaciones and Facultad de Ciencias) and COLCIENCIAS (Project code 120465944147).

ACKNOWLEDGMENTS

The support from Bluelife dive shop (family Garcia) was fundamental to accomplish this study. The San Andres Hospital

kindly supplied medical oxygen for CCR. We are very grateful with Gregg Stanton, Wakulla Dive Center, for continuing support and advise for deep diving. We are thankful with Fabian García, Santiago Herrera, Mariana Gnecco, Manu Forero, Federico Botero, and Camilo Martinez for fieldwork support. We recognize the participation and support from local communities.

REFERENCES

Bayer, F. M. (1961). *The Shallow Water Octocorallia of the West Indian Region.* The Hague: Martinus Nijoff.

Bayer, F. M., and Grasshoff, M. (1994). The genus group taxa of the family Ellisellidae, with clarification of the genera established by JE Gray (*Cnidaria*: *Octocorallia*). *Senckenb. Biol.* 74, 21–45.

Bayer, F. M., and Grasshoff, M. (1995). Two new species of the gorgonacean genus *Ctenocella* (Coelenterata: *Anthozoa, Octocorallia) from deep reefs in the western Atlantic. Bull. Mar. Sci.* 56, 625–652.

Bo, M., Montgomery, A. D., Opresko, D. M., Wagner, D., and Bavestrello, G. (2019). "Antipatharians of the mesophotic zone: four case studies," in *Mesophotic Coral Ecosystems, Coral Reefs of the World*, eds Y. Loya, K. A. Puglise, and T. C. L. Bridge (Cham: Springer Nature Switzerland AG), 683–708.

Bongaerts, P., Ridgway, T., Sampayo, E. M., and Hoegh-Guldberg, O. (2010). Assessing the 'deep reef refugia' hypothesis: focus on Caribbean reefs. *Coral Reefs* 29, 309–327. doi: 10.1007/s00338-009-0581-x

Cairns, S. D. (2000). A revision of the shallow-water Azooxanthellate Scleractinia of the western Atlantic. Revisión de los corales azooxantelados (Scleractinia) de las aguas someras del Atlántico occidental. *Stud. Fauna Curacao Caribbean Islands* 75, 1–231.

Cairns, S. D., Cairns, S. D., Cairns, S. D., and Cairns, S. D. (1986). *A Revision of the Northwest Atlantic Stylasteridae* (Coelenterata: Hydrozoa). Washington, DC: Smithsonian Institution Press.

Chacón-Gómez, I. C., Reyes, J., and Santodomingo, N. (2012). Deep-water octocorals (Anthozoa: Cnidaria) collected from the Colombian Caribbean during'Macrofauna Explorations'1998-2002*. *Bol. Investig. Mar. Costeras-INVEMAR*, 41, 193–211.

Diaz, J. M., Diaz, G., Garzon-Ferreira, J., Geister, J., Sánchez, J. A., and, S., Zea (1996). *Atlas de los arrecifes coralinos del Caribe colombiano.* I. *Archipiélago de San Andrés y Providencia.* Publicaciones Especiales del INVEMAR, Santa Marta.

Díaz, J. M., Garzón-Ferreira, J., and Zea, S. (1995). Los arrecifes coralinos de la Isla de San Andrés, Colombia: estado actual y perspectivas para su conservación. *Colecc. Jorge Alvarez Lleras, Academia Colombiana de Ciencias Exactas, Físicas y Naturales*, 7.

Flórez, P., Reyes, J., and Santodomingo, N. (2010). *Corales Escleractinios de Colombia.* Instituto de Investigaciones Marinas y Costeras-INVEMAR.

Geister, J. (1975). Riffbau und geologische Entwicklungsgeschichte der Insel San Andres (westliches Karibisches meer. Kolurnbien). *Stuttg. Beitr Naturk* 15, 1–203.

Gonzalez-Zapata, F. L., Bongaerts, P., Ramírez-Portilla, C., Adu-Oppong, B., Walljasper, G., Reyes, A., et al. (2018a). Holobiont diversity in a reef-building coral over its entire depth range in the Mesophotic zone. *Front. Mar. Sci.* 5:29. doi: 10.3389/fmars.2018.00029

Gonzalez-Zapata, F. L., Gómez-Osorio, S., and Sánchez, J. A. (2018b). Conspicuous endolithic algal associations in a mesophotic reef-building coral. *Coral Reefs* 37, 705–709. doi: 10.1007/s00338-018-1695-9

Kramer, N., Eyal, G., Tamir, R., and Loya, Y. (2019). Upper mesophotic depths in the coral reefs of Eilat, Red Sea, offer suitable refuge grounds for coral settlement. *Sci. Rep.* 9:2263. doi: 10.1038/s41598-019-38795-1

Luck, D. G., Forsman, Z. H., Toonen, R. J., Leicht, S. J., and Kahng, S. E. (2013). Polyphyly and hidden species among Hawai'i's dominant mesophotic coral genera, *Leptoseris* and *Pavona* (*Scleractinia*: *Agariciidae*). *PeerJ* 1:e132. doi: 10.7717/peerj.132

Opresko, D. M., and Sánchez, J. A. (2005). Caribbean shallow-water black corals (Cnidaria: Anthozoa: Anthipatharia). *Caribb. J. Sci.* 41, 492–507.

Petrescu, I., Chatterjee, T., and Schizas, N. V. (2014). New species of *Cumella* (Crustacea: Cumacea: *Nannastacidae)* from mesophotic habitats of Mona Island, Puerto Rico, Caribbean Sea. *Cah. Biol. Mar.* 55, 183–189. doi: 10.11646/zootaxa.3476.1.2

Sánchez, J. A. (2009). Systematics of the candelabrum gorgonian corals (Eunicea Lamouroux; *Plexauridae*; *Octocorallia*; *Cnidaria*). *Zool. J. Linn. Soc.* 157, 237–263. doi: 10.1111/j.1096-3642.2008.00515.x

Sánchez, J. A. (2017). "Diversity and evolution of octocoral animal forests at both sides of tropical America," i*n Marine Animal Forests,* eds S. Rossi, L. Bramanti, A. Gori, and C. Orejas Saco del Valle (Cham: Springer), 111–143.

Sánchez, J. A., Dueñas, L. F., Rowley, S. J., González, F. L., Vergara, D. C., Montaño-Salazar, S. M., et al. (2019a). "Gorgonian corals (39)," in *Mesophotic Coral Ecosystems*, *Coral Reefs of the World*, eds Y. Loya, K. A. Puglise, and T. C. L. Bridge (Cham: Springer Nature Switzerland AG), 727–745.

Sánchez, J. A., Gómez-Corrales, M., Gutierrez-Cala, L., Vergara, D. C., Roa, P., González-Zapata, F. L., et al. (2019b). Steady decline of corals and other benthic organisms in the seaflower biosphere reserve (Southwestern Caribbean). *Front. Mar. Sci.* 6:73. doi: 10.3389/fmars.2019.00073

Sánchez, J. A., and Wirshing, H. H. (2005). A field key to the identification of tropical western Atlantic zooxanthellate octocorals (*Octocorallia*: *Cnidaria*). *Caribb. J. Sci.* 41, 508–522.

Santodomingo, N., Reyes, J., Flórez, P., Chacón-Gómez, I. C., van Ofwegen, L. P., and Hoeksema, B. W. (2013). Diversity and distribution of azooxanthellate corals in the Colombian Caribbean. *Mar. Biodivers.* 43, 7–22. doi: 10.1007/s12526-012-0131-6

Ziegler, M., Roder, C., Büchel, C., and Voolstra, C. R. (2015). Mesophotic coral depth acclimatization is a function of host-specific symbiont physiology. *Front. Mar. Sci.* 2:4. doi: 10.3389/fmars.2015.00004

Conflict of Interest Statement: The authors declare that the research was conducted in the absence of any commercial or financial relationships that could be construed as a potential conflict of interest.

frontiers in Marine Science

DATA REPORT
published: 22 January 2020
doi: 10.3389/fmars.2019.00817

Sea Turtles at Serrana Island and Serranilla Island, Seaflower Biosphere Reserve, Colombian Caribbean

Cristian Ramirez-Gallego [1] and Karla G. Barrientos-Muñoz [1,2]*

[1] Fundación Tortugas del Mar, Envigado, Colombia, [2] Wider Caribbean Sea Turtle Conservation Network Colombia, Envigado, Colombia

Keywords: sea turtles, loggerhead turtle (*Caretta caretta*), green turtle (*Chelonia mydas*), hawksbill turtle (*Eretmochelys imbricata*), distribution and abundance, nests, conservation

OPEN ACCESS

Edited by:
Sonia Bejarano, Leibniz Centre for Tropical Marine Research (LG), Germany

Reviewed by:
Dalia C. Barragán-Barrera, University of Los Andes, Colombia
Roldan A. Valverde, Southeastern Louisiana University, United States

****Correspondence:***
Cristian Ramirez-Gallego
ramirezgallego.cristian@gmail.com

Specialty section:
This article was submitted to Marine Conservation and Sustainability, a section of the journal Frontiers in Marine Science

Received: *26 May 2019*
Accepted: *17 December 2019*
Published: *22 January 2020*

Citation:
Ramirez-Gallego C and Barrientos-Muñoz KG (2020) Sea Turtles at Serrana Island and Serranilla Island, Seaflower Biosphere Reserve, Colombian Caribbean. Front. Mar. Sci. 6:817. doi: 10.3389/fmars.2019.00817

BACKGROUND

In Colombia, there are five of the seven living species of sea turtles, all of them under some risk of extinction (Morales-Betancourt et al., 2015). Of these, four species are in the Colombian Caribbean and three in the SeaFlower Biosphere Reserve (SFBR). Particularly, the green turtle (*Chelonia mydas*), hawksbill turtle (*Eretmochelys imbricata*), and loggerhead turtle (*Caretta caretta*) have been reported at Serrana Island (McCormick, 1997, 1998). It is likely that these three species of turtles allowed to the Spanish Captain Pedro Serrano to survive on Serrana Island from his shipwreck in 1526 to 1534, when he was rescued from this island. Some turtles were as big and larger than the largest "adargas" (oval or heart shaped leather shield), and others such as "rodelas" (round and small shield), and "broqueles" (small defensive shield), so that there were all sizes. Thanks to sea turtles, Pedro Serrano had a house and food. The enormous turtle shells served as a den and rainwater collection, eggs and meat as a source of protein, and blood to prevent dehydration (Garcilaso de la Vega, 1609). More recently, during coral reef surveys Bruckner (2012) documented the hawksbill and loggerhead turtles around Serranilla Island, and a couple green turtles mating at Bajo Nuevo. The SFBR was declared in 2000 by UNESCO, has an approximate area of 180,000 km^2 and covers the extension of the department of Colombia, Archipelago of San Andres, Providencia, and Santa Catalina (CORALINA-INVEMAR., 2012). However, since 1998 no studies have been conducted on sea turtles in this area ignoring the current status of these species. Due to this lack of knowledge, initiatives that assess the sea turtle populations in the SFBR, become highly relevant to contribute to the current conservation efforts in the Caribbean. This work provides novel information on the distribution and abundance of sea turtles, as well as identification of sea turtle species in foraging areas around of Serrana and Serranilla islands—the northernmost area of the Colombian Caribbean—during Seaflower Scientific Expeditions 2016 and 2017.

DATA DESCRIPTION

Study Site and Methods

We conducted an analysis of the nesting ecology of the sea turtles in Cayo Serrana Island (14.38333 N, −80.2 W) and Cayo Serranilla Island (15.83333 N, −79.83333 W), within the Seaflower Scientific Expeditions 2016 and 2017, respectively, in order to assess the distribution and abundance of sea turtle species (**Figure 1**). Furthermore, identification and hand-capture of sea turtle species in foraging areas around of both islands were carried out.

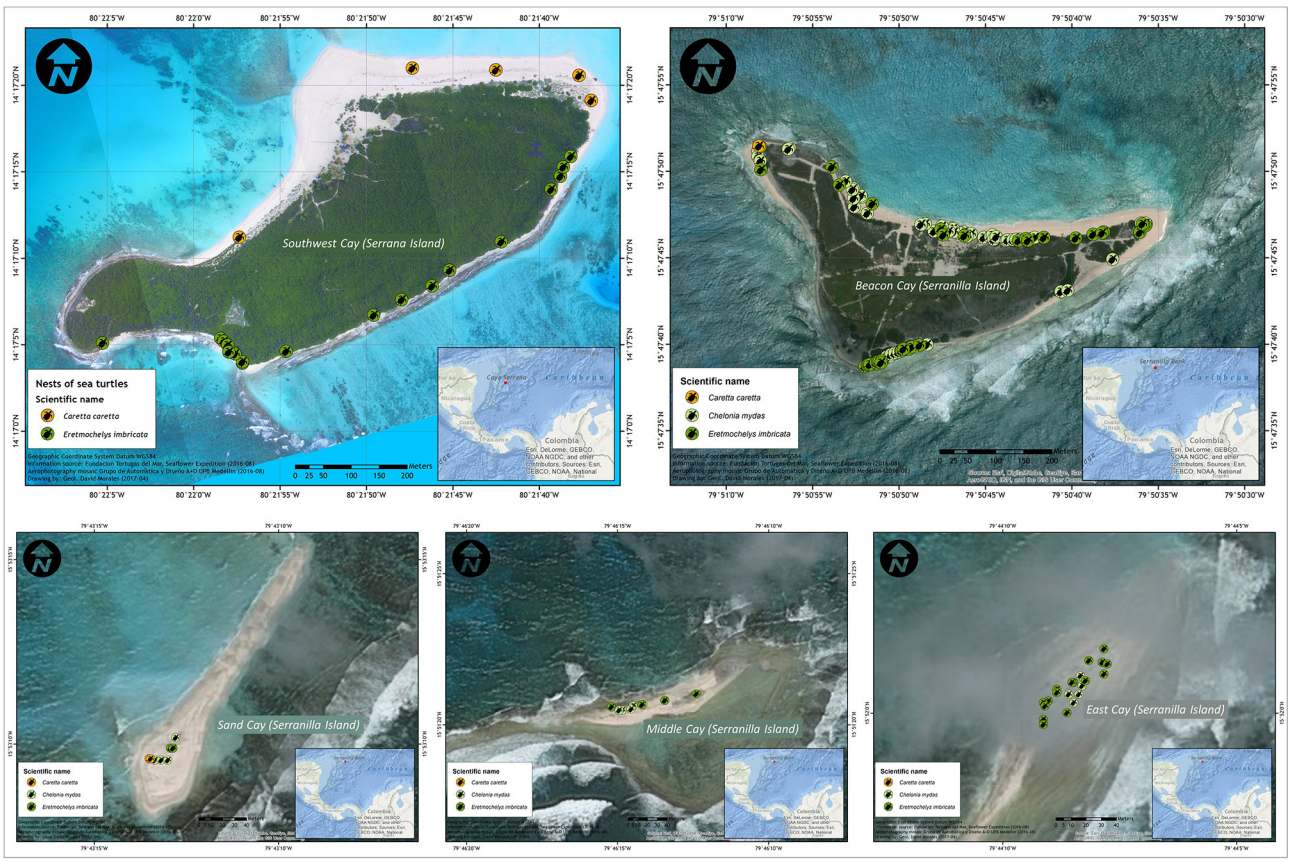

FIGURE 1 | Spatial distribution of sea turtle nests per species in Southwest Cay (Serrana Island, 2016) and Beacon Cay, Sand Cay, Middle Cay, and East Cay (Serranilla Island, 2017) in the Colombian Caribbean. Sea turtle species included *Caretta caretta, Chelonia mydas, and Eretmochelys imbricata*.

Nesting Activity

Systematic diurnal and nocturnal sea turtle monitoring in the beaches of Southwest Cay (14.28913 N, −80.36180 W) with 1,661 m length of coastline (Diaz and Andrade, 2011) located in Serrana Island (8 days: 9–16 August, 2016) and, Beacon Cay (15.79636 N, −79.84686 W) with 1822.79 m length of coastline (González and Pardo, 2017) located in Serranilla Island (24 days: 6–29 September, 2017) (**Figure 1**), were conducted in both areas in order to intercept nesting females, and identify clutches and hatchlings. During both periods, we patrolled the beaches at night (20:00–04:00), and all turtles encountered were tagged and measured, and all nesting events were recorded. Early in the morning (6:00–7:00) and in the afternoon (17:00–18:00), we counted tracks to account for turtles that were missed the previous night, verified successful nesting events (**Figures 2a–c**) and found hatched nests (**Figure 2d**). The records of nesting activity in Sand Cay (15.88616 N, −79.72022 W) with 205 m length of coastline, East Cay (15.86689 N, −79.73565 W) with 516 m length of coastline, and Middle Cay (15.85573 N, −79.77069 W) with 331 m length of coastline (González and Pardo, 2017), all three located in Serranilla Island (**Figure 1**), were carried out in a single beach survey, on September 13, 2017 (12:00–17:00) through the registration and photographic documentation of tracks, nests, and hatchlings. All hatchlings found alive within nests or trapped between roots or rocks were released in the early morning or evening in the company of members of the Expedition and of National Navy Armada República Colombia.

Description of the Dataset

This dataset compiles the lists of sea turtle species in its different life stages, nests, nesting females, and individuals—juveniles or adults—sighted or captured in-water, recorded during the Seaflower Scientific Expeditions 2016 and 2017 (Barrientos-Muñoz and Ramirez-Gallego, 2016; Ramirez-Gallego and Barrientos-Muñoz, 2017). The following 10 fields are included per species within this dataset:

Scientific Name ID: These fields include a unique and stable-through-time alphanumeric identifier (taxonomic identifier) AphiaID provided by World Register of Marine Species (WoRMS).

Basis of record: As the data set includes records based on direct observation in the field or indirect observations (photos), this field contains this specific information for each species.

Institution Code: This field includes the name (or acronym) in use by the institution having custody of the object(s) or information referred to in the record.

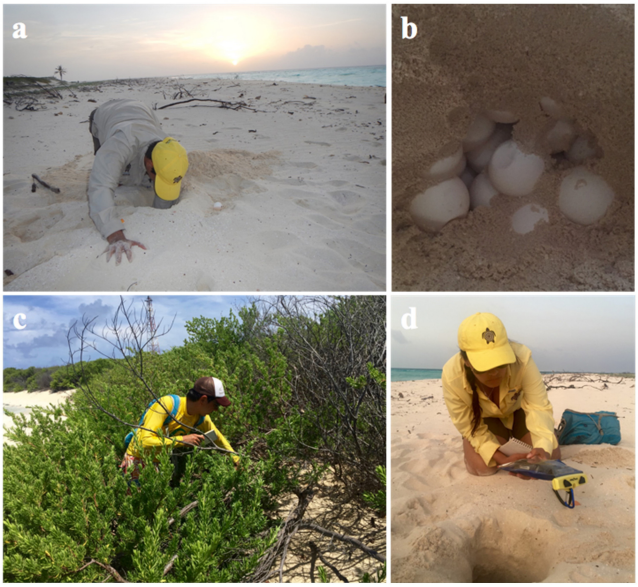

FIGURE 2 | Record of clutches and cleaning of hatched nests. **(a)** identification of loggerhead turtle nest in the middle and exposed area of the beach. **(b)** Confirmation of successful nests. **(c)** Identification of hawksbill turtle nest in vegetation zone. **(d)** Georeferencing and cleaning of hatched nests on Serrana Island (Photos: Karla Barrientos-Muñoz and Cristian Ramirez-Gallego, Fundación Tortugas del Mar).

Event Date: This field includes the date of biological events recorded.

Locality: Specific localities where the species have been recorded in the Serrana and Serranilla islands are presented in this field. Five localities were defined considering the Southwest Cay, Beacon Cay, Sand Cay, Middle Cay, and East Cay.

References: This field includes references that have compiled sea turtle species records during the Expeditions to SFBR in 2016 and 2017.

Life Stage: The age or life stage of the biological entity or entities at the time of the biological registration.

Reproductive Condition: Reproductive condition of the biological entity represented in the biological record.

Habitat: A category (beach of nesting or foraging site) of the habitat in which the event was registered.

Coordinates: Geographical latitude and geographic length (in decimal degrees, using the spatial reference system provided in Geodesic Datum) of the geographic center of a location.

Distribution and Abundance of Sea Turtle Species

In Southwest Cay, Serrana Island, three species were confirmed in the area: the loggerhead turtle (*Caretta caretta*), hawksbill turtle (*Eretmochelys imbricata*), and green turtle (*Chelonia mydas*). The loggerhead and hawksbill used beaches of Southwest Cay as nesting area with five and 20 nests, respectively (**Figure 1**; **Table 1**). Additionally, a hawksbill juvenile and a hawksbill male, as well as a green turtle juvenile were present in foraging areas around of Serrana Island. Meanwhile, at Serranilla Island, which included Beacon Cay, Sand Cay, Middle Cay, and East Cay, a total of 141 nests were confirmed for the green turtle, the hawksbill turtle, and loggerhead turtle (**Figure 1**; **Table 1**). Of the four keys evaluated, Cayo Beacon is the main site for sea turtle nesting in Serranilla, with 71.6% (101 nests) among the three species identified. For the green turtle (*C. mydas*), a total of 78 nests were documented, of which 63 nests (80.8%) were spawned on the beaches of Beacon Cay, followed by six nests (7.7%) spawned in Middle Cay. For the hawksbill turtle (*E. imbricata*), 58 nests were recorded, of which 35 nests (60.3%) were spawned in Beacon Cay and 16 nests (27.6%) in East Cay. For the loggerhead turtle (*C. caretta*), five nests were recorded, three nests (60%) were spawned in Beacon Cay and two nests (40%) in Sand Cay (see **Figure 1**). Furthermore, we confirmed that the marine habitats of Serranilla Island are used as feeding grounds by the presence of a hawksbill turtle juvenile captured meanwhile its was feeding sponges.

In the 1997 nesting season, McCormick reported nine hawksbill nests, four loggerhead turtles, and two green turtles nests in Serrana Island (McCormick, 1997). Nineteen years later in the Seaflower Expedition 2016, we confirmed the presence of nesting hawksbill and loggerhead sea turtle. Our monitoring effort was only 8 days (August 8–16), which may explain not having found any green turtle nest. However, green turtles have been observed in foraging areas around the island (Barrientos-Muñoz and Ramirez-Gallego, 2016). Also, Bruckner (2012) reported for Serrana Island and Bajo Nuevo, these three sea turtle species in marine habitats during the surveys of coral reefs.

The presence of five loggerhead turtles nests in Serrana and five nests in Serranilla with only a few days of effort and both at the end of the nesting season (∼4 months, from May to August), is a sign that it is essential to implement monitoring, research, and long-term conservation actions with this species in the entire Seaflower Biosphere Reserve. These monitoring may be the greatest opportunity to recover loggerhead turtle populations in Colombia, where in the continental area are on board a local extinction (Páez et al., 2015a). The nesting populations of this species in the continental area of Colombia (departments of Magdalena and La Guajira) is restricted to no more than a dozen nests per year (Moreno-Munar et al., 2014; Merizalde, 2017). For the critically endangered hawksbill turtle (Barrientos-Muñoz et al., 2015), Beacon Cay in Serranilla Island together with Southwest Cay in Serrana Island, represent the most conserved places for nesting in Colombia. This is because the hawksbill turtle prefer the vegetation zone for nesting, which is covered mainly by the shade of the coastal and native Caribbean plant *Suriana maritima* that was predominant in both keys (**Figure 2c**). The high presence of *S. maritima* in Beacon Cay, its good development and state of conservation around the whole cay, protects the nests from coastal erosion. Therefore Beacon Cay is the main nesting site in the Colombian Caribbean for the endangered green turtle (Páez et al., 2015b). Although this species prefers to nest in the middle zone of the beach profile, a high percentage of the nests of this species were laid

TABLE 1 | Inventory of three sea turtle species (*Caretta caretta*, *Chelonia mydas*, and *Eretmochelys imbricata*) in different life stages (eggs and nesting females at the sandy beaches, juveniles, and adults at the sea) in Serrana Island and Serranilla Island during the Seaflower Expeditions 2016 and 2017 in the Colombian Caribbean.

Life stage	Scientific name	Location				
		Serrana Island	Serranilla Island			
		Southwest Cay	Beacon Cay	Sand Cay	Middle Cay	East Cay
Eggs (Nests)	*Caretta caretta*	5	3	2	0	0
	Chelonia mydas	0	63	4	6	5
	Eretmochelys imbricata	20	35	3	4	16
	Total nests	25	101	9	10	21
	Reference	1	2	2	2	2
Nesting females	*Caretta caretta*	1	0			
	Chelonia mydas	0	2			
	Eretmochelys imbricata	0	2			
	Total of nesting females	1	4			
	Reference	1	2			
Juveniles	*Caretta caretta*	0	0			
	Chelonia mydas	1	0			
	Eretmochelys imbricata	1	1			
	Total juveniles	2	1			
	Reference	1	2			
Adults	*Caretta caretta*	0	0			
	Chelonia mydas	0	0			
	Eretmochelys imbricata	1	0			
	Total adults	1	0			
	Reference	1	2			

Reference 1 corresponds to Barrientos-Muñoz and Ramirez-Gallego (2016), and the reference 2 corresponds to Ramirez-Gallego and Barrientos-Muñoz (2017).

in the vegetation zone, under the shadow of *S. maritima* and *Conocarpus erectus*.

SFBR Is Synonymous of Hope for the Recovery and Conservation of Sea Turtles

Our records indicated that Serranilla Island is currently the main nesting site for the green turtle. Serrana and Serranilla are possibly the most important nesting sites for the hawksbill turtle in the Colombian Caribbean. Southwest Cay (Serrana Island), Beacon Cay, and Sand Cay (Serranilla Island) are currently the main nesting sites for the loggerhead turtle in the Colombian Caribbean. This represents a hope for this species with greater probability of local extinction in Colombia. The significant presence of loggerheads observed in these cays indicates the importance that SFBR represent for the survival of this species in the Caribbean. However, it is necessary to carry out a complete monitoring in all the cays of the SFBR to determine nesting trends by these three species. Our results are a valuable contribution to knowledge regarding the presence of reproductive and foraging sites for three sea turtle species, and demonstrate the relevance of implementing a long-term monitoring and research studies of these nesting colonies in the SFBR. These studies should strengthen the management of these species, which will contribute to the recovery of sea turtles population in the region.

DATA AVAILABILITY STATEMENT

The dataset Sea turtles at the Serrana Island and Serranilla Island, Seaflower Biosphere Reserve, Colombian Caribbean, was assembled using the Darwin Core standard (DwC) and is available through the Integrated Publishing Tool of the OBIS and the Global Biodiversity Information Facility (GBIF) Colombian nodes (SIBM -SIB Colombia) (IPT link: https://ipt.biodiversidad.co/sib/resource?r=ftm_tortugas_seaflower_2016, https://ipt.biodiversidad.co/sib/resource?r=ftm_tortugas_seaflower_2017; GBIF Portal: https://www.gbif.org/dataset/44c28cce-f455-4002-b6d3-96ccdd30e8b3, https://www.gbif.org/dataset/29e92c92-eee8-49f6-a43d-907cc37027d1; DOI: https://doi.org/10.15472/p9w6sj, https://doi.org/10.15472/tjc0hg).

ETHICS STATEMENT

Ethical review and approval was not required for the animal study because this article was based solely on the registration of sea turtles in nesting and foraging areas. There was no collection of individuals.

AUTHOR CONTRIBUTIONS

CR-G and KB-M collected and identified sea turtle species during expeditions to Serrana and Serranilla Islands (2016 and

2017), collected and processed the information for the biological records and the checklist dataset, compiled the complete checklist dataset, performed the descriptive analyses, wrote the manuscript, and reviewed and approved the manuscript.

FUNDING

This work was possible thanks to funding from Fundación Tortugas del Mar, Comisión Colombiana del Océano through Colombia Bio-Colciencias project (agreement No. 341 of 2017), the National Navy Armada República Colombia, Dirección General Marítima—DIMAR, Governorate of the Archipiélago de San Andrés, Providencia y Santa Catalina, Universidad de los Andes, CORALINA, National Oceanic and Atmospheric Administration—NOAA, The Ocean Foundation, and the Archie Carr Center for Sea Turtle Research.

ACKNOWLEDGMENTS

We thank the institutions and people who organized and participated in SeaFlower Expeditions. Thanks to ARC Providencia crew, ARC 20 de Julio crew, and ARC Roncador crew. Special thanks to T. Forbes, J. Paramo, and D. Cardeñosa, who support the inventories with some photographic records or hand capture of sea turtles in -water. Also thank to J. Leal, N. Bolaños, and R. Vazquez, who were crucial in the process of data collection, and D. Morales, who helped with the nesting sea turtle maps.

REFERENCES

Barrientos-Muñoz, K. G., Páez, V. P., and Ramirez-Gallego, C. (2015). "Tortugacarey. *Eretmochelys imbricata* (Linnaeus, 1766)," in *Libro rojo de reptiles de Colombia (2015)*, eds M. A. Morales- Betancourt, C. A. Lasso, V. P. Páez, and B. Bock (Bogotá: Instituto de Investigación de Recursos Biológicos Alexander von Humboldt (IAvH), Universidad de Antioquia), 127–131.

Barrientos-Muñoz, K. G., and Ramirez-Gallego, C. (2016). *Tortugas marinas de la Isla Cayo Serrana durante la Expedición Seaflower 2016 – Proyecto Colombia BIO*. Version 2.2. Fundación Tortugas del Mar. Ocurrence dataset. doi: 10.15472/p9w6sj

Bruckner, A. (2012). *Global Reef Expedition: San Andres Archipelago, Colombia*. Field Report. April 9-24, 2012. Khaled bin Sultan Living Oceans Foundation, Landover, MD, Unite States, 52.

CORALINA-INVEMAR. (2012). "Atlas de la reserva de Biósfera Seaflower. Archipiélago de San Andrés, providencia y Santa Catalina," in *Serie de Publicaciones Especiales* de INVEMAR No. 28, eds D. I. Gómez-López, C. Segura-Quintero, P. C. Sierra-Correa, and J. Garay-Tinoco (Santa Marta: Instituto de Investigaciones Marinas y Costeras "José Benito Vives De Andréis"-INVEMAR y Corporación para el Desarrollo Sostenible del Archipiélago de San Andrés, Providencia y Santa Catalina-CORALINA). Available online at: http://www.invemar.org.co/redcostera1/invemar/docs/10447AtlasSAISeaflower.pdf

Diaz, A., and Andrade, C. (2011). Variación de la línea de costa en Cayo Serrana y estrategias para su conservación ante las amenazas de origen natural. *Boletín Científico CIOH* 72–86.

Garcilaso de la Vega (1609). *Comentarios Reales de los Incas, Tomo I. Edición, índice analítico y glosario de Carlos Araníbar*. Lima: Fondo de Cultura Económica – Colección Historia, 1991, Libro Primero, Capítulos VII-VIII, 23–28.

González, S. J., and Pardo, Y. (2017). *Expedición Seaflower - Isla Cayo Serranilla, 2017*. Dirección General Marítima-DIMAR. Available online at: http://arcg.is/19HXSn

McCormick, C. C. (1997). "Porque ellas también tienen derecho a seguir dejando huella," in *Diagnóstico actual de las tortugas marinas del archipiélago de San Andrés, Providencia y Santa Catalina, Fase II* (San Andrés: CORALINA), 67.

McCormick, C. C. (1998). *Diagnóstico actual de las tortugas marinas del archipiélago de San Andrés, Providencia y Santa Catalina*. San Andrés: CORALINA, 41.

Merizalde, L. A. (2017). *Informe Final Año 2017, Alianza Interinstitucional para el manejo, la conservación y el desarrollo sostenible de la Guajira (Fase VI)*. Bogotá: Programa conservación para el desarrollo Alianza Fondo Acción - Conservación Internacional Colombia, 38.

Morales-Betancourt, M. A., Lasso, C. A., Páez, V. P., and Bock, B. (eds.). (2015). *Libro rojo de reptiles de Colombia (2015)*. Bogotá: Instituto de Investigación de Recursos Biológicos Alexander von Humboldt (IAvH), Universidad de Antioquia.

Moreno-Munar, A. A., Ospina-Sanchez, S. C., Jauregui-Romero, G. A., and Alvarez, R. (2014). Monitoreamiento de poblaciones de tortugas marinas en los sectores de Arrecifes y Cañaveral, Parque Nacional Natural Tayrona, Colombia. *Arq. Cien. Mar. Fortaleza* 47, 19–30. Available online at: http://www.repositorio.ufc.br/bitstream/riufc/28712/1/2014_art_aammunar.pdf

Páez, V. P., Ramirez-Gallego, C., and Barrientos-Muñoz, K. G. (2015a). "Tortuga caguama. *Careta caretta* (Linnaeus, 1758)," in *Libro rojo de reptiles de Colombia (2015)*, eds M. A. Morales-Betancourt, C. A. Lasso, V. P. Páez, and B. Bock (Bogotá: Instituto de Investigación de Recursos Biológicos Alexander von Humboldt (IAvH), Universidad de Antioquia), 118–121.

Páez, V. P., Ramirez-Gallego, C., and Barrientos-Muñoz, K. G. (2015b). "Tortuga verde. *Chelonia mydas* (Linnaeus, 1758)," in *Libro rojo de reptiles de Colombia (2015),* eds M. A. Morales-Betancourt, C. A. Lasso, V. P. Páez, and B. Bock (Bogotá: Instituto de Investigación de Recursos Biológicos Alexander von Humboldt (IAvH), Universidad de Antioquia), 153–156.

Ramirez-Gallego, C., and Barrientos-Muñoz, K. G. (2017). *Tortugas marinas de la Isla Cayos de Serranilla durante la Expedición Seaflower 2017 – Proyecto Colombia BIO*. Version 3.1. Fundación Tortugas del Mar. Ocurrence dataset. doi: 10.15472/tjc0hg

Conflict of Interest: The authors declare that the research was conducted in the absence of any commercial or financial relationships that could be construed as a potential conflict of interest.

frontiers in Marine Science

ORIGINAL RESEARCH
published: 16 June 2020
doi: 10.3389/fmars.2020.00385

Circulation in the Seaflower Reserve and Its Potential Impact on Biological Connectivity

Luisa Lopera[1]*, *Yuley Cardona*[1] and *Paula A. Zapata-Ramírez*[2]

[1] *Departamento de Geociencias y Medio Ambiente, Facultad de Minas, Universidad Nacional de Colombia, Sede Medellín, Medellín, Colombia,* [2] *Escuela de Ingeniería, Grupo de Automática y Diseño A + D, Universidad Pontificia Bolivariana, Medellín, Colombia*

The influence of ocean currents on marine population connectivity is critical to territory planning, and such phenomena should be considered in the design and implementation of marine protected areas (MPAs), marine spatial planning strategies, and restoration plans, among other developments. Knowledge of the influence of currents is also vital in understanding the relationship between oceanographic drivers and ecosystem configurations. However, despite their importance, ocean currents and their role in coral connectivity remain poorly constrained in the Seaflower Marine Reserve, an area that hosts the most productive open-ocean coral reef system in the Caribbean and that was declared a biosphere reserve in 2000. We herein characterize the larva transport patterns associated with surface currents that control connectivity in the reserve. To achieve this aim, we simulated the advection of buoyant coral larvae of *Acropora palmata* during nine spawning events. Larval dispersal patterns were obtained through offline coupling of a high-spatiotemporal resolution hydrodynamic field and a biophysical Lagrangian model for particle dispersion. Ocean current fields were generated using a Regional Ocean Modeling System (ROMS) that was appropriately configured for the region. Larval dispersion was simulated using an Individual-Based Model (Ichthyop). Our results show that there are heterogeneous connectivity patterns during the spawning events at seasonal and inter-annual scales. This seems to be associated with high spatiotemporal dynamic variability in the region, such as the Caribbean Current bifurcation close to the Nicaraguan Rise, the intrusion-formation of mesoscale and sub-mesoscale eddies, and the semi-permanent presence of the Panama-Colombia Gyre. We also found that Serranilla, Providencia, Quitasueño, and Serrana act as the most important sinks. In contrast, the northernmost reefs, Serranilla, B. Alicia, and B. Nuevo, seem to be the most important sources of larvae, highlighting that these areas need to be incorporated into the current MPA zonification and that this could lead to the improvement of MPA effectiveness. Our findings also suggest the need to implement MPA networks between Jamaica and Colombia to allow biological populations to become resilient to environmental changes and less prone to local extinctions.

Keywords: seaflower, ocean modeling, coral dispersal, surface currents, recruitment, eddies

OPEN ACCESS

Edited by:
Sonia Bejarano, Leibniz Centre for Tropical Marine Research (LG), Germany

Reviewed by:
Pablo Saenz-Agudelo, Austral University of Chile, Chile
Timothée Brochier, IRD UMR209 Unité de Modélisation Mathématique et Informatique de Systèmes Complexes (UMMISCO), France

***Correspondence:**
Luisa Lopera
lfloperag@unal.edu.co

Specialty section:
This article was submitted to Marine Conservation and Sustainability, a section of the journal Frontiers in Marine Science

Received: *07 June 2019*
Accepted: *05 May 2020*
Published: *16 June 2020*

Citation:
Lopera L, Cardona Y and Zapata-Ramírez PA (2020) Circulation in the Seaflower Reserve and Its Potential Impact on Biological Connectivity. Front. Mar. Sci. 7:385. doi: 10.3389/fmars.2020.00385

1. INTRODUCTION

The Seaflower Biosphere Reserve (SFBR) is located at the southwestern side of the Caribbean Sea and has an area of 180,000 km^2, one-third of which (65,000 km^2) is part of the Marine Protected Area (MPA) declared by the Colombian government in 2005. The zonation within the MPA comprises 0.2% of No-entry zone, 3.4% of No-take, 3.1% of Artisanal Fishing, 0.1% of Special Use, and 93.2% of General Use (Sánchez-Jabba, 2012). Due to its geographical location and jurisdictional framework, the SFBR is highly vulnerable to political decisions, resulting in Colombia, Jamaica, and Nicaragua all having jurisdiction over it. Each country has its own rules for environmental regulation, and these are not necessarily compatible. **Figure 1** shows the boundaries of the SBRF, the MPA, and the common regime area. The SFBR system comprises two oceanic islands (San Andrés y Providencia) and a series of atolls and banks (Quitasueño, Serrana, Roncador, Serranilla, Albuquerque, Bajo Nuevo, Bajo Alicia, and Bolívar). Those geoforms are characterized by their associated ecosystems, which include mangroves, seagrasses, and coral reefs. The SFBR hosts ∼77% from the total Colombian reef area and the largest and the most productive open-ocean coral reefs in the Caribbean (Díaz et al., 2000; CORALINA-INVEMAR, 2012). According to Prato and Rixcie (2015), the economic value of these coral reefs is between USD 270,900 and USD 353,000 million per year, i.e., they correspond to ∼70% of the total contribution attributed to the Colombian Caribbean marine territory. However, the importance of the coral reefs is not only economic; the SFBR also hosts high biodiversity and contributes to shoreline protection (Prato and Rixcie, 2015).

The SFBR coral reef complex includes extensive benthic habitats, such as barrier reefs, reef lagoons, reef, slopes, forereefs, deep coral plateaus, seamounts, deep coral reefs, bank reefs, patch reefs, and atolls, while the most recurrent bottoms in them are: (i) calcareous matrixes, (ii) sand and coral debris, and (iii) calcareous, metamorphic, and basaltic rocks; all of them present low to medium inclinations, and their depth usually does not exceed 20 m (Díaz et al., 1997; Geister and Díaz, 2007; CORALINA-INVEMAR, 2012). This coral reef formation is a product of the oceanic location and strong wave exposure due to swells generated by the trend winds; as a result, turbulence controls the distribution of organisms in the reefs. The substrates are constituted principally by: *Millepora complanate*, *zoanthids*, *Diploria strigosa*, *Diploria clivosa*, *Montastraea cavernosa*, *Colpophyllia natans*, *Siderastrea spp*, *Acropora palmata*, *Acropora cervicornis*, sponges, and octocorallia. In the Seaflower MPA, 48 sclerictian corals species have been documented (of ∼60–70 species known to exist in the Caribbean), 54 octocoral species with high endemism, 3 black coral species, 300 fish (one endemic fish), and 124 sponge species, among others (Díaz et al., 2000; Geister and Díaz, 2007). Among the most important species of corals throughout the Greater Caribbean is *Acropora palmata*, a major reef-builder in the Caribbean that contributes to reef growth, island formation, coastal protection, and sustaining the habitat of fisheries. Its three-dimensional thickets are present in intermediate waters of the forereef zone (1–20 m) (Díaz et al., 2000; Johnson et al., 2011; Rodríguez-Martínez et al., 2014; NMFS, 2015).

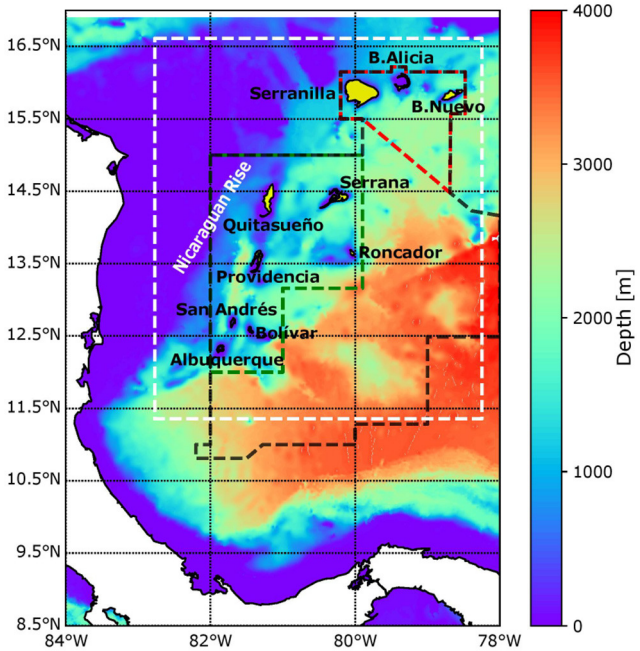

FIGURE 1 | Parent domain for numerical integrations. White dashed lines indicate the nested domain, black dashed lines enclose the Seaflower Reserve, and green and red lines show the MPA and common regime area between Colombia and Jamaica, respectively. Background bathymetry and the black polygons indicating release and recruitment zones in the Lagrangian Model are from the Millennium Coral Reef Mapping Project.

Despite being among the most representative icons of the Colombian marine protection areas, knowledge about the Seaflower area is limited to biological inventories, some of which were led by the Comisiõn Colombiana del Océano (CCO) through Seaflower expeditions (Bolaños et al., 2015; Vega et al., 2015; Acero P. et al., 2019) and geological characterization (Díaz et al., 2000; Idárraga-García and León, 2019). The mesoscale surface circulation across the Colombian Caribbean has been studied by several authors, e.g., Andrade (2000), Richardson (2005), Ruiz (2011), but small-scale dynamic features and circulation in the water column remain unknown or poorly constrained. The surface circulation over Seaflower is driven by two features. The first is an east–west zonal current (the Caribbean Current) that, due to bathymetric configurations, is forced to split into two sections when it reaches the Nicaraguan Rise. One section flows toward the Caimán Sea, and the second enters a cyclonic gyre in the southwestern Caribbean. The latitude over which the bifurcation occurs is not well-known. The second feature driving surface circulation is the Panama-Colombia Gyre (PCG), a semi-permanent cyclonic gyre located in the southwestern Caribbean (Andrade, 2000; CORALINA-INVEMAR, 2012).

The influence of ocean currents on the distribution and abundance of marine organisms has been investigated since

the 1980s. For example, Roughgarden et al. (1988) concluded that regional patterns of coastal circulation partially determine the ecological structure of marine organisms. An understanding of how reef systems are connected through ocean currents at different spatiotemporal scales has nonetheless greatly benefitted from the development of numerical models (Wood et al., 2014; Mayorga-Adame et al., 2017; Lequeux et al., 2018; Romero et al., 2018; Sanvicente-Añorve et al., 2018). Though the understanding of these biogeographic patterns is of key importance in territory planning (e.g., MPA design), particle dispersion patterns, connectivity, and their oceanographic drivers at the SFBR remain poorly understood. Schill et al. (2015) studied connectivity in the wider Caribbean and Gulf of Mexico in order to design and evaluate MPAs. Using a 10 × 10 km 2D daily current field and an explicit larval dispersal model, they aimed to identify the regional coral reef MPA network for conservation goals. Their results suggested the need to quantify connectivity information by marine eco-regions and at the level of Exclusive Economic Zones (EZZ). Despite their findings, the resolution of the results is not sufficiently high to be applied to local exercises since it does not reproduce smaller-scale processes, such as sub-mesoscale fronts, eddies, and filaments. Zhong et al. (2012), Zhong and Bracco (2013), Raitsos et al. (2017), and Medel et al. (2018) have highlighted the importance of small-scale processes, such as fronts, sub-mesoscale eddies, and filaments in larval and plankton dispersal.

Lonin et al. (2010) characterized the dispersion of queen conch *Strombus gigas* larvae in the SFBR during 2007 and 2009 using daily data from the Princeton Ocean Model (POM) at 18-km horizontal resolution. They found monthly connectivity patterns between the southernmost reefs to Providencia and Roncador, links amongst the Quitasueño–Serrana–Roncador system, and links between Serranilla, B. Alicia, and B. Nuevo. Links were particularly evident during the peak reproductive periods of *strombus gigas* (April and September). Larval connectivity has also been studied through genetic analysis of reefs. Foster et al. (2012) evaluated the connectivity of Caribbean coral populations in 26 sites outside the SFBR and found an east–west barrier of connectivity in the southern Caribbean resulting from low salinity and high sediment plume activity in the Colombian Basin, associated with the Magdalena River.

In this work, we characterized the mesoscale and sub-mesoscale dynamic conditions of the Seaflower Reserve in order to i) determine whether connectivity exists between reefs through the ocean currents and ii) provide information about the physical drivers that control larval distribution in the SFBR. To achieve this aim, we used a regional ocean model (ROMS) setup with horizontal resolutions of 5 and 1.7 km and an Individual-Based Model (Ichthyop). Using a fine spatiotemporal current field and parametrized larvae, we simulated nine spawning events for *A. palmata* in the SFBR during neutral (2003, 2008, 2014), El Niño (2002, 2009, 2015), and La Niña (2000, 2007, 2010) phases. In this regard, the impact of the ENSO in the Caribbean is not yet very clear. However, in the tropical Atlantic, the effect has been reported mainly to comprise changes in rainfall, sea surface temperature (SST), and sea level pressure (SLP). The ENSO phenomenon and the induced variability over the subtropical North Atlantic high sea level pressure affects the rainfall in the Caribbean region and the trade wind strength as a reversal in the sign of the correlation. Warm ENSO conditions lead to SST warming in the Caribbean, which is overlain by rainfall reductions, weaker trade winds, and consequent reduction in surface fluxes (Giannini et al., 2000, 2001a,b; Alexander et al., 2002). Our findings are the first concerning the regional patterns that lead to coral larva connectivity in the SFBR and are based on a 3D high-spatio-temporal resolution model. Thus, they provide information that is useful for the identification of critical areas requiring ecological protection through either the redesign or the incorporation of new MPA areas and/or protection co-management zones. Furthermore, our results could also be useful for identifying areas requiring restoration.

2. MATERIALS AND METHODS

To identify hydrodynamic connectivity in the SFBR, a biophysical modeling approach was employed, using a Lagrangian tool (Ichthyop) forced by a regional ocean numerical model (ROMS). We simulated *A. palmata* particle dispersal during spawning events in 2000, 2002, 2003, 2007, 2008, 2009, 2010, 2014, and 2015. This methodological approach, together with the selected events, allowed determination of the influence of circulation patterns and their modifications due to macro-climatic phenomena (ENSO) that lead to larval dispersion and connectivity. The configurations of models used to assess connectivity driven by oceanographic conditions are described below.

2.1. Ocean Model Configuration

The model we used in this study to reproduce the hydrodynamic conditions for different spawning events in the SFBR was the Regional Ocean Modeling System (ROMS-Agrif v3.1.1). ROMS is a 3D free surface and hydrostatic regional oceanic model that solves primitive momentum equations in sigma terrain-following coordinates (S-levels) and orthogonal cartesian coordinates over the vertical and horizontal axes, respectively (Penven et al., 2008). In this study, ROMS was configured in a two-way nesting procedure using a high-resolution child model in a coarser parent model in order to represent small-scale features of SFBR dynamics in more detail. The parent grid has a horizontal resolution of 5 km in a domain extending from 84 to 78°W and from 8 to 17°N. The child grid, with a horizontal resolution of 1.7 km, is bounded by the white dashed line in **Figure 1**. Along the vertical axis, 35 s-levels were distributed in both grids, enhancing the resolution close to the surface (upper 100 m). The parent model was integrated using a time-step of 120 s, providing boundary conditions for the child model with a time step of 40 s. Then, the child model updates the parent model, and the process is repeated. For grid construction, GEBCO 30 arc-second (1-km resolution) was used to derive bathymetry, and a Shapiro smoother of 0.45 was applied to avoid pressure gradient errors (Weatherall et al., 2015). In addition, an Hmin value of 2 m was used for the parent model. First of all, to ensure suitable representation of the mean circulation conditions in the domain and the numerical stability of the model, a climatological

simulation was integrated over 15 years. The run was forced at the surface using monthly climatological mean fields from the Era-Interim dataset, which covers the period 1979–2017 (Dee et al., 2011) and QuikSCAT/ASCAT wind forcing data, which covers the period 2000–2016 (Ricciardulli et al., 2011; Abderrahim and Fillon, 2012). The model was forced at the open boundaries (east and north) through monthly-average fields of temperature, salinity, sea surface height (SSH), and current components from GLORYS reanalysis (Ferry et al., 2010), which covers the period 2000-2015. All of the described databases have a spatial resolution of 0.25°. The initial condition was obtained from the climatological mean for the month of January. We simulated 9 years for the period comprising the timing of spawning (July to September) of *A. palmata* in the Caribbean Sea (section 2.2). For time-dependent simulations, daily surface forcing from QuikSCAT/ASCAT and Era-Interim were used, while 5-days average fields from GLORYS were imposed at the boundaries. The initial condition for each time-dependent simulation was obtained as the last June record during the climatological run; in this way, we ensure the proper start of each simulation. Three-hour averages of the velocity fields and state variables reproduced by the model were stored for use by the biophysical model in the subsequent modeling stages.

2.2. Lagrangian Particle Dispersion Model

Icthyop was used to model the buoyant and Lagrangian advection of coral larvae during the spawning events of 2000, 2002, 2003, 2007, 2008, 2009, 2010, 2014, and 2015. Icthyop is an individual-based model (IBM) developed to study the influence of physical factors and basic biological parameters on ichthyoplankton dynamics (Lett et al., 2008). It also allows the characterization of other marine species, such as coral larvae. Along the vertical axis, Icthyop simulates dispersion, buoyancy, and larval migration processes, while on the horizontal axis, it simulates advection and diffusion (Peliz et al., 2007; Lett et al., 2008; North et al., 2009).

The parameters we used to characterize *A. palmata* in our simulations are as follows.

2.2.1. Species

The Elkhorn coral *Acropora palmata* is historically considered a dominant reef-building coral in wave-exposed and high-surge reef zones, typically at depths of <10 m, and it is also considered a habitat provider for marine organisms in the Caribbean Sea (Rodríguez-Martínez et al., 2014). It is predominantly located close to the reef crest and the shallowest zone of the outer reef. In addition, rehabilitation initiatives have been conducted to restore populations of *A. palmata* in the Caribbean (Chamberland et al., 2015). According to Díaz et al. (2000), *A. palmata* has been identified in almost all marine coral areas of Colombia. The Quitasueño, Providencia, Serrana, Albuquerque, and San Andrés regions show the highest occurrences of *A. palmata* in the SFBR. Due to its widespread presence in the Colombian Caribbean, its ecological importance, and the fact that it has been widely studied, we chose the Elkhorn Coral as the species on which to based our biophysical model.

TABLE 1 | Full moon and spawning event dates.

Full moon date	Spawning event date	ENSO phase
08/15/2000	08/19/2000—09:00 p.m.	La Niña
08/22/2002	08/26/2002—09:00 p.m.	El Niño
08/12/2003	08/10/2008—09:00 p.m.	Neutral
08/28/2007	09/01/2007—09:00 p.m.	La Niña
08/16/2008	08/20/2008—09:00 p.m.	Neutral
08/06/2009	08/10/2009—09:00 p.m.	El Niño
08/24/2010	08/28/2010—09:00 p.m.	La Niña
08/10/2014	08/14/2014—09:00 p.m.	Neutral
08/29/2015	09/02/2015—09:00 p.m.	El Niño

2.2.2. Pelagic Larval Duration (PLD)

This parameter is defined as the period between spawning and the juvenile stage of coral larvae, i.e., it is the maximum time that the larvae spend in the water column as plankton. If larvae do not find a suitable zone within which to be recruited during their PLD, they will die. According to Baums et al. (2006) and Japaud et al. (2013), the timescale of the *A. palmata* PLD may oscillate between 20 and 30 days; hence, we used a PLD of 25 days.

2.2.3. Timing of Spawning

According to Jordan (2018), the spawning peak for *A. palmata* in the Caribbean lies between the third and the fifth day after the August full moon. Spawning was found to occur between 30 and 260 min after sunset. Consequently, in our models, we chose for spawning events to occur 4 days after the full moon of August and 150 min after sunset, which, for the Caribbean, occurs between 6:20 and 6:50 p.m. We chose an average value at 6:35 p.m.; thus, particle release was carried out at 9:00 p.m. Although the oceanic numerical model forcing did not include intra-day variability, performance of a linear interpolation between two closest data points as well as the storage record allowed us to obtain output data in a specific moment of the day that coincides with the spawning. **Table 1** shows the full moon and spawning event dates and the corresponding ENSO phase.

2.2.4. Pre-competency Period (PP)

This is the period before the coral larvae settle. According to Randall and Szmant (2009) and Japaud et al. (2013), the PP for *A. palmata* oscillates between 3 and 5 days, so we used a PP of 3 days in our study.

2.2.5. Release and Recruitment Zones

We used the Millennium Coral Reef Mapping and Global Distribution of Coral Reef databases to build a habitat layer of *A. palmata*, which is shown by the black and yellow polygons in **Figure 1**. More detailed release and recruitment zones can be found in the **Supplementary Material**. The databases are based on Landsat 7 images with a resolution of 30 m [Institute for Marine Remote Sensing, University of South Florida (IMaRS/USF), Institut de Recherche pour le Développement (IRD), UNEP-WCMC, The WorldFish Center, and WRI, 2011; UNEP-WCMC, WorldFish Centre, WRI, TNC, 2018].

TABLE 2 | Area of each zone and number of particles released.

Zone	Area (km^2)	Number of particles
Albuquerque	25.4	84
B. Alicia	91.7	406
Bolivar	24.9	108
B. Nuevo	194.6	849
Providencia	118.9	535
Quitasueño	332.2	1,523
Roncador	43.2	202
San Andrés	23.0	120
Serrana	140.0	720
Serranilla	1202.3	5,453

2.2.6. Release Depth

We released passive particles without ontogenetic, vertical migration, or swimming capabilities between 1.5 and 15 m, i.e., the depth range within which *A. palmata* has been registered by Díaz et al. (2000). Particles were modeled to have a constant size during all PLD, and no mortality rate was included online in the Lagrangian model. Ichthyop conducted the release depending on the total coral area; this means that the number of particles released at each polygon was proportional to its area and at a random position within it (horizontal and vertical). Both the area and the number of particles released in each zone are displayed in **Table 2**.

2.2.7. Number of Released Particles

A sensitivity analysis for the number of released particles was carried out in order to choose the sample size. We released between 10,000 and 100,000 particles to detect differences in connectivity patterns during 2015; however, the connections obtained were shown to be almost the same, so the relative importance of reef connections in both cases is nearly identical, and the strongest/weakest links are the same. Consequently, and due to the constraints of computational time, the release of 10,000 particles was deemed sufficient for our modeling.

2.3. Mortality Rate

Connectivity results excluding mortality are associated with potential connectivity since they allowed the identification of the entire larvae-current interaction during the PLD. Nonetheless, the first stages of larval life are characterized by high daily mortality rates that vary between 10 and 20% (Becker et al., 2007; Schill et al., 2015). For this reason, we included mortality rates to quantify effective connectivity during spawning events. Mortality is included to remove daily, and randomly, a sample of 10, 15, or 20% from the current population. Following this, an ensemble of five hundred runs was used to obtain new connectivity measures. Here we present the effective connectivity results when considering a daily mortality of 15%.

2.4. Connectivity Matrices

Connectivity matrices were used to quantify the release-recruitment strength between two reefs at the end of the PLD. This approach assesses the percentage of larvae that arrive at a reef j (x-axis) from another reef i (y-axis) and allows the distinction of reefs as either sinks or sources. The diagonal of the matrix indicates reefs where local retention occurs (Mayorga-Adame et al., 2017; Lequeux et al., 2018). The reefs are ordered over the vertical axis based on their latitudinal position, from south to north.

2.5. Congruence Among Distance Matrices Test

In order to evaluate the existence of connectivity patterns according to the ENSO phases, we used the Congruence Among Distance Matrices (CADM) tool. CADM is a statistical test used to assess the concordance level of matrices using the distance between them. CADM tests the complete incongruence hypothesis (null hypothesis) between distance matrices by calculating the Kendall's W statistic. The W value provides an estimation of the degree of congruence among matrices on a scale between 0 (no congruence) and 1 (complete congruence) (Legendre, 2005; Campbell et al., 2011).

Distance matrices were calculated using the Euclidean Distance (ED) method, which is one of the most used distance metrics between n-dimensional matrices to determine how dissimilar they are. It is defined as the straight-line distance between two points in an n-dimensional space. Given two n-dimensional matrices in a Euclidean n-space, the ED is calculated following the Pythagorean metric or Euclidean norm.

With:

$\mathbf{X} = (X_1, X_2 \ldots X_n)$

$\mathbf{Y} = (Y_1, Y_2 \ldots Y_n)$

$$ED = \sqrt[2]{(Y_1 - X_1)^2 + (Y_2 - X_2)^2 + (Y_n - X_n)^2} \quad (1)$$

In general:

$$ED = \sqrt[2]{\sum_{i=1}^{n} (Y_i - X_i)^2} \quad (2)$$

3. RESULTS

3.1. Surface Circulation Under Climatological Conditions

The dominant circulation features in the region can be identified from the integration of climatological conditions. **Figure 2** shows the seasonality of mesoscale surface currents in the southwestern Caribbean, calculated from the model (upper part of the figure) and AVISO satellite data (lower part of the figure). Model data (5 km) were interpolated to AVISO resolution in order to make comparisons between them. According to model results and in agreement with available satellite data, there is a semi-permanent cyclonic gyre located in the southwestern of the region, known as the Panama-Colombia Gyre (PCG). The PCG reaches its highest current magnitudes (0.7 m/s) during September, October, and November (SON) and is at its weakest (0.4 m/s) during December, January, and February (DJF). Generally, the PCG is

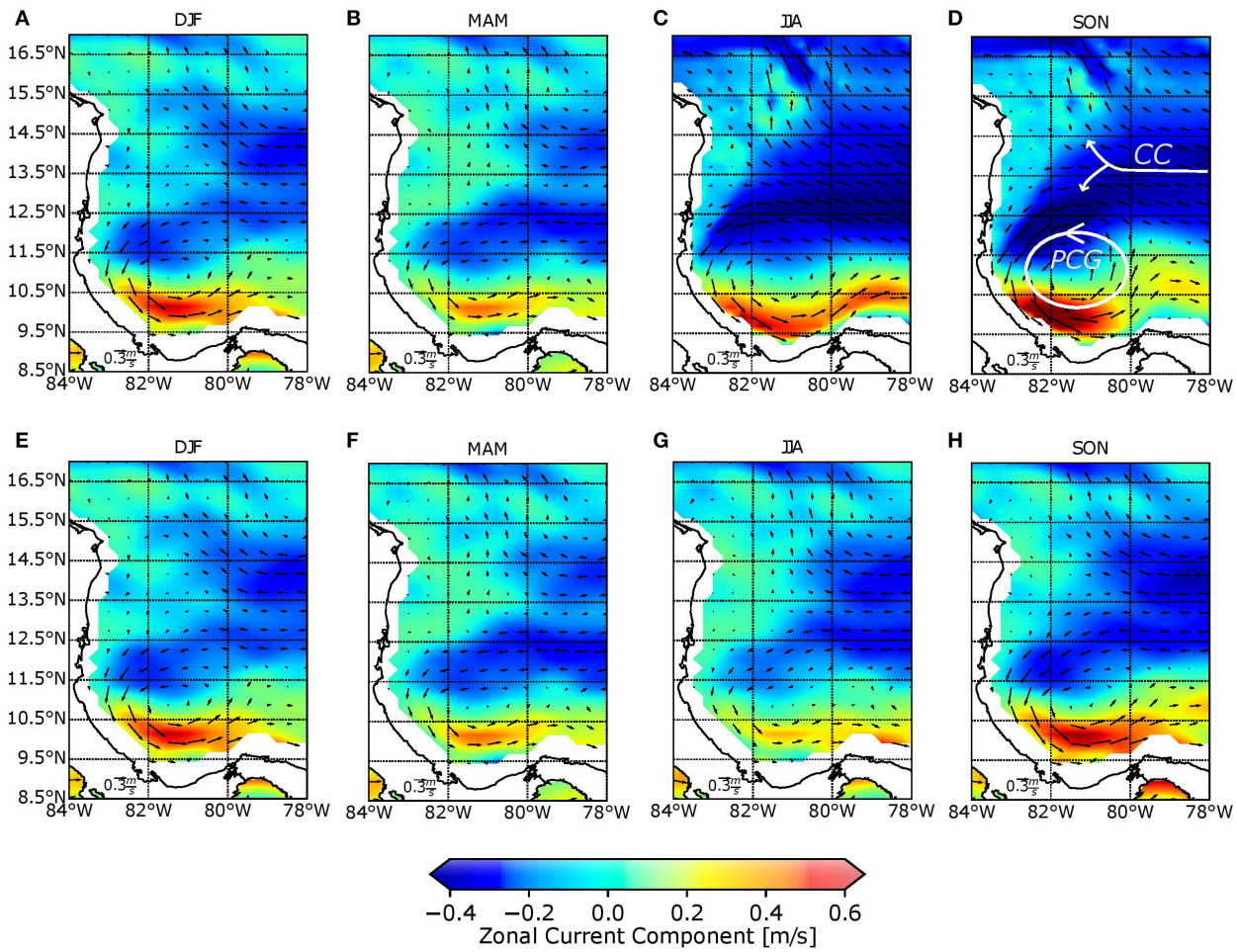

FIGURE 2 | Seasonal behavior of surface currents from model data (upper panels) for: **(A)** DJF, **(B)** MAM, **(C)** JJA, **(D)** SON and AVISO satellite data (lower panels) for: **(E)** DJF, **(F)** MAM, **(G)** JJA, and **(H)** SON. DJF, December, January, and February; MAM, March, April, and May; JJA, June, July, and August; and SON, September, October, and November.

located between 80 and 84°W and between 8 and 13°N, with its center located at 82°W during DJF and March, April, and May (MAM), before moving eastward during June, July, and August (JJA) and SON.

A strong zonal current traveling in an east-west direction is permanently represented in the model. This current, known as the Caribbean Current (CC), occurs between 11.5 and 15.5°N. It reaches its highest magnitudes during JJA (0.5 m/s) and is weakest during MAM (0.4 m/s). As shown in **Figure 2**, during JJA, the current along the SFBR is at its strongest, and this coincides with *A. palmata* spawning events. The presence of the Nicaraguan Rise causes the CC to split into two sections; the first flows toward the north and becomes the Loop Current, whereas the second flows toward the PCG. The bifurcation position associated with bathymetry has a climatological behavior, as shown in **Figure 3**. Red boxes enclose the latitudinal position of the CC bifurcation over 82°W. The arrows indicate the flow direction, and their lengths indicate current magnitude. During MAM and JJA, the position of the bifurcation is located around 13°N, whereas in SON and DJF, the bifurcation is displaced northward, almost at 14°N.

By comparison to AVISO satellite data, it can be seen that the most important features of the surface circulation (the CC, the CC bifurcation, and the PCG) were well-represented by the model. **Figure 4** displays the kinetic energy (KE) differences between the model and AVISO, where kinetic energy was calculated as $KE = \frac{1}{2}(u^2 + v^2)$. Red coloration corresponds to KE overestimation, whereas blue coloration reflects KE underestimation. In general terms, for all of the four seasons, the model overestimated the KE and consequently overestimated the magnitude of the currents. Differences between 0.1 and 0.2 m^2/s^2 prevail in almost the entire domain over the year. The highest differences (more than 0.2 m^2/s^2) are located (i) close to 81°W–16°N due to the bathymetric effect generated by the Nicaraguan Rise (**Figure 1**) and the proximity of the northern boundary and (ii) close to the coast as a result of interpolation errors. During DJF and MAM, the lower portion of the PCG was underestimated by around 0.1 m^2/s^2 in the model. Additionally, red coloration

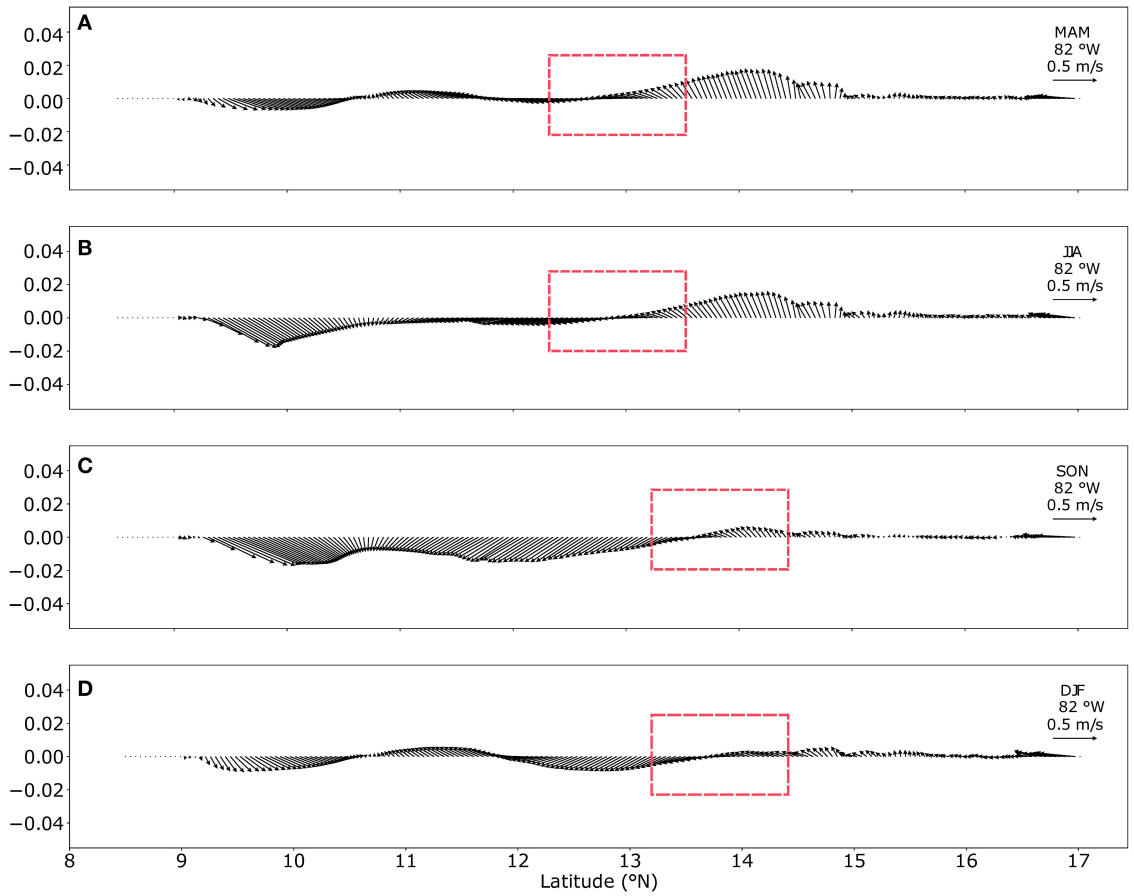

FIGURE 3 | Seasonal position of the CC bifurcation. Transects over 82°W during the climatological seasons **(A)** March–April–May, **(B)** June–July–August, **(C)** September–October–November, and **(D)** December–January–February. The arrows show the direction of the flow, and arrow length corresponds to current speed (magnitude).

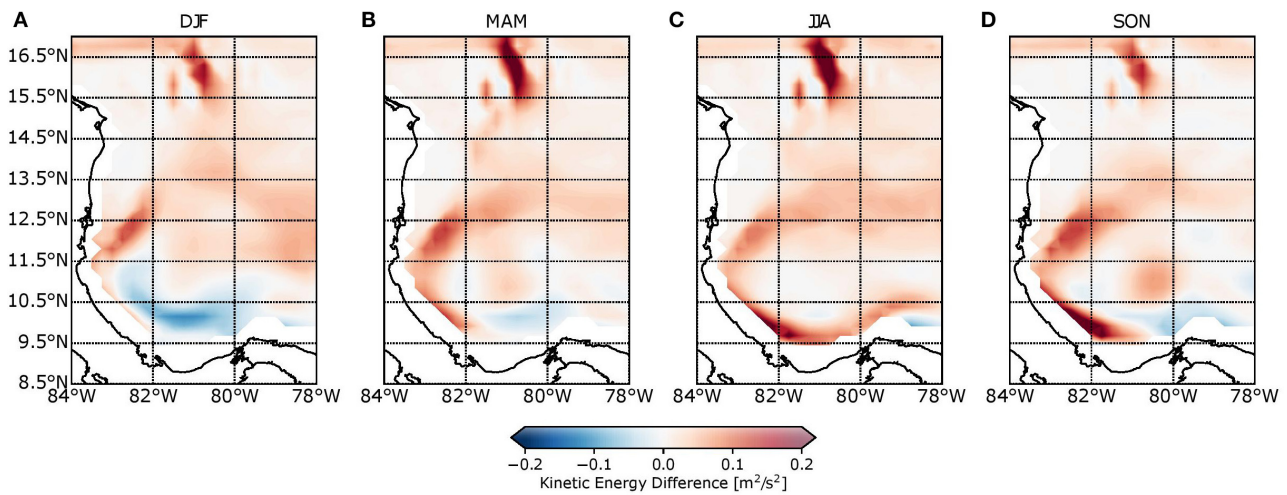

FIGURE 4 | Seasonal kinetic energy difference between model and AVISO satellite data for **(A)** December–January–February, **(B)** March–April–May, **(C)** June–July–August, and **(D)** September–October–November. Red coloration is associated with kinetic energy overestimation, while blue coloration is associated with its underestimation.

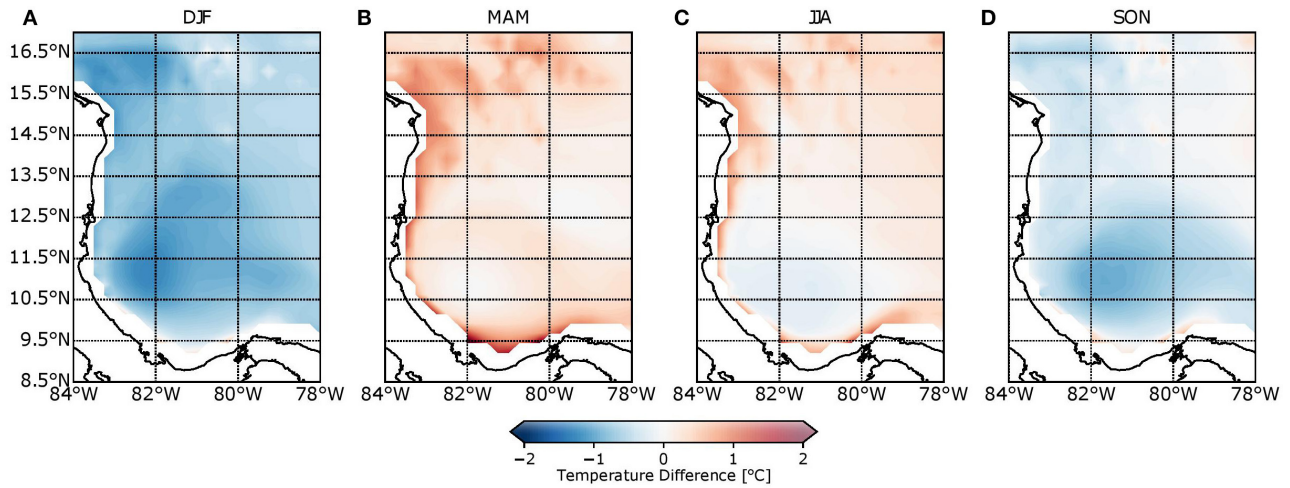

FIGURE 5 | Seasonal temperature difference between model and REYNOLDS data for **(A)** December–January–February, **(B)** March–April–May, **(C)** June–July–August, and **(D)** September–October–November. Red coloration associated with temperature overestimation, while blue coloration is associated with its underestimation.

above 12.5°N is consistent with an overestimation of the PCG not only in terms of magnitude but also in terms of spatial extension. AVISO data show a less expanded gyre in almost 0.5°.

Figure 5 shows seasonal differences in sea surface temperature (SST) between the model and REYNOLDS data. Red colors are associated with an overestimation of SST, whereas blue colors correspond to underestimation. The model underestimated SST during DJF and SON but overestimated them during MAM and JJA when compared to REYNOLDS data. The model underestimation (across almost the entire domain) was around 1.5°C during DJF, while in SON, the differences were between 0 and 0.8°C close to the PCG. Positive differences (i.e., overestimations) were obtained during MAM and JJA, with values lower than 1°C in both trimesters. The lowest differences between the model and satellite data resulted in JJA values that coincided with *A. palmata* spawning events. Model results, therefore, show good performance when compared with REYNOLDS data.

In-situ measurements over the water column are not available for the study zone; therefore, the model validation for this work is limited satellite-derived data for the surface layer. However, according to Montoya (2014), the mixed layer depth in the Colombian Caribbean has been found to be only around 25 m during JJA, so an accurate representation of the surface layer is sufficient to account for the depths of interest (1.5–15 m). In addition, most of the particles (more than 70%) remain in the upper 30 m during the PLD. This can be seen for some particles during the 2015 spawning event in the **Supplementary Material**.

3.2. Mesoscale and Sub-mesoscale Circulation During Spawning Events in the SFBR

At different spatio-temporal scales at the surface, the circulation over the Seaflower Reserve exhibits different characteristics. To track them, we used the model results from the nested grid (1.7 km resolution), which allowed the observation and accurate representation of small features close to the reefs. Dynamics during the spawning events were affected by eddy intrusion, and the presence of eddies was therefore considered to be vital for reef connectivity. To identify mesoscale and sub-mesoscale coherent structures (eddies), we calculated the Okubo Weiss (OW) parameter and vorticity (ξ) fields as follows:

$$\xi = \frac{\partial v}{\partial x} - \frac{\partial u}{\partial y}$$

$$OW = (\frac{\partial v}{\partial x} - \frac{\partial u}{\partial y})^2 + [(\frac{\partial u}{\partial x} - \frac{\partial v}{\partial y}) + (\frac{\partial u}{\partial y} - \frac{\partial v}{\partial x})]^2$$

where u and v are the eastward and northward velocity components, respectively. The OW parameter is used to distinguish strain-dominated areas from vorticity-dominated areas, while vorticity enables quantification of the local spinning motion.

In general terms, all modeled spawning events coincided with the presence of mesoscale and sub-mesoscale eddies. Here, we summarize the most significant cases. During 2009, we identified the presence of three structures, one anticyclonic and two cyclonic, all of which were present since the beginning of the spawning event. The anticyclonic eddy had a diameter of ∼80 km, and its center was located over 82°W and 14°N, close to Serrana. Eddy deformation began after 9 days (21/08/2009) when the feature was proximal to the Nicaraguan Rise. The eddy transported larvae through its rotation and, due to its presence, the self-recruitment in Serrana was around 2%, whereas the recruitment in Serranilla was 6% of the total released larvae in Serrana. With a diameter of almost 70 km, the northernmost cyclonic eddy was located close to B. Nuevo and left the domain 10 days (22/08/2009) after the beginning of the event. This cyclonic eddy allowed self-recruitment in B. Alicia corresponding to 3% of the total amount of larvae. In B. Nuevo, the recruitment was around 8%. These data are presented in **Figure 6B**, and the output of the simulation during the spawning event can be observed in the **Supplementary Material**.

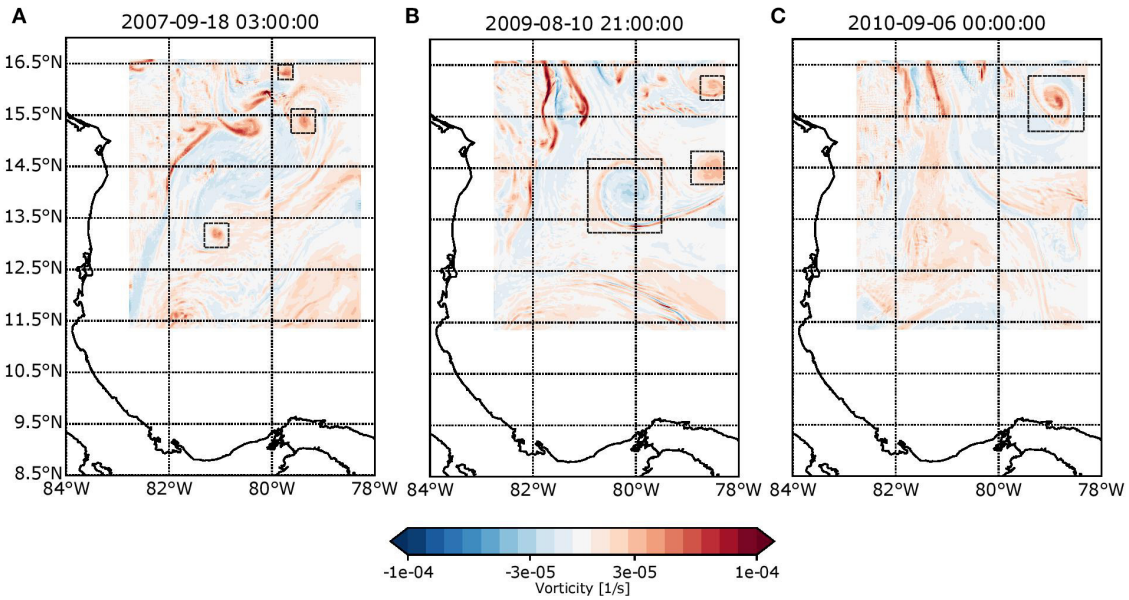

FIGURE 6 | Vorticity fields for **(A)** 2009-08-10 21:00, **(B)** 2007-09-18 21:00, and **(C)** 2010-09-05 21:00. Red coloration indicates anticyclonic spin zones, while blue coloration shows cyclonic spin zones.

In 2010, a cyclonic eddy with a diameter of 60 km influenced the northernmost Seaflower reefs. As it entered lower depths, it lost coherence and was rapidly dissipated (**Figure 6C**). The recruitment associated with this eddy in B. Alicia was around 4% of the total larvae, whereas the self-recruitment in B. Nuevo was ∼12%. Finally, we identified an anticyclonic eddy during 2002 with a diameter of ∼50 km. This began to dissipate in Serranilla and disappeared when close to Quitasueño.

Sub-mesoscale eddies with diameters of <15 km were also common in the SFBR. In particular, we found that almost all spawning events were associated with the presence of cyclonic and anticyclonic sub-mesoscale eddies close to Serranilla, B. Alicia, and B. Nuevo, where abrupt bathymetry changes favor their formation. During 2007, we identified at least three sub-mesoscale cyclonic eddies with diameters between 10 km and 15 km moving in a north–south direction and lasting between 15 and 20 days. Two of these eddies entered through the north boundary and strengthened over Serranilla, B. Alicia, and B. Nuevo. The third was formed close to these reefs (**Figure 6A**). These sub-mesoscale structures linked isolated reefs from north to south, such as B. Nuevo-Albuquerque, B. Nuevo-San Andrés, Quitasueño-Serrana, and Serranilla-Serrana. These results highlight the influence of small-scale eddies on rates of recruitment and self-recruitment since, without their presence, the connections reported here would not have occurred.

The position of the CC bifurcation induced by the presence of the Nicaraguan Rise exhibited highly dynamic behavior during simulated spawning events. During 2000, 2003, 2010, and 2014, the bifurcation occurred close to 15, 14, 14.5, and 15°N, respectively (2, 1, 1.5, and 2° above the mean). During these years, the bifurcation was located in a more northern position in comparison to the mean, and the east side of the SFBR was dominated by a current toward the north, while the current at the west side (and below 14.5°N) was toward the south. During 2007 and 2008, the CC split at 12.5°N, whereas, in 2015, this occurred close to 11.5°N (0.5 and 1.5° below the mean). Cases showing this southernmost position of bifurcation were characterized by an important component of currents toward the south. Finally, 2002 and 2009 were distinguished by a bifurcation that was close to average conditions, which is evident in the significant zonal component of the CC.

At the southwestern margin of the domain, the PCG, a semi-permanent cyclonic gyre, has an influence between 8 and 12.5°N. Nevertheless, this feature may expand or contract; this defines the dynamics of the southernmost reefs (San Andrés, Albuquerque, and Bolívar). In the case of most simulated events, the PCG exerted influence until 12.5°N, for example, during 2000, 2002, 2003, 2008, and 2009, which is similar to its mean (climatological) behavior. During the 2015 event, the PCG contracted until 11.5°N, although during 2014, it expanded to 13°N. During the 2007 and 2010 events, the gyre was not well-defined.

3.3. Connectivity Patterns

Figure 7 shows potential connectivity matrices for each spawning event during El Niño (upper panels), La Niña (middle panels), and neutral ENSO years (lower panel). From these matrices, it is possible to determine that there is connectivity among coral reefs of the SFBR during the simulated spawning events. However, the number of successful links was highly variable over time; for example, in 2000 and 2003, there were only three and four links, respectively, while during 2007 and 2015, there were 24 and 21 successful links between the reefs. In addition,

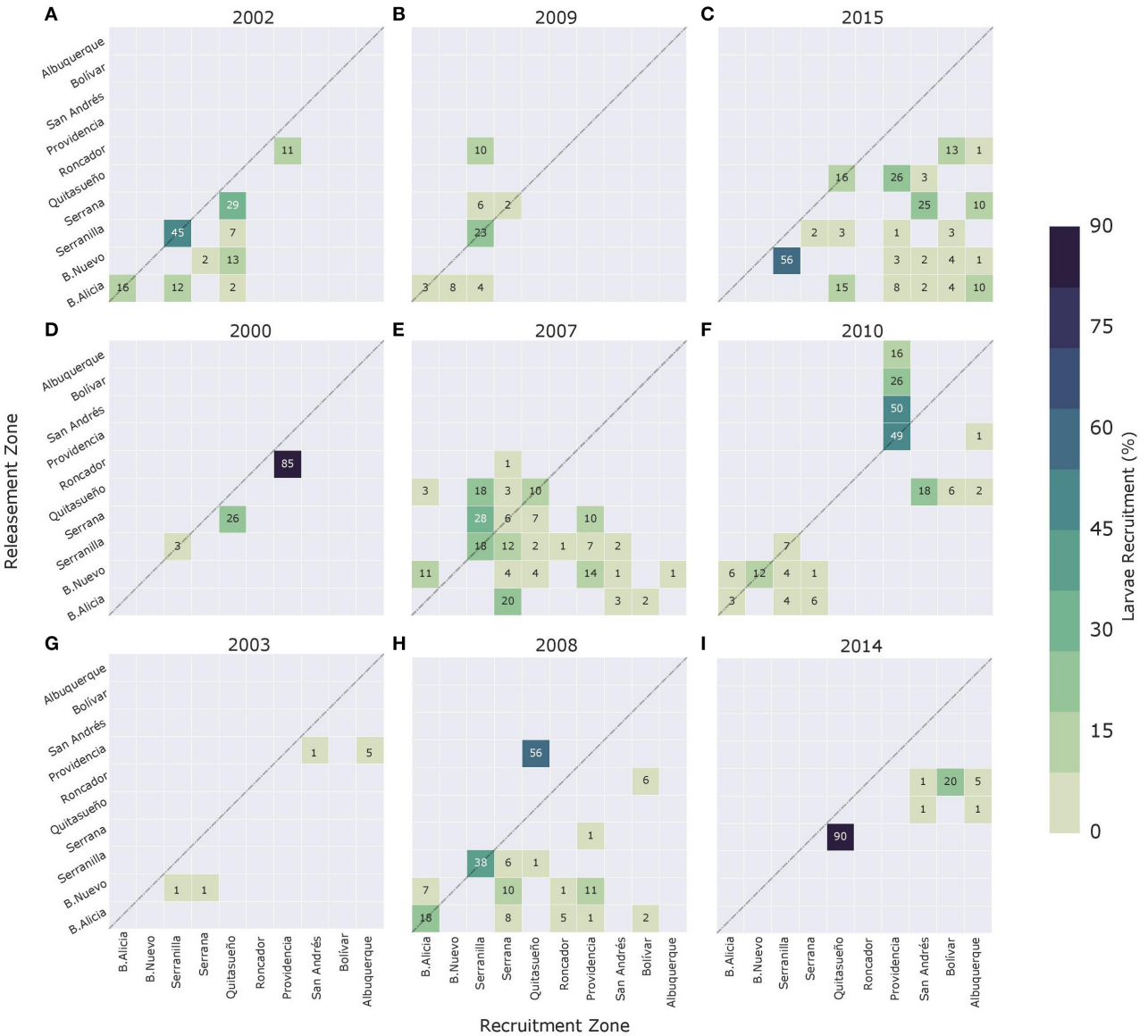

FIGURE 7 | Connectivity matrices for **(A)** 2002, **(B)** 2009, **(C)** 2015, **(D)** 2000, **(E)** 2007, **(F)** 2010, **(G)** 2003, **(H)** 2008, and **(I)** 2014 spawning events. Upper panels correspond to El Niño years, middle panels to La Niña years, and bottom panels to neutral ENSO condition years. Connectivity matrix shows the strength of each connection based on the amount received by reef *j* (x-axis) and contributed by reef *i* (y-axis). The diagonal of the matrix indicates reefs where local retention occurs.

the connection strength was irregular, not only during the same event but also between years. For example, in 2008 there was a wide range of larva recruitment percentages, such as: 1% (B. Alicia-Providencia), 6% (Roncador-Bolívar), 11% (B. Nuevo-Providencia), 18% (self-recruitment in B. Alicia), 38% (self-recruitment in Serranilla), and 56% (Providencia-Quitasueño). Among events, for example, the larva recruitment between Serrana and Quitasueño oscillated between 0% (in 2003, 2007, 2008, 2009, 2010, and 2015) and higher values, i.e., 26% (2000), 29% (2002), and 90% (2014).

Most of the successful connections were concentrated over the sources of B. Alicia, B. Nuevo, and Serranilla (northernmost reefs) as well as in the self-recruitment cases. In the case of the sinks, the larvae were mainly received by the reefs located in the mid-zone, Quitasueño, Serrana, and Providencia. During the 2007, 2008, and 2015 events, the northernmost reefs, B. Alicia, B. Nuevo, and Serranilla, acted as the most important sources for the reefs located in the mid and southernmost zones. In 2000, 2003, 2010, and 2014, the connections were divided into two groups: (i) among the northernmost reefs and (ii) among the mid and southernmost reefs. Finally, during eight of the nine spawning events, the southernmost reefs were not larval sources.

Figure 8A displays the number of events where *i-j* connection occurred successfully, while **Figure 8B** shows the contribution

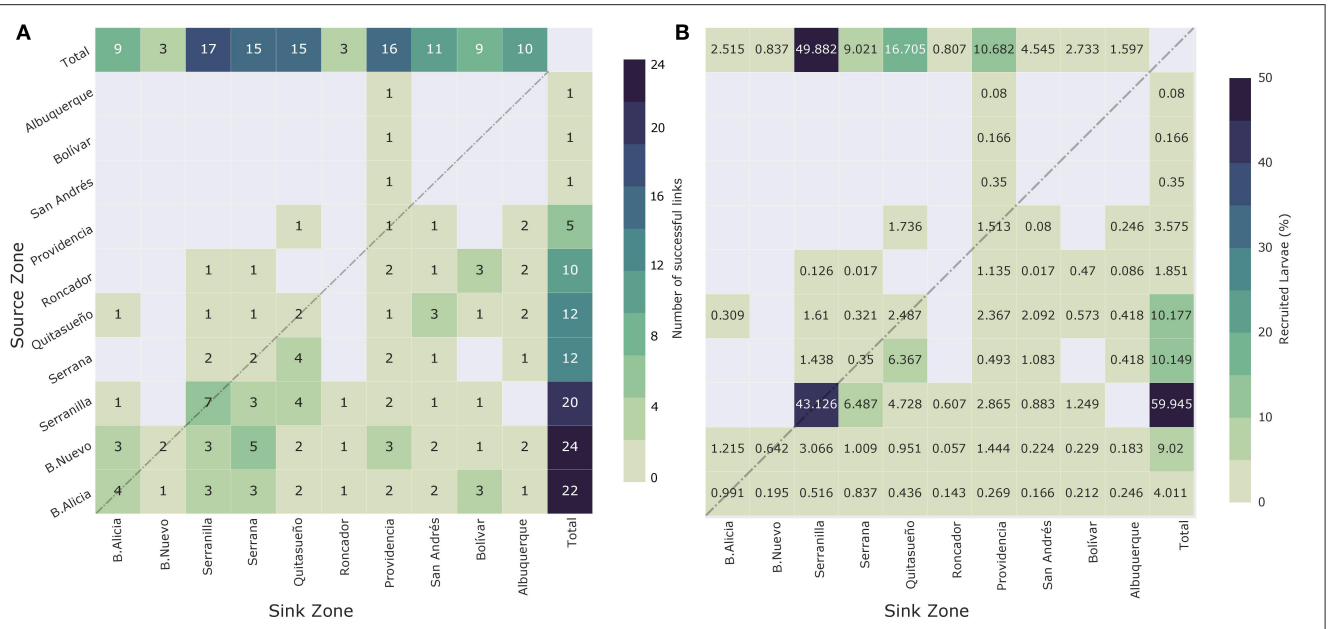

FIGURE 8 | (A) Connectivity summary matrix for all spawning events. Row sums show the number of times that reef *i* acts as a source for all the reefs. Column sums indicate the number of times that reef *j* acts as a sink for all reefs (including self-recruitment). **(B)** Contribution of each *i-j* connection with respect to the overall recruitment across SFBR for all spawning events. Row sums indicate the percentage contribution of each source *i* to the total amount of recruited larvae. Column sums indicate the proportion of larvae received by the sink *j*.

of each *i-j* connection with respect to the overall recruitment across the SFBR for the simulated spawning events. The row sum indicates the number of times in which reef *i* acts as a source for all reefs (including self-recruitment) and its percentage contribution based on the total amount of recruited larvae in the reserve. On the other hand, the column sum shows the number of times in which reef *j* acts as a sink and the proportion of larvae received. For instance, B. Nuevo, B. Alicia, and Serranilla were more frequent sources (23, 22, and 18 occasions, respectively) in comparison to other reefs in the reserve. In contrast, the southernmost reefs, i.e., San Andrés, Bolívar, and Albuquerque, were the least frequent sources, with only one successful link during all simulated events. Serrana, Quitasueño, Roncador, and Providencia made 12, 12, 10, and 5 connections, respectively. However, based on the net larva exchange between reefs, Serranilla was the biggest contributor, with an amount close to 60% of larvae, during the simulated spawning events, of which 43% were associated with self-recruitment processes. With a difference close to 50% in the number of larvae provided to the system, reefs, such as B. Nuevo, Quitasueño, and Serrana supplied around 30% of larvae during the simulated events. Finally, the reefs providing the smallest amount of larvae to the system were the southernmost reefs, Albuquerque, San Andrés, and Bolívar, whose contribution was close to 1% each.

The most recurrent as a sink were Serranilla, Providencia, Quitasueño, and Serrana, acting as such on 16, 16, 15, and 15 occasions across all events. In contrast, B. Nuevo and Roncador functioned as sinks only three times during all of the events. Finally, the B. Alicia, Bolivar, Albuquerque, and San Andres reefs acted as sinks 8, 9, 10, and 11 times, respectively. From a larva exchange point of view, the reef that received the most larvae was Serranilla, receiving ∼50% of the total. As mentioned previously, around 43% were associated with self-recruitment processes. Quitasueño, Providencia, and Serrana were also important sinks for the system, receiving 17, 10, and 10% of the total amount of recruited larvae, respectively. The easternmost sinks, B. Nuevo and Roncador, received a lower number of larvae during the events. They received around 2% of the total recruited larvae across all reefs of the SFBR.

The information provided by **Figure 8B** is partially consistent with the results of **Figure 8A**. We identified the northernmost reefs B. Nuevo (23), B. Alicia (22), and Serranilla (18) as the most recurrent sources for the system; however, based on the net larva contribution during the simulated spawning events, Serranilla provided most of the larvae. It is essential to highlight that this is the biggest releasement zone (1202.3 km^2) in which more larvae were released (> 50%). Therefore, the probability of becoming a relevant source for the system would have been increased. From the net larva contribution, Quitasueño and Serrana exceeded by about 5% the supply made by B. Alicia, which was the second most recurrent larva source; nevertheless, as in the previous case, the two releasement zones exceed the number of larvae released in B. Alicia in 3.5 and 1.5 times, respectively. These results suggest that there is not necessarily equivalence between link recurrence and net larva exchange. For example, the link between Serranilla and Serrana occurred three times, as among B. Alicia and Serrana, but the first linkage with Serranilla as a source amounted to 6.5% of the total quantity of recruits, whereas, for B. Alicia, this was <1%. In contrast, the less frequent sources are consistent with the reefs that provide fewer larvae to the system, i.e., the

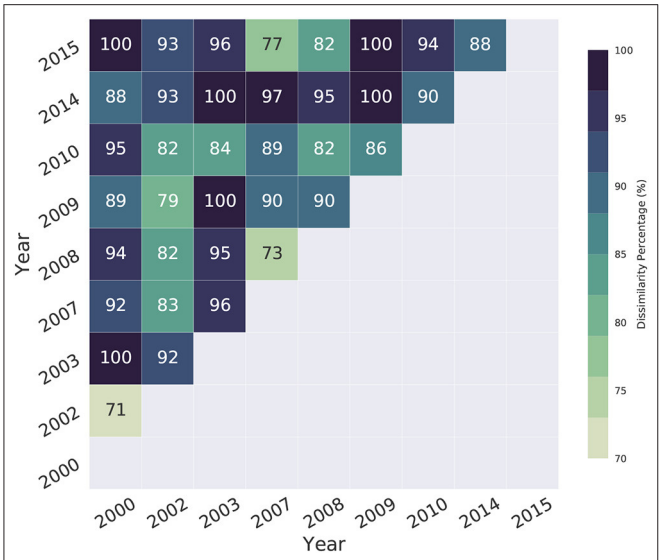

FIGURE 9 | Dissimilarity percentage between pairs of events. This shows the percentage of reef connections between events whose *i-j* position in the connectivity matrices differs.

southernmost reefs Albuquerque, San Andrés, and Bolívar. It is important to note that they have the smallest reef areas in the reserve, and in consequence, fewer larvae were released from them (around 3% from the total). Also, they are highly influenced by the semi-permanent presence of the PCG.

On the other hand, looking at the sinks, the recurrence and net exchange among the reefs allowed us to identify that those located in the middle of the reserve and also the biggest zones (i.e., Providencia, Quitasueño, Serrana, and Serranilla) were the most important during the simulated events. In contrast, the weakest and least frequent sinks were those located on the easternmost (B. Nuevo and Roncador) side of the domain where the east–west direction of the currents does not favor larva recruitment. It is noteworthy that, for example, in B. Nuevo, more than 50% of recruited larvae were supported by self-recruitment processes due to the strong influence of mesoscale eddies. In general terms, the most frequent sink reefs were those in which more larvae were recruited during the simulated spawning events.

We simulated spawning events during El Niño, La Niña, and under neutral ENSO conditions in order to assess the influence of macro-climatic phenomena on surface dynamics and the resulting connectivity patterns, which are shown in **Figure 7**. Our hydrodynamic results suggest that surface dynamics did not suffer significant changes due to atmospheric fluctuations associated with the ENSO. Consequently, the way in which reefs are connected did not exhibit any pattern since there is high variability in the surface circulation of the domain. To quantitatively evaluate the existence of patterns in connectivity matrices, we applied the CADM test to the distance matrices calculated through Equation 2 for El Niño, La Niña, and neutral ENSO conditions. We got Kendall coefficients of 0.68, 0.65, and 0.65, respectively, with *p*-values of 0 in all cases. The obtained W coefficients, as well as the *p*-values, reject the null hypothesis of the complete incongruence of matrices; this evidence suggests the existence of congruence in connectivity matrices based on ENSO conditions. This congruence is linked to the abundant presence of zeros (non-connections) in them; the above implies the existence of a non-connection pattern during the ENSO, given the lack of larva transfer among reefs. We also evaluated differences in the successful connections between pairs of events. **Figure 9** indicates the percentage of connections whose *i-j* position between events is different. For example, between 2002, 2009, and 2015 (El Niño events), the CADM test suggests high congruence due to the number of non-connections in them; however, at least 73% of the successful connections occur in different positions in the matrices. In the case of La Niña, at least 89% of the links differ in position, while for neutral years, it is 95%. In all cases, the percentage of dissimilarity in links is at least 70%, while in some cases, 100% of the connections differ in their position, for example, during 2009–2015, 2003–2014, or 2000–2003. This fact demonstrates high variability in the way the reefs connect over time.

3.4. Potential Connectivity vs. Effective Connectivity

Effective connectivity matrices for a daily mortality rate of 15% during the nine spawning events are shown in **Figure 10**. In general, and as expected, when the mortality rate is included in connectivity measures, links in the matrices are sparser. Weak potential connections (below 5%) are more susceptible to disappearing when mortality is taken into account. The links between Providencia and San Andrés, B. Nuevo and Serranilla, and B. Nuevo and Serrana during the 2003 event (**Figure 7G**) disappeared when mortality was applied (**Figure 10**); however, other stronger links, such as B. Nuevo-Quitasueño (13%) in 2002 or Serrana-Providencia (10%) in 2007 also disappeared when using a daily mortality rate of 15%. On the other hand, where potential larval exchange was stronger, the connections lasted but in smaller proportions, and a large number of links with <5% total exchange were found to arise. For effective connectivity, the most recurrent sources are the northernmost reefs, whereas the least recurrent are the southernmost. Serranilla, Providencia, Quitasueño, and Serrana were the most recurrent sinks, whereas B. Nuevo and Roncador were the least common in this regard.

4. DISCUSSION

Appropriate representation of the SFBR dynamics at high spatiotemporal scales allowed us to determine that there is indeed reef connectivity in the SFBR. Potential and effective connectivity were found for *A. palmata* species using a pre-competency period of 3 days and a pelagic larval duration of 25 days.

Connectivity behavior was found to be dynamically associated with: (i) the latitudinal migration of the CC bifurcation, which is itself linked to bathymetric forcing by the Nicaraguan Rise, (ii) the presence of mesoscale and sub-mesoscale coherent structures (eddies), and (iii) the expansion-contraction of the semi-permanent PCG. The patterns described for the CC and

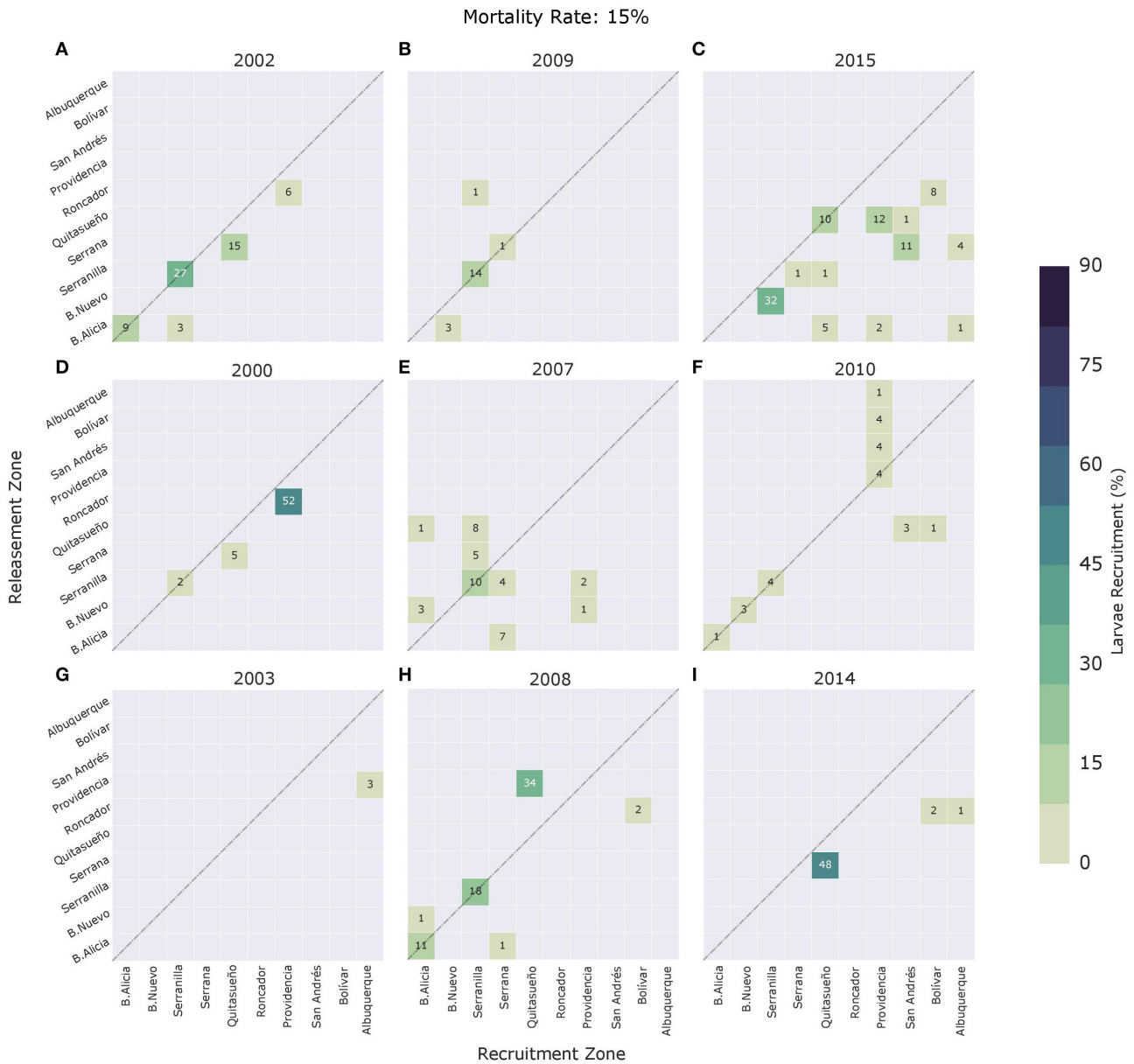

FIGURE 10 | Connectivity matrices for the **(A)** 2002, **(B)** 2009, **(C)** 2015, **(D)** 2000, **(E)** 2007, **(F)** 2010, **(G)** 2003, **(H)** 2008, and **(I)** 2014 spawning events, using a daily mortality rate of 15%. Upper panels correspond to El Niño years, middle panels to La Niña years, and bottom panels to neutral ENSO condition years. Connectivity matrix shows the strength of each connection based on the amount received by reef *j* (x-axis) and contributed by reef *i* (y-axis). The diagonal of the matrix indicates reefs where local retention occurs.

the PCG concur with previous findings reported by Andrade (2000, 2001), who reported a dominant CC with an effect in the upper 700 m, high mesoscale variability associated with eddies entering the region through the Antilles Islands, and an intense cyclonic gyre (PCG). Jouanno et al. (2008, 2009) also reported the influence of mesoscale eddies in the Colombian Caribbean and noted that these eddies either came from Brazil or were generated by CC instabilities in Colombian or Venezuelan basins.

Our model suggests that the position of CC bifurcation induced by the bathymetric effect of the Nicaraguan Rise is critical in the configuration of the dynamic system and is a crucial parameter when identifying potential connections among reefs. The bifurcation of the CC controls the larva dispersal patterns in almost all modeled events. Similar behavior was identified in the tropical Atlantic by Endo et al. (2019), where the latitudinal variability in the South Equatorial Current bifurcation was crucial to the meridional transport of individuals. When the CC bifurcation occurs at its northernmost locations (>13°N), such as in 2000, 2003, 2010, and 2014, it acts as a barrier between the southern and northern reefs and

favors the links between the middle and southern reefs. This pattern is associated with a current toward the north in B. Nuevo, B. Alicia, and Serranilla that rapidly transports a large amount of the larvae released in these reefs out of the domain. Notwithstanding, the southward current in the west favors connections between middle and southernmost reefs, such as Providencia-Albuquerque, Providencia-San Andrés, and Roncador-Bolívar. In this sense, Sanvicente-Añorve et al. (2018) reported that the mean circulation patterns in the Gulf of Mexico are also associated with complex bathymetry and act as an oceanographic barrier for larval dispersal in the Mississippi Canyon. In contrast, when the CC bifurcation reaches its southernmost positions (i.e., $<13°$N), for example, in 2007, 2008, and 2015, the predominant connectivity direction is from north to south. During these events, the northernmost reefs of B. Alicia, B. Nuevo, and Serranilla appear to be a source of larvae for reefs located in more southern positions, e.g., Albuquerque, Providencia, Bolívar, and San Andrés, due to the southward current over the domain.

Mesoscale and sub-mesoscale eddies were seen to have significant importance in the connection of isolated reefs and to favor self-recruitment, even when the general circulation patterns did not facilitate it. A large number of sub-mesoscale eddies were generated in the northern part of the domain, where abrupt changes in bathymetry occur (**Figure 1**). In this regard, Zatsepin et al. (2018) also found that bathymetric roughness associated with underwater banks and its interaction with currents were important factors in sub-mesoscale eddy formation. This fact highlights the importance of studying the role of sub-mesoscale structures in oceanic matter dispersion (e.g., nutrients, sediments) in the SFBR.

Regarding the PCG, it influenced the southernmost reefs (San Andrés, Albuquerque, and Bolívar) and rapidly removed larvae from the domain. It is important to note that the evaluation of the larval re-circulation due to expansion-contraction of the PCG is crucial for understanding the connectivity pattern behavior in the domain; this fact has also been reported, for example, by Staaterman et al. (2012) in the Florida Keys, where the semi-permanent presence of a gyre in the Dry Tortugas region allows more larva retention, resulting in higher self-recruitment rates.

The resulting connectivity measures are highly variable, which is evident both in the existence of the link and its varying strength between individual years. For instance, variability in the Roncador-Bolívar link is seen from the way in which they are connected. In 2008, the connection amounted to 6%, in 2014 it was 20%, and in 2015 it was 13%. No connection existed between them in the other years. Siegel et al. (2008) also demonstrated in California that larval connectivity is inherently an intermittent and heterogeneous process on annual time scales, i.e., it is a stochastic process driven by the interaction between coastal circulation and organisms' life histories. Similarly, Watson et al. (2010) identified variable connectivity in the Southern California Bight (SCB), with the strength of sources and sinks varying between locations and between years. The reason for such heterogeneity lies in the patterns of ocean circulation in the SCB. In the SFBR, the ocean circulation (CC, eddies, and PCG) did not show relationships with ENSO phases; as a consequence, and supported by dissimilarity percentages, the connectivity matrices show high variability in the way the reefs connect over time. In all cases, the difference for connected reefs among events was at least 70%, reaching 100% values in some cases; this implies that linked reefs do not exhibit predictable behavior.

The surface circulation features in the SFBR allowed 105 links in potential connectivity and 52 effective (including self-recruitment) links among the reefs during all of the spawning events modeled. Despite not being part of the MPA (**Figure 1**), the northernmost reefs, Serranilla, B. Nuevo, and B. Alicia, acted as a larval source, accounting for ∼60 and 50% (in potential and effective connectivity, respectively) of the total number of connections. These findings highlight not only the ecological importance of these reefs in long-term system resilience but also illustrate the need to include them within the MPA framework. The integration of reefs into the MPA could be achieved through the redesign of preexisting MPA zonation. As suggested by Schill et al. (2015), the integration of larval dispersal data into a decision-making framework is useful for determining the prioritization of conservation areas and maintenance of the MPA. Herein, we have highlighted the need to include a full 3D high-resolution hydrodynamic field that allows us to take small-scale features into account as well, as they play a key role in the connectivity of coral reefs.

However, based on the total amount of recruited larvae across all reefs, the most significant source was Serranilla, which provided ∼60% of larvae to the system. It is important to note that without self-recruitment processes, Serranilla would have supplied around 17% of larvae, a contribution that is very close to those of Serrana, Quitasueño, and B. Nuevo. We also highlight the need to protect the northernmost reefs of Seaflower due to their high self-recruitment rates and the fact that they are high-percentage source regions for reefs, such as Roncador (100%), Serrana (92%), and Bolivar (62%). In this sense, the findings of Suzuki et al. (2011) stand out in suggesting protected area designation where intense self-recruitment occurs, since this is crucial to the resilience of *Acropora* corals.

In general, effective connectivity matrices are more sparse than potential connectivity matrices as a result of mortality incorporation. In addition, a large amount (65%) of links accounted for up to 5% of larva exchange. This demonstrates the importance of protecting SFBR reefs, since their connections are weak and sparse, and, as a consequence, the resilience of the system could potentially be affected by oceanographic events.

The results of the biophysical modeling presented herein have several limitations and sources of uncertainty. (i) The minimum value among the range of the PP was chosen, which could have led to overestimated recruitment rates (including self-recruitment). However, it is noteworthy that the Colombian Caribbean is a highly energetic basin, and the larvae are rapidly expelled from the domain. In addition, numerical models tend to overestimate current magnitude, as can be seen in **Figure 3** through seasonal kinetic energy differences. Due to these factors, the use of higher PP values could lead to underestimation of recruitment percentages and loss of information. Nevertheless, this could be an important source of uncertainty. (ii) We used a mean value of 25 days for the pelagic larval duration parameter. Other calculations showed us that $<10\%$ of recruited larvae were recruited 20 days after the

releasement; therefore, the impact of the PLD is not bigger, as could be expected. (iii) The polygons used and provided by the Coral Millennium databases do not always account for the precise location of *A. palmata* and its abundance; this could lead to an overestimation or underestimation of the larval source areas in the Seaflower Reserve. (iv) The absence of genetic analyses limits the model validation.

5. CONCLUSIONS

This work has identified the existence of reef connectivity and has characterized the dynamic conditions leading to such connectivity in the SFBR using a numerical modeling approach with high spatio-temporal resolution. This has allowed, for the first time, the exploration of the impact of mesoscale and sub-mesoscale structures on coral larva transport and reef connectivity during nine modeled spawning events. Understanding of the physical drivers and their influence over reef connectivity has been enhanced through the representation of small-scale features present in the region, thus, providing useful information for the identification of critical areas for ecological protection and their incorporation into conservation plans. Despite being a model-based result that may require genetic validation, the results compiled present the most extensive high-resolution connectivity information for this region.

Coral larva transport in the SFBR is highly modulated by the position of CC bifurcation. In cases where the CC bifurcation reaches its northernmost position in comparison to the mean, it acts as a barrier between the northern and southern reefs, whereas its southernmost bifurcation favors connectivity from north to south. The high current speeds and the expansion and contraction of the PCG enable larval release from the San Andrés, Albuquerque, and Bolivar reefs, and these larvae are rapidly trapped on the PCG and removed from the domain.

Alongside with CC and PCG, the region is characterized by mesoscale and sub-mesoscale eddies. The lower part of the Caribbean is constantly populated by large-scale eddies that transit westward and lose coherence as they strike the Nicaraguan Rise. We found a large presence of sub-mesoscale eddies close to Serranilla, B. Alicia, and B. Nuevo, where the abrupt bathymetry changes favor their formation. These mesoscale and sub-mesoscale eddies allow self-recruitment in the northern part of the reserve and are also important larval sources to the southern reefs.

Our results indicate that Serranilla, B. Alicia, and B. Nuevo are key larval sources in the SFBR and contribute to potential and effective connectivity from the recurrence point of view. However, they currently lie outside the MPA protection framework and are located in a common regime area between Colombia and Jamaica. Therefore, we advise that these areas be included in an MPA zonation, as this could consequently improve the effectiveness of the reserve. Our results also suggest the importance of implementation of MPA frameworks between the countries concerned with the reserve, since these could allow the coral populations to be more resilient to environmental changes and less prone to local extinctions.

The existence of links and their strength in connectivity matrices demonstrated high variability between the years and a lack of relation with atmospheric forcing imposed by ENSO phases; therefore, there is no predictable pattern in connected reefs. Nevertheless, the presented matrices are a useful tool for easily interpreting reef to reef connections for ecological managers and decision-makers.

DATA AVAILABILITY STATEMENT

The datasets generated for this study are available on request to the corresponding author.

AUTHOR CONTRIBUTIONS

LL performed the calculations and analyzed the data. YC, PZ-R, and LL conceived and designed the main research ideas and methods, and worked on the main discussions and conclusions.

ACKNOWLEDGMENTS

LL thanks COLCIENCIAS for its economic support through Convocatoria 812 de 2018. PAZ-R acknowledge the support from the Royal Academy of Engineering (Project Award IAPP18-19\210). We thank Dr. ANASTAZIA BANASZAK for her valuable comments and suggestions to the document, in particular to the issue related to the species studied and we thank the two reviewers for insightful comments that significantly improved the manuscript.

SUPPLEMENTARY MATERIAL

The Supplementary Material for this article can be found online at: https://www.frontiersin.org/articles/10.3389/fmars.2020.00385/full#supplementary-material

Video S1 | Vorticity fields and particle dispersion during 2009 spawning event.

Image S1 | Serranilla, *B. Alicia*, and *B. Nuevo* location.

Image S2 | Quitasueño, Serrana, Providencia and Roncador location.

Image S3 | San Andrés, Bolívar, and Albuquerque location.

Image S4 | Vertical behavior for some particles during 2015 spawning event.

REFERENCES

Abderrahim, B., and Fillon, C. (2012). Gridded surface wind fields from METOP/ASCAT measurements. *Int. J. Rem. Sens.* 33, 1729–1754. doi: 10.1080/01431161.2011.600348

Acero, P. A., Tavera, J. J., Polanco, F. A., and Bolaños-Cubillos, N. (2019). Fish biodiversity in three northern islands of the seaflower biosphere reserve (Colombian Caribbean). *Front. Mar. Sci.* 6:113. doi: 10.3389/fmars.2019.00113

Alexander, M. A., Bladé, I., Newman, M., Lanzante, J. R., Lau, N.-C., and Scott, J. D. (2002). The atmospheric bridge: the influence of enso

teleconnections on air–sea interaction over the global oceans. *J. Clim.* 15, 2205–2231. doi: 10.1175/1520-0442(2002)015<2205:TABTIO>2.0.CO;2

Andrade, C. (2000). *The circulation and variability of the Colombian Basin in the Caribbean Sea* (Ph.D. thesis), University of Wales, Cardiff, United Kingdom.

Andrade, C. (2001). Las corrientes superficiales en la cuenca de colombia observadas con boyas de deriva. *Rev. Acad. Colomb. Cien. Exact. Físic. Nat.* 96, 321–335.

Baums, I. B., Paris, C. B., and Chérubin, L. M. (2006). A bio-oceanographic filter to larval dispersal in a reef-building coral. *Limnol. Oceanogr.* 51, 1969–1981. doi: 10.4319/lo.2006.51.5.1969

Becker, B. J., Levin, L. A., Fodrie, F. J., and McMillan, P. A. (2007). Complex larval connectivity patterns among marine invertebrate populations. *Proc. Natl. Acad. Sci. U.S.A.* 104, 3267–3272. doi: 10.1073/pnas.0611651104

Bolaños, N., Abril, A., Bent, H., Caldas, J., and Acero, A. (2015). Lista de peces conocidos del archipiélago de san andrés, providencia y santa catalina, reserva de la biosfera seaflower, caribe occidental colombiano. *Bol. Investig. Mar. Cost. José Benito Vives Andrésis (INVEMAR)* 44, 127–162. doi: 10.25268/bimc.invemar.2015.44.1.24

Campbell, V., Legendre, P., and Lapointe, F.-J. (2011). The performance of the congruence among distance matrices (cadm) test in phylogenetic analysis. *BMC Evol. Biol.* 11:64. doi: 10.1186/1471-2148-11-64

Chamberland, V. F., Vermeij, M. J., Brittsan, M., Carl, M., Schick, M., Snowden, S., et al. (2015). Restoration of critically endangered elkhorn coral (*Acropora palmata*) populations using larvae reared from wild-caught gametes. *Glob. Ecol. Conserv.* 4, 526–537. doi: 10.1016/j.gecco.2015.10.005

CORALINA-INVEMAR (2012). *Atlas de la Reserva de Biósfera Seaflower. Archipiélago de San Andrés, Providencia y Santa Catalina*. Santa Marta: Serie de Publicaciones Especiales de INVEMAR # 28.

Dee, D. P., Uppala, S., Simmons, A., Berrisford, P., Poli, P., Kobayashi, S., et al. (2011). The era-interim reanalysis: configuration and performance of the data assimilation system. *Q. J. R. Meteorol. Soc.* 137, 553–597 doi: 10.1002/qj.828

Díaz, J. M., Sánchez, J. A., and Geister, J. (1997). "Development of lagoonal reefs in oceanic reef complexes of the southwestern Caribbean: geomorphology, structure and distribution," in *Proceedings 8th International Coral Reef Symposium, Vol. 1* (Panamá), 779–784.

Díaz, J. M., Barrios, L. M., Cendales, M. H., Garzón-Ferreira, J., Geister, J., Parra-Velandia, F., et al. (2000). Áreas coralinas de colombia. *Invemar Serie Publ. Especial.* 5:176.

Endo, C. A. K., Gherardi, D. F. M., Pezzi, L. P., and Lima, L. N. (2019). Low connectivity compromises the conservation of reef fishes by marine protected areas in the tropical south atlantic. *Sci. Rep.* 9:8634. doi: 10.1038/s41598-019-45042-0

Ferry, N., Parent, L., Garric, G., Barnier, B., Jourdain, N. C., and the Mercator Ocean team (2012). Global eddy permitting ocean reanalysis GLORYS1V1: description and results. *Mercator Q. Newslett.* 36, 15–27.

Foster, N. L., Paris, C. B., Kool, J. T., Baums, I. B., Stevens, J. R., Sanchez, J. A., et al. (2012). Connectivity of caribbean coral populations: complementary insights from empirical and modelled gene flow. *Mol. Ecol.* 21, 1143–1157. doi: 10.1111/j.1365-294X.2012.05455.x

Geister, J., and Díaz, J. (2007). *Ambientes arrecifales y geología de un archipiélago oceánico: San Andrés, Providencia y Santa Catalina (Mar Caribe, Colombia) con guía de campo*. Bogotá: Ingeominas.

Giannini, A., Cane, M. A., and Kushnir, Y. (2001a). Interdecadal changes in the enso teleconnection to the caribbean region and the north atlantic oscillation. *J. Clim.* 14, 2867–2879. doi: 10.1175/1520-0442(2001)014<2867:ICITET>2.0.CO;2

Giannini, A., Chiang, J. C. H., Cane, M. A., Kushnir, Y., and Seager, R. (2001b). The enso teleconnection to the tropical atlantic ocean: contributions of the remote and local ssts to rainfall variability in the tropical americas. *J. Clim.* 14, 4530–4544. doi: 10.1175/1520-0442(2001)014<4530:TETTTT>2.0.CO;2

Giannini, A., Kushnir, Y., and Cane, M. A. (2000). Interannual variability of Caribbean rainfall, ENSO, and the Atlantic Ocean. *J. Clim.* 13, 297–311. doi: 10.1175/1520-0442(2000)013<0297:IVOCRE>2.0.CO;2

Idárraga-García, J., and León, H. (2019). Unraveling the underwater morphological features of roncador bank, Archipelago of Aan Andres, Providencia and Santa Catalina (Colombian Caribbean). *Front. Mar. Sci.* 6:77. doi: 10.3389/fmars.2019.00077

Institute for Marine Remote Sensing, University of South Florida (IMaRS/USF), Institut de Recherche pour le Développement (IRD), UNEP-WCMC, The WorldFish Center, and WRI. (2011). *Global Coral Reefs Composite Dataset Compiled from Multiple Sources for use in the Reefs at Risk Revisited Project Incorporating Products from the Millennium Coral Reef Mapping Project prepared by IMaRS/USF and IRD.*

Japaud, A., Fauvelot, C., and Bouchon, C. (2013). "Populations genetic study of the corals *Acropora palmata* and *Acropora cervicornis* of Guadeloupe (French West Indies) in view of their preservation," in *Proceedings of the 66 th Gulf and Caribbean Fisheries Institute*. doi: 10.1071/MF14181

Johnson, M., Lustic, C., Bartels, E., Baums, I., Gilliam, D., Larson, L., et al. (2011). *Caribbean Acropora Restoration Guide: Best Practices for Propagation and Population Enhancement*. Caribbean Acropora Restoration Guide. The Nature Conservancy.

Jordan, A. (2018). *Patterns in Caribbean coral spawning* (Master's thesis), Nova Southeastern University, Fort Lauderdale, FL, United States.

Jouanno, J., Sheinbaum, J., Barnier, B., and Molines, J.-M. (2009). The mesoscale variability in the caribbean sea. Part II: energy sources. *Ocean Model.* 26, 226–239. doi: 10.1016/j.ocemod.2008.10.006

Jouanno, J., Sheinbaum, J., Barnier, B., Molines, J.-M., Debreu, L., and Lemarié, F. (2008). The mesoscale variability in the caribbean sea. Part I: simulations and characteristics with an embedded model. *Ocean Model.* 23, 82–101. doi: 10.1016/j.ocemod.2008.04.002

Legendre, P. (2005). Species associations: the Kendall coefficient of concordance revisited. *J. Agric. Biol. Environ. Stat.* 10:226. doi: 10.1198/108571105X46642

Lequeux, B. D., Ahumada-Sempoal, M.-A., López-Pérez, A., and Reyes-Hernández, C. (2018). Coral connectivity between equatorial eastern pacific marine protected areas: a biophysical modeling approach. *PLoS ONE* 13:e0202995. doi: 10.1371/journal.pone.0202995

Lett, C., Verley, P., Mullon, C., Parada, C., Brochier, T., Penven, P., et al. (2008). A lagrangian tool for modelling ichthyoplankton dynamics. *Environ. Model. Softw.* 23, 1210–1214. doi: 10.1016/j.envsoft.2008.02.005

Lonin, S. C., Prada, M., and Erick, C. (2010). "Simulación de dispersión de las larvas de caracol pala strombus gigas en la reserva de biósfera seaflower, Caribe occidental Colombiano," in *Boletín Científico CIOH* (Colombia), 8–24. doi: 10.26640/22159045.212

Mayorga-Adame, C. G., Batchelder, H. P., and Spitz, Y. H. (2017). Modeling larval connectivity of coral reef organisms in the Kenya-Tanzania region. *Front. Mar. Sci.* 4:92. doi: 10.3389/fmars.2017.00092

Medel, C., Parada, C., E., Morales, C., Pizarro, O., Ernst, B., and Conejero, C. (2018). How biophysical interactions associated with sub- and mesoscale structures and migration behavior affect planktonic larvae of the spiny lobster in the Juan Fernández Ridge: a modeling approach. *Prog. Oceanogr.* 162, 98–119. doi: 10.1016/j.pocean.2018.02.017

Montoya, R. (2014). *Variabilidad estacional e interanual del balance de calor en la capa de mezcla superficial en el mar caribe* (Master's thesis), Universidad Nacional de Colombia, Bogotá, Colombia.

NMFS (2015). *Recovery Plan for Elkhorn (Acropora palmata) and Staghorn (A. cervicornis) Corals*. Technical report, National Marine Fisheries Service.

North, E. W., Gallego, A., and Petitgas, P. (2009). *Manual of Recommended Practices for Modelling Physical-Biological Interactions During Fish Early Life*. International Council for the Exploration of the Sea.

Peliz, A., Marchesiello, P., Dubert, J., Marta-Almeida, M., Roy, C., and Queiroga, H. (2007). A study of crab larvae dispersal on the Western Iberian shelf: physical processes. *J. Mar. Syst.* 68, 215–236. doi: 10.1016/j.jmarsys.2006.11.007

Penven, P., Marchesiello, P., Debreu, L., and Lefèvre, J. (2008). Software tools for pre-and post-processing of oceanic regional simulations. *Environ. Model. Softw.* 23, 660–662. doi: 10.1016/j.envsoft.2007.07.004

Prato, J., and Rixcie, N. (2015). *Aproximación a la valoración económica ambiental del departamento Archipiélago de San Andrés, Providencia y Santa Catalina–Reserva de la Biósfera Seaflower*. Bogotá: Secretaría Ejecutiva de la Comisión Colombiana del Océano SECCO, Corporación para el desarrollo sostenible del Archipiélago de San Andrés, Providencia y Santa Catalina-CORALINA.

Raitsos, D. E., Brewin, R. J., Zhan, P., Dreano, D., Pradhan, Y., Nanninga, G. B., et al. (2017). Sensing coral reef connectivity pathways from space. *Sci. Rep.* 7:9338. doi: 10.1038/s41598-017-08729-w

Randall, C. J., and Szmant, A. M. (2009). Elevated temperature affects development, survivorship, and settlement of the elkhorn coral, *Acropora palmata* (Lamarck 1816). *Biol. Bull.* 217, 269–282. doi: 10.1086/BBLv217n3p269

Ricciardulli, L., Wentz, F. J., and Smith, D. K. (2011). *Remote Sensing Systems QuikSCAT Ku-2011 Daily. Ocean Vector Winds on 0.25 deg grid, Version 4.* Santa Rosa, CA: Remote Sensing Systems.

Richardson, P. (2005). Caribbean current and eddies as observed by surface drifters. *Deep Sea Res. II Top. Stud. Oceanogr.* 52, 429–463. doi: 10.1016/j.dsr2.2004.11.001

Rodríguez-Martínez, R. E., Banaszak, A. T., McField, M. D., Beltran-Torres, A. U., and Alvarez-Filip, L. (2014). Assessment of acropora palmata in the mesoamerican reef system. *PLoS ONE* 9:e96140. doi: 10.1371/journal.pone.0096140

Romero, M., Treml, E., Acosta, A., and Paz, D. (2018). The eastern tropical pacific coral population connectivity and the role of the eastern pacific barrier. *Sci. Rep.* 8:9354. doi: 10.1038/s41598-018-27644-2

Roughgarden, J., Gaines, S., and Possingham, H. (1988). Recruitment dynamics in complex life cycles. *Science* 241, 1460–1466. doi: 10.1126/science.11538249

Ruiz, M. (2011). *Variabilidad de la Cuenca Colombia (mar Caribe) asociada con El Niño-Oscilación del Sur, vientos Alisios y procesos locales* (Ph.D. thesis), Universidad Nacional de Colombia, Bogotá, Colombia.

Sánchez-Jabba, A. M. (2012). *Manejo ambiental en seaflower, reserva de biosfera en el archipiélago de San Andrés, Providencia y Santa Catalina*. Cartagena: Documentos de Trabajo Sobre Economía Regional y Urbana; No. 176.

Sanvicente-Añorve, L., Zavala-Hidalgo, J., Allende-Arandía, E., and Hermoso-Salazar, M. (2018). Larval dispersal in three coral reef decapod species: influence of larval duration on the metapopulation structure. *PLoS ONE* 13:e0193457. doi: 10.1371/journal.pone.0193457

Schill, S. R., Raber, G. T., Roberts, J. J., Treml, E. A., Brenner, J., and Halpin, P. N. (2015). No reef is an island: integrating coral reef connectivity data into the design of regional-scale marine protected area networks. *PLoS ONE* 10:e0144199. doi: 10.1371/journal.pone.0144199

Siegel, D. A., Mitarai, S., Costello, C. J., Gaines, S. D., Kendall, B. E., Warner, R. R., et al. (2008). The stochastic nature of larval connectivity among nearshore marine populations. *Proc. Natl. Acad. Sci. U.S.A.* 105, 8974–8979. doi: 10.1073/pnas.0802544105

Staaterman, E., Paris, C. B., and Helgers, J. (2012). Orientation behavior in fish larvae: a missing piece to hjort's critical period hypothesis. *J. Theor. Biol.* 304, 188–196. doi: 10.1016/j.jtbi.2012.03.016

Suzuki, G., Arakaki, S., and Hayashibara, T. (2011). Rapid *in situ* settlement following spawning by acropora corals at Ishigaki, Southern Japan. *Mar. Ecol. Prog. Ser.* 421, 131–138. doi: 10.3354/meps08896

UNEP-WCMC, WorldFish Centre, WRI, TNC (2018). *Global Distribution of Warm-water Coral Reefs, Compiled from Multiple Sources Including the Millennium Coral Reef Mapping Project. Version 4.0. Includes contributions from IMaRS-USF and IRD (2005), IMaRS-USF (2005) and Spalding et al. (2001).* Cambridge,UK: UN Environment World Conservation Monitoring Centre. Available online at: http://data.unep-wcmc.org/datasets/1

Vega, J., Díaz, C., Gómez, K., López, T., Díaz, M., and Gómez, I. (2015). Biodiversidad marina en bajo nuevo, bajo alicia, y banco serranilla, reserva de biosfera seaflower. *Bol. Investig. Mar. Costeras José Benito Vives de Andrésis (INVEMAR)* 44, 199–224. doi: 10.25268/bimc.invemar.2015.44.1.27

Watson, J., Mitarai, S., Siegel, D., Caselle, J., Dong, C., and McWilliams, J. (2010). Realized and potential larval connectivity in the southern california bight. *Mar. Ecol. Prog. Ser.* 401, 31–48. doi: 10.3354/meps08376

Weatherall, P., Marks, K. M., Jakobsson, M., Schmitt, T., Tani, S., Arndt, J. E., et al. (2015). A new digital bathymetric model of the world's oceans. *Earth Space Sci.* 2, 331–345. doi: 10.1002/2015EA000107

Wood, S., Paris, C., Ridgwell, A., and Hendy, E. (2014). Modelling dispersal and connectivity of broadcast spawning corals at the global scale. *Glob. Ecol. Biogeogr.* 23, 1–11. doi: 10.1111/geb.12101

Zatsepin, A., Kubryakov, A., Aleskerova, A., Elkin, D., and Kukleva, O. (2018). Physical mechanisms of submesoscale eddies generation: evidences from laboratory modeling and satellite data in the black sea. *Ocean Dyn.* 69, 253–266. doi: 10.1007/s10236-018-1239-4

Zhong, Y., and Bracco, A. (2013). Submesoscale impacts on horizontal and vertical transport in the Gulf of Mexico. *J. Geophys. Res. Oceans* 118, 5651–5668. doi: 10.1002/jgrc.20402

Zhong, Y., Bracco, A., and Villareal, T. A. (2012). Pattern formation at the ocean surface: sargassum distribution and the role of the eddy field. *Limnol. Oceanogr.* 2, 12–27. doi: 10.1215/21573689-1573372

Conflict of Interest: The authors declare that the research was conducted in the absence of any commercial or financial relationships that could be construed as a potential conflict of interest.

frontiers in Marine Science

ORIGINAL RESEARCH
published: 29 July 2020
doi: 10.3389/fmars.2020.00628

Stronger Together: Do Coral Reefs Enhance Seagrass Meadows "Blue Carbon" Potential?

Luis Alberto Guerra-Vargas[1], Lucy Gwen Gillis[2]* and José Ernesto Mancera-Pineda[3]*

[1] Área Curricular de Medio Ambiente, Facultad de Minas, Universidad Nacional de Colombia, Medellín, Colombia, [2] Department of Ecology, Leibniz-Zentrum für Marine Tropenforschung (ZMT), Bremen, Germany, [3] Departamento de Biología, Facultad de Ciencias, Universidad Nacional de Colombia, Bogotá, Colombia

OPEN ACCESS

Edited by:
Juan Armando Sanchez, University of Los Andes, Colombia

Reviewed by:
Megan Irene Saunders, CSIRO Oceans and Atmosphere (O&A), Australia
Inés Mazarrasa, Environmental Hydraulics Institute (IHCantabria), Spain

****Correspondence:***
Luis Alberto Guerra-Vargas
laguerravar@unal.edu.co
Lucy Gwen Gillis
lucy.gillis@leibniz-zmt.de

Specialty section:
This article was submitted to Marine Ecosystem Ecology, a section of the journal Frontiers in Marine Science

Received: *07 February 2020*
Accepted: *09 July 2020*
Published: *29 July 2020*

Citation:
Guerra-Vargas LA, Gillis LG and Mancera-Pineda JE (2020) Stronger Together: Do Coral Reefs Enhance Seagrass Meadows "Blue Carbon" Potential? Front. Mar. Sci. 7:628. doi: 10.3389/fmars.2020.00628

Seagrass meadows are important for carbon storage, this carbon is known as "blue carbon" and represents a vital ecosystem service. Recently there has been growing interest in connectivity between ecosystems and the potential for connected ecosystems to facilitative ecosystem services. Tropical seagrass meadows are connected to coral reefs, as the reef barrier dissipates waves, which facilitates sediment accumulation and avoid erosion and export. Therefore, coral reefs might enhance the seagrass meadows capacity as a blue carbon sink. We tested this hypothesis through an assessment of blue carbon across a gradient of connected seagrass meadow and coral reef sites. We assessed attributes of seagrass meadows along a transect in addition to classifying the sites as exposed and sheltered. Classification of sites was completed through analyzing wave crest density in photographs and using granulometric evenness index. Organic carbon and organic matter were measured in sediment core samples and within seagrass living biomass (both above and below ground). Lastly, we measured changes in above and below ground traits of seagrass plants across the same sites. Gaps in the reef barrier were linked to high wave disturbance and exposed conditions, whilst barrier continuity to low wave disturbance and sheltered conditions. Organic carbon in sediments was 144 Mg ha^{-1} in the most sheltered (with reef barrier) and 91 Mg ha^{-1} in the most exposed (without reef barrier) meadows. Sheltered conditions also showed a redistribution of seagrass biomass to a greater quantity of roots compared to rhizomes. Whilst in exposed conditions the opposite occurred, which could be due to increased rhizome biomass have to enhanced anchorage or greater nutrient availability. This study found that coral reefs facilitate blue carbon potential in seagrass meadows indicating that coral reefs support this important ecosystem service. Also, results suggest that loss of coral reef structure due to bleaching and other stressors will likely result in a reduction of the blue carbon

storage capacity of adjacent seagrass meadow. Further research should investigate how combined global and regional stresses may impact on the potential for coral reefs to buffer seagrass meadows, and how these stresses affect the functional traits of seagrass plants.

Keywords: organic carbon stock, Caribbean, connectivity, ecosystem service, reef lagoon, living biomass, sediments, *Thalassia testudinum*

INTRODUCTION

Seagrass meadows are dominated by ecosystems engineering plants. These ecosystems have among the highest carbon sequestration rates in the sediments across natural-systems and store organic carbon in their living biomass (Mcleod et al., 2011; Fourqurean et al., 2012a). Seagrass meadows are distributed worldwide across a wide range of geomorphic settings and high deviations of organic carbon stock are observed among regions. For example, in the western tropical Atlantic or the Great Caribbean region, seagrass meadows present different environmental settings, ranging from estuarine and continental coastal settings to oceanic and oligotrophic settings as observed in small and remote islands and atolls. Atolls generally have a connected seascape with contiguous seagrass meadows, coral reefs and mangrove forests (Bouillon and Connolly, 2009; Gillis et al., 2014a; Gullström et al., 2018). These differences in physical attributes alter the carbon stock potential of the seagrass meadows.

Organic carbon (Corg) is stored in seagrass plants in two carbon pools: aboveground (AG-) or belowground (BG-) biomass pools (Fourqurean et al., 2012a; Duarte et al., 2013). Carbon in the living biomass of seagrass plants is usually higher in the below ground compartments (rhizomes and roots) than in the above ground compartments (leaves) (Fourqurean et al., 2012a). Seagrass plants are plastic (Arellano-Méndez et al., 2011; McDonald et al., 2016; Barry et al., 2018) and their AG and BG biomass will vary depending on different environmental conditions, like hydrodynamics or nutrients availability. For example, the growth of seagrasses and, therefore, their ability to transform CO_2 into organic carbon is conditioned by the availability of nutrients (Lee et al., 2007; Burkholder et al., 2007) and light (Alcoverro et al., 1995; Collier et al., 2007). An increase in nutrient availability enhance the increase in the ration AG/BG, favoring the sequestration of CO_2 in the above ground biomass pool compared to below ground biomass (Lee and Dunton, 2000; Medina-Gómez et al., 2016). Research in seagrass meadows has shown that increased water flow decreases leaf length to reduce drag force (de los Santos et al., 2016), which would alter carbon stock in the AG. Changes in AG and BG biomass of seagrass plants not only alter organic carbon within the plant but can affect their ability to attenuate waves and enhance organic carbon retention function whilst reducing sediment bed erosion (Duarte et al., 2005, 2013). Seagrass are exposed to the effects of wave energy on their canopies and sediments (Koch et al., 2006). Wind waves generate orbits in seawater column that transmit energy from the sea surface to the bottom. These cause more friction and sediment transport on the sediment bottom in shallow meadows than in the deep meadows. Seagrass and sediments in shallower meadows would be more exposed to disturbance than deeper ones. Physical variables like sediment texture can be used to relate bottom hydrodynamics with sediment type (Paterson and Black, 1992; Wentworth, 1992). Allochthonous organic matter that accumulate in the sediments of seagrass meadows is an important source that contributes significantly to soil Corg stocks as has been demonstrated by Kennedy et al. (2010), using a carbon isotopic approach. The natural trapping capacity of seagrass meadows could be facilitated by the buffering capacity of connected coral reefs, which reduce hydrodynamics allowing for sediment deposition and sediment erosion prevention (Koch et al., 2006; Gillis et al., 2014b).

Coral reefs protect and mitigate effects of normal hydrodynamics (wind and waves) and storm conditions on seagrass meadows and the reef lagoon (Gillis et al., 2014a; Guannel et al., 2016). Sheltered conditions could enhance the particulate organic matter and sediment trapping effects by seagrass canopies, facilitating the storing of organic carbon in seagrass sediments (Gillis et al., 2014b; Guannel et al., 2016). Additionally, Corg in seagrass living biomass may be protected from hydrodynamic damage; therefore, seagrass material export may be reduced in comparison to high exposure conditions, which there is not a barrier coral reef (Folmer et al., 2012; Duarte et al., 2013; Guannel et al., 2016). There is a growing interest in connectivity between coral reefs and seagrass meadows as this connectivity is thought to enhance ecosystem services for the entire seascape (Saunders et al., 2014; Guannel et al., 2016; Gillis et al., 2017).

The blue carbon sink potential of seagrass meadows is considered one of their most important ecosystem services (Arias-Ortiz et al., 2018; Saderne et al., 2019) as this has the potential to mitigate global climate change (Fourqurean et al., 2012a; Serrano et al., 2019). Given that coral reefs in the tropics often occur adjacent to seagrass meadows, they may play an important role in enhancing seagrass blue carbon potential. But there is little understanding of the interactions between reef

Abbreviations: AG-SLB, aboveground – seagrass living biomass; AG-TLB, aboveground – *Thalassia testudinum* living biomass; BG-SLB, belowground – seagrass living biomass; BG-TLB, belowground – *Thalassia testudinum* living biomass; Corg, organic carbon; DBD, dry bulk density of sediments; Gl, biomass of green leaves in seagrass; *H'*, Shannon-Wiener index used to assess granulometric profile of sediments or evenness; LDW, linear density of wave's crest; MUD, sampling site in the island harbor; OM-LOI, organic matter percentage (in sediments) determined by loss on ignition method; OMsed, organic matter in sediments; OPR, sampling site in the marine protected area of Old Point Regional Park of Mangrove; PCV, physical-chemical variables; RCB, sampling site in Rocky Cay bay; Rh, biomass of rhizomes in seagrass; Ro, biomass of roots in seagrass; SLB, seagrass living biomass; SPB, sampling site in Sprat bay; TC, total carbon; TLB, *Thalassia testudinum* living biomass; TN, total nitrogen.

barrier continuity, their attenuation of waves and organic carbon stock of seagrass meadows. Gaps and openings in a reef barrier are common in reef lagoons in the Caribbean. It is important to quantify the potential of Corg sequestration in associated seagrass meadows and sediments, and how it is affected by the disturbance factors linked to wave exposure (Koch et al., 2006; Folmer et al., 2012). Additionally, there are important knowledge gaps on how seagrasses adapt their organs (modules) to local environments (habitats) shaped by the physical conditions promoted by wave attenuation of the reef barrier (Christianen et al., 2013; Lavery et al., 2013; de los Santos et al., 2016).

This study hypothesizes that different wave exposures caused by discontinuous coral reef barriers impact seagrass organic carbon stocks. In particular it is expected that zones under sheltered conditions will increase organic carbon stocks in seagrass biomass and sediments compared to exposed ones. To answer this hypothesis, the study was conducted in the coral reef lagoon of San Andreìs, in the southwestern Caribbean, which has a discontinuous reef barrier located from north to south leading to different waves exposures. Under this rationale we chose seagrass sites with different levels of exposure to waves within the reef lagoon, sheltered or no from the coral reefs. This study goes beyond describing seagrass meadows as a carbon sink and attempts to explain the drivers of seagrass organic carbon storage potential in relation to physical attributes such as exposure to waves. This will improve the current knowledge of carbon stock potential in seagrass meadows at the seascape scale and establish further important facilitative connections between coral reefs and seagrass meadows.

MATERIALS AND METHODS

Study Area

The study was conducted in San Andrés; a small oceanic island located 80 km from the Caribbean coast of Nicaragua and 775 km from the Colombian coast, N 12° 32′ and W 81°43′, in the southwestern Caribbean (IGAC, 1986; **Figure 1**).

San Andrés has a monomodal rainfall pattern. The rainy season is from May to December, with maximum rainfall in October and November. The dry season is from February to April. In the dry season the island has strong trade winds ("Alisios") from the north east. The island is a calcareous sedimentary and karstic formation, elongated from north to south, with a maximum length of 12.5 km and 3 km width. The location of our study was in the reef lagoon on the east coast of the island (**Figure 1**). There are at least 316 ha of seagrass meadows inside the lagoon, and 24 ha in the west coast of island (Guerra-Vargas and Guerra-Vargas, 2017).

Four species of seagrasses have been reported within the lagoon: *Thalassia testudinum* KD Koening 1805, *Syringodium filiforme* Kützing 1860, *Halodule wrightii* Ascherson 1868 and *Halophila decipiens* Ostenfeld 1902, but *T. testudinum* is the most common and dominant seagrass in the area (Díaz et al., 2003).

Within the reef lagoon, four sampling sites in the seagrass meadows, under a different level of exposure to wave energy due to continuity discontinuity characteristics of the reef, were selected. From north to south of the lagoon, these sampling sites are: SPB, Sprat bay; MUD, in the island harbor; OPR, in the marine protected area of Old Point Regional Park of Mangrove; and RCB, in Rocky Cay bay (**Figure 1**). To increase the representativeness within the sampling sites, sampling depth stations were distributed in a balanced number in three intervals of depth in this way: (1) Deep water (4–10 m), (2) Mid water (2–4 m), and (3) Shallow water meadows (0–2 m). These sampling stations quantified the effect of exposure on Corg stock to waves along changes in the depth. The study was conducted over two periods: rainy season (September–November) in 2016 and dry season (January-March) in 2017.

At each sampling sites, hydrodynamic energy and nutrient availability were measured as potential drivers of Corg stocks in seagrass sediments and biomass.

Hydrodynamic Energy

Hydrodynamic energy disturbance per sampling site was assessed through an analysis of the linear density of wave's crest (LDW, crest m^{-1}). To measure disturbance linked to wave intensity, a total of 22 available aerial photographs from 1974, 1980, 1984, and 1996, taken in different seasons, were analyzed (Source: Instituto Geográfico Agustín Codazzi). Wave's crests in ten transect of 500 m were measured in the four sampling sites: SPB, MUD, OPR, RCB (**Figure 2**). Transects were geo-positioned inside 2.5 km^2 rectangles located in the same sampling sites in the four sets of aerial photographs. Directions of the wave's train (e.g., white arrows in **Figure 2**) were defined within rectangles. Transects were plotted parallel crossing the waves train and orthogonal to the first crest. The next step was to count the number of waves crests on each transect. LDW (crest m^{-1}) is a proxy of disturbance factor because waves break at the reef barrier, dissipate energy and are refracted and diffracted to new directions. Waves increase the number of crests in a line in the same direction of their movement (Harris et al., 2018).

Nutrient Availability

In September of 2016, seawater samples were obtained in the four sampling sites (SPB, MUD, OPR, and RCB). Samples of 500 ml were collected in shallow, mid and deep-water sampling stations in the seagrass meadows directly under the seagrass canopy. Samples were stored on ice and transported to the CORALINA (Corporation for Sustainable Development of the Archipelago) laboratory. The seawater was analyzed using the standard methods of American Public Health Association [APHA] (1992), to determine nitrate, nitrite, ammonium, phosphate and sulfide concentrations (mg l^{-1}) by colorimetric protocols. Nitrate, nitrate, nitrite, ammonium, phosphate and sulfide concentrations were documented to characterize seawater properties and test the limitation of nitrogen in the water column over seagrass meadows.

Soil Biogeochemical Properties

Soil Organic Matter and Organic Carbon Content

Three seagrass sediment cores per depth station and per sampling site were extracted using a PVC pipe of 30 cm length and

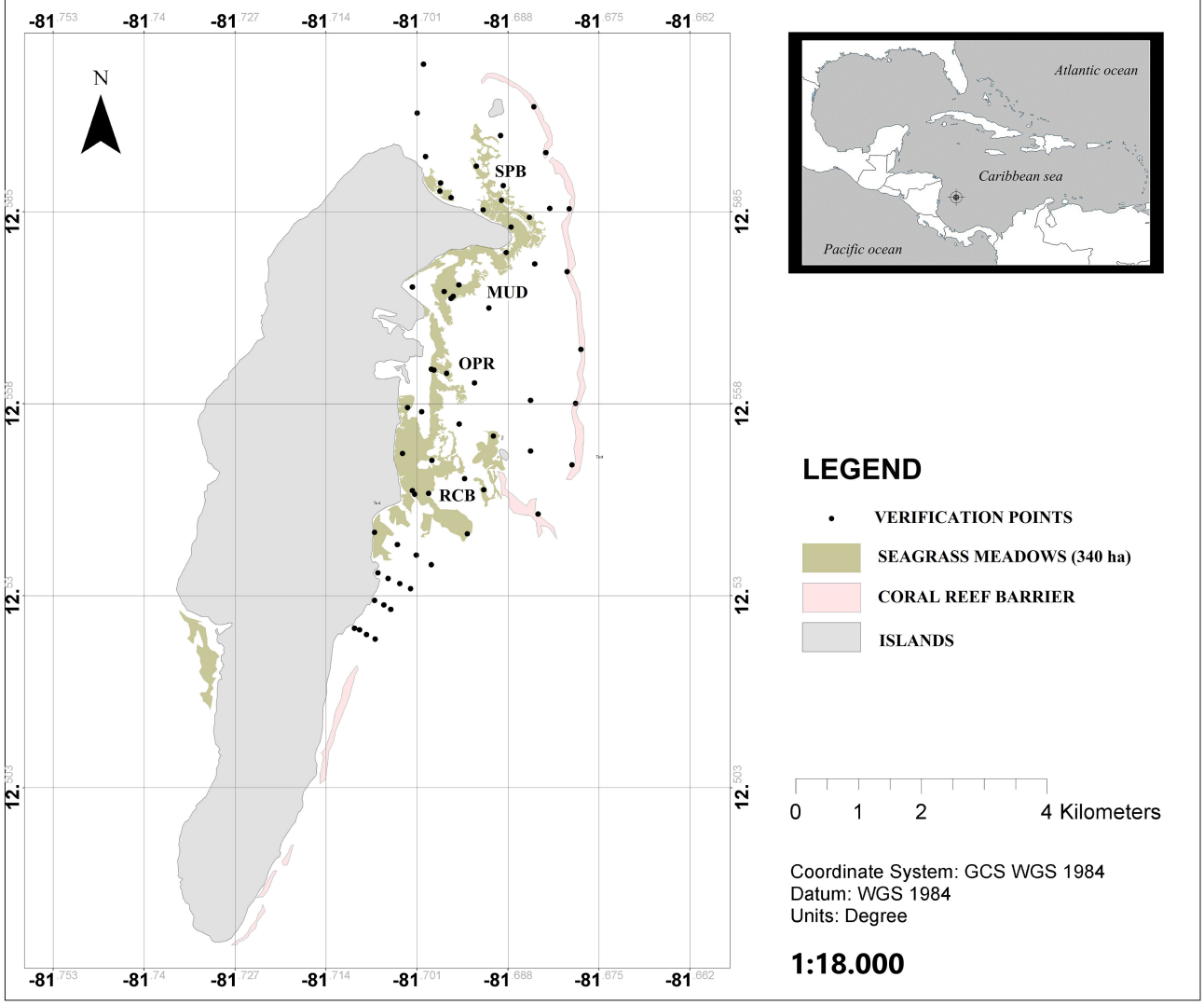

FIGURE 1 | Seagrass meadows in San Andrés island, mapped as green patches. The pink patches are the coral reef barriers. The black circles represent the sampling points used to verify seagrass cover. The four sampled locations are shown on the map; SPB, Sprat bay; MUD, in the island harbor; OPR, in the marine protected area of Old Point Regional Park of Mangrove; and RCB, at Rocky Cay bay. This figure was modified from Guerra-Vargas and Guerra-Vargas (2017).

10.16 cm diameter. So a total of 36 cores were taken for both seasons. Cores were transported on ice to CORALINA's laboratory, where they were frozen for later analysis. In the laboratory, cores were defrosted, and sediments and seagrass plants were separated from other material. The first 10 cm of substrate was excluded to achieve a better comparability among sampling zones and control the effects of biota and recent erosion in that sediment layer. Sediments were homogenized and subsamples were taken to determine organic matter content in sediments (OMsed). OMsed were calculated in sediments samples taken in the wet season of 2016. Dry weight of sediments was determined after 72 h drying at 60°C. Organic matter percentage in sediments (OMsed) was measured using the loss on ignition method (LOI), where mass of volatile organic matter was subtracted from the sediments after burning them in a furnace for 6 h at 450°C. OMsed was determined using this formula:

$$OMsed = \frac{Dry\ weight\ of\ sediments - ashes\ weight\ after\ LOI}{Dry\ weight\ of\ sediments} \times 100\%$$

Organic matter percentage in sediments was also used to calculate the Corg percentage (%) in the three replicate-cores of sediments per depth station (n = 36, only rainy season) using the equation proposed by Fourqurean et al. (2012a):

$$TOC = -0.21 + 0.40\ OMsed$$

For a detailed characterization of soil Corg stocks along the seagrass sediments depth profile, one additional sediment core

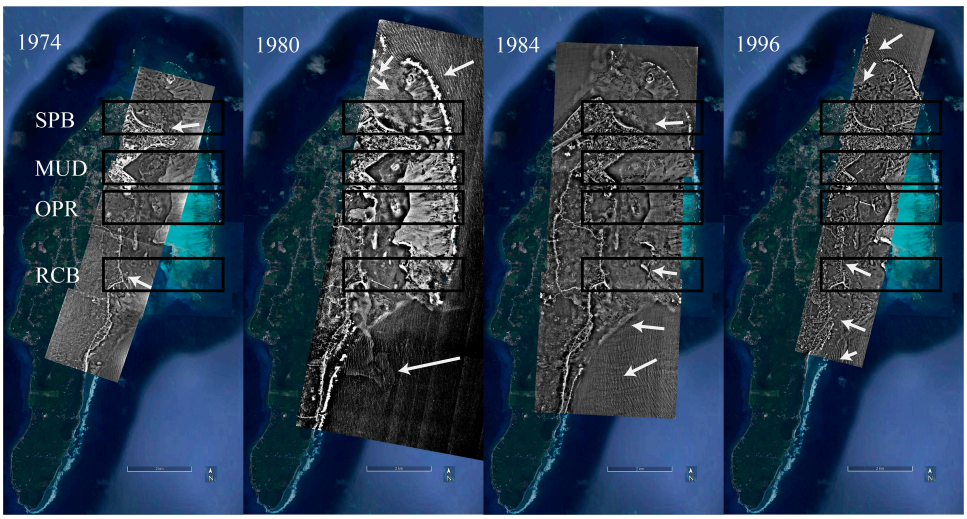

FIGURE 2 | Wave direction (white arrows) in sampling sites (black rectangles: MUD, island harbor; OPR, Old Point Regional Park of Mangrove; RCB, Rocky Cay bay; SPB, Sprat bay), using aerial photographs from the years 1974, 1980, 1984, and 1996 (Source: Instituto Geográfico Agustin Codazzi IGAC).

was extracted from each of the three depth stations at each of the four sampling sites (12 sediment cores in total) using a PVC pipe 30 cm length and 5.8 cm diameter. Cores were extracted in wet season of 2016. These pipes where subsampled with syringes at 5, 10, 15, 20, and 25 cm to determine volume (ml). Subsamples were then transported on ice to the marine biology laboratory of the Universidad Nacional de Colombia, where they were dried for 72 h at 60°C. Dry weights were calculated and means of DBD were obtained from each sampling site.

These subsamples were then transported to the chemistry laboratory of the Leibniz Center for Marine Tropical Research for the total Corg percentage (%) analysis using an elemental auto-analyzer (CN Analyzer Eurovector EA 3000). Then, Corg percentage in subsamples was used to characterize the organic carbon content in the study area.

Corg density (g cm^{-3}) in sediments was calculated in each sample multiplying Corg percentage (%) per DBD (g cm^{-3}). Corg density was multiplied by 100 to obtain top 1 m soil Corg stocks by surface area (g Corg cm^{-2}). Soil Corg stocks are provided in Mg Corg ha^{-1} units (Howard et al., 2014).

Sediment Grain Size

Sediment grain size was determined to support hydrodynamic energy assessment. Granulometric analysis were performed in 200 g (wet weight) sediment subsamples extracted from the soil cores depth fraction between 10 and 20 cm, sampled in both the wet and the dry season. Sediments between 10 and 20 cm depths were treated with sodium hexametaphosphate $(NaPO_3)_6$ 6% (p/v) for 24 h, then dried for 72 h at 60°C. Sediments from the first 10 cm of depth were rejected from the analysis to subtract effects of biota and recent sediment erosion on this layer. Sediments were homogenized and 100 g of dry weight per sample was taken to determine the percentage of the dry weight in seven sediment size ranges, using six sieves following standard grain size ranges (Wentworth, 1992). The smallest sediment grain size (<63 μm) or mud-like sediments were used to assess differences among the sampling periods (dry or wet season), sites and stations. Seven sediment grain size ranges were observed in all the samples. The Shannon-Wiener index (*H'*) was used to assess the granulometric evenness in the sediments:

$$H' = -\sum_{i=1}^{S} (p_i \times log_2 p_i)$$

Where *S* is seven sediment types and it was constant in all samples. Variations in evenness index are attributable to *pi*, or the proportion of dry weight in each assessed sediment type in 100 g of sediments. Granulometric *H'* is close to zero if a sediment type dominates the others and it has a maximum value (*H'* = 2.81 bits) when all sediment types are the same proportion. Grain size analysis using *H'* and proportion of mud-like sediments were used to verify seagrass sediment exposure to waves. Higher granulometric evenness and higher proportions of mud-like sediments are expected in sites where low exposure to waves occurred (Paterson and Black, 1992; Folmer et al., 2012).

Seagrass Biomass

Seagrass biomass were collected over the two sampling seasons (rainy and dry), using PVC corers of 30 cm length and 10.2 cm diameter in the four sampling sites and their three depth stations (**Figure 1**). Three cores were collected per depth station (n = 36 cores, per season). Seagrass living biomass (SLB) was separated from the other material in these cores. SLB was treated with HCl 8% (v/v) to remove carbonates and epiphytes; the SLB was then rinsed in water and classified by seagrass species. Each plant was classified by modules: green leaves (Gl), living rhizomes (Rh) and roots (Ro). Dry weight was determined after seagrass biomass modules were dried at 60°C during 72 h. Rhizomes and roots dry weight (Mg Dry Weight ha^{-1}) was pooled as

belowground (BG-) SLB. Green leaf dry weight was classified as aboveground (AG-) SLB.

Thalassia testudinum is the dominant specie in the area, therefore *T. testudinum* living biomass (TLB) was assessed independently to other species and separated as aboveground *Thalassia* living biomass (AG-TLB) and belowground *Thalassia* living biomass BG-TLB. Dry weight was determined after seagrass samples were dried at 60°C, over 72 h. For the AG-TLB the epiphytes were removed using a razor blade after drying and before the dry weight was measured. Samples from the rainy season were used to determine organic matter (%) in seagrass plants using the LOI method. This method destroys samples. Therefore, samples from the dry season were used to determine percentages of Corg and TN in TLB, using the CN Analyzer Eurovector EA 3000 in the ZMT's chemistry lab. Fifteen random samples of *T. testudinum* were selected across all sampling sites in the dry season, to determine TC, TOC, and TN, and to estimate the mean of these in the study area, and to verify changes in the means of these variables among *Thalassia* organs (green leaf, rhizomes, and roots). Additionally, a 0.34 coefficient was used to estimate organic carbon in seagrass stocks (Duarte, 1990), based on the equation:

$$Corg\ stock = SLB \times 0.34$$

Where *SLB* is seagrass living biomass and Corg stock represents the carbon stock within the seagrass biomass.

Statistical Analysis

Non-parametric analysis of data was used because the data did not fit assumptions required for parametric testing. Two tests were applied according to the objectives of assessing seasonality effects (Wilcoxon test) or spatial/wave exposure effects (Kruskal-Wallis test) on seagrass and sediment variables.

The Wilcoxon test can be used as an alternative non-parametric analysis between similar means from two groups from the same variable using the Student's *t*-test. Seasonality effects were assessed in proportions of mud-like sediments (grain size < 63 μm, %) and granulometric evenness index (*H'*, bits), seagrass living biomass (SLB) and *Thalassia testudinum* living biomass (TLB) in their aboveground and belowground pools.

The Kruskal-Wallis test (K-W test) compares ranks among four sampling sites. To analyze differences between Linear density of wave's crest, a Kruskal-Wallis Rank Sum Test (K-W test, X^2) was applied to compare ranks among Old Point Regional Park of Mangrove (OPR), Rocky Cay bay (RCB) and Sprat bay (SPB) from 1996 data. Nemenyi's (*post hoc*) test were applied to differentiate exposure to wave (Exposure levels). To analyze differences between nitrate, phosphates and sulfide in seawater, we compared ranks among sampling sites: MUD, OPR, RCB and SPB using the K-W test and the Nemenyi's test for each variable. The K-W test and Nemenyi's test were applied to assess effects of reef barrier in seagrass meadows variables, both in sediments and in biomass. Sediment variables analyzed were mud-like sediments, granulometric evenness index, organic matter in sediments (OMsed, %) and dry bulk density (DBD, g cm^{-3}). Biomass variables were seagrass living biomass (SLB) and *Thalassia testudinum* living biomass (TLB), their aboveground (AG) and (BG) belowground pools, and their organic matter (%).

To analyze differences based on ratio among AG and BG pools in SLB, a descriptive approach was used with biomass of green leaves (AG), rhizomes and roots (BG). To assess disturbance factor on seagrass plants variables using the depth factor, a descriptive analysis was applied to compare sampling depth stations using seagrass plants and sediment variables. Seagrass plant variables considered were BG-SLB and BG-TLB. Sediment variables considered were organic carbon stock (Mg Corg ha^{-1}), organic matter (OMsed, %), granulometric evenness *H'* index and mud-like sediments.

Principal Coordinate Analysis (PCA) was used to establish dissimilarities in hydrodynamic conditions across sampling depth stations, based on sediment granulometric profiles. To assess dissimilarity on grain size profile in sediments among the four sampling stations, seven sediment variables were used (as ranges factors of grain size: >2, 2–1, 1–0.5, 0.5–0.25, 0.25–0.125, 0.125–0.063, <0.063 mm) and their proportion of dry mass in 100 g of sediments (as magnitudes).

All tests were conducted in R 3.5.2 and R studio 1.1.463. The *post hoc* testing Nemenyi's All-Pairs Rank Comparison Test (Nemenyi's test) was applied using the PMCMR plus package in R. Principal Coordinate Analysis (PCA) was conducted with this data in Primer v6.1.11 and PERMANOVA+ v1.0.1.

RESULTS

Hydrodynamic Energy

From 1974 to 1984, a comparison of means was only possible between two sampling sites Sprat bay (SPB) and Rocky Cay bay (RCB) because wave crests were not detected in the island harbor (MUD) and Old Point Regional Park of Mangrove (OPR) (**Table 1**). In the photographs from 1996, significant differences were observed among three sampling sites (OPR, SPB and RCB; K-W test, $X^2 = 23.3$, $p < 0.01$). *Post hoc* testing showed OPR was statistically higher than SPB and RCB (Nemenyi, $p < 0.05$). Comparison of means along the four periods suggest three levels of exposure to waves: I lesser exposed conditions (in MUD), II intermediate exposed conditions (in OPR) and III higher exposed conditions (in both RCB and SPB).

Nutrient Availability

In all sampling points dissolved ammonium and nitrite concentration were below the detection limits of the methods (<0.02 mg l^{-1}). Phosphate concentration was in a range of 0.02 to 0.2 mg l^{-1}; nitrate in a range of 0.019 to 0.09 mg l^{-1} and sulfide in a range of 6.3 to 9.9 mg l^{-1} at all sampling points (**Supplementary Table S1**). No significant difference was seen between sampling sites, for sulfide or phosphate (**Supplementary Table S1**).

Soil Biogeochemical Properties

Proportions of mud-like sediments (grain size < 63 μm) showed no significant difference between sampling seasons (Wilcoxon test, $V = 223$, $p > 0.05$, $n = 36$). Similar results were obtained

TABLE 1 | Mean waves crest per meter in sampling sites (MUD, island harbor; OPR, Old Point Regional Park of Mangrove; RCB, Rocky Cay bay; SPB, Sprat bay), using available aerial photographs for the years 1974, 1980, 1984, and 1996.

Year	Sampling sites				Number of photographs	Flight	Scale
	MUD (crest m^{-1})	OPR (crest m^{-1})	RCB (crest m^{-1})	SPB (crest m^{-1})			
1974	0	0	0.06 ± 0.01	0.13 ± 0.03	14	C- 1533	1:10 350
1980	0	0	0.07 ± 0.01	0.13 ± 0.01	6	C- 1956	1:31 000
1984	0	0	0.04 ± 0.01	0.13 ± 0.01	9	C- 2123	1:20 600
1996	0	0.27 ± 0.04	0.15 ± 0.01	0.12 ± 0.02	16	R- 1195	1:10 900
Mean	0	0.27 ± 0.04	0.08 ± 0.05	0.13 ± 0.02			
Exposure	I	II	III	III			

All the values are means of the ten transects ± SD per sampling site. Island harbor (MUD) and Old Point Regional Park of Mangrove (RCB) presented values below detection limits ("0" values). Aerial photographs and their references in the files of the Instituto Geográfico Agustin Codazzi includes the number of photographs, their file ID (Flight) and their geographical scale. Exposure to waves are included as levels from minimum (I) to maximum (III).

using the granulometric evenness index (*H'*) between sampling seasons (V = 378, $p > 0.05$, n = 36). The pooled mud-like sediments, *H'* and organic matter in sediments (OMsed) showed significant differences among sites (**Table 2**). However, dry bulk density (DBD) in sediments showed no significant difference among sampling sites during the rainy season (**Table 2**). Principal coordinates analysis applied to the seven ranges of grain size proportions in sediments results in higher dissimilarities among RCB and SPB shallow water sampling stations compared to others except for the SPB mid water station (2–4 m) (**Figure 3**).

Sediment organic carbon stock has variations within the study area, less exposed and intermediate sites MUD and OPR showed higher sediment organic carbon stocks than more exposed sites SPB and RCB (**Figure 4**). Organic carbon (OC) stocks varied from 122.2 (SD = 9) to 226.9 (SD = 32) Mg Corg ha^{-1} being maximum in MUD and minimum in SPB. OC stock (Mg Corg ha^{-1}) and organic matter (%) in sediments were analyzed along the sampling depth stations per site (**Figure 5** and **Supplementary Table S3**). Both variables showed lower values in the mid (RCB2 and SPB2) and shallow (RCB3 and SPB3) water stations in exposed sites. RCB and SPB sites tended to decrease sediment organic carbon stock and organic matter as the same time as depth decreased.

Seagrass Species

In the study area, three species of seagrasses were found: *Thalassia testudinum* K. D. Koening 1805, *Syringodium filiforme* Kützing 1860, and *Halodule wrightii* Ascherson 1868. Only *T. testudinum* was present at all depths in all sampling sites, while *H. wrightii*, was only observed in SPB2 (mid water sampling station) and *S. filiforme* was absent in MUD1 (deep water station) and RCB2 (mid water station). *Thalassia testudinum* dominated total living biomass of seagrasses (mean 81%, SD = 0.2, n = 72). Therefore, the results obtained in seagrasses living biomass (community scale) and in *T. testudinum* living biomass are presented below independently. *Halophila decipiens* Ostenfeld 1902 was not observed in the sampled meadows.

Seagrass Living Biomass Among Sampling Periods

Significant differences were found in seagrass living biomass (SLB), *T. testudinum* living biomass (TLB), aboveground seagrass living biomass (AG-SLB), aboveground *T. testudinum* living biomass AG-TLB and belowground seagrass living biomass (BG-SLB) across seasons (**Supplementary Figure S1** and **Supplementary Table S4**). Yet no significant difference was seen in belowground *T. testudinum* living biomass across seasons (BG-TLB). Seagrass biomass was always higher in the dry season compared to the rainy season, and this is attributed to the aboveground pools in SLB (**Supplementary Figure S1**). Data were separated by seasons and comparison among sampling sites were conducted (**Supplementary Tables S5, S6**). In both seasons, significant differences in *T. testudinum* living belowground biomass (BG-TLB) across sampling sites, being significantly higher in MUD than in RCB. These differences were attributed to low values in BG-TLB at RCB2 (mid water sampling station) (**Supplementary Tables S5, S6**). Seagrass in the less exposed site (MUD) invested greater biomass in roots than rhizomes in comparison to the other sites where levels of wave exposure were higher (**Figure 6A** and **Supplementary Table S7**). In contrast RCB and SPB had Rh:Ro ratios, which were higher than sites MUD (**Figure 6A** and **Supplementary Table S7**), suggesting that these sites had higher root and belowground biomass with respect to green leaf biomass (**Figures 6B,C**). The descriptive comparison between the ratios showed differences in the distribution of seagrass biomass between their belowground modules (**Supplementary Table S7**).

Organic Matter, Total Organic Carbon and Total Nitrogen in Seagrass Biomass

Organic matter in seagrass living biomass (SLB) and *T. testudinum* living biomass (TLB) showed significant differences among sampling sites for the majority of variables in the rainy season (**Supplementary Table S8**). In AG-SLB and AG-TLB no significant difference was seen (**Supplementary Table S8**). *Post hoc* testing indicated significant differences are attributed to MUD. This sampling site had lower means of organic matter percentage than SPB and OPR. Mean of Corg percentage (%) in the *T. testudinum* organs (34.1 ± 4%) was similar to Duarte's coefficient (34%) used by Fourqurean et al. (2012a) to estimate Corg stock in SLB (**Supplementary Table S9**). Estimated organic carbon stock in seagrass biomass in the study area was 2.4 Mg Corg ha^{-1} (**Supplementary Table S10**).

TABLE 2 | Mean of sediment variables in sampling sites (MUD, OPR, RCB, and SPB). Mud-like sediments (<63 μm) and Granulometric *H'* values are means of 18 replicates.

	Sampling sites					
Variable	**MUD**	**OPR**	**RCB**	**SPB**	**Kruskal Wallis ($p < 0.05$)**	**Nemenyi's *post hoc* ($p < 0.05$)**
Sediments < 63 μm (%)	8.8	5.0	5.2	2.1	$X^2 = 27.4$, $df = 3$, p < 0.00	MUD > SPB; OPR > SPB
±SD	4.5	2.5	3.7	2.2		
Granulometric *H'* (bits)	2.6	2.6	2.3	2.1	$X^2 = 20.4$, $df = 3$, $p < 0.00$	MUD > RCB; MUD > SPB
±SD	0.10	0.08	0.3	0.4		OPR > RCB; OPR > SPB
Organic matter (%)	3.8	3.5	3.0	2.4	$X^2 = 25.2$, $df = 3$ $p < 0.00$	MUD > SPB; OPR > SPB
±SD	0.5	0.9	0.2	0.2		
Dry bulk density (g cm^{-3})	1.7	1.6	1.5	1.6	$X^2 = 2.2$, $df = 3$, $p = 0.5$	NA
±SD	0.1	0.3	0.2	0.1		
Exposure	I	II	III	III		

Sediment organic matter values are means of nine replicates. Dry bulk density values are means of three replicates. Significant pair comparison using the Nemenyi's post hoc test included. NA means not applicable. Exposure to waves levels is included (I, II, and III).

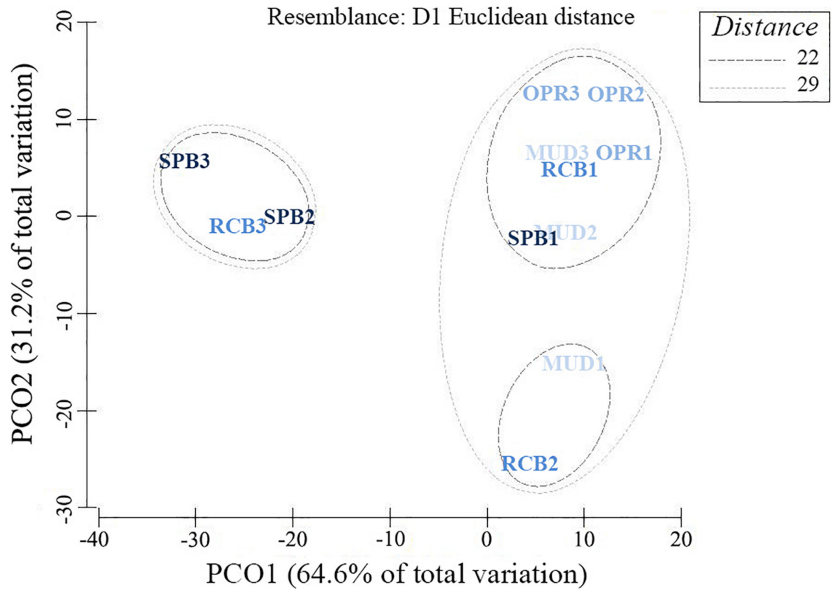

FIGURE 3 | Principal Coordinates Analysis using seven grain-size ranges and their proportion in 100 g dry weight of sediments. Sampling sites differentiated by colors (and exposure levels) as MUD (I), OPR (II), RCB (III) and; SPB (III). And sampling stations (depth factor) differentiated by numbers (site 1 as deep, site 2 as mid and site 3 as shallow water station). Resemblance values based on means from six replicates per sampling station (data from both seasons were pooled).

Depth Effects on Seagrass and Sediments Variables

As there were not significant differences in granulometry (evenness index *H'*), mud-like sediments percentage, SLB and TLB between seasons, the data of these variables were pooled to analyze the effect of depth (**Figure 7**). Descriptive comparisons among evenness index *H'* showed mid and deep-water sampling sites in RCB and SPB were lower in values compared to all sampling stations on MUD and OPR. Mud-like sediments showed the lowest values in the shallow water sampling stations on SPB and RCB, including mid water stations on SPB. Similar values between BG-SLB and BG-TLB were found among all sampling stations on MUD and OPR (**Figure 7**). But SPB and RCB indicated observable differences for BG-SLB and BG-TLB among their shallow and deep-water sampling stations. Except for MUD sampling stations, medians in sediment variables increased with depth whilst BG-SLB and BG-TLB decreased with depth (**Figure 5**).

DISCUSSION

Coral reef barriers and their continuous spatial distribution reflected and broke waves and mitigated wave's disturbance within the reef lagoon. However, gaps and openings at the north and south of the barrier promoted refraction processes and exposed conditions over seagrass meadows inside the reef lagoon. Sites with reduced disturbance enhanced seagrass meadow carbon accumulation in sediments, whilst sites with

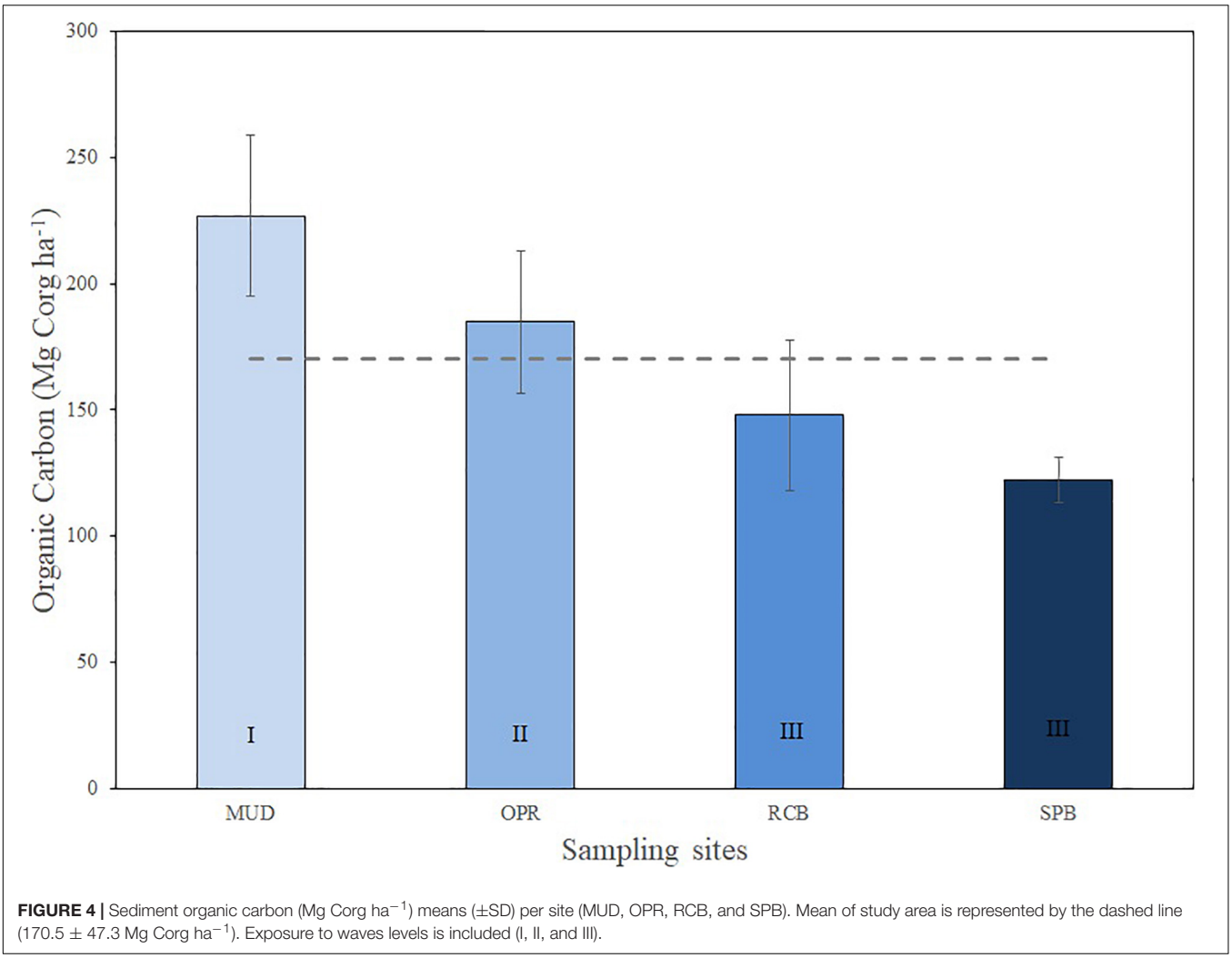

FIGURE 4 | Sediment organic carbon (Mg Corg ha^{-1}) means (±SD) per site (MUD, OPR, RCB, and SPB). Mean of study area is represented by the dashed line (170.5 ± 47.3 Mg Corg ha^{-1}). Exposure to waves levels is included (I, II, and III).

higher disturbance were related with lower organic carbon stock in meadow sediments (**Figure 8**).

This reef barrier function also increased organic carbon stock sequestered by seagrass living biomass in sheltered conditions. Additionally, these conditions promoted responses in *T. testudinum* and other seagrass plants, for example the redistribution of their biomass to rhizomes in exposed conditions (**Figure 5** and **Supplementary Table S7**). Disturbance is a key factor explaining differences in sediment variables inside the reef lagoon.

Wave Disturbance in Seagrass Meadows

Within the reef lagoon, four sampling sites in the seagrass meadows, under a different level of exposure to wave energy due to continuity discontinuity characteristics of the reef, were selected. From north to south of the lagoon, these sampling sites are: SPB, MUD, OPR and RCB (**Figure 1**). The wave's direction within the reef lagoon is from the east in the majority of cases. Differences in the linear density of waves crest among sampling sites were attributed to the coral reef barrier regulation effect (Lugo-Fernández et al., 1992; Hardy and Young, 1996; Ferrario et al., 2014; Harris et al., 2018). Areas where crests cannot be observed correspond with undistinguishable waves and therefore the lowest disturbance factor i.e., sheltered sites, this was found in harbor and Old Point Regional Park where the continuous barrier reduces wave energy in breaking waves. Sprat Bay and Rocky Cay Bay showed higher disturbance factors, because gaps in the barrier permitted waves to enter the reef lagoon and attenuation is lower than at the reef crest. These sites are referred to as exposed sites.

Patterns observed in sediment samples variables supported our classification of exposed or sheltered sites. Granulometric evenness (*H'* index) suggested disturbance factors modulate granulometry in seagrass sediments, where low disturbance factors in sheltered sites corresponds to more even sediment type distribution than in exposed sites (high disturbance), these sites also indicated a lesser capacity to conserve fine sediments than sheltered sites, because this function is modulated by disturbance linked to wave intensity (Folmer et al., 2012). In exposed sites, hydrodynamics were more energetic, and these conditions promoted sandy sediments transported close to the shore because wave action and shallow water currents have sufficient energy

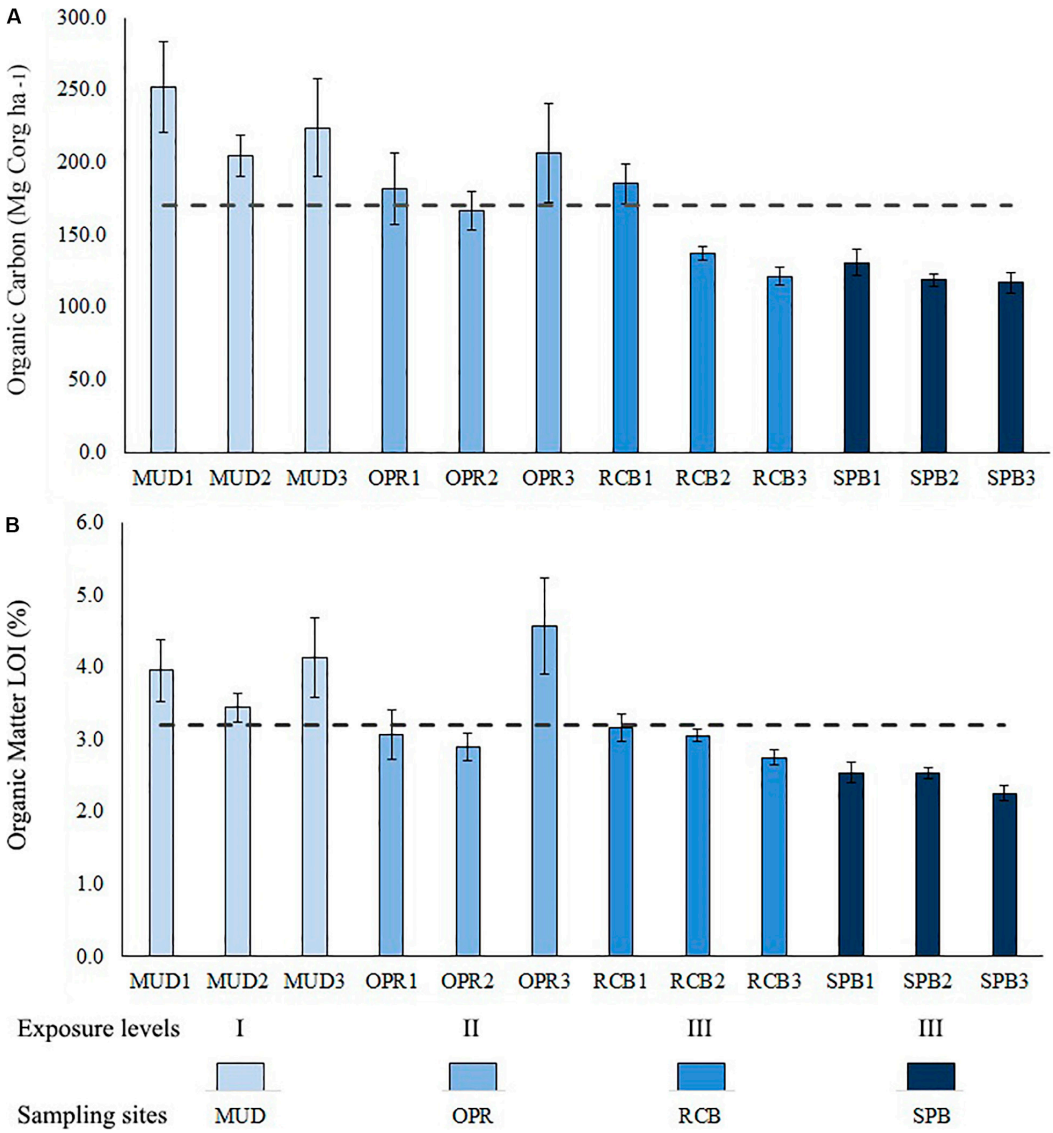

FIGURE 5 | Bar plot showing means (±SD) per depth stations (deep 1, mid 2 and shallow 3) per site (MUD, OPR, RCB, and SPB). **(A)** Sediment organic carbon (Mg Corg ha^{-1}). **(B)** Sediment organic matter (%) determined by LOI method. Means of study area are represented by the dashed lines. Exposure to waves levels is included (I, II and III).

to transport them (de Boer, 2007; Potouroglou et al., 2017). In these sites, medium size sediments dominated the granulometric profile and lower organic matter stock was observed.

Continuous Coral Reef Barrier Increases Sediment Organic Carbon

A vital ecosystem services coral reefs provide is to protect coastal areas from storm surges and hurricanes (Guannel et al., 2016). Within connected coastal seascapes they are also thought to alter hydrodynamic energy sufficiently to allow for establishment and expansion seagrass meadows require (Gillis et al., 2014a,b). Seagrass meadows themselves have been found to be globally important carbon sinks, due to ecosystem engineers (seagrass plants) reducing the water current to allow for carbon accumulation (van Katwijk et al., 2010; Lavery et al., 2013). In this research we have found for the first time, connected coral reefs and seagrass meadows also show enhanced sediment organic carbon. Coral reefs protect coastal areas from sediment erosion from strong hydrodynamics at a seascape scale (Saunders et al., 2014; Guannel et al., 2016). Additionally, coral reefs could prevent sediment erosion which also favors organic carbon burial and stock accumulation in the long-term at a more local scale.

Seagrass meadows within a reef lagoon play a functional role in conserving textural conditions in belowground top sediments (Duarte et al., 2005, 2013; Potouroglou et al., 2017). Sheltered sites tended to accumulate more mud-like sediments and consequently more organic matter in sediments

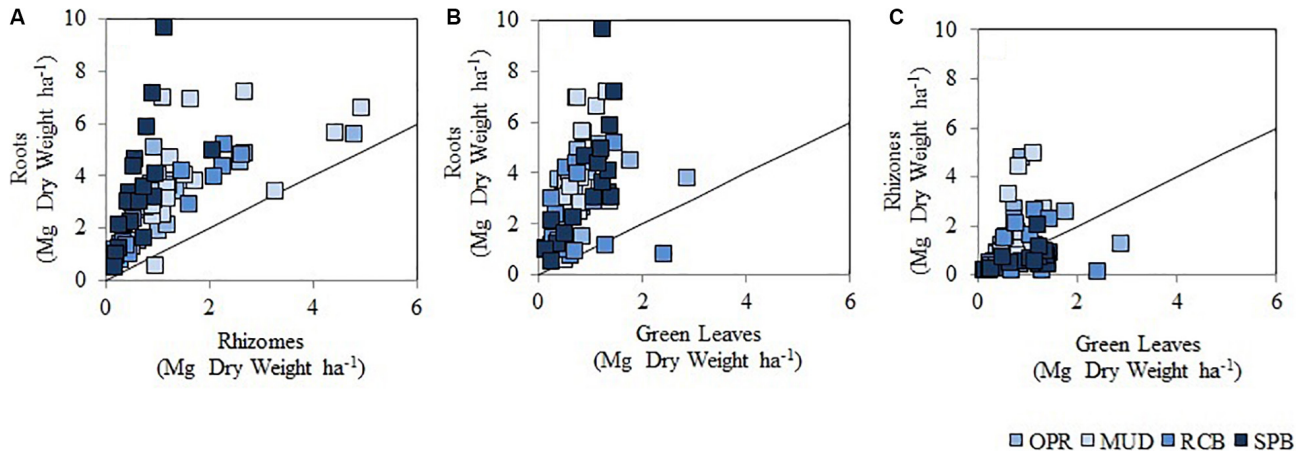

FIGURE 6 | Scatter plot showing living biomass in seagrass modules (all species pooled) in sampling sites. **(A)** It represents roots and rhizomes ratio (Ro:Rh), **(B)** it is roots and green leaves (Ro:Gl), **(C)** shows rhizomes and green leaves (Rh:Gl). Circles in colors respond to sampling sites and waves exposure levels as MUD (I), OPR (II), RCB (III), and SPB (III), from light blue to dark blue. There are 18 replicates per site, data from wet and dry season pooled. The black line indicates a 1:1 relation between the different seagrass modules.

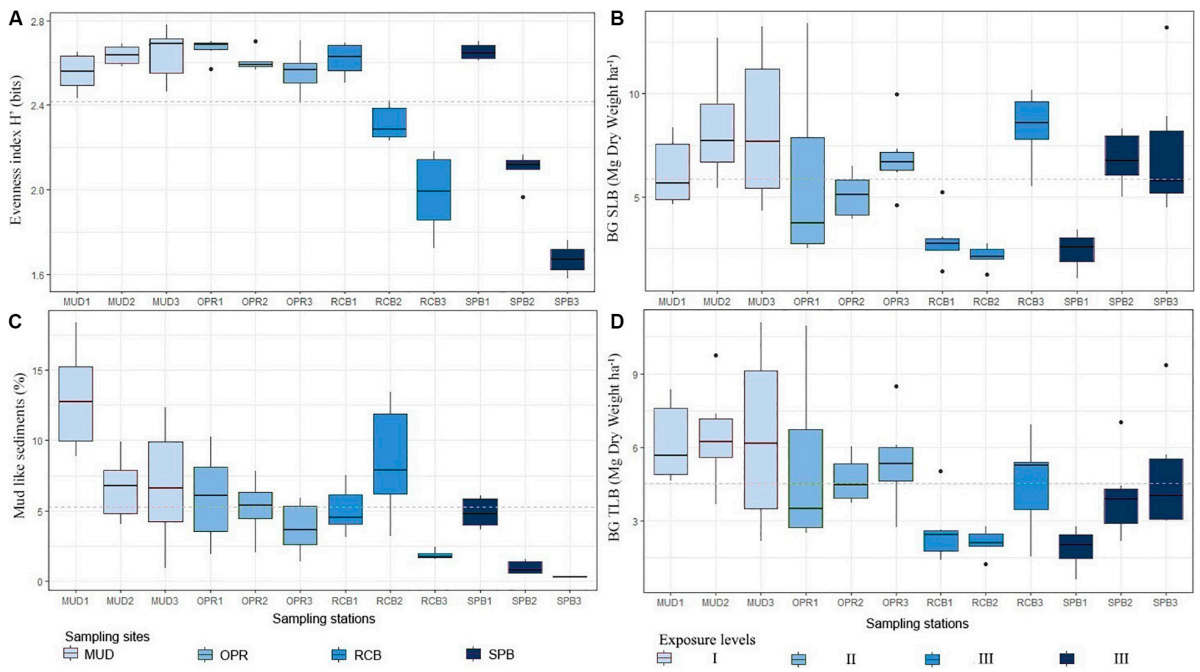

FIGURE 7 | Boxplots by sites (and exposure levels) MUD (I), OPR (II), RCB (III), and SPB (III) and by sampling stations (1 indicates deep water, 2 mid water and 3 shallow water meadows). **(A)** shows evenness index for granulometry profile *H'* (bits), **(B)** shows belowground seagrass living biomass (Mg Dry Weight ha^{-1}), **(C)** is percentage of mud-like sediments per 100 g of dry weight (%) and **(D)** is belowground *T. testudinum* living biomass (Mg Dry Weight ha^{-1}). Each box is based on six replicates per sampling station. Study area means are represented by dashed lines. Exposure to waves levels is included (I, II, and III).

than exposed sites (Folmer et al., 2012; Hossain et al., 2014). This was due to reduced wave intensity, and the disturbance factor had lesser effects on filter capacity of seagrass leaves. Fine sediments are a key factor for conserving organic matter and organic carbon in seagrass meadow sediments, because mud-like sediments prevent organic carbon resuspension and remineralization (Paterson and Black, 1992; Wentworth, 1992; van Katwijk et al., 2010; Folmer et al., 2012).

Our data showed organic matter and organic carbon in sediments had a higher mean in deep water meadows (>4 m depth) than shallow water meadows (<2 m depth) in exposed sites (**Figure 5**). Our data showed organic matter and organic carbon in sediments had a higher mean in deep water meadows

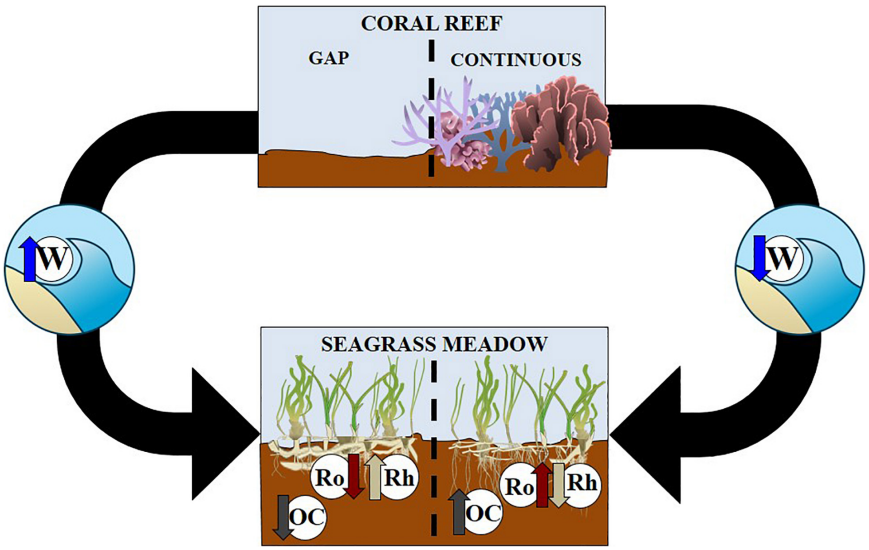

FIGURE 8 | Conceptual diagram showing connected seascape of coral reefs (upper section) and seagrass meadows (lower section). Black arrows indicate connections between coral reefs with a gap (left hand side) and continuous (right hand side) with seagrass meadows. Letters are as follows W is waves, OC is sediment organic carbon, Ro represents roots and Rh is seagrass rhizomes.

(>4 m depth) than shallow water meadows (<2 m depth) in exposed sites (**Figure 5**). Our data showed organic matter and organic carbon in sediments had a higher mean in deep water meadows (>4 m depth) than shallow water meadows (<2 m depth) in exposed sites (**Figure 5**). In this sense, our results differ from those reported in previous studies were authors found lower Corg stocks in deeper meadows compared to shallower ones due to a decrease in seagrass productivity and biomass associated to the decrease in light availability with depth (Alcoverro et al., 1995; Collier et al., 2007; Serrano et al., 2014). However, in tropical latitudes there is a high incidence of light throughout the year, in fact in seagrass meadows from San Andrés island, transparency is 100% up to at least 10 m depth for much of the year (Rodríguez et al., 2010). Thus, in the study area, deep meadows are not limited by light availability and differences in Corg stocks with depth are mainly due to different exposure to hydrodynamic energy.

A higher wave intensity and turbulence in shallow water meadows of exposed sites were linked to greater quantities of sandy sediments in the belowground pool and a reduction in organic matter in sediments. Particulate organic sediments could be more easily trapped in deeper than shallower seagrass meadows because the wave intensity on the seafloor bottom is reduced thus decreasing effects of turbulence and decreasing friction over deposited sediments (Bird, 1994; Folmer et al., 2012). Organic carbon stock in sediments are comparable with regional data from the tropical western Atlantic (**Figure 4** and **Supplementary Table S2**), which is the third highest among bioregions assessed by Fourqurean et al. (2012a). Organic carbon stock in MUD is similar to Corg stock in sediments in the tropical western Atlantic (150.9 ± 26.3 Mg Corg ha^{-1}) and the South Atlantic (137.0 ± 56.8 Mg ha^{-1}), but the other sites assessed in this study showed lower means.

Multi Effects on Seagrass Biomass Carbon Stocks

In this study we found differences across seasons for *Thalassia testudinum*, which has been observed in other studies (van Tussenbroek et al., 2014). Observed differences between *T. testudinum* above ground living biomass in both sampling periods (rainy and dry seasons) were attributable to increases in carbon biomass stock in sheltered sites. Similar to *T. testudinum* living biomass significant differences were observed between rainy and dry seasons for seagrass living biomass. Available data from the Caribbean monitoring of seagrass meadows suggest this oscillation is common and biomass tends to be higher in dry seasons compared to rainy seasons (Pérez et al., 2006; van Tussenbroek et al., 2014).

It was surprising to find no significant differences in values from *T. testudinum* for above ground living biomass among sampling sites, despite green leaves being the most vulnerable to changes in seawater conditions and disturbance factors (Hemminga and Duarte, 2000). However, there were significant differences in *T. testudinum* belowground living biomass related to disturbance factors and sediment variables. In exposed sites decreasing below ground biomass was observed whilst increasing depth correlated with greater biomass among sampling stations (**Figure 7**). The descriptive comparison between the ratios showed differences in the distribution of seagrass biomass between their belowground modules (**Supplementary Table S7**). When investigating further the ratio among living biomass in seagrass modules (roots to green leaves ratio) (**Figure 6** and **Supplementary Table S7**) it was double the biomass in sheltered sites. This indicates seagrass plants invest 2-fold in the biomass of roots for the majority of sheltered sites compared to exposed conditions. This may be because of two reasons.

First seagrass plants in exposed conditions developed greater biomass in rhizomes than in roots, as a strong mechanism is required to anchor in sandy substrate. RCB and SPB had Rh:Ro ratios, which were higher than sites MUD (**Figure 6A** and **Supplementary Table S7**). Rhizome to root ratio in exposed conditions seagrass indicated they invested greater quantities in rhizome than root biomass compared to sheltered conditions. Seagrass response to disturbance in sandy substrates was to produce more rhizomes for anchorage as in agreement with other studies (Hemminga and Duarte, 2000; Hizon-Fradejas et al., 2009). A similar pattern was also seen for depth across sites. Shallower meadows showed higher below ground living biomass than deeper meadows. Because disturbance effects of waves are more intense closer to the shoreline, seagrass therefore increase their belowground biomass (mainly as rhizomes) to tolerate this disturbance (Hemminga and Duarte, 2000).

The second reason is that sediment is richer in organic matter, which could be a source of nitrogen (Fourqurean et al., 2012b; Kindeberg et al., 2018). Data supported the hypothesis that there is low availability of nitrogen in the water column over assessed seagrass meadows (**Supplementary Table S1**). Seagrass in sheltered conditions could use roots to uptake nitrogen, from organic matter available in sediments to sustain biomass especially in oligotrophic seawater around San Andrés island (Gavio et al., 2010; Abdul aziz et al., 2018; **Supplementary Table S1**). Therefore, nitrogen in organic matter could be a source of nitrogen for seagrass plants under sheltered conditions, whilst in exposed conditions waves may facilitate nitrogen uptake from the surrounding water (**Supplementary Figure S2** and **Supplementary Table S11**). In these cases, stronger hydrodynamics are thought to allow for the reduction of the boundary layer thickness surrounding leaves which prevents them up-taking nutrients (Cornelisen and Thomas, 2004; Morris et al., 2008; Gillis et al., 2017).

CONCLUSION

Coral reefs facilitate blue carbon potential in seagrass meadows. Sediments in seagrass meadows protected by a reef barrier avoid erosion and enhance seagrass capacity to retain organic matter in soils. Loss of coral reef structure due to bleaching and other stressors will likely result in a reduction of the blue carbon storage capacity of adjacent seagrass meadow. Given that coral reefs and seagrass meadows in the tropics use to occur together (Huxham et al., 2018), this connective relationship between ecosystems could have global implications for carbon sequestration. Seagrass meadows in the reef lagoon showed a higher potential as a total carbon sink (**Figure 8**), in part because of inorganic sediments from coralline algae and coral fragments from the reef (**Supplementary Table S11**). This suggests these seagrass meadows potential function as an inorganic carbon sink and a particulate carbon filter, as they are retaining and trapping sediments richer in carbonates transported by bottom currents in the reef lagoon (Kennedy et al., 2010; Potouroglou et al., 2017; Saderne et al., 2019).

Here, we showed that traits of seagrass plants alter with exposed and sheltered sites (**Figure 6**), further research could contribute to this topic (Ackerly and Cornwell, 2007). Specifically, how traits may vary across different landscape gradients with different ecosystem matrixes. Traits are plastic and will be altered by environmental factors such as stress, which could come from global climate change or eutrophication. Monitoring programs in seagrass meadows addressing their integrity or health must also investigate measurements in the belowground pool, which are commonly evaded. New studies conducted in reef lagoons similar to this study must consider the high variability within the seagrass living biomass affected by factors as disturbance (wave's intensity), depth and distance to the shore. Studies need to be holistic and monitor the entire seascape; in this research we did not consider the connectivity with mangrove forests. But previous research has found that seagrass carbon sequestration increases when seagrass meadows and mangrove forests are adjacent to each other (Chen et al., 2017; Huxham et al., 2018). Therefore, connectivity with all three systems needs to be further explored.

DATA AVAILABILITY STATEMENT

The datasets generated for this study are available on request to the corresponding author, in the **Supplementary Material** and in ZMT database (https://www.spatialdatahub.org/pat/zmt-database/) through ID 591.

AUTHOR CONTRIBUTIONS

LG-V conceived the study, performed the research, analyzed the data, contributed to the methods or models, and wrote the manuscript. LG contributed by analyzing the data, contributed to the methods or models, and helped to write the manuscript. JM-P conceived the study, supported the data analyzes, and wrote the manuscript. All authors contributed to the article and approved the submitted version.

FUNDING

Thanks to the Center for Excellence in Marine Science Corporation CEMarin, because the support and co-financing of the project and doctoral thesis in marine sciences "Evaluation of seagrass beds as carbon reservoirs: a case study in the Colombian Caribbean" in Universidad Nacional de Colombia, Contract No. 05-2016. Thanks to the Consejo Profesional de Biología CPBiol, because the partial financial support of this project, through Contract No. 13 of 2015. Thanks to COLCIENCIAS and COLFUTURO, because the co-financing of the project through Call No. 617. Also, thanks to Fundación ECO R-EVOLUTION for its partial financial support in travel expenses during the fieldwork.

ACKNOWLEDGMENTS

We thank ZMT chemistry laboratory to facilitate autoanalyzer use and Dr. B. Gavio for her independent revision of this manuscript.

SUPPLEMENTARY MATERIAL

The Supplementary Material for this article can be found online at: https://www.frontiersin.org/articles/10.3389/fmars.2020.00628/full#supplementary-material

REFERENCES

Abdul aziz, P., Mancera-Pineda, J. E., and Gavio, B. (2018). Rapid assessment of coastal water quality for recreational purposes: methodological proposal. *Ocean Coast. Manag.* 151, 118–126. doi: 10.1016/j.ocecoaman.2017.10.014

Ackerly, D. D., and Cornwell, W. K. (2007). A trait-based approach to community assembly: partitioning of species trait values into within- and among-community components. *Ecol. Lett.* 10, 135–145. doi: 10.1111/j.1461-0248.2006.01006.x

Alcoverro, T., Duarte, C. M., and Romero, J. (1995). Annual growth dynamics of *Posidonia oceanica*: contribution of large-scale versus local factors to seasonality. *Mar. Ecol. Prog. Ser.* 120, 203–210. doi: 10.3354/meps120203

American Public Health Association [APHA], (1992). *Standard Methods For The Examination Of Water And Wastewater*, 20th Edn, Washington, DC: American Public Health Association.

Arellano-Méndez, L. U., Herrera-Silveira, J. A., Montero-Muñoz, J. L., and De los Angeles Liceaga-Correa, M. (2011). Morphometric trait variation in *Thalassia testudinum* (Banks ex König) associated to environmental heterogeneity in a subtropical ecosystem. *J. Ecosyst. Ecogr.* S1:001. doi: 10.4172/2157-7625.S1-001

Arias-Ortiz, A., Serrano, O., Masqué, P., Lavery, P. S., Mueller, U., Kendrick, G. A., et al. (2018). A marine heat wave drives massive losses from the world's largest seagrass carbon stocks. *Nat. Clim. Chang.* 8, 338–344. doi: 10.1038/s41558-018-0096-y

Barry, S. C., Bianchi, T. S., Shields, M. R., Hutchings, J. A., Jacoby, C. A., and Frazer, T. K. (2018). Characterizing blue carbon stocks in *Thalassia testudinum* meadows subjected to different phosphorus supplies: a lignin biomarker approach. *Limnol. Oceanogr.* 63, 2630–2646. doi: 10.1002/lno.10965

Bouillon, S., and Connolly, R. M. (2009). "Carbon exchange among tropical coastal ecosystems" in *Ecological Connectivity Among Tropical Coastal Ecosystems*, ed. I. Nagelkerken, (Dordecht: Springer), 45–70. doi: 10.1007/978-90-481-2406-0

Bird, E. C. (1994). "Physical setting and geomorphology of coastal lagoons (Chapter 2)," in *Coastal Lagoon Processes*, Vol. 60, ed. B. Kjerfve, (Amsterdam: Elsevier Oceanography Series), 9–39. doi: 10.1016/s0422-9894(08)70007-2

Burkholder, J. M., Tomasko, D. A., and Touchette, B. W. (2007). Seagrasses and eutrophication. *J. Exper. Mar. Biol. Ecol.* 350, 46–72. doi: 10.1016/j.jembe.2007.06.024

Chen, G., Huzni Azkab, M., Chmura, G. L., Chen, S., Sastrasuwondo, P., Ma, Z., et al. (2017). Mangroves as a major source of soil carbon storage in adjacent seagrass meadows. *Sci. Rep.* 7:42406. doi: 10.1038/srep42406

Christianen, M. J. A., van Belzen, J., Herman, P. M. J., van Katwijk, M. M., Lamers, L. P. M., van Leent, P. M. J., et al. (2013). Low-canopy seagrass beds still provide important coastal protection services. *PLoS One* 8:e62413. doi: 10.1371/journal.pone.0062413

Collier, C., Lavery, P., Masini, R., and Ralph, P. (2007). Morphological, growth and meadow characteristics of the seagrass *Posidonia sinuosa* along a depth-related gradient of light availability. *Mar. Ecol. Prog. Ser.* 337, 103–115. doi: 10.3354/meps337103

Cornelisen, C. D., and Thomas, F. I. M. (2004). Ammonium and nitrate uptake by leaves of the seagrass *Thalassia testudinum*: impact of hydrodynamic regime and epiphyte cover on uptake rates. *J. Mar. Syst.* 49, 177–194. doi: 10.1016/j.jmarsys.2003.05.008

de Boer, W. F. (2007). Seagrass-sediment interactions, positive feedbacks and critical thresholds for occurrence: a review. *Hydrobiologia* 591, 5–24. doi: 10.1007/s10750-007-0780-9

de los Santos, C. B., Onoda, Y., Vergara, J. J., Pérez-Lloréns, J. L., Bouma, T. J., and La Nafie, Y. A. (2016). A comprehensive analysis of mechanical and morphological traits in temperate and tropical seagrass species. *Mar. Ecol. Prog. Ser.* 551, 81–94. doi: 10.3354/meps11717

Díaz, J. M., Barrios, L. M., and Gómez-López, D. I. (2003). *Las Praderas De Pastos Marinos En Colombia: Estructura Y Distribución De Un Ecosistema Estratégico, Serie Publicaciones Especiales No. 10*. Santa Marta: INVEMAR.

Duarte, C. M. (1990). Seagrass nutrient content. *Mar. Ecol. Prog. Ser.* 67, 201–207. doi: 10.3354/meps067201

Duarte, C. M., Losada, I. J., Hendriks, I. E., Mazarrasa, I., and Marbà, N. (2013). The role of coastal plant communities for climate change mitigation and adaptation. *Nat. Clim. Chang.* 3, 961–968. doi: 10.1038/nclimate1970

Duarte, C. M., Middelburg, J. J., and Caraco, N. (2005). Major role of marine vegetation on the oceanic carbon cycle. *Biogeosciences* 2, 1–8. doi: 10.5194/bg-2-1-2005

Ferrario, F., Beck, M. W., Storlazzi, C. D., Micheli, F., Shepard, C. C., and Airoldi, L. (2014). The effectiveness of coral reefs for coastal hazard risk reduction and adaptation. *Nat. Commun.* 5:3794. doi: 10.1038/ncomms4794

Folmer, E. O., van der Geest, M., Jansen, E. J., Olff, H., Anderson, T. M., Piersma, T., et al. (2012). Seagrass-sediment feedback: an exploration using a non-recursive structural equation model. *Ecosystems* 15, 1380–1393. doi: 10.1007/s10021-012-9591-6

Fourqurean, J. W., Duarte, C. M., Kennedy, H., Marbà, N., Holmer, M., Mateo, M. A., et al. (2012a). Seagrass Meadows as a globally significant carbon stock. *Nat. Geosci.* 5, 505–509.

Fourqurean, J. W., Kendrick, G. A., Collins, L. S., Chambers, R. M., and Vanderklift, M. A. (2012b). Carbon, nitrogen and phosphorus storage in subtropical seagrass meadows: examples from Florida Bay and Shark Bay. *Mar. Freshw. Res.* 63, 967–983.

Gavio, B., Palmer-Cantillo, S., and Mancera, J. E. (2010). Historical analysis (2000-2005) of the coastal water quality in San Andrés Island, SeaFlower biosphere reserve, Caribbean Colombia. *Mar. Pollut. Bull.* 60, 1018–1030. doi: 10.1016/j.marpolbul.2010.01.025

Gillis, L. G., Bouma, T. J., Jones, C. G., van Katwijk, M. M., Nagelkerken, I., Jeuken, C. J. L., et al. (2014a). Potential for landscape-scale positive interactions among tropical marine ecosystems. *Mar. Ecol. Prog. Ser.* 503, 289–303. doi: 10.3354/meps10716

Gillis, L. G., Ziegler, A. D., van Oevelen, D., Cathalot, C., Herman, P. M. J., Wolters, J. W., et al. (2014b). Tiny is mighty: seagrass beds have a large role in the export of organic material in the tropical coastal zone. *PLoS One* 9:e111847. doi: 10.1371/journal.pone.0111847

Gillis, L. G., Paul, M., and Bouma, T. (2017). Opportunities for protecting and restoring tropical coastal ecosystems by utilizing a physical connectivity approach. *Front. Mar. Sci.* 4:374. doi: 10.3389/fmars.2017.00374

Guannel, G., Arkema, K., Ruggiero, P., and Verutes, G. (2016). The power of three: coral reefs seagrasses and mangroves protect coastal regions and increase their resilience. *PLoS One* 11:e0158094. doi: 10.1371/journal.pone.0158094

Guerra-Vargas, V. A., and Guerra-Vargas, L. A. (2017). "Determinación y cartografía del área de los pastos marinos del lagoon arrecifal de la isla de San Andrés," in *VI Seminario Las Ciencias del Mar en la Universidad Nacional de Colombia "20 Años de la sede Caribe"*, ed. CECIMAR (San Andrés Isla: Universidad Nacional de Colombia sede Caribe), 40.

Gullström, M., Lyimo, L. D., Dahl, M., Samuelsson, G. S., Eggertsen, M., Anderberg, E., et al. (2018). Blue carbon storage in tropical seagrass meadows relates to carbonate stock dynamics, plant-sediment processes, and landscape context: insights from the Western Indian Ocean. *Ecosystems* 21, 551–566. doi: 10.1007/s10021-017-0170-8

Hardy, T. A., and Young, I. R. (1996). Field study of water attenuation on an offshore coral reef. *J. Geophys. Res.* 101, 14311–14326. doi: 10.1029/96jc00202

Harris, D. L., Rovere, A., Casella, E., Power, H., Canavesio, R., Collin, A., et al. (2018). Coral reef structural complexity provides important coastal protection from waves under rising sea levels. *Sci. Adv.* 4:eaao4350. doi: 10.1126/sciadv.aao4350

Hemminga, M., and Duarte, C. M. (2000). *Seagrass Ecology*. Cambridge: Cambridge University Press.

Hizon-Fradejas, A. B., Nakano, Y., Nakai, S., Nishijima, W., and Mitsumasa, O. (2009). Anchorage and resistance to uprooting forces of eelgrass (*Zostera marina* L.) shoots planted in slag substrates. *J. Water Environ. Technol.* 7, 91–101. doi: 10.2965/jwet.2009.91

Hossain, M. B., Marshall, D. J., and Venkattramanan, S. (2014). Sediment granulometry and organic matter content in the intertidal zone of the Sungai Brunei estuarine system, northwest coast of Borneo. *Carpathian J. Earth Enviro. Sci.* 9, 231–239.

Howard, J., Hoyt, S., Isensee, K., Pidgeon, E., and Telszewski, M. (2014). "field sampling of soil carbon pools in coastal ecosystems," in *Coastal Blue Carbon: Methods for Assessing Carbon Stocks and Emissions Factors in Mangroves, Tidal Salt Marshes, and Seagrasses*, Chap. 3, eds J. Howard, S. Hoyt, K. Isensee, M. Telszewski, and E. Pidgen, (Arlington, VI: UNESCO).

Huxham, M., Whitlock, D., Githaiga, M., and Dencer-Brown, A. (2018). Carbon in the coastal seascape: how interactions between mangrove forests, seagrass meadows and tidal marshes influence carbon storage. *Curr. Forest. Rep.* 4, 101–110. doi: 10.1007/s40725-018-0077-4

IGAC (1986). *San Andrés y Providencia. Aspectos Geográficos*. Bogotá: Instituto Geográfico Agustín Codazzi (IGAC).

Kennedy, H., Beggins, J., Duarte, C. M., Fourqurean, J. W., Holmer, M., Marbá, N., et al. (2010). Seagrass sediments as a global carbon sink: isotopic constraints. *Glob. Biogeochem. Cycles* 24:GB4026. doi: 10.1029/2010GB003848

Kindeberg, T., Ørberg, S. B., Röhr, M. E., Holmer, M., and Krause-Jensen, D. (2018). Sediment stocks of carbon, nitrogen, and phosphorus in danish eelgrass Meadows. *Front. Mar. Sci.* 5:474. doi: 10.3389/fmars.2018.00474

Koch, E. W., Ackerman, J. D., Verduin, J., and van Keulen, M. (2006). "Fluid dynamics in seagrass ecology-from molecules to ecosystems," in *Seagrasses: Biology, Ecology and Conservation*, eds A. W. D. Larkum, R. J. Orth, and C. M. Duarte, (Amsterdam: Springer), 193–225. doi: 10.1007/1-4020-2983-7_8

Lavery, P. S., Mateo, M. A., Serrano, O., and Rozaimi, M. (2013). Variability in the carbon storage of seagrass habitats and its implications for global estimates of blue carbon ecosystem service. *PLoS One* 8:e73748. doi: 10.1371/journal.pone.0073748

Lee, K., and Dunton, K. H. (2000). Effects of nitrogen enrichment on biomass allocation, growth, and leaf morphology of the seagrass *Thalassia testudinum*. *Mar. Ecol. Prog. Ser.* 196, 39–48. doi: 10.3354/meps196039

Lee, K., Park, S. R., and Kim, Y. K. (2007). Effects of irradiance, temperature, and nutrients on growth dynamics of seagrasses: a review. *J. Exper. Mar. Biol. Ecol.* 350, 144–175. doi: 10.1016/j.jembe.2007.06.016

Lugo-Fernández, A., Roberts, H. H., and Wiseman, W. J. (1992). Tide effects on wave attenuation and wave set-up on a Caribbean coral reef. *Estuar. Coast. Shelf Sci.* 47, 385–393. doi: 10.1006/ecss.1998.0365

McDonald, A. M., Prado, P., Heck, K. L., Fourqurean, J. W., Frankovich, T. A., Dunton, K. H., et al. (2016). Seagrass growth, reproductive, and morphological plasticity across environmental gradients over a large spatial scale. *Aquat. Bot.* 134, 87–96. doi: 10.1016/j.aquabot.2016.07.007

Mcleod, E., Chmura, G. L., Bouillon, S., Salm, R., Björk, M., Duarte, C. M., et al. (2011). A blueprint for blue carbon: toward an improved understanding of the role of vegetated coastal habitats in sequestering CO_2. *Front. Ecol. Environ.* 9, 552–560. doi: 10.1890/110004

Medina-Gómez, I., Madden, C. J., Herrera-Silveira, J., and Kjerfve, B. (2016). Response of Thalassia testudinum morphometry and distribution to environmental drivers in a pristine tropical lagoon. *PLoS One* 11:e0164014. doi: 10.1371/journal.pone.0164014

Morris, E. P., Peralta, G., Brun, F. G., van Duren, L., Bouma, T. J., and Perez-Llorens, J. L. (2008). Interaction between hydrodynamics and seagrass canopy structure: spatially explicit effects on ammonium uptake rates. *Limnol. Oceanogr.* 53, 1531–1539. doi: 10.4319/lo.2008.53.4.1531

Paterson, D., and Black, K. (1992). Water flow, sediment dynamics and benthic biology. *Adv. Ecol. Res.* 29, 155–193. doi: 10.1016/s0065-2504(08)60193-2

Pérez, D., Guevara, M., and Bone, D. (2006). Temporal variation of biomass and productivity of *Thalassia testudinum* (Hydrocharitaceae) in Venezuela, Southern Caribbean. *Intern. J. Trop. Biol.* 54, 329–339.

Potouroglou, M., Bull, J. C., Krauss, K. W., Kennedy, H., Fusi, M., Dafonchio, D., et al. (2017). Measuring the role of seagrasses in regulating sediment surface elevation. *Sci. Rep.* 7:11917. doi: 10.1038/s41598-017-12354-y

Rodríguez, A., Mancera, P. J. E., and Gavio, B. (2010). Survey of benthic dinoflagellates associated to beds of *Thalassia testudinum* in San Andrés island, Seaflower biosphere reserve, Caribbean Colombia. *Acta biol. Colomb.* 15, 231–248.

Saderne, V., Geraldi, N. R., Macreadie, P. I., Maher, D. T., Middelburg, J. J., Serrano, O., et al. (2019). Role of carbonate burial in blue carbon budgets. *Nat. Commun.* 10:1106. doi: 10.1038/s41467-019-08842-6

Saunders, M. I., Leon, J. X., Callaghan, D. P., Roelfsema, C. M., Hamilton, S., Brown, C. J., et al. (2014). Interdependency of tropical marine ecosystems in response to climate change. *Nat. Clim. Chang.* 4, 724–729. doi: 10.1038/nclimate2274

Serrano, O., Lavery, P. S., Rozaimi, M., and Mateo, M. A. (2014). Influence of water depth on the carbon sequestration capacity of seagrasses. *Glob. Biogeochem. Cycles* 28, 950–961. doi: 10.1002/2014GB004872

Serrano, O., Lovelock, C. E., Atwood, T., Macreadie, P., Canto, R., Phinn, S., et al. (2019). Australian vegetated coastal ecosystems as global hotspots for climate change mitigation. *Nat. Commun.* 10:4313. doi: 10.1038/s41467-019-12176-8

van Katwijk, M. M., Bos, A. R., Hermus, D. C. R., and Suykerbuyk, W. (2010). Sediment modification by seagrass beds: muddification and sandification induced by plant cover and environmental conditions. *Estuar. Coast. Shelf Sci.* 89, 175–181. doi: 10.1016/j.ecss.2010.06.008

van Tussenbroek, B., Cortés, J., Collin, R., Fonseca, A. C., Gayle, P. M., Guzmán, H. M., et al. (2014). Caribbean-wide, long-term study of seagrass beds reveals local variations, shifts in community structure and occasional collapse. *PLoS One* 9:e90600. doi: 10.1371/journal.pone.0090600

Wentworth, C. A. (1992). Scale of grade and class terms for clastic sediments. *Geology* 30, 377–392. doi: 10.1086/622910

Conflict of Interest: The authors declare that the research was conducted in the absence of any commercial or financial relationships that could be construed as a potential conflict of interest.

frontiers in Marine Science

DATA REPORT
published: 31 August 2020
doi: 10.3389/fmars.2020.00646

Multi-Year Density Variation of Queen Conch (*Aliger gigas*) on Serrana Bank, Seaflower Biosphere Reserve, Colombia: Implications for Fisheries Management

Néstor E. Ardila[1], Hernando Hernández[1], Astrid Muñoz-Ortiz[2], Óscar J. Ramos[2], Erick Castro[3], Nacor Bolaños[3], Anthony Rojas[4] and Juan A. Sánchez[5]*

[1] División de Biología Marina, ECOMAR Consultoría Ambiental, Bogotá, Colombia, [2] Departamento de Ciencias Básicas, Universidad de La Salle, Bogotá, Colombia, [3] Corporación para el Desarrollo Sostenible del Departamento Archipiélago de San Andrés Providencia y Santa Catalina, CORALINA, San Andrés, Colombia, [4] Secretaria de Agricultura y Pesca de la Gobernación del Departamento Archipiélago de San Andrés Providencia y Santa Catalina, San Andrés, Colombia, [5] Laboratorio de Biología Molecular Marina (BIOMMAR), Departamento de Ciencias Biológicas, Facultad de Ciencias, Universidad de los Andes, Bogotá, Colombia

Keywords: spatial distribution, density, marine protected area—MPA, fishery resource, caribbean sea

OPEN ACCESS

Edited by:
Jesper H. Andersen, NIVA Denmark Water Research, Denmark

Reviewed by:
Paulo Vasconcelos, Portuguese Institute of Ocean and Atmosphere (IPMA), Portugal
Francesco Tiralongo, Ente Fauna Marina Mediterranea (EFMM), Italy

****Correspondence:***
Néstor E. Ardila
nestorardila@ecomar.com.co

Specialty section:
This article was submitted to Marine Ecosystem Ecology, a section of the journal Frontiers in Marine Science

Received: *28 February 2020*
Accepted: *14 July 2020*
Published: *31 August 2020*

Citation:
Ardila NE, Hernández H, Muñoz-Ortiz A, Ramos ÓJ, Castro E, Bolaños N, Rojas A and Sánchez JA (2020) Multi-Year Density Variation of Queen Conch (Aliger gigas) on Serrana Bank, Seaflower Biosphere Reserve, Colombia: Implications for Fisheries Management. Front. Mar. Sci. 7:646. doi: 10.3389/fmars.2020.00646

BACKGROUND

Queen conch *Aliger gigas* (Linnaeus, 1758), formerly known as *Strombus gigas*, constitute a valuable commercial and cultural resource for native communities since pre-Hispanic times (Baisre, 2010). Populations of this marine gastropod are registered for 36 countries in the Caribbean, extending from Florida to the northern coast of South America and live mainly on sandy bottoms, in clear waters down to a depth of 100 m (CITES, 2003). Mating and spawning usually take place during the warmer months of the year, although in some areas, mainly in the western Caribbean, the breeding activity is continuous at low reproduction levels throughout the year (Avila-Poveda and Baqueiro-Cardenas, 2009; Aldana-Aranda et al., 2014; Boman et al., 2018). Moreover, some populations migrate seasonally from open waters to shallower waters for spawning (Appeldoorn, 1993).

Over the past decades, intensive overfishing has led to population decline, collapse of stocks, and temporary closure of fisheries in different locations at Bermuda, Cuba, Colombia, Florida, Mexico, Netherlands Antilles, Virgin Islands and Venezuela (Stoner and Schwarte, 1994; Stoner et al., 2018). Studies indicate that most populations of *A. gigas* continue their decline despite having been listed in the CITES appendices for being threatened by local fisheries in countries like Belize, Colombia, Dominican Republic, Haiti, Honduras, Panama, Puerto Rico and the Virgin Islands, as well as the support by regional fisheries management agencies (Stoner et al., 2012; Prada et al., 2017; Tewfik et al., 2019).

In the Colombian Caribbean, *A. gigas* has been one of the most significant fishery resources for many years, being therefore subject to large-scale exploitation. Specifically, for the Seaflower Biosphere Reserve, which included the archipelago of San Andrés, Providencia and Santa Catalina, the landings reached a maximum of 813 tons in 1988, decreasing to 465 tons in 1993 and 81 tons in 2003 (Prada et al., 2009). Restricted access to this resource was enforced in this region between 2005–2007 and 2011–2013. The fishery was reopened between 2008 and 2010 in the areas of Serrana and Roncador banks, and in 2013 only for Serrana bank (Prada et al., 2009; Castro et al., 2011).

In terms of conservation activities, following the guidelines of FAO and CITES, efforts for the responsible management of the queen conch have been implemented in Colombia, which enforced

fishing management and regulations since 1977 (Castro et al., 2011). In recent years, studies have estimated densities and abundances of the queen conch throughout habitat and depth strata on different banks of the Seaflower Biosphere Reserve at least once every 3 years (Castro et al., 2011). With the new ecosystem-based management approach, the 8% control rule proposed by Medley (2008) was incorporated as a criterion of sustainability to regulate the intensity of fishing activity. This increased the restriction for fishing in small banks, taking into account the recruitment of juveniles, the zoning of the Marine Protected Areas (MPA's), and illegal fishing. With this model, it was possible to define the fishery closing and reopening cycles, which have shown positive effects on species recovery (Castro et al., 2011).

The combination of overfishing and the loss and disturbance of habitats are the main factors influencing the population decrease of the queen conch. The current study presents a multi-temporal analysis of *A. gigas* populations on Serrana bank, which is an atoll in the western Caribbean that is included into the Seaflower Biosphere Reserve. This reserve was declared a Marine Protected Area since 2005. The main objective was to release raw data from these valuable observations and assess whether the management tools in the MPA are having positive effects on the recovery and conservation of juvenile and adult populations of *A. gigas*.

DATA COLLECTION

Serrana bank is a triangular bank of 15.5 km in maximum length in the direction SW-NE, originated from an atoll partially dissected to leeward (Díaz et al., 2000). The bank platform has a volcanic form with a strong slope emerging from 1,500 m depth (Geister and Díaz, 2007). Despite its isolation from human populations, coral reef habitats have been declining in the last three decades on Serrana Bank following the Caribbean-wide trend (Sánchez et al., 2019). A total of 72 sampling sites were established on Serrana Bank, which were monitored five times over a period of 10 years (2003, 2007, 2010, 2011, and 2013), although only 69 sampling sites were monitored during 2003. Monitoring consisted in observations of the distribution and density of the queen conch during each season. Estimates of abundance and density of queen conch were made from diver-based visual surveys along 4 strip-transects of 30 × 8 m. Data collected during observations included georeferencing, depth, habitat type (seagrass habitat is not present on Serrana bank, probably replaced by the ruffled form of *Lobophora variegata*, see additional details in Sánchez et al., 2005, 2019), zoning regarding conservation, and density of adults and juveniles of the conch estimated as number of individuals per hectare (ind. ha^{-1}). All conch encountered were counted and lip thickness was measured (nearest 0.1 mm) with a caliper by placing it as far as possible onto the middle of the shell lip. Adults were defined as individuals with flared lips ≥5 mm thick (Brownell, 1977). This criterion was adopted since 2003 although more recently higher values have been proposed (e.g., ≥13 mm; Avila-Poveda and Baqueiro-Cardenas, 2006). The difference in these criteria are due to the fact that the first reference of sexual maturity was based on the evaluation of external macroscopic characteristics and the second work was based on histological methods.

STATISTICAL ANALYSIS AND SPATIAL DESCRIPTION

To establish relationships between depth and adult and juvenile densities of the queen conch, Spearman rank correlations were calculated for the five different samplings given the lack of normality of the data (Shapiro Wilk test). Additionally, to describe and characterize changes in the conch density among habitat types, sampling periods and zoning with respect to conservation, a factorial analysis of variance was performed. The estimations were made using R (R Development Core Team, 2015) with statistical significance level considered for $p < 0.05$. Based on the information obtained from the 72 sites, and using their respective georeference, densities (ind. ha^{-1}) were mapped for juvenile and adult populations. As a geographical reference, the maps illustrate the −100 m depth. Specifically, for representative effects on the map, the density was represented as interpolations with the point kriging method using software Surfer 10. In order to optimize the analysis, the habitat at each sampling site was classified into four categories of substrate type: sand, sand and macroalgae, sand and debris and mixed coral. Additionally, each of the 72 sampling points was classified according to its location in the Serrana Bank MPA within the following categories: recovery and sustainable use (artisanal fishing), preservation and open area to the fishing activity.

MULTI-YEAR DENSITY VARIATION OF QUEEN CONCH (*ALIGER GIGAS*)

A total of 352 observations were made during five sampling years between 2003 and 2013 at depths ranging from 2 to 23 m. The average population density was 123.4 ind. ha^{-1} for juveniles, 96.0 ind. ha^{-1} for adults and 219.4 ind. ha^{-1} for the total population. During the sampling period, the analysis showed that the population density doubled, with a considerable increase of adults and juveniles in 2013 and a minimum average population density for 2010 (**Figure 1** and **Supplementary Figure 1**). At the southeastern and western sectors, the sites with the highest juvenile's density during the study period had averages of 1398 ind. ha^{-1} (site 50) and 1221 ind. ha^{-1} (site 8). For adults, the highest average densities were 583 ind. ha^{-1} (site 8) and 494 ind. ha^{-1} (site 31) (**Figure 2A**). The general description of the density in each period and type of habitat showed that juveniles were more abundant in sandy bottoms with macroalgae, whereas adults preferred sand debris bottoms.

Juvenile density was not associated with the depth of the sampling sites ($r^2 = 0.249$, $p < 0.0001$) (**Figure 2**). On the other hand, there was a significant relationship between adults' densities and sampling depth ($r^2 = 0.080$, $p < 0.001$). Results showed that more adults than juveniles were found at greater depths (**Figure 2**).

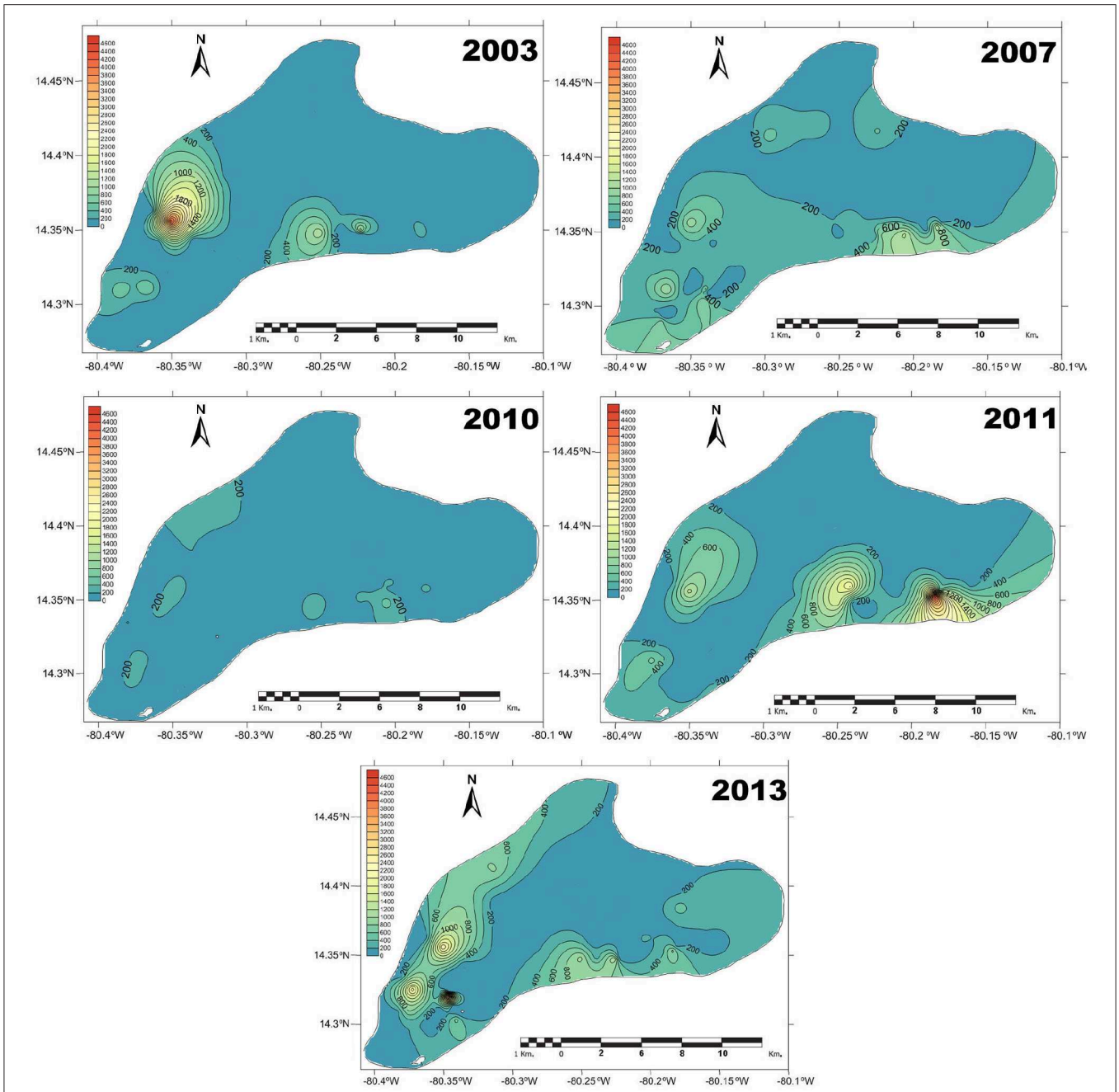

FIGURE 1 | Digital maps of *A. gigas* total density (ind. ha^{-1}) on Serrana Bank (2003–2013) using kriging prediction.

Adult and total snail densities were associated with habitat type, sampling year and zoning with respect to conservation ($p < 0.001$), whereas juveniles were only affected by the type of habitat. Regarding the sampling year, the highest densities were observed in 2007, 2011, and 2013 (**Figure 1** and **Supplementary Figure 1**). The highest densities of adults and juveniles were found in the sand and debris habitat (**Supplementary Table 1**). Finally, open areas presented the highest densities of the snail, indicating preliminarily that the definition of conservation areas have not been efficient for the protection of the resource. The recovery of the resource in the years 2007, 2011, and 2013 is highlighted, which overlaps with the fishery closed seasons on Serrana bank area. Adults were most sparsely distributed in the west sector of Serrana Bank reaching high densities between 400 and 1,800 ind. ha^{-1} (standard error = 0.120–0.132, **Supplementary Figure 1**). Density of adults in the east section of the bank was close to middle part of the bank. Juveniles presented a more

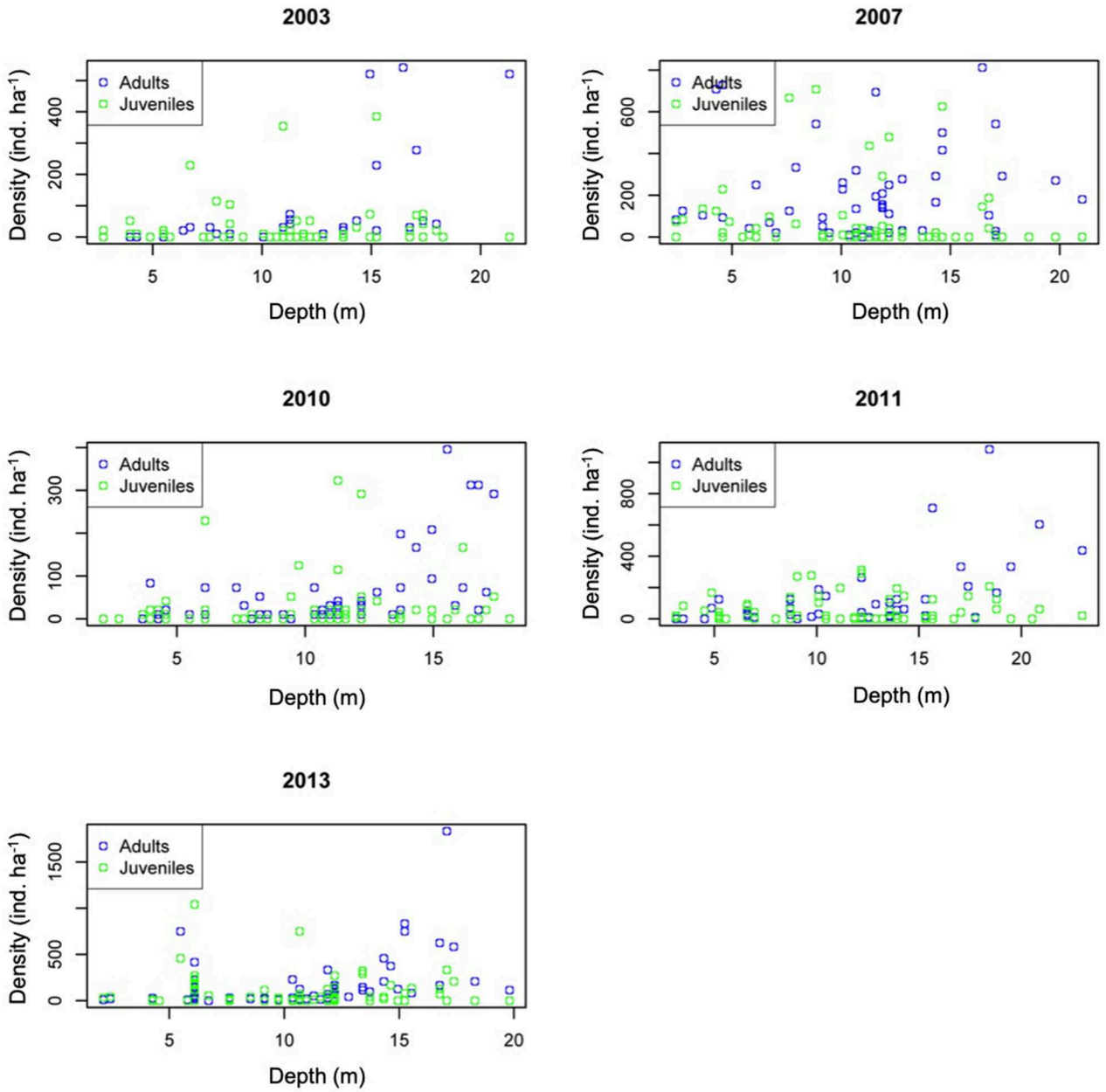

FIGURE 2 | Relationships between sampling depth and densities (ind. ha^{-1}) of *A. gigas* throughout the study period (2003–2013) in Serrana Bank.

dispersed distribution especially in the south of the bank in the last years (2007–2013; standard error = 0.128–0.132, **Supplementary Figure 2**).

IMPLICATIONS FOR FISHERIES MANAGEMENT

The highest densities of adults were observed in 2007 and 2013, with the sand-debris habitat displaying higher densities. On the contrary, the lowest densities were registered in 2003 and 2010. For juveniles, the densities were variable and presented highest values on sand-macroalgae, sand-debris and sand. The highest densities of juveniles were recorded in 2007, 2011, and 2013 and the lowest densities of juveniles were markedly recorded in 2010. Rapid increase in adult queen conch density is probably a direct function of fishing effort limitation due to the closure of the fishery. Several authors have suggested that these deep-water conchs, inhabiting beyond the depth range accessible to free divers, are the primary source of larvae for shallower populations and thus allow for the recovery of the resource (Stoner et al., 2018).

Densities recorded in Serrana bank are similar to those reported for Bahamas during 2011 (Stoner et al., 2012) and

can be up to 10–100 times higher than those reported for adults and juveniles in other studies in the Caribbean, such as in Guadalupe (Saha et al., 2013) and Archipelago Nuestra Señora del Rosario (Gómez-Campo et al., 2010). Likewise, the increase in adults density recorded between 2007 and 2013 can be associated with fishery closures between 2005–2007 and 2011–2013, which has been also noted in closures elsewhere in the Caribbean (Saha et al., 2013). These fishing regulations provided a better conservation strategy for the resource in this region, where the definition of conservation areas did not produce positive outcomes.

The significant relationship between the density of adults and sampling depth corroborated previous studies (García, 1991; Gómez-Campo et al., 2010) that concluded that the species distribution is depth-dependent. In different areas of San Andrés and Providencia Archipelago, it was observed that juveniles and pre-adults are located between 5 and 10 m depth and adults between 18 and 25 m depth (García, 1991). Nursery areas are often very shallow (<5 m), whereas larger organisms are distributed in deeper waters, including mesophotic environments down to approximately 60 m (Stoner and Schwarte, 1994; Garcia-Sais et al., 2012). The greatest association of adults with the "sand and debris" habitat, is due to the species reproductive activity associated with coarse sand and gravel bottoms (Glazer and Kidney, 2004).

REUSE POTENTIAL

The decrease of queen conch populations in different Caribbean areas is imminent and has led to the collapse of fisheries in many locations. The populations in Bermuda, Dominican Republic, Florida (USA), Haiti, Costa Rica, Puerto Rico, Trinidad & Tobago, Venezuela and those of the northern coast of Cuba and the Morrosquillo Gulf in Colombia are diminished and almost exhausted (CITES, 2003; Gómez-Campo et al., 2010). Serrana bank populations comprise an ideal reference dataset for comparisons, where some management measures delivered the expected positive results in recovering the queen conch stocks. In addition, Coralina (Corporación para el Desarrollo Sostenible del Departamento Archipiélago de San Andrés Providencia y Santa Catalina) is monitoring this population every year and this solid and extensive dataset will be needed to ensure continuity and to provide better predictions on this valuable resource.

DATA AVAILABILITY STATEMENT

All datasets generated for this study are included in the article/**Supplementary Material**.

AUTHOR CONTRIBUTIONS

EC, NB, and JS conceived the study. EC, NB, and AR collected the data. NA, HH, AM-O, and ÓR analyzed the data. NA, HH, and JS wrote the manuscript. All authors contributed to the article and approved the submitted version.

FUNDING

This work was supported by an agreement between Corporación para el Desarrollo Sostenible del Departamento Archipiélago de *San Andrés* Providencia y Santa Catalina, CORALINA-Universidad de los Andes (Convenios No. 13, 2014 and No. 21, 2015). Coralina and *Secretaria de Agricultura y Pesca* collected the data.

ACKNOWLEDGMENTS

Secretatria de Agricultura y Pesca de la Gobernación del Archipiélago de San Andrés, Providencia y Santa Catalina. Logistics and boat crew from CORALINA are greatly appreciated. Members of BIOMMAR, particularly J. Andrade helped with logistics and early stages of the study.

SUPPLEMENTARY MATERIAL

The Supplementary Material for this article can be found online at: https://www.frontiersin.org/articles/10.3389/fmars.2020.00646/full#supplementary-material

Supplementary Figure 1 | *A. gigas* average density (ind. ha^{-1}) by site (Juveniles and Adults) on Serrana Bank in the Seaflower Biosphere Reserve 2003–2013.

Supplementary Figure 2 | Adults density (ind. ha^{-1}) on Serrana Bank (2003–2013) using kriging prediction.

Supplementary Figure 3 | Juveniles density (ind. ha^{-1}) on Serrana Bank (2003–2013) using kriging prediction.

Supplementary Table 1 | Total, juveniles and adults densities by sites, coordinates, depth and bottoms types on Serrana Bank (2003–2013).

REFERENCES

Aldana-Aranda, D, Oxenford, H. A., Bissada, C., Enriquez Díaz, M., Brulé, T., Delgado, G. A., Martínez Morales, I., et al. (2014). Reproductive patterns of queen conch, Strombus gigas (Mollusca, Gastropoda), across the wider Caribbean region. *Bull. Mar. Sci.* 90, 813–831. doi: 10.5343/bms.2013.1072

Appeldoorn, R. S. (1993). *Reproduction, Spawning Potential Ratio and Larval Abundance of queen Conch of La Parguera, Puerto Rico*. Report Caribb. Fish. Manage. Counc. Hato Rey (P. R.).

Avila-Poveda, O.H., and Baqueiro-Cardenas, E. R. (2006). Size at sexual maturity in the queen conch Strombus gigas fron Colombia. *Bol. Invest. Mar. Cost.* 35, 223–233. doi: 10.25268/bimc.invemar.2006.35.0.225

Avila-Poveda, O.H., and Baqueiro-Cardenas, E. R. (2009). Reproductive cycle of *Strombus gigas* Linnaeus 1758 (Caenogastropoda strombidae) from archipelago of San andres, Providencia and Santa Catalina, Colombia. *Invertebr. Reprod. Dev.* 53, 1–12. doi: 10.1080/07924259.2009.9652284

Baisre, J. A. (2010). Setting a baseline for Caribbean fisheries. *J. Island Coastal Archaeol.* 5, 120–147. doi: 10.1080/15564891003663943

Boman, E. M., de Graaf, M., Nagelkerke, L. A. J., Stoner, A. W., Bissada, C. E., Avila-Poveda, O. H., et al. (2018). Variability in size at maturity and reproductive season of queen conch Lobatus gigas (Gastropoda: Strombidae) in the wider Caribbean region. *Fisher. Res.* 201, 18–25. doi: 10.1016/j.fishres.2017.12.016

Brownell, W. N. (1977). Reproduction, laboratory culture, and growth of Strombus gigas, S. costatus and S. pugilis in Los Roques, Venezuela. *Bull. Mar. Sci.* 27, 668–680.

Castro, E., Rojas, A., Prada, M., Forbes, T., Lasso, J., and Manrique, Y. M. (2011). Estado actual de las poblaciones del caracol Strombus gigas en el sector norte del área marina protegida Seaflower. Reporte Técnico. Departamento Archipiélago de San Andrés, Providencia y Santa Catalina. Coralina. Universidad Nacional de Colombia. *San Andrés isla* 23.

CITES (2003). *Review of Significant Trade in specimens of Appendix-II species (Resolution Conf. 12.8 and Decision 12.75)*. Nineteenth meeting of the Animals Committee (Geneva), 71.

Díaz, J. M., Barrios, L. M., Cendales, M. H., Garzón-Ferreira, J., Geister, J., López-Victoria, M., et al. (2000). *Áreas Coralinas de Colombia. Invemar, Serie Publicaciones Especiales No. 5*. Santa Marta, 176.

García, M. I. (1991). *Biología y Dinámica Poblacional del Caracol pala Strombus Gigas L., 1758 (Mollusca, Mesogastropoda) en las Diferentes Áreas del Archipiélago de San Andrés y Providencia*. (Tesis, Univ. del Valle, Fac. de Ciencias, Cali), 183.

Garcia-Sais, J. R., Sabater-Clavell, J., Esteves, R., and Carlo, M. (2012). Fishery independent survey of commercially exploited fish and shellfish populations from mesophotic reefs within the Puertorican EEZ. *Submitted CFMC San Juan PR*. 91.

Geister, J., and Díaz, J. M. (2007). Ambientes arrecifales y geología de un archipiélago oceánico: San Andrés, Providencia y Santa Catalina (mar Caribe, Colombia) con guía de campo. *Ingeominas Bogotá* 114. Available online at: https://www2.sgc.gov.co/Publicaciones/Cientificas/NoSeriadas/Documents/AmbGeolArch-SAnd-Prov-SCat-.pdf

Glazer, R., and Kidney, J. (2004). Habitat associations of adult queen conch (Strombus gigas L.) in an unfished Florida Keys back reef: applications to essential fish habitat. *Bull. Mar. Sci.* 75, 205–224. Available online at: https://www.ingentaconnect.com/content/umrsmas/bullmar/2004/00000075/00000002/art00005

Gómez-Campo, K., Rueda, M., and García-Valencía, C. (2010). Distribucón espacial, abunancia y reación con características del hábitat del caracol pala Eustrombus gigas (Linnaeus) (Mollusca: Strombidae) en el archipiélago Nuestra Señora del Rosario, Caribe colombiano. *Bol. Invest. Mar. Cost.* 39, 137–159. doi: 10.25268/bimc.invemar.2010.39.1.146

Linnaeus, C. (1758). *Systema Naturae per Regna Tria Naturae, Secundum Classes, Ordines, Genera, Species, Cum Characteribus, Differentiis, Synonymis, Locis. Editio Decima, Reformata*, 10th Revised ed. Vol. 1, 824. Available online at: https://biodiversitylibrary.org/page/726886

Medley, P. (2008). *Monitoring and Managing Queen Conch Fisheries: A Manual*. FAO Fisheries Technical Paper No. 514. Rome: FAO, 78.

Prada, M., Castro, E., Taylor, E., Puentes, V., and Daves, N. (2009). *Non Detriment Findings for the Queen Conch in Colombia*. Colombia: NOAA Fisheries – Blue Dream Ltd. 51.

Prada, M. C., Appeldoorn, R. S., VanEijs, S., and Perez, M. M. (2017). *Regional Queen Conch Fisheries Management and Conservation Plan*. Rome: Food and Agriculture Organization of the United Nations.

R Development Core Team (2015). *R: A Language and Environment for Statistical Computing*. Vienna: R Foundation for Statistical Computing.

Saha, W., Díaz, N., and Vincent, C. (2013). "Effects of the annual closure of the queen conch (Strombus gigas) fishery in guadeloupe (FWI)," in *Proceedings of the 65th Gulf and Caribbean Fisheries Institute* (Marathon, FL), 458–469.

Sánchez, J. A., Gómez-Corrales, M., Gutierrez-Cala, L. M., Vergara, D. C., Roa, P., Gonzalez, F. L., et al. (2019). Steady decline of corals and other benthic organisms in the SeaFlower Biosphere reserve (Southwestern Caribbean). *Front. Mar. Sci.* 6:73. doi: 10.3389/fmars.2019.00073

Sánchez, J. A. V., Pizarro, A. R., Acosta, P. A., Castillo, P., Herron, J. C., Martínez, P., et al. (2005). Evaluating coral reef benthic communities in remote atolls (Quitasueño, Serrana, and Roncador Banks) to recommend marine-protected areas for the Seaflower Biosphere Reserve. *Atoll Res. Bull.* 531, 1–66. doi: 10.5479/si.00775630.531.1

Stoner, A.W., and Schwarte, K.C. (1994). Queen conch, *Strombus gigas*, reproductive stocks in the central Bahamas: distribution and probable sources. *Fish. Bull.* 92, 171–179.

Stoner, A. W., Davis, M. H., and Booker, C. J. (2012). Abundance and population structure of queen conch inside and outside a marine protected area: repeat surveys show significant declines. *Mar. Ecol. Progress Ser.* 460, 101–114. doi: 10.3354/meps09799

Stoner, A. W., Davis, M. H., and Kough, A. S. (2018). Relationships between fishing pressure and stock structure in queen conch (Lobatus *gigas*) populations: synthesis of long-term surveys and evidence for overfishing in the bahamas. *Rev. Fish. Sci. Aquac.* 27, 51–71. doi: 10.1080/23308249.2018.1480008

Tewfik, A., Babcock, E., Appeldoorn, R. S., and Gibson, J. (2019). Declining size of adults and juvenile harvest threatens. *Aquatic Conserv. Mar. Freshw. Ecosyst.* 29, 1–21. doi: 10.1002/aqc.3147

Conflict of Interest: NA, HH, AM-O, and ÓR were contracted as consultants from ECOMAR Consultoría Ambiental.

The remaining authors declare that the research was conducted in the absence of any commercial or financial relationships that could be construed as a potential conflict of interest.

Advantages of publishing in Frontiers

OPEN ACCESS
Articles are free to read for greatest visibility and readership

FAST PUBLICATION
Around 90 days from submission to decision

HIGH QUALITY PEER-REVIEW
Rigorous, collaborative, and constructive peer-review

TRANSPARENT PEER-REVIEW
Editors and reviewers acknowledged by name on published articles

Frontiers
Avenue du Tribunal-Fédéral 34
1005 Lausanne | Switzerland

Visit us: www.frontiersin.org
Contact us: frontiersin.org/about/contact

REPRODUCIBILITY OF RESEARCH
Support open data and methods to enhance research reproducibility

DIGITAL PUBLISHING
Articles designed for optimal readership across devices

FOLLOW US
@frontiersin

IMPACT METRICS
Advanced article metrics track visibility across digital media

EXTENSIVE PROMOTION
Marketing and promotion of impactful research

LOOP RESEARCH NETWORK
Our network increases your article's readership